

Herbal medical products for metabolic diseases - new integrated pharmacological approaches

Edited by

Stalin Antony, Avdesh Mishra, Abd El-Latif Hesham,
Quan Zou and Savarimuthu Ignacimuthu

Published in

Frontiers in Pharmacology



FRONTIERS EBOOK COPYRIGHT STATEMENT

The copyright in the text of individual articles in this ebook is the property of their respective authors or their respective institutions or funders. The copyright in graphics and images within each article may be subject to copyright of other parties. In both cases this is subject to a license granted to Frontiers.

The compilation of articles constituting this ebook is the property of Frontiers.

Each article within this ebook, and the ebook itself, are published under the most recent version of the Creative Commons CC-BY licence. The version current at the date of publication of this ebook is CC-BY 4.0. If the CC-BY licence is updated, the licence granted by Frontiers is automatically updated to the new version.

When exercising any right under the CC-BY licence, Frontiers must be attributed as the original publisher of the article or ebook, as applicable.

Authors have the responsibility of ensuring that any graphics or other materials which are the property of others may be included in the CC-BY licence, but this should be checked before relying on the CC-BY licence to reproduce those materials. Any copyright notices relating to those materials must be complied with.

Copyright and source acknowledgement notices may not be removed and must be displayed in any copy, derivative work or partial copy which includes the elements in question.

All copyright, and all rights therein, are protected by national and international copyright laws. The above represents a summary only. For further information please read Frontiers' Conditions for Website Use and Copyright Statement, and the applicable CC-BY licence.

ISSN 1664-8714
ISBN 978-2-8325-5343-5
DOI 10.3389/978-2-8325-5343-5

About Frontiers

Frontiers is more than just an open access publisher of scholarly articles: it is a pioneering approach to the world of academia, radically improving the way scholarly research is managed. The grand vision of Frontiers is a world where all people have an equal opportunity to seek, share and generate knowledge. Frontiers provides immediate and permanent online open access to all its publications, but this alone is not enough to realize our grand goals.

Frontiers journal series

The Frontiers journal series is a multi-tier and interdisciplinary set of open-access, online journals, promising a paradigm shift from the current review, selection and dissemination processes in academic publishing. All Frontiers journals are driven by researchers for researchers; therefore, they constitute a service to the scholarly community. At the same time, the *Frontiers journal series* operates on a revolutionary invention, the tiered publishing system, initially addressing specific communities of scholars, and gradually climbing up to broader public understanding, thus serving the interests of the lay society, too.

Dedication to quality

Each Frontiers article is a landmark of the highest quality, thanks to genuinely collaborative interactions between authors and review editors, who include some of the world's best academicians. Research must be certified by peers before entering a stream of knowledge that may eventually reach the public - and shape society; therefore, Frontiers only applies the most rigorous and unbiased reviews. Frontiers revolutionizes research publishing by freely delivering the most outstanding research, evaluated with no bias from both the academic and social point of view. By applying the most advanced information technologies, Frontiers is catapulting scholarly publishing into a new generation.

What are Frontiers Research Topics?

Frontiers Research Topics are very popular trademarks of the *Frontiers journals series*: they are collections of at least ten articles, all centered on a particular subject. With their unique mix of varied contributions from Original Research to Review Articles, Frontiers Research Topics unify the most influential researchers, the latest key findings and historical advances in a hot research area.

Find out more on how to host your own Frontiers Research Topic or contribute to one as an author by contacting the Frontiers editorial office: frontiersin.org/about/contact

Herbal medical products for metabolic diseases - new integrated pharmacological approaches

Topic editors

Stalin Antony — University of Electronic Science and Technology of China, China

Avdesh Mishra — Texas A&M University Kingsville, United States

Abd El-Latif Hesham — Beni-Suef University, Egypt

Quan Zou — University of Electronic Science and Technology of China, China

Savarimuthu Ignacimuthu — St. Xavier's College, Palayamkottai, India

Citation

Antony, S., Mishra, A., Hesham, A. E.-L., Zou, Q., Ignacimuthu, S., eds. (2024). *Herbal medical products for metabolic diseases - new integrated pharmacological approaches*. Lausanne: Frontiers Media SA. doi: 10.3389/978-2-8325-5343-5

Table of contents

- 05 **Editorial: Herbal medical products for metabolic diseases - new integrated pharmacological approaches**
Antony Stalin, Abd El-Latif Hesham, Avdesh Mishra, Quan Zou and Savarimuthu Ignacimuthu
- 08 **Metabolomics analysis delineates the therapeutic effects of Yinlan Tiaozhi capsule on triton WR-1339 -induced hyperlipidemia in mice**
Guanlin Xiao, Aili Xu, Jieyi Jiang, Zhao Chen, Yangxue Li, Sumei Li, Weitao Chen, Jingnian Zhang, Canchao Jia, Zhihao Zeng and Xiaoli Bi
- 21 **Role of anthraquinones in combating insulin resistance**
Wanru Xia, Shuqian Li, LinZehao Li, Shibo Zhang, Xiaolei Wang, Wenyu Ding, Lina Ding, Xiandang Zhang and Zhibin Wang
- 37 **Methylsulfonylmethane ameliorates metabolic-associated fatty liver disease by restoring autophagy flux via AMPK/mTOR/ULK1 signaling pathway**
Daewon Han, Deokryong Kim, Haeil Kim, Jeonga Lee, Jungmook Lyu, Jong-Seok Kim, Jongdae Shin, Jeong Sig Kim, Do Kyung Kim and Hwan-Woo Park
- 51 **Pharmacological therapy of metabolic dysfunction-associated steatotic liver disease-driven hepatocellular carcinoma**
Yumin Wang, Joshua S. Fleishman, Tongda Li, Yulin Li, Zhao Ren, Jichao Chen and Mingchao Ding
- 66 **Shizao decoction for cirrhotic ascites: assessing potential targets based on network analysis combined with pharmacokinetics and metabolomics**
Wenjing Li, Yujiao Hou, Yanping Wang, Ronghong Liu, Han Zhang, Yanqiong Luo, Qian Li, Mosesmanaanye Njolibimi, Bo Hong and Tao Xu
- 84 **Efficacy of a vaginal suppository formulation prepared with *Acacia arabica* (Lam.) Willd. gum and *Cinnamomum camphora* (L.) J. Presl. in heavy menstrual bleeding analyzed using a machine learning technique**
Mohamed Joonus Aynul Fazmiya, Arshiya Sultana, Md Belal Bin Heyat, Saba Parveen, Khaleequr Rahman, Faijan Akhtar, Azmat Ali Khan, Amer M. Alanazi, Zaheer Ahmed, Isabel de la Torre Díez, Julián Brito Ballester and Tirumala Santhosh Kumar Saripalli
- 107 **Traditional Chinese medicine and its active substances reduce vascular injury in diabetes via regulating autophagic activity**
Yankui Gao, Lei Zhang, Fei Zhang, Rong Liu, Lei Liu, Xiaoyan Li, Xiangdong Zhu and Yonglin Liang
- 125 **The efficacy of botanical drugs in orchestrating epigenetic modifications for ameliorating metabolic disorders**
Eko Fuji Ariyanto

- 130 **Progress of medicinal plants and their active metabolites in ischemia-reperfusion injury of stroke: a novel therapeutic strategy based on regulation of crosstalk between mitophagy and ferroptosis**
Guozhen Zhang, Qiang Wang, Bing Jiang, Lihe Yao, Wenjuan Wu, Xiaoyan Zhang, Dongjun Wan and Youquan Gu
- 150 **Ji-Ni-De-Xie ameliorates type 2 diabetes mellitus by modulating the bile acids metabolism and FXR/FGF15 signaling pathway**
Yiwen Tao, Fang Peng, Lijie Wang, Jiayi Sun, Yin Ding, Shuangfeng Xiong, Ugen Tenzin, MiMa, Tsedien Nhamdriel and Gang Fan
- 168 **Psyllium fiber improves hangovers and inflammatory liver injury by inhibiting intestinal drinking**
Keungmo Yang, Tom Ryu and Beom Sun Chung



OPEN ACCESS

EDITED AND REVIEWED BY
Michael Heinrich,
University College London, United Kingdom

*CORRESPONDENCE

Antony Stalin,
✉ a.stalin@gmail.com,
✉ antonystalin@uestc.edu.cn

RECEIVED 13 July 2024
ACCEPTED 30 July 2024
PUBLISHED 09 August 2024

CITATION

Stalin A, Hesham AE-L, Mishra A, Zou Q and
Ignacimuthu S (2024) Editorial: Herbal medical
products for metabolic diseases - new
integrated pharmacological approaches.
Front. Pharmacol. 15:1464176.
doi: 10.3389/fphar.2024.1464176

COPYRIGHT

© 2024 Stalin, Hesham, Mishra, Zou and
Ignacimuthu. This is an open-access article
distributed under the terms of the [Creative
Commons Attribution License \(CC BY\)](#). The use,
distribution or reproduction in other forums is
permitted, provided the original author(s) and
the copyright owner(s) are credited and that the
original publication in this journal is cited, in
accordance with accepted academic practice.
No use, distribution or reproduction is
permitted which does not comply with these
terms.

Editorial: Herbal medical products for metabolic diseases - new integrated pharmacological approaches

Antony Stalin^{1*}, Abd El-Latif Hesham², Avdesh Mishra³,
Quan Zou¹ and Savarimuthu Ignacimuthu⁴

¹Institute of Fundamental and Frontier Sciences, University of Electronic Science and Technology of China, Chengdu, China, ²Genetics Department, Faculty of Agriculture, Beni-Suef University, Beni-Suef, Egypt, ³Department of Electrical Engineering and Computer Science, Texas A&M University Kingsville, Kingsville, TX, United States, ⁴Xavier Research Foundation, St. Xavier's College, Palayamkottai, Tamil Nadu, India

KEYWORDS

metabolic diseases, natural compounds, artificial intelligence, bioinformatics (computational biopharmaceutics and modeling), pharmaceutical chemistry, network pharmacology

Editorial on the Research Topic

[Herbal medical products for metabolic diseases - new integrated pharmacological approaches](#)

Type 2 diabetes mellitus (T2DM), obesity, non-alcoholic fatty liver disease (NAFLD), metabolic dysfunction-associated fatty liver disease (MAFLD) and metabolic dysfunction-associated steatotic liver disease (MASLD) are interrelated metabolic disorders that significantly affect global health (Younossi et al., 2019; Chan et al., 2023). These diseases often lead to serious complications, including cancer and diabetic vascular problems, and are closely linked to autophagic activity, mitophagy and ferroptosis. Insulin resistance and other metabolic abnormalities play a central role in these diseases and contribute to their progression and severity. In particular, these metabolic abnormalities are major causes of hepatocellular carcinoma (HCC), highlighting the urgent need for effective interventions (Wang Y. et al., 2023).

Recent research has emphasized the potential of traditional medicines, plant extracts and natural substances for the treatment of these diseases. Of particular note is traditional Chinese medicine (TCM), which offers a variety of treatments that target underlying metabolic disorders (Hwang et al., 2022). Studies have shown that TCM can modulate autophagic activity, promote mitophagy and reduce ferroptosis, thereby alleviating insulin resistance and other metabolic abnormalities (Undamatla et al., 2023; Xie et al., 2023). These findings suggest that the integration of natural products and traditional medicine with modern therapeutic approaches may open new avenues for the treatment of T2DM, obesity, NAFLD/MAFLD and their associated complications, including HCC (Bai et al., 2020; Wang X. et al., 2023). As research progresses, the role of natural agents and traditional medicinal practices in the treatment and potential alleviation of these widespread health problems may become increasingly important.

In the Research Topic “Herbal Medical Products for Metabolic Diseases - New Integrated Pharmacological Approaches”, 11 articles were published, mainly focusing on plant metabolites, including TCM, for the treatment of metabolic diseases.

Ji-Ni-De-Xie (JNDX), a traditional botanical drug preparation from China used in Tibetan medicine for the treatment of T2DM, was studied by Tao et al. to understand its underlying mechanisms. JNDX significantly decreased fasting blood glucose, serum glycosylated protein, insulin resistance, inflammatory cytokines, triglycerides, total cholesterol and low-density lipoprotein cholesterol while increasing insulin sensitivity and high-density lipoprotein cholesterol in T2DM rats. Metagenomic analyses revealed that JNDX improved gut microbiota dysbiosis, specifically by altering bacteria associated with bile acid metabolism. JNDX also corrected disorders of bile acid metabolism by increasing cholic acid levels and decreasing ursodeoxycholic acid levels, and it improved FXR and FGF15 protein and mRNA expression while inhibiting CYP7A1 expression in the liver. This study revealed that JNDX effectively improved insulin resistance, hyperglycemia, hyperlipidemia and inflammation in T2DM rats through its regulation of bile acid metabolism and activation of the FXR/FGF15 pathway.

Similarly, Xia et al. summarized in their review article that botanical drug remedies show promise in combating insulin resistance, with anthraquinone extracts garnering attention for their role in improving insulin sensitivity and treating diabetes. The findings discussed in this review suggest that anthraquinones represent a promising therapeutic strategy for combating insulin resistance and associated metabolic diseases.

Hyperlipidemia is associated with obesity and is a serious health problem for many people. Xiao et al. reported that TCM Yinlan Tiaozhi capsule (YL) significantly reduced the levels of TC, TG, LDL-C, IL6, Tnf- α and Vegfa in mice with Triton WR-1339-induced hyperlipidemia and significantly increased the levels of HDL-C and Alb. The reduction in serum lipids was related to the alteration of metabolic abnormalities and maintenance of the dynamic balance of metabolites.

NAFLD, also known as MAFLD or MASLD, is a global health problem because it is associated with obesity, insulin resistance and other metabolic abnormalities and is also the leading cause of HCC. Methylsulfonylmethane (MSM), an organic sulfur compound found in various plants and animals, exerts antioxidant and anti-inflammatory effects. Han et al. highlighted their ability to assess the anti-obesity activity and autophagy-related mechanisms of MSM and suggested that MSM ameliorates hepatic steatosis by enhancing autophagic flux via an AMPK/mTOR/ULK1-dependent signaling pathway.

In addition, Wang et al. comprehensively discussed recent advances in the possible mechanisms of pathogenesis and progression of MASLD-related HCC in their review article. They also discussed the application of various bioactive metabolites to attenuate MASLD-related HCC through different modulatory mechanisms involving anti-inflammatory, lipid metabolic and microbial pathways in the gut, providing valuable information for the future treatment and prevention of MASLD-related HCC. They also discussed recent findings suggesting that ferroptosis, a form of regulated cell death, plays a role in the progression from MASLD to HCC and is a potential therapeutic target.

Gao et al. reviewed the relationship between diabetic vascular complications and autophagic activity, a process important for cellular homeostasis that involves lysosomal degradation of protein aggregates, damaged organelles and pathogens. Dysregulated autophagy has been associated with vascular abnormalities in both microvessels and large vessels in diabetes. They also discussed the potential of TCMs, with their ability to target multiple metabolic pathways, which offers promising prospects as treatment strategies, especially given the complex etiology of diabetic vascular lesions. This complexity often renders single-target treatments ineffective, whereas TCMs can address multiple autophagic targets simultaneously.

Similarly, Zhang et al. provided an overview of advances in medicinal plants and their active metabolites for the treatment of ischemia–reperfusion injury in stroke, a common and severe neurological disorder that includes ischemic (85% of cases) and hemorrhagic (15% of cases) forms. This review describes in detail how mitophagy and ferroptosis contribute to the pathogenesis of stroke and discusses the potential of medicinal plants to act on these processes, offering new insights for drug development.

The increase in chronic alcohol consumption has become a major global health problem and leads to a number of liver diseases, including steatosis, steatohepatitis, cirrhosis and HCC. Excessive alcohol consumption often causes hangovers and inflammatory liver damage, and current treatment options are inadequate. In their study, Yang et al. investigated the effects of psyllium fiber (PF), known for its gastrointestinal benefits, on hangover symptoms. Excessive alcohol consumption was found to activate alcohol-metabolizing enzymes in the small intestine and liver, leading to inflammatory damage and increased alcohol metabolites such as acetaldehyde and acetone, which correlate with hangover symptoms in mice. Compared with control mice, PF-treated mice exhibited significant improvement in hangover symptoms and reduced hepatic inflammation. *In vitro* experiments with HepG2 cell lines and semipermeable membranes have shown that PF inhibits alcohol absorption.

Shizao decoction (SZD) is a TCM that has a therapeutic effect on cirrhotic ascites (CAS). In their study, Li et al. developed a new integrated strategy involving network analysis combined with pharmacokinetics and metabolomics to investigate the main targets and mechanisms of SZD in the treatment of CAS. The results showed that SZD can reduce liver tissue inflammation, inhibit collagen fiber hyperplasia and improve liver function.

Fazmiya et al. investigated the efficacy of *Acacia arabica* (Lam.) Willd. and *Cinnamomum camphora* (L.) J. Presl. Vaginal suppositories for heavy menstrual bleeding (HMB) and their effects on participants' health-related quality of life (HRQoL) were analyzed using machine learning algorithms, and the results revealed that the use of a vaginal suppository is effective, inexpensive and safe for controlling HMB.

Ariyanto provided an overview of the efficacy of botanical drugs in the treatment of metabolic diseases through epigenetic modifications in his review paper to provide insight into the research and development strategies for botanical drugs as pharmacotherapies for metabolic diseases.

In summary, this Research Topic highlights the key interest as well as the potential of traditional medicine, especially TCM and

other botanical drugs, in modulating metabolic pathways and addressing metabolic disorders. It also discusses the role of autophagy, mitophagy and ferroptosis in the development and treatment of metabolic diseases. In addition, the integration of natural products and traditional medicine with modern therapeutic approaches for comprehensive treatment strategies has been addressed.

Moreover, some areas are not covered, such as detailed research on specific molecular mechanisms and pathways involved in all plant metabolites, comparative studies between botanical drugs and modern pharmacological treatments, long-term clinical trials and safety profiles, standardized formulations, dosages and quality control of botanical drugs, *etc.*, Overall, this Research Topic highlights the recent advances in botanical drugs for various interrelated metabolic diseases such as T2DM, obesity, cancer and NAFLD and emphasizes the importance of further research and integration with modern medicine.

Author contributions

AS: Conceptualization, Data curation, Formal Analysis, Investigation, Methodology, Project administration, Resources, Software, Supervision, Validation, Visualization, Writing–original draft, Writing–review and editing. AH: Data curation, Formal Analysis, Resources, Validation, Visualization, Writing–original draft, Writing–review and editing. AM: Data curation, Formal Analysis, Validation, Writing–review and editing. QZ: Data curation, Formal Analysis, Investigation, Resources, Software, Validation, Visualization, Writing–review and editing. SI: Data curation, Formal Analysis, Validation, Visualization, Writing–original draft, Writing–review and editing.

References

- Bai, Q. Y., Tao, S. M., Tian, J. H., and Cao, C. R. (2020). Progress of research on effect and mechanism of *Scutellariae Radix* on preventing liver diseases. *Zhongguo Zhong Yao Za Zhi* 45, 2808–2816. doi:10.19540/j.cnki.cjcmm.20200224.403
- Chan, W. K., Chuah, K. H., Rajaram, R. B., Lim, L. L., Ratnasingam, J., and Vethakkan, S. R. (2023). Metabolic dysfunction-associated steatotic liver disease (MASLD): a state-of-the-art review. *J. Obes. Metab. Syndr.* 32, 197–213. doi:10.7570/jomes23052
- Hwang, K. A., Hwang, Y., Hwang, H. J., and Park, N. (2022). Hepatoprotective effects of radish (*raphanus sativus* L.) on acetaminophen-induced liver damage via inhibiting oxidative stress and apoptosis. *Nutrients* 14, 5082. doi:10.3390/nu14235082
- Undamatla, R., Fagunloye, O. G., Chen, J., Edmunds, L. R., Murali, A., Mills, A., et al. (2023). Reduced mitophagy is an early feature of NAFLD and liver-specific PARKIN knockout hastens the onset of steatosis, inflammation and fibrosis. *Sci. Rep.* 13, 7575. doi:10.1038/s41598-023-34710-x
- Wang, X., Liu, B., Liu, Y., Wang, Y., Wang, Z., Song, Y., et al. (2023a). Antioxidants ameliorate oxidative stress in alcoholic liver injury by modulating lipid metabolism and phospholipid homeostasis. *Lipids* 58, 229–240. doi:10.1002/lipd.12377
- Wang, Y., Fleishman, J. S., Li, T., Li, Y., Ren, Z., Chen, J., et al. (2023b). Pharmacological therapy of metabolic dysfunction-associated steatotic liver disease-driven hepatocellular carcinoma. *Front. Pharmacol.* 14, 1336216. doi:10.3389/fphar.2023.1336216
- Xie, D., Li, K., Feng, R., Xiao, M., Sheng, Z., and Xie, Y. (2023). Ferroptosis and traditional Chinese medicine for type 2 diabetes mellitus. *Diabetes Metab. Syndr. Obes.* 16, 1915–1930. doi:10.2147/DMSO.S412747
- Younossi, Z. M., Golabi, P., De Avila, L., Paik, J. M., Srishord, M., Fukui, N., et al. (2019). The global epidemiology of NAFLD and NASH in patients with type 2 diabetes: a systematic review and meta-analysis. *J. Hepatol.* 71, 793–801. doi:10.1016/j.jhep.2019.06.021

Funding

The author(s) declare that financial support was received for the research, authorship, and/or publication of this article. The work was supported by the National Natural Science Foundation of China (No. 62131004), and the National Key R&D Program of China (2022ZD0117700).

Acknowledgments

We would like to acknowledge the authors for their valuable publications on this Research Topic.

Conflict of interest

The authors declare that the research was conducted in the absence of any commercial or financial relationships that could be construed as a potential conflict of interest.

The author(s) declared that they were an editorial board member of Frontiers, at the time of submission. This had no impact on the peer review process and the final decision.

Publisher's note

All claims expressed in this article are solely those of the authors and do not necessarily represent those of their affiliated organizations, or those of the publisher, the editors and the reviewers. Any product that may be evaluated in this article, or claim that may be made by its manufacturer, is not guaranteed or endorsed by the publisher.



OPEN ACCESS

EDITED BY

Stalin Antony,
University of Electronic Science and
Technology of China, China

REVIEWED BY

Pandikumar Perumal,
St. Xaviers College, India
Yi Li,
China Pharmaceutical University, China
Ai-Jun Liu,
Second Military Medical University, China

*CORRESPONDENCE

Guanlin Xiao,
✉ 164669079@qq.com
Xiaoli Bi,
✉ zyfxys@gzucm.edu.cn

RECEIVED 03 July 2023

ACCEPTED 18 October 2023

PUBLISHED 30 October 2023

CITATION

Xiao G, Xu A, Jiang J, Chen Z, Li Y, Li S,
Chen W, Zhang J, Jia C, Zeng Z and Bi X
(2023), Metabolomics analysis delineates
the therapeutic effects of Yinlan Tiaozhi
capsule on triton WR-1339 -induced
hyperlipidemia in mice.
Front. Pharmacol. 14:1252146.
doi: 10.3389/fphar.2023.1252146

COPYRIGHT

© 2023 Xiao, Xu, Jiang, Chen, Li, Li, Chen,
Zhang, Jia, Zeng and Bi. This is an open-
access article distributed under the terms
of the [Creative Commons Attribution
License \(CC BY\)](https://creativecommons.org/licenses/by/4.0/). The use, distribution or
reproduction in other forums is
permitted, provided the original author(s)
and the copyright owner(s) are credited
and that the original publication in this
journal is cited, in accordance with
accepted academic practice. No use,
distribution or reproduction is permitted
which does not comply with these terms.

Metabolomics analysis delineates the therapeutic effects of Yinlan Tiaozhi capsule on triton WR-1339 -induced hyperlipidemia in mice

Guanlin Xiao^{1*}, Aili Xu¹, Jieyi Jiang¹, Zhao Chen¹, Yangxue Li¹,
Sumei Li¹, Weitao Chen¹, Jingnian Zhang¹, Canchao Jia²,
Zhihao Zeng² and Xiaoli Bi^{1,2*}

¹Guangdong Province Engineering Technology Research Institute of Traditional Chinese Medicine/
Guangdong Provincial Key Laboratory of Research and Development in Traditional Chinese Medicine,
Guangzhou, China, ²School of the Fifth Clinical Medicine, Guangzhou University of Chinese Medicine,
Guangzhou, China

Hyperlipidemia is a disorder of lipid metabolism resulting from abnormal blood lipid metabolism and is one of the most frequent metabolic diseases that endanger people's health. Yinlan Tiaozhi capsule (YL) is a formulated TCM widely used to treat hyperlipidemia. The purpose of this study was to discover biomarkers utilizing untargeted metabolomics techniques, as well as to analyze the mechanisms underlying the changes in metabolic pathways linked to lipid-lowering, anti-inflammation, and regulation of angiogenesis in hyperlipidemia mice. To assess the efficacy of YL, serum total cholesterol (TC), triglycerides (TG), low-density lipoprotein cholesterol (LDL-c), and high-density lipoprotein cholesterol (HDL-c) levels were measured. Biochemical examinations showed that YL significantly reduced the levels of TC, TG, LDL-c, *Il6*, *Tnf-α*, and *Vegfa* in hyperlipidemia mice ($p < 0.01$). YL also significantly increased the levels of HDL-c and *Alb* ($p < 0.01$). Twenty-seven potential serum biomarkers associated with hyperlipidemia were determined. These differential metabolites were related to the reduction of serum lipid levels in hyperlipidemia mice, probably through metabolic pathways such as linoleic acid metabolism, glycerophospholipid metabolism, phenylalanine metabolism, phenylalanine, tyrosine and tryptophan biosynthesis, and D-glutamine and D-glutamate metabolism. Further correlation analysis showed that the serum lipid reduction through YL was related to the metabolites (amino acid metabolites, phospholipids metabolites, and fatty acids metabolites). The present study reveals that YL has a profound effect on alleviating triton WR-1339-induced hyperlipidemia, inflammation, and angiogenesis and that the positive effects of YL were primarily associated with the correction of metabolic abnormalities and the maintenance of metabolite dynamic balance.

KEYWORDS

Yinlan Tiaozhi capsule, hyperlipidemia, metabolomics, inflammation, angiogenesis

1 Introduction

Hyperlipidemia is a metabolic disorder characterized by abnormally increased levels of plasma total cholesterol (TC), triglycerides (TG), and low-density lipoprotein-cholesterol (LDL-C), accompanied by decreased levels of high-density lipoprotein-cholesterol (HDL-c) (Birger et al., 2021). Hyperlipidemia is a primary reason for many cardiovascular diseases and is closely correlated with diabetes, obesity, and atherosclerosis (Jia et al., 2021). Pharmacological interventions are the main therapy for hyperlipidemia, and the main drugs include statins, fibrates, and cholesterol absorption inhibitors. However, most medications cause adverse effects such as gastrointestinal problems (Tacherfiout et al., 2018). Presently, an appropriate way to alleviate dyslipidemia and avoid adverse effects may be through the use of natural medicines, and the efficacy of TCM in treating hyperlipidemia has been increasingly investigated (Tong et al., 2018).

Yinlan Tiaozi capsule (YL) is a formulated traditional Chinese medicine (TCM) comprising Citri Grandis Exocarpium, Ginkgo Folium, Gynostemma pentaphyllum, and propolis. It has been clinically used for the treatment of hyperlipidemia and is presently in the phase II clinical stage (2012L01011) (Chen et al., 2019; Xiao et al., 2023a; Xiao et al., 2023b). Previously, the chemical constituents of YL were investigated using UPLC-Q-TOF-MS/MS, and an overall of 66 compounds were identified, which mainly included flavonoids, saponins, lactones, and organic acids. The primary components of YL, such as naringenin and ferulic acid, may treat hyperlipidemia by modulating angiogenic mechanisms and suppressing the inflammatory response, according to network pharmacology integrated with molecular docking and experimental verification (Xiao et al., 2023a). Meanwhile, preliminary data showed that the anti-hyperlipidemia actions of YL may be associated with the inhibition of PXR expression, promotion of bile acid excretion, TG hydrolysis, and RCT processes (Xiao et al., 2023a). YL contains multiple active ingredients and achieves its pharmacological effects through multiple pathways and targets. Consequently, it is crucial to understand the integrated mechanism of the overall metabolism of YL under conditions of hyperlipidemia.

Metabolomics, with its systematic perspective and strategy, has been applied to comprehensively characterize and quantify metabolite levels and is the optimum instrument to illuminate the safety and efficacy of TCM, the pathophysiology of diseases, and the mechanism of drug action (Su et al., 2019; Wu et al., 2019; Zhao et al., 2021). Metabolomics is a “top-down” approach to defining the overall alterations in living systems at the metabolic level for complex metabolic diseases (Sun et al., 2012). This study performed serum biochemical analysis, metabolic pathway analysis, and analysis of metabolic changes to identify the underlying biomarkers of hyperlipidemia and to investigate the mechanisms and pathways of lipid-lowering of YL in hyperlipidemia mice.

2 Materials and methods

2.1 Materials and animals

The YL (Batch number: 20220801) was obtained from Guangdong Efang Pharmaceutical Co. Ltd. (Foshan, China). Triton WR-1339 was

purchased from Sigma-Aldrich (Shanghai, China). The chemical profile of YL analyzed by UPLC-QTOF-MS/MS is shown in [Supplementary Figure S1](#). The 24 male Kunming (KM) mice (18–22 g body weight) were obtained from the Guangdong Medical Laboratory Animal Center (Guangzhou, China) (Permit number: 44007200106576). All animal experiments were approved by the Guangdong Provincial Engineering Technology Institute of Traditional Chinese Medicine (Guangzhou, China).

2.2 Animal administration

Combined with the group’s previous research and clinical trials (Chen et al., 2019; Li et al., 2019; Li et al., 2020; Xiao et al., 2023a), the animal experimental process is shown in [Figure 1](#), and the experimental program is specified as follows: The 24 male KM mice were raised in a barrier system under standard room temperature $24^{\circ}\text{C} \pm 2^{\circ}\text{C}$ with the humidity of $70\% \pm 5\%$. The mice were subjected to 12 h light/dark cycle conditions and fed with normal food and water. The experiment mice were randomly divided into the following 4 groups of 6 mice in each group: control group (CG), model group (MG), fenofibrate group (26 mg/kg) (Fenofibrate) (Li et al., 2020), and YL group (144 mg/kg) (YL) (Chen et al., 2019). The administration groups were given corresponding drugs by gavage and once a day for 5 days. On the third day of administration, all groups excluding the CG were administered triton WR-1339 (480 mg/kg) intramuscularly to build an acute hyperlipidemia model. On the fifth day, after gavage administration for 1 hour, all mice were anesthetized with isoflurane and sacrificed through inner canthus artery exsanguination. Blood samples were preserved at room temperature for 30 min and centrifuged at 3,000 rpm at 4°C for 15 min to isolate the serum. Liver tissue was surgically extracted from each mouse. The wet weights of the organs were recorded and the tissues were saved at -80°C until further experiments.

2.3 Biochemical analysis

The levels of TC, TG, HDL-c, and LDL-c in serum were determined by using commercial kits (Nanjing Jiancheng Bioengineering Institute, China) according to the manufacturer’s instructions.

2.4 Histopathology

The liver tissues of mice were fixed with 4% paraformaldehyde solution, then the samples were dehydrated, embedded in paraffin, and sliced into 4 μm thick sections for H&E staining, and the histomorphology of the livers was observed and recorded using a microphotographic operating system.

2.5 Sample preparation

Serum metabolomic analysis was conducted on all mice in each group as individual differences in each group were taken into account. Serum samples were collected and stored at -80°C . Prior to analysis, the

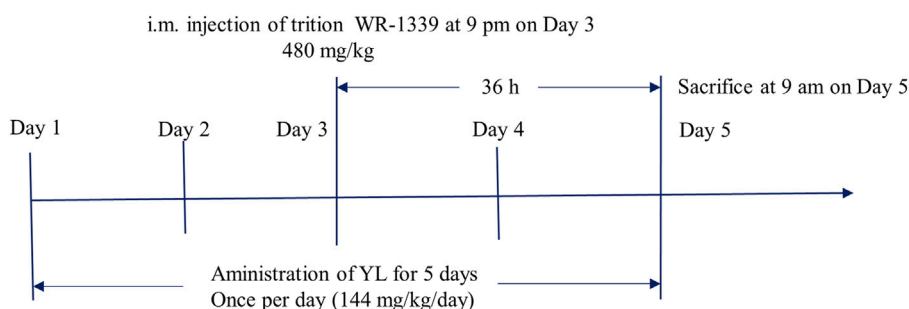


FIGURE 1
Process of administration of YL and hyperlipidemia modeling.

serum samples were defrosted at room temperature, and 100 μ L serum was added to 400 μ L of pre-cooled acetonitrile and water mixture (1:1, v/v) fixed in a 1.5 mL microtubes, placed in -20°C refrigerator for 1 h, centrifuge for 15 min (4°C , 12,000 rpm), transfer the supernatant (400 μ L) to a new 1.5 mL centrifuge tube, and blow dry with nitrogen. Add 100 μ L of pre-cooled acetonitrile and methanol mixture (1:1, v/v), vortex for the 30 s, centrifuge for 15 min (4°C , 12,000 rpm), and accurately absorb 80 μ L of the supernatant into the injection bottle for sample analysis. Quality control (QC) sample was obtained by mixing 10 μ L of serum samples from the above mice, and the sample was prepared as described above. The QC samples were injected at 6 intervals of study samples to assess the stability of the analytical system (Ren et al., 2023).

2.6 UPLC-Q-TOF/MS analysis

The UPLC analysis was carried out on a SHIMADZU ExionLC system (Shimadzu, Japan). The chromatographic separations were achieved on a Waters UPLC BEH C18 column (2.1 mm \times 100 mm, 1.7 μ m), flow rate 0.3 mL min^{-1} , injector temperature 4°C , column temperature 35°C , injection volume 1 μ L. Mobile phase: gradient elution of acetonitrile (A) -0.1% formic acid water (B) (0–1 min, 2% A; 1–3 min, 2%–10% A; 3–7 min, 10%–40% A; 7–16 min, 40%–75% A; 16–20 min, 75%–98% A; 20–23 min, 98% A).

The high-resolution mass detection was performed on an AB SCIEX X500R QTOF-MS/MS system (Sciex, United States). MS was performed both in positive and negative ion modes with electrospray ionization (ESI). The optimization source parameters were set as follows: ion voltage: $-4,500$ V and $+5,500$ V, Gas1: 55 psi; Gas2: 55 psi; curtain gas: 35 psi; de-clustering potential voltage: 60 V; ion source temperature: 500°C ; collision energy: 35 V; collision energy spread: 15 V; full scan: m/z 50–1,000.

2.7 Data processing and multivariate analysis

Multivariate statistical analysis was conducted using SIMCA 14.1 software with unsupervised principal component analysis (PCA) and orthogonal partial least discriminant analysis (OPLS-DA) models, and the results of OPLS-DA needed to be further confirmed by 200 times permutation evaluations. Statistical analyses were then performed using the online tool Metaboanalyst 5.0 for univariate student t -test (t -test) and

finally for difference multiple (FC value) analysis. The metabolites with significantly different (Variable important in projection (VIP) > 1 , $p < 0.05$, Fold change (FC) value < 0.8 , or FC value > 1.2) between MG and CG and between YL and MG were screened for preliminary identification and analysis. Further analysis of these metabolites was performed to screen for metabolites that were significant differences between YL and MG and showed a trend of recovery compared with CG were screened as the differential metabolites for treating hyperlipidemia. Potential biomarkers were characterized according to the METLIN and Human Metabolome Database databases, and pathways of differential metabolites were analyzed using the online software MetaboAnalyst 5.0 (<http://www.metaboanalyst.ca/>) (Shi et al., 2023).

2.8 Quantitative RT-PCR

Approximately 50 mg of liver were transferred to a 1.5 mL grinding tube. Liver samples were acquired by mechanically homogenized under an ice water bath and centrifuged at 12,000 rpm for 10 min at 4°C , and the supernatant was subsequently collected. Extraction of total RNA from liver tissues was performed using Trizol reagent (Dingguo Changsheng, Beijing, China), and reverse transcription was conducted. RT-qPCR reactions were conducted on an IQTM5 RT-Q-PCR system (Bio-Rad, Hercules, California, United States) with SYBR Green detection. The sequences of primers are shown in Table 1.

2.9 Statistical analysis

SPSS software was utilized to analyze the data by one-way ANOVA and all values were presented as means \pm SD. $p < 0.05$ was considered statistically significant. Metabolomics data are normalized by MetaboAnalyst 5.0 and exported into SIMCA-P 14.1 software for processing (Shi et al., 2023).

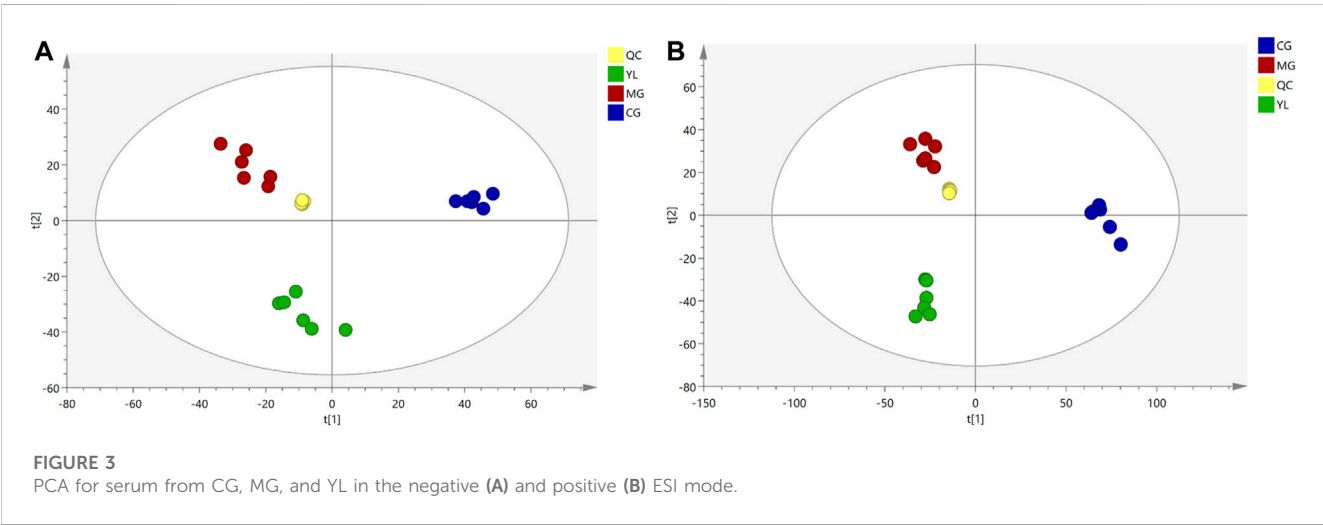
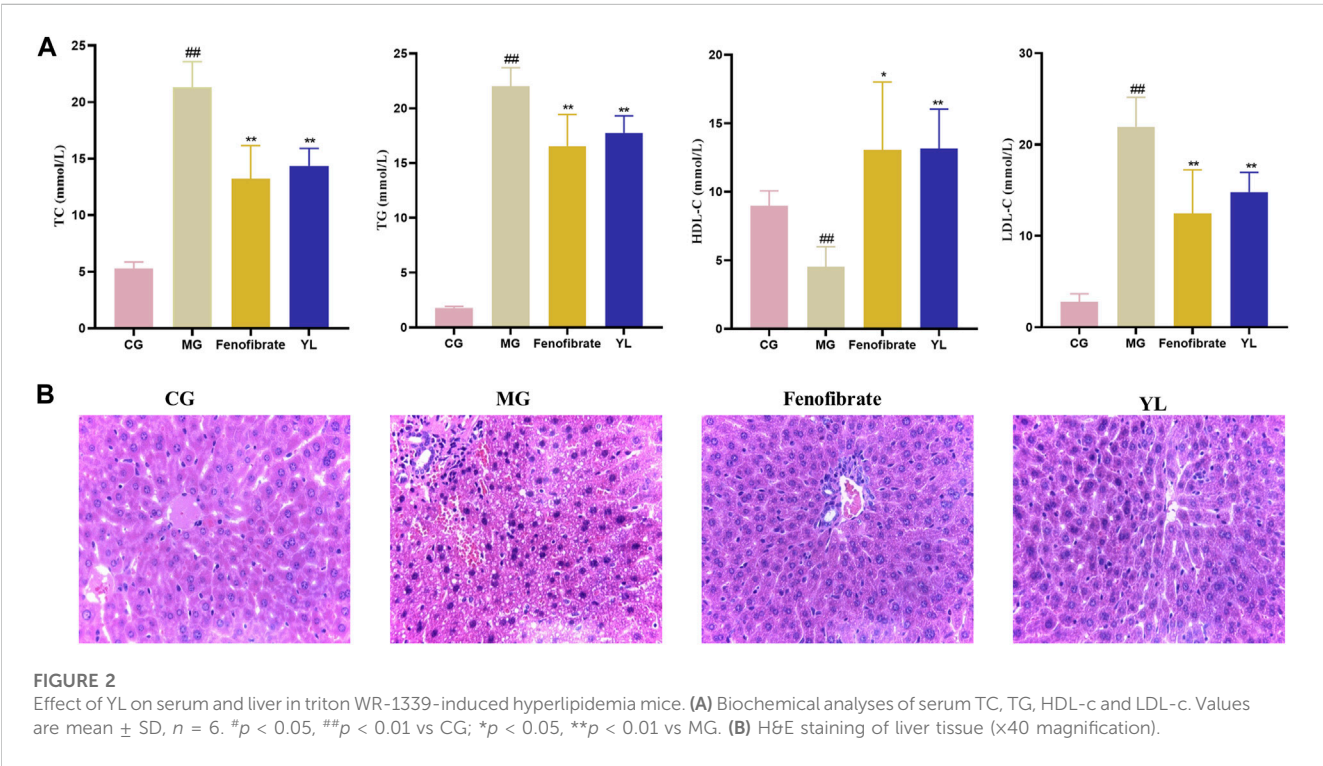
3 Results

3.1 Effect of YL in the treatment of triton WR-1339-induced hyperlipidemia in mice

As shown in Figure 2A, serum TC, TG, and LDL-c levels were significantly higher (all $p < 0.01$), and the serum HDL-c levels

TABLE 1 The primer sequence formation.

Gene name	Forward primer (5'-3')	Reverse primer (5'-3')
<i>Il6</i>	AGTTGTGCAATGGCAATTCTGA	CTCTGAAGGACTCTGGCTTTGTC
<i>Tnf-α</i>	CCCTCACACTCACAAACCACC	CTTTGAGATCCATGCCGTTG
<i>Alb</i>	AACAAGAGCCCGAAAGAAACG	CTGGCAACTTCATGCAAAATAGTG
<i>Vegfa</i>	GTAACGATGAAGCCCTGGAGTG	TCACAGTGAACGCTCCAGGAT
<i>Gapdh</i>	CCTCGTCCCGTAGACAAAATG	TGAGGTCAATGAAGGGGTCGT



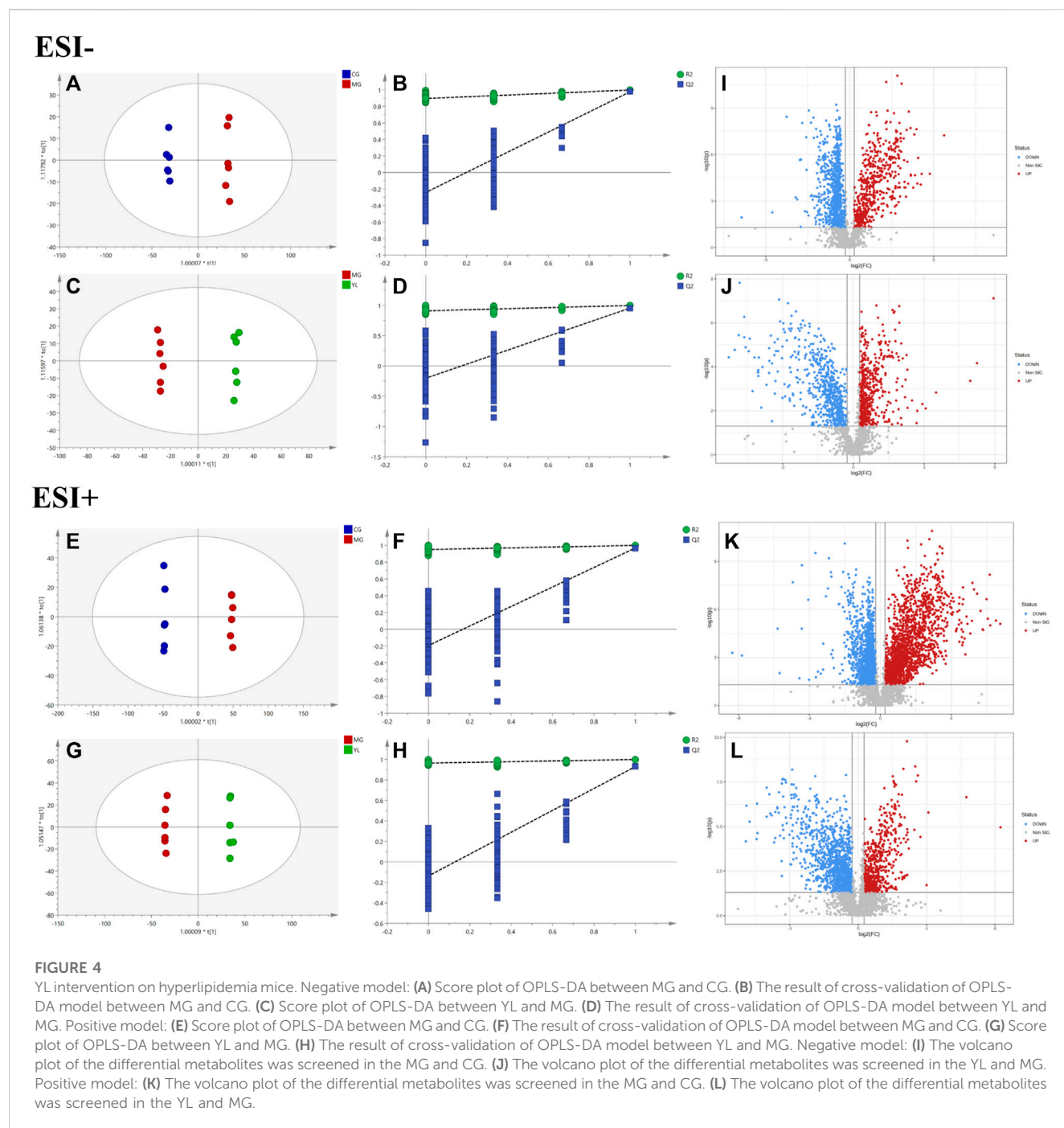


TABLE 2 The parameters of the OPLS-DA model.

Mode	Group	R ² X	R ² Y	Q ²	CV-ANOVA
Positive	MG vs. CG	0.558	0.999	0.968	2.51e ⁻⁵
	YL vs. MG	0.427	0.999	0.929	0.0004
Negative	MG vs. CG	0.596	0.998	0.976	9.29e ⁻⁶
	YL vs. MG	0.535	0.998	0.954	8.85e ⁻⁵

were lower ($p < 0.01$) in the MG compared with mice in the CG. After administration of YL or Fenofibrate, the serum levels of TC, TG, and LDL-c (all $p < 0.01$) were decreased and the serum

HDL-c ($p < 0.05$, $p < 0.01$) levels were increased in mice compared to the MG. These results suggested that YL effectively ameliorated dyslipidemia in hyperlipidemia mice induced by triton WR-1339.

The histologic data were consistent with observations of serum lipid levels in mice. The liver cells of mice in the CG were neatly arranged, with intact nuclei and no inflammatory cell infiltration or vacuolar lesions. The liver cells of mice in the MG were disordered, with unclear cell boundaries, absence of some nuclei, diffuse steatosis of liver cells, and increased vacuolar lesions and inflammatory infiltration. Compared with the MG, the liver cells of the Fenofibrate were neatly arranged, the number of fat vacuoles

TABLE 3 Identification and change trend of potential biomarkers.

Ion mode	HMDB ID	Metabolites	Formula	RT (min)	MG vs. CG	YL vs. MG
ESI ⁻	HMDB0000190	L-Lactic acid	C ₃ H ₆ O ₃	1.27	↓ ^{##}	↑ ^{**}
	HMDB0000148	L-Glutamic acid	C ₅ H ₉ NO ₄	1.47	↓ ^{##}	↑ ^{**}
	HMDB0000159	L-Phenylalanine	C ₉ H ₁₁ NO ₂	4.02	↓ ^{##}	↑ ^{**}
	HMDB0000714	Hippuric acid	C ₉ H ₉ NO ₃	5.80	↓ ^{##}	↑ ^{**}
	HMDB0000826	Pentadecanoic acid	C ₁₅ H ₃₀ O ₂	19.80	↓ ^{##}	↑ ^{**}
	HMDB0000673	Linoleic acid	C ₁₈ H ₃₂ O ₂	18.44	↑ ^{##}	↓ ^{**}
	HMDB0000573	Elaidic acid	C ₁₈ H ₃₄ O ₂	19.58	↑ ^{##}	↓ ^{**}
	HMDB0004669	9-OxoODE	C ₁₈ H ₃₀ O ₃	15.53	↑ ^{##}	↓ ^{**}
	HMDB0004702	12,13-EpOME	C ₁₈ H ₃₂ O ₃	16.03	↑ ^{##}	↓ ^{**}
	HMDB0007855	LysoPA(18:1(9Z)/0:0)	C ₂₃ H ₄₆ NO ₇ P	15.32	↓ ^{##}	↑ ^{**}
ESI ⁺	HMDB0012497	1-Pyrroline	C ₄ H ₇ N	1.04	↓ ^{##}	↑ ^{**}
	HMDB0000097	Choline	C ₅ H ₁₃ NO	0.91	↓ ^{##}	↑ ^{**}
	HMDB0003229	Palmitoleic acid	C ₁₆ H ₃₀ O ₂	19.14	↑ ^{##}	↓ ^{**}
	HMDB0000220	Palmitic acid	C ₁₆ H ₃₂ O ₂	19.15	↑ ^{##}	↓ ^{**}
	HMDB0031934	(9S,10E,12Z,15Z)-9-Hydroxy-10,12,15-octadecatrienoic acid	C ₁₈ H ₃₀ O ₃	15.51	↑ ^{##}	↓ ^{**}
	HMDB0001388	Alpha-Linolenic acid	C ₁₈ H ₃₀ O ₃	16.00	↓ ^{##}	↑ ^{**}
	HMDB0003759	5a-Pregnane-3,20-dione	C ₂₁ H ₃₂ O ₂	18.87	↑ ^{##}	↓ ^{**}
	HMDB0000253	Pregnenolone	C ₂₁ H ₃₂ O ₂	17.94	↑ ^{##}	↓ ^{**}
	HMDB0002395	Ursolic acid	C ₃₀ H ₄₈ O ₃	14.09	↓ ^{##}	↑ ^{**}
	HMDB0011473	LysoPE(0:0/16:0)	C ₂₁ H ₄₄ NO ₇ P	15.19	↓ ^{##}	↑ ^{**}
	HMDB0002815	LysoPC(18:1(9Z))	C ₂₆ H ₅₂ NO ₇ P	15.37	↓ ^{##}	↑ ^{**}
	HMDB0010386	LysoPC(18:2(9Z,12Z))	C ₂₆ H ₅₀ NO ₇ P	13.23	↓ ^{##}	↑ ^{**}
	HMDB0010395	LysoPC(20:4(5Z,8Z,11Z,14Z))	C ₂₈ H ₅₀ NO ₇ P	14.33	↓ ^{##}	↑ ^{**}
	HMDB0010384	LysoPC(18:0)	C ₂₆ H ₅₄ NO ₇ P	14.76	↓ ^{##}	↑ ^{**}
	HMDB0010393	LysoPC(20:3(5Z,8Z,11Z))	C ₂₈ H ₅₂ NO ₇ P	15.12	↓ ^{##}	↑ ^{**}
	HMDB0010392	LysoPC(20:2(11Z,14Z))	C ₂₈ H ₅₄ NO ₇ P	14.77	↓ ^{##}	↑ ^{**}
	HMDB0010391	LysoPC(20:1(11Z))	C ₂₈ H ₅₆ NO ₇ P	15.97	↓ ^{##}	↑ ^{**}

[#]*p* < 0.05, and ^{##}*p* < 0.01, MG, vs. CG.
^{*}*p* < 0.05, and ^{**}*p* < 0.01, YL, vs. MG., the structures, molecular weights, and codes of differential metabolites were assigned according to the human metabolome database and KEGG, compound database.

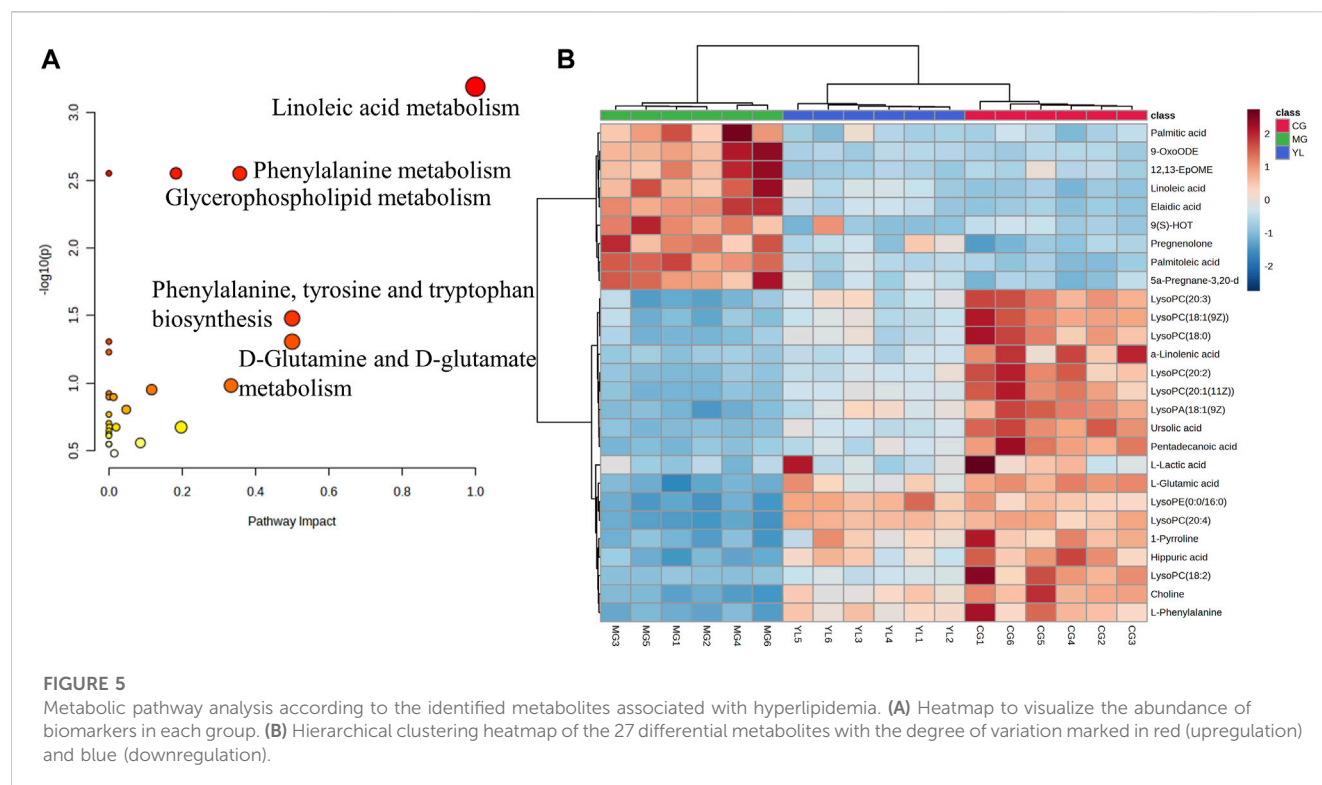
was significantly reduced, and the cell morphology was improved, but there was still inflammatory infiltration; the liver cell morphology of the YL was significantly improved, there was no inflammatory infiltration, and the scope of the lesions was significantly reduced (Figure 2B).

3.2 Quality evaluation of metabolomics data

As illustrated in Figure 3, the QC samples displayed good clustering in the PCA score plot, demonstrating that the pre-processing and experimental conditions of the samples were reliable and the data obtained were accurate.

3.3 YL-modulated serum metabolomic profiling

The PCA results indicated a significant separation of the three groups in positive and negative ion modes (Figure 3). The results indicated that the serum biochemical of hyperlipidemia mice was disordered and the metabolic pattern was significantly altered after oral administration of YL. OPLS-DA models were performed between the CG and MG and the MG and YL, respectively. The results of the OPLS-DA score plot and the 200 permutation test in serum metabolomics were presented in Figures 4A–H. The R²Y, Q², and CV-ANOVA (*p*-values) of the OPLS-DA model for serum metabolomics were presented in Table 2. The data in the table



revealed that the R^2Y values of each model were greater than 0.997 and the Q^2 values were greater than 0.928, indicating that the classification and explanation ability of the models was excellent (Gao et al., 2023). The 200 times permutation tests suggested that the OPLS-DA models established were all reliable and not overfitting (Yang et al., 2020). VIP, P, and FC values were visualized by volcano plot for selecting differential metabolites (Figures 4I–L). 27 differential metabolites were characterized with a VIP >1 and $p < 0.05$ ($FC > 1.2$ or < 0.8) between MG vs CG or YL vs. MG (Table 3).

3.4 YL regulated metabolomic pathways in the hyperlipidemia mice

To obtain a deeper understanding of the molecular mechanisms of YL, pathway analysis was performed on 27 differential metabolites. Metabolite data were imported into pathway analysis to investigate metabolic pathway weights, enriching 26 metabolic pathways, five of which were highly emphasized with raw $p < 0.05$ or pathway impact >0.05 (Sun et al., 2022). They were linoleic acid metabolism, glycerophospholipid metabolism, phenylalanine metabolism, Phenylalanine, tyrosine and tryptophan biosynthesis, and D-Glutamine and D-glutamate metabolism (Figure 5A). As indicated in Figure 5B, the clustering analysis of the heat map for all metabolites showed the differences in relative levels between the three groups. In addition, the heat map was also employed to show the relative abundance of the different metabolites in each sample. Compared with the CG, 9 metabolites were upregulated significantly in the MG, including 9-OxoODE, 12, 13-EpOME, and linoleic acid. The levels of L-Glutamic acid, Phenylalanine, Hippuric acid, LysoPC

(18:0), LysoPC (18:1(9Z)), and Alpha-linolenic acid was significantly decreased. However, the levels of these metabolites in YL were reversed and returned to normal or near-normal levels compared to MG. Therefore, they are considered potential biomarkers for the hypolipidemic effects of YL. Figure 6 shows the trend of biomarker levels in the different groups, which indicates a significant change in the potential biomarkers between CG and MG, and these changes can be reversed by YL treatment.

3.5 Effect of YL on inflammation and angiogenesis

As shown in Figure 7, compared with the CG, the levels of *Il6*, *Vegfa*, and *Tnf-α* mRNA significantly increased in the MG ($p < 0.01$), whereas the *Alb* mRNA was significantly decreased ($p < 0.01$). As expected, YL administration significantly enhanced the expression of *Alb* mRNA and declined *Il6*, *Tnf-α*, and *Vegfa* mRNA expression compared with those in the MG (all $p < 0.01$).

3.6 Correlation analysis

To further investigate the relationship between metabolites, metabolic parameters, and their regulatory effects (including dyslipidemia, inflammation, and angiogenesis), we analyzed the correlation between 27 altered metabolites and 8 metabolic parameters in the hyperlipidemia and YL groups with Spearman correlation analysis. The result suggested that the altered metabolites of amino acid metabolites (L-glutamic acid, L-phenylalanine, hippuric acid, etc.), fatty acid metabolites (linoleic acid, Alpha-Linolenic acid, 9-

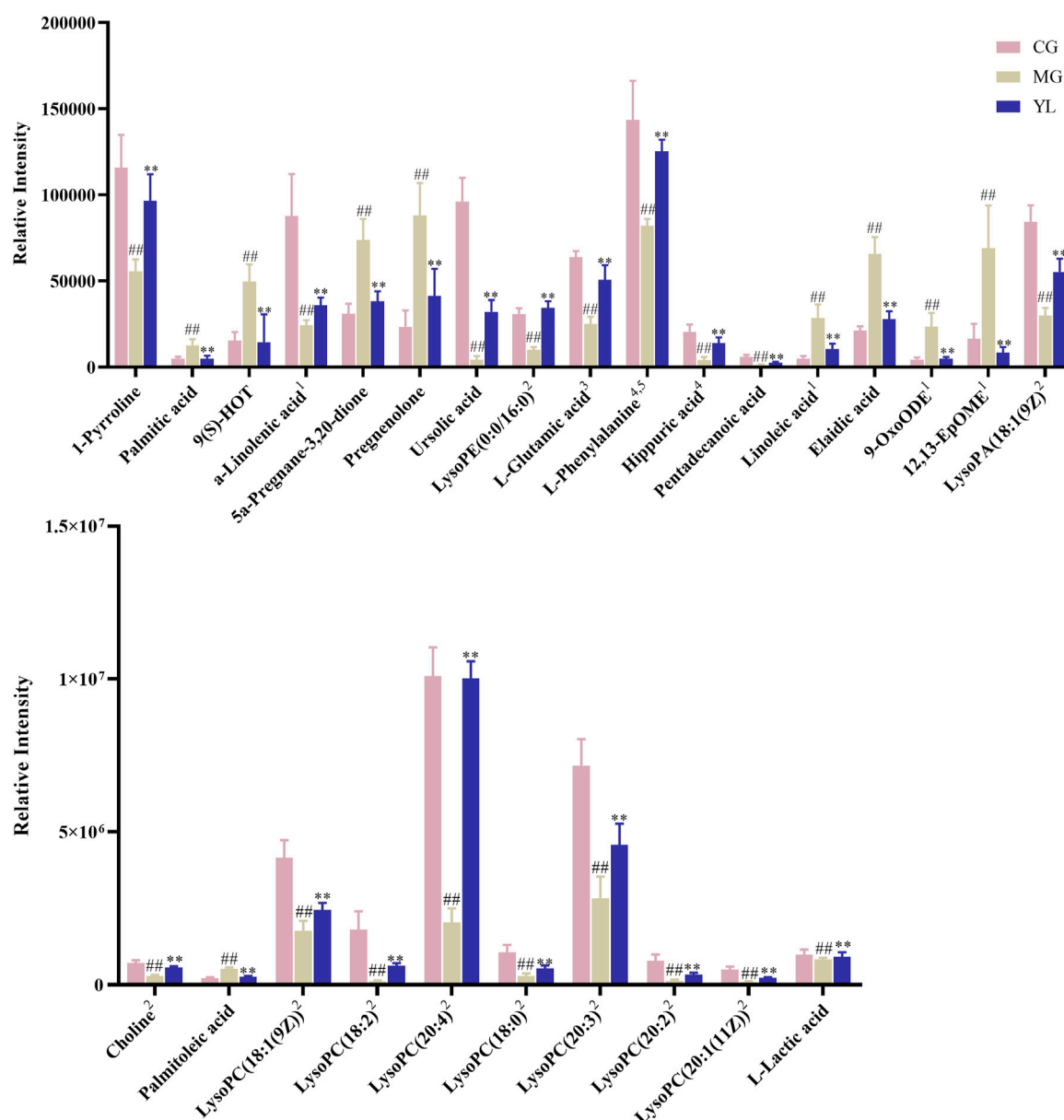


FIGURE 6

The relative contents of potential serum biomarkers in each group. (Compared with CG, $^{\#}p < 0.05$, $^{\#\#}p < 0.01$; compared with MG, $^*p < 0.05$, $^{**}p < 0.01$). ¹Linoleic acid metabolism, ²Glycerophospholipid metabolism, ³D-Glutamine and D-glutamate metabolism, ⁴Phenylalanine metabolism, ⁵Phenylalanine, tyrosine and tryptophan biosynthesis.

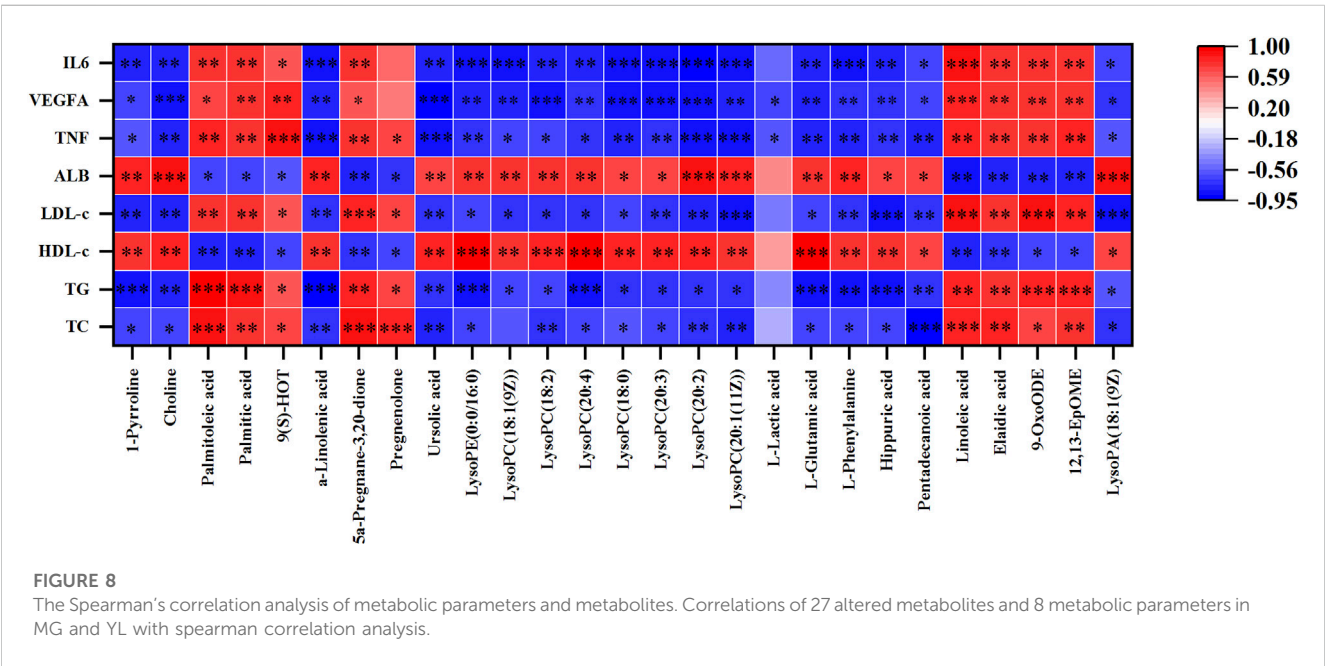
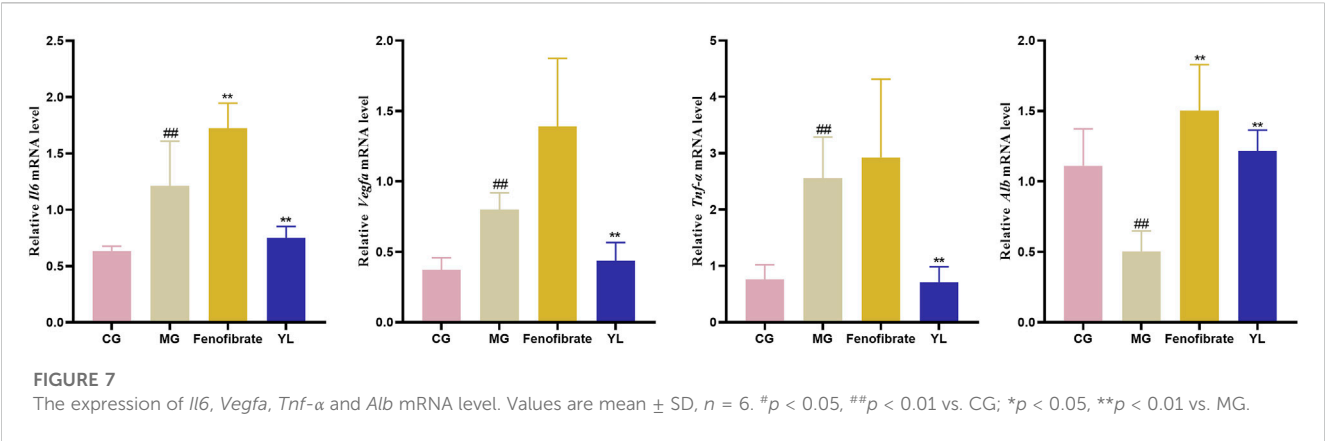
OxoODE, etc.), phospholipids metabolites (LysoPC (18:1(9Z)), LysoPC (18:0), etc.) were significantly associated with blood lipid levels in Figure 8. Positive and negative correlations are represented by red and blue colors, respectively. Furthermore, the stronger the link between the two biomarkers, the deeper the hue (Wang et al., 2022). According to the KEGG database, we graphed the metabolic network associated with the Triton WR-1339-induced hyperlipidemia model and the relevant biomarkers affected by YL (Figure 9). The results implied that YL promoted its anti-hyperlipidemia effect by improving the levels of endogenous metabolites, and anti-inflammatory and modulating angiogenic capacity.

This study illuminated that the intervention of YL could ameliorate dyslipidemia and abnormal metabolites in triton 1339-

WR-induced hyperlipidemia mice. The pathogenesis of hyperlipidemia is mainly associated with disorders of metabolic pathways including linoleic acid metabolism, glycerophospholipid metabolism, phenylalanine metabolism, phenylalanine, tyrosine and tryptophan biosynthesis, and D-glutamine and D-glutamate metabolism.

4 Discussion

Hyperlipidemia is characterized by abnormal lipid levels in the blood and constitutes a potentially harmful disease leading to CVDs with high mortality (Ge et al., 2022). Previous studies found that YL

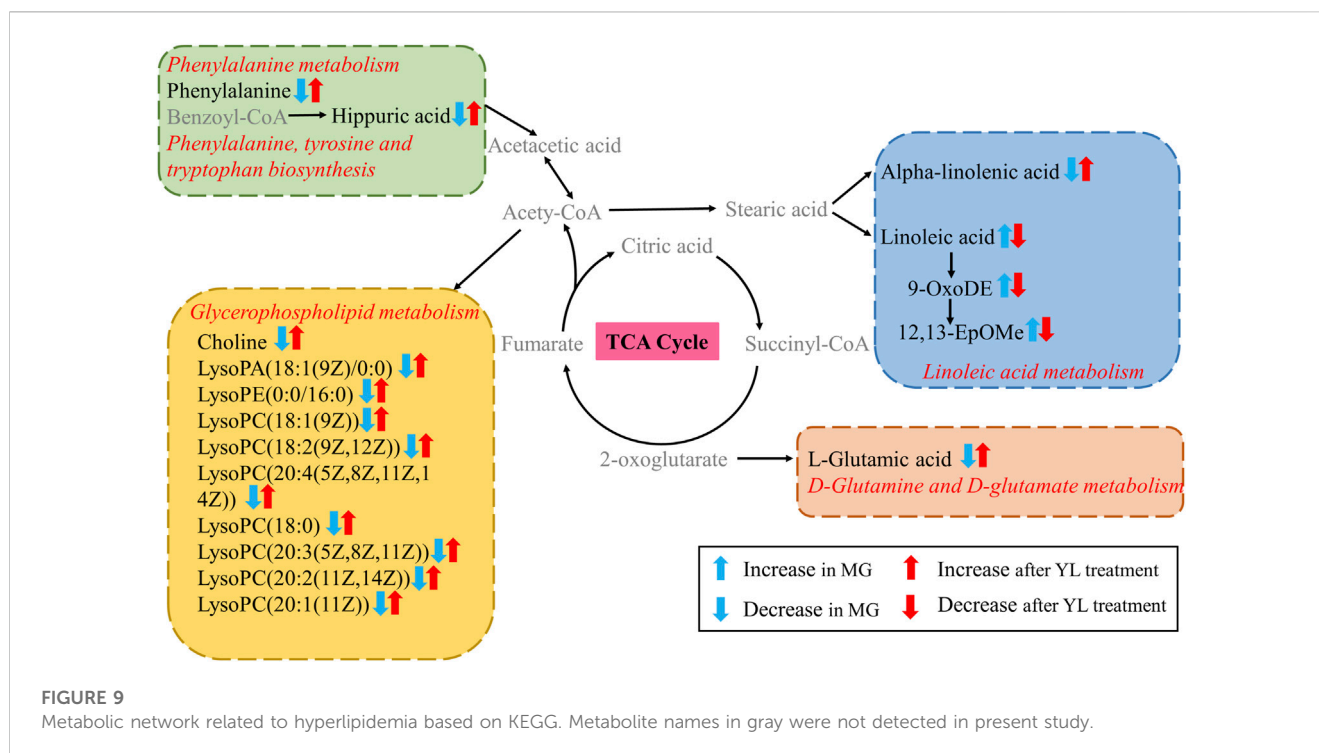


may treat hyperlipidemia by modulating angiogenesis and suppressing inflammatory responses (Chen et al., 2019; Xiao et al., 2023a). Therefore, we investigated the hypolipidemic effects of YL in hyperlipidemia mice to understand whether the YL could reverse triton WR-1339-induced dyslipidemia and metabolic abnormalities and exert anti-inflammatory and angiogenic effects, as well as to observe the changes of metabolites in mice to illuminate the underlying mechanism of hyperlipidemia alleviation. It is critical to investigate the occurrence and progression of lipid metabolism disorder using serum as a research object and metabolomics technology. Our results identified 27 serum biomarkers associated with hyperlipidemia, primarily phospholipids, fatty acids, and amino acid metabolites. Meanwhile, serum lipid levels were significantly improved after YL treatment, which demonstrated the lipid-lowering effect of YL.

Hyperlipidemia is diagnosed in clinical practice by evaluating four lipid indices showing elevated levels of TC, TG, and LDL-c and declined levels of HDL-c (Ta et al., 2023). Our results showed that TC, TG, and LDL-c levels were significantly elevated and HDL-C

levels declined in Triton WR-1339-induced hyperlipidemia mice compared with CG, demonstrating that the hyperlipidemia model was successfully established. However, the levels of TC, TG, and LDL-c were significantly decreased and the levels of HDL-c were significantly increased in the YL compared with the MG. These results proved the lipid-lowering effect of YL.

The most obvious manifestation of the development of hyperlipidemia is the disorder of lipid metabolism. Evidence is growing that hyperlipidemia is involved with phospholipids and fatty acids (Li et al., 2016; Sun et al., 2017; Ren et al., 2023). We have determined some metabolites related to lipid metabolism in the serum of mice treated with YL by serum metabolomics analysis. The results of the clustering analysis showed that the major differential metabolite pathways in the different groups were linoleic acid metabolism, glycerophospholipid metabolism, phenylalanine metabolism, phenylalanine, tyrosine and tryptophan biosynthesis, and glutamine and glutamate metabolism. Alpha-linolenic acid has been shown in studies to dramatically increase insulin sensitivity and anti-inflammatory state, which is crucial for the prevention of



CVDs (Zhang et al., 2016; Yue et al., 2021; Ren et al., 2023). The alpha-linolenic acid diet has also been reported to improve lipid profiles by lowering TG, TC, and LDL levels in patients with hyperlipidemia or hyperglycemia. Furthermore, alpha-linolenic acid dramatically lowered liver weight, hepatic cholesterol levels, and the expression of cholesterol synthase enzymes linked with hyperlipidemia, and it may reduce plasma and liver cholesterol content via modulating RCT (Andersen and Fernandez, 2013; O'Reilly et al., 2020). Conjugated linoleic acids are critical for fat deposition in the liver as well as for the development and improvement of IR (Moon et al., 2009). In addition, studies have indicated that unsaturated fatty acids reduce the incidence of hyperlipidemia, whereas saturated fatty acids have the opposite effect (Ito, 2015; Jenkins et al., 2015; Ren et al., 2023). As downstream products of linoleic acid, 9-OxoDE and 12,13-EpOME were significantly increased in the serum of hyperlipidemic mice. After the treatment of YL, the lipid-related metabolites in the serum of hyperlipidemic mice could be reversed, and the disordered lipid metabolism could be improved, which could play a positive role in hyperlipidemia.

The basic structural components of cell membranes are glycerophospholipids and sphingolipids, and Lysophosphatidylcholine (lysoPCs) is generated by the hydrolysis of oxidized phosphatidylcholine in LDL by phospholipase A2 and act in a range of biological processes (Ren et al., 2023; Zhao et al., 2023). Phosphatidylcholine (PC), phosphatidylglycerol (PG), and phosphatidylethanolamine (PE) are the three types of glycerophospholipids (Rowlett et al., 2017). LysoPCs behave as a direct response molecule, capable of inducing inflammation, cyclooxygenase production, and autoimmune reactions either independently or by activating specific G protein-coupled receptors (Brkic et al., 2012). Furthermore, lysoPCs are the primary metabolic intermediates of glycerophospholipid metabolism, and lysoPC has been linked to CVDs such as atherosclerosis and hyperlipidemia,

with a positive association between hyperlipidemia and glycerophospholipid metabolism problems (Miao et al., 2015; Zhao et al., 2015; Paapstel et al., 2018). YL may perform a critical role in ameliorating disorders of glycerol and phospholipid metabolism, resulting in reduced inflammation and suppression of hyperlipidemia development. Choline is involved in the lipid metabolism pathway of the body, and mice lacking the PEMT gene, which encodes the function of liver choline synthesis, have a large accumulation of fatty fat in the liver, resulting in fatty liver, suggesting that choline plays an essential role in the regulation of lipid metabolism (Song et al., 2005). In the present study, a series of lysophospholipids were significantly decreased in the MG compared with CG and recovered after YL treatment. There is growing evidence that lysophospholipids are implicated in energy metabolism, inflammation, and endothelial damage (Yan et al., 2020). However, the exact mechanisms are still too complex and need to be explored in greater depth.

In addition to glycerophosphate metabolism, changes in amino acid levels can also affect lipid levels. Some studies have shown that amino acids, which are primarily involved in numerous metabolic pathways such as the TCA cycle, gluconeogenesis, and others, play an essential role in metabolism (Wu, 2009; Park and Han, 2018). Through the TCA cycle, glutamic acid can be transformed into aspartic acid, and glutamine synthetase converts glutamate into glutamine, which is crucial for the glycolysis of energy metabolism and lipid metabolism in the body (Davalli et al., 2012). Phenylalanine is a nutritional precursor of metabolites generated by the gut microbiota and is clinically and mechanistically associated with CVDs and the resulting major adverse cardiovascular events through the action of adrenergic receptors (Nemet et al., 2020; Zhang et al., 2022). Phenylalanine is an amino acid precursor to tyrosine, which is biologically transformed into L-tyrosine. Tyrosine is also a precursor of catecholamines, which facilitate lipid metabolism and may be a biomarker of hyperlipidemia (Zhang et al., 2009; Zhang et al., 2022). In

the present study, the serum levels of glutamate and phenylalanine were elevated in YL-treated mice, indicating that the favorable effects of YL may be attributed to the regulation of phenylalanine metabolism and phenylalanine, tyrosine and tryptophan biosynthesis under hyperlipidemia conditions.

Inflammation, combined with the occurrence and progression of hyperlipidemia, can hasten fat accumulation in liver cells, whereas massive fat creation constantly exacerbates inflammation, resulting in increased blood lipids (Tietge, 2014). Furthermore, YL may treat hyperlipidemia by modulating inflammatory and angiogenesis mechanisms (Xiao et al., 2023a). We found that the expression of *Il6*, *Vegfa*, and *Tnf- α* mRNA were significantly enhanced ($p < 0.01$), and the expression of *Alb* mRNA ($p < 0.01$) was significantly reduced in the MG compared with those in the CG. After treatment with YL, the expression of *Il6*, *Vegfa*, and *Tnf- α* mRNA ($p < 0.01$) were inhibited and promoted the expression of *Alb* mRNA ($p < 0.01$). Therefore, the effects of YL can effectively ameliorate hyperlipidemia by regulating angiogenesis and anti-inflammatory mechanisms. Besides, in connection with the correlation analysis, YL may synergistically affect amino acid, phospholipid, and fatty acid levels and regulate lipid levels in hyperlipidemia mice through metabolic pathways such as linoleic acid metabolism, glycerophospholipid metabolism, phenylalanine metabolism, phenylalanine, tyrosine and tryptophan biosynthesis, and glutamine and glutamate metabolism.

In summary, YL can significantly reverse the triton WR-1339-induced abnormal levels of the metabolites linoleic acid, 12,13-EpOME, lysoPC(18:1(9Z)), lysoPC(18:0), choline, L-phenylalanine, and L-glutamic acid, and thereby interfere with the signaling pathways of linoleic acid metabolism, glycerophospholipid metabolism, phenylalanine metabolism, phenylalanine, tyrosine and tryptophan biosynthesis, and glutamine and glutamate metabolism, resulting in effective treatment of hyperlipidemia. However, the exact mechanism is far too complex, and further study is needed to validate the levels of the target gene or protein expression associated with the altered pathway and demonstrate how YL can lipid-lowering at the molecular level. Furthermore, further studies are also required to analyze the active constituents of YL and its relationship with key metabolites and lipid metabolism parameters, and to identify the biological activity and mechanism of action.

5 Conclusion

YL could effectively ameliorate the hyperlipidemia resulting from triton WR-1339-induced. The beneficial actions of YL have been primarily associated with the correction of metabolic disorders and the maintenance of the dynamic balance of metabolites, which mainly involve linoleic acid metabolism, glycerophospholipid metabolism, phenylalanine metabolism, phenylalanine, tyrosine and tryptophan biosynthesis, and glutamine and glutamate metabolism pathways. The current study suggests that YL can be used as a TCM prescription for the treatment of hyperlipidemia, and the results might provide novel insights into the lipid-lowering effect of YL, and expand the comprehension of the relationship between metabolites and lipid-lowering effects, as well as provide new scientific evidence for clinical application and promotion of YL.

Data availability statement

The original contributions presented in the study are included in the article/Supplementary Material, further inquiries can be directed to the corresponding authors.

Ethics statement

All animal experiments were approved by the Guangdong Provincial Engineering Technology Institute of Traditional Chinese Medicine (Guangzhou, China). The study was conducted in accordance with the local legislation and institutional requirements.

Author contributions

GX, XB, AX, JJ, ZC, CJ, and YL designed the study, implemented, and performed the material preparation, data collection and analysis, GX wrote the manuscript. Animal experiment were performed by GX, AX, JJ, and ZC. GX, YL, SL, WC, ZZ, and JZ prepared the tables and figures under the supervision of XB. All authors contributed to the article and approved the submitted version.

Funding

We gratefully acknowledge the support of the Scientific Research Project of Traditional Chinese Medicine Bureau of Guangdong Province (Number 20222016).

Conflict of interest

The authors declare that the research was conducted in the absence of any commercial or financial relationships that could be construed as a potential conflict of interest.

Publisher's note

All claims expressed in this article are solely those of the authors and do not necessarily represent those of their affiliated organizations, or those of the publisher, the editors and the reviewers. Any product that may be evaluated in this article, or claim that may be made by its manufacturer, is not guaranteed or endorsed by the publisher.

Supplementary material

The Supplementary Material for this article can be found online at: <https://www.frontiersin.org/articles/10.3389/fphar.2023.1252146/full#supplementary-material>

References

- Andersen, C. J., and Fernandez, M. L. (2013). Dietary approaches to improving atheroprotective HDL functions. *Food Funct.* 4, 1304–1313. doi:10.1039/c3fo60207a
- Birger, M., Kaldjian, A. S., Roth, G. A., Moran, A. E., Dieleman, J. L., and Bellows, B. K. (2021). Spending on cardiovascular disease and cardiovascular risk factors in the United States: 1996 to 2016. *Circulation* 144, 271–282. doi:10.1161/CIRCULATIONAHA.120.053216
- Brkic, L., Riederer, M., Graier, W. F., Malli, R., and Frank, S. (2012). Acyl chain-dependent effect of lysophosphatidylcholine on cyclooxygenase (COX)-2 expression in endothelial cells. *Atherosclerosis* 224, 348–354. doi:10.1016/j.atherosclerosis.2012.07.038
- Chen, Z., Sun, D., Bi, X., Luo, W., Xu, A., Chen, W., et al. (2019). Selection and evaluation of quality markers from Yinlan capsule and its LXRA-mediated therapy for hyperlipidemia. *Phytomedicine* 59, 152896. doi:10.1016/j.phymed.2019.152896
- Davalli, A. M., Perego, C., and Folli, F. B. (2012). The potential role of glutamate in the current diabetes epidemic. *Acta Diabetol.* 49, 167–183. doi:10.1007/s00592-011-0364-z
- Gao, Y., Qian, Q., Xun, G., Zhang, J., Sun, S., Liu, X., et al. (2023). Integrated metabolomics and network analysis reveal changes in lipid metabolisms of tripterygium glycosides tablets in rats with collagen-induced arthritis. *Comput. Struct. Biotechnol. J.* 21, 1828–1842. doi:10.1016/j.csbj.2023.02.050
- Ge, S., Liao, C., Su, D., Mula, T., Gegen, Z., Li, Z., et al. (2022). Wuwei qingzhao san ameliorates hyperlipidemia in mice fed with HFD by regulating metabolomics and intestinal flora composition. *Front. Pharmacol.* 13, 842671. doi:10.3389/fphar.2022.842671
- Ito, M. K. (2015). Long-chain omega-3 fatty acids, fibrates and niacin as therapeutic options in the treatment of hypertriglyceridemia: a review of the literature. *Atherosclerosis* 242, 647–656. doi:10.1016/j.atherosclerosis.2015.06.012
- Jenkins, B., West, J. A., and Koulman, A. (2015). A review of odd-chain fatty acid metabolism and the role of pentadecanoic Acid (c15:0) and heptadecanoic Acid (c17:0) in health and disease. *Molecules* 20, 2425–2444. doi:10.3390/molecules20022425
- Jia, X., Xu, W., Zhang, L., Li, X., Wang, R., and Wu, S. (2021). Impact of gut microbiota and microbiota-related metabolites on hyperlipidemia. *Front. Cell Infect. Microbiol.* 11, 634780. doi:10.3389/fcimb.2021.634780
- Li, S., Jin, S., Song, C., Chen, C., Zhang, Y., Xiang, Y., et al. (2016). The metabolic change of serum lysophosphatidylcholines involved in the lipid lowering effect of triterpenes from *Alismatis rhizoma* on high-fat diet induced hyperlipidemia mice. *J. Ethnopharmacol.* 177, 10–18. doi:10.1016/j.jep.2015.11.017
- Li, Y., Cai, D., Zhan, X., Zheng, L., Huang, J., Huang, X., et al. (2019). Lipid metabolism and inflammatory changes in mice with hyperlipidemia induced by Triton WR-1339. *J. Guangdong Pharm. Univer* 35, 793–797. doi:10.16809/j.cnki.2096-3653.2019101504
- Li, Y., Chen, Y., Huang, X., Huang, D., Gan, H., Yao, N., et al. (2020). Tanshinol A ameliorates triton-1339W-induced hyperlipidemia and liver injury in C57BL/6J mice by regulating mRNA expression of lipemic-oxidative injury genes. *Lipids* 55, 127–140. doi:10.1002/lipd.12217
- Miao, H., Chen, H., Pei, S., Bai, X., Vaziri, N. D., and Zhao, Y. Y. (2015). Plasma lipidomics reveal profound perturbation of glycerophospholipids, fatty acids, and sphingolipids in diet-induced hyperlipidemia. *Chem. Biol. Interact.* 228, 79–87. doi:10.1016/j.cbi.2015.01.023
- Moon, H. S., Lee, H. G., Seo, J. H., Chung, C. S., Kim, T. G., Choi, Y. J., et al. (2009). Antiobesity effect of PEGylated conjugated linoleic acid on high-fat diet-induced obese C57BL/6J (ob/ob) mice: attenuation of insulin resistance and enhancement of antioxidant defenses. *J. Nutr. Biochem.* 20, 187–194. doi:10.1016/j.jnutbio.2008.02.001
- Nemet, I., Saha, P. P., Gupta, N., Zhu, W., Romano, K. A., Skye, S. M., et al. (2020). A cardiovascular disease-linked gut microbial metabolite acts via adrenergic receptors. *Cell* 180, 862–877. doi:10.1016/j.cell.2020.02.016
- O'Reilly, M. E., Lenighan, Y. M., Dillon, E., Kajani, S., Curley, S., Bruen, R., et al. (2020). Conjugated linoleic acid and alpha linolenic acid improve cholesterol homeostasis in obesity by modulating distinct hepatic protein pathways. *Mol. Nutr. Food Res.* 64, e1900599. doi:10.1002/mnfr.201900599
- Paapstel, K., Kals, J., Eha, J., Tootsi, K., Ottas, A., Piir, A., et al. (2018). Inverse relations of serum phosphatidylcholines and lysophosphatidylcholines with vascular damage and heart rate in patients with atherosclerosis. *Nutr. Metab. Cardiovasc Dis.* 28, 44–52. doi:10.1016/j.numecd.2017.07.011
- Park, J. E., and Han, J. S. (2018). A *Portulaca oleracea* L. extract promotes insulin secretion via a K(+)(ATP) channel dependent pathway in INS-1 pancreatic beta-cells. *Nutr. Res. Pract.* 12, 183–190. doi:10.4162/nrp.2018.12.3.183
- Ren, J., Fang, H., Yang, L., Sun, H., Song, H., Yan, G., et al. (2023). Fecal metabolomics analysis for deciphering the lipid-lowering effect of Qizhi capsule on high-fat feed induced hyperlipidemia. *J. Ethnopharmacol.* 308, 116270. doi:10.1016/j.jep.2023.116270
- Rowlett, V. W., Mallampalli, V., Karlstaedt, A., Dowhan, W., Taegtmeier, H., Margolin, W., et al. (2017). Impact of membrane phospholipid alterations in *Escherichia coli* on cellular function and bacterial stress adaptation. *J. Bacteriol.* 199, e00849-16. doi:10.1128/JB.00849-16
- Shi, W. B., Wang, Z. X., Liu, H. B., Jia, Y. J., Wang, Y. P., Xu, X., et al. (2023). Study on the mechanism of Fufang E'jiao Jiang on precancerous lesions of gastric cancer based on network pharmacology and metabolomics. *J. Ethnopharmacol.* 304, 116030. doi:10.1016/j.jep.2022.116030
- Song, J., da Costa, K. A., Fischer, L. M., Kohlmeier, M., Kwock, L., Wang, S., et al. (2005). Polymorphism of the PEMT gene and susceptibility to nonalcoholic fatty liver disease (NAFLD). *FASEB J.* 19, 1266–1271. doi:10.1096/fj.04-3580com
- Su, G., Wang, H., Bai, J., Chen, G., and Pei, Y. (2019). A metabolomics approach to drug toxicology in liver disease and its application in traditional Chinese medicine. *Curr. Drug Metab.* 20, 292–300. doi:10.2174/1389200220666181231124439
- Sun, H., Zhang, A., and Wang, X. (2012). Potential role of metabolomic approaches for Chinese medicine syndromes and herbal medicine. *Phytother. Res.* 26, 1466–1471. doi:10.1002/ptr.4613
- Sun, J. H., Liu, X., Cong, L. X., Li, H., Zhang, C. Y., Chen, J. G., et al. (2017). Metabolomics study of the therapeutic mechanism of Schisandra Chinensis lignans in diet-induced hyperlipidemia mice. *Lipids Health Dis.* 16, 145. doi:10.1186/s12944-017-0533-3
- Sun, Y., Cheng, G., Du, L., Gan, Y., Li, B., Yan, S., et al. (2022). Chuanzhitongluo capsule ameliorates microcirculatory dysfunction in rats: efficacy evaluation and metabolic profiles. *Front. Pharmacol.* 13, 1011333. doi:10.3389/fphar.2022.1011333
- Ta, N., Lisha, A. L., Erdunduleng, E., Qi, R., Mu, X., Feng, L., et al. (2023). Metabolomics analysis reveals amelioration effects of yellowhorn tea extract on hyperlipidemia, inflammation, and oxidative stress in high-fat diet-fed mice. *Front. Nutr.* 10, 1087256. doi:10.3389/fnut.2023.1087256
- Tacherfiout, M., Petrov, P. D., Mattonai, M., Ribechini, E., Ribot, J., Bonet, M. L., et al. (2018). Antihyperlipidemic effect of a *Rhamnus alaternus* leaf extract in Triton-induced hyperlipidemic rats and human HepG2 cells. *Biomed. Pharmacother.* 101, 501–509. doi:10.1016/j.biopha.2018.02.106
- Tietge, U. J. (2014). Hyperlipidemia and cardiovascular disease: inflammation, dyslipidemia, and atherosclerosis. *Curr. Opin. Lipidol.* 25, 94–95. doi:10.1097/MOL.0000000000000051
- Tong, X., Xu, J., Lian, F., Yu, X., Zhao, Y., Xu, L., et al. (2018). Structural alteration of gut microbiota during the amelioration of human type 2 diabetes with hyperlipidemia by metformin and a traditional Chinese herbal formula: a multicenter, randomized, open label clinical trial. *mBio* 9, e02392-17. doi:10.1128/mBio.02392-17
- Wang, Q., Luo, Z., Li, D., Qin, J., Pan, Z., Guo, B., et al. (2022). Investigation of the therapeutic effect of total alkaloids of *Corydalis saxicola* bunting on CCl(4)-induced liver fibrosis in rats by LC/MS-Based metabolomics analysis and network pharmacology. *Metabolites* 13, 9. doi:10.3390/metabo13010009
- Wu, G. (2009). Amino acids: metabolism, functions, and nutrition. *Amino Acids* 37, 1–17. doi:10.1007/s00726-009-0269-0
- Wu, G., Zhang, W., and Li, H. (2019). Application of metabolomics for unveiling the therapeutic role of traditional Chinese medicine in metabolic diseases. *J. Ethnopharmacol.* 242, 112057. doi:10.1016/j.jep.2019.112057
- Xiao, G., Hu, Z., Jia, C., Yang, M., Li, D., Xu, A., et al. (2023a). Deciphering the mechanisms of Yinlan Tiaozhi capsule in treating hyperlipidemia by combining network pharmacology, molecular docking and experimental verification. *Sci. Rep.* 13, 6424. doi:10.1038/s41598-023-33673-3
- Xiao, G., Li, S., Chen, Z., Yang, M., Qiu, J., and Bi, X. (2023b). Identification of the chemical constituents of Yinlan Tiaozhi capsule and attribution of original herbs. *Chin. Tradit. Pat. Med.* 45, 2420–2427. doi:10.3969/j.issn.1001-1528.2023.07.055
- Yan, Z., Wu, H., Zhou, H., Chen, S., He, Y., Zhang, W., et al. (2020). Integrated metabolomics and gut microbiome to the effects and mechanisms of naoxintong capsule on type 2 diabetes in rats. *Sci. Rep.* 10, 10829. doi:10.1038/s41598-020-67362-2
- Yang, B., Xuan, S., Ruan, Q., Jiang, S., Cui, H., Zhu, L., et al. (2020). UPLC/Q-TOF-MS/MS-based metabolomics revealed the lipid-lowering effect of *Ilicis Rotundae* Cortex on high-fat diet induced hyperlipidemia rats. *J. Ethnopharmacol.* 256, 112784. doi:10.1016/j.jep.2020.112784
- Yue, H., Qiu, B., Jia, M., Liu, W., Guo, X. F., Li, N., et al. (2021). Effects of alpha-linolenic acid intake on blood lipid profiles: systematic review and meta-analysis of randomized controlled trials. *Crit. Rev. Food Sci. Nutr.* 61, 2894–2910. doi:10.1080/10408398.2020.1790496
- Zhang, J., Wang, O., Guo, Y., Wang, T., Wang, S., Li, G., et al. (2016). Effect of increasing doses of linoleic and alpha-linolenic acids on high-fructose and high-fat diet

induced metabolic syndrome in rats. *J. Agric. Food Chem.* 64, 762–772. doi:10.1021/acs.jafc.5b04715

Zhang, Q., Wang, G. J., Ji-Ye, A., Wu, D., Zhu, L. L., Ma, B., et al. (2009). Application of GC/MS-based metabonomic profiling in studying the lipid-regulating effects of Ginkgo biloba extract on diet-induced hyperlipidemia in rats. *Acta Pharmacol. Sin.* 30, 1674–1687. doi:10.1038/aps.2009.173

Zhang, S., Yuan, L., Li, H., Han, L., Jing, W., Wu, X., et al. (2022). The novel interplay between commensal gut bacteria and metabolites in diet-induced hyperlipidemic rats treated with simvastatin. *J. Proteome Res.* 21, 808–821. doi:10.1021/acs.jproteome.1c00252

Zhao, W., An, R., Liu, F., Gu, J., Sun, Y., Xu, S., et al. (2021). Urinary metabolomics analysis of the protective effects of Daming capsule on hyperlipidemia rats using ultra-high-performance liquid chromatography coupled to quadrupole time-of-flight mass spectrometry. *J. Sep. Sci.* 44, 3305–3318. doi:10.1002/jssc.202100113

Zhao, Y., Zhang, Z., Wang, L., Li, W., Du, J., Zhang, S., et al. (2023). Hypolipidemic mechanism of *Pleurotus eryngii* polysaccharides in high-fat diet-induced obese mice based on metabolomics. *Front. Nutr.* 10, 1118923. doi:10.3389/fnut.2023.1118923

Zhao, Y. Y., Miao, H., Cheng, X. L., and Wei, F. (2015). Lipidomics: novel insight into the biochemical mechanism of lipid metabolism and dysregulation-associated disease. *Chem. Biol. Interact.* 240, 220–238. doi:10.1016/j.cbi.2015.09.005



OPEN ACCESS

EDITED BY

Abd El-Latif Hesham,
Beni-Suef University, Egypt

REVIEWED BY

Jia-Wen Shou,
The Chinese University of Hong Kong,
China
Yasmina Esther Hernández-Santana,
APC, Ireland

*CORRESPONDENCE

Xiandang Zhang,
✉ xiandangzh@163.com
Zhibin Wang,
✉ wangzhibin@sdfmu.edu.cn

RECEIVED 10 August 2023

ACCEPTED 06 November 2023

PUBLISHED 20 November 2023

CITATION

Xia W, Li S, Li L, Zhang S, Wang X, Ding W,
Ding L, Zhang X and Wang Z (2023), Role
of anthraquinones in combating
insulin resistance.
Front. Pharmacol. 14:1275430.
doi: 10.3389/fphar.2023.1275430

COPYRIGHT

© 2023 Xia, Li, Li, Zhang, Wang, Ding,
Ding, Zhang and Wang. This is an open-
access article distributed under the terms
of the [Creative Commons Attribution
License \(CC BY\)](https://creativecommons.org/licenses/by/4.0/). The use, distribution or
reproduction in other forums is
permitted, provided the original author(s)
and the copyright owner(s) are credited
and that the original publication in this
journal is cited, in accordance with
accepted academic practice. No use,
distribution or reproduction is permitted
which does not comply with these terms.

Role of anthraquinones in combating insulin resistance

Wanru Xia¹, Shuqian Li², LinZehao Li¹, Shibo Zhang¹,
Xiaolei Wang¹, Wenyu Ding¹, Lina Ding¹, Xiandang Zhang^{2*} and
Zhibin Wang^{1*}

¹Endocrine and Metabolic Diseases Hospital of Shandong First Medical University, Shandong First Medical University and Shandong Academy of Medical Sciences, Jinan, China, ²Shandong First Medical University and Shandong Academy of Medical Sciences, Jinan, China

Insulin resistance presents a formidable public health challenge that is intricately linked to the onset and progression of various chronic ailments, including diabetes, cardiovascular disease, hypertension, metabolic syndrome, nonalcoholic fatty liver disease, and cancer. Effectively addressing insulin resistance is paramount in preventing and managing these metabolic disorders. Natural herbal remedies show promise in combating insulin resistance, with anthraquinone extracts garnering attention for their role in enhancing insulin sensitivity and treating diabetes. Anthraquinones are believed to ameliorate insulin resistance through diverse pathways, encompassing activation of the AMP-activated protein kinase (AMPK) signaling pathway, restoration of insulin signal transduction, attenuation of inflammatory pathways, and modulation of gut microbiota. This comprehensive review aims to consolidate the potential anthraquinone compounds that exert beneficial effects on insulin resistance, elucidating the underlying mechanisms responsible for their therapeutic impact. The evidence discussed in this review points toward the potential utilization of anthraquinones as a promising therapeutic strategy to combat insulin resistance and its associated metabolic diseases.

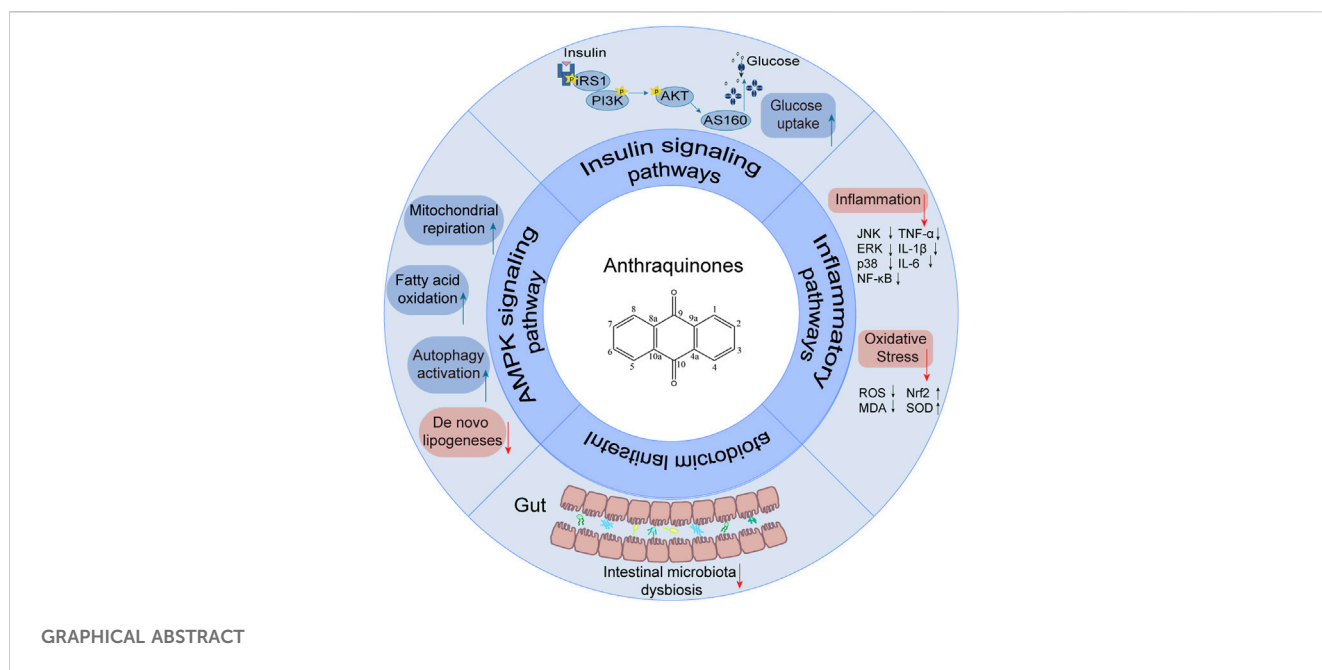
KEYWORDS

anthraquinones, insulin resistance, natural products, intestinal microbiome, antiinflammation

1 Introduction

Insulin resistance is characterized by a persistent loss of insulin sensitivity and is a prevalent risk factor contributing to obesity, hypertension, cardiovascular diseases, and type 2 diabetes (James et al., 2021; Wang et al., 2022; Sasaki et al., 2022). Additionally, insulin resistance increases the susceptibility to heart failure and fuels tumor growth, posing a substantial threat to human health and imposing a considerable economic burden on society and families. Notably, its prevalence is on the rise, reaching 20%–40% among young populations in developing countries (Artunc et al., 2016). Consequently, the implementation of effective strategies to ameliorate insulin resistance has become indispensable.

While no medication specifically targets insulin resistance, several antidiabetic drugs, including insulin sensitizers, insulin secretagogues, and alpha-glucosidase inhibitors, have been utilized to improve insulin resistance. However, these treatments often have some adverse effects and limitations. For instance, insulin sensitizers may lead to heart failure (Arnold et al., 2019) and weight gain (Dutta et al., 2023), insulin secretagogues may cause excessive insulin secretion and damage to pancreatic beta cells (Rustenbeck et al., 2004), and alpha-glucosidase inhibitors may result in diarrhea and gastrointestinal discomfort (Taylor et al., 2019).



Recently, a plethora of studies have indicated that natural products possessing mild pharmaceutical properties can significantly augment insulin sensitivity, suggesting that natural products may be a new strategy for the treatment of insulin resistance (Zhang et al., 2020; Zhang et al., 2020; Wang et al., 2022; Zhou et al., 2022). These findings underscore the considerable potential of natural products as promising alternatives to conventional treatments for metabolic disorders. Notably, a substantial proportion of these natural products known for their efficacy in combating obesity and ameliorating insulin resistance are rich in anthraquinones (Kumar et al., 2019). For instance, *Cassia semen* (Ko et al., 2020), *Rheum palmatum L.* (Cui et al., 2019) and *Aloe vera* (Deora et al., 2021), all of which boast anthraquinones, are prominent examples of natural products that are widely employed for the amelioration of metabolic diseases. Anthraquinones, distinguished by their tricyclic diketone pharmacophoric structure (Alam et al., 2019) (Figure 1), constitute a class of plant secondary metabolites. Several studies have substantiated the capacity of anthraquinones to enhance insulin resistance, thereby signifying their promising candidacy as pharmacological agents for mitigating insulin resistance and associated metabolic disorders.

To date, no comprehensive review has been conducted to explore the mechanisms by which anthraquinones ameliorate insulin resistance. This review endeavors to bridge this knowledge gap by providing a systematic assessment of identified anthraquinones and elucidating their respective mechanisms for improving insulin resistance.

2 Characteristics of anthraquinones

Anthraquinones (9,10-dioxoanthracenes) are plant secondary metabolites containing a tricyclic dione pharmacophore structure. The anthraquinone ring is the fundamental parent structure of anthraquinones. Anthraquinone monomer refers to chemical compounds containing a single anthraquinone ring, whereas two

monomeric anthraquinone units can undergo dehydration and condensation reactions via two distinct pathways to form dimeric anthraquinones (Malik and Müller, 2016). Some studies have revealed that anthraquinones can be substituted with various functional groups, including hydroxyl, alkyl, alkoxy, and sugar units. The specific type, number, and position of substituents on the parent nucleus are critical determinants of natural product bioactivity in this chemical class. For instance, rhein, which has a carboxylic acid group at the sixth substitution position, exhibits significantly greater lipid-lowering activity than aloe-emodin, which has a hydroxyl substitution at the same position (Fang et al., 2022).

Anthraquinones are commonly found in higher plants, such as Polygonaceae, Fabaceae, Rhamnaceae, Rubiaceae, and Liliaceae, either in the form of free anthraquinones or anthraquinone glycosides. Additionally, they are also found in the metabolites of lichens and fungi (Li and Jiang, 2018). It is now well established that anthraquinones exhibit a wide range of biological activities, such as anticancer (Zhang et al., 2021), anti-inflammatory (Xie et al., 2022), antibacterial (Qi et al., 2022), anti-oxidant (Yin et al., 2022), and

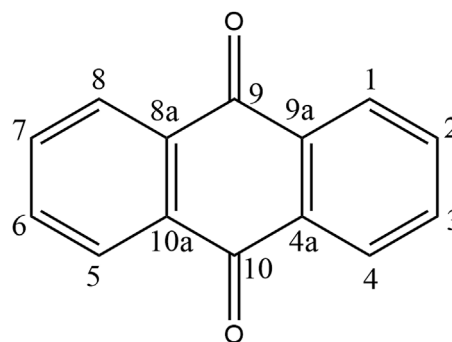


FIGURE 1
Overview diagram of anthraquinones.

antiviral effects (Dai et al., 2017). They have also been shown to have great potential in the prevention and treatment of various diseases, including cancer and diabetes.

Emodin, rhein, chrysophanol, aloe-emodin, and physcion are among the most common and representative anthraquinones found in traditional Chinese medicine. These compounds have been identified as the major bioactive components of *R. palmatum L.*, *Polygonum multiflorum*, *Cassiae semen*, *Aloe vera*, and *Senna* (Khurm et al., 2020; Ma et al., 2022). Research has demonstrated the potential of these natural products to improve insulin resistance, making them promising agents for obesity prevention and treatment. *Rumex dentatus L.* is a natural medicinal plant rich in anthraquinones, including emodin. The study demonstrated its significant potential in reducing homeostatic model assessment of insulin resistance (HOMA-IR) and improving insulin resistance in diabetic rats (Elsayed et al., 2020). *Aloe vera* is rich in anthraquinones, including aloe-emodin and aloin. Some studies indicate that these bioactive molecules possess the potential to regulate pancreatic β cell function, suppress fat accumulation, and lower fasting blood glucose (FBG) levels, thus offering an effective therapeutic approach for alleviating obesity (Deora et al., 2021; Fu et al., 2022). Administration of *Aloe vera* extract in obese mice significantly reduced fasting blood glucose levels, improved glucose tolerance, mitigated adipose tissue inflammation, and subsequently ameliorated insulin resistance (Shin et al., 2011; An et al., 2021). A randomized controlled trial with obese individuals demonstrated that *Aloe vera* extracts significantly reduced body weight and HOMA-IR (Zhang et al., 2016). Anthraquinones are also widely distributed among other traditional herbals. *Rheum palmatum L.* is an herbal medicine rich in anthraquinones, including emodin, rhein, and chrysophanol, that has exhibited significant potential in attenuating adipose tissue inflammation and hepatic accumulation of triglycerides in mice. These findings suggest that *R. palmatum L.* may be a potential preventive and therapeutic strategy for obesity (Régner et al., 2020). Oral administration of *R. palmatum L.* extracts significantly inhibited ectopic fat accumulation and was shown to improve insulin resistance in obese rats (Yang et al., 2016). *Senna*, a natural medicine rich in the anthraquinone-derived natural product sennoside A, has been shown to improve the oxidative stress response and alleviate the inflammatory reaction of adipose tissue, resulting in weight loss in rats (Nayan et al., 2021). Additionally, *Cassiae semen*, a natural medicine rich in anthraquinone-derived natural products such as aurantio-obtusin and alaternin, has been shown to lower FBG and insulin levels and enhance glucose uptake in skeletal muscle in obese mice, thus restoring insulin sensitivity (Wang et al., 2019). Additionally, we have summarized more than ten anthraquinones that can improve insulin resistance through various mechanisms (Table 1).

3 Mechanism of insulin resistance improvement by anthraquinones

3.1 Anthraquinones improve insulin resistance by attenuating impaired insulin signaling pathways

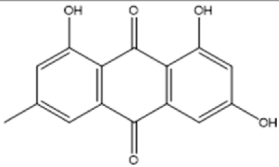
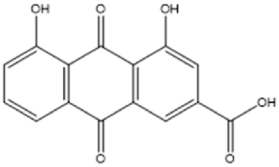
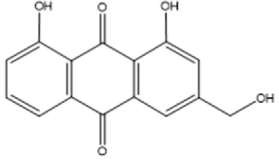
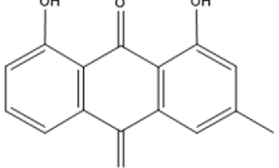
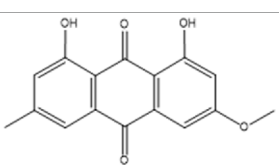
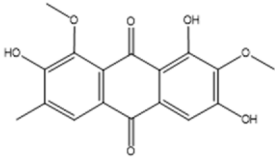
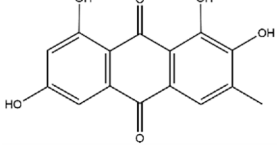
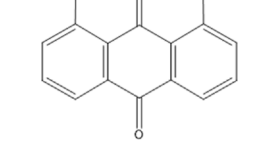
Upon engagement with its receptor, insulin sets in motion a myriad of intricate signaling cascades. Insulin resistance manifests

when this finely tuned pathway falters, impeding the profound physiological effects of insulin. Remarkably, anthraquinones have demonstrated the ability to alleviate insulin resistance through diverse mechanisms. These include the inhibition of protein tyrosine phosphatase 1B (PTP1B) activity and facilitation of glucose transporter type 4 (GLUT4) expression and translocation, thereby potentially restoring the proper conduction of the insulin signaling pathway (Figure 2).

Insulin binding to its receptor initiates a wide range of signaling cascades that ultimately lead to the uptake and utilization of glucose in insulin target tissues, including skeletal muscles, adipose tissue, and liver. PTP-1B, as a downstream regulatory factor, is a crucial negative regulator of insulin signal transduction. Overexpression of PTP-1B in adipose tissue can lead to dephosphorylation of insulin receptors and inhibit insulin signaling (Venable et al., 2000). Conversely, *PTP-1B^{-/-}* mice show enhanced glucose tolerance and increased systemic insulin sensitivity (Elchebly et al., 1999; Behl et al., 2022), indicating that PTP-1B may serve as a potential therapeutic target for improving insulin resistance. Several studies indicate that anthraquinone compounds could inhibit the activity of PTP1B. Studies have demonstrated that (trans)-emodin-physcion bianthrone and (cis)-emodin-physcion bianthrone isolated from *Polygonum cuspidatum* show potent inhibitory effects against PTP-1B, with corresponding IC₅₀ values of 2.77 and 7.29 μ M, respectively (Zhao et al., 2017). Furthermore, enzyme kinetic analysis revealed that alaternin extracted from *Cassiae semen* could competitively inhibit PTP-1B activity, with a corresponding inhibition constant (K_i) value of 1.70 μ M (Jung et al., 2016). Additionally, molecular docking simulations indicated that the interaction between alaternin and PTP-1B was primarily driven by hydrogen bonding and hydrophobic interactions. A study unveiled the steadfast binding of chrysophanol and emodin to the allosteric site of PTP-1B, shedding light on their intricate association. This site acts as a metastable inhibitor and inactivates the enzyme by blocking the mobility of the catalytic ring of the enzyme (Martínez-Aldino et al., 2021). Anthraquinones have been widely studied, and many of these natural products exhibit inhibitory effects against PTP-1B. Currently, most relevant studies have employed enzyme kinetic analysis or molecular docking simulations to explore their underlying mechanisms. Nevertheless, the cellular and animal realms remain relatively uncharted territories in this domain. Consequently, additional endeavors are imperative to unravel the labyrinthine interplay between anthraquinones and PTP-1B, unmasking their manifold effects across diverse model systems.

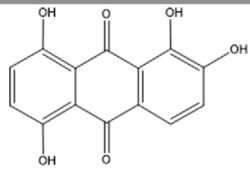
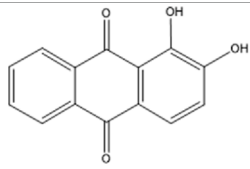
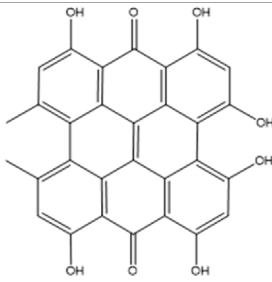
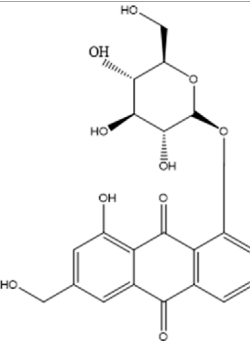
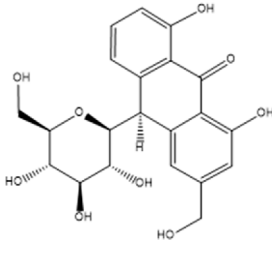
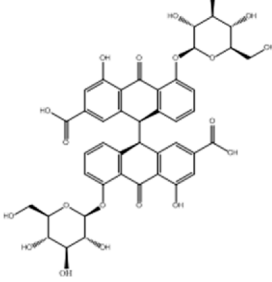
GLUT4 is a protein that facilitates the translocation of glucose across cell membranes and is primarily expressed in adipose and muscle tissues. In these tissues, insulin resistance is associated with impaired insulin-dependent translocation of GLUT4, resulting in decreased glucose uptake (Leto and Saltiel, 2012; Zumbaugh et al., 2022). Aloe-emodin-8-O- β -D-glucoside, derived from *Cassiae semen*, exerts its influence by fostering the cellular uptake of glucose through the activation of the phosphatidylinositol pathway and the upregulation of GLUT4 expression (Anand et al., 2010). Upon subjecting insulin-resistant 3T3-L1 cells to the therapeutic influence of emodin, a marked enhancement in cellular glucose uptake was observed. Notably, this effect was found to be partially attenuated by wortmannin, an inhibitor of

TABLE 1 The Characteristics of Anthraquinones with Improved Insulin Resistance Activity.

Compound	Chemical structure formula	Plant	Overall effect	References
Emodin		<i>Rheum palmatum L.</i> , <i>Polygonum cuspidatum</i> , <i>Cassiae semen</i> , <i>Senna</i> , <i>Aloe vera</i>	Reduced fat storage and promoted cellular glucose uptake	Yang et al. (2007), Tzeng et al. (2012a)
Rhein		<i>Rheum palmatum L.</i> , <i>Polygonum cuspidatum</i> , <i>Cassiae semen</i> , <i>Senna</i> , <i>Aloe vera</i>	Reduced inflammatory response	Ji and Gu (2021)
Aloe-emodin		<i>Rheum palmatum L.</i> , <i>Polygonum cuspidatum</i> , <i>Cassiae semen</i> , <i>Senna</i> , <i>Aloe vera</i>	Reduced inflammatory response	Dou et al. (2019), Quan et al. (2019)
Chrysophanol		<i>Rheum palmatum L.</i> , <i>Polygonum cuspidatum</i> , <i>Cassiae semen</i> , <i>Aloe vera</i>	Enhanced cellular glucose uptake and adipose tissue thermogenesis	Liu et al. (2020), Martínez-Aldino et al. (2021)
Physcion		<i>Rheum palmatum L.</i>	Reduced fat accumulation	Zhao et al. (2017)
Aurantio-obtusin		<i>Cassiae semen</i>	Reduced adipogenesis; promoted cellular glucose uptake; regulated intestinal flora	Guo et al. (2021), Huo et al. (2022), Li et al. (2022)
Alaternin		<i>Cassiae semen</i> , <i>Rhamnus davurica</i>	Promoted cellular glucose uptake	Jung et al. (2016)
Danthron		<i>Rheum palmatum L.</i>	Reduced adipogenesis	(Ma et al., 2021, 2)

(Continued on following page)

TABLE 1 (Continued) The Characteristics of Anthraquinones with Improved Insulin Resistance Activity.

Compound	Chemical structure formula	Plant	Overall effect	References
Quinalizarin		<i>Rubia cordifolia L</i>	Reduced adipogenesis	Yang et al. (2016)
Alizarin		<i>Rubia cordifolia L</i>	Promoted cellular glucose uptake	Xu et al. (2019)
Hypericin		<i>Hypericum perforatum</i>	Improved oxidative stress	Liang et al. (2019)
Aloe-emodin-8-O-β-D-glucoside		<i>Cassiae semen</i>	Promoted cellular glucose uptake	Deora et al. (2021) , Fu et al. (2022)
Aloin		<i>Aloe vera</i>	Reduced free fatty acids	Anand et al. (2010)
Sennoside A		<i>Senna</i>	Regulated intestinal flora	Wei et al. (2020)

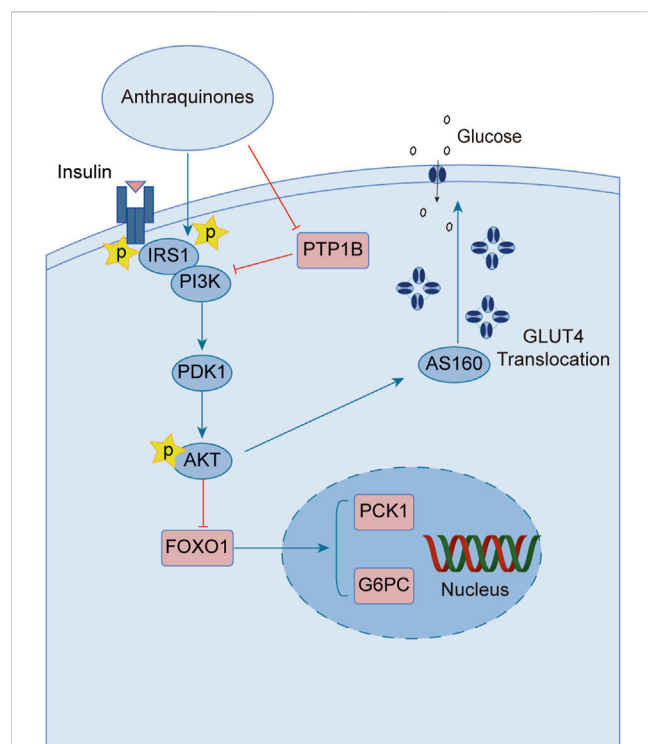


FIGURE 2

Anthraquinones exert a positive influence on insulin resistance by facilitating the transduction of insulin signaling. These bioactive compounds possess the capability to inhibit the activity of PTP-1B and enhance the expression of PI3K, thereby reinstating the effective conduction of the proximal insulin signaling pathway. Moreover, they elevate the levels of AKT phosphorylation, suppress the expression of FOXO1, and attenuate gluconeogenesis. Furthermore, they promote the expression and translocation of GLUT4, consequently augmenting cellular glucose uptake and fortifying the distal signaling pathways associated with insulin signaling.

phosphatidylinositol 3-kinase (PI3K), thereby implicating the PI3K pathway as a crucial route through which emodin stimulates the facilitation of glucose uptake (Yang et al., 2007). The anthraquinone extracts derived from *Cassia semen* elicited a substantial elevation in the phosphorylation states of Akt substrate of 160 kDa (AS160), Akt, and PI3K within the skeletal muscle of diabetic rats. This intricate cascade of events fosters the activation of the PI3K-AKT-AS160 signaling pathway, facilitating the translocation of GLUT4 and concomitantly resulting in a commendable reduction in FBG levels as well as fasting serum insulin (FSI) concentrations (Zhang et al., 2018). Aurantio-obtusin propels the activation of the important PI3K-AKT signaling pathway in both hepatic and adipose tissues. This remarkable orchestration induces a discernible reduction in fasting blood glucose levels while elevating glucose tolerance (Guo et al., 2021). Alizarin exerts a profound influence, effectively lowering fasting and postprandial blood glucose levels in diabetic mice. This versatile compound orchestrates a cascade of molecular events, stimulating the phosphorylation of insulin receptor substrate-1 (IRS-1) and Akt proteins while simultaneously enhancing the expression levels of GLUT4. Collectively, these molecular phenomena synergistically contribute to the amelioration of insulin resistance in mice afflicted with diabetes (Xu et al., 2019).

3.2 Anthraquinones improve insulin resistance by activating the AMPK signaling pathway

The AMPK signaling pathway plays a pivotal role in governing energy metabolism and upholding metabolic equilibrium. Robust evidence supports that AMPK activation enhances insulin sensitivity, promotes glucose uptake, and augments fatty acid oxidation across adipocytes, hepatocytes, and myocytes. Consequently, harnessing the power of AMPK activation has emerged as a potent therapeutic strategy for combating insulin resistance and type 2 diabetes. Notably, several investigations have revealed the ability of anthraquinones, including emodin, aloe emodin, and rhein, to activate the AMPK pathway. These compounds achieve this by increasing the expression and phosphorylation of vital upstream kinases of AMPK, such as protein kinase A (PKA), Ca^{2+} /calmodulin-dependent protein kinase kinases (CaMKKs), and adiponectin. Furthermore, these remarkable agents demonstrate the capacity to ameliorate insulin resistance by orchestrating the AMPK pathway, thereby impeding lipid and cholesterol synthesis, enhancing fatty acid oxidation, and fostering glucose uptake (Figure 3).

The AMPK signaling pathway has emerged as a captivating avenue for the prevention and amelioration of insulin resistance (Towler and Hardie, 2007; Lin and Hardie, 2018; Zhang et al., 2022).

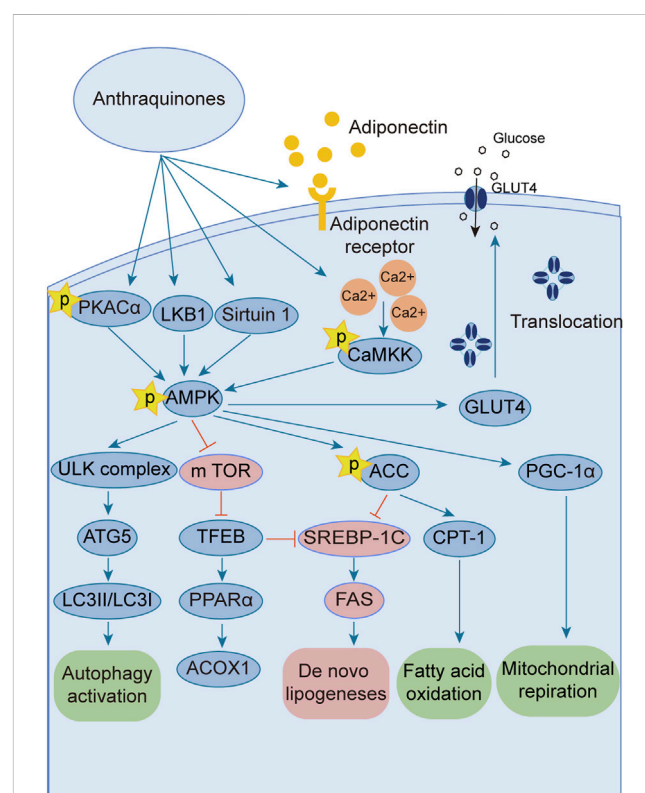


FIGURE 3

Anthraquinones activate the AMPK signaling pathway through various intricate pathways and mechanisms. This activation subsequently enhances lipid metabolism, culminating in a reduction in lipid synthesis and an increase in fatty acid oxidation. Ultimately, these profound effects contribute to the amelioration of insulin resistance.

Positioned as a pivotal kinase regulating energy homeostasis (Diniz et al., 2021), AMPK receives activation signals from an array of influential upstream regulators, including liver kinase B1 (LKB1) (Zhang et al., 2013), CaMKKs (Mungai et al., 2011), transforming growth factor beta-activated kinase1 (TAK1) (Momcilovic et al., 2006), PKA (Hurtado de Llera et al., 2014), and adiponectin (Iwabu et al., 2010; Li et al., 2020). Anthraquinones, including hypericin, danthrone, rhein, and emodin, exhibit the remarkable capacity to augment the expression of key kinases situated upstream of the AMPK signaling pathway, thereby promoting its activation. Through this activation, anthraquinones effectively curtail lipid synthesis, amplify fatty acid oxidation, enhance glucose uptake, and consequently alleviate insulin resistance. Hypericin has garnered attention as a potent agonist of PKA catalytic subunit alpha (PKAC α), manifesting its capability to directly bind to PKAC α . This direct engagement, in turn, sets forth a cascade of events that activate the PKA/AMPK signaling pathway, thereby effectively impeding the detrimental accumulation of ectopic lipids within the hepatic milieu (Liang et al., 2020). Danthron stimulates the AMPK signaling pathway by augmenting the heterodimerization of retinoid X receptor-alpha (RXR α) and peroxisome proliferator-activated receptor alpha (PPAR α) with the adiponectin promoter (Ma et al., 2021). Rhein exhibits the capacity to increase both the expression and phosphorylation of AMPK protein, thereby effectively activating the AMPK pathway (Lu et al., 2022). Within the composition of *R. palmatum* L., emodin has been validated as an activator of the AMPK signaling pathway. Its mode of action involves the facilitation of adiponectin expression and the mitigation of oxygen consumption in insulin-resistant C2C12 and 3T3-L1 cells (Chen et al., 2012; Zhang et al., 2015). Moreover, emodin elicits the activation of CaMKK2, a crucial upstream kinase, through the augmentation of intracellular Ca²⁺ concentration within L6 myotubular cells. This consequential event subsequently triggers the activation of the AMPK signaling pathway (Song et al., 2013).

Excessive energy availability promotes heightened flux of free fatty acids (FFAs) and aberrant lipid deposition, thereby contributing to insulin resistance (Nguyen et al., 2005; Jiao et al., 2011). The AMPK signaling pathway assumes a pivotal role in governing lipid metabolism and preventing undue lipid accumulation. Activation of AMPK effectively curtails the activity of acetyl-CoA carboxylase (ACC), alleviating its inhibitory influence on carnitine palmitoyltransferase 1 (CPT-1) and potentiating fatty acid oxidation (Monsénégro et al., 2012; Sheng et al., 2019). Moreover, AMPK activation downregulates the expression of sterol regulatory element-binding protein-1c (SREBP-1c) (Li et al., 2011) and CCAAT enhancer-binding protein alpha (C/EBP α) (Kawaguchi et al., 2002), transcription factors that orchestrate lipogenic gene expression, thereby diminishing lipid synthesis. Therefore, harnessing the AMPK signaling pathway represents an efficacious strategy to counter insulin resistance, as it heightens fat oxidation, suppresses lipogenesis, and fosters lipid homeostasis. Emodin, a naturally occurring compound found in medicinal plants, has demonstrated the capacity to augment fatty acid oxidation through the activation of the AMPK pathway in rats subjected to a high-fat diet (HFD). Its activation of AMPK leads to the upregulation of CPT-1 expression, concomitant with the downregulation of SREBP-1c and fatty acid synthase (FAS)

expression, effectively inhibiting lipogenesis and curtailing lipid accumulation. As a result, emodin exerts a beneficial effect on insulin resistance (Tzeng et al., 2012b). Furthermore, intravenous administration of emodin has been observed to stimulate AMPK and ACC phosphorylation in skeletal muscle and liver tissue of HFD-fed mice, leading to reduced fasting blood glucose and fasting insulin levels, as well as improved insulin sensitivity (Song et al., 2013). Chrysophanic acid effectively attenuated weight gain in mice with diet-induced obesity. It also mitigated lipid accumulation and downregulated the expression of adipogenesis-associated factors, such as peroxisome proliferator-activated receptor gamma (PPAR γ) and C/EBP α , in 3T3-L1 adipocytes (Lim et al., 2016). In a dose-dependent manner, danthrone exhibited a remarkable capacity to induce the phosphorylation of AMPK and ACC in both HepG2 and C2C12 cells. Furthermore, danthron treatment demonstrated significant efficacy in suppressing lipid synthesis by downregulating the expression of SREBP1c and FAS, thereby leading to reduced levels of total cholesterol (TC) and triglycerides (TGs). Intriguingly, the effects of danthrone on lipid and glucose metabolism were attenuated or reversed when coadministered with the AMPK inhibitor compound C (Zhou et al., 2013). Furthermore, auranthio-obtusin has been shown to induce the phosphorylation of transcription factor EB (TFEB) and bolster autophagic flux within hepatocytes by eliciting AMPK activation. This consequential activation subsequently upregulates the expression of PPAR α and acyl-CoA oxidase 1 (ACOX1), thereby stimulating the oxidation of fatty acids. Concurrently, it inhibits the expression of SREBP-1 and FAS, thus culminating in a reduction in lipid synthesis and a decline in the accumulation of lipids in nonadipose tissues (Zhou et al., 2021). TFEB serves as a crucial regulator of autophagy and lysosomal function. Remarkably, TFEB overexpression has been demonstrated to effectively impede weight gain, curtail lipid accumulation, and ameliorate insulin resistance in mouse models of diet-induced obesity (Settembre et al., 2013). The addition of the Physcion supplement increased energy expenditure, contributing to improvements in plasma lipids, adipokines, cytokines, and fecal lipids. Notably, there was a reduction in hepatic FFA synthesis and an increase in FFA oxidation. A significant decrease in lipid synthesis was observed, while lipolysis and oxidation were enhanced.

Activation of the AMPK signaling pathway upholds energy homeostasis by efficiently dissipating surplus energy as heat (Yang et al., 2021). White adipose tissue (WAT) assumes the role of an energy reservoir, storing excess energy in the form of fat. Its accumulation has been closely associated with metabolic disorders (Maqdasy et al., 2022). Conversely, brown adipose tissue (BAT) expends energy through thermogenesis, exerting an inverse relationship with blood glucose levels, insulin resistance, and obesity (Anhê et al., 2019; Xu et al., 2020; Sugimoto et al., 2022; Villarroya and Gavalda-Navarro, 2022). Certain stimuli, such as cold exposure, exercise, or specific hormonal cues, can instigate a process known as “browning” in WAT (Liu et al., 2022). The process of WAT browning entails the activation of uncoupling protein 1 (UCP-1), a pivotal factor associated with prompt and adaptive thermogenesis (Fedorenko et al., 2012). This process is governed by the transcriptional coactivator peroxisome proliferator-activated receptor- γ co-activator-1 α (PGC-1 α), which exerts crucial regulatory control over UCP-1 expression and thermogenesis in BAT (Boström et al., 2012). Using primary cultured brown adipocytes as *in vitro* models and HFD-induced

obese mice as *in vivo* models, the administration of chrysophanol yielded a notable reduction in weight gain among obese mice. Furthermore, chrysophanol treatment substantially upregulated the expression of UCP1 and PGC1 α . Interestingly, in brown adipocytes, the coadministration of Compound C, an inhibitor of AMPK, effectively nullified the impact of chrysophanol on AMPK α , thereby indicating the partial involvement of the AMPK α pathway in chrysophanol efficacy (Lim et al., 2016). Sirtuin 6 (SIRT6) is a multifunctional enzyme with ADP-ribosyltransferase and histone deacetylase activities that orchestrates the recruitment of phosphorylated transcription factor 2 (ATF2), leading to enhanced expression of PGC-1 α (Yao et al., 2017). The upregulated expression of SIRT6 increases the phosphorylation of AMPK, thereby ameliorating insulin resistance (Luo et al., 2018; Fan et al., 2019). Chrysophanol administration in mice with HFD-induced obesity substantially elevates SIRT6 and UCP-1 expression within WAT. This finding was further supported by metabolic cage data, elucidating the augmentation of thermogenesis. Importantly, these effects were not observed in Sirt6-deficient mice (Sirt6 $^{-/-}$), underscoring the pivotal role of SIRT6 in mediating the impact of chrysophanol. Collectively, these discoveries highlight the therapeutic potential of chrysophanol in combating obesity and related metabolic disorders by virtue of its ability to upregulate SIRT6, subsequently promoting the upregulation of PGC-1 α and UCP-1 in BAT (Liu et al., 2020). Aurantio-obtusin (AO) is a bioactive compound found in Cassiae semen that is a Chinese traditional medicinal herb. It demonstrated remarkable efficacy in enhancing hepatic lipid metabolism in a mouse model of hepatic steatosis. The administration of AO significantly increased mitochondrial metabolism and upregulated UCP1 expression. This effect was achieved through the activation of PPAR α signaling, both *in vivo* and in primary brown adipocytes (Yi-Jie et al., 2023).

3.3 Anthraquinones ameliorate insulin resistance by inhibiting inflammatory pathways

Emerging research has illuminated the pivotal contribution of low-grade chronic inflammation in the development and advancement of insulin resistance. Notably, anthraquinones have demonstrated their potential in mitigating insulin resistance linked to inflammation. These compounds exhibit the ability to ameliorate adipocyte inflammatory infiltration, suppress the secretion of diverse inflammatory factors by adipocytes, induce macrophage M2 polarization, and enhance overall systemic inflammation regulation (Figure 4).

A growing body of evidence highlights the intimate association between low-grade chronic systemic inflammation and insulin resistance (Ahmed et al., 2021). The elevation of FFA triggers the activation of Toll-like receptor 4 (TLR4), initiating a cascade of signaling events involving key regulators such as nuclear factor kappaB (NF- κ B) and c-Jun N-terminal kinase (JNK) (Wang et al., 2017; Li et al., 2020; Zhang et al., 2023). Activation of the NF- κ B and JNK pathways increases the secretion of various inflammatory mediators, including tumor necrosis factor- α (TNF- α), interleukin-1 β (IL-1 β), and interleukin-6 (IL-6) (Glass and Olefsky, 2012; Jiang et al., 2022; Park et al., 2022). These pro-inflammatory factors perpetuate systemic inflammation, thus

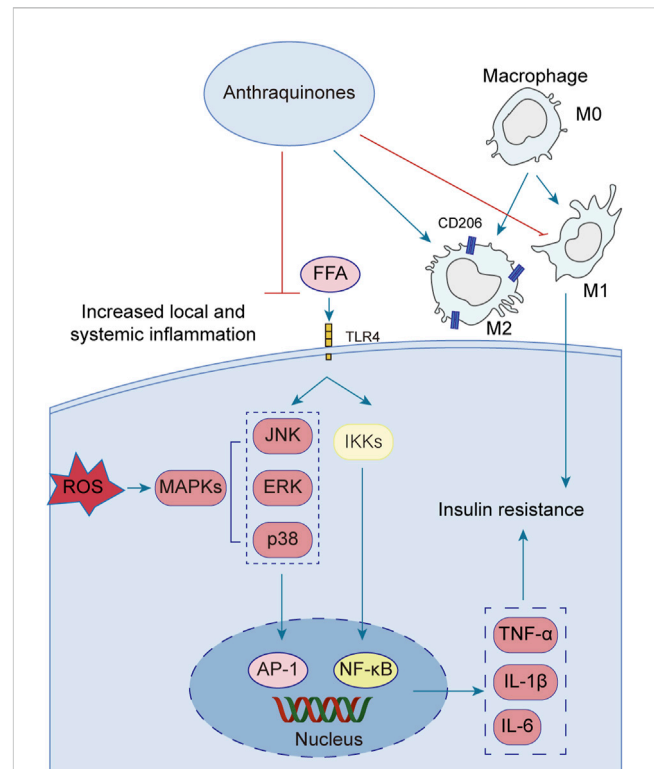


FIGURE 4

Low-grade chronic systemic inflammation is intricately linked to insulin resistance. Anthraquinones exert a direct inhibitory effect on the MAPK and NF- κ B pathways, resulting in the suppression of pro-inflammatory cytokines such as TNF- α , IL-1 β , IL-6, and IL-8. Moreover, anthraquinones effectively reduce ROS levels and foster the polarization of M2 macrophages. By mitigating low-grade chronic systemic inflammation through these mechanisms, anthraquinones contribute to the improvement of insulin resistance.

contributing to the persistence of insulin resistance. Several anthraquinones have emerged as potential therapeutics for reducing pro-inflammatory mediators and improving insulin resistance. For instance, chrysophanol demonstrated efficacy by downregulating the expression of TNF- α , IL-1 β , IL-6, and IL-8 in mice subjected to a HFD (Lian et al., 2017). Similarly, rhein showcased its beneficial effects by attenuating weight gain, lipid accumulation, and IL-6, IL-1 β , and TNF- α levels in adipose tissue and serum of rats with HFD-induced obesity (Ji and Gu, 2021). Molecular docking studies further revealed that rhein effectively bound to TNF- α , IL-6, and NF- κ B, with binding energies of -8.9, -7.1, and -7.6 kcal/mol, respectively, suggesting its potential as a modulator of the TNF signaling pathway (Jiang et al., 2022). Additionally, rhein exhibited inhibitory effects on mitogen-activated protein kinase (MAPK) signaling in macrophages, leading to reduced transcription of the proinflammatory mediators TNF- α and IL-1 β (Chang et al., 2019). Aloe-emodin demonstrated its capability to diminish TNF- α and IL-6 production while suppressing the NF- κ B pathway, thereby restoring insulin signaling and ameliorating insulin resistance (Dou et al., 2019; Quan et al., 2019). Furthermore, emodin was shown to inhibit the expression of adipokines, including TNF- α , IL-1 β , and IL-6, in adipocytes, potentially through the inhibition of p38, extracellular-signal-

regulated kinase (ERK), and JNK phosphorylation (Fang et al., 2022). In a dose-dependent manner, physcion exhibited the capacity to attenuate the gene expression levels of TNF- α , IL-6, and IL-1 β in a hepatocellular carcinoma cell line (HepG2) upon induction of inflammation by lipopolysaccharide (LPS) (Selim et al., 2019). Aloe-emodin significantly attenuated the production of nitric oxide (NO), IL-6, and IL-1 β in LPS-stimulated RAW264.7 cells. Western blot analysis revealed that aloe-emodin suppressed the LPS-induced expression of iNOS protein, degradation of I κ B α , and phosphorylation of ERK, p38, JNK, and Akt. These findings elucidate the anti-inflammatory properties of aloe-emodin, which likely involve the attenuation of proinflammatory cytokine production in LPS-induced RAW264.7 macrophages through the inhibition of the NF- κ B, MAPK, and PI3K signaling pathways (Hu et al., 2014). Furthermore, the nitrogen-containing derivatives of aloe-emodin demonstrated superior efficacy in inhibiting nitric oxide, with an IC₅₀ value of 3.15 μ M. Furthermore, these derivatives exhibited a significant reduction in the levels of the pro-inflammatory cytokines TNF- α , IL-1 β , and IL-6, as well as iNOS and COX-2 enzymes (Shang et al., 2022).

Macrophages can be classified into two distinct subtypes based on their activation state: M1-polarized macrophages and M2-polarized macrophages. In the context of obesity, macrophages tend to favor the M1 phenotype, exacerbating adipose tissue inflammation and contributing to systemic insulin resistance (Li et al., 2018). Conversely, M2 polarization is associated with anti-inflammatory effects, lower body weight, and enhanced insulin sensitivity (Chen et al., 2019). *In vitro* and *in vivo* experiments have demonstrated the inhibitory effects of emodin on the p65-NF- κ B complex, along with its ability to enhance the prevalence of M2 (anti-inflammatory)-like phenotype macrophages (Chen et al., 2022). Rhein possesses the ability to shift macrophages toward the M2 phenotype. This was achieved through the downregulation of the M1 marker inducible nitric oxide synthase (iNOS) in mouse colon tissue and the upregulation of CD206, Arg1, IL-10, and ChIL3, which are indicative of M2 macrophage activation (Zhou et al., 2022). The triggering receptor expressed on myeloid cell 2 (TREM2), a member of the immunoglobulin receptor superfamily, has been found to enhance the production of anti-inflammatory cytokines and the expression of M2 marker genes when overexpressed (Korvatska et al., 2020). Upregulation of TREM2 has been demonstrated to mitigate insulin resistance induced by obesity (Carrasco et al., 2019). In mice with HFD-induced obesity, emodin effectively induced the polarization of M2 macrophages through the upregulation of TREM2 expression. This intervention notably alleviated local and systemic inflammation, curbed weight gain and lipid accumulation, reduced fasting glucose and fasting insulin levels, and improved insulin sensitivity (Yu et al., 2021). Rhein exhibited notable efficacy in reducing tissue inflammation and facilitating the transition of macrophages toward an M2 polarization state in an LPS-induced model. *In vitro* experiments demonstrated that rhein effectively mitigated intracellular ROS levels, suppressed the activation of P65, and thereby hindered macrophage polarization toward an M1 phenotype. Mechanistically, the protective effects of rhein were attributed to its modulation of the nuclear factor of activated T cells c1 (NFATc1)/TREM2 axis, as evidenced by the substantial attenuation observed in blocking experiments targeting both TREM2 and NFATc1 (Li et al., 2023).

The interplay between oxidative stress and inflammation can mutually aggravate insulin resistance. Reactive oxygen species (ROS), such as superoxide dismutase (SOD) and malondialdehyde (MDA), can stimulate the production of inflammatory factors, while cellular inflammatory factors, in turn, promote the generation of free radicals (Kwak et al., 2017). Oxidative stress poses detrimental effects on pancreatic beta cell function, leading to apoptosis and exacerbating insulin resistance (Costes et al., 2006). Notably, aloe-emodin has demonstrated the ability to reduce ROS levels in RIN-5F cells exposed to high glucose conditions, thus safeguarding these cells (Alshatwi and Subash-Babu, 2016). Physcion, a bioactive compound derived from rhubarb, exhibits notable properties, such as antihypertensive, antibacterial, and antitumor activities. Remarkably, physcion demonstrated the capacity to reduce body weight and plasma TG levels in rats subjected to a HFD. Palmitic acid increased the levels of ROS and MDA and reduced the levels of NO, SOD and GSH-Px. These trends were reversed by physcion. In addition, physcion reversed PA-induced activation of the NF- κ B/TNF- α pathway in HUVECs (Wang et al., 2023). The pancreatic and duodenal homeobox-1 (PDX1) protein plays a pivotal role in pancreatic development, maturation, and the functioning of β cells (McKinnon and Docherty, 2001). In the context of glycototoxicity and lipotoxicity, oxidative stress further hinders PDX1 expression, resulting in β cell dysfunction and apoptosis (Hong et al., 2012). Conversely, hypericin enhances PDX1 expression through ERK activation in mice subjected to high-fat and high-glucose diets, thereby ameliorating glucose intolerance and insulin resistance. This intervention also leads to reduced fasting blood glucose levels, attenuation of islet- β cell apoptosis, and inhibition of nitric oxide (NO) production induced by glucotoxicity and lipotoxicity (Liang et al., 2019). Furthermore, *in vivo* experimentation revealed that emodin impeded the manifestation of TNF- α , IL-6, and MDA within both the circulating serum and tissues while concurrently augmenting the concentrations of SOD and GSH (Shang et al., 2021). Rhein exhibited a potent inhibitory effect on LPS-induced intestinal inflammation and oxidative stress. This was evidenced by a significant reduction in serum and intestinal levels of TNF- α , IL-1 β , IL-6, and nitric oxide. Additionally, it downregulated MDA levels in the small intestine. Remarkably, rhein also inhibited the phosphorylation of JNK and p38 MAPK while activating the nuclear factor E2-related factor 2 (Nrf2) pathway (Zhuang et al., 2019).

3.4 Anthraquinones mitigate insulin resistance by regulating the intestinal microbiota

Emerging studies have unveiled the close interconnection between metabolic disorders and the perturbations observed in the composition and functionality of the intestinal microbiota (Ussar et al., 2015; Zeng et al., 2020). Manipulating the gut microbiota has emerged as a promising therapeutic strategy to enhance insulin sensitivity in the host (Chambers et al., 2019; Naderpoor et al., 2019). Anthraquinones have been demonstrated to effectively modulate gut dysbiosis by promoting the proliferation of beneficial bacteria while concurrently suppressing the abundance

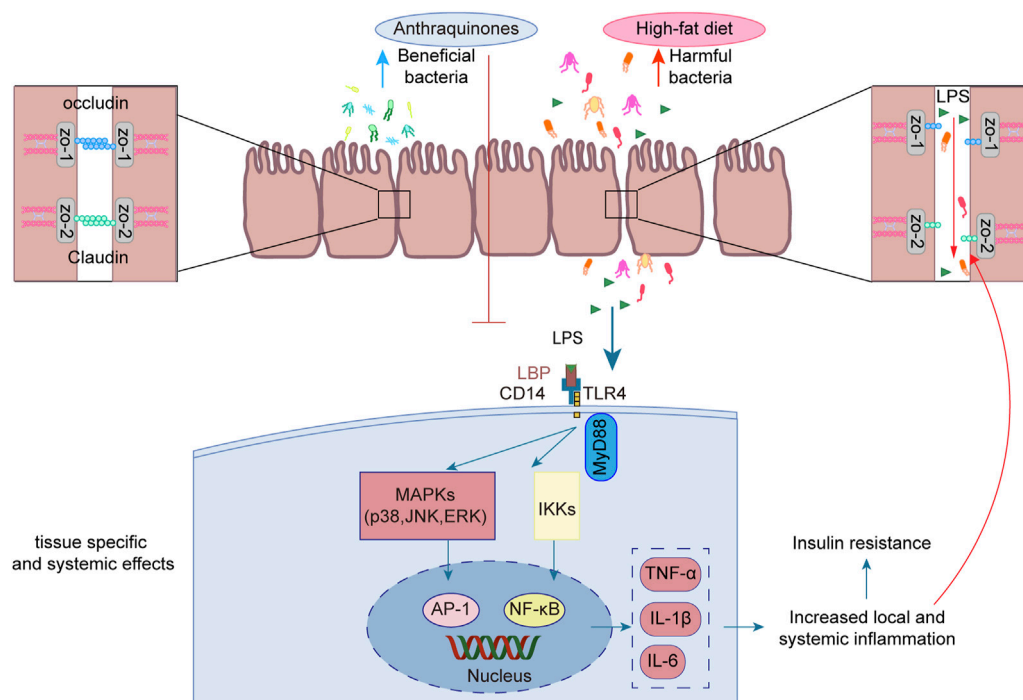


FIGURE 5

Anthraquinones efficiently attenuated the elevation in plasma LPS levels induced by a HFD while simultaneously dampening LPS-induced inflammatory responses in intestinal epithelial cells. Furthermore, these compounds demonstrated the ability to safeguard the continuity and integrity of colonic enterocytes through the upregulation of crucial tight junction proteins, including occludin, claudin, and ZO-1.

of potentially pathogenic counterparts. Notably, these compounds have been shown to enhance insulin resistance through the preservation of gut mucosal integrity and the reduction in metabolic endotoxemia. As such, anthraquinones present a promising approach for restoring the gut microbiota (Figure 5).

LPS, also referred to as endotoxins, is a sizable compound present in the outer membrane of Gram-negative bacteria (Simpson and Trent, 2019). Following the destruction of Gram-negative bacteria, the breakdown of their cell walls results in the release of LPS into the surrounding milieu (Tulkens et al., 2020). High-energy diets have been demonstrated to elicit heightened plasma LPS levels in murine experiments, as well as in a substantial cohort of healthy men drawn from a population-based sample (Amar et al., 2008). The translocation of LPS across the gut lining serves as a hallmark associated with insulin resistance, obesity, and diabetes. The leakage of LPS into the bloodstream initiates a state of low-grade inflammation, exerting profound effects on the liver, adipose tissue, and muscle metabolism (Cani et al., 2008). Long-term subcutaneous infusion of LPS in mice results in various alterations, including elevated weight gain, insulin resistance, WAT inflammation, heightened systemic LPS levels, and increased intestinal permeability (Cani et al., 2007). The regulation of tight junction permeability plays a pivotal role in maintaining the integrity of the intestinal barrier. Disruption of these tight junctions results in compromised barrier function, leading to “leakage” and subsequently causing an elevation in intestinal permeability (Ma et al., 2004). Additionally, an increase in LPS leads to its binding with TLR4, consequently activating the TLR4 signaling pathway. This signaling cascade involves downstream regulators such as NF-κB

and JNK (Płóciennikowska et al., 2015). Rhein demonstrated a salutary influence by promoting body weight reduction and enhancing glucose tolerance in mice with diet-induced obesity. Moreover, it efficiently attenuated the surge in plasma LPS levels induced by a HFD while concurrently mitigating the accumulation of proinflammatory macrophages within the colon (Wang et al., 2016). Another investigation demonstrated the ameliorative effects of rhein on LPS-induced intestinal barrier injury, achieved through the modulation of Nrf2 and MAPK signaling pathways (Zhuang et al., 2019). Rhein restores the expression of claudin-1, E-cadherin, and mucus secretion to reduce intestinal permeability in chronic mouse colitis model induced by dextran sulfate sodium (Wu et al., 2020). Emodin demonstrated the capacity to suppress LPS-induced inflammatory responses in intestinal epithelial cells while simultaneously enhancing intestinal barrier function through the upregulation of ZO-1 and occludin expression (Zhang et al., 2020). Aurantio-obtusin exerts a favorable influence on intestinal barrier function by upregulating the expression of occludin and ZO-1 in HFD-fed mice. Moreover, it reduces serum LPS levels and attenuates the production of inflammatory mediators (Luo et al., 2021). Sennoside A was observed to safeguard the continuity and integrity of colonic enterocytes in mice with diet-induced obesity by upregulating the expression of tight junction proteins, namely, occludin, claudin-2, and ZO-1. This mechanism effectively restores colonic barrier function (Ma et al., 2020).

In murine models, it has been demonstrated that the consumption of a HFD induces notable modifications in the composition of the gut microbiota (Rabot et al., 2016; Tan et al., 2021). This perturbation is characterized by a decline in the

abundance of beneficial bacteria, such as *Bifidobacterium* (Yang et al., 2022) and *Lactobacillus* (Lee et al., 2021), coupled with an elevation in the prevalence of potentially pathogenic microbes, including *Bilophila wadsworthia* (Natividad et al., 2018) and *Ruminococcus gnavus* (Grahnmemo et al., 2022). The intervention of anthraquinones of Cassiae semen effectively increased *Bacteroides*, *Lactobacillus*, and *Parabacteroides* in HFD-fed rats (Mei et al., 2015). Another investigation demonstrated a significant abundance of *Lactobacillus* after rhein treatment (Wu et al., 2020). The modulation of gut microbiota contributed to the amelioration of metabolic syndrome in mice subjected to a HFD (Shi et al., 2019; Wang et al., 2020). In a double-blind randomized placebo-controlled pilot trial utilizing oral fecal microbiota transplantation (FMT) capsules, patients receiving FMT exhibited enduring alterations in their microbiomes linked to obesity, converging toward those characteristic of the lean donor ($p < 0.001$) (Allegretti et al., 2020). An increase in the abundance of potentially advantageous bacteria may ameliorate insulin resistance. *Akkermansia muciniphila* has been identified as a key regulator of energy metabolism, glucose tolerance, and the maturation and functionality of the immune system in human individuals (Yoon et al., 2021). Furthermore, the absence of *A. muciniphila* has been implicated in the disruption of gut barrier integrity, exerting consequential effects on other bacterial populations, ultimately precipitating the development of insulin resistance (Yang et al., 2019). A study demonstrated that aurantio-obtusin significantly augments the abundance of *Akkermansia winderi* in mice fed a HFD (Luo et al., 2021). Rhein effectively restrained the elevated plasma LPS levels induced by a HFD and modulated the gut microbiota by reducing *Bacteroides-Prevotella* spp. and *Desulfovibrio* spp. DNA while simultaneously increasing *Bifidobacterium* spp. and *Lactobacillus* spp. DNA (Wang et al., 2016).

4 Conclusion and future perspectives

In recent years, metabolic disorders have emerged as a pressing global health concern. Projections suggest that obesity will affect approximately one billion individuals by 2030, and diabetes cases will escalate to 783 million by 2045, posing significant challenges to healthcare systems worldwide. Numerous studies have indicated that anthraquinones hold promise in improving insulin resistance, a pivotal factor in preventing and treating various diseases, including diabetes, obesity, and other metabolic syndromes. Thus, this systematic review aims to comprehensively elucidate the mechanisms underlying the potential of anthraquinones in ameliorating insulin resistance, thereby fostering a deeper understanding of their therapeutic applications.

While numerous anthraquinones exhibit potential in ameliorating insulin resistance, the current research predominantly focuses on key compounds such as emodin, chrysophanol, rhein, and aloe-emodin. The precise mechanisms

by which these compounds improve insulin resistance warrant further investigation. Moreover, existing studies primarily utilize animal models, cell culture models, or enzymatic methods to explore the potential of anthraquinone natural products in insulin resistance improvement. Therefore, well-designed, multicenter trials with large sample sizes are imperative to evaluate the effects of anthraquinones in human subjects with insulin resistance. It is hoped that upon integrating anthraquinones as treatment options for insulin resistance, they will prove to be both safer and more efficacious, offering innovative approaches to addressing metabolic disorders.

Overall, the potential of anthraquinones to improve insulin resistance through multiple pathways makes them a promising candidate for the treatment of insulin resistance and related metabolic disorders.

Author contributions

WX: Investigation, Writing—original draft. SL: Writing—original draft, Writing—review and editing. LL: Writing—review and editing. SZ: Writing—review and editing. XW: Writing—review and editing. WD: Writing—review and editing. LD: Writing—review and editing. XZ: Conceptualization, Supervision, Writing—review and editing. ZW: Conceptualization, Supervision, Writing—review and editing.

Funding

The author(s) declare financial support was received for the research, authorship, and/or publication of this article. This work was supported by the Shandong Province “Double-Hundred Talent Plan” on 100 Foreign Experts and 100 Foreign Expert Teams Introduction (WST2018004), the Natural Science Foundation of Shandong Province (ZR2023MH091), and the Innovation Project of Shandong Academy of Medical Sciences (2022).

Conflict of interest

The authors declare that the research was conducted in the absence of any commercial or financial relationships that could be construed as a potential conflict of interest.

Publisher's note

All claims expressed in this article are solely those of the authors and do not necessarily represent those of their affiliated organizations, or those of the publisher, the editors and the reviewers. Any product that may be evaluated in this article, or claim that may be made by its manufacturer, is not guaranteed or endorsed by the publisher.

References

- Ahmed, B., Sultana, R., and Greene, M. W. (2021). Adipose tissue and insulin resistance in obese. *Biomed. Pharmacother.* 137, 111315. doi:10.1016/j.biopha.2021.111315
- Alam, M. B., Bajpai, V. K., Ra, J.-S., Lim, J.-Y., An, H., Shukla, S., et al. (2019). Anthraquinone-type inhibitor of α -glucosidase enhances glucose uptake by activating an insulin-like signaling pathway in C2C12 myotubes. *Food Chem. Toxicol.* 129, 337–343. doi:10.1016/j.fct.2019.05.005
- Allegretti, J. R., Kassam, Z., Mullish, B. H., Chiang, A., Carrellas, M., Hurtado, J., et al. (2020). Effects of fecal microbiota transplantation with oral capsules in obese patients. *Clin. Gastroenterol. Hepatol.* 18, 855–863. doi:10.1016/j.cgh.2019.07.006
- Alshatwi, A. A., and Subash-Babu, P. (2016). Aloe-emodin protects RIN-5F (pancreatic β -cell) cell from glucotoxicity via regulation of pro-inflammatory cytokine and downregulation of bax and caspase 3. *Biomol. Ther. Seoul.* 24, 49–56. doi:10.4062/biomolther.2015.056
- Amar, J., Burcelin, R., Ruidavets, J. B., Cani, P. D., Fauvel, J., Alessi, M. C., et al. (2008). Energy intake is associated with endotoxemia in apparently healthy men. *Am. J. Clin. Nutr.* 87, 1219–1223. doi:10.1093/ajcn/87.5.1219
- An, J., Lee, H., Lee, S., Song, Y., Kim, J., Park, I. H., et al. (2021). Modulation of pro-inflammatory and anti-inflammatory cytokines in the fat by an aloe gel-based formula, QDMC, is correlated with altered gut microbiota. *Immune Netw.* 21, e15. doi:10.4110/in.2021.21.e15
- Anand, S., Muthusamy, V. S., Sujatha, S., Sangeetha, K. N., Bharathi Raja, R., Sudhagar, S., et al. (2010). Aloe emodin glycosides stimulates glucose transport and glycogen storage through PI3K dependent mechanism in L6 myotubes and inhibits adipocyte differentiation in 3T3L1 adipocytes. *FEBS Lett.* 584, 3170–3178. doi:10.1016/j.febslet.2010.06.004
- Anh , F. F., Nachbar, R. T., Varin, T. V., Trotter, J., Dudonn , S., Le Barz, M., et al. (2019). Treatment with camu camu (*Myrciaria dubia*) prevents obesity by altering the gut microbiota and increasing energy expenditure in diet-induced obese mice. *Gut* 68, 453–464. doi:10.1136/gutjnl-2017-315565
- Arnold, S. V., Inzucchi, S. E., Echouffo-Tcheugui, J. B., Tang, F., Lam, C. S. P., Sperling, L. S., et al. (2019). Understanding contemporary use of thiazolidinediones. *Circ. Heart Fail* 12, e005855. doi:10.1161/CIRCHEARTFAILURE.118.005855
- Artunc, F., Schleicher, E., Weigert, C., Fritsche, A., Stefan, N., and H ring, H.-U. (2016). The impact of insulin resistance on the kidney and vasculature. *Nat. Rev. Nephrol.* 12, 721–737. doi:10.1038/nrneph.2016.145
- Behl, T., Gupta, A., Sehgal, A., Albarrati, A., Albratty, M., Meraya, A. M., et al. (2022). Exploring protein tyrosine phosphatases (PTP) and PTP-1B inhibitors in management of diabetes mellitus. *Biomed. Pharmacother.* 153, 113405. doi:10.1016/j.biopha.2022.113405
- Bostr m, P., Wu, J., Jedrychowski, M. P., Korde, A., Ye, L., Lo, J. C., et al. (2012). A PGC1- α -dependent myokine that drives brown-fat-like development of white fat and thermogenesis. *Nature* 481, 463–468. doi:10.1038/nature10777
- Cani, P. D., Amar, J., Iglesias, M. A., Poggi, M., Knauf, C., Bastelica, D., et al. (2007). Metabolic endotoxemia initiates obesity and insulin resistance. *Diabetes* 56, 1761–1772. doi:10.2337/db06-1491
- Cani, P. D., Bibiloni, R., Knauf, C., Waget, A., Neyrinck, A. M., Delzenne, N. M., et al. (2008). Changes in gut microbiota control metabolic endotoxemia-induced inflammation in high-fat diet-induced obesity and diabetes in mice. *Diabetes* 57, 1470–1481. doi:10.2337/db07-1403
- Carrasco, K., Boufenzar, A., Jolly, L., Le Cordier, H., Wang, G., Heck, A. J., et al. (2019). TREM-1 multimerization is essential for its activation on monocytes and neutrophils. *Cell Mol. Immunol.* 16, 460–472. doi:10.1038/s41423-018-0003-5
- Chambers, E. S., Byrne, C. S., Morrison, D. J., Murphy, K. G., Preston, T., Tedford, C., et al. (2019). Dietary supplementation with inulin-propionate ester or inulin improves insulin sensitivity in adults with overweight and obesity with distinct effects on the gut microbiota, plasma metabolome and systemic inflammatory responses: a randomised cross-over trial. *Gut* 68, 1430–1438. doi:10.1136/gutjnl-2019-318424
- Chang, W.-C., Chu, M.-T., Hsu, C.-Y., Wu, Y.-J. J., Lee, J.-Y., Chen, T.-J., et al. (2019). Rhein, an anthraquinone drug, suppresses the NLRP3 inflammasome and macrophage activation in urate crystal-induced gouty inflammation. *Am. J. Chin. Med.* 47, 135–151. doi:10.1142/S0192415X19500071
- Chen, C., Lin, Z., Liu, W., Hu, Q., Wang, J., Zhuang, X., et al. (2022). Emodin accelerates diabetic wound healing by promoting anti-inflammatory macrophage polarization. *Eur. J. Pharmacol.* 936, 175329. doi:10.1016/j.ejphar.2022.175329
- Chen, G., Ni, Y., Nagata, N., Xu, L., Zhuge, F., Nagashimada, M., et al. (2019). Pirfenidone prevents and reverses hepatic insulin resistance and steatohepatitis by polarizing M2 macrophages. *Lab. Invest.* 99, 1335–1348. doi:10.1038/s41374-019-0255-4
- Chen, Z., Zhang, L., Yi, J., Yang, Z., Zhang, Z., and Li, Z. (2012). Promotion of adiponectin multimerization by emodin: a novel AMPK activator with PPAR γ -agonist activity. *J. Cell Biochem.* 113, 3547–3558. doi:10.1002/jcb.24232
- Costes, S., Broca, C., Bertrand, G., Lajoix, A.-D., Bataille, D., Bockaert, J., et al. (2006). ERK1/2 control phosphorylation and protein level of cAMP-responsive element-binding protein: a key role in glucose-mediated pancreatic beta-cell survival. *Diabetes* 55, 2220–2230. doi:10.2337/db05-1618
- Cui, H.-X., Zhang, L.-S., Luo, Y., Yuan, K., Huang, Z.-Y., and Guo, Y. (2019). A purified anthraquinone-glycoside preparation from rhubarb ameliorates type 2 diabetes mellitus by modulating the gut microbiota and reducing inflammation. *Front. Microbiol.* 10, 1423. doi:10.3389/fmicb.2019.01423
- Dai, J.-P., Wang, Q.-W., Su, Y., Gu, L.-M., Zhao, Y., Chen, X.-X., et al. (2017). Emodin inhibition of influenza A virus replication and influenza viral pneumonia via the Nrf2, TLR4, p38/JNK and NF-kappaB pathways. *Molecules* 22, 1754. doi:10.3390/molecules22101754
- Deora, N., Sunitha, M. M., Satyavani, M., Harishankar, N., Vijayalakshmi, M. A., Venkataraman, K., et al. (2021). Alleviation of diabetes mellitus through the restoration of β -cell function and lipid metabolism by Aloe vera (L.) Burm. f. extract in obese genetic WNIN/GR-Ob rats. *J. Ethnopharmacol.* 272, 113921. doi:10.1016/j.jep.2021.113921
- Diniz, T. A., de Lima Junior, E. A., Teixeira, A. A., Biondo, L. A., da Rocha, L. A. F., Valadao, I. C., et al. (2021). Aerobic training improves NAFLD markers and insulin resistance through AMPK-PPAR- α signaling in obese mice. *Life Sci.* 266, 118868. doi:10.1016/j.lfs.2020.118868
- Dou, F., Liu, Y., Liu, L., Wang, J., Sun, T., Mu, F., et al. (2019). Aloe-emodin ameliorates renal fibrosis via inhibiting PI3K/Akt/mTOR signaling pathway *in vivo* and *in vitro*. *Rejuvenation Res.* 22, 218–229. doi:10.1089/rej.2018.2104
- Dutta, D., Bhattacharya, S., Kumar, M., Datta, P. K., Mohindra, R., and Sharma, M. (2023). Efficacy and safety of novel thiazolidinedione lobeiglitazone for managing type-2 diabetes a meta-analysis. *Diabetes Metab. Syndr.* 17, 102697. doi:10.1016/j.dsx.2022.102697
- Elchebly, M., Payette, P., Michaliszyn, E., Cromlish, W., Collins, S., Loy, A. L., et al. (1999). Increased insulin sensitivity and obesity resistance in mice lacking the protein tyrosine phosphatase-1B gene. *Science* 283, 1544–1548. doi:10.1126/science.283.5407.1544
- Elsayed, R. H., Kamel, E. M., Mahmoud, A. M., El-Bassuony, A. A., Bin-Jumah, M., Lamsabhi, A. M., et al. (2020). Rumex dentatus L. phenolics ameliorate hyperglycemia by modulating hepatic key enzymes of carbohydrate metabolism, oxidative stress and PPAR γ in diabetic rats. *Food Chem. Toxicol.* 138, 111202. doi:10.1016/j.fct.2020.111202
- Fan, Y., Yang, Q., Yang, Y., Gao, Z., Ma, Y., Zhang, L., et al. (2019). Sirt6 suppresses high glucose-induced mitochondrial dysfunction and apoptosis in podocytes through AMPK activation. *Int. J. Biol. Sci.* 15, 701–713. doi:10.7150/ijbs.29323
- Fang, J.-Y., Huang, T.-H., Chen, W.-J., Aljuffali, I. A., and Hsu, C.-Y. (2022). Rhubarb hydroxyanthraquinones act as antiobesity agents to inhibit adipogenesis and enhance lipolysis. *Biomed. Pharmacother.* 146, 112497. doi:10.1016/j.biopha.2021.112497
- Fedorenko, A., Lishko, P. V., and Kirichok, Y. (2012). Mechanism of fatty-acid-dependent UCP1 uncoupling in brown fat mitochondria. *Cell* 151, 400–413. doi:10.1016/j.cell.2012.09.010
- Fu, S., Dang, Y., Xu, H., Li, A., Zhou, X., Gao, X., et al. (2022). Aloe vera-fermented beverage ameliorates obesity and gut dysbiosis in high-fat-diet mice. *Foods* 11, 3728. doi:10.3390/foods11223728
- Glass, C. K., and Olefsky, J. M. (2012). Inflammation and lipid signaling in the etiology of insulin resistance. *Cell Metab.* 15, 635–645. doi:10.1016/j.cmet.2012.04.001
- Grahnmemo, L., Nethander, M., Coward, E., Gabrielsen, M. E., Sree, S., Billod, J.-M., et al. (2022). Cross-sectional associations between the gut microbe *Ruminococcus gnavus* and features of the metabolic syndrome. *Lancet Diabetes Endocrinol.* 10, 481–483. doi:10.1016/S2213-8587(22)00113-9
- Guo, C.-Y., Liao, W.-T., Qiu, R.-J., Zhou, D.-S., Ni, W.-J., Yu, C.-P., et al. (2021). Aurantio-obtusin improves obesity and insulin resistance induced by high-fat diet in obese mice. *Phytother. Res.* 35, 346–360. doi:10.1002/ptr.6805
- Hong, S.-W., Lee, J., Park, S. E., Rhee, E.-J., Park, C.-Y., Oh, K.-W., et al. (2012). Repression of sterol regulatory element-binding protein 1-c is involved in the protective effects of exendin-4 in pancreatic β -cell line. *Mol. Cell Endocrinol.* 362, 242–252. doi:10.1016/j.mce.2012.07.004
- Hu, B., Zhang, H., Meng, X., Wang, F., and Wang, P. (2014). Aloe-emodin from rhubarb (*Rheum rhabarbarum*) inhibits lipopolysaccharide-induced inflammatory responses in RAW264.7 macrophages. *J. Ethnopharmacol.* 153, 846–853. doi:10.1016/j.jep.2014.03.059
- Huo, J., Wang, T., Wei, B., Shi, X., Yang, A., Chen, D., et al. (2022). Integrated network pharmacology and intestinal flora analysis to determine the protective effect of Xuanbai-Chengqi decoction on lung and gut injuries in influenza virus-infected mice. *J. Ethnopharmacol.* 298, 115649. doi:10.1016/j.jep.2022.115649
- Hurtado de Llera, A., Martin-Hidalgo, D., Gil, M. C., Garcia-Marin, L. J., and Bragado, M. J. (2014). The calcium/CaMKK α /beta and the cAMP/PKA pathways are essential upstream regulators of AMPK activity in boar spermatozoa. *Biol. Reprod.* 90, 29. doi:10.1095/biolreprod.113.112797
- Iwabu, M., Yamauchi, T., Okada-Iwabu, M., Sato, K., Nakagawa, T., Funata, M., et al. (2010). Adiponectin and AdipoR1 regulate PGC-1 α and mitochondria by Ca(2+) and AMPK/SIRT1. *Nature* 464, 1313–1319. doi:10.1038/nature08991
- James, D. E., St ckli, J., and Birnbaum, M. J. (2021). The aetiology and molecular landscape of insulin resistance. *Nat. Rev. Mol. Cell Biol.* 22, 751–771. doi:10.1038/s41580-021-00390-6

- Ji, L., and Gu, H. (2021). The anti-obesity effects of rhein on improving insulin resistance (IR) and blood lipid levels are involved in endoplasmic reticulum stress (ERs), inflammation, and oxidative stress *in vivo* and *in vitro*. *Bioengineered* 12, 5797–5813. doi:10.1080/21655979.2021.1969196
- Jiang, B., Wang, D., Hu, Y., Li, W., Liu, F., Zhu, X., et al. (2022a). Serum amyloid A1 exacerbates hepatic steatosis via TLR4-mediated NF- κ B signaling pathway. *Mol. Metab.* 59, 101462. doi:10.1016/j.molmet.2022.101462
- Jiang, H., Mao, T., Liu, Y., Tan, X., Sun, Z., Cheng, Y., et al. (2022b). Protective effects and mechanisms of yinchen lingui zhugan decoction in HFD-induced nonalcoholic fatty liver disease rats based on network pharmacology and experimental verification. *Front. Pharmacol.* 13, 908128. doi:10.3389/fphar.2022.908128
- Jiao, P., Ma, J., Feng, B., Zhang, H., Diehl, J. A., Chin, Y. E., et al. (2011). FFA-induced adipocyte inflammation and insulin resistance: involvement of ER stress and IKK β pathways. *Obes. (Silver Spring)* 19, 483–491. doi:10.1038/oby.2010.200
- Jung, H. A., Ali, M. Y., and Choi, J. S. (2016). Promising inhibitory effects of anthraquinones, naphthopyrone, and naphthalene glycosides, from *Cassia obtusifolia* on α -glucosidase and human protein tyrosine phosphatases 1B. *Molecules* 22, 28. doi:10.3390/molecules22010028
- Kawaguchi, T., Osatomi, K., Yamashita, H., Kabashima, T., and Uyeda, K. (2002). Mechanism for fatty acid “sparing” effect on glucose-induced transcription: regulation of carbohydrate-responsive element-binding protein by AMP-activated protein kinase. *J. Biol. Chem.* 277, 3829–3835. doi:10.1074/jbc.M107895200
- Khurm, M., Wang, X., Zhang, H., Hussain, S. N., Qaisar, M. N., Hayat, K., et al. (2020). The genus *Cassia* L.: ethnopharmacological and phytochemical overview. *Phytother. Res.* 35, 2336–2385. doi:10.1002/ptr.6954
- Ko, E., Um, M. Y., Choi, M., Han, T., Kim, I.-H., and Shin, S. (2020). *Cassia tora* seed improves pancreatic mitochondrial function leading to recovery of glucose metabolism. *Am. J. Chin. Med.* 48, 615–629. doi:10.1142/S0192415X20500317
- Korvatska, O., Kianitsa, K., Ratushny, A., Matsushita, M., Beeman, N., Chien, W.-M., et al. (2020). Triggering receptor expressed on myeloid cell 2 R47H exacerbates immune response in alzheimer's disease brain. *Front. Immunol.* 11, 559342. doi:10.3389/fimmu.2020.559342
- Kumar, R., Singh, A. K., Gupta, A., Bishayee, A., and Pandey, A. K. (2019). Therapeutic potential of *Aloe vera*-A miracle gift of nature. *Phytomedicine* 60, 152996. doi:10.1016/j.phymed.2019.152996
- Kwak, H. J., Yang, D., Hwang, Y., Jun, H.-S., and Cheon, H. G. (2017). Baicalein protects rat insulinoma INS-1 cells from palmitate-induced lipotoxicity by inducing HO-1. *PLoS One* 12, e0176432. doi:10.1371/journal.pone.0176432
- Lee, J., Park, S., Oh, N., Park, J., Kwon, M., Seo, J., et al. (2021). Oral intake of *Lactobacillus plantarum* L-14 extract alleviates TLR2-and AMPK-mediated obesity-associated disorders in high-fat-diet-induced obese C57BL/6J mice. *Cell Prolif.* 54, e13039. doi:10.1111/cpr.13039
- Leto, D., and Saltiel, A. R. (2012). Regulation of glucose transport by insulin: traffic control of GLUT4. *Nat. Rev. Mol. Cell Biol.* 13, 383–396. doi:10.1038/nrm3351
- Li, B., Leung, J. C. K., Chan, L. Y. Y., Yiu, W. H., and Tang, S. C. W. (2020a). A global perspective on the crosstalk between saturated fatty acids and Toll-like receptor 4 in the etiology of inflammation and insulin resistance. *Prog. Lipid Res.* 77, 101020. doi:10.1016/j.plipres.2019.101020
- Li, C., Xu, M. M., Wang, K., Adler, A. J., Vella, A. T., and Zhou, B. (2018). Macrophage polarization and meta-inflammation. *Transl. Res.* 191, 29–44. doi:10.1016/j.trsl.2017.10.004
- Li, X., Xiao, C., Yuan, J., Chen, X., Li, Q., and Shen, F. (2023). Rhein-attenuates LPS-induced acute lung injury via targeting NFATc1/Trem2 axis. *Inflamm. Res.* 72, 1237–1255. doi:10.1007/s00011-023-01746-8
- Li, X., Zhang, D., Vatner, D. F., Goedeke, L., Hirabara, S. M., Zhang, Y., et al. (2020b). Mechanisms by which adiponectin reverses high fat diet-induced insulin resistance in mice. *Proc. Natl. Acad. Sci. U. S. A.* 117, 32584–32593. doi:10.1073/pnas.1922169117
- Li, Y., and Jiang, J.-G. (2018). Health functions and structure-activity relationships of natural anthraquinones from plants. *Food Funct.* 9, 6063–6080. doi:10.1039/c8fo01569d
- Li, Y., Xu, S., Mihaylova, M. M., Zheng, B., Hou, X., Jiang, B., et al. (2011). AMPK phosphorylates and inhibits SREBP activity to attenuate hepatic steatosis and atherosclerosis in diet-induced insulin-resistant mice. *Cell Metab.* 13, 376–388. doi:10.1016/j.cmet.2011.03.009
- Li, Y., Yu, Z., Liu, Y., Wang, T., Liu, Y., Bai, Z., et al. (2022). Dietary α -linolenic acid-rich flaxseed oil ameliorates high-fat diet-induced atherosclerosis via gut microbiota-inflammation-artery Axis in ApoE $-/-$ mice. *Front. Cardiovasc. Med.* 9, 830781. doi:10.3389/fcvm.2022.830781
- Lian, Y., Xia, X., Zhao, H., and Zhu, Y. (2017). The potential of chrysophanol in protecting against high fat-induced cardiac injury through Nrf2-regulated anti-inflammation, anti-oxidant and anti-fibrosis in Nrf2 knockout mice. *Biomed. Pharmacother.* 93, 1175–1189. doi:10.1016/j.biopha.2017.05.148
- Liang, C., Hao, F., Yao, X., Qiu, Y., Liu, L., Wang, S., et al. (2019). Hypericin maintains PDX1 expression via the Erk pathway and protects islet β -cells against glucotoxicity and lipotoxicity. *Int. J. Biol. Sci.* 15, 1472–1487. doi:10.7150/ijbs.33817
- Liang, C., Li, Y., Bai, M., Huang, Y., Yang, H., Liu, L., et al. (2020). Hypericin attenuates nonalcoholic fatty liver disease and abnormal lipid metabolism via the PKA-mediated AMPK signaling pathway *in vitro* and *in vivo*. *Pharmacol. Res.* 153, 104657. doi:10.1016/j.phrs.2020.104657
- Lim, H., Park, J., Kim, H.-L., Kang, J., Jeong, M.-Y., Youn, D.-H., et al. (2016). Chrysophanic acid suppresses adipogenesis and induces thermogenesis by activating AMP-activated protein kinase α *in vivo* and *in vitro*. *Front. Pharmacol.* 7, 476. doi:10.3389/fphar.2016.00476
- Lin, S.-C., and Hardie, D. G. (2018). AMPK: sensing glucose as well as cellular energy status. *Cell Metab.* 27, 299–313. doi:10.1016/j.cmet.2017.10.009
- Liu, K., Liu, X., Deng, Y., Li, Z., and Tang, A. (2022). CircRNA-mediated regulation of brown adipose tissue adipogenesis. *Front. Nutr.* 9, 926024. doi:10.3389/fnut.2022.926024
- Liu, X., Yang, Z., Li, H., Luo, W., Duan, W., Zhang, J., et al. (2020). Chrysophanol alleviates metabolic syndrome by activating the SIRT6/AMPK signaling pathway in Brown adipocytes. *Oxid. Med. Cell Longev.* 2020, 7374086. doi:10.1155/2020/7374086
- Lu, W., Zhu, H., Wu, J., Liao, S., Cheng, G., and Li, X. (2022). Rhein attenuates angiotensin II-induced cardiac remodeling by modulating AMPK-FGF23 signaling. *J. Transl. Med.* 20, 305. doi:10.1186/s12967-022-03482-9
- Luo, H., Wu, H., Wang, L., Xiao, S., Lu, Y., Liu, C., et al. (2021). Hepatoprotective effects of *Cassia Semen* on mice with non-alcoholic fatty liver disease based on gut microbiota. *Commun. Biol.* 4, 1357. doi:10.1038/s42003-021-02883-8
- Luo, P., Qin, C., Zhu, L., Fang, C., Zhang, Y., Zhang, H., et al. (2018). Ubiquitin-specific peptidase 10 (USP10) inhibits hepatic steatosis, insulin resistance, and inflammation through Sirt6. *Hepatology* 68, 1786–1803. doi:10.1002/hep.30062
- Ma, C., Wang, Z., Xia, R., Wei, L., Zhang, C., Zhang, J., et al. (2021). Danthron ameliorates obesity and MAFLD through activating the interplay between PPAR α /RXR α heterodimer and adiponectin receptor 2. *Biomed. Pharmacother.* 137, 111344. doi:10.1016/j.biopha.2021.111344
- Ma, L., Cao, X., Ye, X., Qi, Y., Zhu, Y., Ye, J., et al. (2020). Sennoside A restores colonic barrier function through protecting colon enterocytes from ROS-induced mitochondrial damage in diet-induced obese mice. *Biochem. Biophys. Res. Commun.* 526, 519–524. doi:10.1016/j.bbrc.2020.03.117
- Ma, Q., Wang, C.-Z., Sawadogo, W. R., Bian, Z.-X., and Yuan, C.-S. (2022). Herbal medicines for constipation and phytochemical comparison of active components. *Am. J. Chin. Med.* 50, 723–732. doi:10.1142/S0192415X2250029X
- Ma, T. Y., Iwamoto, G. K., Hoa, N. T., Akotia, V., Pedram, A., Boivin, M. A., et al. (2004). TNF- α -induced increase in intestinal epithelial tight junction permeability requires NF- κ B activation. *Am. J. Physiol. Gastrointest. Liver Physiol.* 286, G367–G376. doi:10.1152/ajpgi.00173.2003
- Malik, E. M., and Müller, C. E. (2016). Anthraquinones as pharmacological tools and drugs. *Med. Res. Rev.* 36, 705–748. doi:10.1002/med.21391
- Maqdasly, S., Lecoutre, S., Renzi, G., Frendo-Cumbo, S., Rizo-Roca, D., Moritz, T., et al. (2022). Impaired phosphocreatine metabolism in white adipocytes promotes inflammation. *Nat. Metab.* 4, 190–202. doi:10.1038/s42255-022-00525-9
- Martínez-Aldino, I. Y., Villaseca-Murillo, M., Morales-Jiménez, J., and Rivera-Chávez, J. (2021). Absolute configuration and protein tyrosine phosphatase 1B inhibitory activity of xanthopocin, a dimeric naphthopyrone from *Penicillium* sp. IQ-429. *Bioorg. Chem.* 115, 105166. doi:10.1016/j.bioorg.2021.105166
- McKinnon, C. M., and Docherty, K. (2001). Pancreatic duodenal homeobox-1, PDX-1, a major regulator of beta cell identity and function. *Diabetologia* 44, 1203–1214. doi:10.1007/s001250100628
- Mei, L., Tang, Y., Li, M., Yang, P., Liu, Z., Yuan, J., et al. (2015). Co-administration of cholesterol-lowering probiotics and anthraquinone from *Cassia obtusifolia* L. Ameliorate non-alcoholic fatty liver. *PLoS One* 10, e0138078. doi:10.1371/journal.pone.0138078
- Momcilovic, M., Hong, S.-P., and Carlson, M. (2006). Mammalian TAK1 activates Snf1 protein kinase in yeast and phosphorylates AMP-activated protein kinase *in vitro*. *J. Biol. Chem.* 281, 25336–25343. doi:10.1074/jbc.M604399200
- Monsénégro, J., Mansouri, A., Akkaoui, M., Lenoir, V., Esnous, C., Fauveau, V., et al. (2012). Enhancing liver mitochondrial fatty acid oxidation capacity in obese mice improves insulin sensitivity independently of hepatic steatosis. *J. Hepatol.* 56, 632–639. doi:10.1016/j.jhep.2011.10.008
- Mungai, P. T., Waypa, G. B., Jairaman, A., Prakriya, M., Dokic, D., Ball, M. K., et al. (2011). Hypoxia triggers AMPK activation through reactive oxygen species-mediated activation of calcium release-activated calcium channels. *Mol. Cell Biol.* 31, 3531–3545. doi:10.1128/MCB.05124-11
- Naderpoor, N., Mousa, A., Gomez-Arango, L. F., Barrett, H. L., Dekker Nitert, M., and de Courten, B. (2019). Faecal microbiota are related to insulin sensitivity and secretion in overweight or obese adults. *J. Clin. Med.* 8, 452. doi:10.3390/jcm8040452
- Natividad, J. M., Lamas, B., Pham, H. P., Michel, M.-L., Rainteau, D., Bridonneau, C., et al. (2018). *Bilophila wadsworthia* aggravates high fat diet induced metabolic dysfunctions in mice. *Nat. Commun.* 9, 2802. doi:10.1038/s41467-018-05249-7

- Nayan, S. I., Chowdhury, F. I., Akter, N., Rahman, M. M., Selim, S., Saffoon, N., et al. (2021). Leaf powder supplementation of *Senna alexandrina* ameliorates oxidative stress, inflammation, and hepatic steatosis in high-fat diet-fed obese rats. *PLoS One* 16, e0250261. doi:10.1371/journal.pone.0250261
- Nguyen, M. T. A., Satoh, H., Favellyukis, S., Babendure, J. L., Imamura, T., Sbodio, J. I., et al. (2005). JNK and tumor necrosis factor- α mediate free fatty acid-induced insulin resistance in 3T3-L1 adipocytes. *J. Biol. Chem.* 280, 35361–35371. doi:10.1074/jbc.M504611200
- Park, J. E., Kang, E., and Han, J. S. (2022). HM-chromanone attenuates TNF- α -mediated inflammation and insulin resistance by controlling JNK activation and NF- κ B pathway in 3T3-L1 adipocytes. *Eur. J. Pharmacol.* 921, 174884. doi:10.1016/j.ejphar.2022.174884
- Plóciennikowska, A., Hromada-Judycka, A., Borzęcka, K., and Kwiatkowska, K. (2015). Co-operation of TLR4 and raft proteins in LPS-induced pro-inflammatory signaling. *Cell Mol. Life Sci.* 72, 557–581. doi:10.1007/s00018-014-1762-5
- Qi, Y., Liu, Y., Zhang, B., Wang, M., Cao, L., Song, L., et al. (2022). Comparative antibacterial analysis of the anthraquinone compounds based on the AIM theory, molecular docking, and dynamics simulation analysis. *J. Mol. Model* 29, 16. doi:10.1007/s00894-022-05406-2
- Quan, Y., Gong, L., He, J., Zhou, Y., Liu, M., Cao, Z., et al. (2019). Aloe emodin induces hepatotoxicity by activating NF- κ B inflammatory pathway and P53 apoptosis pathway in zebrafish. *Toxicol. Lett.* 306, 66–79. doi:10.1016/j.toxlet.2019.02.007
- Rabot, S., Membrez, M., Blancher, F., Berger, B., Moine, D., Krause, L., et al. (2016). High fat diet drives obesity regardless the composition of gut microbiota in mice. *Sci. Rep.* 6, 32484. doi:10.1038/srep32484
- Régnier, M., Rastelli, M., Morissette, A., Suriano, F., Le Roy, T., Pilon, G., et al. (2020). Rhubarb supplementation prevents diet-induced obesity and diabetes in association with increased *Akkermansia muciniphila* in mice. *Nutrients* 12, 2932. doi:10.3390/nu12102932
- Rustenbeck, I., Krauthelm, A., Jörns, A., and Steinfeldt, H. J. (2004). Beta-cell toxicity of ATP-sensitive K⁺ channel-blocking insulin secretagogues. *Biochem. Pharmacol.* 67, 1733–1741. doi:10.1016/j.bcp.2004.01.016
- Sasaki, N., Maeda, R., Ozono, R., Yoshimura, K., Nakano, Y., and Higashi, Y. (2022). Adipose tissue insulin resistance predicts the incidence of hypertension: the Hiroshima Study on Glucose Metabolism and Cardiovascular Diseases. *Hypertens. Res.* 45, 1763–1771. doi:10.1038/s41440-022-00987-0
- Selim, N. M., Elgazar, A. A., Abdel-Hamid, N. M., El-Magd, M. R. A., Yasri, A., Hefnawy, H. M. E., et al. (2019). Chrysophanol, physcion, hesperidin and curcumin modulate the gene expression of pro-inflammatory mediators induced by LPS in HepG2: *in silico* and molecular studies. *Anti-oxidants (Basel)* 8, 371. doi:10.3390/antiox8090371
- Settembre, C., De Cegli, R., Mansueto, G., Saha, P. K., Vetrini, F., Visvikis, O., et al. (2013). TFEB controls cellular lipid metabolism through a starvation-induced autoregulatory loop. *Nat. Cell Biol.* 15, 647–658. doi:10.1038/ncb2718
- Shang, H., Guo, J., Wang, P., Li, L., Tian, Y., Li, X., et al. (2022). Design, synthesis and anti-inflammatory evaluation of aloe-emodin derivatives as potential modulators of Akt, NF- κ B and JNK signaling pathways. *Eur. J. Med. Chem.* 238, 114511. doi:10.1016/j.ejmech.2022.114511
- Shang, L., Liu, Y., Li, J., Pan, G., Zhou, F., and Yang, S. (2021). Emodin protects sepsis associated damage to the intestinal mucosal barrier through the VDR/Nrf2/HO-1 pathway. *Front. Pharmacol.* 12, 724511. doi:10.3389/fphar.2021.724511
- Sheng, D., Zhao, S., Gao, L., Zheng, H., Liu, W., Hou, J., et al. (2019). BabaoDan attenuates high-fat diet-induced non-alcoholic fatty liver disease via activation of AMPK signaling. *Cell Biosci.* 9, 77. doi:10.1186/s13578-019-0339-2
- Shi, X., Zhou, X., Chu, X., Wang, J., Xie, B., Ge, J., et al. (2019). Allicin improves metabolism in high-fat diet-induced obese mice by modulating the gut microbiota. *Nutrients* 11, 2909. doi:10.3390/nu11122909
- Shin, E., Shin, S., Kong, H., Lee, S., Do, S.-G., Jo, T. H., et al. (2011). Dietary aloe reduces adipogenesis via the activation of AMPK and suppresses obesity-related inflammation in obese mice. *Immune Netw.* 11, 107–113. doi:10.4110/in.2011.11.2.107
- Simpson, B. W., and Trent, M. S. (2019). Pushing the envelope: LPS modifications and their consequences. *Nat. Rev. Microbiol.* 17, 403–416. doi:10.1038/s41579-019-0201-x
- Song, P., Kim, J. H., Ghim, J., Yoon, J. H., Lee, A., Kwon, Y., et al. (2013). Emodin regulates glucose utilization by activating AMP-activated protein kinase. *J. Biol. Chem.* 288, 5732–5742. doi:10.1074/jbc.M112.441477
- Sugimoto, S., Mena, H. A., Sansbury, B. E., Kobayashi, S., Tsuji, T., Wang, C.-H., et al. (2022). Brown adipose tissue-derived MaR2 contributes to cold-induced resolution of inflammation. *Nat. Metab.* 4, 775–790. doi:10.1038/s42255-022-00590-0
- Tan, R., Dong, H., Chen, Z., Jin, M., Yin, J., Li, H., et al. (2021). Intestinal microbiota mediates high-fructose and high-fat diets to induce chronic intestinal inflammation. *Front. Cell Infect. Microbiol.* 11, 654074. doi:10.3389/fcimb.2021.654074
- Taylor, S. I., Blau, J. E., Rother, K. I., and Beitelshes, A. L. (2019). SGLT2 inhibitors as adjunctive therapy for type 1 diabetes: balancing benefits and risks. *Lancet Diabetes Endocrinol.* 7, 949–958. doi:10.1016/S2213-8587(19)30154-8
- Towler, M. C., and Hardie, D. G. (2007). AMP-activated protein kinase in metabolic control and insulin signaling. *Circ. Res.* 100, 328–341. doi:10.1161/01.RES.0000256090.42690.05
- Tulkens, J., Vergauwen, G., Van Deun, J., Geerickx, E., Dhondt, B., Lippens, L., et al. (2020). Increased levels of systemic LPS-positive bacterial extracellular vesicles in patients with intestinal barrier dysfunction. *Gut* 69, 191–193. doi:10.1136/gutjnl-2018-317726
- Tzeng, T.-F., Lu, H.-J., Liou, S.-S., Chang, C. J., and Liu, I.-M. (2012a). Emodin, a naturally occurring anthraquinone derivative, ameliorates dyslipidemia by activating AMP-activated protein kinase in high-fat-diet-fed rats. *Evid. Based Complement. Altern. Med.* 2012, 781812. doi:10.1155/2012/781812
- Tzeng, T.-F., Lu, H.-J., Liou, S.-S., Chang, C. J., and Liu, I.-M. (2012b). Emodin protects against high-fat diet-induced obesity via regulation of AMP-activated protein kinase pathways in white adipose tissue. *Planta Med.* 78, 943–950. doi:10.1055/s-0031-1298626
- Ussar, S., Griffin, N. W., Bezy, O., Fujisaka, S., Vienberg, S., Softic, S., et al. (2015). Interactions between gut microbiota, host genetics and diet modulate the predisposition to obesity and metabolic syndrome. *Cell Metab.* 22, 516–530. doi:10.1016/j.cmet.2015.07.007
- Venable, C. L., Frevert, E. U., Kim, Y. B., Fischer, B. M., Kamatkar, S., Neel, B. G., et al. (2000). Overexpression of protein-tyrosine phosphatase-1B in adipocytes inhibits insulin-stimulated phosphoinositide 3-kinase activity without altering glucose transport or Akt/Protein kinase B activation. *J. Biol. Chem.* 275, 18318–18326. doi:10.1074/jbc.M908392199
- Villarroya, F., and Gavalda-Navarro, A. (2022). Brown fat resolves hepatic inflammation in obesity. *Nat. Metab.* 4, 649–650. doi:10.1038/s42255-022-00596-8
- Wang, C., Ha, X., Li, W., Xu, P., Gu, Y., Wang, T., et al. (2017). Correlation of TLR4 and KLF7 in inflammation induced by obesity. *Inflammation* 40, 42–51. doi:10.1007/s10753-016-0450-z
- Wang, H., Zhang, H., Gao, Z., Zhang, Q., and Gu, C. (2022a). The mechanism of berberine alleviating metabolic disorder based on gut microbiome. *Front. Cell Infect. Microbiol.* 12, 854885. doi:10.3389/fcimb.2022.854885
- Wang, P., Gao, J., Ke, W., Wang, J., Li, D., Liu, R., et al. (2020). Resveratrol reduces obesity in high-fat diet-fed mice via modulating the composition and metabolic function of the gut microbiota. *Free Radic. Biol. Med.* 156, 83–98. doi:10.1016/j.freeradbiomed.2020.04.013
- Wang, Q.-Y., Tong, A.-H., Pan, Y.-Y., Zhang, X.-D., Ding, W.-Y., and Xiong, W. (2019). The effect of cassia seed extract on the regulation of the LKB1-AMPK-GLUT4 signaling pathway in the skeletal muscle of diabetic rats to improve the insulin sensitivity of the skeletal muscle. *Diabetol. Metab. Syndr.* 11, 108. doi:10.1186/s13098-019-0504-0
- Wang, S., Huang, X.-F., Zhang, P., Wang, H., Zhang, Q., Yu, S., et al. (2016). Chronic rhein treatment improves recognition memory in high-fat diet-induced obese male mice. *J. Nutr. Biochem.* 36, 42–50. doi:10.1016/j.jnutbio.2016.07.008
- Wang, T., Li, M., Zeng, T., Hu, R., Xu, Y., Xu, M., et al. (2022b). Association between insulin resistance and cardiovascular disease risk varies according to glucose tolerance status: a nationwide prospective cohort study. *Diabetes Care* 45, 1863–1872. doi:10.2337/dc22-0202
- Wang, Y.-H., Liu, Y.-P., Zhu, J.-Q., Zhou, G. H., Zhang, F., An, Q., et al. (2023). Physcion prevents high-fat diet-induced endothelial dysfunction by inhibiting oxidative stress and endoplasmic reticulum stress pathways. *Eur. J. Pharmacol.* 943, 175554. doi:10.1016/j.ejphar.2023.175554
- Wei, Z., Shen, P., Cheng, P., Lu, Y., Wang, A., and Sun, Z. (2020). Gut bacteria selectively altered by sennoside A alleviate type 2 diabetes and obesity traits. *Oxid. Med. Cell Longev.* 2020, 2375676. doi:10.1155/2020/2375676
- Wu, J., Wei, Z., Cheng, P., Qian, C., Xu, F., Yang, Y., et al. (2020). Rhein modulates host purine metabolism in intestine through gut microbiota and ameliorates experimental colitis. *Theranostics* 10, 10665–10679. doi:10.7150/thno.43528
- Xie, P., Yan, L.-J., Zhou, H.-L., Cao, H.-H., Zheng, Y.-R., Lu, Z.-B., et al. (2022). Emodin protects against lipopolysaccharide-induced acute lung injury via the JNK/Nur77/c-Jun signaling pathway. *Front. Pharmacol.* 13, 717271. doi:10.3389/fphar.2022.717271
- Xu, L., Xing, M., Xu, X., Saadeldin, F. S., Liu, Z., Wei, J., et al. (2019). Alizarin increase glucose uptake through PI3K/Akt signaling and improve alloxan-induced diabetic mice. *Future Med. Chem.* 11, 395–406. doi:10.4155/fmc-2018-0515
- Xu, Y., Wang, N., Tan, H.-Y., Li, S., Zhang, C., Zhang, Z., et al. (2020). Panax notoginseng saponins modulate the gut microbiota to promote thermogenesis and beige adipocyte reconstruction via leptin-mediated AMPK/STAT3 signaling in diet-induced obesity. *Theranostics* 10, 11302–11323. doi:10.7150/thno.47746
- Yang, B., Yu, Q., Chang, B., Guo, Q., Xu, S., Yi, X., et al. (2021). MOTSC-c interacts synergistically with exercise intervention to regulate PGC-1 α expression, attenuate insulin resistance and enhance glucose metabolism in mice via AMPK signaling pathway. *Biochim. Biophys. Acta Mol. Basis Dis.* 1867, 166126. doi:10.1016/j.bbdis.2021.166126
- Yang, J., Ma, Y., Li, T., Pang, Y., Zhang, H., Xie, Y., et al. (2022). Ameliorative effects of *Bifidobacterium animalis* subsp. *lactis* J-12 on hyperglycemia in pregnancy and pregnancy outcomes in a high-fat-diet/streptozotocin-induced rat model. *Nutrients* 15, 170. doi:10.3390/nu15010170
- Yang, M., Li, X., Zeng, X., Ou, Z., Xue, M., Gao, D., et al. (2016). Rheum palmatum L. Attenuates high fat diet-induced hepatosteatosis by activating AMP-activated protein kinase. *Am. J. Chin. Med.* 44, 551–564. doi:10.1142/S0192415X16500300

- Yang, Y., Shang, W., Zhou, L., Jiang, B., Jin, H., and Chen, M. (2007). Emodin with PPARgamma ligand-binding activity promotes adipocyte differentiation and increases glucose uptake in 3T3-L1 cells. *Biochem. Biophys. Res. Commun.* 353, 225–230. doi:10.1016/j.bbrc.2006.11.134
- Yang, Y., Zhong, Z., Wang, B., Xia, X., Yao, W., Huang, L., et al. (2019). Early-life high-fat diet-induced obesity programs hippocampal development and cognitive functions via regulation of gut commensal *Akkermansia muciniphila*. *Neuropsychopharmacology* 44, 2054–2064. doi:10.1038/s41386-019-0437-1
- Yao, L., Cui, X., Chen, Q., Yang, X., Fang, F., Zhang, J., et al. (2017). Cold-inducible SIRT6 regulates thermogenesis of Brown and beige fat. *Cell Rep.* 20, 641–654. doi:10.1016/j.celrep.2017.06.069
- Yi-Jie, L., Rui-Yu, W., Run-Ping, L., Kai-Yi, W., Ming-Ning, D., Rong, S., et al. (2023). Aurantio-obtusin ameliorates obesity by activating PPARα-dependent mitochondrial thermogenesis in brown adipose tissues. *Acta Pharmacol. Sin.* 44, 1826–1840. doi:10.1038/s41401-023-01089-4
- Yin, Z., Gao, D., Du, K., Han, C., Liu, Y., Wang, Y., et al. (2022). Rhein ameliorates cognitive impairment in an APP/PS1 transgenic mouse model of Alzheimer's disease by relieving oxidative stress through activating the SIRT1/PGC-1α pathway. *Oxid. Med. Cell Longev.* 2022, 2524832. doi:10.1155/2022/2524832
- Yoon, H. S., Cho, C. H., Yun, M. S., Jang, S. J., You, H. J., Kim, J.-H., et al. (2021). *Akkermansia muciniphila* secretes a glucagon-like peptide-1-inducing protein that improves glucose homeostasis and ameliorates metabolic disease in mice. *Nat. Microbiol.* 6, 563–573. doi:10.1038/s41564-021-00880-5
- Yu, F., Yu, N., Peng, J., Zhao, Y., Zhang, L., Wang, X., et al. (2021). Emodin inhibits lipid accumulation and inflammation in adipose tissue of high-fat diet-fed mice by inducing M2 polarization of adipose tissue macrophages. *FASEB J.* 35, e21730. doi:10.1096/fj.202100157RR
- Zeng, S.-L., Li, S.-Z., Xiao, P.-T., Cai, Y.-Y., Chu, C., Chen, B.-Z., et al. (2020). Citrus polymethoxyflavones attenuate metabolic syndrome by regulating gut microbiome and amino acid metabolism. *Sci. Adv.* 6, eaax6208. doi:10.1126/sciadv.aax6208
- Zhang, C.-S., Li, M., Wang, Y., Li, X., Zong, Y., Long, S., et al. (2022). The aldolase inhibitor aldometanib mimics glucose starvation to activate lysosomal AMPK. *Nat. Metab.* 4, 1369–1401. doi:10.1038/s42255-022-00640-7
- Zhang, H., Yi, J.-K., Huang, H., Park, S., Park, S., Kwon, W., et al. (2021). Rhein suppresses colorectal cancer cell growth by inhibiting the mTOR pathway *in vitro* and *in vivo*. *Cancers (Basel)* 13, 2176. doi:10.3390/cancers13092176
- Zhang, K., Qin, X., Qiu, J., Sun, T., Qu, K., Din, A. U., et al. (2023). *Desulfovibrio desulfuricans* aggravates atherosclerosis by enhancing intestinal permeability and endothelial TLR4/NF-κB pathway in *Apoe*^{-/-} mice. *Genes Dis.* 10, 239–253. doi:10.1016/j.gendis.2021.09.007
- Zhang, L., Wu, X., Yang, R., Chen, F., Liao, Y., Zhu, Z., et al. (2020a). Effects of berberine on the gastrointestinal microbiota. *Front. Cell Infect. Microbiol.* 10, 588517. doi:10.3389/fcimb.2020.588517
- Zhang, M., Li, X., Liang, H., Cai, H., Hu, X., Bian, Y., et al. (2018). Semen Cassiae extract improves glucose metabolism by promoting GLUT4 translocation in the skeletal muscle of diabetic rats. *Front. Pharmacol.* 9, 235. doi:10.3389/fphar.2018.00235
- Zhang, X., Zhang, R., Lv, P., Yang, J., Deng, Y., Xu, J., et al. (2015). Emodin up-regulates glucose metabolism, decreases lipolysis, and attenuates inflammation *in vitro*. *J. Diabetes* 7, 360–368. doi:10.1111/1753-0407.12190
- Zhang, X.-Y., Chen, J., Yi, K., Peng, L., Xie, J., Gou, X., et al. (2020b). Phlorizin ameliorates obesity-associated endotoxemia and insulin resistance in high-fat diet-fed mice by targeting the gut microbiota and intestinal barrier integrity. *Gut Microbes* 12, 1–18. doi:10.1080/19490976.2020.1842990
- Zhang, Y., Liu, W., Liu, D., Zhao, T., and Tian, H. (2016). Efficacy of aloe vera supplementation on prediabetes and early non-treated diabetic patients: a systematic review and meta-analysis of randomized controlled trials. *Nutrients* 8, 388. doi:10.3390/nu8070388
- Zhang, Y.-L., Guo, H., Zhang, C.-S., Lin, S.-Y., Yin, Z., Peng, Y., et al. (2013). AMP as a low-energy charge signal autonomously initiates assembly of AXIN-AMPK-LKB1 complex for AMPK activation. *Cell Metab.* 18, 546–555. doi:10.1016/j.cmet.2013.09.005
- Zhao, Y., Chen, M. X., Kongstad, K. T., Jäger, A. K., and Staerk, D. (2017). Potential of *Polygonum cuspidatum* root as an antidiabetic food: dual high-resolution α-glucosidase and PTP1B inhibition profiling combined with HPLC-MS/MS and NMR for identification of antidiabetic constituents. *J. Agric. Food Chem.* 65, 4421–4427. doi:10.1021/acs.jafc.7b01353
- Zhou, F., Ding, M., Gu, Y., Fan, G., Liu, C., Li, Y., et al. (2021). Aurantio-obtusin attenuates non-alcoholic fatty liver disease through AMPK-mediated autophagy and fatty acid oxidation pathways. *Front. Pharmacol.* 12, 826628. doi:10.3389/fphar.2021.826628
- Zhou, R., Wang, L., Xu, X., Chen, J., Hu, L., Chen, L., et al. (2013). Danthron activates AMP-activated protein kinase and regulates lipid and glucose metabolism *in vitro*. *Acta Pharmacol. Sin.* 34, 1061–1069. doi:10.1038/aps.2013.39
- Zhou, W., Yang, T., Xu, W., Huang, Y., Ran, L., Yan, Y., et al. (2022a). The polysaccharides from the fruits of *Lycium barbarum* L. confer anti-diabetic effect by regulating gut microbiota and intestinal barrier. *Carbohydr. Polym.* 291, 119626. doi:10.1016/j.carbpol.2022.119626
- Zhou, Y., Gao, C., Vong, C. T., Tao, H., Li, H., Wang, S., et al. (2022b). Rhein regulates redox-mediated activation of NLRP3 inflammasomes in intestinal inflammation through macrophage-activated crosstalk. *Br. J. Pharmacol.* 179, 1978–1997. doi:10.1111/bph.15773
- Zhuang, S., Zhong, J., Bian, Y., Fan, Y., Chen, Q., Liu, P., et al. (2019). Rhein ameliorates lipopolysaccharide-induced intestinal barrier injury via modulation of Nrf2 and MAPKs. *Life Sci.* 216, 168–175. doi:10.1016/j.lfs.2018.11.048
- Zumbaugh, M. D., Johnson, S. E., Shi, T. H., and Gerrard, D. E. (2022). Molecular and biochemical regulation of skeletal muscle metabolism. *J. Anim. Sci.* 100, skac035. doi:10.1093/jas/skac035

Glossary

ACC	Acetyl-CoA carboxylase
ACOX1	Acyl-CoA oxidase 1
AMPK	AMP-activated protein kinase
AS160	Akt substrate of 160 kDa
ATF2	Activating transcription factor 2
BAT	Brown adipose tissue
CaMKKs	Ca ²⁺ /calmodulin-dependent protein kinase kinases
C/EBPα	CCAAT enhancer-binding protein alpha
CPT-1	Carnitine palmitoyltransferase 1
ERK	Extracellular-signal-regulated kinase
FAS	Fatty acid synthase
FBG	Fasting blood glucose
FFA	Free fatty acids
FSI	Fasting serum insulin
GLUT4	Glucose transporter type 4
HFD	High-fat diet
HOMA-IR	Homeostatic model assessment of insulin resistance
IL-1β	Interleukin-1beta
IL-6	Interleukin-6
iNOS	Inducible nitric oxide synthase
IR	Insulin resistance
IRS-1	Insulin receptor substrate-1
JNK	C-Jun N-terminal kinase
LKB1	Liver kinase B1
LPS	Lipopolysaccharide
MAPK	Mitogen-activated protein kinases
MDA	Malondialdehyde
Mn-SOD	Manganese superoxide dismutase
NF-κB	Nuclear factor kappaB
NO	Nitric oxide
PDX1	Pancreatic and duodenal homeobox 1
PGC-1α	Peroxisome proliferator-activated receptor-γ co-activator-1α
PI3K	Phosphatidylinositol 3-kinase
PKA	Protein kinase A
PPARα	Peroxisome proliferator-activated receptor alpha
PTP1B	Protein tyrosine phosphatase 1B
ROS	Reactive oxygen species
RXRα	Retinoid X receptor-alpha
SIRT6	Sirtuin 6
SOD	Superoxide dismutase

SREBP-1c	Sterol regulatory element-binding protein-1c
TAK1	Transforming growth factor beta-activated kinase1
TFEB	Transcription factor EB
TLR4	Toll-like receptor 4
TNF-α	Tumor necrosis factor-alpha
TREM2	Triggering receptor expressed on myeloid cell 2
UCP-1	Uncoupling protein 1
WAT	White adipose tissue
ZO-1	Zona occludens-1



OPEN ACCESS

EDITED BY

Abd El-Latif Hesham,
Beni-Suef University, Egypt

REVIEWED BY

David Dolivo,
Greenstone Biosciences, United States
Ruichao Yue,
University of North Carolina at
Greensboro, United States

*CORRESPONDENCE

Hwan-Woo Park,
✉ hwanwoopark@konyang.ac.kr

[†]These authors have contributed equally
to this work

RECEIVED 26 September 2023

ACCEPTED 20 November 2023

PUBLISHED 30 November 2023

CITATION

Han D, Kim D, Kim H, Lee J, Lyu J,
Kim J-S, Shin J, Kim JS, Kim DK and
Park H-W (2023), Methylsulfonylmethane
ameliorates metabolic-associated fatty
liver disease by restoring autophagy flux
via AMPK/mTOR/ULK1 signaling pathway.
Front. Pharmacol. 14:1302227.
doi: 10.3389/fphar.2023.1302227

COPYRIGHT

© 2023 Han, Kim, Kim, Lee, Lyu, Kim, Shin,
Kim, Kim and Park. This is an open-access
article distributed under the terms of the
[Creative Commons Attribution License
\(CC BY\)](https://creativecommons.org/licenses/by/4.0/). The use, distribution or
reproduction in other forums is
permitted, provided the original author(s)
and the copyright owner(s) are credited
and that the original publication in this
journal is cited, in accordance with
accepted academic practice. No use,
distribution or reproduction is permitted
which does not comply with these terms.

Methylsulfonylmethane ameliorates metabolic-associated fatty liver disease by restoring autophagy flux via AMPK/mTOR/ULK1 signaling pathway

Daewon Han^{1,2†}, Deokryong Kim^{1†}, Haeil Kim¹, Jeonga Lee¹,
Jungmook Lyu³, Jong-Seok Kim², Jongdae Shin^{1,2},
Jeong Sig Kim⁴, Do Kyung Kim⁵ and Hwan-Woo Park^{1,2*}

¹Department of Cell Biology, Konyang University College of Medicine, Daejeon, Republic of Korea,

²Myunggok Medical Research Institute, Konyang University College of Medicine, Daejeon, Republic of Korea, ³Department of Medical Science, Konyang University, Daejeon, Republic of Korea, ⁴Department of Obstetrics and Gynecology, Soonchunhyang University Seoul Hospital, Seoul, Republic of Korea,

⁵Department of Anatomy, Konyang University College of Medicine, Daejeon, Republic of Korea

Introduction: Metabolism-associated fatty liver disease (MAFLD) is a global health concern because of its association with obesity, insulin resistance, and other metabolic abnormalities. Methylsulfonylmethane (MSM), an organic sulfur compound found in various plants and animals, exerts antioxidant and anti-inflammatory effects. Here, we aimed to assess the anti-obesity activity and autophagy-related mechanisms of Methylsulfonylmethane.

Method: Human hepatoma (HepG2) cells treated with palmitic acid (PA) were used to examine the effects of MSM on autophagic clearance. To evaluate the anti-obesity effect of MSM, male C57/BL6 mice were fed a high-fat diet (HFD; 60% calories) and administered an oral dose of MSM (200 or 400 mg/kg/day). Moreover, we investigated the AMP-activated protein kinase (AMPK)/mechanistic target of rapamycin complex 1 (mTORC1)/UNC-51-like autophagy-activating kinase 1 (ULK1) signaling pathway to further determine the underlying action mechanism of MSM.

Results: Methylsulfonylmethane treatment significantly mitigated PA-induced protein aggregation in human hepatoma HepG2 cells. Additionally, Methylsulfonylmethane treatment reversed the PA-induced impairment of autophagic flux. Methylsulfonylmethane also enhanced the insulin sensitivity and significantly suppressed the HFD-induced obesity and hepatic steatosis in mice. Western blotting revealed that Methylsulfonylmethane improved ubiquitinated protein clearance in HFD-induced fatty liver. Remarkably, Methylsulfonylmethane promoted the activation of AMPK and ULK1 and inhibited mTOR activity.

Conclusion: Our study suggests that MSM ameliorates hepatic steatosis by enhancing the autophagic flux via an AMPK/mTOR/ULK1-dependent signaling pathway. These findings highlight the therapeutic potential of MSM for obesity-related MAFLD treatment.

KEYWORDS

methylsulfonylmethane, obesity, autophagy, AMPK/mTOR, ULK1

1 Introduction

Metabolism-associated fatty liver disease (MAFLD), characterized by excessive accumulation of fat in the liver associated with obesity and insulin resistance, is a serious global health concern (Diehl and Day, 2017). MAFLD encompasses several conditions, including metabolic-associated steatohepatitis, advanced liver fibrosis, cirrhosis, and hepatocellular carcinoma, and is closely associated with various risk factors, such as obesity, type 2 diabetes mellitus, cardiovascular complications, and metabolic syndrome (Loomba et al., 2020; Sheka et al., 2020). The strong association between obesity and MAFLD suggests obesity-associated inflammation and insulin resistance as key factors that trigger or worsen this condition (Marra and Svegliati-Baroni, 2018). Lipotoxicity, oxidative stress, inflammation, genetics, and metabolism play important roles in the pathogenesis of MAFLD (Park et al., 2014a; Cho et al., 2018; Marra and Svegliati-Baroni, 2018); however, the exact mechanism underlying MAFLD development remains elusive.

Autophagy is a conserved catabolic process that is crucial for degrading and recycling unnecessary intracellular components, such as excessive lipid droplets, misfolded protein aggregates, and damaged organelles, to maintain the liver metabolic homeostasis (Klionsky and Emr, 2000; Khambu et al., 2018). Impaired autophagy hinders the clearance of excess lipids from lipid droplets, inclusion bodies, and toxic protein aggregates, thereby contributing to MAFLD development (Park et al., 2014b; Park and Lee, 2014; Zhang et al., 2018). Sequestosome-1 (p62/SQSTM1; hereafter referred to as p62) is an autophagy adaptor protein responsible for autophagic degradation of polyubiquitinated substrates (Pankiv et al., 2007). p62 binds to polyubiquitinated substrates via its ubiquitin-associated domain and interacts with microtubule-associated protein light chain 3 (LC3) on the autophagosome (Bjorkoy et al., 2009; Isogai et al., 2011). Impaired autophagy contributes to several pathological conditions, including fatty liver disease and hepatocellular carcinoma progression (Mizushima and Klionsky, 2007; Niture et al., 2021).

Recent studies are focusing on identifying natural compounds that are relatively safe and have potentially beneficial effects in obesity-related diseases. Methylsulfonylmethane (MSM) is an organosulfur compound found in various plant and animal tissues that has been investigated for its potential biological benefits, including its anti-inflammatory, antioxidant, and analgesic effects (Kim et al., 2009; Nakhostin-Roohi et al., 2011; Ahn et al., 2015). MSM exerts beneficial effects on obesity-induced hepatic steatosis and insulin resistance (Sousa-Lima et al., 2016; Miller et al., 2021). However, the action mechanism of MSM in metabolic syndrome remains unknown. Therefore, in this study, we aimed to explore the role of autophagy in the treatment of MAFLD with MSM.

In this study, we investigated the potential effects of MSM treatment on autophagic clearance in vitro models of obesity using palmitic acid (PA)-treated human hepatoma (HepG2) cell lines and diet-induced obese mice. Furthermore, the molecular mechanisms by which MSM regulates autophagy were studied. We observed that MSM reduced obesity-induced insulin resistance and hepatic steatosis. Mechanistically, MSM treatment markedly enhanced autophagic flux, subsequently inhibiting the

accumulation of protein inclusions via the AMP-activated protein kinase (AMPK)/mechanistic target of rapamycin kinase (mTOR)/UNC-51-like autophagy-activating kinase 1 (ULK1) signaling pathway. Our findings provide a better understanding of the role of autophagy in the pharmacological treatment of MAFLD and its associated metabolic disorders using MSM-based medicine.

2 Materials and methods

2.1 Materials

MSM, fatty acid-free bovine serum albumin (BSA), and PA were purchased from Sigma-Aldrich (MO, United States). Torin 1 was purchased from Cayman Chemical (MI, United States). Bafilomycin A1, Rapamycin and AICAR were purchased from LC Laboratories (MA, United States). Compound C was purchased from Tokyo Chemical Industry (Japan). Ubiquitin (sc-8017) and ribosomal protein S6 (sc-74459) were purchased from Santa Cruz Biotechnology (CA, United States). LC-3 (2775), p62 (5114), phospho-ULK1 (5869), ULK1 (8054), phospho-AMPK (2535), AMPK (2532), phospho-p70S6K (9205), p70S6K (9202), phospho-ribosomal protein S6 (2211), and TSC2 (4308) were purchased from Cell Signaling Technology (MA, United States). β -actin (JLA20) and α -Tubulin (12G10) were purchased from Developmental Studies Hybridoma Bank (IA, United States). GAPDH (OAEA00006) was purchased from Aviva Systems Biology (CA, United States).

2.2 Cell culture and treatment

Human hepatoma (HepG2) cells were cultured in Dulbecco's Modified Eagle Medium (Welgene, South Korea) supplemented with 10% fetal bovine serum (Welgene) and 100 U/mL penicillin-streptomycin (Welgene) at 37°C and 5% CO₂. For PA treatment, the cells were incubated for the indicated time points with 500 μ M PA, as previously described (Lee et al., 2019). Control cell cultures containing fatty acid-free bovine serum albumin (Sigma-Aldrich) as a vehicle were incubated along with the treated cultures.

2.3 Animal experiments

Eight-week-old male C57BL/6 mice were purchased from Samtako (Osan, South Korea). The mice were kept in a controlled environment at a temperature of 21°C–24°C and humidity of 50% \pm 5%. They followed a 12-h light/dark cycle and had *ad libitum* access to water and a standard rodent low-fat diet (LFD) or high-fat diet (HFD; containing 60% of calories from fat, Research Diets, New Brunswick, NJ, United States of America). MSM (200 mg/kg body weight or 400 mg/kg body weight) was administered via daily oral gavage for 4 weeks after 9 weeks of HFD intake. The mice were euthanized by CO₂ asphyxiation and their blood samples, liver tissues, and epididymal white adipose tissues were harvested, stored at –80°C, and then used for further molecular analysis.

2.4 Cell viability

Cell viability was measured using a water-soluble tetrazolium salt (WST)-8 cell counting kit (catalog no. QM2500; Daeil Lab Service, South Korea), according to the manufacturer's instructions. Briefly, HepG2 cells were plated at a final density of 1×10^4 cells/well in a 96-well plate. After 24 h of incubation, the cells were treated with MSM or phosphate-buffered saline (PBS; vehicle) as indicated. Subsequently, 10 μ L of WST-8 solution was added to each well and incubated for 30 min in a humidified atmosphere (37°C and 5% CO₂). Absorbance was measured at 450 nm using an Epoch2 microplate reader (Bio-Tek Instruments, Winooski, VT, United States). Absorbance values of treated cells were expressed as a percentage of the absorbance value of the control.

2.5 Solubility fractionation

Solubility fractionation was performed as previously described (Kim et al., 2023). Liver tissues and HepG2 cells were washed and lysed in a lysis buffer containing 20 mM Tris-Cl pH 7.5, 150 mM NaCl, 1 mM EDTA, 1 mM EGTA, 2.5 mM NaPPi, 1 mM β -glycerophosphate, 1 mM Na₃VO₄, 1% Triton X-100, and a protease inhibitor cocktail. After 30 min of incubation on ice, lysates were centrifuged at $12,000 \times g$ for 15 min at 4°C. The supernatant was collected as the Triton X-100-soluble fraction. The pellets were resuspended again in a lysis buffer containing 2% sodium dodecyl sulfate (Triton X-100-insoluble fraction). Samples were boiled in Laemmli's sample buffer and subjected to sodium dodecyl sulfate-polyacrylamide gel electrophoresis (SDS-PAGE) and immunoblotting.

2.6 Glucose and insulin tolerance tests

For the glucose tolerance test (GTT), the mice were fasted for 6 h and intraperitoneally injected with D-glucose (1 g/kg body weight). For the insulin tolerance test (ITT), mice were fasted for 6 h and intraperitoneally injected with insulin (0.65 U/kg body weight). At the specified time intervals, blood samples were collected from the tail, and blood glucose levels were assessed using an Accu-Chek glucometer (Roche Diagnostics, Germany).

2.7 Biochemical measurements

Blood samples were collected and left to coagulate for 30 min at room temperature (22°C–26°C). Subsequently, the samples were centrifuged at $1,000 \times g$ for 15 min to collect the serum. Serum alanine aminotransferase (ALT), aspartate aminotransferase (AST), and alkaline phosphatase (ALP) levels were determined using assay kits (ALT, catalog no. K752-100; AST, catalog no. K753-100; ALP, catalog no. K412-500; BioVision, United States).

2.8 Western blotting

Frozen liver tissues and HepG2 cells were homogenized on ice in a radioimmunoprecipitation assay buffer containing a cOmplete™

EDTA-free protease inhibitor cocktail (Roche, Switzerland). Lysates were then sonicated and centrifuged at $18,000 \times g$ for 15 min at 4°C to remove the cell debris. Total protein concentration was determined using bicinchoninic acid protein (Thermo Fisher Scientific, United States). Laemmli sample buffer was added to the samples and the mixture was boiled for 5 min. Proteins were separated via SDS-PAGE and transferred onto polyvinylidene fluoride membranes (Merck Millipore, Germany). Membranes were incubated with the appropriate primary antibodies against ubiquitin, p62, phospho-ULK1, ULK1, LC-3, phospho-AMPK, AMPK, phospho-p70S6K, p70S6K, phospho-ribosomal protein S6, ribosomal protein S6, TSC2, and β -actin in TBS containing 5% non-fat milk powder or BSA for 1 h at room temperature. The membranes were then washed thrice and incubated with the appropriate horseradish peroxidase-conjugated secondary antibodies. The membranes were again washed thrice and the protein bands were detected via enhanced chemiluminescence assay using the Clarity ECL Western blotting Substrate (Bio-Rad, United States). Band densities were quantified using the ImageJ software (National Institutes of Health, United States).

2.9 Plasmids and virus production

HEK293T cells were co-transfected with the following lentiviral and packaging vectors using a polyethyleneimine reagent: sh-Luciferase (sh-Luc), sh-ULK1, and sh-TSC2 (kindly provided by Andrei V. Budanov, Trinity College Dublin) (Park et al., 2014a). Lentiviral supernatants were collected 48 and 72 h after transfection and further concentrated using a Lenti-X concentrator (Takara, Japan), according to the manufacturer's protocol. HepG2 cells were transduced with the concentrated lentivirus in the presence of 4 μ g/mL polybrene.

2.10 Immunocytochemistry

HepG2 cells were fixed with 4% paraformaldehyde (pH 7.4) for 15 min at room temperature, washed thrice with PBS, and permeabilized with methanol at -20°C . The cells were incubated for 1 h in a blocking solution with a combination of anti-p62 (1:400), anti-ubiquitin (1:400), anti-LC3B (1:400), and anti-lysosomal-associated membrane protein 1 (LAMP1, 1:400) antibodies at 4°C in a humidified chamber. The cells were again washed thrice with PBS and incubated with the appropriate combination of secondary antibodies (1: 400, Alexa Fluor 488-conjugated goat anti-mouse or anti-rabbit and Alexa Fluor 549-conjugated goat anti-mouse or anti-rabbit secondary antibodies; Thermo Fisher Scientific) for 1.5 h. Nuclei were counterstained with 1 μ g/mL Hoechst 33342 (Thermo Fisher Scientific) and mounted on slides using the ProLong Gold antifade reagent (Thermo Fisher Scientific). Fluorescent images were obtained using a laser scanning confocal microscope (LSM 700; Carl Zeiss, Germany).

2.11 Histological analysis

Liver tissues were prepared for histological examination and stained with hematoxylin and eosin (H&E; Sigma-Aldrich) and Oil red O

(Sigma-Aldrich) as previously described (Lee et al., 2019). The tissues were fixed with 10% neutral buffered formalin, embedded in paraffin, and stained with H&E. Paraffin-embedded sections were deparaffinized, rehydrated, and subjected to heat-induced epitope retrieval using a citrate buffer. Endogenous peroxidase activity was blocked by incubating the tissue sections with 3% hydrogen peroxide. The sections were incubated with a blocking solution for 60 min at room temperature. Subsequently, sections were incubated overnight at 4°C with the primary antibody against anti-p62. The sections were then washed thrice with PBS and incubated with a biotinylated anti-rabbit secondary antibody (Vector Laboratories, Burlingame, CA, United States of America). The antibodies were detected using streptavidin-horseradish peroxidase (BD Biosciences) and 3,3'-diaminobenzidine (Sigma-Aldrich). The sections were counterstained with hematoxylin. Frozen liver tissues embedded in OCT were sectioned and stained with Oil red O (Sigma-Aldrich). All samples were examined under a light microscope equipped with a digital camera (Leica, Germany).

2.12 Reverse transcription-quantitative polymerase chain reaction (RT-qPCR)

Total RNA was extracted from the liver tissue homogenates and HepG2 cells using the TRIzol reagent (Takara), following the manufacturer's instructions. Total RNA was reverse-transcribed into complementary DNA using a cDNA synthesis kit (catalog no. BR123; BioFact, Korea). To determine the relative gene expression, real-time PCR was performed using the SYBR Green qPCR Master Mix (BioFact) on a real-time PCR system (Life Technologies, United States). Relative fold changes in the expression of target genes were calculated using the comparative threshold cycle (Ct) method with cyclophilin A as an internal control gene to normalize the target gene expression levels. Primers used in this study are listed in [Supplementary Table S1](#).

2.13 Statistical analysis

The results are presented as mean \pm standard error of the mean. Unless otherwise indicated, data depicted in the figures represent at least three independent experiments. The significance of the differences between two experimental groups was determined using a two-tailed Student's *t*-test. Multiple comparisons were conducted using one-way analysis of variance, followed by Tukey's *post hoc* test. Differences among means were considered statistically significant at $p < 0.05$.

3 Results

3.1 MSM inhibits PA-induced accumulation of protein inclusions

Saturated fatty acids suppress the autophagic degradation of ubiquitinated proteins (Park et al., 2014b; Lee et al., 2019; Kim et al., 2023). To investigate the effect of MSM on the autophagic clearance of ubiquitinated proteins in PA-treated HepG2 cells, ubiquitinated

protein and p62 levels in detergent-soluble and detergent-insoluble fractions were analyzed via immunoblotting. No significant differences were observed in the levels of ubiquitinated proteins or p62 in the detergent-soluble fractions of HepG2 cells treated with MSM at any dose ([Figures 1A, B](#)). However, pretreatment with MSM significantly reduced the levels of ubiquitinated proteins and p62 in the detergent-insoluble fraction of PA-treated HepG2 cells in a dose-dependent manner ([Figures 1C, D](#)). To exclude the inhibitory effect of MSM on protein aggregation induced by cytotoxicity, a cell viability test was carried out 12 h after the treatment of HepG2 cells with various doses of MSM (0–400 mM). MSM treatment exerted no cytotoxicity up to 200 mM, whereas significant cytotoxicity was observed at 400 mM ([Supplementary Figure S1](#)). Using immunocytochemistry, we further investigated the effects of MSM on the formation of protein aggregates. Pretreatment with MSM decreased the aggregation of PA-induced ubiquitin- and p62-positive proteins ([Figures 1E, F](#)). However, this decrease was not attributed to a reduction in p62 expression ([Supplementary Figure S2](#)). These findings suggest that MSM improves the autophagic clearance of ubiquitinated proteins.

3.2 MSM prevents PA-induced impairment of autophagic flux

Exposure to PA suppresses autophagic flux in hepatocytes by impairing autophagosome-lysosome fusion (Park et al., 2014b; Park and Lee, 2014). To investigate the effect of MSM on autophagic flux, we assessed MSM-induced autophagic activity using a flux assay based on the immunoblotting of LC3-II and p62. We treated HepG2 cells with bafilomycin A1, a specific inhibitor of vacuolar-type H (+)-ATPase, which inhibits lysosomal enzyme activity and the fusion of autophagosomes with lysosomes. PA-treated cells showed no increase in LC3-II and p62 levels after bafilomycin A1 treatment, whereas MSM pretreatment significantly increased LC3-II and p62 levels in the presence of bafilomycin A1 ([Figures 2A, B](#)), suggesting that increased autophagosome degradation, rather than decreased autophagosome formation, was the cause of autophagic degradation by MSM. Confocal fluorescence imaging showed that pretreatment with MSM reduced the number of GFP-LC3 puncta in PA-treated HepG2 cells, whereas treatment with bafilomycin A1 caused a marked accumulation of GFP-LC3 puncta in HepG2 cells co-treated with MSM and PA ([Figures 2C, D](#)). To determine whether MSM influenced the fusion of autophagosomes and lysosomes, we analyzed the co-localization of LC3 with the lysosomal marker LAMP-1. Immunofluorescence staining revealed that the colocalization of LC3 puncta with LAMP-1 was significantly reduced in PA-treated HepG2 cells compared to that in control cells, whereas MSM treatment prevented the decrease in PA-treated HepG2 cells ([Figures 2E, F](#)). These findings suggest that MSM treatment potentially restores the defective autophagosome-lysosome fusion.

3.3 MSM inhibits obesity-induced insulin resistance and hepatic steatosis

To investigate whether oral administration of MSM affected glucose tolerance and insulin sensitivity in HFD-induced obese

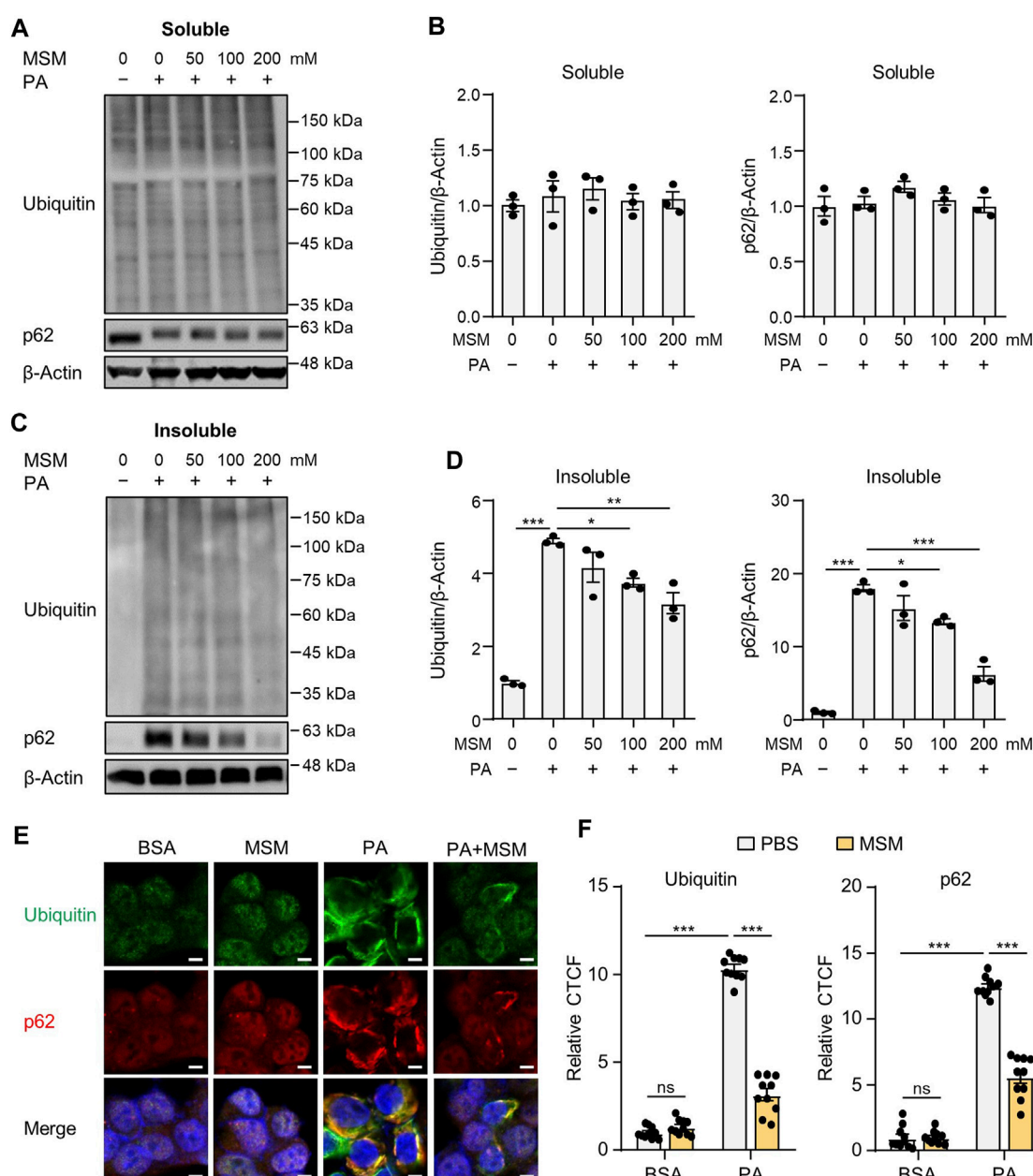


FIGURE 1

Methylsulfonylmethane (MSM) mitigates palmitic acid (PA)-induced protein aggregation. (A,C) Immunoblots for ubiquitin and sequestosome-1 (p62/SQSTM1) from Triton X-100-soluble and -insoluble fractions of HepG2 cells pretreated with the indicated concentrations of MSM (50–200 mM) for 1 h followed by 500 μ M PA treatment for 12 h. β -actin was used as a loading control. (B,D) Band intensities were quantified and normalized to the control levels. (E) Immunofluorescence staining for ubiquitin (green) and p62 (red) in HepG2 cells pretreated with 200 mM MSM for 1 h followed by 500 μ M PA treatment for 12 h. Nuclei were stained with 4',6-diamidino-2-phenylindole (DAPI; blue). Scale bar, 5 μ m. (F) Images were quantified for corrected total cell fluorescence (CTCF) per unit area. Data are represented as the mean \pm standard error of the mean (SEM). * p < 0.05, ** p < 0.01, and *** p < 0.001 (one-way (B,D) or two-way (F) analysis of variance [ANOVA] followed by Tukey's test).

mice, we fed male mice an HFD or LFD for 9 weeks and gavaged them daily with a vehicle control or 200 or 400 mg/kg body weight MSM for 4 weeks. The glucose tolerance test and calculated area under the curve revealed that MSM-treated HFD-fed mice displayed an elevated clearance rate of blood glucose after injection compared to PBS-treated HFD-fed mice (Figures 3A, B). To determine whether MSM reduces HFD-induced insulin resistance, we conducted a glucose tolerance

test in each group. The results revealed that administration of 400 mg/kg MSM significantly enhanced the insulin-mediated glucose-lowering effects (Figures 3C, D). The 200 mg/kg MSM-treated mice also showed improved insulin sensitivity compared to the PBS-treated HFD-fed mice, although the difference was not significant. In lean mice fed LFD, insulin sensitivity and glucose tolerance were unaffected by MSM (Supplementary Figure S3).

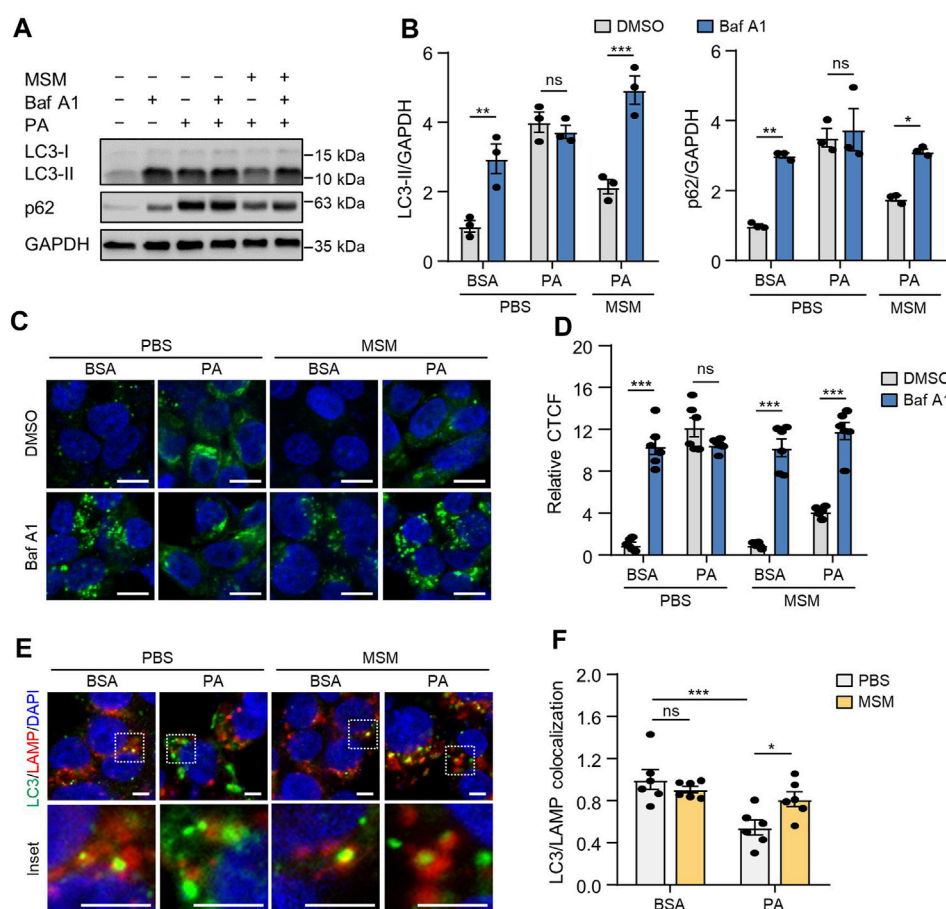


FIGURE 2

MSM reverses PA-induced impairment of autophagic flux in HepG2 cells. (A) Immunoblots of light chain 3 (LC3) and p62 in the cell lysates of HepG2 cells pretreated with 100 mM MSM for 1 h followed by 500 μ M PA treatment for 12 h with or without 100 nM bafilomycin A1 for the last 3 h. (B) Band intensities were quantified and normalized to the control levels. (C) Confocal fluorescence imaging of HepG2 cells transiently transfected with the GFP-LC3 plasmid with the indicated treatments. Nuclei were stained with DAPI (blue). Scale bar, 10 μ m. (D) Images were quantified for CTCF per unit area. (E) Immunofluorescence staining for LC3 (green) and lysosomal-associated membrane protein (LAMP; red) in HepG2 cells with the indicated treatments. Nuclei were stained with DAPI (blue). Boxed areas are magnified in the bottom panels. Scale bar, 5 μ m. (F) Images were quantified for CTCF per unit area. Data are represented as the mean \pm SEM. * p < 0.05, ** p < 0.01, and *** p < 0.001 (two-way ANOVA, followed by Tukey's (B,D) or Fisher's least significant difference [LSD] (F) test).

We investigated the effects of MSM on obesity-associated metabolic phenotypes. Treatment of mice with 400 mg/kg significantly reduced the weight gain produced by the HFD (Figure 4A). However, the food intake was not affected by MSM administration (Figure 4B). While the livers of obese mice treated with PBS appeared pale, those of obese mice treated with MSM exhibited a reddish-brown color (Figure 4C). In this model, MSM treatment significantly reduced the liver weight (Figure 4D). Serum levels of ALT, AST, and ALP were significantly lower after administration of MSM (Figures 4E–G). Histological staining of liver tissue sections was performed using hematoxylin and eosin and Oil Red O. PBS-treated obese mice showed signs of hepatocellular ballooning and steatosis, whereas MSM-treated obese mice showed a significant reduction in hepatocellular steatosis and ballooning compared to PBS-treated obese mice (Figures 4H, I). Oil Red O staining revealed a remarkable decrease in hepatic lipid accumulation in MSM-treated obese mice compared to that in PBS-treated obese mice (Figures 4H, J). The expression of genes

involved in lipogenesis were reduced in the livers of obese mice treated with MSM (Figure 4K).

3.4 MSM attenuates ubiquitinated protein accumulation and inflammation in HFD-induced fatty liver

We investigated whether administration of MSM influenced autophagy clearance in the livers of HFD-fed mice. Immunoblotting analysis revealed that the levels of ubiquitinated proteins and p62 in the detergent-soluble fractions from liver tissues were not significantly different between PBS- and MSM-treated obese mice (Figures 5A, B). However, MSM administration reduced the elevated levels of ubiquitinated proteins and p62 in the detergent-insoluble fractions of the HFD-fed mouse liver tissues (Figures 5C, D). Immunohistochemical analysis also revealed that the administration of MSM resulted in a significant reduction in

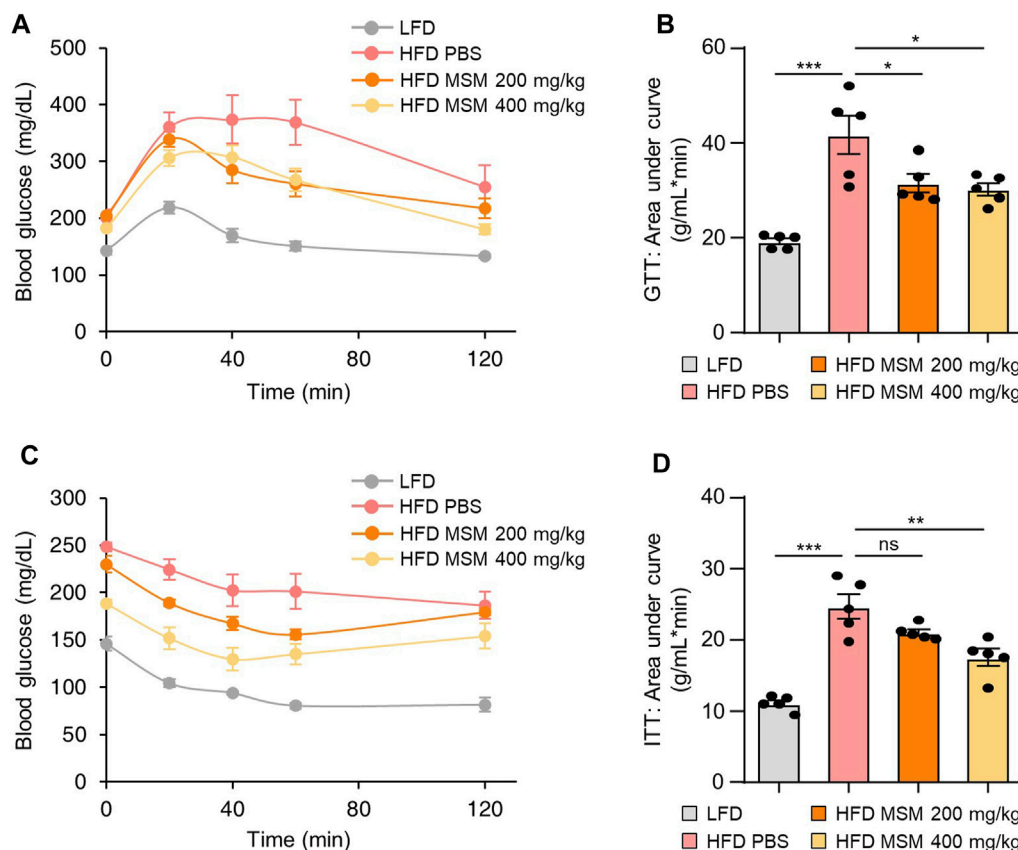


FIGURE 3

MSM improves the glucose tolerance and insulin sensitivity of mice. (A–D) C57BL/6 male mice fed a high-fat diet (HFD) were treated with phosphate-buffered saline (PBS), 200 mg/kg/day p.o. MSM, or 400 mg/kg/day p.o. MSM for 4 weeks. Low-fat diet (LFD)-fed mice of the same age were used as a negative control. Glucose tolerance test (GTT) (A) and insulin tolerance test (ITT) (C) were conducted using LFD- or HFD-fed mice treated as indicated. The area under the curve was quantified from GTT (B) and ITT data (D). Data are represented as the mean \pm SEM. * $p < 0.05$, ** $p < 0.01$, and *** $p < 0.001$ (one-way ANOVA, followed by Tukey's test).

p62 staining in the cytoplasm of hepatocytes in HFD-fed mice (Figures 5E, F). Consistent with this, MSM administration significantly alleviated LC3-II protein levels in HFD-fed mouse liver tissues (Figures 5G, H), suggesting that treatment with MSM enhanced the autophagic degradation of ubiquitinated proteins in HFD-induced fatty liver. To evaluate whether MSM administration influenced hepatic inflammation, we measured the expression of inflammatory genes in the livers of lean and obese mice treated with PBS or MSM, using qRT-PCR. Obese mice treated with MSM showed reduced expression of several inflammatory genes, including *Emr1* (also known as *F4/80*), *Tnfa*, *Col1a1*, *Tgfb1*, *Il-1b*, and *Il-6*, compared to PBS-treated obese mice (Supplementary Figure S4).

3.5 MSM regulates the AMPK/mTOR/ULK1 signaling pathway

AMPK positively regulates autophagy by detaching mTORC1 from the ULK1 complex (Salminen and Kaarniranta, 2012). To explore the potential mechanisms by which MSM enhances autophagy, we investigated the signaling pathways

involving AMPK and mTORC1, two key upstream signaling molecules responsible for regulating autophagy. Immunoblotting analysis revealed increased phosphorylation of AMPK (Supplementary Figures S5A–D) and decreased phosphorylation of p70S6K (Supplementary Figures S6A–D) in HepG2 cells by MSM in a dose- and time-dependent manner. Next, we examined the effects of MSM on the activities of AMPK and mTORC1 in PA-treated HepG2 cells and livers of HFD-fed mice. MSM treatment increased AMPK activation (Figures 6A, B) but suppressed the phosphorylation of p70S6K and ribosomal protein S6 in PA-treated HepG2 cells (Figures 6C, D). Correspondingly, obese mice treated with MSM showed a significant increase in phosphorylated AMPK levels (Figures 6E, F) and a reduction in the levels of phosphorylated p70S6K and ribosomal protein S6 compared to those in PBS-treated obese mice (Figures 6G, H). To further determine whether ULK1 signaling is involved in MSM attenuation of impaired autophagy in MAFLD, the phosphorylation of ULK1 at Serine-555 (S555) was assessed. We observed a dose- and time-dependent increase in ULK1 S555 phosphorylation in MSM-treated HepG2 cells (Supplementary Figures S7A–D). Immunoblotting analysis revealed that MSM treatment enhanced ULK1 S555 phosphorylation in PA-treated

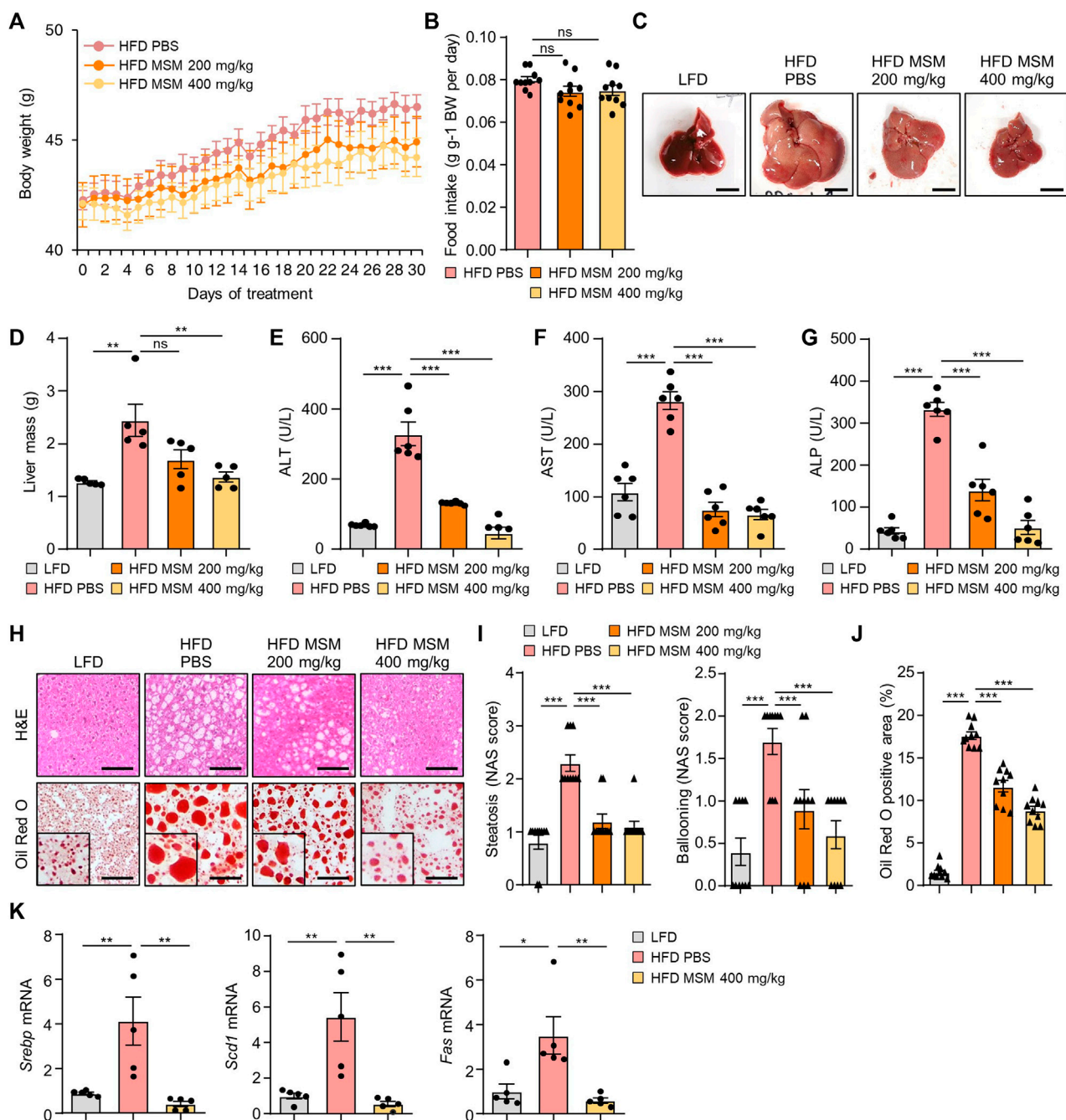


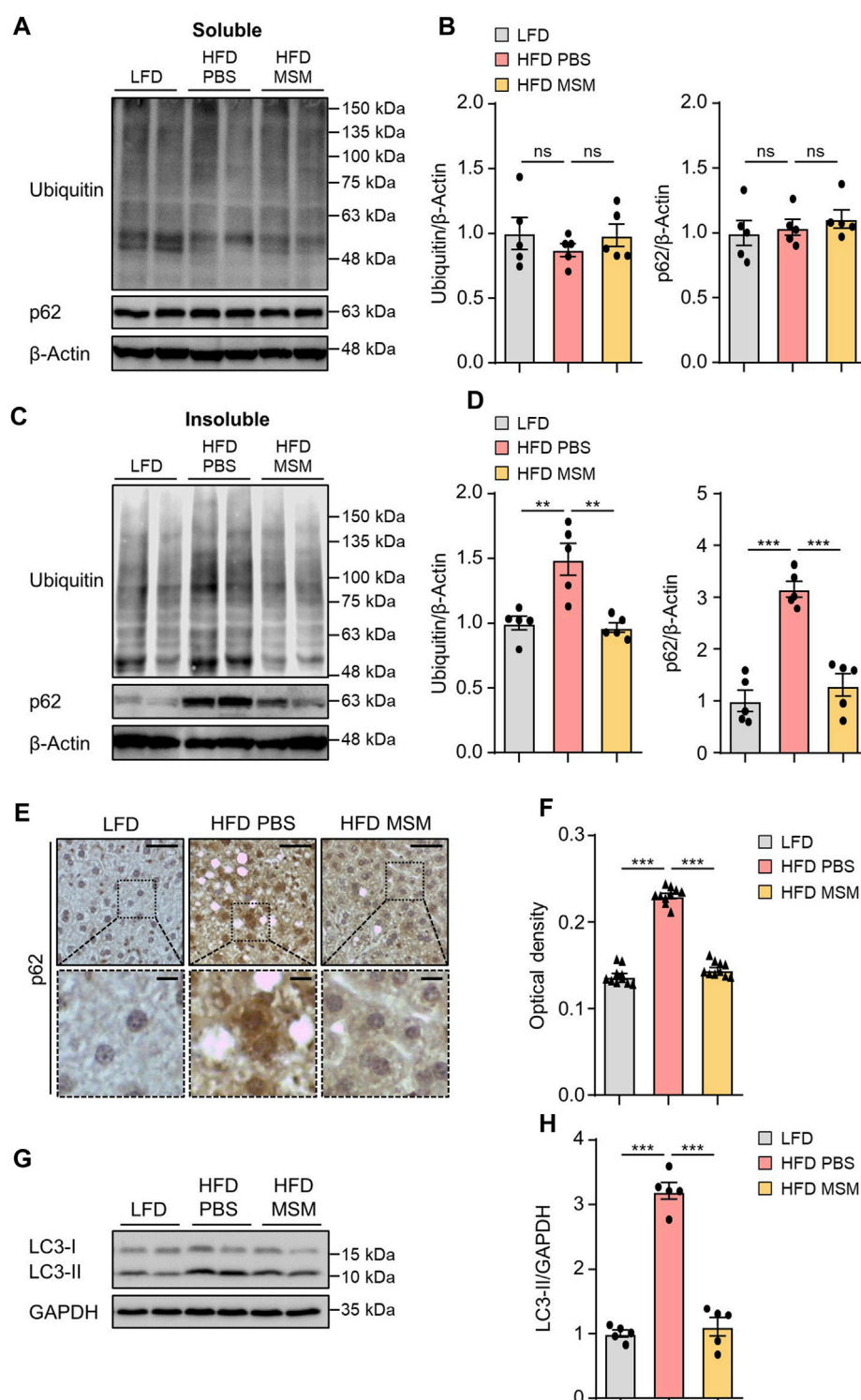
FIGURE 4

MSM ameliorates HFD-induced obesity and hepatic steatosis. (A–K) C57BL/6 male mice fed HFD were treated with PBS, 200 mg/kg/day p.o. MSM, or 400 mg/kg/day p.o. MSM for 4 weeks. LFD-fed mice of the same age were used as a negative control. (A) Body weight of mice treated as indicated. (B) Food intake during the treatment period. Gross liver morphology (C) and total liver mass (D) of mice in each group indicated. (E–G) Serum alanine aminotransferase (ALT), aspartate aminotransferase (AST), and alkaline phosphatase (ALP) levels. (H) Hematoxylin and eosin staining and Oil red O staining of liver sections from mice in each group as indicated. Scale bar, 100 μ m. (I) Histological non-alcoholic fatty liver disease (NAFLD) activity score (NAS). (J) Quantified Oil red O-stained area. (K) RT-qPCR analysis of hepatic lipogenic gene expression from mice in each group as indicated. Data are represented as the mean \pm SEM. * p < 0.05, ** p < 0.01, and *** p < 0.001 (one-way ANOVA, followed by Tukey's test).

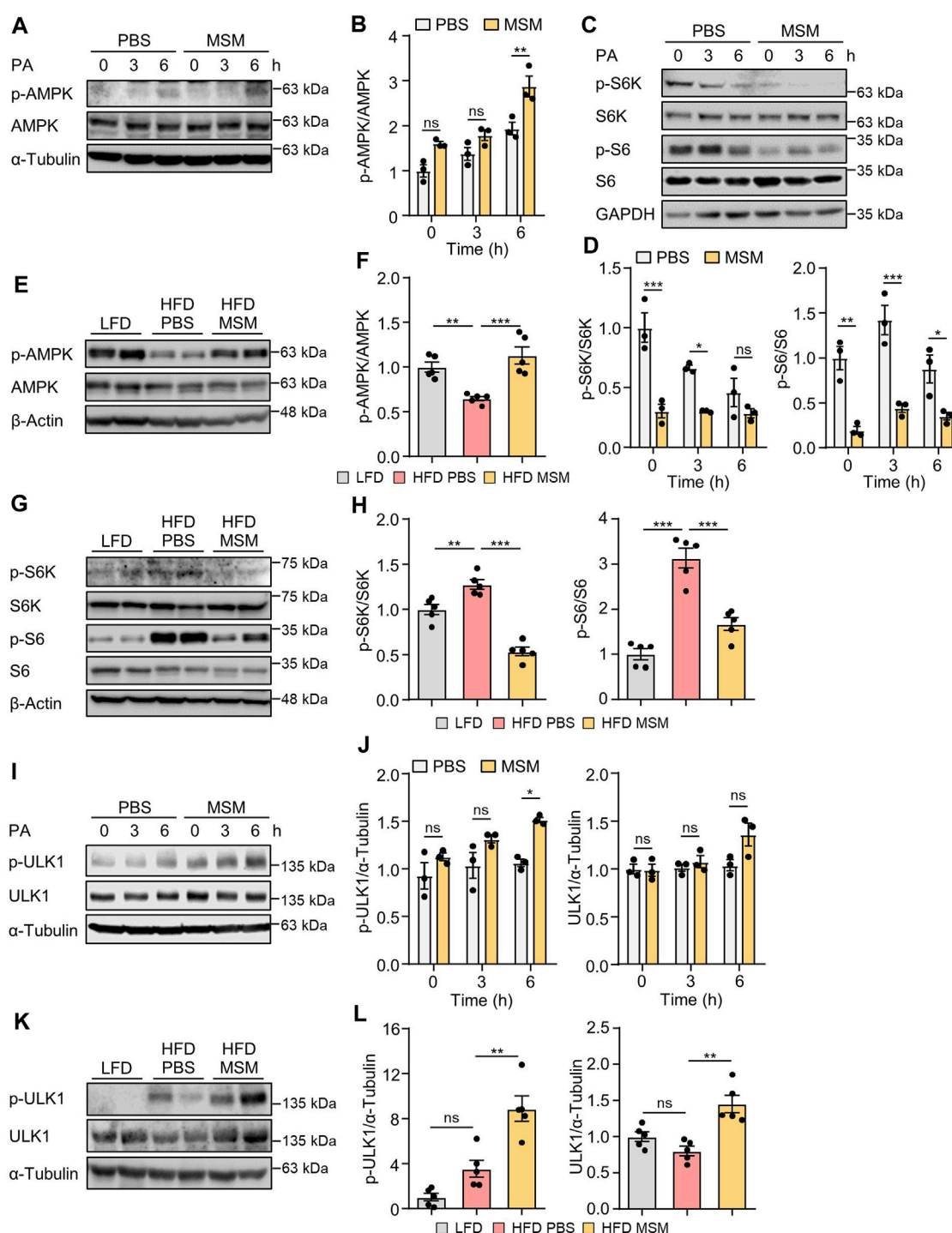
HepG2 cells (Figures 6I, J). Consistently, ULK1 S555 phosphorylation was significantly higher in the livers of obese mice treated with MSM than in those treated with PBS (Figures 6K, L). Collectively, these data suggest that the AMPK/mTOR/ULK1 signaling pathway is involved in MSM-mediated enhancement of hepatic autophagy.

3.6 MSM enhances autophagy via an AMPK/mTORC1-dependent pathway

To determine whether AMPK signaling in MSM-treated cells influences the autophagic degradation of p62, we pretreated HepG2 cells with the AMPK α inhibitor compound C.

**FIGURE 5**

MSM improves the ubiquitinated protein clearance in diet-induced fatty liver. (A–H) C57BL/6 male mice fed HFD were treated with PBS or 400 mg/kg/day p.o. MSM for 4 weeks. LFD-fed mice of the same age were used as a negative control. (A,C) Immunoblots of ubiquitin and p62 from Triton X-100-soluble and -insoluble fractions of liver tissue lysates. β -actin was used as a loading control. (B,D) Band intensities were quantified and normalized to the control levels. (E) Immunohistochemical staining for p62 in the liver tissues of mice in each group. Boxed areas are magnified in the bottom panels. Scale bars, 50 and 10 μ m (insets). (F) Optical density of p62 immunoreactivity. (G) Immunoblots of LC3 in the liver tissue lysates of mice in each group. Glyceraldehyde 3-phosphate dehydrogenase (GAPDH) was used as a loading control. (H) Band intensities were quantified and normalized to the control levels. Data are represented as the mean \pm SEM. * $p < 0.05$, ** $p < 0.01$, and *** $p < 0.001$ (one-way ANOVA, followed by Tukey's test).

**FIGURE 6**

Effects of MSM on the AMP-activated protein kinase (AMPK)/mechanistic target of rapamycin kinase (mTOR)/UNC-51-like autophagy-activating kinase 1 (ULK1) signaling pathway in PA-treated HepG2 cells and in the livers of HFD-fed mice. **(A, C and I)** HepG2 cells were pretreated with 100 mM MSM for 1 h followed by 500 μ M PA treatment for the indicated time points. Cell lysates were immunoblotted with the indicated antibodies. GAPDH or α -tubulin served as a loading control. **(B, D and J)** Band intensities were quantified and normalized to the control levels. **(E, G and K)** C57BL/6 male mice fed HFD were treated with PBS or 400 mg/kg/day p.o. MSM for 4 weeks. LFD-fed mice of the same age were used as a negative control. Liver tissue lysates were immunoblotted with the indicated antibodies. β -actin or α -tubulin served as a loading control. **(F, H, and L)** Band intensities were quantified and normalized to the control levels. Data are represented as the mean \pm SEM. * p < 0.05, ** p < 0.01, and *** p < 0.001 (one-way ANOVA, followed by Tukey's test).

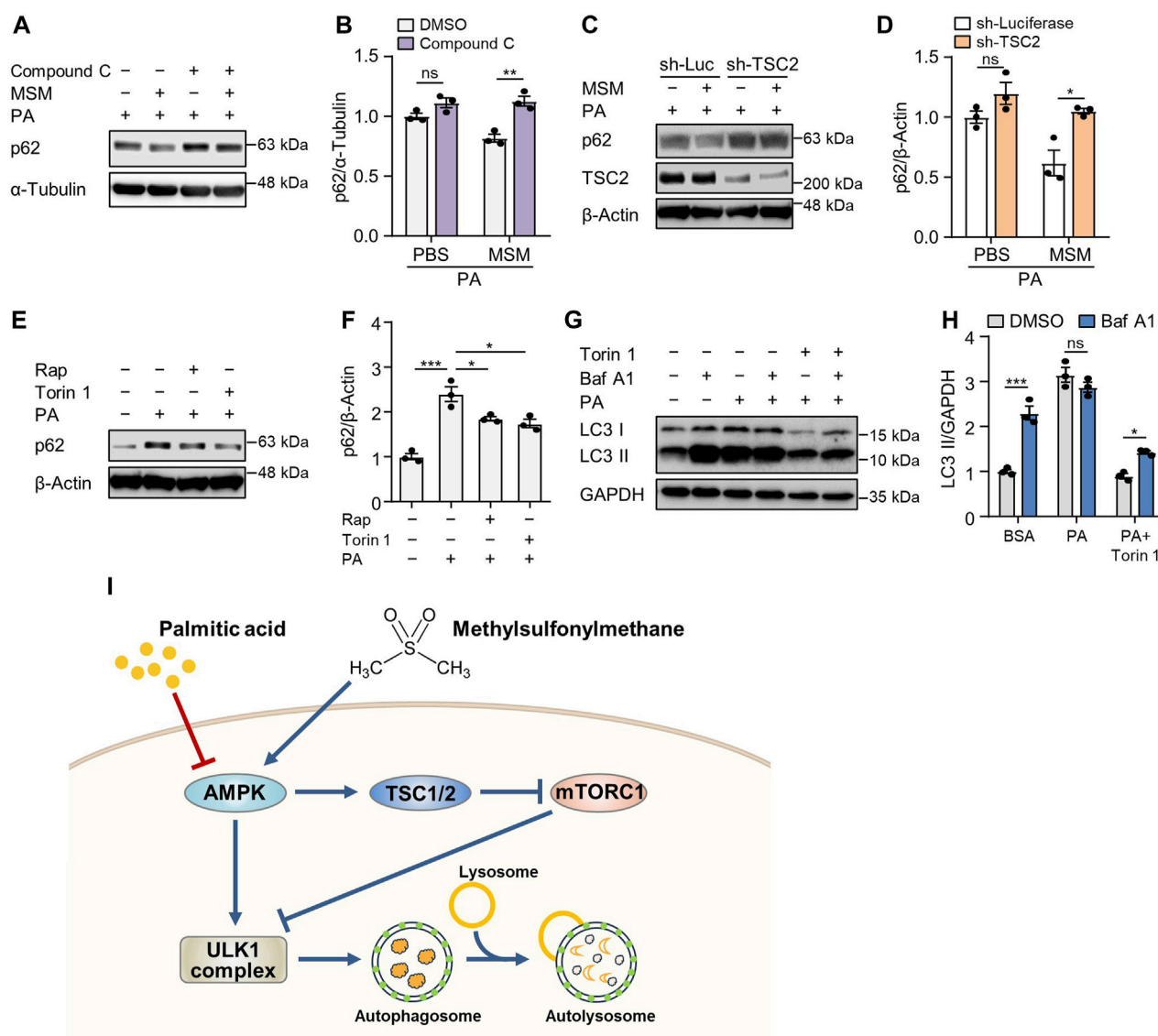


FIGURE 7

MSM enhances autophagy by regulating the AMPK/mTOR signaling pathway. (A) Immunoblots of p62 in the cell lysates of HepG2 cells pretreated with 20 μM compound C or 100 mM MSM for 30 min followed by 500 μM PA treatment for 9 h. (C) Immunoblots of p62 and TSC2 in the cell lysates of lentiviral sh-Luc- or sh-TSC2-infected HepG2 cells pretreated with 100 mM MSM for 30 min followed by 500 μM PA treatment for 9 h. (E) Immunoblots of p62 in the cell lysates of HepG2 cells pretreated with 100 nM rapamycin or 250 nM Torin 1 for 30 min followed by 500 μM PA treatment for 9 h. (G) Immunoblots of LC3 and p62 in the cell lysates of HepG2 cells pretreated with 250 nM Torin 1 for 1 h followed by 500 μM PA treatment for 12 h with or without bafilomycin A1 (100 nM) for the last 3 h (B,D,F and H) Band intensities were quantified and normalized to the control levels. Data are represented as the mean ± SEM. **p* < 0.05, ***p* < 0.01, and ****p* < 0.001 (one-way ANOVA, followed by Tukey's test). (I) Schematic diagram of the underlying mechanism of the protective effects of MSM against obesity-induced metabolic dysregulation in hepatocytes.

Immunoblotting analysis revealed that pretreatment with compound C abrogated MSM-induced reduction of p62 levels in PA-treated cells (Figures 7A, B). Next, we investigated whether the enhancement of autophagy by MSM treatment was associated with mTORC1 signaling. We found that the lentiviral knockdown of TSC2 did not have any significant effect on MSM-induced autophagic degradation in PA-treated HepG2 cells (Figures 7C, D). Consistent with the inhibitory effect of MSM on mTORC1 signaling, the mTOR inhibitors, rapamycin, and Torin 1, significantly reduced the accumulation of p62 in PA-treated cells (Figures 7E, F). Next, we monitored the autophagic flux by analyzing the LC3 turnover in HepG2 cells

cotreated with Torin 1 and PA. In the presence of Torin 1 and PA, HepG2 cells treated with bafilomycin A1 had higher expression of LC3-II than those without bafilomycin A1 treatment (Figures 7G, H). Collectively, these data suggest that MSM-enhanced hepatic autophagy is mediated by the AMPK/mTOR signaling pathway.

4 Discussion

Owing to the increasing prevalence of obesity and metabolic syndrome, MAFLD has emerged as the most common chronic liver

ailment in both industrialized and developing nations (Adams et al., 2020). No specific medicine can suppress the progression of MAFLD, and existing drugs with therapeutic effects have many limitations. Several natural compounds have been shown to exert therapeutic effects against MAFLD. Although MSM holds promise as a potential therapeutic modality for mitigating obesity-associated metabolic disorders, including type 2 diabetes and fatty liver disease (Sousa-Lima et al., 2016; Miller et al., 2021), the precise underlying mechanism by which it exerts its beneficial effects on obesity-induced metabolic perturbations remains unclear. In this study, we investigated the potential therapeutic effects of MSM on MAFLD and the underlying mechanisms involving autophagic flux via the AMPK/mTOR/ULK1 signaling pathway. We found that MSM treatment effectively ameliorated MAFLD-associated pathological changes. Moreover, obesity-induced insulin resistance, hepatic steatosis, and inflammation were noticeably attenuated in the MSM-treated group than in the vehicle-treated control group. These findings are consistent with those of previous studies showing the beneficial effects of MSM on various metabolic and inflammatory disorders (Ahn et al., 2015; Sousa-Lima et al., 2016; Miller et al., 2021). The present study further expands these observations by demonstrating the potential of MSM to mitigate MAFLD progression.

MSM has gained significant attention as a dietary supplement because of its potential therapeutic effects on various health conditions, primarily those related to joint health and inflammation (Kim et al., 2009; Nakhostin-Roohi et al., 2011). MSM is generally well tolerated and recognized as safe by the FDA. Other studies have demonstrated the beneficial impact of sulfur-containing amino acids, such as methionine, cysteine, and taurine, on glucose homeostasis in patients with diabetes and animal models (Ribeiro et al., 2009; Manna et al., 2013; Dahlhoff et al., 2014; Xu et al., 2015). Owing to the presence of two methyl groups within their structure, MSM potentially function as a source of methyl donation, thereby mitigating hepatic steatosis (Sousa-Lima et al., 2016). Interestingly, methyl donors have been shown to mitigate hepatic lipid accumulation in numerous nutritional models (Song et al., 2007; Kwon et al., 2009; Wang et al., 2010). Consistent with this finding, we found that hepatocellular ballooning and steatosis decreased in MSM-treated obese mice in this study. Solubility is a crucial factor influencing the bioavailability and efficacy of MSM. MSM exhibits high solubility in aqueous solutions in the neutral to slightly alkaline pH range, facilitating its absorption and potential therapeutic action (Kaiser et al., 2020). Therefore, consideration of the formulation and administration methods of MSM is important to optimize its solubility and subsequent absorption. Its reported adverse effects, including gastrointestinal discomfort, bloating, and headache, are typically mild (Liu et al., 2018; Crawford et al., 2019). However, the limited long-term safety data on MSM necessitates further research to facilitate its long-term use.

Autophagy plays a crucial role in maintaining cellular homeostasis by regulating the turnover of organelles and various macromolecules, including proteins and lipids (Choi et al., 2013; Gatica et al., 2018). In various liver diseases, impaired autophagic flux is involved in the accumulation of lipid droplets in hepatocytes, progression of hepatic steatosis, and hepatic inflammation (Park et al., 2014b; Kim et al., 2018; Nitire et al., 2021). We and other researchers have previously reported that increased autophagic activity enhances the metabolic profile of

mice with metabolic syndrome and obesity (Park and Lee, 2014; Lim et al., 2018; Kim et al., 2023). In the present study, MSM restored the autophagic flux in PA-treated HepG2 cells and HFD-fed mouse liver tissues. The observed reduction in ubiquitinated protein and p62 levels in the detergent-insoluble fractions of cells and liver tissues in MSM-treated group suggests that MSM promotes autophagic degradation in MAFLD. This effect is likely to contribute to a reduction in lipid accumulation and an overall improvement in hepatic function.

AMPK/mTOR/ULK1 signaling pathway is a well-established regulator of autophagy. AMPK, a highly conserved serine/threonine-protein kinase throughout evolution, serves as a key energy sensor regulating metabolic processes and inflammatory responses (Paquette et al., 2021). AMPK directly phosphorylates several components of the mTORC1 pathway, leading to the downregulation of mTORC1 activity and subsequent promotion of cellular autophagy (Inoki et al., 2003; Holczer et al., 2019). Autophagy initiation is also hindered by mTOR activation via the regulation of ULK1 ubiquitylation (Nazio et al., 2013). Furthermore, autophagy is enhanced by the suppression of the activation of p70S6K, a pivotal kinase downstream of mTOR (Sun et al., 2018). Here, phosphorylated AMPK level was increased, whereas phosphorylated p70S6K and ribosomal protein S6 levels were reduced by MSM treatment (Figure 7I). Moreover, compound C, an inhibitor of AMPK α , abrogated MSM-induced autophagy in PA-treated HepG2 cells. Consistent with this finding, lentiviral knockdown of *TSC2* did not significantly affect the autophagic degradation promoted by MSM treatment in HepG2 cells exposed to PA. Therefore, the correlation between MSM-induced autophagy and the AMPK/mTOR axis suggests that the beneficial effects of MSM may be due to its ability to enhance autophagy via the AMPK/mTOR/ULK1 pathway.

Despite the promising findings, our study has limitations. First, our study was conducted on mice, so it is unclear whether the same results would be observed in humans. Future research should use clinical trials to validate the therapeutic potential of MSM in a more physiologically relevant context. Additionally, investigating the long-term effects of MSM on metabolic parameters and liver function will be crucial for establishing its clinical relevance. Second, the study did not explore the possibility that other mechanisms, including inflammation, may be involved in the improved insulin sensitivity caused by MSM treatment. Cytokines secreted by activated Kupffer cells and adipocytes can further exacerbate inflammation and insulin resistance (de Luca and Olefsky, 2008). Therefore, understanding the specific interactions among inflammation, insulin resistance, and defective autophagy will provide deeper insights into the mechanisms of action.

5 Conclusion

Taken together, this study highlights the beneficial effects of MSM in ameliorating MAFLD by restoring the autophagic flux via the AMPK/mTOR/ULK1 signaling pathway. These findings provide a mechanistic basis for the observed improvements in obesity-induced insulin resistance and hepatic steatosis. The potential translational implications of our findings further highlight the importance of exploring the therapeutic potential of MSM in MAFLD and related metabolic disorders.

Data availability statement

The raw data supporting the conclusion of this article will be made available by the authors, without undue reservation.

Ethics statement

The animal study was approved by the Animal Ethics Committee of Konyang University. The study was conducted in accordance with the local legislation and institutional requirements.

Author contributions

DH: Conceptualization, Writing—original draft, Writing—review and editing, Formal Analysis, Investigation. DK: Formal Analysis, Investigation, Methodology, Validation, Writing—review and editing. HK: Formal Analysis, Investigation, Writing—review and editing. JeL: Formal Analysis, Investigation, Writing—review and editing. JuL: Writing—review and editing, Methodology, Validation. J-SK: Methodology, Validation, Writing—review and editing. JS: Funding acquisition, Methodology, Validation, Writing—review and editing. JK: Funding acquisition, Methodology, Validation, Writing—review and editing. DK: Methodology, Validation, Writing—review and editing. H-WP: Writing—review and editing, Conceptualization, Funding acquisition, Project administration, Resources, Supervision, Writing—original draft.

Funding

The author(s) declare financial support was received for the research, authorship, and/or publication of this article. This research was supported by grants from the National Research Foundation of

Korea (NRF), funded by the Ministry of Education (NRF-2023R1A2C1005469, NRF-2017R1A6A1A03015713, and NRF-2020R1A2C1102244).

Acknowledgments

We thank Jae-Eun Jo from Soonchunhyang University for preparing the histology slides. Additionally, we would like to thank Editage (www.editage.co.kr) for editing and reviewing this manuscript for English language.

Conflict of interest

The authors declare that the research was conducted in the absence of any commercial or financial relationships that could be construed as a potential conflict of interest.

Publisher's note

All claims expressed in this article are solely those of the authors and do not necessarily represent those of their affiliated organizations, or those of the publisher, the editors and the reviewers. Any product that may be evaluated in this article, or claim that may be made by its manufacturer, is not guaranteed or endorsed by the publisher.

Supplementary material

The Supplementary Material for this article can be found online at: <https://www.frontiersin.org/articles/10.3389/fphar.2023.1302227/full#supplementary-material>

References

- Adams, L. A., Roberts, S. K., Strasser, S. I., Mahady, S. E., Powell, E., Estes, C., et al. (2020). Nonalcoholic fatty liver disease burden: Australia, 2019–2030. *J. Gastroenterol. Hepatol.* 35, 1628–1635. doi:10.1111/jgh.15009
- Ahn, H., Kim, J., Lee, M. J., Kim, Y. J., Cho, Y. W., and Lee, G. S. (2015). Methylsulfonylmethane inhibits NLRP3 inflammasome activation. *Cytokine* 71, 223–231. doi:10.1016/j.cyto.2014.11.001
- Bjorkoy, G., Lamark, T., Pankiv, S., Overvatn, A., Brech, A., and Johansen, T. (2009). Monitoring autophagic degradation of p62/SQSTM1. *Methods Enzymol.* 452, 181–197. doi:10.1016/S0076-6879(08)03612-4
- Cho, C. S., Park, H. W., Ho, A., Semple, I. A., Kim, B., Jang, I., et al. (2018). Lipotoxicity induces hepatic protein inclusions through TANK binding kinase 1-mediated p62/sequestosome 1 phosphorylation. *Hepatology* 68, 1331–1346. doi:10.1002/hep.29742
- Choi, A. M., Ryter, S. W., and Levine, B. (2013). Autophagy in human health and disease. *N. Engl. J. Med.* 368, 1845–1846. doi:10.1056/NEJMc1303158
- Crawford, P., Crawford, A., Nielson, F., and Lystrup, R. (2019). Methylsulfonylmethane for treatment of low back pain: a safety analysis of a randomized, controlled trial. *Complement. Ther. Med.* 45, 85–88. doi:10.1016/j.ctim.2019.05.022
- Dahlhoff, C., Worsch, S., Sailer, M., Hummel, B. A., Fiamoncini, J., Uebel, K., et al. (2014). Methyl-donor supplementation in obese mice prevents the progression of NAFLD, activates AMPK and decreases acyl-carnitine levels. *Mol. Metab.* 3, 565–580. doi:10.1016/j.molmet.2014.04.010
- De Luca, C., and Olefsky, J. M. (2008). Inflammation and insulin resistance. *FEBS Lett.* 582, 97–105. doi:10.1016/j.febslet.2007.11.057
- Diehl, A. M., and Day, C. (2017). Cause, pathogenesis, and treatment of nonalcoholic steatohepatitis. *N. Engl. J. Med.* 377, 2063–2072. doi:10.1056/NEJMra1503519
- Gatica, D., Lahiri, V., and Klionsky, D. J. (2018). Cargo recognition and degradation by selective autophagy. *Nat. Cell Biol.* 20, 233–242. doi:10.1038/s41556-018-0037-z
- Holczer, M., Hajdu, B., Lorincz, T., Szarka, A., Banhegyi, G., and Kapuy, O. (2019). A double negative feedback loop between mTORC1 and AMPK kinases guarantees precise autophagy induction upon cellular stress. *Int. J. Mol. Sci.* 20, 5543. doi:10.3390/ijms20225543
- Inoki, K., Zhu, T., and Guan, K. L. (2003). TSC2 mediates cellular energy response to control cell growth and survival. *Cell* 115, 577–590. doi:10.1016/S0092-8674(03)00929-2
- Isogai, S., Morimoto, D., Arita, K., Unzai, S., Tenno, T., Hasegawa, J., et al. (2011). Crystal structure of the ubiquitin-associated (UBA) domain of p62 and its interaction with ubiquitin. *J. Biol. Chem.* 286, 31864–31874. doi:10.1074/jbc.M111.259630
- Kaiser, L. G., Russell, D., Maschmeyer, T., Redfern, R. L., and Inglis, B. A. (2020). Methylsulfonylmethane (MSM): a chemical shift reference for (1) H MRS of human brain. *Magn. Reson. Med.* 83, 1157–1167. doi:10.1002/mrm.27997
- Khambhu, B., Yan, S., Huda, N., Liu, G., and Yin, X. M. (2018). Autophagy in non-alcoholic fatty liver disease and alcoholic liver disease. *Liver Res.* 2, 112–119. doi:10.1016/j.livres.2018.09.004
- Kim, D. K., Han, D., Bae, J., Kim, H., Lee, S., Kim, J. S., et al. (2023). Verapamil-loaded supramolecular hydrogel patch attenuates metabolic dysfunction-associated fatty liver disease via restoration of autophagic clearance of aggregated proteins and inhibition of NLRP3. *Biomater. Res.* 27, 4. doi:10.1186/s40824-023-00342-5

- Kim, S., Han, S. Y., Yu, K. S., Han, D., Ahn, H. J., Jo, J. E., et al. (2018). Impaired autophagy promotes bile acid-induced hepatic injury and accumulation of ubiquitinated proteins. *Biochem. Biophys. Res. Commun.* 495, 1541–1547. doi:10.1016/j.bbrc.2017.11.202
- Kim, Y. H., Kim, D. H., Lim, H., Baek, D. Y., Shin, H. K., and Kim, J. K. (2009). The anti-inflammatory effects of methylsulfonylmethane on lipopolysaccharide-induced inflammatory responses in murine macrophages. *Biol. Pharm. Bull.* 32, 651–656. doi:10.1248/bpb.32.651
- Klionsky, D. J., and Emr, S. D. (2000). Autophagy as a regulated pathway of cellular degradation. *Science* 290, 1717–1721. doi:10.1126/science.290.5497.1717
- Kwon, D. Y., Jung, Y. S., Kim, S. J., Park, H. K., Park, J. H., and Kim, Y. C. (2009). Impaired sulfur-amino acid metabolism and oxidative stress in nonalcoholic fatty liver are alleviated by betaine supplementation in rats. *J. Nutr.* 139, 63–68. doi:10.3945/jn.108.094771
- Lee, S., Han, D., Kang, H. G., Jeong, S. J., Jo, J. E., Shin, J., et al. (2019). Intravenous sustained-release nifedipine ameliorates nonalcoholic fatty liver disease by restoring autophagic clearance. *Biomaterials* 197, 1–11. doi:10.1016/j.biomaterials.2019.01.008
- Lim, H., Lim, Y. M., Kim, K. H., Jeon, Y. E., Park, K., Kim, J., et al. (2018). A novel autophagy enhancer as a therapeutic agent against metabolic syndrome and diabetes. *Nat. Commun.* 9, 1438. doi:10.1038/s41467-018-03939-w
- Liu, X., Eyles, J., McLachlan, A. J., and Mobasheri, A. (2018). Which supplements can I recommend to my osteoarthritis patients? *Rheumatol. Oxf.* 57, iv75–iv87. doi:10.1093/rheumatology/key005
- Loomba, R., Lim, J. K., Patton, H., and El-Serag, H. B. (2020). AGA clinical practice update on screening and surveillance for hepatocellular carcinoma in patients with nonalcoholic fatty liver disease: expert review. *Gastroenterology* 158, 1822–1830. doi:10.1053/j.gastro.2019.12.053
- Manna, P., Das, J., and Sil, P. C. (2013). Role of sulfur containing amino acids as an adjuvant therapy in the prevention of diabetes and its associated complications. *Curr. Diabetes Rev.* 9, 237–248. doi:10.2174/1573399811309030005
- Marra, F., and Svegliati-Baroni, G. (2018). Lipotoxicity and the gut-liver axis in NASH pathogenesis. *J. Hepatol.* 68, 280–295. doi:10.1016/j.jhep.2017.11.014
- Miller, L., Thompson, K., Pavlenko, C., Mettu, V. S., Haverkamp, H., Skaufel, S., et al. (2021). The effect of daily methylsulfonylmethane (MSM) consumption on high-density lipoprotein cholesterol in healthy overweight and obese adults: a randomized controlled trial. *Nutrients* 13, 3620. doi:10.3390/nu13103620
- Mizushima, N., and Klionsky, D. J. (2007). Protein turnover via autophagy: implications for metabolism. *Annu. Rev. Nutr.* 27, 19–40. doi:10.1146/annurev.nutr.27.061406.093749
- Nakhostin-Roohi, B., Barmaki, S., Khoshkharesh, F., and Bohlooli, S. (2011). Effect of chronic supplementation with methylsulfonylmethane on oxidative stress following acute exercise in untrained healthy men. *J. Pharm. Pharmacol.* 63, 1290–1294. doi:10.1111/j.2042-7158.2011.01314.x
- Nazio, F., Strappazzon, F., Antonioli, M., Bielli, P., Cianfanelli, V., Bordi, M., et al. (2013). mTOR inhibits autophagy by controlling ULK1 ubiquitylation, self-association and function through AMBRA1 and TRAF6. *Nat. Cell Biol.* 15, 406–416. doi:10.1038/ncb2708
- Niture, S., Lin, M., Rios-Colon, L., Qi, Q., Moore, J. T., and Kumar, D. (2021). Emerging roles of impaired autophagy in fatty liver disease and hepatocellular carcinoma. *Int. J. Hepatol.* 2021, 6675762. doi:10.1155/2021/6675762
- Pankiv, S., Clausen, T. H., Lamark, T., Brech, A., Bruun, J. A., Outzen, H., et al. (2007). p62/SQSTM1 binds directly to Atg8/LC3 to facilitate degradation of ubiquitinated protein aggregates by autophagy. *J. Biol. Chem.* 282, 24131–24145. doi:10.1074/jbc.M702824200
- Paquette, M., El-Houjeiri, L., Puustinen, P., Blanchette, P., Jeong, H., Dejgaard, K., et al. (2021). AMPK-dependent phosphorylation is required for transcriptional activation of TFEB and TFE3. *Autophagy* 17, 3957–3975. doi:10.1080/15548627.2021.1898748
- Park, H. W., and Lee, J. H. (2014). Calcium channel blockers as potential therapeutics for obesity-associated autophagy defects and fatty liver pathologies. *Autophagy* 10, 2385–2386. doi:10.4161/15548627.2014.984268
- Park, H. W., Park, H., Ro, S. H., Jang, I., Semple, I. A., Kim, D. N., et al. (2014a). Hepatoprotective role of Sestrin2 against chronic ER stress. *Nat. Commun.* 5, 4233. doi:10.1038/ncomms5233
- Park, H. W., Park, H., Semple, I. A., Jang, I., Ro, S. H., Kim, M., et al. (2014b). Pharmacological correction of obesity-induced autophagy arrest using calcium channel blockers. *Nat. Commun.* 5, 4834. doi:10.1038/ncomms5834
- Ribeiro, R. A., Bonfleur, M. L., Amaral, A. G., Vanzela, E. C., Rocco, S. A., Boschero, A. C., et al. (2009). Taurine supplementation enhances nutrient-induced insulin secretion in pancreatic mice islets. *Diabetes Metab. Res. Rev.* 25, 370–379. doi:10.1002/dmrr.959
- Salminen, A., and Kaarniranta, K. (2012). AMP-activated protein kinase (AMPK) controls the aging process via an integrated signaling network. *Ageing Res. Rev.* 11, 230–241. doi:10.1016/j.arr.2011.12.005
- Sheka, A. C., Adeyi, O., Thompson, J., Hameed, B., Crawford, P. A., and Ikramuddin, S. (2020). Nonalcoholic steatohepatitis: a review. *JAMA* 323, 1175–1183. doi:10.1001/jama.2020.2298
- Song, Z., Deaciuc, I., Zhou, Z., Song, M., Chen, T., Hill, D., et al. (2007). Involvement of AMP-activated protein kinase in beneficial effects of betaine on high-sucrose diet-induced hepatic steatosis. *Am. J. Physiol. Gastrointest. Liver Physiol.* 293, G894–G902. doi:10.1152/ajpgi.00133.2007
- Sousa-Lima, I., Park, S. Y., Chung, M., Jung, H. J., Kang, M. C., Gaspar, J. M., et al. (2016). Methylsulfonylmethane (MSM), an organosulfur compound, is effective against obesity-induced metabolic disorders in mice. *Metabolism* 65, 1508–1521. doi:10.1016/j.metabol.2016.07.007
- Sun, J., Mu, Y., Jiang, Y., Song, R., Yi, J., Zhou, J., et al. (2018). Inhibition of p70 S6 kinase activity by A77 1726 induces autophagy and enhances the degradation of superoxide dismutase 1 (SOD1) protein aggregates. *Cell Death Dis.* 9, 407. doi:10.1038/s41419-018-0441-0
- Wang, Z., Yao, T., Pini, M., Zhou, Z., Fantuzzi, G., and Song, Z. (2010). Betaine improved adipose tissue function in mice fed a high-fat diet: a mechanism for hepatoprotective effect of betaine in nonalcoholic fatty liver disease. *Am. J. Physiol. Gastrointest. Liver Physiol.* 298, G634–G642. doi:10.1152/ajpgi.00249.2009
- Xu, L., Huang, D., Hu, Q., Wu, J., Wang, Y., and Feng, J. (2015). Betaine alleviates hepatic lipid accumulation via enhancing hepatic lipid export and fatty acid oxidation in rats fed with a high-fat diet--CORRIGENDUM. *Br. J. Nutr.* 114, 995–996. doi:10.1017/S0007114515002901
- Zhang, Y., Sowers, J. R., and Ren, J. (2018). Targeting autophagy in obesity: from pathophysiology to management. *Nat. Rev. Endocrinol.* 14, 356–376. doi:10.1038/s41574-018-0009-1



OPEN ACCESS

EDITED BY

Stalin Antony,
University of Electronic Science and
Technology of China, China

REVIEWED BY

Vineet Mahajan,
University of Pittsburgh, United States
Evangelos Cholongitas,
National and Kapodistrian University of Athens,
Greece

*CORRESPONDENCE

Yumin Wang,
✉ 721wangym@aliyun.com
Jichao Chen,
✉ chen_hxzxy@sina.com
Mingchao Ding,
✉ dmc_zxl@vip.sina.com

[†]These authors have contributed equally to
this work

RECEIVED 10 November 2023

ACCEPTED 31 December 2023

PUBLISHED 19 January 2024

CITATION

Wang Y, Fleishman JS, Li T, Li Y, Ren Z, Chen J
and Ding M (2024), Pharmacological therapy of
metabolic dysfunction-associated steatotic
liver disease-driven hepatocellular carcinoma.
Front. Pharmacol. 14:1336216.
doi: 10.3389/fphar.2023.1336216

COPYRIGHT

© 2024 Wang, Fleishman, Li, Li, Ren, Chen and
Ding. This is an open-access article distributed
under the terms of the [Creative Commons
Attribution License \(CC BY\)](#). The use,
distribution or reproduction in other forums is
permitted, provided the original author(s) and
the copyright owner(s) are credited and that the
original publication in this journal is cited, in
accordance with accepted academic practice.
No use, distribution or reproduction is
permitted which does not comply with these
terms.

Pharmacological therapy of metabolic dysfunction-associated steatotic liver disease-driven hepatocellular carcinoma

Yumin Wang^{1†}, Joshua S. Fleishman^{2†}, Tongda Li^{3†}, Yulin Li¹,
Zhao Ren⁴, Jichao Chen^{1*} and Mingchao Ding^{5*}

¹Department of Respiratory and Critical Care Medicine, Aerospace Center Hospital, Peking University
Aerospace School of Clinical Medicine, Beijing, China, ²Department of Pharmaceutical Sciences, College
of Pharmacy and Health Sciences, St. John's University, Queens, NY, United States, ³Department of
Traditional Chinese Medicine, Beijing Geriatric Hospital, Beijing, China, ⁴Department of Pharmacy,
Aerospace Center Hospital, Peking University Aerospace School of Clinical Medicine, Beijing, China,
⁵Department of Peripheral Vascular Intervention, Aerospace Center Hospital, Peking University
Aerospace School of Clinical Medicine, Beijing, China

In light of a global rise in the number of patients with type 2 diabetes mellitus (T2DM) and obesity, non-alcoholic fatty liver disease (NAFLD), now known as metabolic dysfunction-associated fatty liver disease (MAFLD) or metabolic dysfunction-associated steatotic liver disease (MASLD), has become the leading cause of hepatocellular carcinoma (HCC), with the annual occurrence of MASLD-driven HCC expected to increase by 45%–130% by 2030. Although MASLD has become a serious major public health threat globally, the exact molecular mechanisms mediating MASLD-driven HCC remain an open problem, necessitating future investigation. Meanwhile, emerging studies are focusing on the utility of bioactive compounds to halt the progression of MASLD to MASLD-driven HCC. In this review, we first briefly review the recent progress of the possible mechanisms of pathogenesis and progression for MASLD-driven HCC. We then discuss the application of bioactive compounds to mitigate MASLD-driven HCC through different modulatory mechanisms encompassing anti-inflammatory, lipid metabolic, and gut microbial pathways, providing valuable information for future treatment and prevention of MASLD-driven HCC. Nonetheless, clinical research exploring the effectiveness of herbal medicines in the treatment of MASLD-driven HCC is still warranted.

KEYWORDS

hepatocellular carcinoma, non-alcoholic fatty liver disease, metabolic dysfunction-associated steatotic liver disease, natural products, treatment

Introduction

As the most common type of primary liver cancer, hepatocellular carcinoma (HCC) represents the fifth most common cancer worldwide (Akinyemiju et al., 2017). Currently, HCC is on the path to globally becoming the second most common cause of cancer-related death. Historically, cirrhosis induced by chronic infections (such as hepatitis B/C virus) and alcoholic hepatotoxicity are the two major causes of HCC (Villanueva, 2019). However, the incidence of chronic infection-associated HCC is decreasing with the development of anti-

HCV drugs and anti-HBV vaccines (Akinyemiju et al., 2017). Accumulating evidence suggests that HCC-associated mortality is increasing steadily, indicating that other risk factors besides alcohol and viral hepatitis drive HCC pathogenesis.

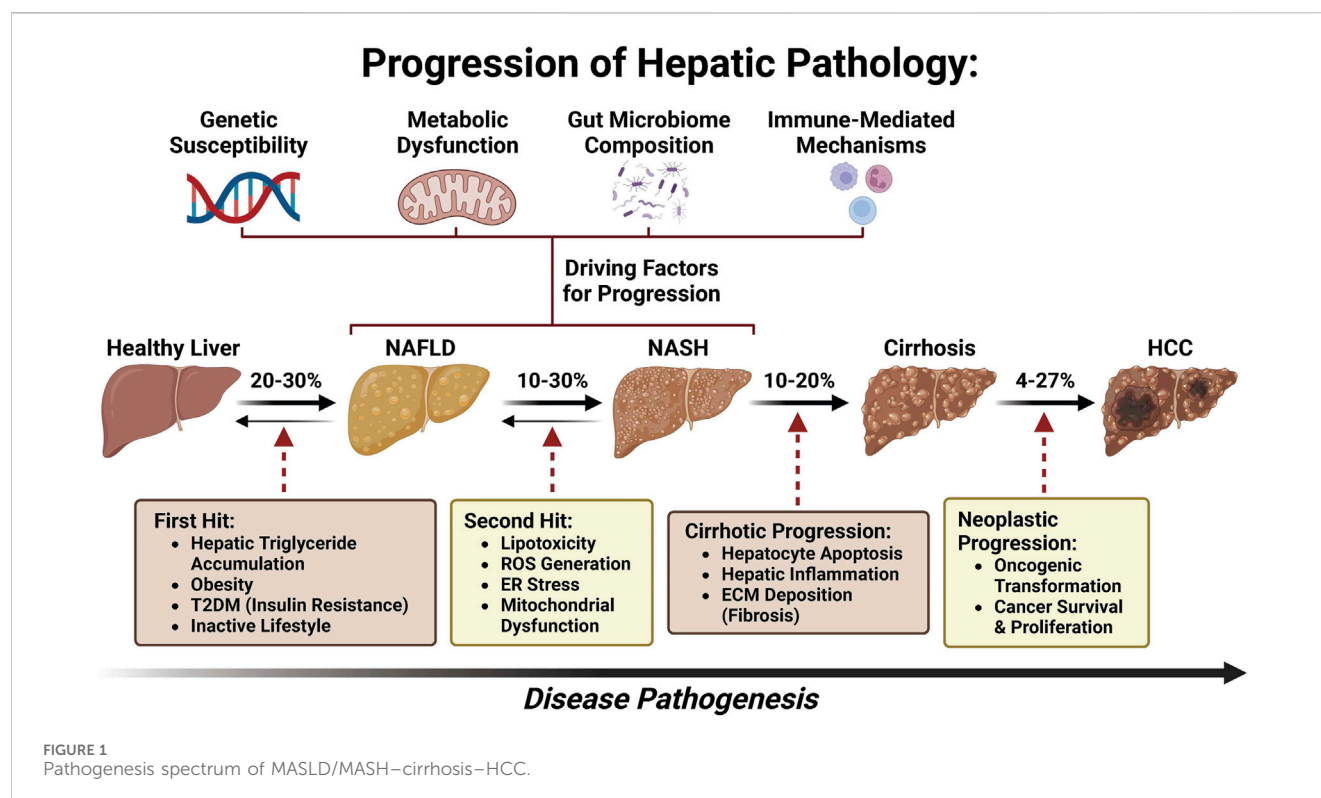
With a global rise in the number of patients with type 2 diabetes mellitus (T2DM) and obesity, non-alcoholic fatty liver disease (NAFLD), now named metabolic dysfunction-associated fatty liver disease (MAFLD) (Eslam et al., 2020a; Eslam et al., 2020b; Lim et al., 2021; Pirola and Sookoian, 2022; Sangro et al., 2023) or metabolic dysfunction-associated steatotic liver disease (MASLD) (Yang et al., 2023; Rinella et al., 2023a; Rinella et al., 2023b; Rinella et al., 2023c; Noureddin et al., 2023; He et al., 2023; Chan et al., 2023; Hagström et al., 2023), has been postulated to become the leading etiology of HCC, leading to MASLD-associated hepatocellular carcinoma (MASLD-HCC) (Younossi et al., 2018; Zhou et al., 2019; Sarin et al., 2020; Talamantes et al., 2023). The prevalence of MASLD-HCC is increasing in most countries worldwide and presents a major healthcare burden (Koh et al., 2024). However, the underlying molecular mechanism of MASLD progression to HCC remains largely unknown (Yu et al., 2020; Di Maira et al., 2022). As a disease continuum progressing from simple steatosis to non-alcoholic steatohepatitis (NASH), now named as metabolic dysfunction-associated steatohepatitis (MASH) and fibrosis, MASLD affects 25% of adults and is one of the most common chronic liver diseases globally (Bence and Birnbaum, 2021; Powell et al., 2021; Kalligeros et al., 2023). Approximately 27% of cirrhosis induced by MASH could progress to MASLD-HCC (Ioannou, 2021) (Figure 1). Although several drugs are being tested for MASLD/MASH treatment, no curative agents are effective against MASLD-HCC (Wong, 2018). Therefore, there is an unmet need for the discovery of novel and safe drugs for MASLD-HCC. Meanwhile,

emerging bioactive compounds have been shown to halt the progression of MASLD to MASLD-driven HCC (Khairnar et al., 2023).

This article aims to assess the recent advancements in pharmacological therapy against MASLD-HCC. In this review, we first briefly review the possible main mechanisms of the progression and pathogenesis of MASLD-HCC. Then, we overview the application of bioactive compounds in mitigating MASLD-HCC. We categorize drugs that treat MASLD-HCC by their mechanisms (anti-inflammatory, lipid metabolism, and gut microbiota), providing valuable information for future treatment and prevention of MASLD-HCC.

Distinctive features of MASLD-HCC

Patient demographics have revealed that patients with MASLD and HCC are mainly White, male, and older than patients with HCC from other origins (Degasperis and Colombo, 2016). A prospective multicenter study in Italy indicates that compared to patients with hepatitis C-related tumors, 54% of MASLD-HCC patients had no evidence of cirrhosis histologically or clinically, were younger, and were less frequently diagnosed during surveillance (Piscaglia et al., 2016). MASLD-HCC tumors tended to be larger and fell less frequently within the Milan criteria or in BCLC stage 0. Compared to HCV-related HCC, MASLD-HCC manifested an infiltrative pattern (Piscaglia et al., 2016). This observation was corroborated by a retrospective cohort HCC study at the Veterans Affairs Hospitals in the United States, in which patients with hepatitis C HCC were younger than those with MASLD-HCC (Mittal et al., 2015). HCC in veterans with MASLD was



Pathogenic Mechanisms of NAFLD-HCC Progression:

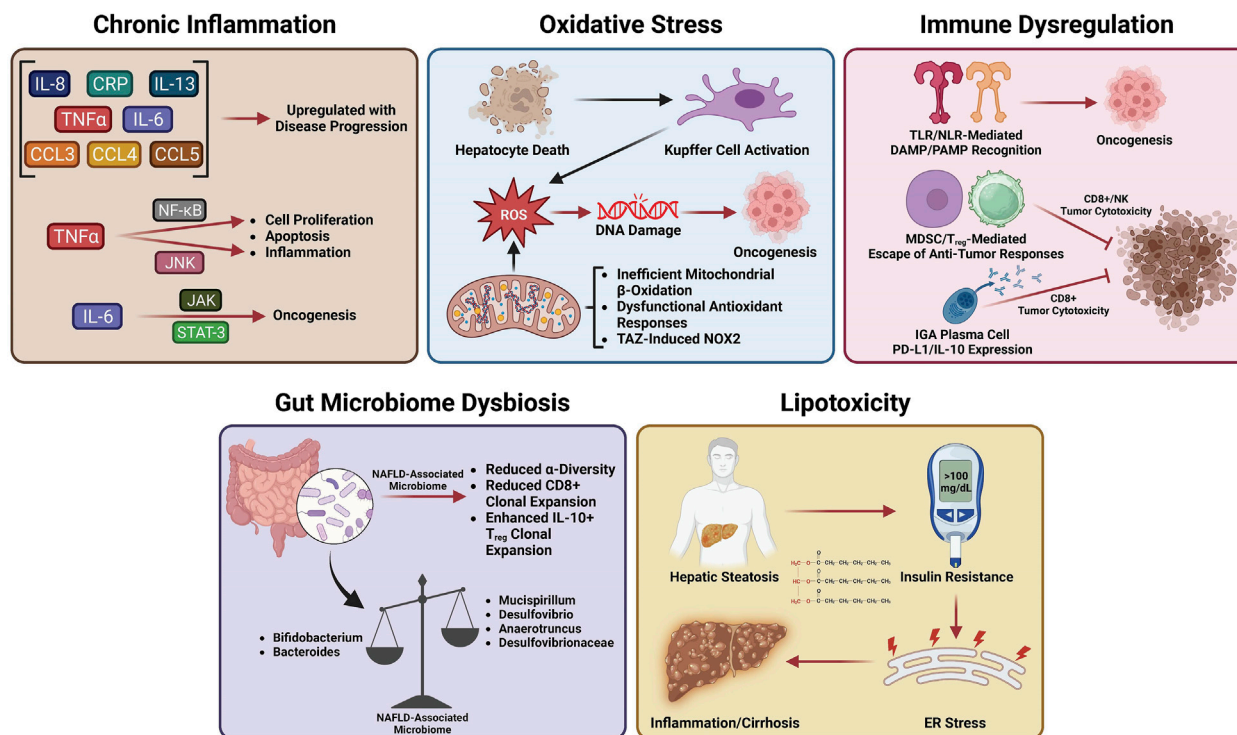


FIGURE 2
Pathogenic mechanisms of MASLD-HCC progression.

distinctively characterized by diabetes and dysmetabolism, including peripheral arteriopathy, myocardial infarction, and congestive heart failure. Owing to the burdens of age and comorbidities, patients in the hepatitis C group had a higher likelihood of curative treatment than those with MASLD-HCC (22% VS 11%) (Mittal et al., 2015). A more recent study provided compelling evidence that HCC may also develop in MASLD patients with persistently normal values of transaminase activity (Natarajan et al., 2020).

It has been shown in both population-based and large cohort studies that MASLD patients have an increased risk for metabolic syndrome and diabetes complication-associated cardiovascular comorbidities compared with patients with HCC without MASLD. The median age was 73 years and 66 years in patients with MASLD and hepatitis C, respectively, as per the SEER Registry (Younossi et al., 2015). White patients accounted for 57% (1,560/2,536) of 2,536 patients with hepatitis C and 76% (532/701) of 701 cases with MASLD (Younossi et al., 2015). These results aligned well with the findings of the cohort study of 1,500 American veterans with HCC, where it was reported that the prevalence of arterial hypertension (95% vs 70%) and diabetes (89% vs 33%) was higher in the MASLD patient group than in patients with hepatitis C (Mittal et al., 2015). MASLD patients had significantly higher rates of cardiovascular disease and peripheral vascular disease. Mittal's study uncovered that a poor prognosis in patients with MASLD results from the burden of comorbidities, leading to limited access to more radical treatments, such as

hepatic resection or transplantation (Mittal et al., 2015). A recent retrospective study replicated these findings, which compared the clinicopathological characteristics and prognosis of patients undergoing surgical resection in MASLD/MASH-associated HCC and other HCC etiologies (Pal Chaudhary et al., 2023). A total of 110 HCC patients had MASLD/MASH, and 150 patients had other etiologies. The median age at diagnosis was lower in the other etiology cohort than in the MASLD/MASH-HCC cohort, with a decreased number of female patients (Pal Chaudhary et al., 2023). The diameter of tumors induced by MASLD/MASH was more commonly >5 cm. There were no significant differences in rates of lymphovascular or perineural invasion, histologic grade, or serum AFP levels. There was a lower rate of background liver fibrosis, lower aspartate transaminase, lower alanine aminotransferase, and higher platelet counts in the MASLD/MASH cohort (Pal Chaudhary et al., 2023). These findings suggest that patients with MASLD/MASH-HCC more commonly presented with larger HCC tumors and lacked liver fibrosis than those with HCC due to other etiologies.

Pathogenesis of MASLD-driven HCC

Many studies have investigated the specific mechanisms of transition from MASLD/MASH to HCC. It is thought that this process involves multiple factors including oxidative stress, lipotoxicity, gut dysbiosis, metabolic imbalances, chronic injury,

and hypoxia, which, in turn, stimulate chronic inflammation, tissue scarring, and HCC pathogenesis (Cannito et al., 2023). In this section, we will summarize the current knowledge about these factors and how they may be involved in the transition from MASLD/MASH to HCC (Figure 2).

Chronic inflammation in MASLD-HCC

Many variables play a role in the MASLD to MASH transition, including metabolic dysfunction, oxidative stress, gut dysbiosis, lipotoxicity, and hepatocellular necrosis, all of which induce chronic inflammation, leading to perpetual tissue injury, parenchymal cell regeneration, mutagenesis, and HCC tumorigenesis. Hepatic oxidative stress, inflammation, and insulin resistance (IR) are important features and hallmarks of MASLD-HCC (Talamantes et al., 2023). Enhanced inflammation and IR are found in patients with HCC, evidenced by elevated levels of pro-inflammatory cytokines such as interleukin-6 (IL-6), tumor necrosis factor- α (TNF- α), and C-reactive protein (Aleksandrova et al., 2014; Duan et al., 2022). Both obesity and IR systemically are responsible for HCC tumorigenesis as they induce inflammation and activate oncogenic pathways (Margini and Dufour, 2016). The chronic low-grade inflammation that has been linked to HCC development is a distinctive feature of MASLD (Talamantes et al., 2023). Hepatocellular injury due to persistent stimulation of innate and adaptive immune pathways, gut dysbiosis, and low-grade chronic systemic inflammation in MASLD (Cannito et al., 2023) all contribute to the pathogenesis of MASLD-HCC (Marengo et al., 2016; Polyzos et al., 2023; Talamantes et al., 2023). The liver is chronically exposed to TNF- α and IL-6, the two major obesity-associated adipose-derived pro-inflammatory cytokines (Avgerinos et al., 2019; Potoupni et al., 2021). Cytokines facilitate inflammatory and immune tolerance in the liver microenvironment. Chemokines have also been associated with the pathogenesis of MASLD-HCC. It was found that MASLD-HCC patients have higher plasma levels of IL-8, IL-13, chemokine (C-C motif) ligand (CCL-3), CCL-4, and CCL-5, which are correlated with activated circulating monocytes (Ponziani et al., 2019). Several signaling pathways linked to inflammation, steatosis, and oncogenes can be activated by IL-6 and TNF- α in hepatocytes. Upregulation of TNF- α and IL-6 promoted hepatic steatosis and inflammation in a mouse obesity model (Park et al., 2010). Of note, Janus kinase/signal transducer and activator of transcription 3 (JAK/STAT-3) and c-Jun N-terminal kinase/nuclear factor kappa B (JNK/NF- κ B) pathways are commonly activated in HCC (Llovet et al., 2021). TNF- α activates the NF- κ B and JNK pathways, inducing the transcription of genes involved in hepatic cell proliferation, inflammation, and apoptosis (Yu et al., 2013). IL-6 activates the JAK/STAT-3 pathway, which is linked to cell differentiation and cell growth (Grohmann et al., 2018). Furthermore, oncogenic STAT3 activity associated with HCC pathogenesis is induced by both the inflammatory response and steatosis (Park et al., 2010). The detailed role of intracellular mitogenic, anti-apoptotic, and other signaling pathways involved in the pathogenesis of MASLD-HCC has been recently reviewed [see (Polyzos et al., 2023; Talamantes et al., 2023) for a recent review].

Oxidative stress in MASLD-HCC

Accumulating evidence reveals that the role of oxidative stress in the pathogenesis of MASLD-HCC is well-elucidated and established, with precise mechanistic exploration recently published (Brahma et al., 2021; Gabbia et al., 2021). Excessive hepatic lipid exposure triggers oxidative stress-dependent cell damage through different mechanisms (Bessone et al., 2019). Oxidative stress and ensuing hepatocyte death substantially promote cell proliferation and activate hepatic resident Kupffer cells simultaneously, which secrete chemokines and cytokines to recruit other immune cells, thereby intensifying inflammation and further facilitating the production of reactive oxygen species (ROS) (Wen et al., 2021). At the same time, chronic oxidative stress promotes genomic DNA mutations and upregulates HCC development-related genes (Wen et al., 2021). Increased lipid accumulation can generate pathogenic drivers of carcinogenesis in hepatocytes, in particular oxidative DNA damage (Tanaka et al., 2013; Masarone et al., 2018), which has been found higher in the hepatocytes of MASH-HCC patients than in the hepatocytes of MASH patients without HCC (Tanaka et al., 2013). Inadequate mitochondrial respiratory chain activity and elevated mitochondrial fatty acid β -oxidation (FAO) lead to production of ROS in hepatocytes that can damage DNA in MASLD (Begrache et al., 2013). Dysfunction of antioxidant cellular mechanisms can result in an elevation in fatty acid (FA) metabolism-associated pathways, which causes fatty acid accumulation, steatosis, and metabolic stress (Masarone et al., 2018). Enhanced FA accumulation leads to *de novo* lipogenesis (DNL) and FAO, which promotes ROS generation (Perla et al., 2017). Hepatic steatosis functions as a precursor for ROS generation and can promote STAT-1 and STAT-3 activity through oxidizing constitutively active phosphatases, driving MASH, fibrosis, and HCC pathogenesis (Grohmann et al., 2018). Since increased oxidative stress and ROS have been linked to the transition from MASLD to HCC, emerging studies have focused on uncovering the role of NADPH oxidases (NOXs) in MASLD-HCC. Wang et al. (2022) have shown that the transducer of the Hippo pathway, transcriptional co-activator with PDZ binding motif (TAZ), contributes to MASH-associated HCC in pre-tumor MASH hepatocytes via induction of Cybb and NOX2-mediated DNA damage. This interesting study provided compelling evidence that TAZ plays a role in the progression of MASH to HCC and suggested a future therapeutic option for treating MASH-HCC by targeting MASH through TAZ. Wang et al. (2022) provided a new research paradigm to assess the molecular mechanisms related to MASLD/MASH-HCC, observing pathogenesis by modulating TAZ-mediated NOX2-derived oxidative damage to the DNA of hepatocytes. The author suggested that TAZ-mediated therapies may be a potential avenue for MASH-HCC treatment.

Immune dysregulation in MASLD-HCC

The role of the immune response in the pathogenesis of MASLD-HCC has been comprehensively revealed and summarized elsewhere [see (Anstee et al., 2019; Hirsova et al., 2021; Zhang and Yang, 2021; Riaz et al., 2022; Yahoo et al., 2023) for a recent review]. In short, chronic inflammation

induced by pathogen-associated molecular patterns (PAMPs) and damage-associated molecular patterns (DAMPs) serves as a significant driver of hepatocarcinogenesis (Park et al., 2010; Arrese et al., 2016). Vital immunosuppression by T regulatory cells (Tregs) and myeloid-derived suppressor cells (MDSCs) on cytotoxic CD8⁺ T cells and natural killer (NK) cells mediates immune escape from antitumor responses. Targeting the recruitment of MDSCs and Tregs into the liver is a potentially druggable step in the pathogenesis of MASH-HCC, especially after observing that platelet-derived platelet glycoprotein Iba (GPIIb) proved critical for the development of MASH-HCC (Malehmir et al., 2019). The role of adaptive immunity in the pathogenesis of MASLD-HCC has also been revealed, showing that IgA⁺ plasma cells accumulate in MASH fibrosis and lead to MASLD-HCC by inhibiting CD8⁺ T cells via IL-10 and programmed cell death ligand 1 (PD-L1) expression (Shalapour et al., 2017). These immunosuppressive IgA⁺ plasma cells may play a key role in the gut microbiome–liver axis, contributing to HCC carcinogenesis by providing mucosal IgA exposure.

Gut microbiome dysbiosis in MASLD-HCC

Recent studies have shown that gut microbiota dysbiosis contributes to MASLD-HCC formation, even in the absence of cirrhosis (Xie et al., 2016; Sydor et al., 2020; Yahoo et al., 2023). Emerging studies demonstrate that the intestinal microbiota play a role in stimulating and maintaining liver inflammation, which becomes more pro-inflammatory as the disease progresses toward HCC (Xie et al., 2016; Sydor et al., 2020). This initial animal study was corroborated by a clinical study, which reported a decreased abundance of *Bifidobacterium* and an elevated abundance of Ruminococcaceae and *Bacteroides* in MASLD-HCC patients compared to patients with cirrhosis, which did not progress to MASLD-HCC (Ponziani et al., 2019). Decreased α -diversity (a measure of microbiome diversity applicable to a single sample) was found in patients with MASLD-HCC (Ponziani et al., 2019). Later work elaborated on this finding, demonstrating that a decreased α -diversity and the Chao-1 richness index were found in patients with MASLD-HCC (Behary et al., 2021). In addition, there is a relationship between the gut microbiota and several inflammatory cytokines such as higher levels of IL-8 and CCL-3 in patients with MASLD-HCC (Ponziani et al., 2019). This suggests that inflammation driven by gut microbiota may aggravate the progression of MASLD-HCC. This dysbiosis was confirmed by Behary et al. (2021) in MASLD-HCC and MASLD-cirrhosis patients. An increased rarity index was found in patients with MASH-HCC with cirrhosis (Sydor et al., 2020). Gut microbiota also function as cofactors in the pathogenesis of MASLD-HCC via interaction with immune cells. A recent study on 32 MASLD-HCC patients indicates that gut microbiota augment the expansion of IL-10⁺ Treg cells but reduce the expansion of CD8⁺ T cells (Behary et al., 2021). Gut microbiota dysbiosis contributes to the pathogenesis of MASLD-HCC in a spontaneous MASLD-HCC mouse model. Dietary cholesterol can trigger MASLD-HCC tumorigenesis by enhancing the abundance of *Desulfovibrio*, *Mucispirillum*, *Desulfovibrionaceae*, and *Anaerotruncus* and decreasing levels of *Bacteroides* and *Bifidobacterium* (Odenwald

and Turner, 2017). Gut microbiota dysbiosis and alteration of gut bacterial metabolites contribute to the pathogenesis of MASLD-HCC in mice, and several probiotics including *Lactobacillus* and *Bifidobacterium* strains were identified as depleted in MASLD-HCC (Zhang X. et al., 2021).

Role of lipotoxicity and glucotoxicity in MASH and HCC development

Hepatocytes function as a major site for fat accumulation, making them a main target of lipotoxicity (Rao et al., 2023; Yahoo et al., 2023). IR in adipose tissue results in enhanced release of free FAs and delivery to the liver, allowing for excessive lipid accumulation and toxic metabolite-induced lipotoxicity, causing mitochondrial dysfunction and endoplasmic reticulum stress (ERS) (Venkatesan et al., 2023; Yahoo et al., 2023). Increased free FA flux to the mitochondria enhances the rates of FAO, leading to increased ROS production (Serviddio et al., 2013). In MASLD, the damage in balance between antioxidant mechanisms and ROS production results in oxidative stress and thereby further induces mitochondrial dysfunction. Uncontrolled ROS production and the ensuing oxidative stress directly cause damage to cellular macromolecules such as DNA, proteins, and lipids (Chen et al., 2020). Lipotoxicity mediated by diacylglycerol and non-esterified FAs facilitates hepatic IR and ERS, which results in chronic inflammation, hepatic fibrosis, hepatic cirrhosis, and ultimately HCC (Samuel et al., 2010; Hardy et al., 2016; Piscaglia et al., 2016; Foerster et al., 2022). A recent study has revealed that decreased lysine-specific demethylase 6B (KDM6B), a key mediator of gene transcription, contributes to the development of MASLD-related HCC. This is accomplished by acquiring resistance to lipotoxicity via epigenetic downregulation of G0S2 expression-mediated activation of adipose triglyceride lipase/patatin-like phospholipase domain containing 2 (ATGL/PNPLA2) (Hatano et al., 2023). KDM6B loss may promote cell survival through activation of ATGL/PNPLA2 in NASH-related HCC. A high ATGL/PNPLA2 activation level was found in KDM6B-KO cells. Genetic or pharmacological inhibition of ATGL/PNPLA2 increased lipid accumulation and decreased cell proliferation in KDM6B-KO cells. ATGL/PNPLA2 overexpression facilitates the growth of HCC cells (Liu et al., 2019). Silencing G0S2 conferred lipotoxicity resistance in KDM6B-expressed HCC cells, whereas ATGL/PNPLA2 inhibition in the KDM6B-KO cells reduced these effects. These results indicate that targeting the KDM6B–G0S2–ATGL/PNPLA2 pathway may be a useful therapeutic strategy for MASLD-related HCC. Pharmacologically induced lipotoxicity comprising LXR agonists and Raf inhibitors represents a promising therapeutic strategy for the treatment of MASLD-related HCC (Rudalska et al., 2021).

Current pharmacological therapies for MASH-driven HCC

Following a better understanding of the molecular mechanisms behind MASLD/MASH-HCC progression, research on anti-MASLD/MASH-HCC small molecules has intensified, resulting

TABLE 1 List of available potential compounds targeting different mechanisms to treat MASLD-driven HCC.

Compound	Experimental model	Involved mechanism	Effects	Ref
Saroglitazar	DEN + CDAHFD/C57BL/6 mice	Anti-inflammation	↓ Liver injury markers (serum ALT and AST); ↓ hepatic steatosis; ↓ pro-inflammatory cytokines like TNF- α in the liver; ↑ serum adiponectin and osteopontin levels; ↓ hepatic tumors; ↓ hepatic tumorigenesis	Giri et al. (2023)
9-Xanthylacetic acid	CDAHFD/C57BL/6J male mice	Anti-inflammation; anti-fibrosis	↓ Hepatic TAG accumulation; ↓ collagen α 1 content; ↓ F4/80-positive liver parenchyma; ↓ HCC development; ↓ body weight of mice; ↓ serum TGFA	Gnocchi et al. (2023)
Scoparone	HFD/DEN/C57BL/6J mice	Anti-inflammation	↓ Hepatic pathological changes; ↓ incidence and multiplicity of the tumor; ↑ liver functions; ↓ hepatic inflammation; ↓ NF- κ B p65; ↓ TNF- α , MCP-1, iNOS, COX-2, NF- κ B, and MMP-9; ↓ activation of the MAPK/Akt	Ye et al. (2023)
Tipifarnib	CDAHFD/DEN/C57BL/6J mice	Anti-inflammation	↓ HIF-1 α ; ↓ cell proliferation; ↑ apoptosis; ↓ IL-6; ↓ phosphorylated NF- κ B; ↓ TGF- β ; ↓ tumor nodule formation	Yamada et al. (2023a)
Eicosapentaenoic acid	DEN + HFD-fed mice	Anti-inflammation	↓ Hepatocarcinogenesis; ↓ activation of the pro-tumorigenic IL-6 effector STAT3	Inoue-Yamauchi et al. (2018)
Probiotics	Hepatocyte-specific PTEN knockout mouse	Anti-inflammation Antioxidant	↓ Serum transaminase levels; ↓ MASLD activity score; ↓ pro-inflammatory cytokines; ↓ liver fibrosis grade; ↓ the number of liver tumors; ↓ oxidative stress	Arai et al. (2022)
Metformin	HFD-fed mice	Anti-inflammation	↓ Hepatocarcinogenesis; ↓ fat accumulation in the liver, associated with the suppression of adipose tissue inflammation	Tajima et al. (2013)
Apo-10'-lycopenoic acid	DEN + HFD-fed mice	Anti-inflammation	↓ Hepatic tumorigenesis and lung tumor incidence; ↑ hepatic SIRT1 protein and deacetylation of SIRT1 targets; ↓ caspase-1 activation and SIRT1 protein cleavage; ↑ glucose intolerance; ↓ hepatic inflammation	Ip et al. (2013)
Liraglutide	STZ + HFD-fed mice	Anti-inflammation	↓ Steatosis, inflammation, and hepatocyte ballooning; ↓ hepatocarcinogenesis	Kojima et al. (2020)
Vildagliptin	HFD-fed rat	Anti-inflammation	↓ Tumor progression by mediating the pro-angiogenic role of CCL2	Qin et al. (2018)
Rosuvastatin	HFD-fed mice	Anti-inflammation	↓ Hepatocarcinogenesis; ↓ TNF- α , IL-6, and TGF- β 1; ↓ VEGFR, EGFR, and PDGF	Yokohama et al. (2016)
Lycopene	STZ + HFD-fed mice	Anti-inflammation	↓ Hepatocarcinogenesis; ↓ IL6; ↓ NF- κ B p65 (Ser536) phosphorylation; ↓ STAT3 (Tyr705) phosphorylation	Ip et al. (2014)
Berberine	STZ + HFHC	Anti-inflammation; anti-angiogenesis	↓ Hepatocarcinogenesis; ↓ the expressions of genes related to lipogenesis, inflammation, fibrosis, and angiogenesis; ↓ phosphorylation of p38MAPK and ERK as well as COX2 expression	Luo et al. (2019)
Lycopene and tomato extract	DEN + HFD-fed rat	Antioxidant	↓ Hepatocarcinogenesis; ↓ glutathione S-transferase; ↓ cyclin D1; ↓ ERK; ↓ nuclear NF- κ B; ↓ lipid peroxidation; ↓ cytochrome P450 2E1; ↓ inflammatory foci; ↓ mRNA expression of pro-inflammatory cytokines (TNF- α , IL-1 β , and IL-12); ↑ nuclear Nrf2 and HO-1	Wang et al. (2010)

(Continued on following page)

TABLE 1 (Continued) List of available potential compounds targeting different mechanisms to treat MASLD-driven HCC.

Compound	Experimental model	Involved mechanism	Effects	Ref
Curcumin	DEN + HFD-fed mice	Antioxidant	↓ Steatosis, fibrosis associated with decreasing serum aminotransferases; ↓ IFN γ , IL-1 β , and IFN γ -inducible protein 10; ↓ VEGF, glypican-3, and prothrombin; ↑ Nrf2; ↓ hepatic C/EBP β , CYP2E1, p-ERK1/2, and p67phox; ↓ SREBP1c	Afrin et al. (2017)
		Anti-inflammation		
		Anti-fibrosis		
		Inhibit lipogenesis		
NV556	STZ + HFD-fed mice	Anti-fibrosis	↓ The number and diameter of tumorous nodules; ↓ collagen deposition	Kuo et al. (2019)
Pioglitazone	DEN + CDAHFD-fed mice	Anti-fibrosis	↓ HCC development in both models; ↓ gross tumor nodules; ↓ fibrosis progression; ↓ activation of MAPK; ↑ AMPK	Li et al. (2019)
Ezetimibe	Pten ^{Δhep} mice were fed a HFD	Anti-fibrosis	↓ Tumor growth; ↓ cholesterol levels; ↓ angiogenetic processes; ↓ inflammation, liver fibrosis	Miura et al. (2019)
		Regulating lipid metabolism		
n-3 PUFAs	STZ/HFD-treated mice	Regulating lipid metabolism	↑ Survival of these mice; ↓ tumor size, and tumor number; ↑ hepatic n-3 PUFA content and n-3/n-6 PUFA ratio; ↓ hepatic lipid accumulation	Liebig et al. (2019)
Mulberry (<i>Morus alba</i> L.) leaf powder	STZ/HFD-treated mice	Regulating lipid metabolism	↓ Hepatocarcinogenesis; ↓ fat deposition	Wakame et al. (2022)
Daikenchuto (TU-100)	Spontaneous MASH TSOD mouse	Anti-inflammation	↓ The expression of IL6, IL1B, and ACTA2 mRNA in the liver; ↓ levels of serum alanine aminotransferase; ↓ MASH; ↓ tumor diameter; ↑ intestinal microbiome, the genera <i>Blautia</i> and <i>Ruminococcus</i> ; ↓ Dorea and Erysipelotrichaceae	Yamada et al. (2023b)
		Regulating gut microbiota		
Curcuma	DEN + HFD-fed rat	Anti-inflammation	↓ IL-1 β , IL-6, TNF- α , IL-2, and IL-7 in the serum and hepatic tissue; ↑ IL-10 in the serum and hepatic tissue; ↓ COX-2, PGE2, and NF- κ B in the serum and hepatic tissue; ↑ gut microbial diversity and richness; ↓ abundance of genera <i>Mucispirillum</i> and <i>Clostridium</i>	Zhang et al. (2021b)
		Regulating gut microbiota		
Dietary tomato powder	DEN + HFD BCO1/BCO2 double knockout mice	Anti-inflammation	↓ HCC development (incidence, multiplicity, and tumor volume); ↓ hepatic inflammatory foci development; ↓ IL-1 β , IL-6, IL-12 α , monocyte chemoattractant protein-1, and iNOS (mRNA); ↑ sirtuin mRNA; ↑ hepatic circadian clock genes; ↑ gut microbial richness and diversity; ↓ relative abundance of the genera <i>Clostridium</i> and <i>Mucispirillum</i>	Xia et al. (2018)
		Regulating gut microbiota		
<i>B. pseudolongum</i>	DEN + HFHC-fed C57BL/6	Regulating gut microbiota	↓ MASLD-HCC formation in two mouse models; ↑ healthy gut microbiome composition; ↑ gut barrier function. Mechanistically, <i>B. pseudolongum</i> -produced acetate entered the portal vein to reach to the liver and bind to G coupled-protein receptor 43 (GPR43) on hepatocytes. GPR43 activation suppressed the IL-6/JAK1/STAT3 signaling pathway, thereby preventing MASLD-HCC progression	Song et al. (2023)
<i>B. pseudolongum</i>	MASLD-HCC cell lines (HKIC2 and HKIC10)	Regulating gut microbiota	MASLD-HCC cell co-incubation with <i>B.p</i> CM significantly suppressed cell proliferation, inhibited the G1/S phase transition, and induced apoptosis	Song et al. (2023)

(Continued on following page)

TABLE 1 (Continued) List of available potential compounds targeting different mechanisms to treat MASLD-driven HCC.

Compound	Experimental model	Involved mechanism	Effects	Ref
Acetate	MASLD-HCC cell lines (HKCI2 and HKCI10)	Regulating gut microbiota	↓ Cell proliferation and induced cell apoptosis	Song et al. (2023)
Acetate	DEN + HFHC-fed C57BL/6	Regulating gut microbiota	↓ MASLD-HCC tumor formation <i>in vivo</i>	Song et al. (2023)
Mebendazole	Human MASLD-HCC cell lines (HKCI2 and HKCI10); MASLD-HCC xenografts	Inducing apoptosis	↓ MASLD-HCC growth; ↑ apoptosis; ↑ cellular senescence. Mebendazole synergized with navitoclax to inhibit MASLD-HCC cell growth via the induction of intrinsic and extrinsic apoptosis pathways	Yang et al. (2023b)
Metformin	Intrahepatic RIL-175 tumors of mice fed with MCD	Regulating immunity	Metformin treatment rescued the efficacy of anti-PD-1 therapy against liver tumors in MASH	Wabitsch et al. (2022)
AM06	STZ + HFD-fed mice	Regulating immunity	↓ MASH severity; ↓ progression of MASH to HCC; ↑ hepatic CXCR6+ natural killer T (NKT) cell; ↓ macrophage infiltration	Li et al. (2022)
Losartan	HFD/MUP-uPA mice	Regulating immunity	↓ Liver and peritumoral fibrosis; ↑ anti-PD-1-induced tumor regression; ↑ HCC infiltration by effector CD8 ⁺ T cells compared to the PD-1 blockade alone. The beneficial effects of losartan correlated with blunted TGF-β receptor signaling, reduced collagen deposition, and depletion of immunosuppressive fibroblasts	Gu et al. (2023)
Anti-CD122 antibody	High-fat/high-sucrose diet/C57BL/6 N	Regulating immunity	↓ Number of CXCR6+PD-1+ cells; ↑ OVA-specific CD8 activity; ↓ HCC growth compared to untreated MASH mice	Lacotte et al. (2023)
Metformin	HFD/transgenic zebrafish	Regulating immunity	↓ Macrophage polarization, liver size, and micronuclei formation in MASLD-associated HCC larvae; ↑ T-cell density in the liver, which was reversed by treatment with metformin	de Oliveira et al. (2019)
Honokiol	HFD-fed mice	—	↓ Hepatocarcinogenesis; ↓ EGFR signaling; ↓ nuclear translocation of GR; ↑ MIG6/ERRFI1 expression, leading to EGFR degradation	Okuda et al. (2021)
Gallic acid	HFD-fed male C57BL/6J mice	—	MASLD-HCC progression	Zhang et al. (2023a)
T0901317-sorafenib	CD-HFD-fed male C57BL/6 mice	Inducing lipotoxicity	↓ MASH-induced tumor development	Rudalska et al. (2021)

AM06, breast milk-isolated *Akkermansia muciniphila*; AMPK, AMP-activated protein kinase; CCL2, chemokine ligand 2; CDAA, choline-deficient L-amino acid-defined diet; CDAHFD, choline-deficient, L-amino acid-defined, high-fat diet; CD-HFD, choline-deficient high-fat diet; COX-2, cyclooxygenase; DEN, diethylnitrosamine; EGFR, epidermal growth factor receptor; ERRFI1, ERBB receptor feedback inhibitor 1; HFHC, high-fat and high-cholesterol diet; HFD, high-fat diet; FNY, interferon γ; GR, glucocorticoid receptor; IL-1β, interleukin-1β; IL-6, interleukin-6; iNOS, inducible NO synthase; MAPK, mitogen-activated protein kinase; MCD, methionine/choline-deficient diet; MIG6, mitogen-inducible gene 6; NF-κB, nuclear factor kappa B; PDGF, platelet-derived growth factor; PGE2, prostaglandin E2; STZ, streptozotocin; TNF-α, tumor necrosis factor-α; VEGFR, vascular endothelial growth factor receptor.

in an exponentially increasing number of published articles on this field. We present newly identified small molecules for the inhibition of MASLD-HCC disease progression (Table 1; Figure 3), describing drugs targeting anti-inflammatory, antioxidant, anti-fibrotic, anti-lipid metabolic, microbiota-pertaining, and immunomodulatory mechanisms.

Anti-inflammatory drugs

Saroglitazar, a novel PPAR-α/γ agonist with predominant PPAR-α activity, has been shown to inhibit symptoms of MASH.

A recent study has shown that it prevents the development of MASLD-HCC in rodents (Giri et al., 2023). Saroglitazar significantly reversed hepatic steatosis, reduced hepatic injury, and decreased the levels of pro-inflammatory cytokines in the livers of diethylnitrosamine (DEN)-treated, choline-deficient, L-amino acid-defined, high-fat diet (CDAHFD)-fed C57BL/6 mice. Saroglitazar completely prevented hepatic tumorigenesis (Giri et al., 2023). The compound 9-xanthylacetic acid (XAA) inhibits the development of MASLD-HCC (Gnocchi et al., 2023). The choline-deficient L-amino acid-defined diet (CDAAD) induced metabolic imbalance by stimulating lysophosphatidic acid receptor 6 (LPAR6) expression in mice. XAA reverses CDAAD-induced

Mechanistic Classes of Example Agents Against NAFLD-Driven HCC

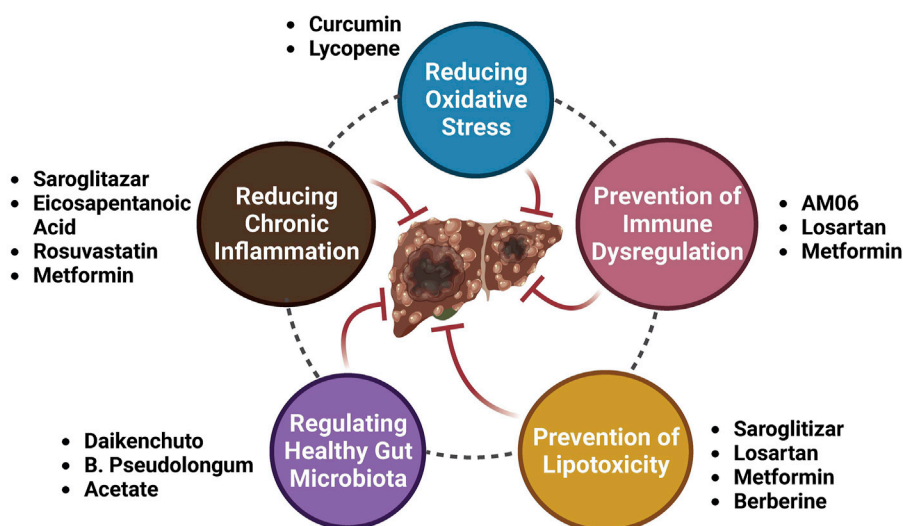


FIGURE 3
Mechanistic classes of example agents against MASLD-driven HCC.

increase in hepatic lipid accumulation, inflammation, fibrosis, and HCC development. These findings are corroborated by the results of gain- and loss-of-function of LPAR6 in HCC cells (Gnocchi et al., 2023). Scoparone (SCO), a compound originating from the leaves and stems of *Artemisia capillaris*, has many pharmacological effects such as anti-tumor, lipid-lowering, anti-hypotensive, anti-inflammatory, analgesic, anti-coagulant, and anti-asthmatic (Li et al., 2021; Jiang et al., 2022; Wei et al., 2022; Wu X. et al., 2023; Shen et al., 2023; Zhou et al., 2023). The most recent study showed that scoparone attenuates the pathological alterations observed in MASLD-HCC mouse models. Scoparone inhibits activation of mitogen-activated protein kinase (MAPK)/Akt signaling and reverses upregulation of NF- κ B p65 and its target genes, including NF- κ B, TNF- α , cyclooxygenase (COX-2), MCP-1, iNOS, and MMP-9, in MASLD-HCC models (Ye et al., 2023). These results suggest that scoparone is a potential therapeutic agent for MASLD-HCC as it inhibits MAPK/Akt/NF- κ B-mediated inflammatory pathways. Tipifarnib is a farnesyltransferase inhibitor (FTI) possessing anti-inflammatory and anti-tumor effects (Untch et al., 2018; Egawa et al., 2021; Shu et al., 2021; Greenberg et al., 2022; Smith et al., 2023). Tipifarnib significantly reduced tumor nodule formation and exhibited anti-tumor and anti-inflammatory effects in a MASH-related HCC mouse model challenged with DEN and a high-fat diet (HFD), primarily by decreasing serum IL-6 (Yamada et al., 2023). Tipifarnib strongly inhibited cell proliferation, decreased the expression of HIF-1 α , and induced apoptosis. Tipifarnib suppressed IL-6 secretion *in vitro* and *in vivo* (Yamada et al., 2023). Additionally, tipifarnib suppressed the expression of phosphorylated NF- κ B and TGF- β (Yamada et al., 2023). The omega-3 polyunsaturated fatty acid eicosapentaenoic acid (EPA) inhibits the development of HCC induced by DEN and HFD, suggesting that EPA attenuates the development of obesity-

related MASLD-HCC by suppressing STAT3 (Inoue-Yamauchi et al., 2018). An increasing number of studies have shown that probiotics can prevent and mitigate the development of cancer (Deng et al., 2023; Zhao et al., 2023). Probiotics suppressed HCC pathogenesis by inhibiting the gene expression of pro-inflammatory cytokines and reducing oxidative stress in a hepatocyte-specific PTEN knockout mouse MASLD model (Arai et al., 2022). Metformin, a promising antidiabetic medication for cancer treatment, inhibits long-term HFD-induced HCC tumorigenesis by inhibiting liver fat accumulation in the early stage (before the onset of MASLD) in C57Bl/6 mice (Tajima et al., 2013; Saengboonmee et al., 2021; Wu et al., 2023; Georgopoulos et al., 2023). Apo-10'-lycopenoic acid (APO10LA), a cleavage metabolite of lycopene, significantly reduced hepatic tumorigenesis and lung metastasis in C57Bl/6J mice challenged with DEN and HFD. This was accomplished by increasing hepatic SIRT1 protein activity, deacetylating SIRT1 targets, decreasing caspase-1 activation, and reducing hepatic inflammation, indicating APO10LA as having anti-inflammatory and anti-tumor effects in MASLD-HCC models (Ip et al., 2013). Liraglutide, a glucagon-like peptide-1 receptor agonist used for the treatment of T2DM, obesity, and chronic weight management, completely suppressed hepatic tumorigenesis in mice with streptozotocin (STZ) and HFD-induced MASH models through ameliorating steatosis, inflammation, and hepatocyte ballooning (Kojima et al., 2020). The dipeptidyl peptidase 4 (DPP4) inhibitor vildagliptin prevented MASLD-HCC in mouse models challenged with DEN and HFD by reversing HFD-induced CCL-2 production and angiogenesis, suggesting that the DPP4/CCL2/angiogenesis axis plays a key role in inhibiting MASLD-HCC. Targeting DPP4 may represent a novel therapeutic regimen for MASLD-HCC (Qin et al., 2018). As a 3-hydroxy-3-methyl-glutaryl-coenzyme-A (HMG-CoA) reductase inhibitor,

rosuvastatin inhibited hepatic tumorigenesis in an STAM mouse model challenged with a HFD by decreasing the expression of pro-inflammatory cytokines, suggesting that rosuvastatin may function as a preventive drug against MASLD-HCC (Yokohama et al., 2016). Lycopene suppresses hepatic tumorigenesis in HFD-promoted HCC by inactivating hepatic pro-inflammatory signaling and inflammatory foci (Ip et al., 2014). Berberine reduced the incidence of tumors and mitigated MASH in a STZ high-fat high-cholesterol diet (HFHC) mice model, suppressing lipogenesis, inflammation, fibrosis, and angiogenesis (Luo et al., 2019). Meanwhile, berberine inhibited the phosphorylation of p38 MAPK, extracellular signal-regulated kinase (ERK), and suppressed expression of COX2, suggesting berberine attenuates MASH-HCC by halting inflammation and angiogenesis via p38 MAPK/ERK-COX2 pathways (Luo et al., 2019).

Antioxidant drugs

Dietary lycopene and tomato extract halt MASH-HCC in rats through antioxidant activity (Wang et al., 2010). Dietary lycopene from either tomato extract or pure compounds inhibited hepatic tumorigenesis in an MASLD-related HCC rat model challenged with DEN and a HFD. This was accomplished by inhibiting the activation of ERK and NF- κ B, decreasing the expression of CYP2E1, reducing inflammatory foci, reducing pro-inflammatory cytokines, and increasing nuclear NF-E2-related factor-2 (Nrf2) and heme oxygenase-1 (HO-1) expression, suggesting that lycopene and tomato extract can inhibit MASH-HCC by reducing oxidative stress (Wang et al., 2010). Curcumin inhibits MASH-HCC pathogenesis in rats through antioxidant activity (Afrin et al., 2017). Curcumin inhibited hepatic tumorigenesis in a C57BL/6J male mice MASLD-related HCC model challenged with STZ and a HFD by inhibiting hepatic C/EBP β , CYP2E1, p-ERK1/2, and p67phox, while upregulating Nrf2 (Afrin et al., 2017). Curcumin significantly reduced the translocation of high-mobility group box 1 (HMGB1) into the cytosol and decreased the protein expression of toll-like receptor 4 (TLR4). Curcumin reduced MASH-HCC by downregulating the protein expression of glypican-3, prothrombin, and vascular endothelial growth factor (VEGF) (Afrin et al., 2017).

Anti-fibrosis drugs

The cyclophilin inhibitor derived from sanglifehrins NV556 reduces MASH-HCC by inhibiting fibrosis (Kuo et al., 2019). NV556 inhibited hepatic tumorigenesis in a mice model challenged with STZ and a HFD by inhibiting fibrosis, rather than altering inflammation, steatosis, and systemic cytokine generation, suggesting NV556 as a promising agent for the treatment of MASH-driven fibrosis and HCC (Kuo et al., 2019). Pioglitazone effectively reduced hepatic tumorigenesis in an MASH-related HCC mice model challenged with DEN and choline-deficient, L-amino acid-defined, high-fat diet (CDAHFD) by inhibiting fibrosis via inactivating MAPK and upregulating the hepatoprotective AMP-activated protein kinase (AMPK) pathway (Li et al., 2019). An inhibitor of cholesterol absorption, ezetimibe, reduces MASH-

HCC by inhibiting fibrosis (Miura et al., 2019). Ezetimibe inhibited hepatic tumorigenesis in hepatocyte-specific phosphatase and tensin homolog (Pten)-deficient (Pten^{Δhep}) mice challenged with a HFD by suppressing liver fibrosis and inflammation (Miura et al., 2019).

Drugs regulating lipid metabolism

Dietary n-3 polyunsaturated fatty acids (PUFAs) reduced hepatic tumorigenesis in an MASLD-related HCC mice model challenged with STZ and a HFD by regulating lipid metabolism, evidenced by decreased hepatic lipid accumulation and increased hepatic content of n-3 PUFAs and a higher n-3/n-6 PUFA ratio, suggesting n-3 PUFAs as a new therapeutic regimen for MASLD-HCC (Liebig et al., 2019). Dietary mulberry (*Morus alba* L.) leaf powder reduced hepatic tumorigenesis in an MASLD-related HCC C57L/6J mice model challenged with STZ and a HFD by regulating lipid metabolism, evidenced by reduced fat deposition and adenoma. This study suggests that the administration of mulberry leaf powder in STAM mice inhibits the progression of MASH-HCC, highlighting that it may be effective in preventing the development of MASH-HCC in humans (Wakame et al., 2022).

Regulating gut microbiota

Daikenchuto (TU-100) reduced hepatic tumorigenesis in Tsumura-Suzuki obese diabetes mice with the spontaneous onset of MASH and HCC by modulating the intestinal microbiome, evidenced by increased *Blautia* and *Ruminococcus* genera and decreased *Dorea* and *Erysipelotrichaceae* genera (Yamada et al., 2023). Curcuma reduced hepatic tumorigenesis in an MASLD-related HCC mice model challenged with DEN and a HFD by suppressing the levels of pro-inflammatory cytokines and inflammatory mediators including prostaglandin E2 (PGE2), COX-2, and NF- κ B and additionally augmented the level of IL-10 in the hepatic tissue and serum. Furthermore, Curcuma enhanced the diversity and richness of gut microbiota and decreased the relative abundance of *Clostridium* and *Mucispirillum* (Zhang et al., 2021). This study suggests that Curcuma attenuates MASLD-HCC via regulating gut microbiota, along with inhibiting oxidative stress and its associated inflammation. Dietary tomato powder inhibits MASLD-HCC by regulating gut microbiota in mice with loss of carotenoid cleavage enzymes (Xia et al., 2018). Dietary tomato powder reduced hepatic tumorigenesis in a β -carotene-15, 15'-oxygenase (BCO1)/BCO2 double-knockout mice model challenged with DEN and HFD. This was accomplished by decreasing hepatic inflammatory foci development and expression of pro-inflammatory genes, increasing the expression of SIRT1, hepatic circadian clock genes, and nicotinamide phosphoribosyltransferases (Xia et al., 2018). Dietary tomato powder also increased gut microbial diversity and richness, significantly decreasing the relative abundance of the genera *Clostridium* and *Mucispirillum* (Xia et al., 2018). This study indicates that dietary tomato powder prevents MASLD-HCC by

inhibiting inflammation and modulating gut microbiota independent of carotenoid cleavage enzymes (Xia et al., 2018). Recent studies have shown that *Bifidobacterium pseudolongum* is a potential novel probiotic for the prevention of MASLD-HCC. Mechanistically, it was found to suppress MASLD-HCC progression by secreting acetate, which by binding to the hepatic G-coupled-protein receptor 43 (GPR43) suppresses the activation of hepatic oncogenic IL-6/JAK1/STAT3 signaling pathways (Song et al., 2023).

Regulating immunity

MASH impaired the effect of anti-PD-1 therapy by inducing a pro-inflammatory phenotypic change and impairing the metabolism of hepatic CD8⁺ T cells in multiple murine MASH liver cancer models. Reduced motility of intratumoral CD8⁺ T cells was found through *in vivo* imaging analysis. Metformin was found to modulate the anti-PD-1 therapy efficacy against liver tumors in MASH models (Wabitsch et al., 2022). HFD alters macrophage polarization and promotes the liver inflammatory microenvironment, exacerbating cancer progression in MASLD/MASH-associated zebrafish HCC models. Metformin reversed MASLD/MASH-HCC by modulating the immune response via altering T-cell infiltration and macrophage polarization (de Oliveira et al., 2019). Gut *Akkermansia muciniphila* is reduced in mice and patients with MASH-related HCC (Li et al., 2022). Breast milk-isolated *A. muciniphila* (AM06) improved the severity of MASH, in addition to inhibiting the pathogenesis of MASH-HCC, indicated by decreased macrophage infiltration and an increased level of hepatic CXCR6⁺ natural killer T (NKT) cells (Li et al., 2022). The anti-tumor effects of *A. muciniphila* were attenuated by NKT cell deficiency in mice (CD1d^{-/-} and CXCR6^{-/-}). *A. muciniphila* enhanced the NKT cell-mediated killing of HepG2 cells (Li et al., 2022). Peritumoral fibrosis exerts an obstacle to T-cell-mediated tumor regression in mouse models of MASH-HCC. The antihypertensive drug angiotensin II receptor inhibitor losartan inhibited liver and peritumoral fibrosis, thereby substantially boosting tumor regression induced by anti-PD-1 therapy, mostly by facilitating effector CD8⁺ T-cell-mediated infiltration. The beneficial effects of losartan are associated with blunting of TGF- β receptor signaling, reduced fibrosis, and depletion of immunosuppressive fibroblasts (Gu et al., 2023).

Conclusion and future perspectives

This review summarizes the recent progress of research on the pathological pathways and underlying mechanisms of MASLD/MASH-HCC and reviews the application of compounds in the treatment of MASLD-HCC. This review is expected to improve our knowledge of the molecular mechanisms of MASLD/MASH-HCC and highlight strategies for targeting MASLD/MASH-HCC by pharmacological modulation as potential novel therapeutic targets. The progression of MASLD/MASH to HCC is still an international research hotspot, and there has been some progress in elucidating metabolic disorder/gut microbiota imbalance and immune factors in the progression of MASLD/MASH to HCC.

However, the exploration of treatment for MASLD/MASH-HCC is still in its infancy. In this article, based on a brief review of the latest research on the pathogenesis and progress of MASLD-HCC, we further summarize and organize the latest results of compounds in the treatment of MASLD-HCC. Based on the main mechanisms of anti-inflammatory, antioxidant, gut microbiota regulation, lipid metabolism regulation, and liver fibrosis inhibition, we classified the drugs used to treat MASLD/MASH-HCC and elucidated their pharmacological effects and related mechanisms of action. Adding further complexity, the same drug may inhibit MASLD/MASH-HCC through one or more of the above mechanisms, adding new insights for future polyreceptor pharmacology. Although continuous exploratory experimental research is still ongoing, the exact molecular mechanisms of these drugs in treating MASLD/MASH-HCC still need to be further explored.

After our detailed discussion, it is important to recall limitations that still plague the field of MASLD/MASH-HCC research. The first limitation is that the etiology of MASLD/MASH-HCC remains largely unclear, and further research is still needed. Recent studies have shown that new mechanisms of regulated cell death, such as ferroptosis, can be involved in the development and progression of MASLD (Feng et al., 2022; Wang et al., 2022; Zhang et al., 2023b; Zou et al., 2023) to HCC (Cong et al., 2022; Wang et al., 2023a; Wang et al., 2023b; Xu et al., 2023), and modulating ferroptosis may be a potential novel therapeutic target for MASLD and HCC (Yin et al., 2022; Ajoalabady et al., 2023; Cheng et al., 2023). However, mechanistic details relating to ferroptosis and the molecular pathways concerning transition of MASLD to HCC have been lacking. It is of fundamental importance to understand the importance of ferroptosis in the pathogenesis of MASLD-HCC. The second limitation is that the mechanism of specific genetic factors in the progression of MASLD/MASH to HCC and the exact downstream molecules are currently unclear, and further research is needed. The third limitation is that there is a lack of large-scale clinical trials on targeted MASLD/MASH-HCC drugs. The fourth limitation is that it is still largely unclear how one may develop or repurpose existing drugs for new clinical indications.

Due to a significant increase in obesity and T2DM globally, MASLD has gradually become an important cause of HCC, leading to the occurrence of MASLD-HCC. To note, HCC is characterized by high heterogeneity and different genetic mutations that could damage the effectiveness of current treatments. Therefore, future clinical trials should consider the most representative genetic mutations and find new strategies to identify biomarkers to guide personalized and precision treatment for HCC. Currently, there are no approved effective drugs to treat MASLD/MASH, implying that the targeted inhibition of MASLD/MASH and preventing disease progression to HCC have important social significance and are worthy of further exploration.

Author contributions

YW: conceptualization, funding acquisition, and writing—original draft. JF: visualization and writing—review and editing. TL: conceptualization and writing—review and editing.

YL: data curation and writing–review and editing. ZR: data curation and writing–review and editing. JC: funding acquisition, project administration, and writing–review and editing. MD: investigation and writing–review and editing.

Funding

The author(s) declare that financial support was received for the research, authorship, and/or publication of this article. This work was supported in part by the Science Foundation of CASIC (2020-LCYL-009), the Science Foundation of ASCH (YN202104), and the Hygiene and Health Development Scientific Research Fostering Plan of Haidian District, Beijing (HP2021-19-50701).

References

- Afrin, R., Arumugam, S., Rahman, A., Wahed, M. I. I., Karuppagounder, V., Harima, M., et al. (2017). Curcumin ameliorates liver damage and progression of NASH in NASH-HCC mouse model possibly by modulating HMGB1-NF- κ B translocation. *Int. Immunopharmacol.* 44, 174–182. doi:10.1016/j.intimp.2017.01.016
- Ajoolabady, A., Tang, D., Kroemer, G., and Ren, J. (2023). Ferroptosis in hepatocellular carcinoma: mechanisms and targeted therapy. *Br. J. Cancer.* 128, 190–205. doi:10.1038/s41416-022-01998-x
- Akinyemiju, T., Abera, S., Ahmed, M., Alam, N., Alemayohu, M. A., Allen, C., et al. (2017). The burden of primary liver cancer and underlying etiologies from 1990 to 2015 at the global, regional, and national level: results from the global burden of disease study 2015. *JAMA Oncol.* 3 (12), 1683–1691. doi:10.1001/jamaoncol.2017.3055
- Aleksandrova, K., Boeing, H., Nöthlings, U., Jenab, M., Fedirko, V., Kaaks, R., et al. (2014). Inflammatory and metabolic biomarkers and risk of liver and biliary tract cancer. *Hepatology* 60, 858–871. doi:10.1002/hep.27016
- Anstee, Q. M., Reeves, H. L., Kotsiliti, E., Govaere, O., and Heikenwalder, M. (2019). From NASH to HCC: current concepts and future challenges. *Nat. Rev. Gastroenterol. Hepatol.* 16, 411–428. doi:10.1038/s41575-019-0145-7
- Arai, N., Miura, K., Aizawa, K., Sekiya, M., Nagayama, M., Sakamoto, H., et al. (2022). Probiotics suppress nonalcoholic steatohepatitis and carcinogenesis progression in hepatocyte-specific PTEN knockout mice. *Sci. Rep.* 12, 16206. doi:10.1038/s41598-022-20296-3
- Arrese, M., Cabrera, D., Kalergis, A. M., and Feldstein, A. E. (2016). Innate immunity and inflammation in NAFLD/NASH. *Dig. Dis. Sci.* 61, 1294–1303. doi:10.1007/s10620-016-4049-x
- Avgerinos, K. I., Spyrou, N., Mantzoros, C. S., and Dalamaga, M. (2019). Obesity and cancer risk: emerging biological mechanisms and perspectives. *Metab. Clin. Exp.* 92, 121–135. doi:10.1016/j.metabol.2018.11.001
- Begrache, K., Massart, J., Robin, M. A., Bonnet, F., and Fromenty, B. (2013). Mitochondrial adaptations and dysfunctions in nonalcoholic fatty liver disease. *Hepatology* 58, 1497–1507. doi:10.1002/hep.26226
- Behary, J., Amorim, N., Jiang, X. T., Raposo, A., Gong, L., McGovern, E., et al. (2021). Gut microbiota impact on the peripheral immune response in non-alcoholic fatty liver disease related hepatocellular carcinoma. *Nat. Commun.* 12 (1), 187. doi:10.1038/s41467-020-20422-7
- Bence, K. K., and Birnbaum, M. J. (2021). Metabolic drivers of non-alcoholic fatty liver disease. *Mol. Metab.* 50, 50101143. doi:10.1016/j.molmet.2020.101143
- Bessone, F., Razori, M. V., and Roma, M. G. (2019). Molecular pathways of nonalcoholic fatty liver disease development and progression. *Cell. Mol. Life Sci.* 76, 99–128. doi:10.1007/s00018-018-2947-0
- Brahma, M. K., Gilgioni, E. H., Zhou, L., Trépo, E., Chen, P., and Gurzov, E. N. (2021). Oxidative stress in obesity-associated hepatocellular carcinoma: sources, signaling and therapeutic challenges. *Oncogene* 40, 5155–5167. doi:10.1038/s41388-021-01950-y
- Cannito, S., Dianzani, U., Parola, M., Albano, E., and Sutti, S. (2023). Inflammatory processes involved in NASH-related hepatocellular carcinoma. *Biosci. Rep.* 43, BSR20221271. doi:10.1042/BSR20221271
- Chan, W. K., Chuah, K. H., Rajaram, R. B., Lim, L. L., Ratnasingam, J., and Vethakkan, S. R. (2023). Metabolic dysfunction-associated steatotic liver disease (MASLD): a state-of-the-art review. *J. Obes. Metab. Syndr.* 32, 197–213. doi:10.7570/jomes23052
- Chen, Z., Tian, R., She, Z., Cai, J., and Li, H. (2020). Corrigendum to "Role of oxidative stress in the pathogenesis of nonalcoholic fatty liver disease" [Free Radic. Biol. Med. 152

Conflict of interest

The authors declare that the research was conducted in the absence of any commercial or financial relationships that could be construed as a potential conflict of interest.

Publisher's note

All claims expressed in this article are solely those of the authors and do not necessarily represent those of their affiliated organizations, or those of the publisher, the editors, and the reviewers. Any product that may be evaluated in this article, or claim that may be made by its manufacturer, is not guaranteed or endorsed by the publisher.

(2020) 116–141]. *Free Radic. Biol. Med.* 152, 174–141. doi:10.1016/j.freeradbiomed.2020.06.011

Cheng, Z., Chu, H., Zhu, Q., and Yang, L. (2023). Ferroptosis in non-alcoholic liver disease: molecular mechanisms and therapeutic implications. *Front. Nutr.* 10, 1090338. doi:10.3389/fnut.2023.1090338

Cong, T., Luo, Y., Fu, Y., Liu, Y., Li, Y., and Li, X. (2022). New perspectives on ferroptosis and its role in hepatocellular carcinoma. *Chin. Med. J.* 135, 2157–2166. doi:10.1097/CM9.0000000000002327

Degasper, E., and Colombo, M. (2016). Distinctive features of hepatocellular carcinoma in non-alcoholic fatty liver disease. *Lancet Gastroenterology Hepatology* 1 (2), 156–164. doi:10.1016/S2468-1253(16)30018-8

Deng, X., Yang, J., Zhang, Y., Chen, X., Wang, C., Suo, H., et al. (2023). An update on the pivotal roles of probiotics, their components, and metabolites in preventing colon cancer. *Foods* 12, 3706. doi:10.3390/foods12193706

de Oliveira, S., Houseright, R. A., Graves, A. L., Golenberg, N., Korte, B. G., Miskolci, V., et al. (2019). Metformin modulates innate immune-mediated inflammation and early progression of NAFLD-associated hepatocellular carcinoma in zebrafish. *J. Hepatol.* 70 (4), 710–721. doi:10.1016/j.jhep.2018.11.034

Di Maira, G., Foglia, B., Napione, L., Turato, C., Maggiora, M., Sutti, S., et al. (2022). Oncostatin M is overexpressed in NASH-related hepatocellular carcinoma and promotes cancer cell invasiveness and angiogenesis. *J. Pathol.* 257, 82–95. doi:10.1002/path.5871

Duan, Y., Pan, X., Luo, J., Xiao, X., Li, J., Bestman, P. L., et al. (2022). Association of inflammatory cytokines with non-alcoholic fatty liver disease. *Front. Immunol.* 13, 880298. doi:10.3389/fimmu.2022.880298

Egawa, N., Tanaka, T., Matsufuji, S., Yamada, K., Ito, K., Kitagawa, H., et al. (2021). Antitumor effects of low-dose tipifarnib on the mTOR signaling pathway and reactive oxygen species production in HIF-1 α -expressing gastric cancer cells. *FEBS Open Bio* 11, 1465–1475. doi:10.1002/2211-5463.13154

Eslam, M., Newsome, P. N., Sarin, S. K., Anstee, Q. M., Targher, G., Romero-Gomez, M., et al. (2020a). A new definition for metabolic dysfunction-associated fatty liver disease: an international expert consensus statement. *J. Hepatol.* 73 (1), 202–209. doi:10.1016/j.jhep.2020.03.039

Eslam, M., Sanyal, A. J., George, J., and International Consensus Panel (2020b). MAFLD: a consensus-driven proposed nomenclature for metabolic associated fatty liver disease. *Gastroenterology* 158 (7), 1999–2014.e1. doi:10.1053/j.gastro.2019.11.312

Feng, G., Byrne, C. D., Targher, G., Wang, F., and Zheng, M. H. (2022). Ferroptosis and metabolic dysfunction-associated fatty liver disease: is there a link. *Liver Int.* 42, 1496–1502. doi:10.1111/liv.15163

Foerster, F., Gairing, S. J., Müller, L., and Galle, P. R. (2022). NAFLD-driven HCC: safety and efficacy of current and emerging treatment options. *J. Hepatol.* 76, 446–457. doi:10.1016/j.jhep.2021.09.007

Gabbia, D., Cannella, L., and De Martin, S. (2021). The role of oxidative stress in NAFLD-NASH-HCC transition-focus on NADPH oxidases. *Biomedicine* 9, 687. doi:10.3390/biomedicine9060687

Georgopoulos, N. S., Tolia, M., Mauri, D., Kamposioras, K., Charalampakis, N., Tsoukalas, N., et al. (2023). Metformin: a promising radiosensitizer in neoadjuvant rectal cancer treatment. *Rev. Recent Clin. Trials* 18, 172–180. doi:10.2174/1574887118666230428114349

Giri, S. R., Bhoi, B., Trivedi, C., Rath, A., Rathod, R., Sharma, A., et al. (2023). Saroglitazar suppresses the hepatocellular carcinoma induced by intraperitoneal

injection of diethylnitrosamine in C57BL/6 mice fed on choline deficient, l-amino acid-defined, high-fat diet. *BMC Cancer* 23, 59. doi:10.1186/s12885-023-10530-0

Gnocchi, D., Afonso, M. B., Cavalluzzi, M. M., Lentini, G., Ingravallo, G., Sabbà, C., et al. (2023). Inhibition of lysophosphatidic acid receptor 6 upregulated by the choline-deficient l-amino acid-defined diet prevents hepatocarcinogenesis in mice. *Mol. Carcinog.* 62 (5), 577–582. doi:10.1002/mc.23516

Greenberg, J. W., Kim, H., Ahn, M., Moustafa, A. A., Zhou, H., Barata, P. C., et al. (2022). Combination of tipifarnib and sunitinib overcomes renal cell carcinoma resistance to tyrosine kinase inhibitors via tumor-derived exosome and T cell modulation. *Cancers (Basel)* 14, 903. doi:10.3390/cancers14040903

Grohmann, M., Wiede, F., Dodd, G. T., Gurzov, E. N., Ooi, G. J., Butt, T., et al. (2018). Obesity drives STAT-1-dependent NASH and STAT-3-dependent HCC. *Cell* 175, 1289–1306. doi:10.1016/j.cell.2018.09.053

Gu, L., Zhu, Y., Lee, M., Nguyen, A., Ryujin, N. T., Huang, J. Y., et al. (2023). Angiotensin II receptor inhibition ameliorates liver fibrosis and enhances hepatocellular carcinoma infiltration by effector T cells. *Proc. Natl. Acad. Sci. U.S.A.* 120 (19), e2300706120. doi:10.1073/pnas.2300706120

Hagström, H., Vessby, J., Eksted, M., and Shang, Y. (2023). 99% of patients with NAFLD meet MASLD criteria and natural history is therefore identical. *J. Hepatol.* 2023 (23), 05080–05088. [pii]. doi:10.1016/j.jhep.2023.08.026

Hardy, T., Oakley, F., Anstee, Q. M., and Day, C. P. (2016). Nonalcoholic fatty liver disease: pathogenesis and disease spectrum. *Annu. Rev. Pathol.* 11, 451–496. doi:10.1146/annurev-pathol-012615-044224

Hatano, M., Akiyama, Y., Shimada, S., Yagi, K., Akahoshi, K., Itoh, M., et al. (2023). Loss of KDM6B epigenetically confers resistance to lipotoxicity in nonalcoholic fatty liver disease-related HCC. *Hepatol. Commun.* 7, e0277. doi:10.1097/HC9.0000000000000277

He, L., Zheng, W., Qiu, K., Kong, W., and Zeng, T. (2023). Changing from NAFLD to MASLD: the new definition can more accurately identify individuals at higher risk for diabetes. *J. Hepatol.* S0168-8278 (23), 05164. [pii]. doi:10.1016/j.jhep.2023.09.035

Hirsova, P., Bamidele, A. O., Wang, H., Povero, D., and Revelo, X. S. (2021). Emerging roles of T cells in the pathogenesis of nonalcoholic steatohepatitis and hepatocellular carcinoma. *Front. Endocrinol. (Lausanne)* 12, 760860. doi:10.3389/fendo.2021.760860

Inoue-Yamauchi, A., Itagaki, H., and Oda, H. (2018). Eicosapentaenoic acid attenuates obesity-related hepatocellular carcinogenesis. *Carcinogenesis* 39 (1), 28–35. doi:10.1093/carcin/bgx112

Ioannou, G. N. (2021). Epidemiology and risk-stratification of NAFLD-associated HCC. *J. Hepatol.* 75 (6), 1476–1484. doi:10.1016/j.jhep.2021.08.012

Ip, B. C., Hu, K. Q., Liu, C., Smith, D. E., Obin, M. S., Ausman, L. M., et al. (2013). Lycopene metabolite, apo-10'-lycopenoic acid, inhibits diethylnitrosamine-initiated, high fat diet-promoted hepatic inflammation and tumorigenesis in mice. *Cancer Prev. Res. (Phila)* 6 (12), 1304–1316. doi:10.1158/1940-6207.CAPR-13-0178

Ip, B. C., Liu, C., Ausman, L. M., von Lintig, J., and Wang, X. D. (2014). Lycopene attenuated hepatic tumorigenesis via differential mechanisms depending on carotenoid cleavage enzyme in mice. *Cancer Prev. Res. (Phila)* 7 (12), 1219–1227. doi:10.1158/1940-6207.CAPR-14-0154

Jiang, Y., Xu, J., Huang, P., Yang, L., Liu, Y., Li, Y., et al. (2022). Scoparone improves nonalcoholic steatohepatitis through alleviating JNK/sab signaling pathway-mediated mitochondrial dysfunction. *Front. Pharmacol.* 13, 863756. doi:10.3389/fphar.2022.863756

Kalligeros, M., Vassilopoulos, A., Vassilopoulos, S., Victor, D. W., Mylonakis, E., and Nouredin, M. (2023). Prevalence of steatotic liver disease (MASLD, MetALD, and ALD) in the United States: NHANES 2017–2020. *Clin. Gastroenterol. Hepatol.* S1542-3565 (23), 00914–00914X. [pii]. doi:10.1016/j.cgh.2023.11.003

Khairnar, R., Islam, M. A., Fleishman, J., and Kumar, S. (2023). Shedding light on non-alcoholic fatty liver disease: pathogenesis, molecular mechanisms, models, and emerging therapeutics. *LIFE Sci.* 312, 121185. doi:10.1016/j.lfs.2022.121185

Koh, J. H., Wang, M., Suzuki, H., Muthiah, M., Ng, C. H., and Huang, D. Q. (2024). NAFLD and NAFLD-related HCC in asia: burden and surveillance. *J. Clin. Exp. Hepatol.* 14, 101213. doi:10.1016/j.jceh.2023.06.013

Kojima, M., Takahashi, H., Kuwashiro, T., Tanaka, K., Mori, H., Ozaki, I., et al. (2020). Glucagon-like peptide-1 receptor agonist prevented the progression of hepatocellular carcinoma in a mouse model of nonalcoholic steatohepatitis. *Int. J. Mol. Sci.* 21 (16), 5722. doi:10.3390/ijms21165722

Kuo, J., Serrano, S. S., Grönberg, A., Massoumi, R., Hansson, M. J., and Galloway, P. (2019). Cyclophilin inhibitor NV556 reduces fibrosis and hepatocellular carcinoma development in mice with non-alcoholic steatohepatitis. *Front. Pharmacol.* 10, 1129. doi:10.3389/fphar.2019.01129

Lacotte, S., Slits, F., Moeckli, B., Peloso, A., Koenig, S., Tihy, M., et al. (2023). Anti-CD122 antibody restores specific CD8(+) T cell response in nonalcoholic steatohepatitis and prevents hepatocellular carcinoma growth. *Oncoimmunology* 12 (1), 2184991. doi:10.1080/2162402X.2023.2184991

Li, N., Yang, F., Liu, D. Y., Guo, J. T., Ge, N., and Sun, S. Y. (2021). Scoparone inhibits pancreatic cancer through PI3K/Akt signaling pathway. *World J. Gastrointest. Oncol.* 13, 1164–1183. doi:10.4251/wjgo.v13.i9.1164

Li, S., Ghoshal, S., Sojoodi, M., Arora, G., Masia, R., Erstad, D. J., et al. (2019). Pioglitazone reduces hepatocellular carcinoma development in two rodent models of cirrhosis. *J. Gastrointest. Surg.* 23 (1), 101–111. doi:10.1007/s11605-018-4004-6

Li, T., Lin, X., Shen, B., Zhang, W., Liu, Y., Liu, H., et al. (2022). Akkermansia muciniphila suppressing nonalcoholic steatohepatitis associated tumorigenesis through CXCR6(+) natural killer T cells. *Front. Immunol.* 13, 1047570. doi:10.3389/fimmu.2022.1047570

Liebig, M., Dannenberger, D., Vollmar, B., and Abshagen, K. (2019). n-3 PUFAs reduce tumor load and improve survival in a NASH-tumor mouse model. *Ther. Adv. Chronic Dis.* 10, 2040622319872118. doi:10.1177/2040622319872118

Lim, S., Kim, J. W., and Targher, G. (2021). Links between metabolic syndrome and metabolic dysfunction-associated fatty liver disease. *Trends Endocrinol. Metabolism* TEM 32, 500–514. doi:10.1016/j.tem.2021.04.008

Liu, M., Yu, X., Lin, L., Deng, J., Wang, K., Xia, Y., et al. (2019). ATGL promotes the proliferation of hepatocellular carcinoma cells via the p-AKT signaling pathway. *J. Biochem. Mol. Toxicol.* 33, e22391. doi:10.1002/jbt.22391

Llovet, J. M., Kelley, R. K., Villanueva, A., Singal, A. G., Pikarsky, E., Roayaie, S., et al. (2021). Hepatocellular carcinoma. *Nat. Rev. Dis. Prim.* 7, 6. doi:10.1038/s41572-020-00240-3

Luo, Y., Tian, G., Zhuang, Z., Chen, J., You, N., Zhuo, L., et al. (2019). Berberine prevents non-alcoholic steatohepatitis-derived hepatocellular carcinoma by inhibiting inflammation and angiogenesis in mice. *Am. J. Transl. Res.* 11 (5), 2668–2682.

Malehmir, M., Pfister, D., Gallage, S., Szydłowska, M., Inverso, D., Kotsiliti, E., et al. (2019). Platelet GPIIb is a mediator and potential interventional target for NASH and subsequent liver cancer. *Nat. Med.* 25, 641–655. doi:10.1038/s41591-019-0379-5

Marengo, A., Rosso, C., and Bugianesi, E. (2016). Liver cancer: connections with obesity, fatty liver, and cirrhosis. *Annu. Rev. Med.* 67, 103–117. doi:10.1146/annurev-med-090514-013832

Margini, C., and Dufour, J. F. (2016). The story of HCC in NAFLD: from epidemiology, across pathogenesis, to prevention and treatment. *Liver Int.* 36, 317–324. doi:10.1111/liv.13031

Masarone, M., Rosato, V., Dallio, M., Gravina, A. G., Aglitti, A., Loguercio, C., et al. (2018). Role of oxidative stress in pathophysiology of nonalcoholic fatty liver disease. *Oxid. Med. Cell Longev.* 2018, 9547613. doi:10.1155/2018/9547613

Mittal, S., Sada, Y. H., El-Serag, H. B., Kanwal, F., Duan, Z., Temple, S., et al. (2015). Temporal trends of nonalcoholic fatty liver disease-related hepatocellular carcinoma in the veteran affairs population. *Clin. Gastroenterol. Hepatol.* 13 (3), 594–601. doi:10.1016/j.cgh.2014.08.013

Miura, K., Ohnishi, H., Morimoto, N., Minami, S., Ishioka, M., Watanabe, S., et al. (2019). Ezetimibe suppresses development of liver tumors by inhibiting angiogenesis in mice fed a high-fat diet. *Cancer Sci.* 110 (2), 771–783. doi:10.1111/cas.13902

Mu, W., Jiang, Y., Liang, G., Feng, Y., and Qu, F. (2023). Metformin: a promising antidiabetic medication for cancer treatment. *Curr. Drug Targets* 24, 41–54. doi:10.2174/1389450124666221104094918

Natarajan, Y., Kramer, J. R., Yu, X., Li, L., Thrift, A. P., El-Serag, H. B., et al. (2020). Risk of cirrhosis and hepatocellular cancer in patients with NAFLD and normal liver enzymes. *Hepatology* 72 (4), 1242–1252. doi:10.1002/hep.31157

Nouredin, M., Wei, L., Castera, L., and Tsochatzis, E. A. (2023). Embracing change: from NAFLD to MASLD under the steatotic liver disease umbrella. *Clin. Gastroenterol. Hepatol.* S1542-3565 (23), 00833–00839. [pii].

Odenwald, M. A., and Turner, J. R. (2017). The intestinal epithelial barrier: a therapeutic target. *Nat. Rev. Gastroenterol. Hepatol.* 14 (1), 9–21. doi:10.1038/nrgastro.2016.169

Okuda, K., Umemura, A., Umemura, S., Kataoka, S., Taketani, H., Seko, Y., et al. (2021). Honokiol prevents non-alcoholic steatohepatitis-induced liver cancer via EGFR degradation through the glucocorticoid receptor-MIG6 Axis. *Cancers (Basel)* 13 (7), 1515. doi:10.3390/cancers13071515

Pal Chaudhary, S., Reyes, S., Chase, M. L., Govindan, A., Zhao, L., Luther, J., et al. (2023). Resection of NAFLD/NASH-related hepatocellular carcinoma (HCC): clinical features and outcomes compared with HCC due to other etiologies. *Oncologist* 28 (4), 341–350. doi:10.1093/oncolo/oyac251

Park, E. J., Lee, J. H., Yu, G. Y., He, G., Ali, S. R., Holzer, R. G., et al. (2010). Dietary and genetic obesity promote liver inflammation and tumorigenesis by enhancing IL-6 and TNF expression. *Cell* 140, 197–208. doi:10.1016/j.cell.2009.12.052

Perla, F. M., Prelati, M., Lavorato, M., Visicchio, D., and Anania, C. (2017). The role of lipid and lipoprotein metabolism in non-alcoholic fatty liver disease. *Child. (Basel, Switz.)* 4, 46. doi:10.3390/children4060046

Pirola, C. J., and Sookoian, S. (2022). Metabolic dysfunction-associated fatty liver disease: advances in genetic and epigenetic implications. *Curr. Opin. Lipidol.* 33, 95–102. doi:10.1097/MOL.0000000000000814

Piscaglia, F., Svegliati-Baroni, G., Barchetti, A., Pecorelli, A., Marinelli, S., Tiribelli, C., et al. (2016). Clinical patterns of hepatocellular carcinoma in nonalcoholic fatty liver disease: a multicenter prospective study. *Hepatology* 63 (3), 827–838. doi:10.1002/hep.28368

- Polyzos, S. A., Chrysavgis, L., Vachliotis, I. D., Chartampilas, E., and Cholongitas, E. (2023). Nonalcoholic fatty liver disease and hepatocellular carcinoma: Insights in epidemiology, pathogenesis, imaging, prevention and therapy. *Semin. Cancer Biol.* 93, 20–35. doi:10.1016/j.semcancer.2023.04.010
- Ponziani, F. R., Bhoori, S., Castelli, C., Putignani, L., Rivoltini, L., Del Chierico, F., et al. (2019). Hepatocellular carcinoma is associated with gut microbiota profile and inflammation in nonalcoholic fatty liver disease. *Hepatology* 69, 107–120. doi:10.1002/hep.30036
- Potoupni, V., Georgiadou, M., Chatzigriva, E., Polychronidou, G., Markou, E., Zapantis Gakis, C., et al. (2021). Circulating tumor necrosis factor- α levels in non-alcoholic fatty liver disease: a systematic review and a meta-analysis. *J. Gastroenterol. Hepatol.* 36, 3002–3014. doi:10.1111/jgh.15631
- Powell, E. E., Wong, V. W., and Rinella, M. (2021). Non-alcoholic fatty liver disease. *Lancet* 397 (10290), 2212–2224. doi:10.1016/S0140-6736(20)32511-3
- Qin, C. J., Zhao, L. H., Zhou, X., Zhang, H. L., Wen, W., Tang, L., et al. (2018). Inhibition of dipeptidyl peptidase IV prevents high fat diet-induced liver cancer angiogenesis by downregulating chemokine ligand 2. *Cancer Lett.* 420, 26–37. doi:10.1016/j.canlet.2018.01.064
- Rao, G., Peng, X., Li, X., An, K., He, H., Fu, X., et al. (2023). Unmasking the enigma of lipid metabolism in metabolic dysfunction-associated steatotic liver disease: from mechanism to the clinic. *Front. Med. (Lausanne)*. 10, 1294267. doi:10.3389/fmed.2023.1294267
- Riaz, F., Wei, P., and Pan, F. (2022). Fine-tuning of regulatory T cells is indispensable for the metabolic steatosis-related hepatocellular carcinoma: a review. *Front. Cell Dev. Biol.* 10, 949603. doi:10.3389/fcell.2022.949603
- Rinella, M. E., Lazarus, J. V., Ratzliff, V., Francque, S. M., Sanyal, A. J., Kanwal, F., et al. (2023a). A multi-society Delphi consensus statement on new fatty liver disease nomenclature. *J. Hepatol.* S0168-8278 (23), 1966–1986. [pii]. doi:10.1097/hep.0000000000000520
- Rinella, M. E., Lazarus, J. V., Ratzliff, V., Francque, S. M., Sanyal, A. J., Kanwal, F., et al. (2023b). A multi-society Delphi consensus statement on new fatty liver disease nomenclature. *Ann. Hepatol.* 29, 101133. doi:10.1016/j.aohp.2023.101133
- Rinella, M. E., Lazarus, J. V., Ratzliff, V., Francque, S. M., Sanyal, A. J., Kanwal, F., et al. (2023c). A multi-society Delphi consensus statement on new fatty liver disease nomenclature. *Hepatology* 79, 1542–1556. doi:10.1016/j.jhep.2023.06.003
- Rudalska, R., Harbig, J., Snaebjornsson, M. T., Klotz, S., Zwirner, S., Taranets, L., et al. (2021). LXRA activation and Raf inhibition trigger lethal lipotoxicity in liver cancer. *Nat. Cancer* 2, 201–217. doi:10.1038/s43018-020-00168-3
- Saengboonmee, C., Sanlung, T., and Wongkham, S. (2021). Repurposing metformin for cancer treatment: a great challenge of a promising drug. *Anticancer Res.* 41, 5913–5918. doi:10.21873/anticancer.15410
- Samuel, V. T., Petersen, K. F., and Shulman, G. I. (2010). Lipid-induced insulin resistance: unravelling the mechanism. *Lancet* 375, 2267–2277. doi:10.1016/S0140-6736(10)60408-4
- Sangro, P., de la Torre Aláez, M., Sangro, B., and D'Avola, D. (2023). Metabolic dysfunction-associated fatty liver disease (MAFLD): an update of the recent advances in pharmacological treatment. *J. Physiol. Biochem.* 79, 869–879. doi:10.1007/s13105-023-00954-4
- Sarin, S. K., Kumar, M., Eslam, M., George, J., Al Mahtab, M., Akbar, S. M. F., et al. (2020). Liver diseases in the asia-pacific region: a lancet gastroenterology and hepatology commission. *Lancet Gastroenterol. Hepatol.* 5 (2), 167–228. doi:10.1016/S2468-1253(19)30342-5
- Serviddio, G., Bellanti, F., and Vendemiale, G. (2013). Free radical biology for medicine: learning from nonalcoholic fatty liver disease. *Free Radic. Biol. Med.* 65, 952–968. doi:10.1016/j.freeradbiomed.2013.08.174
- Shalapour, S., Lin, X. J., Bastian, I. N., Brain, J., Burt, A. D., Aksenov, A. A., et al. (2017). Inflammation-induced IgA+ cells dismantle anti-liver cancer immunity. *Nature* 551, 340–345. doi:10.1038/nature24302
- Shen, H., Wei, Y., Yang, Q., Cai, Y., Zhu, K., and Chen, X. (2023). Scoparone induces both apoptosis and ferroptosis via multiple mechanisms in non-small-cell lung cancer cells. *Toxicol. Vitro* 91, 105627. doi:10.1016/j.tiv.2023.105627
- Shu, L., Wang, D., Nannapaneni, S., Sun, Y., Griffith, C. C., Wang, X., et al. (2021). Tipifarnib enhances anti-EGFR activity of cetuximab in non-HRAS mutated head and neck squamous cell carcinoma cancer (HNSCC). *Oral Oncol.* 122, 105546. doi:10.1016/j.oraloncology.2021.105546
- Smith, A. E., Chan, S., Wang, Z., McCloskey, A., Reilly, Q., Wang, J. Z., et al. (2023). Tipifarnib potentiates the antitumor effects of PI3K α inhibition in PIK3CA- and HRAS-dysregulated HNSCC via convergent inhibition of mTOR activity. *Cancer Res.* 83, 3252–3263. doi:10.1158/0008-5472.CAN-23-0282
- Song, Q., Zhang, X., Liu, W., Wei, H., Liang, W., Zhou, Y., et al. (2023). Bifidobacterium pseudolongum-generated acetate suppresses non-alcoholic fatty liver disease-associated hepatocellular carcinoma. *J. Hepatol.* S0168-8278 (23), 1352–1365. [pii]. doi:10.1016/j.jhep.2023.07.005
- Sydor, S., Best, J., Messerschmidt, I., Manka, P., Vilchez-Vargas, R., Brodesser, S., et al. (2020). Altered microbiota diversity and bile acid signaling in cirrhotic and noncirrhotic NASH-HCC. *Clin. Transl. Gastroenterol.* 11 (3), e00131. doi:10.14309/ctg.0000000000000131
- Tajima, K., Nakamura, A., Shirakawa, J., Togashi, Y., Orime, K., Sato, K., et al. (2013). Metformin prevents liver tumorigenesis induced by high-fat diet in C57BL/6 mice. *Am. J. Physiol. Endocrinol. Metab.* 305 (8), E987–E998. doi:10.1152/ajpendo.00133.2013
- Talamantes, S., Lisjak, M., Gilgioni, E. H., Llamaza-Torres, C. J., Ramos-Molina, B., and Gurzov, E. N. (2023). Non-alcoholic fatty liver disease and diabetes mellitus as growing aetiologies of hepatocellular carcinoma. *JHEP Rep.* 5, 100811. doi:10.1016/j.jhepr.2023.100811
- Tanaka, S., Miyamishi, K., Kobune, M., Kawano, Y., Hoki, T., Kubo, T., et al. (2013). Increased hepatic oxidative DNA damage in patients with nonalcoholic steatohepatitis who develop hepatocellular carcinoma. *J. Gastroenterol.* 48, 1249–1258. doi:10.1007/s00535-012-0739-0
- Untch, B. R., Dos Anjos, V., Garcia-Rendueles, M., Knauf, J. A., Krishnamoorthy, G. P., Saqceña, M., et al. (2018). Tipifarnib inhibits HRAS-driven dedifferentiated thyroid cancers. *Cancer Res.* 78, 4642–4657. doi:10.1158/0008-5472.CAN-17-1925
- Venkatesan, N., Doskey, L. C., and Malhi, H. (2023). The role of endoplasmic reticulum in lipotoxicity during metabolic dysfunction-associated steatotic liver disease (MASLD) pathogenesis. *Am. J. Pathol.* 193, 1887–1899. doi:10.1016/j.ajpath.2023.08.007
- Villanueva, A. (2019). Hepatocellular carcinoma. *N. Engl. J. Med.* 380 (15), 1450–1462. doi:10.1056/NEJMra1713263
- Wabitsch, S., McCullen, J. D., Kamenyeva, O., Ruf, B., McVey, J. C., Kabat, J., et al. (2022). Metformin treatment rescues CD8(+) T-cell response to immune checkpoint inhibitor therapy in mice with NAFLD. *J. Hepatol.* 77 (3), 748–760. doi:10.1016/j.jhep.2022.03.010
- Wakame, K., Sato, K., Kasai, M., Kikuchi, E., Shimizu, K., Kudo, A., et al. (2022). Oral administration of Mulberry (morus alba L.) Leaf powder prevents the development of hepatocellular carcinoma in stelic animal model (STAM) mice. *Anticancer Res.* 42 (8), 4055–4062. doi:10.21873/anticancer.15902
- Wang, S., Liu, Z., Geng, J., Li, L., and Feng, X. (2022). An overview of ferroptosis in non-alcoholic fatty liver disease. *Biomed. Pharmacother.* 153, 113374. doi:10.1016/j.biopha.2022.113374
- Wang, X., Zeldin, S., Shi, H., Zhu, C., Saito, Y., Corey, K. E., et al. (2022). TAZ-induced Cybb contributes to liver tumor formation in non-alcoholic steatohepatitis. *J. Hepatol.* 76, 910–920. doi:10.1016/j.jhep.2021.11.031
- Wang, Y., Ausman, L. M., Greenberg, A. S., Russell, R. M., and Wang, X. D. (2010). Dietary lycopene and tomato extract supplementations inhibit nonalcoholic steatohepatitis-promoted hepatocarcinogenesis in rats. *Int. J. Cancer* 126 (8), 1788–1796. doi:10.1002/ijc.24689
- Wang, Y., Hu, J., Wu, S., Fleishman, J. S., Li, Y., Xu, Y., et al. (2023b). Targeting epigenetic and posttranslational modifications regulating ferroptosis for the treatment of diseases. *Signal Transduct. Target Ther.* 8, 449. doi:10.1038/s41392-023-01720-0
- Wang, Y., Wu, X., Ren, Z., Li, Y., Zou, W., Chen, J., et al. (2023a). Overcoming cancer chemotherapy resistance by the induction of ferroptosis. *Drug resist. updat.* 66, 100916. doi:10.1016/j.drug.2022.100916
- Wei, M., Li, T., Cao, H., He, H., Yang, C., Yin, Y., et al. (2022). The effects of scoparone on alcohol and high-fat diet-induced liver injury revealed by RNA sequencing. *Biomed. Pharmacother.* 155, 113770. doi:10.1016/j.biopha.2022.113770
- Wen, Y., Lambrecht, J., Ju, C., and Tacke, F. (2021). Hepatic macrophages in liver homeostasis and diseases-diversity, plasticity and therapeutic opportunities. *Cell. Mol. Immunol.* 18, 45–56. doi:10.1038/s41423-020-00558-8
- Wong, V. W. (2018). Current prevention and treatment options for NAFLD. *Adv. Exp. Med. Biol.* 157, 1061149–1061157. doi:10.1007/978-981-10-8684-7_12
- Wu, X., Li, X., Li, J., Zhao, X., Cui, Y., and Eerdun, C. (2023a). Scoparone inhibits breast cancer cell viability through the NF- κ B signaling pathway. *Exp. Ther. Med.* 26, 328. doi:10.3892/etm.2023.12027
- Wu, Z., Wang, W., Wei, L., and Zhu, S. (2023b). Current status and frontier tracking of clinical trials on Metformin for cancer treatment. *J. Cancer Res. Clin. Oncol.* 149, 16931–16946. doi:10.1007/s00432-023-05391-w
- Xia, H., Liu, C., Li, C. C., Fu, M., Takahashi, S., Hu, K. Q., et al. (2018). Dietary tomato powder inhibits high-fat diet-promoted hepatocellular carcinoma with alteration of gut microbiota in mice lacking carotenoid cleavage enzymes. *Cancer Prev. Res. (Phila)* 11 (12), 797–810. doi:10.1158/1940-6207.CAPR-18-0188
- Xie, G., Wang, X., Liu, P., Wei, R., Chen, W., Rajani, C., et al. (2016). Distinctly altered gut microbiota in the progression of liver disease. *Oncotarget* 7 (15), 19355–19366. doi:10.18632/oncotarget.8466
- Xu, Q., Ren, L., Ren, N., Yang, Y., Pan, J., Zheng, Y., et al. (2023). Ferroptosis: a new promising target for hepatocellular carcinoma therapy. *Mol. Cell. Biochem.* doi:10.1007/s11010-023-04893-y
- Yahoo, N., Dudek, M., Knolle, P., and Heikenwälder, M. (2023). Role of immune responses in the development of NAFLD-associated liver cancer and prospects for therapeutic modulation. *J. Hepatol.* 79, 538–551. doi:10.1016/j.jhep.2023.02.033
- Yamada, K., Tanaka, T., Kai, K., Matsufuji, S., Ito, K., Kitajima, Y., et al. (2023a). Suppression of NASH-related HCC by farnesyltransferase inhibitor through inhibition

- of inflammation and hypoxia-inducible factor-1 α expression. *Int. J. Mol. Sci.* 24 (14), 11546. doi:10.3390/ijms241411546
- Yamada, S., Morine, Y., Imura, S., Ikemoto, T., Saito, Y., Shimizu, M., et al. (2023b). Effect of daikenchuto (TU-100) on carcinogenesis in non-alcoholic steatohepatitis. *J. Med. Invest.* 70 (1.2), 66–73. doi:10.2152/jmi.70.66
- Yang, A., Zhu, X., Zhang, L., and Ding, Y. (2023a). Transitioning from NAFLD to MAFLD and MASLD: consistent prevalence and risk factors in a Chinese cohort. *J. Hepatol.* S0168-8278 (23), 05161–05169. [pii]. doi:10.1016/j.jhep.2023.09.033
- Yang, Z., Gao, S., Wong, C. C., Liu, W., Chen, H., Shang, H., et al. (2023b). TUBB4B is a novel therapeutic target in non-alcoholic fatty liver disease-associated hepatocellular carcinoma. *J. Pathol.* 260 (1), 71–83. doi:10.1002/path.6065
- Ye, M., Liu, C., Liu, J., Lu, F., Xue, J., Li, F., et al. (2023). Scoparone inhibits the development of hepatocellular carcinoma by modulating the p38 MAPK/Akt/NF- κ B signaling in nonalcoholic fatty liver disease mice. *Environ. Toxicol.* doi:10.1002/tox.23851
- Yin, L., Liu, P., Jin, Y., Ning, Z., Yang, Y., and Gao, H. (2022). Ferroptosis-related small-molecule compounds in cancer therapy: strategies and applications. *Eur. J. Med. Chem.* 244, 114861. doi:10.1016/j.ejmech.2022.114861
- Yokohama, K., Fukunishi, S., Ii, M., Nakamura, K., Ohama, H., Tsuchimoto, Y., et al. (2016). Rosuvastatin as a potential preventive drug for the development of hepatocellular carcinoma associated with non-alcoholic fatty liver disease in mice. *Int. J. Mol. Med.* 38 (5), 1499–1506. doi:10.3892/ijmm.2016.2766
- Younossi, Z., Anstee, Q. M., Marietti, M., Hardy, T., Henry, L., Eslam, M., et al. (2018). Global burden of NAFLD and NASH: trends, predictions, risk factors and prevention. *Nat. Rev. Gastroenterol. Hepatol.* 15 (1), 11–20. doi:10.1038/nrgastro.2017.109
- Younossi, Z. M., Otgonsuren, M., Henry, L., Venkatesan, C., Mishra, A., Erario, M., et al. (2015). Association of nonalcoholic fatty liver disease (NAFLD) with hepatocellular carcinoma (HCC) in the United States from 2004 to 2009. *Hepatology* 62 (6), 1723–1730. doi:10.1002/hep.28123
- Yu, J., Shen, J., Sun, T. T., Zhang, X., and Wong, N. (2013). Obesity, insulin resistance, NASH and hepatocellular carcinoma. *Semin. Cancer Biol.* 23, 483–491. doi:10.1016/j.semcancer.2013.07.003
- Yu, X., Lin, Q., Wu, Z., Zhang, Y., Wang, T., Zhao, S., et al. (2020). ZHX2 inhibits SREBP1c-mediated *de novo* lipogenesis in hepatocellular carcinoma via miR-24-3p. *J. Pathol.* 252, 358–370. doi:10.1002/path.5530
- Zhang, C., and Yang, M. (2021). Targeting T cell subtypes for NAFLD and NAFLD-related HCC treatment: an opinion. *Front. Med. (Lausanne)* 8, 789859. doi:10.3389/fmed.2021.789859
- Zhang, J., Xie, H., Yao, J., Jin, W., Pan, H., Pan, Z., et al. (2023b). TRIM59 promotes steatosis and ferroptosis in non-alcoholic fatty liver disease via enhancing GPX4 ubiquitination. *Hum. Cell.* 36, 209–222. doi:10.1007/s13577-022-00820-3
- Zhang, J., Zhang, W., Yang, L., Zhao, W., Liu, Z., Wang, E., et al. (2023a). Phytochemical gallic acid alleviates nonalcoholic fatty liver disease via AMPK-ACC-PPAR α axis through dual regulation of lipid metabolism and mitochondrial function. *Phytomedicine* 109, 154589. doi:10.1016/j.phymed.2022.154589
- Zhang, X., Coker, O. O., Chu, E. S., Fu, K., Lau, H., Wang, Y. X., et al. (2021a). Dietary cholesterol drives fatty liver-associated liver cancer by modulating gut microbiota and metabolites. *Gut* 70 (4), 761–774. doi:10.1136/gutjnl-2019-319664
- Zhang, Y., Li, X., and Li, X. (2021b). Curcuma ameliorates diethylnitrosamine-induced hepatocellular carcinoma via alteration of oxidative stress, inflammation and gut microbiota. *J. Inflamm. Res.* 14, 5551–5566. doi:10.2147/JIR.S330499
- Zhao, J., Liao, Y., Wei, C., Ma, Y., Wang, F., Chen, Y., et al. (2023). Potential ability of probiotics in the prevention and treatment of colorectal cancer. *Clin. Med. Insights-Oncology* 17, 11795549231188225. doi:10.1177/11795549231188225
- Zhou, F., Zhou, J., Wang, W., Zhang, X. J., Ji, Y. X., Zhang, P., et al. (2019). Unexpected rapid increase in the burden of NAFLD in China from 2008 to 2018: a systematic review and meta-analysis. *Hepatology* 70 (4), 1119–1133. doi:10.1002/hep.30702
- Zhou, Y., Han, Z., Zhao, Z., and Zhang, J. (2023). Scoparone attenuates glioma progression and improves the toxicity of temozolomide by suppressing RhoA/ROCK1 signaling. *Environ. Toxicol.* doi:10.1002/tox.23882
- Zou, L., Shi, Q., Li, Y., Yuan, Z., Peng, L., Lu, J., et al. (2023). FMO1 promotes nonalcoholic fatty liver disease progression by regulating PPAR α activation and inducing ferroptosis. *Discov. Med.* 35, 612–622. doi:10.24976/Descov.Med.202335177.60



OPEN ACCESS

EDITED BY

Abd El-Latif Hesham,
Beni-Suef University, Egypt

REVIEWED BY

Jianguo Sun,
China Pharmaceutical University, China
Fei Luan,
Shaanxi University of Chinese Medicine, China

*CORRESPONDENCE

Bo Hong,
✉ bohong200630174@163.com
Tao Xu,
✉ 19304661649@163.com

RECEIVED 22 September 2023

ACCEPTED 04 January 2024

PUBLISHED 23 January 2024

CITATION

Li W, Hou Y, Wang Y, Liu R, Zhang H, Luo Y, Li Q,
Njolibimi M, Hong B and Xu T (2024), Shizao
decoction for cirrhotic ascites: assessing
potential targets based on network analysis
combined with pharmacokinetics
and metabolomics.
Front. Pharmacol. 15:1298818.
doi: 10.3389/fphar.2024.1298818

COPYRIGHT

© 2024 Li, Hou, Wang, Liu, Zhang, Luo, Li,
Njolibimi, Hong and Xu. This is an open-access
article distributed under the terms of the
[Creative Commons Attribution License \(CC BY\)](https://creativecommons.org/licenses/by/4.0/).
The use, distribution or reproduction in other
forums is permitted, provided the original
author(s) and the copyright owner(s) are
credited and that the original publication in this
journal is cited, in accordance with accepted
academic practice. No use, distribution or
reproduction is permitted which does not
comply with these terms.

Shizao decoction for cirrhotic ascites: assessing potential targets based on network analysis combined with pharmacokinetics and metabolomics

Wenjing Li¹, Yujiao Hou¹, Yanping Wang², Ronghong Liu³,
Han Zhang¹, Yanqiong Luo¹, Qian Li¹, Mosesmanaanye Njolibimi¹,
Bo Hong^{1*} and Tao Xu^{1*}

¹School of Pharmacy, Qiqihar Medical University, Qiqihar, China, ²Comprehensive Support Center, Arongqi Medical Security Bureau, Hulunbuir, China, ³Pharmacy Department, Xichong Traditional Chinese Medicine Hospital, Nanchong, China

Introduction: Shizao decoction (SZD) is a traditional Chinese medicine decoction that has therapeutic effects on cirrhotic ascites (CAS). Because of the unclear treatment mechanism, in the current study, the anti-CAS activity of SZD and molecular mechanisms were analyzed by network analysis combined with pharmacokinetics and metabolomics.

Methods: Firstly, we assessed the anti-CAS efficacy of SZD by hematoxylin-eosin (H&E), liver function tests, NO and ET-1 levels, and portal venous pressure. Secondly, network analysis was applied to dig out the metabolites, targets, and pathways related to SZD and CAS. Then, the pharmacokinetics of the pharmacokinetically relevant metabolites (PRM) were analyzed. Thirdly, the serum and urine metabolic biomarkers of rats with CAS were identified using metabolomics by comparing them with the SZD treatment group. In addition, MetaboAnalyst was utilized to conduct metabolic pathway analysis. Finally, the correlation analysis established a dynamic connection between absorbed PRM from SZD and CAS-associated endogenous metabolites.

Results: Pharmacodynamic analysis indicated that SZD effectively mitigated liver injury symptoms by ameliorating inflammatory cell infiltration in CAS rats. The network analysis results indicated that twelve RPM contribute to the therapeutic efficacy of SZD against CAS; the key signaling pathways involved might be hepatitis B and PI3K-Akt. Pharmacokinetics results showed that the 12 RPM were efficiently absorbed into rat plasma, ensuring desirable bioavailability.

Abbreviations: ALT, Alanine aminotransferase; ALB, Albumin; AST, Aspartate transaminase; AUC, Area under curve; CA, Caffeic acid; CAS, Cirrhotic ascites; CHA, Chlorogenic acid; DHA, Docosahexaenoic acid; FA, formic acid; GLB, Globulin; RSD, Relative standard deviations; C_{max}, Maximum concentration after oral dosing; SZD, Shizao decoction; LLOQ, Lower limit of quantification; OPLS-DA, Orthogonal correction partial least squares-discriminant analysis; PA, Protocatechuic acid; PCA, Principal component analysis; TBIL, Total bilirubin; 9,10-EPOME, 9,10-Epoxyoctadecenoic acid; T_{1/2}, Half-life, ESI, Electrospray ionization; T_{max}, Time of apparent maximum concentration measured; UPLC-Q-TOF/MS, Ultra high performance liquid chromatography coupled with quadrupole-time-of-flight mass spectrometry; IS, Internal standard; LA, Linoleic acid; LA-HPOD, 8(R)-Hydroperoxylinoleic acid; VIP, Variable significance analysis; ULOQ, Upper Limit of quantitation; UL, Umbelliferone; UPLC-MS/MS, Ultra-high Performance Liquid Chromatography tandem Mass Spectrometry.

The metabolomic analysis yielded 21 and 23 significantly distinct metabolites from the serum and urine, respectively. The 12 bioavailable SZD-PRM, such as luteolin, apigenin, and rutin, may be associated with various CAS-altered metabolites related to tryptophan metabolism, alpha-linolenic acid metabolism, glycine metabolism, etc.

Discussion: A novel paradigm was provided in this study to identify the potential mechanisms of pharmacological effects derived from a traditional Chinese medicine decoction.

KEYWORDS

Shizao decoction, pharmacokinetics, metabolomic, network analysis, cirrhotic ascites

1 Introduction

Chronic liver disease can irreversibly lead to cirrhosis, the most common and clinically relevant complication of cirrhosis (Gallo et al., 2020). Dysregulation of multiple intersecting biological pathways is intimately linked to the development of CAS. Current scientific strategies to discover therapeutic approaches for CAS usually focus on a single target: dehydration, so diuretic therapy is the standard traditional treatment method (Li et al., 2023). However, long-term use of diuretics can lead to endocrine disorders, diarrhea, and abdominal pain. Traditional Chinese Medicine (TCM) is multi-targeted and has been used clinically for thousands of years (Gao and Yao, 2019). Hence, exploring bioactive metabolites extracted from classical formulations of TCM with good therapeutic effects is a potentially effective way to discover novel therapeutics for CAS.

SZD, a very famous water-removing formula, is from “Treatise on Febrile Diseases” and has also been found in “Synopsis of the Golden Chamber” (Zhou et al., 2012). It comprises 4 botanical drugs: euphorbia (*Euphorbia pekinensis* Rupr.), flos genkwa (*Daphne genkwa* Siebold & Zucc.), gansui (*Euphorbia kansui* S.L.Liou ex S.B.Ho.), and jujube (*Ziziphus jujuba* Mill.). It is commonly used clinically to treat CAS and has achieved significant efficacy with few side effects (Zhao et al., 2018). Euphorbia has been widely used to treat urinary retention, malignant ascites, and edema because of its diuretic and decongestive properties. Euphorbia has been included in many formulas, such as the Ji Dai formula and Modified Shi Zao Decoction, for treating malignant ascites (Luo, 2013; He, 2015; He et al., 2017). The extracts of euphorbia have been found to have a variety of activities, such as antiviral and anti-inflammatory effects. Flos genkwa, a traditional laxative and water-removing medicine, is mainly used to treat the syndrome of fluid retained in the chest, hypochondrium, and abdominal fluid (Jiang et al., 2015). Gansui is a dry root derived from *Euphorbia kansui* T., which is toxic and commonly used to treat pleural effusion, ascites, and edema (Zhao et al., 2019a). Euphorbia, *Euphorbia kansui*, and flos genkwa in SZD are toxic to the intestinal tract. Adding jujube can enhance immunity and show network analysis of the anti-inflammatory effects by regulating the gut microbiota and metabolites (Gao et al., 2023).

“Holistic regulation,” which views the organism as a whole, is what distinguishes Chinese herbal medicine. CHM practitioners focus more on the patients with diseases than on the ailments themselves, using the human body’s homeostasis as their guidance. It is challenging for a single medication to meet the needs of patients with variable and complex conditions due to the diversity of pathogenesis and the complexity of patients’ conditions. The TCM formula is derived

from the wealth of rich experience in long-term clinical practice by fully utilizing the benefits of TCM differentiation and treatment. A large number of studies have confirmed the multi-target and multi-level characteristics of the mechanism of action of traditional Chinese medicine compounding, which means that modern scientific analysis should be used to study the active ingredients of compounding and the mechanism of compounding action. The characteristics of the mechanism of action of traditional Chinese medicine formulas are very similar to the completeness, systematicity, and comprehensiveness of network pharmacology, so network analysis is very suitable for the study of the pharmacological mechanism of traditional Chinese medicine formulas (Wang et al., 2022; Shang et al., 2023). There are multiple metabolites in TCM formulations. Network analysis can be used to screen potential metabolites and targets, while the potential PRM absorbed into the bloodstream at an effective concentration is a prerequisite for the therapeutic effects of TCM formulation. Therefore, pharmacokinetics revealed the exposure levels of the absorbed PRM from SZD (Zhao et al., 2021). Metabolic markers and pathways that may predict drug responses can be identified by metabolomics (Pang et al., 2019). Subsequently, integrating network analysis, pharmacokinetics, and metabolomics is a practical method to predict pharmacodynamic PRM and explore the effects of PRM.

To our knowledge, pharmacokinetic studies of CAS have never been reported before. In this paper, the metabolites and targets of SZD were screened by network analysis, and pharmacokinetic studies of the PRM of SZD were performed to explore the exposure levels in the blood. Comprehensive metabolomic studies of CAS in serum and urine were used to identify potential biomarkers of CAS. Finally, we explored the possible mechanisms of SZD for treating CAS by integrating pharmacokinetics and metabolomics. These findings contribute to the development of new therapeutic targets and treatments for CAS.

2 Methods

2.1 Reagents and chemical

Euphorbia (root, Lot: 20210324, 20210515), flos genkwa (bud, Lot: 20210427, 20210509), gansui (root tuber, Lot: 20210612, 20210718) and jujube (fruit, Lot: 20210728) were all purchased from Nanjing Tongrentang Pharmaceutical Co., Ltd. (Nanjing, China). The plant name has been checked with <http://www.worldfloraonline.org>. (Note: website accessed on 27 August 2023). Moreover, it was identified by Prof. Lina Guo (School of

Traditional Chinese Materia Medica, Qiqihar Medical University, Qiqihar, China) as the dried root of *Euphorbia peginensis* Rupr., the dried flower bud of *D. genkwa* Siebold & Zucc., the dried tuberous root of *Euphorbia kansui* Liou ex S.B.Ho., and the ripe fruit of *Z. jujuba* Mill., respectively, and placed in the herbarium of Chinese herbs of Qiqihar Medical University. Preparation of SZD: *Euphorbia* and *gansui* were removed from the non-medicinal parts, impurities, and foreign matter, and *flos genkwa* was removed from the impurities to produce the raw drinkable tablets of each herb. Pure *flos genkwa* was placed in a hot pan, heated with mild fire, and stir-fried until it changed color, removed, and allowed to cool, resulting in boiled *flos genkwa*. The above tablets were pulverized and then passed through a 200-mesh sieve. 3 g of *euphorbia*, *gansui*, and *flos genkwa* were accurately weighed, and 3 g of *jujube* was removed from the pit and weighed. The mixture was boiled in two batches and concentrated to 500 mL. Finally, SZD was obtained. The extraction rate of the extract was 31%.

Colchicine tablets (Lot: 120994) were produced by Kunming Pharmaceutical Group Co., Ltd. (Kunming, China). Colchicine tablets (Lot: 120994, packing specification of 0.5 mg × 100) were produced by Kunming Pharmaceutical Group Co., Ltd. (Kunming, China). The reference substances were supplied by Xinyang Zhongjian Quantitative Biotechnology Co., Ltd. (Henan, China), including PA (protocatechuic acid, Lot: 200406), CHA (chlorogenic acid, Lot no: 191110), CA (caffeic acid, Lot: 190503), rutin (Lot no: 200404), isovitexin (Lot: 191218), galuteolin (Lot no: 190721), UL (Umbelliferone, Lot: 190621), Luteolin (Lot: 190711), Naringenin (Lot no: 191224), Apigenin (Lot: 200824), Daphnoretin (Lot: 200516), Genkwanin (Lot no: 200518), and Schisandrin (Lot: 21022452) (internal standard, IS). The purity of all reference substances was >98%. Methanol and acetonitrile (Lot: 348604, 142085) were from high-performance liquid chromatography (HPLC, Fairfield Reagent Co., Ltd.). Formic acid (chromatographically pure, Lot: 095224) was purchased from the American Dikma Corporation.

2.2 Animals and groups

2.2.1 Animals

Sprague Dawley rats (220 ± 20 g) of half gender were supplied by the Animal Experimental Center of Qiqihar Medical University and Beijing Weitong Lihua Laboratory Animal Co., Ltd., respectively (animal license No. SCXK (Beijing) 2007-0001, SYXK (Hei) 2021-013). Rats had free access to water. Animal room temperature: 20–22°C, humidity: 40%–70%. All protocols for animal studies were approved by the Animal Ethics Committee of Qiqihar Medical University and conducted according to the guidelines (approval number: QMU-AECC-2022-13; time: 3/6/2022).

2.2.2 Grouping of rats and establishment of the CAS model

The rats were randomly divided into different groups. For pharmacokinetics, the blank group can test the comprehensive impact of factors such as instrument noise, reagents, environment, and contamination during operation on sample determination. Meanwhile, the blank experiment can reduce the

experimental error, which is essential to improving the accuracy of the test results. The experimental group was given 2 mL of SZD sample solution (5 mg/kg), and the same amount of water was given to the blank group. The rats for metabolomics research were in the normal group (A), CAS model group (B) (Fortea et al., 2018), SZD treatment group (C), and colchicine treatment group (D). After the rats were acclimated in the laboratory for 1 week, the normal rats were given water, and the other groups were given 35% phenobarbital solution (first week) for 1 week of induction. Intraperitoneal injection of 10% CCL₄ oil solution twice a week (week 2–3), the dose is 1 mL/kg, and the first dose is double; 12% CCL₄ oil solution (week 4–5); 14% CCL₄ oil solution (week 6–7); 16% CCL₄ oil solution (week 8–9); 18% CCL₄ oil solution (week 10–11); 20% CCL₄ oil solution (week 12–14). Liver pathology was examined in 2 animals every 2–3 weeks, starting from the fourth week, to observe the dynamic changes in liver pathology during the modeling process. Colchicine solution (a mixture of colchicine tablet 13.44 mg and water 168 mL) and SZD were given to groups D and C separately from the 10th week. 1 mL/kg of drug solution was gavagely administered every time, twice a week.

10 of the 100 SD rats were chosen in the normal group, and the other 90 rats were used to establish the CAS model. The rats for pharmacodynamic research were in the same four groups as those for metabolomic experiments. During the modeling period, the body weight of the rats was closely monitored, with the abdominal circumference measured before each injection and compared with that before the last injection. The intraperitoneal injection was suspended in rats with significant body weight loss.

2.2.3 Modeling standards and inspection indicators

Modeling standards (Fortea et al., 2018; Zhao et al., 2019b): ① The urine volume was significantly reduced; ② The amount of ascites increased significantly; ③ The regenerative nodules on the liver were observed with the naked eye. ④ The fibrous septa expanded and connected in liver tissue sections, and the hepatic lobules were divided to form pseudolobuli.

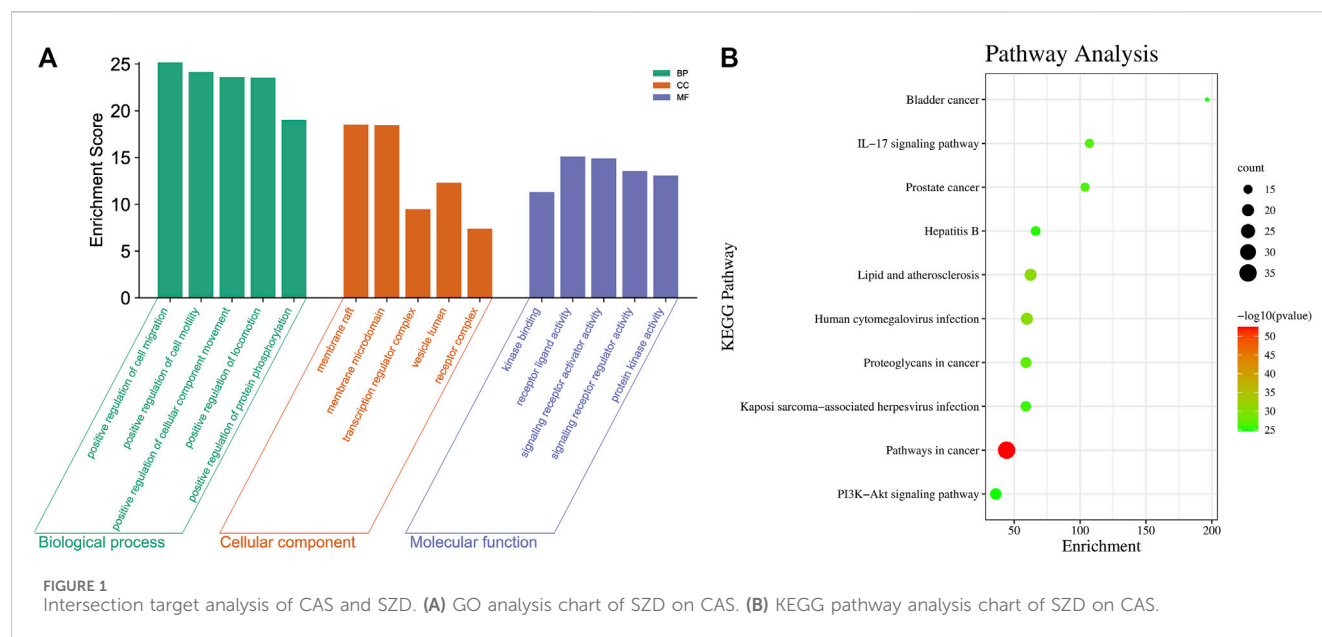
2.3 Pharmacodynamics study

2.3.1 Abdominal water volume

After 14 weeks, the rats were anesthetized with ether. A 3.0 cm incision was made along the abdominal midline, and then a weighed filter paper (2.5 cm × 5.0 cm) was inserted into the abdominal cavity. After 3 min, the filter paper with fully absorbed ascites was taken out and weighed, and the difference between the two masses was calculated.

2.3.2 NO and ET-1 contents and portal vein pressure

After 14 weeks of treatment, the rats in Groups A, B, C, and D were fasted and given an intraperitoneal injection of chloral hydrate (3 mL/kg) for anesthesia. After opening the abdomen, the portal vein was isolated to measure the pressure. After manometry, portal blood was collected to measure liver function and levels of vasoactive substances (NO and ET-1).



2.3.3 H&E experiment

Liver tissue was taken and fixed in formalin. After dehydration with different alcohol concentrations, xylene permeabilization, and paraffin embedding, hematoxylin-eosin staining was performed, and the slide was sealed. According to animal experimental guidelines, the rats were finally euthanized.

2.4 Network analysis studies

Metabolites-target-pathway networks by Cytoscape 3.9.1 were constructed. Perform the following operations in sequence to draw the network: (1) The TCMSP (<http://lsp.nwu.edu.cn/tcmspsearch.php>) and BindingDB (<https://www.bindingdb.org/bind/index.jsp>) databases were used to find metabolites of SZD. The protein targets of these metabolites were predicted through the PubChem (<https://pubchem.ncbi.nlm.nih.gov/>) and Swiss Target Prediction (<http://www.swisstargetprediction.ch/>) databases. Then, the disease targets were filtered on the Gene Cards (<https://www.genecards.org/>) and Online Mendelian Inheritance in Man (OMIM, <https://omim.org/>) databases. (2) After screening the SZD-CAS crossover targets, we performed the enrichment analysis using the Cytoscape database (<https://metascape.org/gp/index.html>). (3) The intersection targets, drugs, metabolites, and KEGG pathways were used to establish a metabolites-targets-pathways-disease network.

2.5 Serum and urine sample preparation for pharmacokinetic and metabolomic analysis

Blood samples for pharmacokinetics: Approximately 500 μ L of blood was collected from the ocular venous plexus at 0.08, 0.25, 0.50, 1.0, 2.0, 3.0, 4.0, 6.0, 8.0, 12.0, and 24 h after administration and placed in a centrifuge tube after rinsing with heparin. Plasma samples (200 μ L) were spiked with 20 μ L of schisandrin, 20 μ L of

hydrochloric acid solution, and 1 mL of ethyl acetate. The mixture was vortexed for 2 min and centrifuged at 12,000 rpm for 5 min at 4°C. The supernatant was removed and blown with nitrogen at 40°C. The residue was reconstituted with 200 μ L of methanol and centrifuged (12,000 rpm, 5 min) to obtain the supernatant for analysis.

Blood samples for metabolomics were placed in a 4°C non-heparinized tube. After 2 h, the serum samples were separated by centrifugation (10 min, 3,500 r min⁻¹, 4°C). Add three times the amount of methanol to the serum sample (600 μ L). After vortexing for 1 min, centrifugation (4°C, 12,000 rpm, 12 min) was performed. The supernatant was collected and filtered with a microporous membrane for analysis. Urine samples for metabolomic analysis (200 μ L) were diluted with 800 μ L of water. The mixed solution was vortexed for 1 min and then centrifuged at 12,000 rpm for 12 min. The supernatant was analyzed using the UPLC-Q-TOF/MS method. Quality control (QC) samples for validation consisted of 50 μ L of mixed serum and urine samples taken separately.

2.6 Plasma pharmacokinetic analysis by UPLC-MS/MS

A SHIMADZU LC-30AD UPLC system and a SCIEX QTRAP 6500+ mass spectrometer were used for UPLC-MS/MS analysis. The chromatographic conditions were as follows: Waters T3 C18 column (2.1 mm \times 100 mm, 1.7 μ m), column temperature: 40°C; flow rate: 0.4 mL/min; injection volume: 1 μ L. The mobile phases consisted of phase A (0.1% formic acid in water) and phase B (acetonitrile): 0–10 min, 95%–0% A; 10–12 min, 0%–0% A; 12–13 min, 0%–95% A; 13–16 min, 95%–95% A. The mass spectrometry conditions are: condition scan mode: MRM mode; source temperature: 550°C; electrospray voltage: 5,500 V; nebulizing gas and cone gas: 50 and 20 psi. The mass spectrometry parameters of each RPM are listed in [Supplementary Table S1](#).

In the PK study, non-compartmental analysis was performed using Drugs and Statistics version 3.0 (DAS 3.0) software to show the results of the time of maximum plasma concentration (T_{max}), the maximum concentration of the PRM (C_{max}), the terminal elimination half-life ($t_{1/2}$), and the area under the concentration-time curve (AUC).

2.7 Urinary and plasma metabolomic analysis by UPLC-Q-TOF/MS

The SCIEX Triple TOFR 4600 AB ACQUITY UPLC system (AB Corp., Milwaukee, WI, United States) was used in conjunction with a Micromass Quattro Micro API mass spectrometer (AB Corp., Milwaukee, WI, United States) for UPLC-Q-TOF/MS analysis. A T3 column (2.1 mm \times 100 mm, 1.7 μ m) was used in the UPLC analysis system. The flow rate: 0.4 mL min⁻¹; injection volume: 5 μ L; system temperature: 40°C; sample temperature: 4°C. A gradient elution was used, with mobile phase A (0.1% formic acid-water, FA) and phase B consisting of acetonitrile, ACN (0.1% formic acid). The gradient elution procedure is shown in [Supplementary Table S2](#). The MS method was used to identify the obtained metabolites in serum and urine analyses. The ion source was electrospray ionization (ESI) in positive and negative detection mode; source temperature: 530°C; acquisition range: m/z 50–1,200; ion spray voltage: 4,500 V; capillary voltage: 2.5 kV (positive); 2.2 kV (negative); MS/MS collision energy: 20–50 eV; nebulizing gas flow rate: 500 L h⁻¹, cone gas flow rate: 50 L h⁻¹. Cone voltage: 25 V for positive mode, 40 V for negative mode.

2.8 Metabolomic data analysis

Micromass Marker View Applications Manager version 1.2.1 (AB Corp., Milwaukee, WI, United States) and SIMCA-P 13.0 software were used to analyze the raw data. Unsupervised principal component analysis (PCA) and orthogonal partial least-squares discriminant analysis (OPLS-DA) using SIMCA 14.1 (Umetrics AB, Umea, Sweden) were shown as the result data matrix. A joint scoring plot (S-plot) was used to find variables that contributed to differences among different groups by performing a variable significance analysis (VIP) > 1. The accuracy of the results was evaluated by parameters such as R² and Q². For putative identification, the mass of potential biomarkers was first determined; in particular, MS/MS information on marker fragmentation patterns was obtained. Then, we define the structure from MS/MS spectra, databases (METLIN and HMDB), and literature. The identified potential biomarkers were directed to the online website of MetaboAnalyst for metabolic pathway analysis.

2.9 Statistical analysis

Drug concentration-time curves and pharmacokinetic parameters were analyzed using Drug and Statistics (DAS) 3.0 software. Other data were shown as the average \pm SD ($\bar{x} \pm s$) and analyzed by SPSS 20.0 software.

3 Results

3.1 Pharmacodynamic study results

3.1.1 Performance of rats

Compared with the blank group, the rats in the model group had lusterless fur, decreased activity, weight loss, and diluted feces. Compared with the model group, the abdominal water volume was significantly reduced in the SZD and colchicine groups. ([Supplementary Table S3](#)).

3.1.2 HE staining

For group A, the liver lobules were intact and clear; the liver plates were strips, with irregular hepatic sinusoids between the plates; and only a few collagen fibers were present in the confluent area and central vein. For group B, most of the typical lobular structures were destroyed; thick collagen fibrous cords were extended from the confluent area, with the central vein dividing and encircling the lobules; disorganized hepatic cords; obvious hepatocyte edema; extensive steatosis; and some necrosis; inflammatory cells infiltrated the fibrous septum. Compared with group B, the rats in the treatment groups showed significantly less structural damage to the liver lobules and narrower fibrous strips with improved hepatocyte edema; degeneration was significantly improved, and inflammatory cell infiltration was reduced ([Supplementary Figure S2](#)).

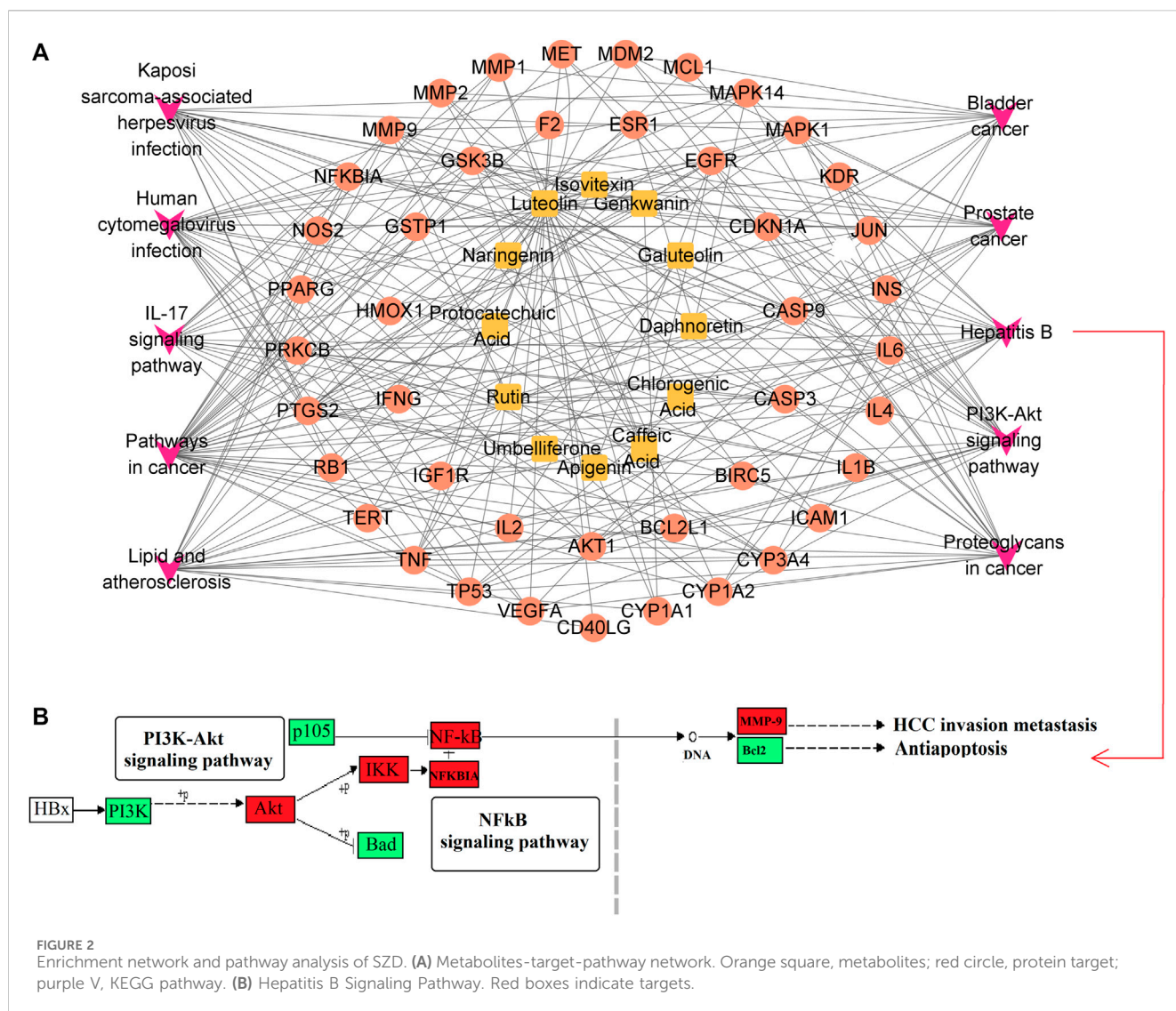
3.1.3 Effect of SZD on liver function in CAS rats

The comparison of liver function levels in rats in each group is shown in [Supplementary Figure S3](#). The levels of ALT, AST, GLB, and TBIL in group B were higher than in group A ($p < 0.01$), while the levels were downregulated after administration of SZD and colchicine (groups C and D). The ALB level in group B was lower than group A ($p < 0.01$), while the levels of ALB in groups C and D were upregulated.

Compared with the normal group, NO and ET-1 levels and portal pressure were increased in the model group. In groups C and D, NO and ET-1 levels and portal pressure decreased ([Supplementary Figure S4](#)). SZD significantly reduced the NO and ET-1 contents and decreased portal vein pressure in rats with CAS, which indicated that the SZD group showed good therapeutic effects.

3.2 Network analysis

Through the TCMSP and Binding DB databases, 74 and 800 targets of SZD and CAS were obtained, respectively. There were 45 intersecting targets between SZD and CAS that were likely to be potential targets of SZD for treating CAS. In addition, 12 metabolites related to the above intersection targets in SZD, which may be related to the treatment of CAS, were screened. To further systematically explore the mechanisms of SZD, 45 intersecting targets were uploaded into the Metascape database. The top 5 GO enrichment items are shown in [Figure 1A](#), and the top 10 KEGG pathways are shown in [Figure 1B](#). Among these pathways, the PI3K-Akt and hepatitis B signaling pathways may be important ways to improve CAS.



A metabolite-target-pathway network was constructed to further explore the mechanism of SZD in improving CAS using the top 10 items in the enrichment pathway. The network topology analysis showed that the metabolites of SZD with the top-degree values for treating CAS were luteolin and rutin. The key targets of SZD may be TNF, CYP3A4, and CYP1A2. In the target, the targets and pathways were directly related (Figure 2A). Finally, 12 metabolites (PA, CHA, CA, rutin, isovitexin, galuteolin, UL, luteolin, naringenin, apigenin, daphnoretin, and genkwanin) were screened as the potentially active metabolites of SZD in treating CAS. As the highest-degree metabolite, luteolin acted on 40 targets (TP53, AKT1, IL6, etc.). MMP9 was associated with three metabolites (rutin, galuteolin, and CA). Moreover, we found that hepatitis B and PI3K-Akt, two closely linked signaling pathways, may be associated with the effects on CAS of SZD. Therefore, we separately intercepted their relationships and further analyzed them through KEGG pathway annotation. The network analysis highlighted the interactions between the PI3K-Akt signaling pathway, the hepatitis B signaling pathway, and key targets (Figure 2B).

3.3 Validation of the UPLC-MS/MS method

The method was validated according to the Drugs and Biologics Method Validation Guidelines of the FDA. The validation parameters were as follows:

Specificity: The ion mass spectra of those PRM are presented in Supplementary Figure S5. The typical MRM chromatograms of 12 analytes and IS are shown in Figure 3. No endogenous species were observed within the 12 PRM and IS, indicating good specificity of the method.

Linearity and LOQ: The linear regression equations, correlation coefficients ($R^2 > 0.99$), linear ranges, ULOQ, and LLOQ values for the 12 PRM showed quantified calibration curves (Supplementary Table S4).

Accuracy and precision: Experimental concentrations should not deviate more than $\pm 15\%$ from their theoretical concentrations. The precision and accuracy results of the 12 PRM are shown in Supplementary Table S5. The within-run precision (CV) range of the 12 PRM was 1.9–11.5%. The between-run precision (CV) range was 2.8–14.9%. The results indicated that the within-run and between-run precisions, given as CV (%), did not exceed 15%.

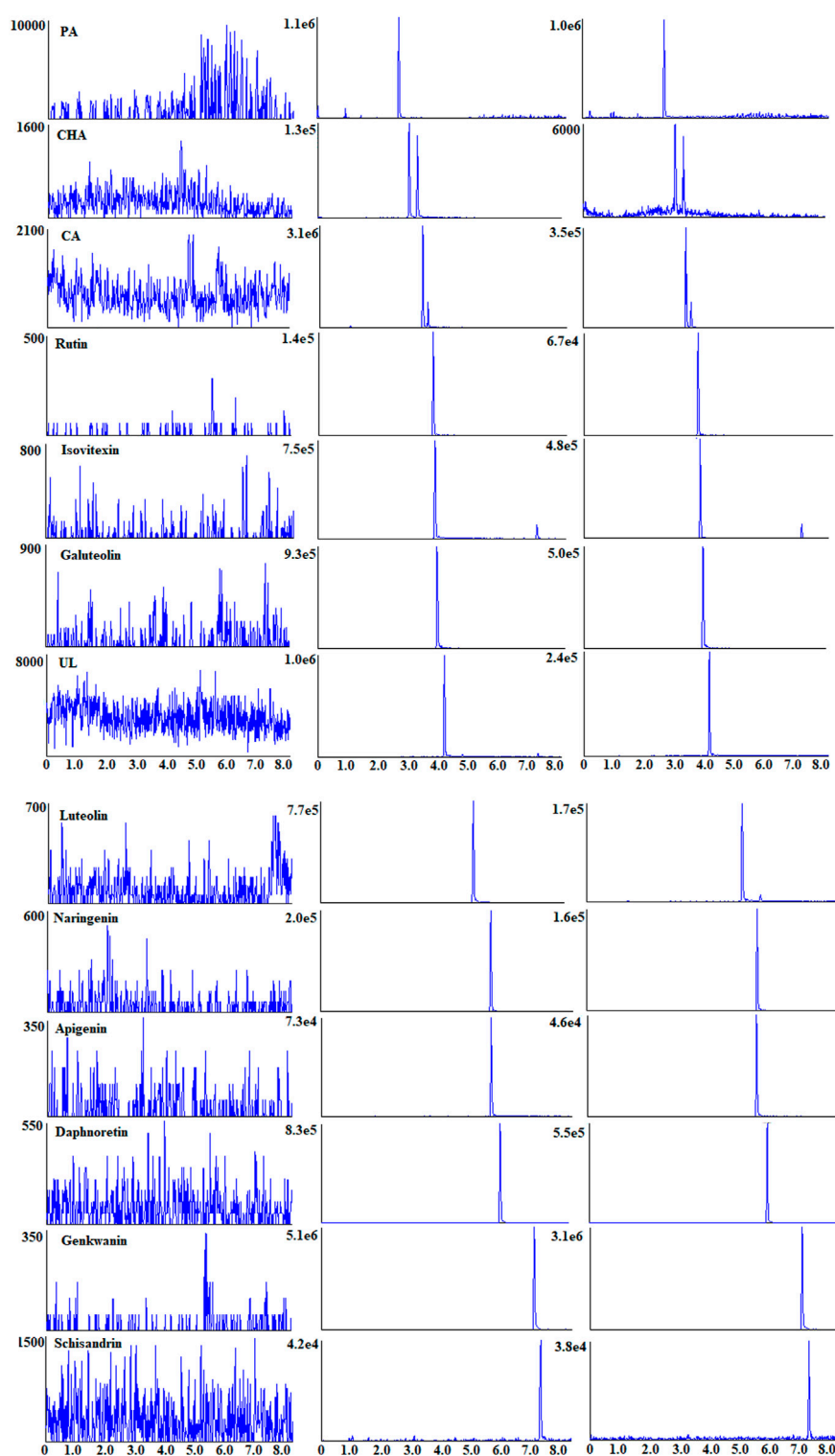


FIGURE 3
Typical MRM chromatograms of 12 analytes and IS in rat plasma.

The results confirmed the excellent reproducibility and reliability in the analytical range.

Extraction recovery and matrix effect: As shown in [Supplementary Table S6](#), the RSDs of extraction recoveries

(70.3–84.2%) were less than 13.0% with consistent, accurate, and repeatable results. The matrix effects were 86.9–114.2%, and the RSDs were less than 15.0%, which showed that the established method meets the requirements.

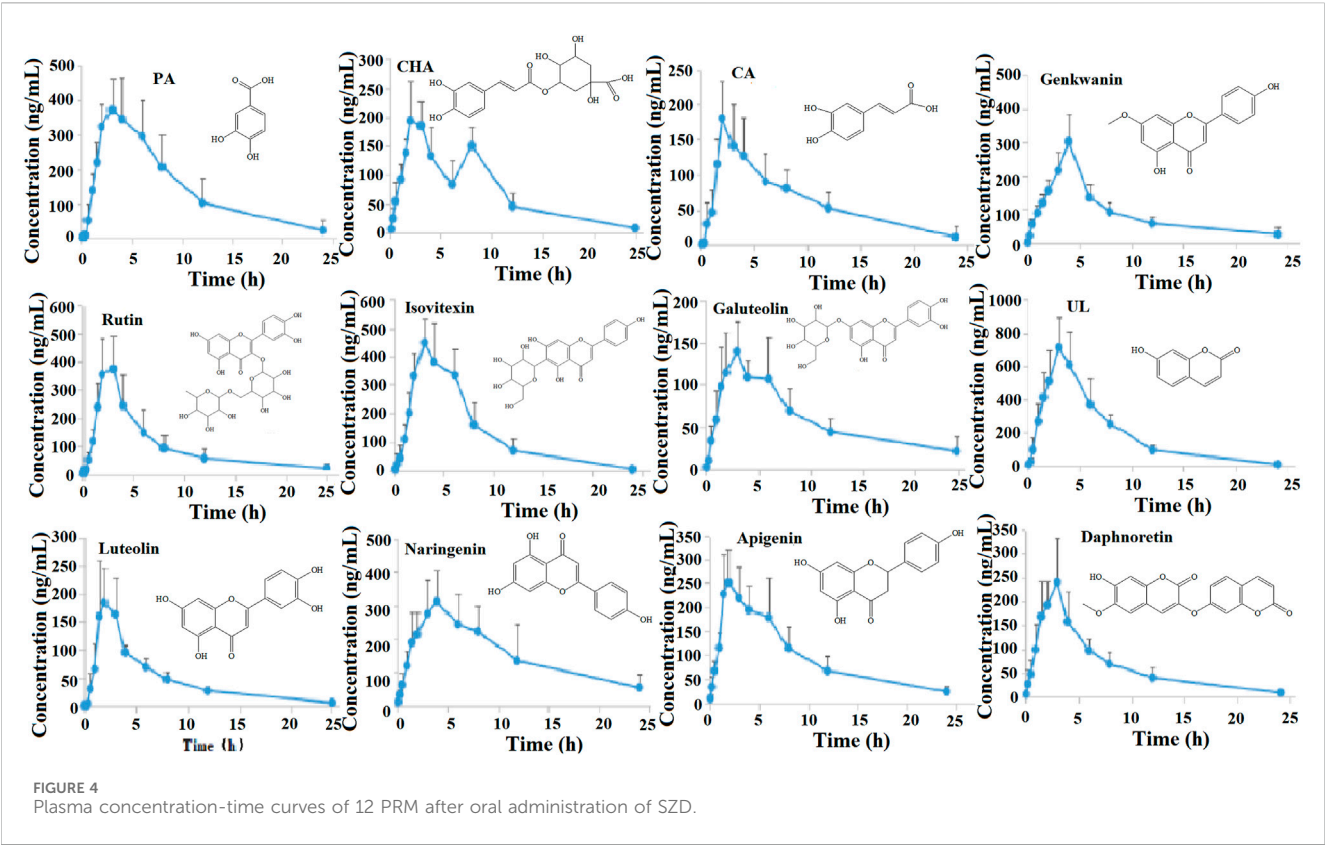


FIGURE 4 Plasma concentration-time curves of 12 PRM after oral administration of SZD.

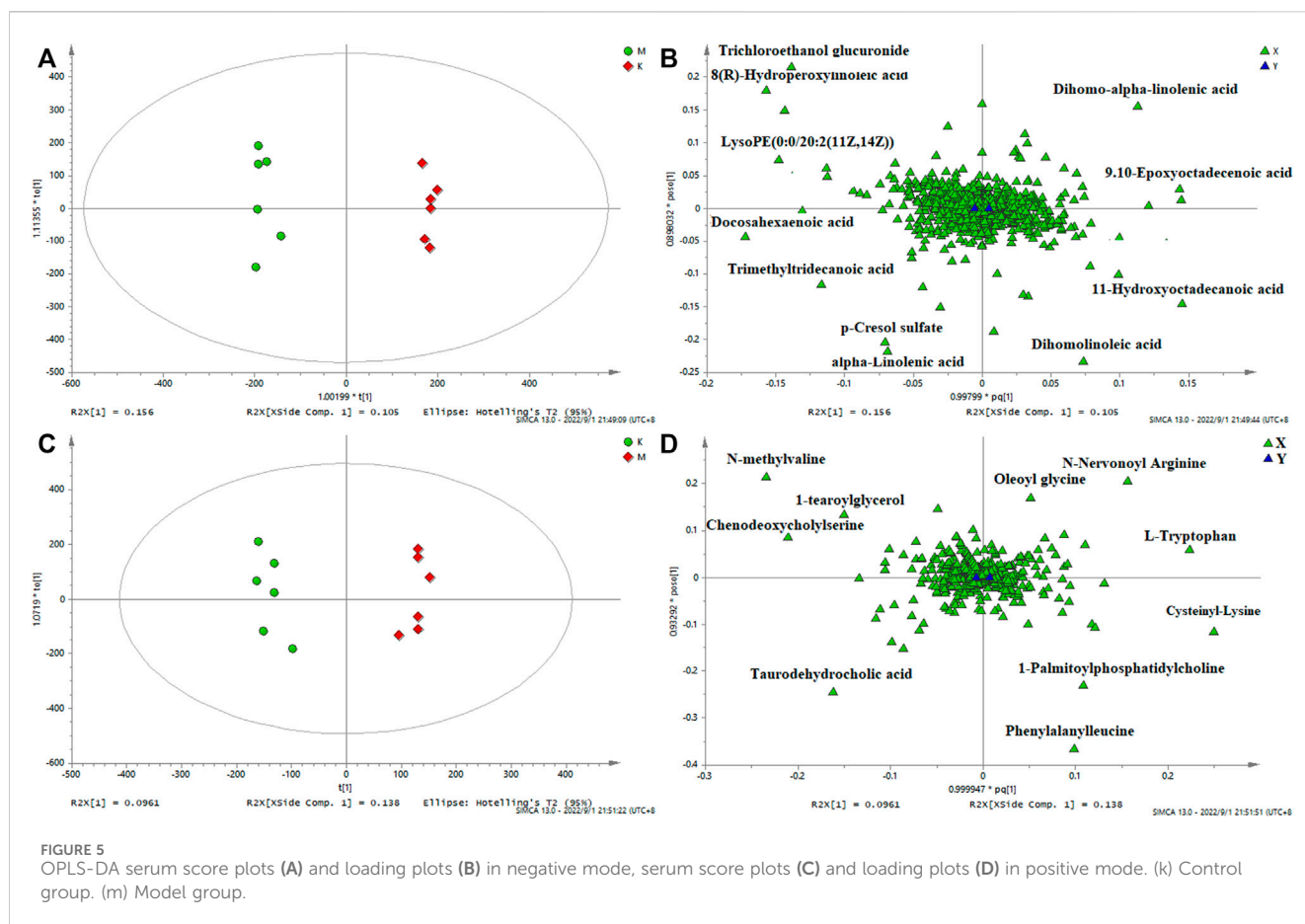
TABLE 1 Pharmacokinetic parameters of 12 analytes in different group.

PRM	AUC _(0-t) (ng·h/mL)	AUC _(0-∞) (ng·h/mL)	T _{1/2} (h)	T _{max} (h)	C _{max} (ng/mL)
PA	3,493.30 ± 1,505.41	3,641.33 ± 1725.92	9.68 ± 2.89	3.88 ± 2.10	347.09 ± 113.56
CHA	1,680.19 ± 564.17	1724.35 ± 570.50	5.85 ± 1.41	2.25 ± 0.93	193.75 ± 59.55
CA	1,610.09 ± 558.05	1833.80 ± 942.07	6.20 ± 3.19	2.19 ± 1.30	180.30 ± 89.43
Rutin	2,384.35 ± 1,086.08	2,568.17 ± 1,380.14	5.35 ± 2.78	2.44 ± 0.62	374.49 ± 122.35
Isovitexin	3,170.12 ± 1,121.18	3,191.18 ± 1,111.83	7.31 ± 1.31	3.50 ± 1.07	448.58 ± 202.57
Galuteolin	1,379.81 ± 463.96	1,492.72 ± 501.32	6.41 ± 3.26	3.13 ± 1.53	139.52 ± 63.34
UL	4,629.52 ± 1,187.68	4,661.42 ± 1,185.75	6.34 ± 0.89	3.19 ± 0.84	710.60 ± 351.36
Luteolin	1,087.29 ± 188.46	1,119.48 ± 193.52	4.5 ± 2.61	2.06 ± 0.62	184.34 ± 68.60
Naringenin	3,637.69 ± 1,667.01	4,406.82 ± 1878.00	10.78 ± 1.87	4.00 ± 1.69	311.72 ± 130.04
Apigenin	2,278.47 ± 655.45	2,492.03 ± 738.98	7.05 ± 3.39	2.04 ± 0.88	250.69 ± 53.25
Daphnoretin	1,572.20 ± 424.58	1,626.87 ± 419.31	6.17 ± 2.41	2.81 ± 0.75	240.57 ± 111.33
Genkwanin	2077.08 ± 640.03	2,314.22 ± 884.40	5.52 ± 2.39	3.88 ± 0.52	301.84 ± 130.33

Stability: The stability results are shown in [Supplementary Table S7](#), including short-term stability, post-preparation stability, freeze-thaw cycle stability, and long-term stability. None of the 12 analytes showed significant degradation (short-term stability: $RSD \leq 11.6\%$, $RE \leq 11.5\%$; post-preparation stability: $RSD \leq 11.6\%$, $RE < 11.3\%$; freeze-thaw cycles: $RSD \leq 12.6\%$, $RE < 10.8\%$; long-term stability: $RSD \leq 12.5\%$, $RE < 12.8\%$).

3.4 Pharmacokinetic analysis of blood RPM after administration of SZD

The concentration-time curves and pharmacokinetic parameters are shown in [Figure 4](#) and [Table 1](#), respectively. The half-life ($T_{1/2}$) and time to peak (T_{max}) of naringenin were approximately 10.78 h and 4.00 h, respectively, which were



longer than the other PRM. The $T_{1/2}$ and T_{max} of luteolin were the shortest, at approximately 4.5 h and 2.06 h, respectively; UL had a higher AUC, and the $AUC_{(0-\infty)}$ of luteolin, PA, CHA, CA, galuteolin, naringenin, and apigenin were $1,119.48 \pm 193.52$, $3,641.33 \pm 1725.92$, 1724.35 ± 570.50 , 1833.80 ± 942.07 , $1,492.72 \pm 501.32$, $4,406.82 \pm 1878$, and $2,492.03 \pm 738.98$ ng/h/mL, respectively. Interestingly, these 12 RPM screened by network analysis were fully exposed to plasma, indicating that after intragastric administration of SZD in rats, the 12 RPM can be absorbed into the blood to exert a therapeutic effect on CAS.

3.5 Metabolic profiling

3.5.1 Metabonomic method validation

Supplementary Figure S6 (in Supplement) shows the chromatograms of serum and urine. Selected ion chromatographic peaks were extracted separately from serum and urine (six positive and six negative ion modes) for method validation. QC samples were applied to investigate precision, repeatability, and stability. The RSDs of retention time for instrument precision, repeatability, and system stability were 0.1%–0.3%, 0.1%–0.3%, and 0.1%–0.4%, respectively, and the RSDs of peak area were 1.9%–8.6%, 3.3%–7.3%, and 3.1%–9.3%, respectively. RE values of –7.7%–6.6% and –7.7%–9.1% were used to

evaluate post-preparative stability and freeze-thaw cycle stability. The results of serum and urine samples are presented in Supplementary Table S8, which shows that the reasonable and reliable method is suitable for metabolomic analysis.

3.5.2 Liver metabolic profile and potential biomarkers

The PCA score chart showed that the normal group, CAS model group, colchicine positive group, and SZD group had been separated because of the significant differences in the metabolic situation. The result showed that the metabolic environment in rats had changed in the four groups after drug administration (Supplementary Figure S7). The SZD administration group was different from the model group. It closed to normal, indicating that the metabolic situation shifted to normal after SZD treatment and that SZD could regulate the metabolic disorder in rats with CAS, consistent with the results of pharmacodynamic studies. The liver structure (Supplementary Figure S2) of Group A was intact, Group B was severely damaged, the damaged liver in Groups C and D was significantly improved, and the inflammatory cell infiltration was also significantly reduced. The concentrated quality control points indicated the good stability of the instrument.

In order to identify the potential biomarkers, supervised OPLS-DA analysis was used to analyze significantly different metabolites in different groups, and S-plots were used to identify variables that affected the metabolic profiles. S-plot results are shown in Figure 5 and Figure 6, which prove the successful establishment of the CAS

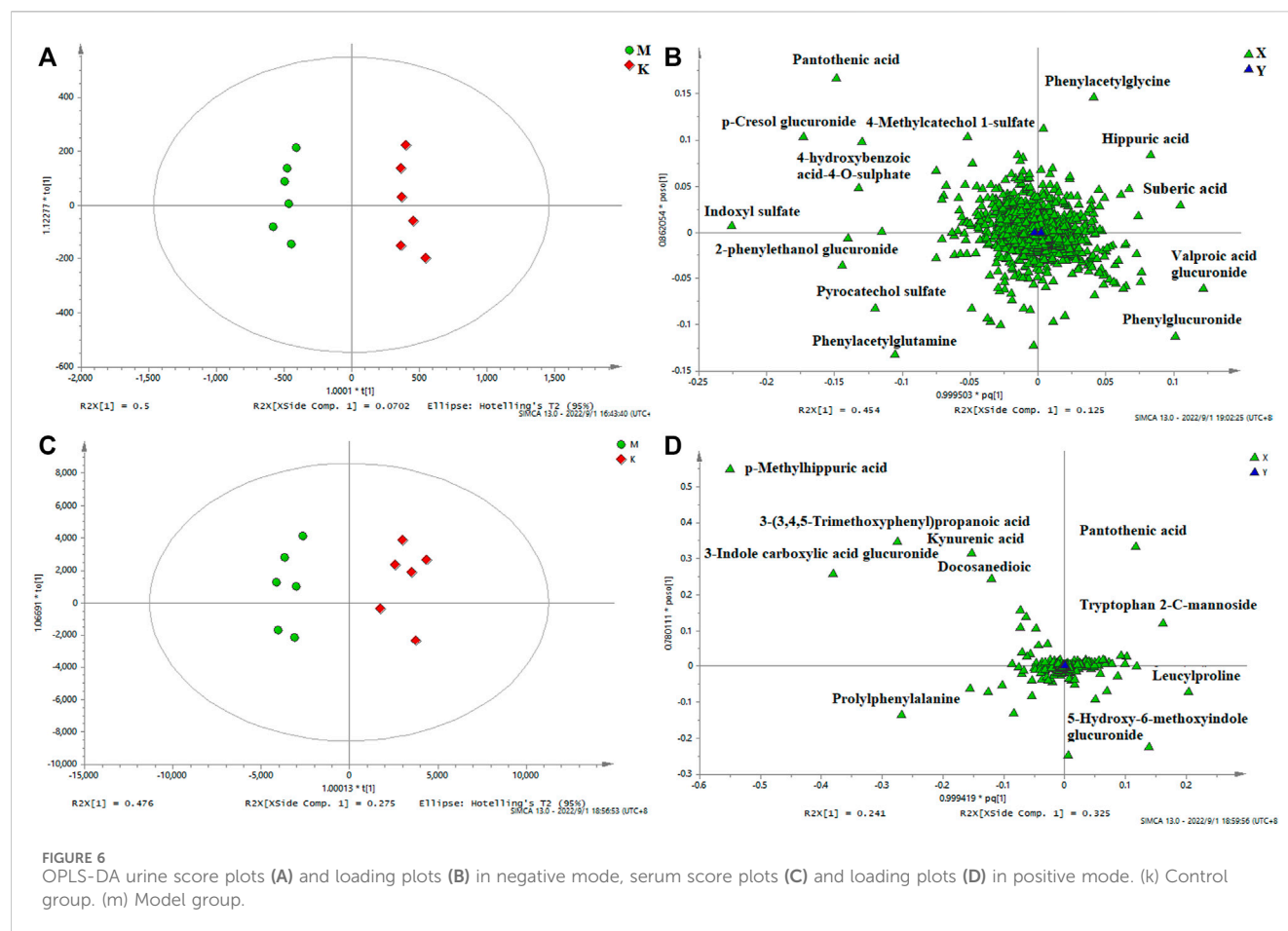


FIGURE 6
OPLS-DA urine score plots (A) and loading plots (B) in negative mode, serum score plots (C) and loading plots (D) in positive mode. (K) Control group. (M) Model group.

model. It was necessary to evaluate the reliability of the model by cross-testing. The results of the parameters used to evaluate model quality are summarized in [Supplementary Table S9](#) (in the Supplement). In general, when R^2 and $Q^2 > 0.9$, the model had excellent explanation and predictive power. R^2 and $Q^2 > 0.5$ indicated that the model had good explanation and predictive ability.

In the research process of non-targeted metabolomics, the variable importance in the projection (VIP) value was usually used as the criterion for judging potential biomarkers. By t -test, $VIP > 1$, $p < 0.05$ between the normal and model groups was used as the screening condition for potential biomarkers. Difference variables were evaluated according to the mass tolerance between the obtained m/z values. Exact masses of RPM within 5 ppm (e^{-6}) were used to infer metabolites. Potential biomarkers were screened and identified based on the above screening criteria and by accurately matching mass and MS/MS fragment information from the online databases HMDB (www.hmdb.ca) and METLIN (metlin.scripps.edu). Finally, 20 metabolites were screened in positive ion mode, and 24 were screened out in negative mode (Table 2). The metabolites in the serum and urine of the drug administration group were significantly different ($**p < 0.01$, $*p < 0.05$), which indicated the preventive and therapeutic effects of SZD. A heat map using MetaboAnalyst showed the metabolic patterns of 44 biomarkers (Figure 7), and the hierarchical clustering results provided a visualization of both groups.

As shown in Figure 8A, five pathways, including tryptophan metabolism, arginine biosynthesis, alpha-linolenic acid metabolism, pantothenic acid biosynthesis, and arginine and proline metabolism, were significantly affected, among which alpha-linolenic acid metabolism had the most significant influence. The correlation between metabolites and metabolic pathways was analyzed by combining the experimental results of network analysis and metabolomics, as well as relevant literature, and the metabolic network analysis diagram is detailed in Figure 8B.

3.6 Comprehensive analysis of network analysis and metabolomics

To fully understand the mechanism of SZD in treating CAS, an interaction network was constructed based on metabolomics and network analysis (Figure 9). The differential metabolites were imported into MetScape, a plug-in of Cytoscape, to obtain a PRM-targets-pathways-disease network. By matching the potential targets found in the network analysis with the genes analyzed by MetScape, two key targets (CYP3A4 and CYP1A2) were identified. The related metabolites were 9,10-epoxyoctadecenoic acid, docosahexaenoic acid (DHA), and tryptophan, which affected the following metabolic pathways: omega-3 fatty acid metabolism, linoleate metabolism, tryptophan

TABLE 2 Potential biomarkers in serum and urine of CAS rats induced by SZD.

t _R (min)	m/z (Da)	Putative identification	M/C	T/M	t _R (min)	m/z (Da)	Putative identification	M/C	T/M
Positive mode in rat serum sample					Negative mode in rat serum sample				
2.09	132.1022	N-methylvaline	↑**	↓*	5.68	322.9486	Trichloroethanol glucuronide	↓**	↑*
4.24	205.0958	L-Tryptophan	↓**	↑**	8.8	327.2334	Docosahexaenoic acid	↓**	↑
6.78	250.123	Cysteinyl-Lysine or Lysylcysteine	↑**	↓**	9.01	279.2325	Dihomolinoleic acid (LA)	↓**	↑**
8.14	279.168	Phenylalanyl-leucine	↑**	↓**	5.83	187.0075	p-Cresol sulfate	↑**	↓**
5.69	340.2839	Oleoyl glycine	↓**	↑**	8.65	277.2182	alpha-Linolenic acid	↓**	↑*
9.94	359.3125	1-Stearoylglycerol	↓**	↑**	7.51	311.2217	8(R)-Hydroperoxylinoleic acid (LA-HPOD)	↓*	↑*
7.85	480.3332	Chenodeoxycholic acid	↑**	↓**	8.18	299.2593	11-Hydroxyoctadecanoic acid	↓**	↑**
7.91	496.3425	1-Palmitoylphosphatid-ylcholine	↑**	↓**	8.19	295.2279	9,10-Epoxyoctadecenoic acid (9, 10-EPOME)	↓**	↑*
6.02	510.254	Taurodehydrocholic acid	↑**	↓**	7.42	504.3083	LysoPE (0:0/20:2 (11Z,14Z))	↑**	↓*
7.84	523.4609	N-Nervonoyl Arginine	↑**	↓**	9.38	305.2487	Dihomo-alpha-linolenic acid	↓**	↑**
					9.45	255.2319	Trimethyltridecanoic acid	↓**	↑
Positive mode in rat urine sample					Negative mode in rat urine sample				
5.79	194.0827	p-Methylhippuric acid	↑**	↓**	4.96	212.0025	Indoxyl sulfate	↑**	↓**
5.41	338.0853	3-Indole carboxylic acid glucuronide	↓**	↑**	5.69	192.0677	Phenylacetyl-glycine	↑**	↓**
4.33	241.1061	3-(3,4,5-Trimethoxyphenyl) propanoic acid	↑**	↓**	5.77	283.0827	p-Cresol glucuronide	↑**	↓**
4.87	190.0517	Kynurenic acid	↑**	↓*	4.01	188.9869	Pyrocatechol sulfate	↓**	↑**
2.95	367.1512	Tryptophan 2-C-mannoside	↑*	↓*	6.04	297.0995	2-Phenylethanol glucuronide	↓**	↑*
10.68	371.3157	Docosanedioic acid	↓**	↑*	5.29	178.0518	Hippuric acid	↓**	↑*
2.38	229.1558	Leucylproline	↑**	↓*	5.87	173.0824	Suberic acid	↓**	↑**
3.56	220.118	Pantothenic acid	↓**	↑**	4.17	216.9817	4-hydroxybenzoic acid -4-O-sulphate	↑**	↓**
5.58	263.1396	Prolylphenylalanine	↑*	↓**	4.94	269.0683	Phenylglucuronide	↑*	↓*
3.09	340.1016	5-Hydroxy-6-methoxyindole glucuronide	↓**	↑*	5.65	203.0013	4-Methylcatechol 1-sulfate	↑**	↓**
					6.29	319.1373	Valproic acid glucuronide	↑**	↓*
					3.5	218.1035	Pantothenic acid	↓**	↑*
					5.4	263.1035	Phenylacetylglutamine	↑**	↓*

Note: M/C, change trend of model group vs. control group; T/M, change trend of SZD, treatment group vs. model group; * Metabolite has significant difference between two group ($p < 0.05$); ** Metabolite has significant difference between two group ($p < 0.01$).

metabolism, and pantothenic acid biosynthesis. They may be the key points in the pharmacological effect of SZD on CAS.

3.7 The correlation between SZD PRM and CAS-related metabolic changes

We performed Pearson correlation analysis to investigate the biological relationship between the CAS-altered endogenous metabolites and the absorbed SZD PRM (Wang et al., 2023a). Interestingly, the concentrations of the absorbed SZD PRM were significantly correlated with the 17 metabolites ($|r| \geq 0.7$ and $p <$

0.05), with negative correlations indicated in blue and positive correlations in red (Figure 10). It was found that the RPM from SZD was mainly positively correlated with taurodehydrocholic acid, DHA, L-tryptophan, kynurenic acid, cysteinyl-lysine, 8(R)-hydroperoxylinoleic acid (LA-HPOD), pantothenic acid, dihomolinoleic acid, phenylacetylglutamine, leucylproline, and oleoyl glycine, and were negatively correlated with indoxyl sulfate, hippuric acid, chenodeoxycholic, 9,10-EPOME, alpha-linolenic acid, and N-nervonoyl arginine. According to the above correlation studies, it was shown that the 12 phytochemicals of SZD have different functions and efficacy and can synergistically resist CAS.

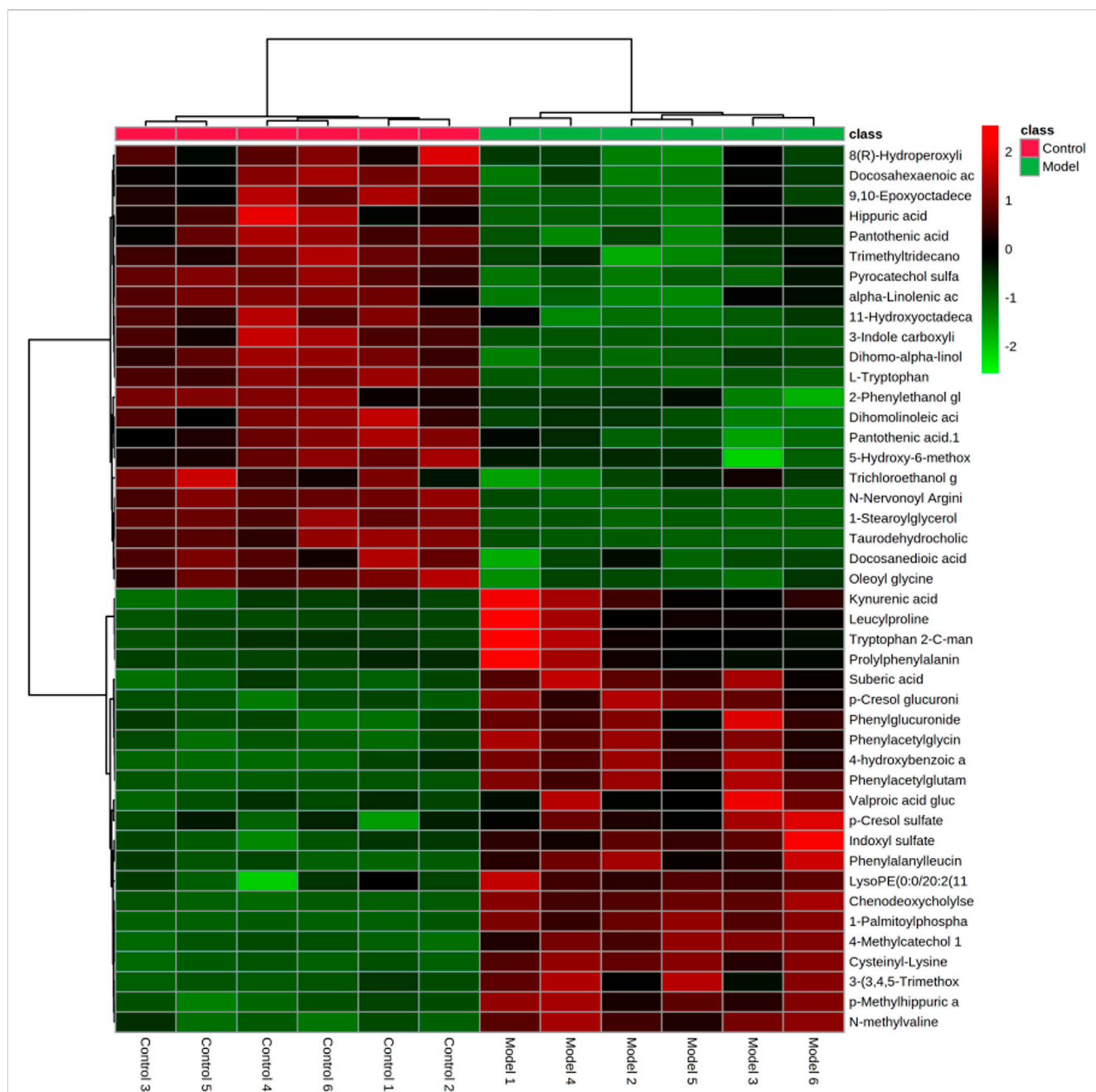


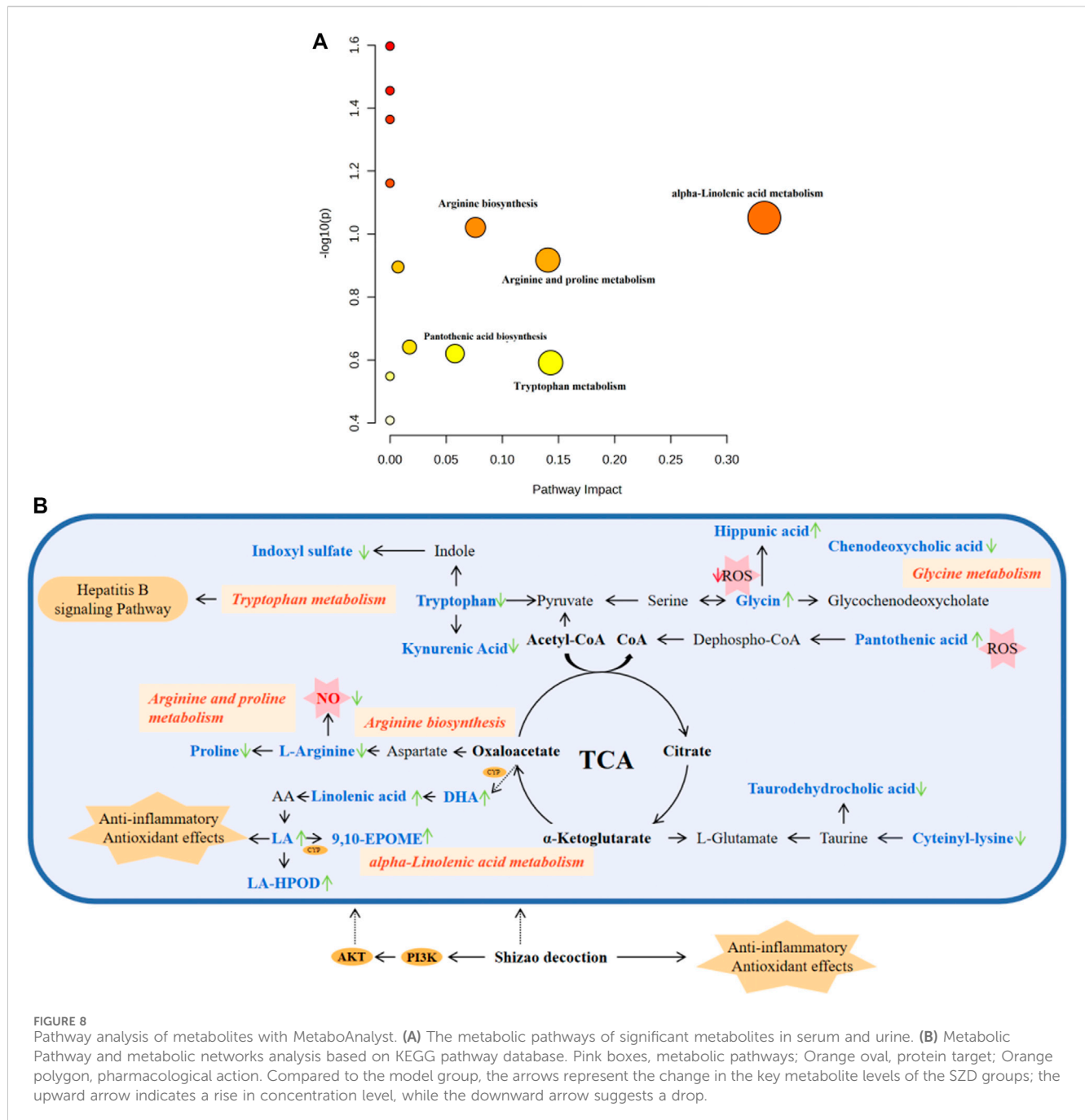
FIGURE 7 Heatmap of differential metabolite levels. With the deepening of red, the expression level of endogenous substances gradually increased, and with the deepening of green, the expression level of endogenous substances gradually decreased.

4 Discussion

The study confirmed that SZD significantly reduced liver injury and inflammatory cell infiltration in CAS rats, improved liver function, reduced ALT, AST, GLB, and TBIL levels, increased ALB levels, and also reduced NO and ET-1 levels in peripheral blood and portal vein pressure. However, systematic studies on the pharmacokinetics and metabolomics of SZD-treated CAS still need to be completed. In this study, 12 metabolites were screened through network analysis, and all have been found to have anti-CAS pharmacological effects according to relevant literature. Moreover,

the pharmacokinetic parameters of the 12 potential PRM of SZD were revealed for the first time after intragastric administration. All these findings shed light on the pathogenesis of CAS and the mechanism of action of the RPM of SZD in the metabolic system of CAS.

The results of the pharmacodynamics showed that SZD could significantly attenuate liver injury and improve liver function in CAS rats. Pharmacokinetic studies indicated PA, CHA, CA, rutin, isovitexin, galuteolin, UL, luteolin, naringenin, apigenin, daphnoretin, and genkwanin have good blood exposure. Studies have shown that these 12 potential PRM of SZD have therapeutic effects on liver diseases such as hepatitis, hepatic cholestasis, cirrhosis, *etc.* While



most chronic liver diseases have the pathological process of hepatitis to hepatic fibrosis to cirrhosis to hepatic carcinoma and cirrhotic ascites is one of the standard clinical manifestations of cirrhosis in its decompensated stage, these 12 potential PRM may hinder the development of cirrhotic ascites by acting on the compensatory stage of cirrhosis. So, we investigated these 12 metabolites. In addition, the metabolites with disordered expression levels were analyzed, which were mainly in the tryptophan metabolism, alpha-linolenic acid metabolism, glycerophospholipid metabolism, pantothenate and CoA biosynthesis, arginine biosynthesis and arginine, and proline metabolism.

High levels of NO production, as an important toxicity executor, play an important role in hepatotoxicity (Harstad and Klaassen, 2002;

Hirunpanich et al., 2008). Arginine is a NO originator, and it can generate NO under the action of the NOS enzyme (Morris et al., 2017). To verify the effect of SZD on NO synthesis, we collected rat portal vein blood and detected the NO content. The NO level in the CAS group was significantly higher than in group A, and the NO content could be improved after SZD treatment (Supplementary Figure S4). Isovitexin can inhibit the expression of iNOS in cells and reduce NO production (Lin et al., 2005; Quintieri et al., 2008; Lucas et al., 2010). In the metabolomic study, SZD treatment led to a significant decrease in the arginine metabolite N-nervonoyl arginine. Arginine is a substrate for NO synthesis, and its downregulation can reduce NO production. Also, the changes in the levels of N-nervonoyl arginine were positively correlated with isovitexin, suggesting the

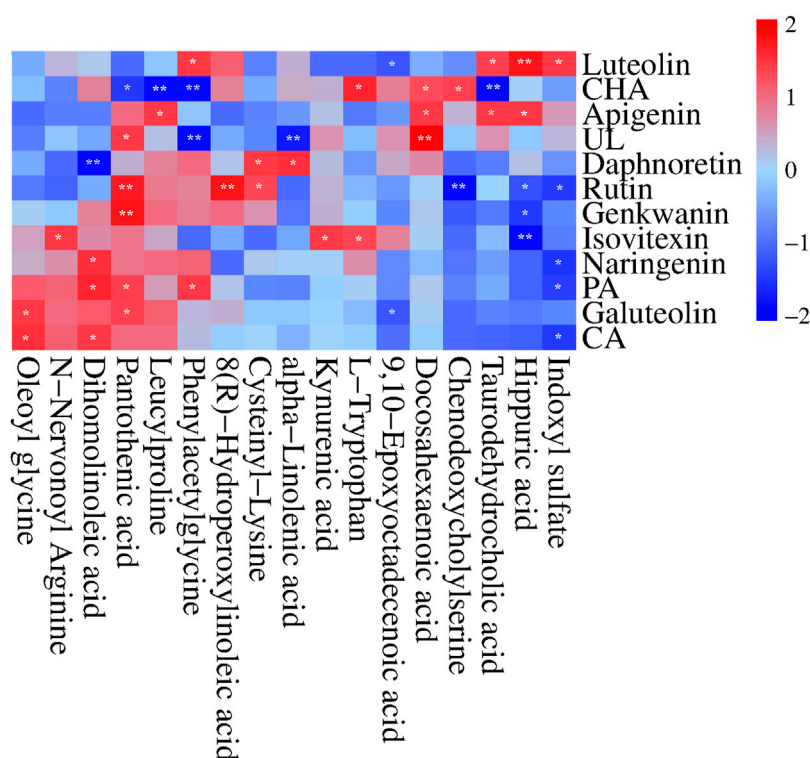


FIGURE 10
Correlation heatmap (Pearson correlation) between the 12 SZD Pharmacokinetic-markers and the plasma CAS-altered metabolites in response to SZD administration. Red and blue squares represent the positive and negative correlations between SZD-RPM and CAS-associated endogenous metabolites, respectively. $n = 10$, $*p < 0.05$, $**p < 0.01$.

where CA can be used in combination with DHA to alleviate oxidative stress damage. In this study, the $AUC_{(0-\infty)}$ of luteolin, PA, CHA, CA, galuteolin, naringenin, and apigenin were $1,119.48 \pm 193.52$, $3,641.33 \pm 1725.92$, 1724.35 ± 570.50 , 1833.80 ± 942.07 , $1,492.72 \pm 501.32$, $4,406.82 \pm 1878$, and $2,492.03 \pm 738.98$ ng h/mL, respectively (Table 1). The AUC values were all larger. A larger AUC indicates greater drug absorption and increased bioavailability. Metabolomic results showed that ω -3 fatty acid metabolism (ω -3 PUFA) may be a potential metabolic pathway for SZD-treated CAS because of α -linolenic acid as the main precursor of ω -3 PUFA metabolites. Moreover, ω -3 PUFA can be metabolized to DHA by Cytochrome P450 (CYP) enzymes (Shoieb et al., 2020). In a CAS model, DHA inhibits fiber formation and prevents the development of cirrhosis by interfering with NF- κ B and TGF β signaling pathways. From the references, we know that CAS models are often induced by CCL₄, which upregulates the inflammatory cytokine TNF, while DHA ameliorates TNF (Boyer-Diaz et al., 2020). In conclusion, there was significant DHA depletion in the livers of patients with advanced cirrhosis. Studies have shown that the development of cirrhosis can be mitigated by enhancing antioxidant capacity. Linoleic acid (LA), or dihomolinoleic acid, is the most consumed PUFA in the human diet and can enhance liver cells' antioxidant capacity and metabolism (Chen et al., 2019; Cai et al., 2022). LA-HPOD can be metabolized into LA in the body, and LA can be metabolized into 9,10-EPOME by CYP enzymes. Enguita et al. evaluated the association between LA and its derived lipid metabolite 9,10-EpOME and biomarkers of liver injury and

systemic inflammation and showed that 9,10-EpOME was reduced in patients. In addition, metabolites associated with anti-inflammation in CAS rats, including DHA, α -linolenic acid, LA-HPOP, LA, and 9,10-EPOME, were found to be significantly altered by metabolomics studies, and administration of SZD significantly improved the changes of these metabolites. Interestingly, positive or negative correlations were found between α -linolenic acid, LA, DHA, LA-HPOD, and 9,10-EPOME and eight absorbed SZD pharmacokinetics markers, including luteolin, PA, CHA, CA, UL, galuteolin, naringenin, and apigenin (Figure 10). In summary, we believe that the occurrence of CAS may be related to inflammation caused by disorders of linolenic and linoleic acid metabolism. These results indicate that SZD may increase the metabolism of linolenic acid to produce DHA by promoting CYP enzymes, thus restoring the normal level of DHA in CAS rats and achieving therapeutic effects.

Through network analysis research, it was hypothesized that hepatitis B might be a key signaling pathway for SZD to treat CAS. HBV may cause cirrhosis or even liver cancer. Besides, some experiments have demonstrated that the RPM of SZD has obvious anti-HBV effects. Through pharmacokinetic studies, the $T_{1/2}$ and T_{max} of luteolin were the shortest, at approximately 4.5 ± 2.61 h and 2.06 ± 0.62 h, respectively, which indicates that luteolin was rapidly absorbed into the bloodstream and reached the site of action. Luteolin inhibits the production of TNF- α , IL-6, and IFN- γ in the blood and has potent anti-HBV effects (Wu et al., 2005; Wu et al., 2022). In addition, studies have shown that PRM PA, rutin,

naringenin, isovitexin, CA, and CHA also exhibit anti-HBV effects (Dai et al., 2017; Jose-Abrego et al., 2022). HBV infection tends to lead to metabolic disorders, in which tryptophan metabolism can produce indoxyl sulfate and kynurenic acid (Kyn). Kyn can inhibit T-cell function and lead to T-cell apoptosis. This reaction puts the body in an immunosuppressed state and severely hinders liver function, so that tryptophan levels are consistently low in CAS patients (Jiang et al., 2020). Our experiment found that, compared with normal rats, CAS rats had higher levels of kynurenic acid and indoxyl sulfate and lower levels of tryptophan. Interestingly, SZD could regulate the levels of tryptophan, kynurenic acid, and indoxyl in CAS rats to return them to normal. Also, the contents of tryptophan, kynurenic acid, and indoxyl sulfate in serum and urine after SZD treatment were positively correlated with those of luteolin, isovitexin, and CHA, while indoxyl sulfate was negatively correlated with CA, PA, naringenin, and rutin (Figure 10). Based on the above results, it can be hypothesized that the PRM of SZD may act on the HBV signaling pathway by binding to the TNF target and interfering with the metabolism of tryptophan to exert anti-HBV effects and stop the progression of HBV to CAS.

Through network analysis, we hypothesized that the PI3K-Akt signaling pathway may play an essential role in SZD to treat CAS (Figure 1; Figure 2). In addition, many studies have shown that CHA, galuteolin (Ho et al., 2021), rutin, and genkwanin (Kim et al., 2023) can exert antioxidant effects by activating this pathway. CHA also prevents CCL₄-induced liver fibrosis by suppressing oxidative stress in the liver and hepatic stellate cells (Shi et al., 2021). Our pharmacokinetic results revealed a significant bimodal peak after CHA absorption into the blood, possibly caused by reabsorption from the enterohepatic circulation (Xu et al., 2020). The enterohepatic circulation of CHA can prolong the half-life and maintenance time of the drug, which is generally beneficial for exerting its therapeutic effect. Through metabolomics research, we found that the content of pantothenic acid in CAS rats was lower than that in the normal group. However, SZD can improve the metabolism of pantothenic acid. Studies have shown that pantothenic acid can prevent CCL₄-induced hepatotoxicity and oxidative stress (Eidi et al., 2012). In addition, pantothenic acid reduces oxidative stress levels mainly through the ROS-mediated PI3K-Akt signaling pathway, which may be the reason why pantothenic acid is resistant to CAS (Ya et al., 2021). Also, pantothenic acid has a positive correlation with the four active PRM of SZD, including rutin, galuteolin, and genkwanin, while CHA is negatively correlated with pantothenic acid (Figure 10). These demonstrate that SZD exerts its therapeutic effects by modulating pantothenic acid biosynthesis.

In this article, we refer to the studies in recent years that only combined network analysis and metabolomics. Our article identifies the potential RPM of SZD anti-CAS through network analysis and analyzes their migration in the bloodstream via pharmacokinetics. Additionally, an integrated network of metabolomics and network analysis was constructed using Cytoscape, ultimately hypothesizing that the key targets might be CYP3A4 and CYP1A2. This study preliminarily explored the possible mechanisms of SZD anti-CAS. In our future research, we will consider utilizing Western blot or PCR methods to validate the signaling pathways that were

identified by network analysis. This would enhance the reliability of our results.

5 Conclusion

In this study, we first established a new integrated strategy to investigate the key targets and mechanisms of SZD in treating CAS. The results revealed that SZD can reduce liver tissue inflammation, inhibit collagen fiber hyperplasia, and improve liver function. In addition, we speculate that the effective RPM of SZD may have significant regulatory effects on the Hepatitis B signaling pathway, PI3K-Akt signaling pathway, tryptophan metabolism, arginine biosynthesis, alpha-linolenic acid metabolism, pantothenic acid biosynthesis, arginine, and proline metabolism through key targets. The data and theories provided in this study help to study the mechanism in depth and lay the foundation for clinical application.

Data availability statement

The datasets presented in this study can be found in online repositories. The names of the repository/repositories and accession number(s) can be found in the article/Supplementary Material.

Ethics statement

The animal studies were approved by No. SCXK (Beijing) 2007-0001, SYXK (Hei) 2021-013, QMU-AECC-2022-13. The studies were conducted in accordance with the local legislation and institutional requirements. Written informed consent was obtained from the owners for the participation of their animals in this study.

Author contributions

WL: Supervision, Writing—original draft. YH: Software, Validation, Writing—review and editing. YW: Investigation, Methodology, Writing—review and editing. RL: Data curation, Software, Writing—review and editing. HZ: Data curation, Software, Writing—review and editing. YL: Data curation, Software, Writing—review and editing. QL: Data curation, Writing—review and editing. MN: Software, Validation, Writing—review and editing. BH: Formal Analysis, Funding acquisition, Project administration, Writing—review and editing. TX: Data curation, Software, Writing—review and editing.

Funding

The author(s) declare financial support was received for the research, authorship, and/or publication of this article. The work was supported by Key Cultivation Project of Qiqihar Academy of

Medical Sciences (2022-ZDPY-003), Scientific research project of Heilongjiang Provincial Health Commission (20210202040072, 20220202040636), Qiqihar Science and Technology Plan Joint Guidance Project (LSFGG-2022042, LSFGG-2022048) and in part by Post-doctoral general program supported by Heilongjiang Province (LBH-Z21226), Heilongjiang Province's Basic Research Support Program for Excellent Young Teachers (YQJH2023117).

Conflict of interest

The authors declare that the research was conducted in the absence of any commercial or financial relationships that could be construed as a potential conflict of interest.

References

- Boeing, T., Souza, P., Specia, S., Somensi, L. B., Mariano, L. N. B., Cury, B. J., et al. (2020). Luteolin prevents irinotecan-induced intestinal mucositis in mice through antioxidant and anti-inflammatory properties. *Br. J. Pharmacol.* 177, 2393–2408. doi:10.1111/bph.14987
- Boyer-Diaz, Z., Morata, P., Aristu-Zabalza, P., Gibert-Ramo, A., Bosch, J., and Gracia-Sancho, J. (2020). Oxidative stress in chronic liver disease and portal hypertension: potential of DHA as nutraceutical. *Nutrients* 12, 2627. doi:10.3390/nu12092627
- Cai, Y. L., Zhang, F., Dou, X. X., Zeng, H. W., Wu, G. S., Liang, Y. L., et al. (2022). Integrated metabolomics and network pharmacology to reveal the therapeutic mechanism of Dingkun Pill on polycystic ovary syndrome. *J. Ethnopharmacol.* 295, 115442. doi:10.1016/j.jep.2022.115442
- Chen, Y. Y., Cao, Y. J., Tang, Y. P., Yue, S. J., and Duan, J. A. (2019). Comparative pharmacodynamic, pharmacokinetic and tissue distribution of Dahuang-Gancao decoction in normal and experimental constipation mice. *Chin. J. Nat.* 17, 871–880. doi:10.1016/S1875-5364(19)30104-9
- Dai, X. Q., Cai, W. T., Wu, X., Chen, Y., and Han, F. M. (2017). Protocatechuic acid inhibits hepatitis B virus replication by activating ERK1/2 pathway and down-regulating HNF4 α and HNF1 α *in vitro*. *Life Sci.* 180, 68–74. doi:10.1016/j.lfs.2017.05.015
- De Simone, G., Balducci, C., Forloni, G., Pastorelli, R., and Brunelli, L. (2021). Hippuric acid: could become a barometer for frailty and geriatric syndromes? *Ageing Res. Rev.* 72, 101466. doi:10.1016/j.arr.2021.101466
- Eidi, A., Mortazavi, P., Tehrani, M. E., Rohani, A. H., and Safi, S. (2012). Hepatoprotective effects of pantothenic acid on carbon tetrachloride-induced toxicity in rats. *EXCLI J.* 11, 748–759.
- Fortea, J. I., Fernández-Mena, C., Puerto, M., Ripoll, C., Almagro, J., Bañares, J., et al. (2018). Comparison of two protocols of carbon tetrachloride-induced cirrhosis in rats - improving yield and reproducibility. *Sci. Rep.* 8, 9163. doi:10.1038/s41598-018-27427-9
- Gallo, A., Dedionigi, C., Civitelli, C., Panzeri, A., Corradi, C., and Squizzato, A. (2020). Optimal management of cirrhotic ascites: a review for internal medicine physicians. *J. Transl. Int. Med.* 8 (4), 220–236. doi:10.2478/jtim-2020-0035
- Gao, H., and Yao, X. S. (2019). Strengthen the research on the medicinal and edible substances to advance the development of the comprehensive healthcare industry of TCMs. *Chin. J. Nat. Med.* 17, 1–2. doi:10.1016/S1875-5364(19)30002-0
- Gao, X. Q., Xu, J. D., Zhou, S. K., Zhang, Y., and Zhang, L. (2023). Jujubae Fructus alleviates intestinal injury caused by toxic medicinals in Shizao Decoction based on correlation between intestinal flora and host metabolism. *China J. Chin. Materia Medica* 48, 2792–2802. doi:10.19540/j.cnki.cjmm.20230111.401
- Harstad, E. B., and Klaassen, C. D. (2002). iNOS-null mice are not resistant to cadmium chloride-induced hepatotoxicity. *Toxicology* 175, 83–90. doi:10.1016/S0300-483X(02)00068-9
- He, J., Bai, K., Hong, B., Zhang, F., and Zheng, S. (2017). Docosahexaenoic acid attenuates carbon tetrachloride-induced hepatic fibrosis in rats. *Int. Immunopharmacol.* 53, 56–62. doi:10.1016/j.intimp.2017.09.013
- He, N. Y. (2015). Clinical observations of the external application of Jidai formula and thermal therapy in the treatment of malignant ascites in 25 cases. *Hebei J. Traditional Chin. Med.* 37, 190–191.
- Heidari, R., Jamshidzadeh, A., Niknahad, H., Safari, F., Azizi, H., Abdoli, N., et al. (2016). The hepatoprotection provided by taurine and glycine against antineoplastic drugs induced liver injury in an ex vivo model of normothermic recirculating isolated perfused rat liver. *Trend. Pharm. Sci.* 2, 59–76.
- Hiranpanich, V., Murakoso, K., and Sato, H. (2008). Inhibitory effect of docosahexaenoic acid (DHA) on the intestinal metabolism of midazolam: *in vitro* and *in vivo* studies in rats. *Int. J. Pharm.* 351, 133–143. doi:10.1016/j.ijpharm.2007.09.037
- Ho, H. Y., Chen, P. J., Lo, Y. S., Lin, C. C., Chuang, Y. C., Hsieh, M. J., et al. (2021). Luteolin-7-O-glucoside inhibits cell proliferation and modulates apoptosis through the AKT signaling pathway in human nasopharyngeal carcinoma. *Environ. Toxicol.* 36, 2013–2024. doi:10.1002/tox.23319
- Jiang, C., Bian, Y., and Fan, X. (2015). History of incompatibility among medicinals of "Glycyrrhiza antagonistic to Sargassum, Euphorbia Pekinensis, Kansui, and Genkwa" and its modern recognition. *Zhonghua Yi Shi Za Zhi* 45, 131–136.
- Jiang, Y. C., Li, Y. F., Zhou, L., and Zhang, D. P. (2020). Comparative metabolomics unveils molecular changes and metabolic networks of syringin against hepatitis B mice by untargeted mass spectrometry. *RSC Adv.* 10, 461–473. doi:10.1039/c9ra06332c
- Jose-Abrego, A., Rivera-Iñiguez, I., Torres-Reyes, L. A., and Roman, S. (2022). Anti-hepatitis B virus activity of food nutrients and potential mechanisms of action. *Ann. Hepatol.* 28, 100766. doi:10.1016/j.aohp.2022.100766
- Kim, M., Lee, E., and Kim, Y. B. (2023). Elucidating anti-aging and antioxidant activity of *Hydnocarpus anthelmintica* on skin aging and cosmeceutical potentials: *in silico* and *in vitro* study. *Comb. Chem. High. Throughput Screen* 26. doi:10.2174/1386207326666230901092247
- Li, B. S., Zhu, R. Z., Lim, S. H., Seo, J. H., and Choi, B. M. (2021a). Apigenin alleviates oxidative stress-induced cellular senescence via modulation of the SIRT1-NAD [formula: see text]-CD38 Axis. *Am. J. Chin. Med.* 49, 1235–1250. doi:10.1142/S0192415X21500592
- Li, T., Zhang, W., Hu, E., Sun, Z., Li, P., Yu, Z., et al. (2021b). Integrated metabolomics and network pharmacology to reveal the mechanisms of hydroxysafflower yellow A against acute traumatic brain injury. *Comput. Struct. Biotechnol. J.* 19, 1002–1013. doi:10.1016/j.csbj.2021.01.033
- Li, X., Liu, S., Xu, H., and Zhou, W. (2023). Curative effect and safety of tolvaptan combined with traditional diuretics in treatment of patients with cirrhotic ascites and relevant research on its dose. *Am. J. Ther.* 30, 158–162. doi:10.1097/MJT.0000000000001327
- Lin, C. M., Huang, S. T., Liang, Y. C., Lin, M. S., Shih, C. M., Chang, Y. C., et al. (2005). Isovitexin suppresses lipopolysaccharide-mediated inducible nitric oxide synthase through inhibition of NF- κ B in mouse macrophages. *Planta Med.* 71, 748–753. doi:10.1055/s-2005-871287
- Lucas, D., Goulitquer, S., Marienhagen, J., Fer, M., Dreano, Y., Schwaneberg, U., et al. (2010). Stereoselective epoxidation of the last double bond of polyunsaturated fatty acids by human cytochromes P450. *J. Lipid Res.* 51, 1125–1133. doi:10.1194/jlr.M003061
- Luo, Y. H. (2013). Clinical effect of integrated traditional Chinese and Western medicine therapy in treatment of cirrhotic ascites: a report of 54 cases. *Hunan J. Traditional Chin. Medicine (In Chinese)* 29, 20–22.
- Morris, C. R., Hamilton-Reeves, J., Martindale, R. G., Sarav, M., and Ochoa Gautier, J. B. (2017). Acquired amino acid deficiencies: a focus on arginine and glutamine. *Nutrition in Clinical Practice* 32, 30S–47S. doi:10.1177/0884533617691250
- Motallebi, M., Bhia, M., Rajani, H. F., Bhia, I., Tabarraei, H., Mohammadkhani, N., et al. (2022). Naringenin: a potential flavonoid phytochemical for cancer therapy. *Life Sci* 305, 120752. doi:10.1016/j.lfs.2022.120752

Publisher's note

All claims expressed in this article are solely those of the authors and do not necessarily represent those of their affiliated organizations, or those of the publisher, the editors and the reviewers. Any product that may be evaluated in this article, or claim that may be made by its manufacturer, is not guaranteed or endorsed by the publisher.

Supplementary material

The Supplementary Material for this article can be found online at: <https://www.frontiersin.org/articles/10.3389/fphar.2024.1298818/full#supplementary-material>

- Pal, P. B., Pal, S., Das, J., Sil, P. C., and Das, J. (2011). Modulation of mercury-induced mitochondria-dependent apoptosis by glycine in hepatocytes. *Amino Acids* 42, 1669–1683. doi:10.1007/s00726-011-0869-3
- Pang, H., Jia, W., and Hu, Z. (2019). Emerging applications of metabolomics in clinical pharmacology. *Clin. Pharmacol. Ther.* 106, 544–556. doi:10.1002/cpt.1538
- Quintieri, L., Palatini, P., Nassi, A., Ruzza, P., and Floreani, M. (2008). Flavonoids diosmetin and luteolin inhibit midazolam metabolism by human liver microsomes and recombinant CYP 3A4 and CYP3A5 enzymes. *Biochem. Pharmacol* 75, 1426–1437. doi:10.1016/j.bcp.2007.11.012
- Shang, L., Wang, Y., Li, J., Zhou, F., Xiao, K., Liu, Y., et al. (2023). Mechanism of Sijunzi Decoction in the treatment of colorectal cancer based on network pharmacology and experimental validation. *J Ethnopharmacol* 302, 115876. doi:10.1016/j.jep.2022.115876
- Shi, A., Li, T., Zheng, Y., Song, Y., Wang, H., Wang, N., et al. (2021). Chlorogenic acid improves NAFLD by regulating gut microbiota and GLP-1. *Front Pharmacol* 12, 693048. doi:10.3389/fphar.2021.693048
- Shoieb, S. M., El-Ghiaty, M. A., Alqahtani, M. A., and El-Kadi, A. O. S. (2020). Cytochrome P450-derived eicosanoids and inflammation in liver diseases. *Prostaglandins Other Lipid Mediat* 147, 106400. doi:10.1016/j.prostaglandins.2019.106400
- Wang, X. B., Wang, M. L., Chu, Y. J., Zhou, P. P., Zhang, X. Y., Zou, J., et al. (2023a). Integrated pharmacokinetics and pharmacometabolomics to reveal the synergistic mechanism of a multicomponent Chinese patent medicine, Mailuo Shutong pills against thromboangiitis obliterans. *Phytomedicine* 112, 154709. doi:10.1016/j.phymed.2023.154709
- Wang, Y., Cheng, W., Wang, X., He, T., Liu, J., Chen, S., et al. (2023b). Integrated metabolomics and network pharmacology revealing the mechanism of arsenic-induced hepatotoxicity in mice. *Food Chem Toxicol* 178, 113913. doi:10.1016/j.fct.2023.113913
- Wang, Y., Yuan, Y., Wang, W., He, Y., Zhong, H., Zhou, X., et al. (2022). Mechanisms underlying the therapeutic effects of Qingfei Yin in treating acute lung injury based on GEO datasets, network pharmacology and molecular docking. *Comput. Biol Med* 145, 105454. doi:10.1016/j.compbiomed.2022.105454
- Wu, M. J., Weng, C. Y., Ding, H. Y., and Wu, P. J. (2005). Anti-inflammatory and antiviral effects of *Glossogyne tenuifolia*. *Life Sci* 76, 1135–1146. doi:10.1016/j.lfs.2004.08.017
- Wu, W., Li, K., Ran, X., Wang, W., Xu, X., Zhang, Y., et al. (2022). Combination of resveratrol and luteolin ameliorates α -naphthylisothiocyanate-induced cholestasis by regulating the bile acid homeostasis and suppressing oxidative stress. *Food Funct* 13, 7098–7111. doi:10.1039/d2fo00521b
- Xu, D., Zhang, G. Q., Zhang, T. T., Jin, B., and Ma, C. (2020). Pharmacokinetic comparisons of naringenin and naringenin-nicotinamide cocrystal in rats by LC-MS/MS. *J Anal Methods Chem* 2020, 8364218. doi:10.1155/2020/8364218
- Ya, F., Li, K., Chen, H., Tian, Z., Fan, D., Shi, Y., et al. (2021). Protocatechuic acid protects platelets from apoptosis via inhibiting oxidative stress-mediated PI3K/Akt/GSK3 β signaling. *Thromb Haemost* 121, 931–943. doi:10.1055/s-0040-1722621
- Yin, J. N., Wang, H. Q., and Lu, G. Y. (2018). Umbelliferone alleviates hepatic injury in diabetic db/db mice via inhibiting inflammatory response and activating Nrf2-mediated antioxidant. *Bioscience reports* 38. doi:10.1042/BSR20180444
- Zhao, C., Jia, Z., Li, E., Zhao, X., Han, T., Tian, J., et al. (2019a). Hepatotoxicity evaluation of *Euphorbia kansui* on zebrafish larvae *in vivo*. *Phytomedicine* 62, 152959. doi:10.1016/j.phymed.2019.152959
- Zhao, K. F., Tan, R., Li, F., and Shi, R. S. (2019b). Research on the ascitic fluid model of rat liver cirrhosis with the combination of CCl₄, phenobarbitone and ethylal. *Jilin Medical Journal* 40, 1170–1172.
- Zhao, Q., Xing, F., and Liu, C. H. (2018). Research progress of traditional Chinese medicine treatment of liver cirrhosis ascites. *Chinese Journal of Chinese Medicine* 33, 4557–4559.
- Zhao, T., Mao, L., Yu, Z., Hui, Y., Feng, H., Wang, X., et al. (2021). Therapeutic potential of bicyclol in liver diseases: lessons from a synthetic drug based on herbal derivative in traditional Chinese medicine. *Int Immunopharmacol* 91, 107308. doi:10.1016/j.intimp.2020.107308
- Zheng, S., Cao, P., Yin, Z., Wang, X., Chen, Y., Yu, M., et al. (2021). Apigenin protects mice against 3,5-diethoxycarbonyl-1,4-dihydrocollidine-induced cholestasis. *Food Funct* 12, 2323–2334. doi:10.1039/d0fo02910f
- Zhou, M. D., Tong, Q. Y., and Zhou, G. (2012). Observation on the effect of Shizao decoction on Shenque point on the navel in the treatment of liver cirrhosis and ascites. *Emergencies of Chinese Medicine* 21, 1166.
- Zhu, L., Wang, L., Cao, F., Liu, P., Bao, H., Yan, Y., et al. (2018). Modulation of transport and metabolism of bile acids and bilirubin by chlorogenic acid against hepatotoxicity and cholestasis in bile duct ligation rats: involvement of SIRT1-mediated deacetylation of FXR and PGC-1 α . *J Hepatobiliary Pancreat Sci* 25, 195–205. doi:10.1002/jhbp.537



OPEN ACCESS

EDITED BY

Abd El-Latif Hesham,
Beni-Suef University, Egypt

REVIEWED BY

Alex Boye,
University of Cape Coast, Ghana
Muhammad Umar Aftab,
National University of Computer and Emerging
Sciences, Pakistan

*CORRESPONDENCE

Arshiya Sultana,
✉ drarshiya@yahoo.com
Md Belal Bin Heyat,
✉ belalheyat@gmail.com

[†]These authors have contributed equally to
this work

RECEIVED 01 November 2023

ACCEPTED 16 January 2024

PUBLISHED 12 February 2024

CITATION

Fazmiya MJA, Sultana A, Heyat MBB, Parveen S,
Rahman K, Akhtar F, Khan AA, Alanazi AM,
Ahmed Z, Diez IdIT, Ballester JB and
Saripalli TSK (2024), Efficacy of a vaginal
suppository formulation prepared with *Acacia
arabica* (Lam.) Willd. gum and *Cinnamomum
camphora* (L.) J. Presl. in heavy menstrual
bleeding analyzed using a machine
learning technique.
Front. Pharmacol. 15:1331622.
doi: 10.3389/fphar.2024.1331622

COPYRIGHT

© 2024 Fazmiya, Sultana, Heyat, Parveen,
Rahman, Akhtar, Khan, Alanazi, Ahmed, Diez,
Ballester and Saripalli. This is an open-access
article distributed under the terms of the
[Creative Commons Attribution License \(CC BY\)](https://creativecommons.org/licenses/by/4.0/).
The use, distribution or reproduction in other
forums is permitted, provided the original
author(s) and the copyright owner(s) are
credited and that the original publication in this
journal is cited, in accordance with accepted
academic practice. No use, distribution or
reproduction is permitted which does not
comply with these terms.

Efficacy of a vaginal suppository formulation prepared with *Acacia arabica* (Lam.) Willd. gum and *Cinnamomum camphora* (L.) J. Presl. in heavy menstrual bleeding analyzed using a machine learning technique

Mohamed Joonus Aynul Fazmiya^{1†}, Arshiya Sultana^{1*†},
Md Belal Bin Heyat^{2*†}, Saba Parveen^{3†}, Khaleequr Rahman⁴,
Faijan Akhtar⁵, Azmat Ali Khan⁶, Amer M. Alanazi⁶,
Zaheer Ahmed⁷, Isabel de la Torre Díez⁸,
Julián Brito Ballester^{9,10,11} and
Tirumala Santhosh Kumar Saripalli¹²

¹Department of Ilmul Qabalat wa Amraze Niswan, National Institute of Unani Medicine, Ministry of AYUSH, Bengaluru, India, ²CenBRAIN Neurotech Center of Excellence, School of Engineering, Westlake University, Hangzhou, China, ³College of Electronics and Information Engineering, Shenzhen University, Shenzhen, China, ⁴Department of Ilmul Saidla, National Institute of Unani Medicine, Ministry of AYUSH, Bengaluru, India, ⁵School of Computer Science and Engineering, University of Electronic Science and Technology of China, Chengdu, China, ⁶Pharmaceutical Biotechnology Laboratory, Department of Pharmaceutical Chemistry, College of Pharmacy, King Saud University, Riyadh, Saudi Arabia, ⁷Central Council for Research in Unani Medicine, New Delhi, India, ⁸Department of Signal Theory and Communications, University of Valladolid, Valladolid, Spain, ⁹Research Group on Foods, Nutritional Biochemistry and Health, Universidad Europea del Atlántico, Santander, Spain, ¹⁰Research Group on Foods, Nutritional Biochemistry and Health, Universidad Internacional Iberoamericana, Arecibo, PR, United States, ¹¹Research Group on Foods, Nutritional Biochemistry and Health, Universidad de La Romana, La Romana, Dominican Republic, ¹²Regional Research Institute of Unani Medicine, Chennai, India

Objective: This study aims to determine the efficacy of the *Acacia arabica* (Lam.) Willd. and *Cinnamomum camphora* (L.) J. Presl. vaginal suppository in addressing heavy menstrual bleeding (HMB) and their impact on participants' health-related quality of life (HRQoL) analyzed using machine learning algorithms.

Method: A total of 62 participants were enrolled in a double-dummy, single-center study. They were randomly assigned to either the suppository group (SG), receiving a formulation prepared with *Acacia arabica* gum (*Gond Babul*) and camphor from *Cinnamomum camphora* (*Kafoor*) through two vaginal suppositories (each weighing 3,500 mg) for 7 days at bedtime along with oral placebo capsules, or the tranexamic group (TG), receiving oral tranexamic acid (500 mg) twice a day for 5 days and two placebo vaginal suppositories during menstruation at bedtime for three consecutive menstrual cycles. The primary outcome was the pictorial blood loss assessment chart (PBLAC) for HMB, and secondary outcomes included hemoglobin level and SF-36 HRQoL questionnaire

scores. Additionally, machine learning algorithms such as k-nearest neighbor (KNN), AdaBoost (AB), naive Bayes (NB), and random forest (RF) classifiers were employed for analysis.

Results: In the SG and TG, the mean PBLAC score decreased from 635.322 ± 504.23 to 67.70 ± 22.37 and 512.93 ± 283.57 to 97.96 ± 39.25 , respectively, at post-intervention (TF3), demonstrating a statistically significant difference ($p < 0.001$). A higher percentage of participants in the SG achieved normal menstrual blood loss compared to the TG (93.5% vs 74.2%). The SG showed a considerable improvement in total SF-36 scores (73.56%) compared to the TG (65.65%), with a statistically significant difference ($p < 0.001$). Additionally, no serious adverse events were reported in either group. Notably, machine learning algorithms, particularly AB and KNN, demonstrated the highest accuracy within cross-validation models for both primary and secondary outcomes.

Conclusion: The *A. arabica* and *C. camphora* vaginal suppository is effective, cost-effective, and safe in controlling HMB. This botanical vaginal suppository provides a novel and innovative alternative to traditional interventions, demonstrating promise as an effective management approach for HMB.

KEYWORDS

female disorder, heavy menstrual bleeding, Unani system of medicine, drug design, artificial intelligence with botanical drug, medical intelligence, *Acacia arabica* gum, *Cinnamomum camphora*

1 Introduction

Heavy menstrual bleeding (HMB) is diagnosed as excessive or prolonged uterine bleeding per menstruation of more than 80 mL or for 7 days in a normal cycle (Magnay et al., 2020). Approximately 10%–35% of women visit the hospital with complaints of HMB throughout their reproductive years, and 5% seek medical attention to have HMB investigated (Chaplin, 2018). HMB has a substantial influence on a woman's quality of life (QoL); hence, essential intervention must focus on QoL rather than just blood loss (Azizkhani et al., 2018). According to Unani medicine, HMB is characterized by excessive or prolonged menstrual blood loss during the menstrual cycle (Al-Jurjāni, 2010; Majusi, 2010). Unani scholars posit that the primary cause of HMB is weak retentive power, excessive excretory power, or a combination of both. Additionally, any deviation from normal temperament (*Mizaj*), particularly a hot (*Harr*) and dry (*Yabis*) disposition, is believed to weaken the uterus and its vessels, impacting the uterine excretory power. This, in turn, leads to the opening and dilation of the mouths of uterine vessels, resulting in heavy menstrual flow (Jurjani, 2010; Sina, 2010). Since there is no universally accepted test-and-treat strategy for HMB in women, the first line of defense is typically empiric pharmacological treatment without further research (Azizkhani et al., 2018). Due to the limitations of current medications, the absence of specific treatment strategies, and limited studies on side effects and drug interactions, the full spectrum of complementary and alternative systems has grown immensely and gained popularity (Tansaz et al., 2016). Plant products act through four strategies to regulate irregular uterine bleeding: estrogenic action, inflammatory process inhibition, inhibition of prostaglandin formation, and anti-proliferative effect on human cervical cancer cells (Magnay et al., 2020).

India uniquely possesses its own recognized traditional medicine systems: Ayurveda, Yoga, Unani, Siddha, and Homeopathy

(AYUSH) (Ahmad et al., 2021). Unani researchers provide valuable insights into the diagnosis and treatment of menstrual diseases, considering regular menstruation as a crucial indicator of a woman's health (Sina, 2010; Al-Jurjāni, 2010). Unani medicine offers effective treatments for HMB in various forms, including oral single or compound form and/or topical vaginal pessary, vaginal suppository, sitz bath, lotion, and balm. In Unani texts, a vaginal suppository of *Acacia arabica* (Lam.) Willd. [Fabaceae] gum (Acacia gum) and camphor from *Cinnamomum camphora* (L.) J. Presl. [Lauraceae] is recommended for controlling HMB. Acacia gum (*Gond Babul*) possesses astringent, anti-inflammatory, styptic, and desiccant properties (Farzana and Sultana, 2020) and is known for treating abnormal vaginal discharge and heavy menstrual bleeding. Unani researchers explain that hemostatic drugs typically have a dry and cold temperament, facilitating capillary constriction and surrounding structure support (Tansaz et al., 2016). Camphor (*Kafoor*) possesses ethnomedicinal properties such as astringent (*Qabis*), anti-inflammatory (*Muhallil*) (Khan and Muhammad, 2018), and external anesthetic and analgesic (*Musakhin*) properties (Kabir al-Din, 2007). Acacia gum and camphor contain tannins that contribute to the coagulation of cellular proteins and the constriction of the capillary endothelium (Tansaz et al., 2016). *A. arabica* gum is pharmacologically reported to have powerful astringent, styptic, analgesic, antioxidant, and anti-inflammatory properties (Massiha and Muradov, 2015; Garg and Jain, 2016). *C. camphora* has potent prostaglandin inhibitors that are astringent, hemostatic, and anti-inflammatory (Daffalah and al-Mustafa, 1996; Karashima et al., 2007; Fan et al., 2020; Hussain et al., 2021; Lee et al., 2022). Acacia gum is rich in tannin with bioactive molecules such as ellagic acid, gallic acid, and tannic acid, which have astringent properties (Ali, 2012; Elgailani and Ishak, 2014; Saeedi et al., 2020). Acacia gum's aqueous extracts contain polymeric content that shortens the activated partial thromboplastin time (aPTT) and prothrombin time (PT), has hemostatic effects, and

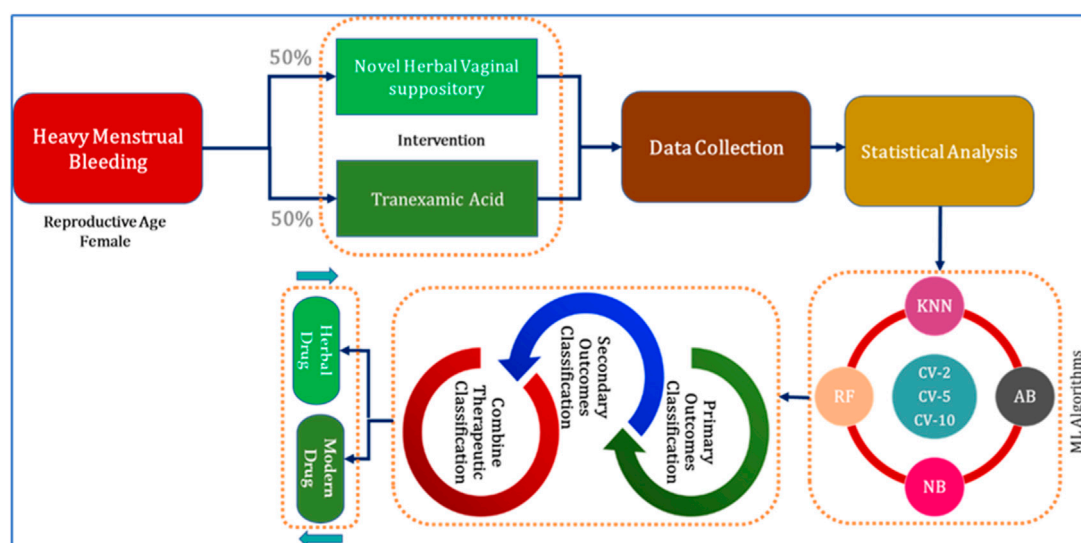


FIGURE 1
Organizational diagram of the present study.

accelerates blood coagulation (Bhatnagar et al., 2013). *A. arabica* was reported to be safe in a single dose in experimental animal mice (Alli et al., 2015), and camphor was safe in a proper dose in adult humans. The lethal dose of camphor has been reported to be 5 to 20 gm (Nadkarni KM, 2004).

Various Unani formulations such as *Sharbat-i-Anjabar* (Jahan et al., 2016), *Safuf-i-Hābis* (Fathima and Sultana, 2012), *Qurs-i-Hābis* (Mukhtar et al., 2019), *Gulnār* (Goshtasebi et al., 2015), and dry cupping (*Hijama bila Shart*) (Sultana and Rahman, 2012) have been validated and clinically proven for their effectiveness in treating HMB. Few studies on female disorders included machine learning methods in their clinical trials, including pelvic inflammatory disease (Qayyum et al., 2023) and premenstrual syndrome (Sultana et al., 2022b). However, to date, there has been no study assessing the efficacy of a vaginal suppository formulation prepared with *A. arabica* gum and *C. camphora* camphor in addressing HMB (Khan, 2006) using a machine learning model.

This study intended to compare the efficacy of the formulation prepared with acacia gum (*Gond Babul*) and camphor (*Kafoor*) vaginal suppository with tranexamic acid on the pictorial blood loss assessment score (PBLAC), health-related quality of life (HRQoL), and hemoglobin levels in human participants with HMB. The research question was “whether acacia gum and camphor vaginal suppositories would be efficacious to reduce HMB and, thereby, improve the participant’s HRQoL.” Beyond conventional methods, artificial intelligence (AI) (Benifa et al., 2023), particularly machine learning models, was utilized to classify experimental and standard groups. Additionally, this study used experimental data related to heavy menstrual bleeding for the classification of the vaginal suppository group (SG) as an experimental group and tranexamic group (TG) as a standard control group. The present study used four types of machine learning algorithms, namely, k-nearest neighbor (KNN), AdaBoost (AB), naive Bayes (NB), and random forest (RF) (Belal Bin Heyat et al., 2022; Bin Heyat et al., 2022; Pal et al., 2022; Tripathi et al., 2022; Qayyum et al., 2023).

It makes significant contributions by proposing an improved alternative treatment for HMB through the utilization of acacia gum (*Gond Babul*) and camphor (*Kafoor*) vaginal suppositories. Additionally, it involves the design and development of this innovative botanical drug vaginal suppository with a focus on standardization and purity testing, including microbial loads, heavy metal, and HPTLC fingerprint analysis. This study also explores the application of AI for the classification of experimental data through machine learning models. Moreover, the research delves into understanding the role of oxidative stress, inflammation, and immune responses in abnormal uterine bleeding. It also seeks to elucidate the mechanism of action for the bioactive metabolites and molecules present in camphor and acacia gum, highlighting their potential as anti-inflammatory, antioxidant, and hemostatic agents.

The proposed study is organized in the standard format, including introduction, materials and methods, results, discussion, and conclusion.

2 Materials and methods

This study included stages such as protocol designing, approval from the scientific review committee, ethical approval, clinical trial registry, participant enrollment, data collection, and analysis of data results (Figure 1).

2.1 Ethical statement

The protocol was completed in line with the principles of the “Declaration of Helsinki” (2013) and the “GCP guidelines of the Ministry of AYUSH.” This study was approved by the institutional review and ethics committees. Informed consent was obtained from all randomized participants.

2.2 Experimental design and data collection

The study followed the design of a single-center, randomized, double-dummy, standard-controlled study with two parallel arms (1:1) in the National Institute of Unani Medicine, Bengaluru. Married women with regular cycles (21–35 days) within the reproductive age group of 18–45 years and complaints of HMB for more than 7 days, an amount of flow >80 mL, or both (Yousefi et al., 2020) were included. Participants were excluded if they had pelvic pathology (uterine fibroids >3 cm and/or >3 in number, polyp, and PID) and malignancy. Diagnosed cases of bleeding disorders, severe anemia (Hb < 7 g%), chronic renal disease, endocrine disorders (uncontrolled thyroid dysfunction), liver disease, uncontrolled hypertension, and diabetes mellitus, along with individuals with a history of using hormonal contraceptives in the last 3 months, pregnant women, and lactating mothers, were also excluded. Throughout the study, every participant had the choice to discontinue at any point.

We collected the demographic, clinical, and behavioral characteristic data during the recruitment interview of both the suppository and tranexamic groups. Kuppaswamy's scale of 2020 was used for assessing socioeconomic status (Saleem and January 2021). A general physical examination, bimanual examination, and PBLAC score for HMB were recorded. Furthermore, laboratory investigations such as hemogram, random blood sugar, clotting time, bleeding time, platelet count, thyroid-stimulating hormone, and abdominopelvic ultrasound sonography (USG) were conducted at baseline to exclude general diseases and pelvic diseases. During the trial period, the participants were instructed to use the barrier method for contraception and refrain from using any other medicines during the menstrual phase. Participants included in the study were asked to report any treatment-related adverse effects.

2.3 Intervention protocol

2.3.1 Selection of novel vaginal suppository

After reviewing the literature, the formulation of acacia gum (*Gond Babul*) and camphor (*Kafoor*) vaginal suppository was selected for the management of HMB as they possess astringent, hemostatic, and anti-inflammatory properties (Kabir al-Din, 2007; Saeedi et al., 2020). Furthermore, scientific studies on Acacia gum reported its powerful astringent, anti-inflammatory, antimicrobial, styptic, and analgesic properties (Saeedi et al., 2020). Camphor, a terpenoid with the chemical formula $C_{10}H_{16}O$, is obtained by distillation of the wood of *C. camphora* and has been traditionally employed to address various symptoms, including inflammation, infection, congestion, and muscle pain (Lee et al., 2022). Camphor is proven to have anti-inflammatory, analgesic, antioxidant, and astringent properties (Karashima et al., 2007; Fan et al., 2020; Hussain et al., 2021; Lee et al., 2022). Acacia gum was confirmed and verified through authentication procedures. It was labeled as *Acacia arabica* (Lam.) Willd. [Fabaceae] with an authentication number FRLHT No. 5575. Camphor was identified and authenticated in the Regional Research Institute of Unani Medicine, Chennai, India, with no. DSRU/DTL No.09, 10/2022-23. In addition, the plant's scientific

names were cross-checked in “Kew Plants of the World Online” and “World Flora Online.” For further reference, the specimens of camphor and *A. arabica* gum were submitted to our institute's pharmacology department with voucher specimen number 104/UQ/Res/2021.

2.3.2 Standardization of the vaginal suppository drugs

The qualitative and quantitative analysis of vaginal suppositories was carried out at the “Regional Research Institute of Unani Medicine, Chennai.” Microbial load testing for the vaginal suppository encompassed assessments for total fungal count, total bacterial count, Enterobacteriaceae, *E. coli*, *Salmonella* spp., and *S. aureus*. Results indicated that the total bacterial and fungal counts in the vaginal suppository sample were less than 1 cfu/g, well within permissible limits. Furthermore, the samples were found to be free from microbes such as *Salmonella* spp., *E. coli*, Enterobacteriaceae, and *S. aureus*. In addition, heavy metal analysis, encompassing lead, cadmium, arsenic, and mercury, was conducted. The analysis of the vaginal suppository revealed the absence of lead, cadmium, arsenic, and mercury.

The qualitative densitometry HPTLC analysis of the vaginal suppository was carried out at the Drug Safety Research Unit at the Regional Research Institute of Unani Medicine, Chennai, India. One gram of the vaginal suppository was separately dissolved in a mobile phase prepared with toluene:ethyl acetate:methanol (9:0.7:0.3). Solvent systems were sampled in various volume ratios, viz., toluene:ethyl acetate (7:3), toluene:ethyl acetate (9:1), toluene:ethyl acetate:methanol (7:2:1), toluene:ethyl acetate:ethyl formate:formic acid (6:2:1:1), and toluene:ethyl acetate:methanol (9:0.7:0.3). The most appropriate solvent system was toluene:ethyl acetate:methanol 9:0.7:0.3 (v/v/v).

Analysis was completed on 10 × 10 cm silica gel 60 F254 plates. The sample solution, Linomat 5 (CAMAG, Switzerland), an automated spray-on band applicator equipped with a 100-μL Hamilton syringe, was used and operated with the following settings: a band width of 8 mm, distance from the plate edge of 12.5 mm, migration of 8 cm, and distance from the bottom of the plate of 10 mm. The test sample solution (5 μL) was applied on tracks A and B for vaginal suppositories, respectively, on the TLC plate using the HPTLC ATS4 system. Development of the plates was carried out after allowing a twin trough chamber (CAMAG, Switzerland) for saturation at room temperature for 20 min. After development, the plates were allowed to air-dry at room temperature. Subsequently, fingerprints and densitometric chromatograms were recorded under UV 254 nm and 366 nm and visible light, and after derivatization with anisaldehyde sulfuric acid, the plates were kept in an oven at 110°C. The process was monitored using the CAMAG TLC Visualizer and scanned using the CAMAG TLC Scanner 3. The R_f values of the spots were calculated as follows: $R_f = \text{distance traveled by the spot} / \text{distance traveled by the solvent front}$ (Sethi, 1996).

A significant color variation in HPTLC of vaginal suppository was observed on tracks A and B under UV 254. The spot with R_f values of 0.70 and 0.92 is light black. It was also observed that on tracks A and B under UV 366, a lack of spots appeared in the absorbance mode. However, in the case of fluorescence mode track A under UV 366, three spots with R_f values of 0.34 (light blue), 0.98

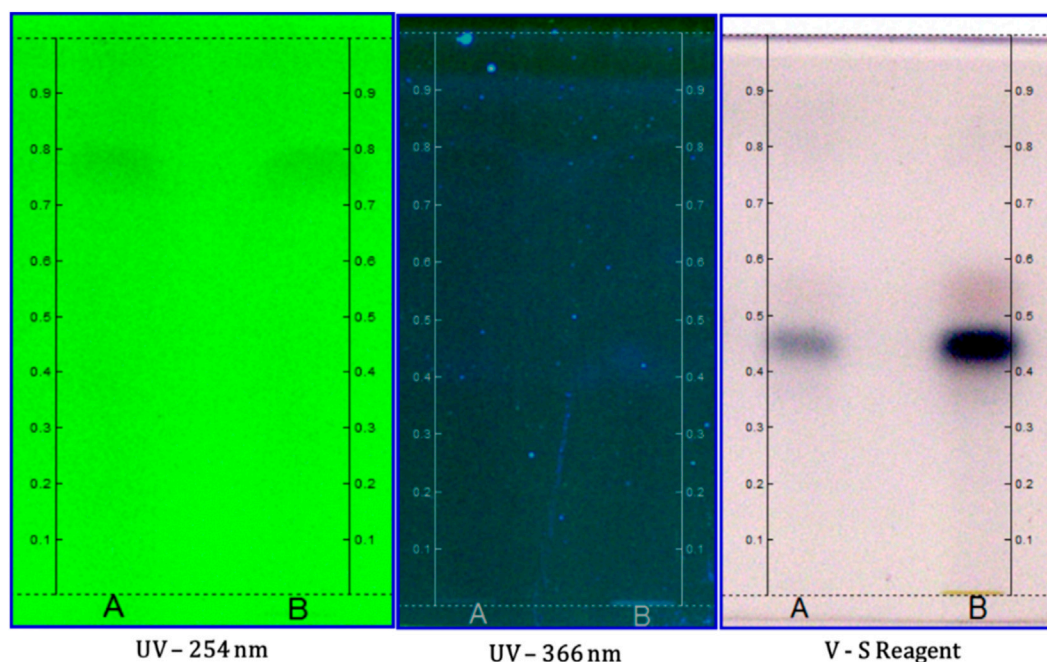


FIGURE 2
HPTLC fingerprint analysis of the suppository with tracks A and B at different wavelengths.



FIGURE 3
Preparation of the novel vaginal suppository of Acacia gum (*Gond Babul*) and Camphor (*Kafoor*).

(light blue), and 0.97 (light blue) were observed. In addition, in track B under UV 366, three spots with R_f values of 0.38 (light blue), 0.87 (light blue), and 0.98 (light blue) are observed. After derivatization under white light, spots with R_f values of 0.45 (dark blue) and 0.55 (light pink) were observed on tracks A and B. The chromatograms of acacia gum and vaginal suppository at UV 254 and 366 nm revealed that all sample constituents were separated without any tailing or diffuseness.

In the HPTLC fingerprinting analysis, various peaks were detected, and it was found that some metabolites with various colors under the UV wavelength appeared in track B in comparison to track A. Thus, the developed chromatogram will be specific to the selected solvent system: toluene:ethyl acetate:methanol (9:0.7:0.3), providing an R_f value, and serves as a better tool for the standardization of the drug (Figure 2).

2.3.3 Preparation of the vaginal suppository

The vaginal suppository was made at the National Institute of Unani Medicine, India (Figure 3). Acacia gum and camphor crude plant materials were purchased from the local market and were cleaned. After cleaning, the medicine was finely powdered separately in the powder-making machine. The powder was passed through a sieve, with a mesh size of 80. Then, the fine powder of both plant materials was thoroughly mixed. The mixture of camphor and acacia gum was tightly filled in a brass suppository mold with six holes and sealed to make a vaginal suppository. Cellulose powder (500 mg) was filled in capsules (size 0) using a capsule filling machine.

2.3.4 Dosage of the SG and TG

During the initial 5 days of the menstrual cycle, participants in the SG received one oral placebo capsule twice a day. Simultaneously, from the first day to the seventh day of the menstrual cycle, two vaginal suppositories (each weighing 3,500 mg) were administered per vaginum at bedtime for three consecutive cycles. On the other hand, participants in the TG were administered the standard drug, tranexamic acid (500 mg), orally twice a day from day one to day five of the menstrual cycle. Simultaneously, from day one to day seven of the menstrual cycle, two placebo vaginal suppositories made of palm sugar were administered per vaginum at bedtime for three consecutive cycles.

2.4 Pictorial blood loss assessment chart for HMB

The first PBLAC, created in 1990 by Higham et al. (1990), featured three graphics (icons) that represented different brands of feminine products that had been progressively stained with blood (Magnay et al., 2020). Towels received 1, 5, and 20 points on the icon scale, whereas tampons received 1, 5, and 10 points. Different blood quantities resulted in visually comparable stain sizes. As a result, the score given to each icon was based on the applied blood volume in mL; however, it was not always equal to that amount. Although there were no linked scores, the diameter of the currency was compared to the size of the blood clot, and the number of flooding incidents was noted (Magnay et al., 2020). The PBLAC's specificity and sensitivity for detecting menorrhagia are 80% and 88%, respectively (Yousefi et al., 2020). During each follow-up, a change in the PBLAC mean score was determined. Additionally, calculations were performed for PBLAC scores categorized as either <100 or >100. Participants with a PBLAC score of less than 100 were considered to have normal menstrual bleeding. A score surpassing 100 was regarded as indicative of heavy menstrual bleeding.

All participants were evaluated at baseline (BL) and treatment follow-up (TF1, TF2, and TF3) every month for three successive menstrual cycles after menstruation to assess the PBLAC score and adverse events. A follow-up without treatment (FF1) was conducted after menstruation in the fifth cycle to determine the sustained effect of vaginal suppository and tranexamic acid.

2.5 SF-36 HRQoL questionnaire and hemoglobin (HB %) estimation

During each follow-up, a change in the SF-36 HRQoL score was determined. The total score and eight health-related dimensions that contribute to the scores were assessed at the baseline and post-intervention (TF3). To further categorize the SF-36 dimensions, the physical component summary (PCS) for physical functioning and the mental component summary (MCS) for emotional wellbeing were also assessed in both groups at the baseline and post-intervention (Qaraaty et al., 2014). All participants were evaluated at baseline and treatment follow-up (TF3) after menstruation to assess the SF-36 score and hemoglobin levels.

Hemoglobin estimation was carried out at baseline and post-intervention to observe the improvement in HB% post-intervention from baseline.

2.6 Assessment of the safety of the SG and TG

Medication safety was assessed by clinical history, physical examination, measuring vital signs, and monitoring adverse events at each follow-up.

2.7 Assessment of hematological and safety biochemical markers

Hematological and safety biochemical markers were measured at baseline in the SG and TG. At the pre-screening visit, blood was collected from recruited participants and was permitted to clot for 15–30 min at room temperature. For serum preparation, the clotted blood sample was centrifuged at 3,000–3,500 rpm for 5–10 min. Biochemical marker evaluation was performed with kits purchased from BioSystems, manufactured by BioSystems Diagnostics Pvt. Ltd., India, using the BA 200 LED Technology Automatic Biochemistry Analyzer. The glucose oxidase/peroxidase method was used to measure glucose (Trinder, 1969). Alanine aminotransferase (ALT) and aspartate aminotransferase (AST) levels were measured using the IFCC method (Schumann et al., 2010). The alkaline phosphatase (ALP) level was predicted using the 2-amino-2-methyl-1-propanol buffer (IFCC) (Tietz et al., 2011). The urease/glutamate dehydrogenase method was used to estimate blood urea levels (Gutman, n.d.). S. creatinine levels were assessed using Jaffe's method (M Peake, 2006).

2.8 Sample size estimation

For an outcome variable on the SF-36 score with a minimum difference of 52 post-treatment in a two-group randomized study with a 5% level of significance and 90% statistical power, the sample size of 62 (31 in each group) was estimated with a 10% attrition rate (Goshtasebi et al., 2015).

2.9 Randomization and allocation concealment

The second investigator, using randomization software, generated a random list. The randomization process employed a simple random sampling method, creating an open list of random numbers within a single block. The allocation ratio was 1:1, and the randomization order was kept confidential from the initial investigator until each patient was allocated to receive an intervention.

2.10 Masking and blinding

The participants were blinded using a process that included masking and matching, achieved by administering the medication in a non-transparent sachet to both groups. A double-dummy technique was also employed to maintain blinding in a trial, as the interventions being compared had different routes of administration. In this technique, the SG received placebo oral capsules and a per-vaginal research suppository, while the TG was given oral standard tranexamic acid capsules and a placebo suppository per-vaginal. However, the double-dummy technique adds complexity to the trial design and involves more intensive monitoring to ensure compliance and assess outcomes accurately. Despite this challenge, this technique was adopted to maintain blinding, as it is crucial for the validity of study results. The analyst conducting the study was also blinded and unaware of the group assignments.

2.11 Treatment adherence

Every month, participants were given research and standard control drugs in a pouch until their next planned visit. They were trained to return all unused medicine at each visit. To determine the number of medicines taken, the remaining suppository and tablets/capsules were counted and subtracted from the number provided. In addition, to enhance compliance, each participant was called on their mobile at the time of menstruation to take their medication.

2.12 Statistical methods

The statistical program SPSS version 28.0.0 was used. The mean (standard deviation) of the quantitative variables was displayed. The alpha error was established at 0.05 with a 95% confidence level; a two-sided *p*-value was employed; and 80% of the study's power was achieved. In view of the design of this study, the Mann–Whitney U test was used to compare the effect of vaginal suppositories vs tranexamic acid on primary and secondary efficacy parameters. For intragroup and inter-group comparison, repeated measures of ANOVA were analyzed for follow-up data of each group. All efficacy parameters were analyzed as per intention-to-treat principles using data from all randomized participants who have taken treatment for at least one menstrual cycle. The last observation carried forward (LOCF) approach was used to impute missing data.

2.13 Machine learning techniques

In the current study, we used four types of machine learning algorithms, namely, KNN, AB, NB, and RF, to analyze the experimental research data (AlShorman et al., 2022; Sultana et al., 2022a; Iqbal et al., 2022; Ullah et al., 2022).

2.13.1 K-nearest neighbor classifier

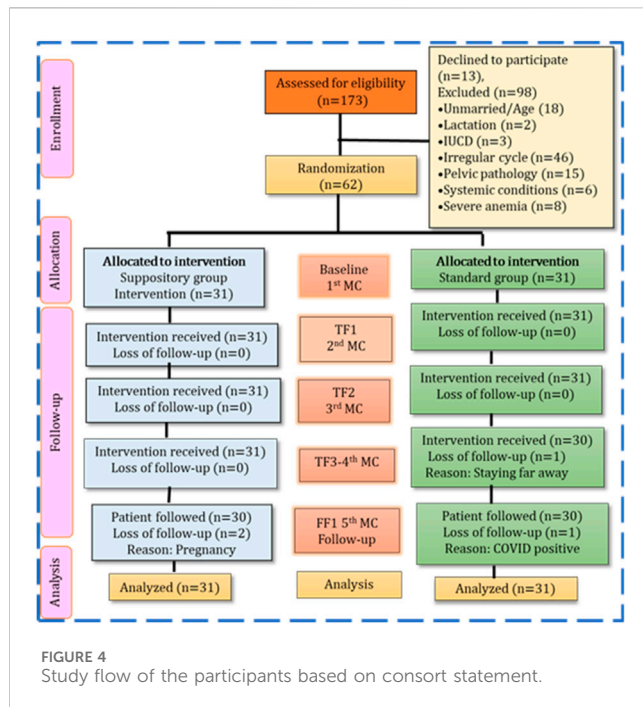
The KNN classifier is an extensively used machine learning algorithm employed for both classification and regression tasks, particularly valuable in scenarios where data exhibit intricate and non-linear relationships. The underlying principle of the KNN classifier revolves around the concept of similarity. When tasked with classifying a new data point, the algorithm identifies the 'k' closest neighbors from the training dataset, where 'k' is a user-defined parameter. The selection of neighbors is determined by a chosen distance metric, often the Euclidean or Manhattan distance, which quantifies the dissimilarity between data points based on their feature values. During the training phase, KNN stores the entire training dataset, retaining its respective class labels for reference (Lai et al., 2019).

In the prediction phase, KNN calculates the distances between the new data point and every point in the training dataset. The 'k' data points with the smallest distances to the new point are chosen as neighbors. The class label for the new data point is then determined by a majority vote among these 'k' neighbors. This flexible approach allows KNN to adapt to varying data distributions and decision boundaries, making it effective at capturing complex patterns in the data. However, the algorithm does come with certain considerations. For instance, the choice of 'k' can significantly impact the model's performance, influencing its sensitivity to noise and overfitting. Additionally, KNN can be computationally expensive, particularly when dealing with large datasets, and requires careful preprocessing steps such as feature scaling to ensure that no single feature dominates the distance calculations.

2.13.2 AdaBoost classifier

The AdaBoost classifier is a prominent ensemble learning algorithm for its remarkable ability to enhance the accuracy of weak learners and improve overall predictive performance. Introduced by Yoav Freund and Robert Schapire in the mid-1990s, AdaBoost addresses the task of combining multiple weak learners—individual models that perform slightly better than random chance—to create a single, robust model with strong predictive capabilities. At its core, AdaBoost functions through an iterative process that emphasizes the misclassified instances in each successive round. During each iteration, the algorithm assigns higher weights to misclassified data points, compelling subsequent weak learners to focus on those difficult examples. This adaptive weight assignment effectively directs the attention of the algorithm toward the instances that present the greatest challenge. Consequently, the ensemble model evolves to excel at handling complex decision boundaries and capturing intricate data patterns (Pal et al., 2023).

Throughout the iterations, AdaBoost trains a sequence of weak learners, often simple decision trees or stumps, and progressively combines their outputs to create an ensemble prediction. Importantly, each weak learner contributes to the final prediction with a weight proportional to its accuracy, ensuring that the most



reliable models hold the most influence. AdaBoost's strengths lie not only in its capacity to amplify the performance of modest models but also in its relative insensitivity to overfitting. It avoids the pitfalls of overfitting by focusing on difficult instances, which helps prevent the algorithm from becoming overly tailored to the training data. While AdaBoost does exhibit exceptional performance in many scenarios, it may be sensitive to noisy data and outliers, potentially leading to undue emphasis on misclassified instances and affecting overall accuracy.

2.13.3 Naive Bayes classifier

The naive Bayes classifier is a machine learning algorithm renowned for its simplicity and efficiency in handling classification tasks. Rooted in Bayesian probability theory, naive Bayes operates to make predictions. Despite its "naive" assumption of feature independence, which may not hold in all cases, naive Bayes often yields impressive results and serves as a strong baseline model (AlShorman et al., 2022).

The algorithm's working principle involves estimating the probability of a given class label for a new data instance based on the joint probabilities of its features. Naive Bayes makes use of Bayes' theorem to compute these probabilities. In the prediction phase, the algorithm applies Bayes' theorem to compute the posterior probabilities for each class and assigns the class label with the highest probability to the new data instance.

2.13.4 Random forest classifier

The random forest classifier stands as a cornerstone in the realm of ensemble learning, offering a robust and versatile approach to classification tasks. Rooted in the concept of decision tree ensembles, random forest addresses the limitations of individual trees by combining the predictive power of multiple trees, thereby mitigating issues of overfitting and enhancing overall accuracy. This algorithm,

introduced by Leo Breiman and Adele Cutler, operates by constructing a multitude of decision trees during both the training and prediction phases (Heyat et al., 2019).

In a random forest, each tree is built using a bootstrapped subset of the original training data, ensuring diversity among the trees. Moreover, during the tree-building process, a random subset of features is selected for each split, promoting different paths of decision making and reducing the likelihood of a single dominant feature dictating the outcome. Once all trees are constructed, the algorithm aggregates their predictions through a majority vote (for classification tasks) or an average (for regression tasks) to arrive at a final prediction. This ensemble approach lends itself to improved generalization and robustness.

3 Results

The study duration was from 2 February 2021 to 17 February 2022. In this study, a total of 173 participants with HMB were screened according to inclusion criteria. Ninety-eight participants were omitted from the trial for different reasons, and 13 participants declined to participate. The remaining 62 participants were randomly assigned to the study. The randomly assigned 62 participants were divided into two groups: the suppository group and tranexamic acid group (standard control). The loss to follow-up is summarized in Figure 4.

3.1 Baseline sociodemographic, clinical, and temperament parameters

Statistical tests demonstrated the insignificant difference between the SG and TG ($p > 0.05$) in the baseline sociodemographic parameters in terms of age, religion, habitat, duration of illness, diet, BMI, and socioeconomic characteristics. The mean age in the SG and TG was 35.61 ± 6.27 and 35.61 ± 5.54 years, respectively. A significant proportion of participants were identified as Muslim, with 74.19% in the SG and 83.87% in the TG. Additionally, the majority of participants in both groups belonged to the upper-lower socioeconomic status, comprising 74.1% in the SG and 70.9% in the TG. The details can be found in Table 1.

3.2 Efficacy parameters

3.2.1 Primary outcome results

In the SG, the mean PBLAC score at baseline was 635.322 ± 504.23 . Subsequently, at post-intervention (TF3) and the fifth cycle (FF1), it decreased to 67.70 ± 22.37 and 70.51 ± 33.23 , respectively, demonstrating a statistically extremely significant reduction from the baseline ($p < 0.0001$). In the TG, the PBLAC score was 512.93 ± 283.57 at baseline, and it notably decreased to 97.96 ± 39.25 at post-intervention (TF3) and 104.64 ± 47.81 during the fifth cycle (FF1), indicating a statistically extremely significant reduction from the baseline ($p < 0.0001$) (Table 2 (a)). A higher percentage of participants in the SG achieved normal menstrual blood loss compared to the TG (93.5% vs 74.2%) at post-intervention (TF3) (Table 2 (b)). A statistically significant

TABLE 1 Statistical analysis of the suppository and tranexamic acid groups based on baseline sociodemographic parameters.

Parameter	Suppository group (n = 31)	Tranexamic group (n = 31)	Total (n = 62)	p-value
Age (years)				
20–29	6 (19.35)	6 (19.35)	12 (19.35)	0.83 ^a
30–39	16 (51.61)	18 (58.06)	34 (54.83)	
40–45	9 (29.03)	7 (22.58)	16 (25.80)	
Religion no. (%)				
Muslim	23 (74.19)	26 (83.87)	49 (79.03)	0.53 ^a
Hindu	8 (25.8)	5 (16.12)	13 (20.96)	
Habitat				0.70 ^a
Urban	28 (90.32)	26 (83.87)	54 (87.10)	
Rural	3 (9.68)	5 (16.12)	8 (12.90)	
Duration of illness (months)	19 ± 4.40	14.12 ± 2.75	-	0.35 ^b
Diet				
Vegetarian	4 (12.90)	3 (9.6)	7 (11.29)	0.99 ^a
Non-vegetarian	18 (58.06)	20 (64.51)	38 (61.29)	
Mixed	9 (29.03)	8 (25.80)	17 (27.42)	
BMI (Kg/m²)	26.92 ± 4.66	28.43 ± 4.89	-	0.21 ^b
Socioeconomic status				
Upper I	0	0	0	0.44 ^c
Upper middle II	1 (3.23)	2 (6.25)	3 (4.84)	
Lower middle III	5 (16.13)	7 (22.58)	12 (19.35)	
Upper lower IV	23 (74.19)	22 (70.97)	45 (72.58)	
Lower V	2 (6.25)	0	2 (3.22)	

^aChi-square test
^bUnpaired *t*-test.
^cFisher exact test; data are presented as the mean ± SD or no. %.

reduction in the mean PBLAC score was observed at each follow-up in the SG compared to the TG ($p < 0.001$). Table 3 provides a summary of the cycle duration as well as the duration and amount of menstrual blood flow in both the SG and TG.

3.2.2 Secondary outcome results

A significant improvement in the SF-36 HRQoL score in the SG compared to the TG was noted in the sub-score of the physical health composite score ($p = 0.01$), mental health component score ($p = 0.01$), and total SF-36 score ($p = 0.02$) at post-intervention (TF3). Furthermore, significant improvement in physical function ($p = 0.04$), general health ($p = 0.01$), the role of limitation of the emotional problem ($p = 0.04$), and social function ($p = 0.02$) in the SG was noted in comparison with the TG at post-intervention. The intragroup comparison of both groups at post-intervention from baseline showed extremely significant improvement ($p < 0.0001$) in all parameters of the SF-36 score (Table 4). At post-intervention (TF3), the hemoglobin level was increased in 11 participants (35.48%) in the SG and 10 participants (32.25%) in the TG, with a significant difference ($p < 0.05$) (Table 5).

3.3 Hematological, coagulation profile, safety biochemical markers, and ultrasonography of the abdomen in the SG and TG

All parameters (thyroid-stimulating hormone, clotting time, bleeding time, and platelet count) were within the normal limit at the baseline in the suppository and tranexamic acid groups with an insignificant difference ($p > 0.05$) (Table 5). Hepatic (AST, ALT, and ALP) and renal (blood urea and S. creatinine) safety parameters were within normal limits at baseline.

3.4 Classification (SG vs. TG) results using machine learning algorithms

3.4.1 Primary outcome classification

The current study employed a combination of three distinct cross-validation (CV) strategies: CV-2, CV-5, and CV-10, in primary outcome classification (SG vs. TG) analysis (Table 6).

TABLE 2 PBLAC score of both groups.

(a) PBLAC mean score at each follow-up in both groups							
Follow-up	Suppository group (n = 31)	95% CI (L-U)	Difference from BL	Tranexamic group (n = 31)	95% CI (L-U)	Difference from BL	p-value
BL	635.322 ± 504.23	450.40–820.25	-	512.93 ± 283.57	408.94–616.93	-	0.50 ^a
TF1	96.93 ± 52.98***	77.50–116.37	538.39	144.87 ± 67.73***	120.03–169.71	368.06	0.002*** ^a
TF2	75.74 ± 29.08***	65.07–86.41	559.58	110.709 ± 45.55***	94.00–127.42	402.23	0.0009*** ^a
TF3	67.70 ± 22.37***	59.50–75.91	567.61	97.96 ± 39.25***	83.56–112.37	414.97	0.0018*** ^a
FF1	70.51 ± 33.23***	58.32–87.70	564.81	104.64 ± 47.81**	87.10–122.18	408.29	0.0003*** ^a
(b) Participants with normal PBLAC scores (<100) and HMB (>100) in both groups							
Follow-up	Suppository group (n = 31)		Tranexamic group (n = 31)				
	<100 (normal menstrual bleeding)	>100 (heavy menstrual bleeding)	<100 (normal menstrual bleeding)	>100 (heavy menstrual bleeding)			
BL	0	31 (100)	0	31 (100)			
TF1	19 (61.3)	12 (38.7)	10 (32.3)	21 (67.7)			
TF2	27 (87.1)	4 (12.9)	19 (61.3)	12 (38.7)			
TF3	29 (93.5)	2 (6.5)	23 (74.2)	8 (25.8)			
FF1	29 (93.5)	2 (6.5)	20 (64.5)	11 (35.5)			

^aMann-Whitney U test; ** $p < 0.001$ is considered strongly significant; *** $p < 0.0001$ is considered extremely significant from baseline; **BL**, baseline; **TF1**, **TF2**, and **TF3**, treatment follow-up months; **FF1**, follow-up without treatment; **PBLAC**, pictorial blood loss assessment chart. Data are presented as the mean ± SD and no. %.

TABLE 3 Statistical analysis of both groups based on different variables.

Variable	Suppository group (n = 31)	95% CI (L-U)	Difference from BL	Tranexamic group (n = 31)	95% CI (L-U)	Difference from BL	p-value
Duration of the cycle							
BL	28.54 ± 3.1	27.40–29.68		28.45 ± 1.52	27.89–29.01		0.70 ^a
TF3	28.87 ± 2.34	28.96–2.3	–0.33	29.19 ± 2.33	27.58–29.44	–0.74	0.90 ^a
p-value	0.49			0.85			
Overall p-value between the groups = 0.24 ^b							
Duration of flow							
BL	10.8 ± 5.17	8.43–12.14		8.67 ± 3.9	7.23–10.11		0.07 ^a
TF1	5.44 ± 1.55***	8.33–6.00	5.36	5.51 ± 1.56***	4.94–6.09	3.16	0.76 ^a
TF2	5.16 ± 1.44***	4.79–6.18	5.64	5.51 ± 1.56***	4.91–6.09	3.16	0.16 ^a
TF3	5.16 ± 1.31***	4.68–5.63	5.64	5.16 ± 1.09***	5.09–5.93	3.51	0.62 ^a
FF1	5.36 ± 1.44***	4.61–5.70	5.44	5.22 ± 1.25***	4.75–5.56	3.45	0.96 ^a
Overall p-value between the groups = 0.04 ^b							
Amount of flow (no. of pads/cycle)							
BL	34.16 ± 25.49	24.81–43.51		27.45 ± 14.84	22.00–32.89		0.35 ^a
TF1	8.64 ± 2.8***	7.60–9.68	25.52	9.54 ± 4.30***	7.97–11.12	17.91	0.69 ^a
TF2	7.74 ± 2.12***	6.96–8.52	26.42	8.83 ± 3.23***	7.65–10.02	18.62	0.29 ^a
TF3	7.48 ± 1.69***	6.86–8.10	26.68	8.09 ± 2.05***	7.34–8.85	19.36	0.20 ^c
FF1	7.70 ± 1.9***	6.98–8.43	26.46	8.41 ± 2.95***	7.33–9.50	19.04	0.27 ^c

^aMann–Whitney U test.
^bRMANOVA.
^cUnpaired *t*-test. ****p* < 0.0001 is considered extremely significant from baseline; BL, baseline; TF, treatment follow-up; FF, first follow-up without treatment.

Each model was evaluated across various performance metrics, including AUC, accuracy, precision, recall, and specificity. In the context of the CV-2 model, the AB classifier emerged as the top performer, exhibiting exceptional results across all measures: AUC (57.90%), accuracy (57.80%), precision (58.20%), recall (57.80%), and specificity (60.00%). Within the CV-5 framework, the KNN classifier took the lead, achieving the highest scores for AUC (52.10%), accuracy (57.10%), precision (57.00%), recall (57.10%), and specificity (58.50%). Remarkably, in the CV-10 configuration, the AB classifier excelled with remarkable prowess, yielding superior performance metrics, including AUC (58.60%), accuracy (60.30%), precision (60.00%), recall (60.30%), and specificity (61.60%).

Upon examining the collective outcomes, the AB classifier demonstrated its prowess by achieving the highest accuracy (60.30%) within the CV-10 model, showcasing its efficacy in this specific setting (Figure 5). Conversely, the NB classifier, operating within the CV-10 model, exhibited the lowest accuracy (4.80%), underlining its limitations within this context. This in-depth exploration of classification results elucidates the varying capabilities of machine learning models under different cross-validation scenarios and provides insights into their strengths and weaknesses in accurately categorizing the given data.

3.4.2 Secondary outcome classification

The current study employed a combination of three distinct CV strategies: CV-2, CV-5, and CV-10, in secondary outcome classification (SG vs. TG) analysis (Table 7). Each model was evaluated across various performance metrics, including AUC, accuracy, precision, recall, and specificity. In the context of the CV-2 model, the AB classifier emerged as the top performer, exhibiting exceptional results across all measures: AUC (53.40%), accuracy (54.00%), precision (53.30%), recall (54.00%), and specificity (55.40%). Within the CV-5 framework, the RF classifier took the lead, achieving the highest scores for AUC (60.40%), accuracy (57.10%), precision (56.20%), recall (57.10%), and specificity (58.50%). Remarkably, in the CV-10 configuration, the KNN classifier excelled with remarkable prowess, yielding superior performance metrics, including AUC (59.10%), accuracy (57.10%), precision (57.40%), recall (57.10%), and specificity (58.50%).

Upon examining the collective outcomes, the KNN classifier demonstrated its prowess by achieving the highest accuracy (57.10%) within the CV-10 model, showcasing its efficacy in this specific setting (Figure 5). Conversely, the NB classifier, operating within the CV-10 model, exhibited the lowest accuracy (4.80%), underlining its limitations within this context. This in-depth exploration of classification results

TABLE 4 SF-36 HRQoL health survey using statistical techniques in secondary outcomes.

Domain	Period	Suppository group (n = 31)	Tranexamic group (n = 31)	p-value
Physical function (PF)	Baseline	68.70 ± 19.53	69.51 ± 18.04	0.99 ^a
	TF3	88.22 ± 12.14	79.35 ± 20.19	0.04 ^a
	p-value	<0.0001 ^b	<0.0001 ^b	
Role limitation due to physical problems (RF)	Baseline	37.09 ± 43.71	34.35 ± 38.46	0.96 ^a
	TF3	81.45 ± 33.52	72.25 ± 35.8	0.28 ^a
	p-value	<0.0001 ^b	<0.0001 ^b	
Bodily pain (BP)	Baseline	48.7 ± 17.11	45.64 ± 13.52	0.96 ^a
	TF3	67.82 ± 14.54	59.75 ± 12.84	0.28 ^a
	p-value	<0.0001 ^c	<0.0001 ^b	
General health (GH)	Baseline	38.96 ± 9.65	39.63 ± 9.32	0.78 ^d
	TF3	62.14 ± 11.78	55.64 ± 10.89	0.01 ^a
	p-value	<0.0001 ^c	<0.0001 ^b	
Role limitation due to emotional problems	Baseline	54.83 ± 39.95	47.30 ± 42.83	0.48 ^a
	TF3	96.77 ± 10.02	73.11 ± 38.89	0.04 ^a
	p-value	<0.0001 ^b	<0.0001 ^b	
Energy/fatigue/vitality (VT)	Baseline	48.83 ± 11.27	48.38 ± 12.40	0.71 ^a
	TF3	63.70 ± 10.56	63.70 ± 11.75	0.9 ^d
	p-value	<0.0001 ^b	<0.0001 ^c	
Emotional wellbeing (mental Health-MH)	Baseline	53.58 ± 11.36	54.70 ± 11.28	0.69 ^d
	TF3	63.83 ± 10.25	64.58 ± 9.5	0.92 ^a
	p-value	0.0001 ^c	0.0001 ^c	
Social functioning (SF)	Baseline	48.95 ± 14.60	47.98 ± 12.11	0.85 ^a
	TF3	64.51 ± 12.54	56.85 ± 9.5	0.02 ^a
	p-value	<0.0001 ^b	0.0002 ^b	
Physical health composite score (PCS)	Baseline	48.36 ± 17.43	47.28 ± 14.77	0.79 ^d
	TF3	74.91 ± 14.93	66.75 ± 16.44	0.01 ^a
	p-value	<0.0001 ^c	<0.0001 ^b	
Mental health composite score (MCS)	Baseline	51.15 ± 15.30	49.59 ± 16.53	0.70 ^d
	TF3	72.20 ± 8.26	64.56 ± 15.55	0.01 ^d
	p-value	<0.0001 ^c	<0.0001 ^b	
Total score	Baseline	49.76 ± 15.57	48.44 ± 14.51	0.73 ^d
	TF3	73.56 ± 11.09	65.65 ± 14.81	0.02 ^d
	p-value	<0.0001 ^c	<0.0001 ^c	

TF3: Post-intervention (third treatment follow-up).
^aMann–Whitney U test.
^bWilcoxon matched pair test.
^cPaired Student’s ‘t’ test.
^dUnpaired Student’s ‘t’ test; TF, treatment follow-up.

elucidates the varying capabilities of machine learning models under different cross-validation scenarios and provides insights into their strengths and weaknesses in accurately categorizing the given data.

3.4.3 Combine therapeutic classification

In current research, comprehensive combined therapeutic classification (TG vs. SG) analysis employed a combination of three distinct CV strategies: CV-2, CV-5, and CV-10 (Table 8).

TABLE 5 Hematological and safety biochemical markers of the SG and TG.

Variable (mean \pm SD)	Suppository group (n = 31)	Tranexamic group (n = 31)	p-value
Hemoglobin (g/dL)			
Baseline	11.06 \pm 1.36	10.6 \pm 1.38	0.21 ^a
Fourth cycle (TF3)	11.01 \pm 1.33	10.79 \pm 1.21	0.49 ^a
p-value	0.26 ^b	0.39 ^b	
Coagulation profile			
Platelet count	3.17 \pm 0.60	3.35 \pm 0.70	0.30 ^a
Lakhs/cu mm			
Bleeding time (min)	2.05 \pm 0.19	2.13 \pm 0.34	0.61 ^c
Clotting time (min)	5.44 \pm 0.46	5.34 \pm 0.43	0.43 ^c
Random blood sugar (mg/dL)	100.48 \pm 19.48	98.88 \pm 14.80	0.80 ^c
Thyroid-stimulating hormone (μ U/mL)	2.68 \pm 1.10	2.55 \pm 1.30	0.65 ^a
Safety profile			
Alanine aminotransferase (IU/L)	22.93 \pm 7.5	24.67 \pm 9.59	0.76 ^c
Aspartate aminotransferase (IU/L)	31.54 \pm 8.3	32.51 \pm 10.69	0.69 ^a
Alkaline phosphatase (IU/L)	100.35 \pm 19.83	112.38 \pm 35.29	0.10 ^a
Blood urea (mg/dL)	20.70 \pm 5.56	21.29 \pm 5.45	0.67 ^c
Serum creatinine (mg/dL)	0.87 \pm 0.13	1.05 \pm 1.11	0.95 ^c
Ultrasonography of the abdomen			
USG abdomen no. (%)			
Normal 1)	19 (61.29)	21 (67.74)	0.89 ^d
Bulky 2)	2 (6.45)	2 (6.45)	
Fibroid 3)	3 (9.67)	1 (3.25)	
Adenomyosis 4)	3 (9.67)	3 (9.67)	
Mixed 5)	4 (12.90)	4 (12.90)	

^aUnpaired Student's 't'.^bPaired student's 't' test.^cMann-Whitney U test.^dChi-square test.

Each model was evaluated across various performance metrics, including AUC, accuracy, precision, recall, and specificity. In the context of the CV-2 model, the RF classifier emerged as the top performer, exhibiting exceptional results across all measures: AUC (47.60%), accuracy (49.20%), precision (48.40%), recall (49.20%), and specificity (50.80%). Within the CV-5 framework, the AB classifier took the lead, achieving the highest scores for AUC (53.20%), accuracy (52.40%), precision (54.80%), recall (52.40%), and specificity (58.40%). Notably, in the CV-10 configuration, the KNN classifier excelled with remarkable prowess, yielding superior performance metrics, including AUC (55.80%), accuracy (52.40%), precision (52.00%), recall (52.40%), and specificity (53.90%).

Upon examining the collective outcomes, the AB classifier demonstrated its prowess by achieving the highest accuracy (52.40%) within the CV-5 model, showcasing its efficacy in this specific setting (Figure 5). Conversely, the NB classifier, operating within the CV-10 model, exhibited the lowest accuracy (6.30%), underlining its limitations within this context. This in-depth exploration of classification results elucidates the varying capabilities of machine learning models under different cross-validation scenarios and provides insights into their strengths and weaknesses in accurately categorizing the given data.

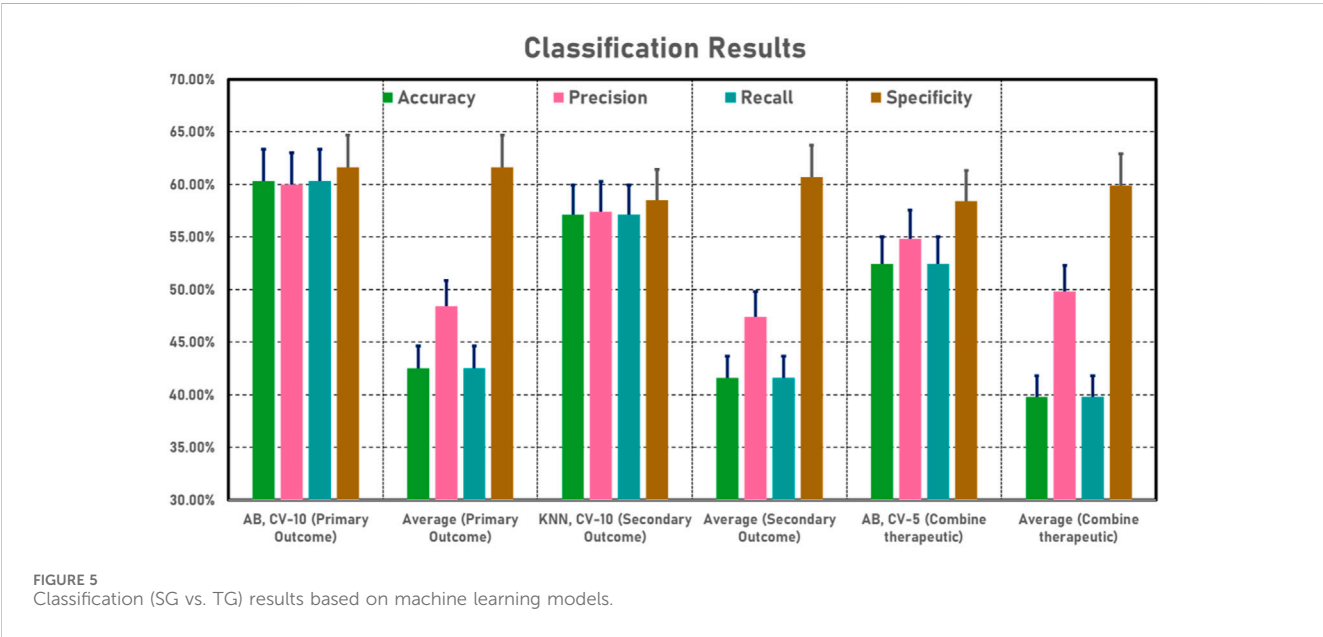
4 Discussion

The present study found that the PBLAC score was meaningfully reduced in the SG and TG from the baseline measurement at each follow-up, showing a reduction in HMB. At post-intervention (TF3), 29 participants (93.5%) in the test group and 23 participants (74.2%) in the tranexamic group had normal MBL (less than 80 mL), showing that the SG was more effective than the TG. In the second (TF1), third (TF2), fourth (TF3), and fifth (FF1) cycles, PBLAC scores decreased significantly in the SG compared to the TG. In the SG and TG, the mean PBLAC score decreased from 635.322 \pm 504.23 to 67.70 \pm 22.37 and 512.93 \pm 283.57 to 97.96 \pm 39.25, respectively, at post-intervention (TF3), demonstrating a statistically significant difference ($p < 0.001$). A higher percentage of participants in the SG achieved normal menstrual blood loss compared to the TG (93.5% vs 74.2%). The SG showed a considerable improvement in total SF-36 scores (73.56%) compared to the TG (65.65%), with a statistically significant difference ($p < 0.001$). Additionally, no serious adverse events were reported in either group. Notably, machine learning algorithms, particularly AB and KNN,

TABLE 6 Primary outcome classification (SG vs. TG) based on different machine learning models.

Classifier	Model	AUC	Accuracy	Precision	Recall	MCC	Specificity
KNN	CV-2	0.484	0.460	0.453	0.460	−0.064	0.477
AB		0.579	0.578	0.582	0.578	0.191	0.600
NB		0.454	0.254	0.503	0.254	−0.007	0.746
RF		0.518	0.524	0.532	0.524	0.075	0.539
KNN	CV-5	0.521	0.571	0.570	0.571	0.162	0.585
AB		0.466	0.476	0.469	0.476	−0.032	0.493
NB		0.487	0.079	0.375	0.079	−0.082	0.864
RF		0.558	0.556	0.552	0.556	0.129	0.569
KNN	CV-10	0.436	0.429	0.414	0.429	−0.134	0.446
AB		0.586	0.603	0.600	0.603	0.224	0.616
NB		0.470	0.048	0.246	0.048	−0.066	0.924
RF		0.495	0.524	0.515	0.524	0.063	0.539
Mean		0.504	0.425	0.484	0.425	0.038	0.616
±SD		0.046	0.184	0.097	0.185	0.113	0.144

Bold values mean highest value.



demonstrated the highest accuracy within cross-validation models for both primary and secondary outcomes. There was an insignificant difference in the duration of the cycle ($p = 0.240$) between the SG and TG. Moreover, participants receiving suppositories reported statistically clinically significant improvements in HRQoL compared to those receiving tranexamic acid.

A noteworthy reduction in the PBLAC score was noted during treatment from baseline to post-intervention follow-up ($p < 0.001$). This finding aligns with the previous studies (Imdad et al., 2017;

Azizkhani et al., 2018; Yousefi et al., 2020). According to the work of Goshtasebi et al. (2015), there was an insignificant difference between *Punica granatum* and tranexamic acid on HMB and quality-of-life improvement. Imdad et al. (2017) confirmed that Qurs Gulnar was more effective than tranexamic acid for HMB. Yousefi et al. (2020) reported no significant difference between the efficacy of the Golnar tablet with tranexamic acid in HMB. As per the work of Azizkhani et al. (2018), women treated with cupping experienced significantly lower PBLAC scores at one and 3 months compared to those treated with medroxyprogesterone acetate. In the

TABLE 7 Secondary outcome classification (SG vs. TG) based on different machine learning models.

Classifier	Model	AUC	Accuracy	Precision	Recall	MCC	Specificity
KNN	CV-2	0.538	0.476	0.469	0.476	−0.031	0.493
AB		0.534	0.540	0.533	0.540	0.095	0.554
NB		0.512	0.270	0.514	0.270	0.022	0.761
RF		0.475	0.444	0.434	0.444	−0.095	0.462
KNN	CV-5	0.563	0.508	0.502	0.508	0.032	0.523
AB		0.421	0.429	0.421	0.429	−0.125	0.446
NB		0.490	0.095	0.410	0.095	−0.045	0.880
RF		0.604	0.571	0.562	0.571	0.157	0.585
KNN	CV-10	0.591	0.571	0.574	0.571	0.166	0.585
AB		0.526	0.540	0.531	0.540	0.094	0.554
NB		0.487	0.048	0.246	0.048	−0.066	0.924
RF		0.550	0.508	0.503	0.508	0.032	0.523
Mean		0.524	0.416	0.474	0.416	0.019	0.607
±SD		0.049	0.173	0.085	0.173	0.091	0.152

Bold values mean highest value.

TABLE 8 Combined therapeutic (SG vs. TG) classification based on different machine learning models.

Classifier	Model	AUC	Accuracy	Precision	Recall	MCC	Specificity
KNN	CV-2	0.489	0.460	0.452	0.460	−0.066	0.477
AB		0.468	0.429	0.457	0.429	−0.047	0.522
NB		0.490	0.238	0.451	0.238	−0.035	0.731
RF		0.476	0.492	0.484	0.492	0.000	0.508
KNN	CV-5	0.534	0.492	0.486	0.492	0.000	0.508
AB		0.532	0.524	0.548	0.524	0.104	0.584
NB		0.473	0.127	0.609	0.127	0.030	0.910
RF		0.530	0.508	0.499	0.508	0.032	0.523
KNN	CV-10	0.558	0.524	0.520	0.524	0.066	0.539
AB		0.401	0.413	0.404	0.413	−0.160	0.431
NB		0.473	0.063	0.574	0.063	−0.016	0.940
RF		0.526	0.508	0.500	0.508	0.031	0.523
Mean		0.495	0.398	0.498	0.398	−0.005	0.599
±SD		0.040	0.155	0.054	0.155	0.065	0.161

Bold values mean highest value.

current study, the secondary endpoints were HRQoL and Hb%. It was noticeable that the suppository group showed significant improvement in women’s QoL in all parameters at TF3 and FF1 from baseline. These findings were similar to the previous study (Jahan et al., 2016). At post-intervention (TF3), the Hb% was increased by 35.48% in the SG and 32.25% in the TG, with a significant difference ($p < 0.05$).

4.1 Role of inflammation, oxidative stress, and immune responses in uterine bleeding and the possible mechanisms of action of botanical drugs to ameliorate HMB

Intrauterine leukocytes and their molecular by-products play an essential inflammatory role in both normal and pathological uterine

hemorrhage. According to current data, immune cell disruption and associated cytokine mediators are causal factors for abnormal uterine bleeding (AUB) and pelvic pain (Berbic et al., 2014). Intrauterine leucocytes and their derivatives play main 'inflammatory' roles in normal menstruation and AUB. Menstruation has recently been linked to an increase in tissue leukocyte counts and their pro-inflammatory mediator. They are crucial in endometrial breakdown, proliferation, and remodeling. Endothelial cells secrete various pro-inflammatory cytokines during mitochondrial failure, including IL-6, IL-1, and TNF- α , as well as an elevation of ICAM-1 expression, which attracts monocyte activation and adhesion. During the menstrual cycle in the endometrium, macrophages, NKc, large granular lymphocytes, eosinophils, and mast cells are explicitly increased. In addition, during the proliferative phase following an endometrial breakdown, to expedite clearance of the endometrial cavity, CD8 cytotoxic T-cell activity is enhanced, which shows that this factor supports the concept of an activated adaptive component of the immune system. During normal menstruation, the immune responses seem to be tightly regulated. It is believed that MMP-2 and MMP-9 (matrix metalloproteinase) expression levels interfere with hemorrhage (Berbic et al., 2014). As per another study, compared to normal women, women with HMB have higher serum levels of prostaglandin E2 and prostacyclin, which cause localized vasodilation and platelet accumulation, and lower levels of prostaglandin F2, which cause vasoconstriction and PGE2 receptors (Kashefi et al., 2015). The current evidence emphasizes the importance of mitochondrial function in immune cell activity. During immunological reactions, mitochondrial physiology, morphology, and metabolism are tightly regulated. T-cell activation necessitates the formation of ROS, whereas activated T cells can use both OXPHOS and glycolysis for proliferation (Chen et al., 2018). According to research, foods that cause inflammatory reactions in the body contribute to HMB. In exchange, natural remedies or pharmaceutical drugs that prevent the production of PGs and leukotrienes may have an anti-inflammatory impact and reduce menstrual blood loss (Berbic et al., 2014). ROS accumulation, which causes oxidative stress, has been linked to improper oocyte maturation, decreased fertilization, and the formation of endometriosis. The balance of ROS and antioxidants is critical for the health of women. Mumford et al. (2016) contend that the interactions between serum antioxidants and endogenous hormones are critical for the menstrual cycles of premenopausal women (Mumford et al., 2016).

Unani treatments have the potential to treat HMB as they have astringent, analgesic, and anti-inflammatory properties and avoid hormonal side effects. Unani scholars mention the use of acacia gum to treat hemoptysis and menorrhagia (Yousefi et al., 2020) as it possesses ethnomedicinal activities such as astringent, styptic, and anti-inflammatory (Kabir al-Din, 2007), with specific therapeutic action that is useful in stopping menstrual bleeding (Kabir al-Din, 2007). Additionally, acacia gum possesses pharmacological and therapeutic potential, including anti-inflammatory, analgesic (Fan et al., 2020), prostaglandin inhibiting (Lee et al., 2006), hepatoprotective (Johari et al., 2015), vasoconstrictor (Amos et al., 1999), hemostatic, and astringent properties. Acacia gum has been documented to have plant metabolites such as phenolics, saponins, alkaloids, flavonoids, tannins (gallic acid, ellagic acid, and tannic acid), vitamin C, stearic acid, Arabin, carotene, crude protein, carbohydrates crude fiber, calcium, magnesium, and selenium (Ali, 2012). Tannins, gallic acid, and other flavonoids are considered to have strong astringent and styptic activities

and, thus, can cause the contraction of the capillary endothelium (Tansaz et al., 2016). The astringent 0 exerts an impact on the biosynthesis of prostaglandins and reduces uterine bleeding (Livdands-Forret et al., 2007). The calcium in the acacia gum helps maintain the hemostatic mechanism (Nadkarni KM, 2004). Vitamin C with bioflavonoids helps decrease HMB by making the capillaries stronger and also preventing their fragility (Livdands-Forret et al., 2007). Camphor possesses ethnomedicinal properties such as astringent, disinfectant, and neutralizing blood actions due to its cold and dry, anti-inflammatory (Khan and Muhammad, 2018), and externally anesthetic and analgesic properties (Kabir al-Din, 2007). Camphor research studies show that it possesses pharmacological and therapeutic potential such as anti-inflammatory (Liu et al., 2020), analgesic (Fan et al., 2020), hepatoprotective, antioxidant (Muhamad et al., 2019), estrogenic (Maerkel et al., 2007), and prostaglandin inhibiting properties (Liu et al., 2020). Camphor has phenols, flavonoids (tannins), saponins, alkaloids, and carbohydrates. The effect of camphor on estrogenic gene expression was studied (Maerkel et al., 2007). According to their findings, 4-MBC administration in rats had sex- and region-specific effects on the mRNA levels of PPE, ER- α , PR, and IGF-I (Maerkel et al., 2007). A variety of liver illnesses have been treated using camphor as a hepatoprotective drug.

Tannin, a plant secondary metabolite, has analgesic, hemostatic, and anti-inflammatory properties. Flavonoids have anti-inflammatory, antioxidant, and analgesic properties (Safari et al., 2016). Flavonoids can scavenge lipid peroxyl, hydroxyl, and superoxide anion radicals, and they play an important role in the prevention of illnesses caused by oxidative damage to membranes, proteins, and DNA. Alkaloids and saponins possess anti-inflammatory properties. Anti-inflammatory activity is aided by antioxidant properties (Abdulhamid et al., 2019). Polyphenols, which are natural plant metabolites found in plants, have a wide range of biological activities. Before cell viability is seriously compromised, phenolic plant metabolites and flavonoids can interact with ROS/RNS to stop the chain reaction (Taghvaei and Jafari, 2015). Several authors have established a link between inflammation and oxidative stress. Evidence suggests that oxidative stress is pathogenic in chronic inflammatory diseases (Hussain et al., 2016). Antioxidants have anti-inflammatory actions that limit nociceptor activity and reduce the production and/or release of prostaglandins, which act as inflammatory pain mediators. By blocking the NF- κ B pathway, a substance can exhibit both antioxidant and anti-inflammatory characteristics (Agnieszka and Skrzydlewska, 2022). A study mentioned that the production of the inflammatory cytokines TNF- α and IL-6 can be reduced by taking vitamin C (an antioxidant) orally. When given intravenously, it can help prevent cytokine storms. *C. camphora* contains cineol, borneol, and citronellal, which inhibit inflammatory cytokine, chemokine production, and PGE-2 production (Fazmiya et al., 2022). *C. camphora* has potent anti-inflammatory (Kang et al., 2019) and antioxidant properties (Zafar et al., 2012). Eucalyptol, camphor, and linalool were extracted, and nine terpenoids were obtained from the essential oil of *C. camphora* (Wu et al., 2020). These inhibit the production of TNF- α , IL-6, and PGE2 and improve the increase of mRNA and protein levels of iNOS, COX-2, and MMP-9 in LPS-stimulated RAW 264.7 macrophages (Li et al., 2018). *C. camphora* has anti-inflammatory mechanisms that limit the synthesis of NO and PGE2 in LPS/IFN-activated macrophages. Its MeOH extract inhibits 70% of the synthesis of PGE2 in LPS/IFN-

activated macrophages. Another study found that *C. camphora* has anti-inflammatory properties due to its ability to modulate cytokine production, NO and PGE2 release, functional activation of adhesion molecules, and oxidative stress. Additionally, *C. camphora* can significantly modulate numerous inflammatory responses at the transcriptional level (Lee et al., 2006).

Oxidative stress has been linked to several diseases' pathogenesis, including cardiovascular disease, renal disease, atherosclerosis, hypertension, premenstrual syndrome, and aging (Sultana et al., 2022b). The PAs of *C. camphora* also showed strong antioxidant capacity with the scavenging of DPPH, FRAP, and ABTS assays (Yang et al., 2021). Liu et al. (2019) confirmed that flavonoids extracted from *C. camphora* have antioxidant capacity (Fu et al., 2016). From *C. camphora* ethanolic extract, phenolic plant metabolites, including linalool, nerolidol, and borneol, were extracted (Muhamad et al., 2019) that have antioxidant and remove free radical potential (Fazmiya et al., 2022). Kaddam et al. demonstrated the unique effect of acacia gum as an antioxidant among sickle cell anemic patients, as it increases TAC levels and decreases oxidative stress markers. In addition, acacia gum has immune-modulatory and anti-inflammatory effects. It controls immunity in mice by reducing TNF α and CRP while increasing the IL-10 anti-inflammatory cytokine. It exerts local anti-inflammatory effects by modifying NF- κ B in the small intestine (Ali et al., 2020). Kaur et al. (2022) reported the anti-inflammatory and antioxidant activities of the bioactive molecule betulin isolated from *Acacia arabica* bark. Betulin exhibited moderate-to-strong antioxidant potential in a lipid peroxidation assay and was a selective inhibitor of COX-2 (Kaur et al., 2022). Flavonoids and other phenolic plant metabolites are known to target cyclooxygenase-mediated inflammation. A study found that acacia gum has protective and antioxidant effects on the blood,

liver, kidney, and cardiovascular system in experimentally induced injuries to these organs and tissues (Hassanien et al., 2019). Methanolic crude extracts (MCEs) of acacia gum demonstrated anti-inflammatory activity at 300 mg/kg, comparable to indomethacin, which suppresses PG synthesis while also inhibiting the initiatory inflammation process, in which histamine, serotonin, and kinin are the primary mediators. Flavonoids, alkaloids, β -carotene, phenolic acids, and tannins are the phytochemical constituents of Acacia gum. Furthermore, acacia gum has higher antioxidant activity than standard gallic acid and has a strong relationship with total phenolic content (AM Elnour et al., 2018). The mechanism of the suppositories as an anti-inflammatory agent is described in Figure 6, and Figure 7 depicts the antioxidant mechanism of camphor and acacia.

Synchronized prothrombotic and antithrombotic reactions involve a coagulation system, platelets, fibrinolysis system, and vessel wall, which maintain the hemostatic balance in the body. However, in the event of oxidative stress, inflammation, and an altered blood flow state inside the vessel, this balance shifts toward prothrombotic, which is exhibited by impaired platelet and leukocyte adhesion, impaired synthesis of PGI $_2$ and NO, and disturbed fibrinolysis (Marcinićzyk et al., 2022). Fibrinolysis is a physiologic factor of hemostasis that contributes to the formation of border clots. Nonetheless, excessive fibrinolysis following tissue injury caused by ischemia and reperfusion, trauma, or surgery may contribute to coagulopathy, bleeding, and inflammatory responses (Levy et al., 2018). The thrombin–thrombomodulin complex, when activated, leads to the activation of thrombin fibrinolysis inhibitor and removes lysine residues on fibrin, removing binding sites for plasminogen, and could play an important role in modifiable cross-talk between inflammation and coagulation. After massive trauma, surgery, or ischemia, the

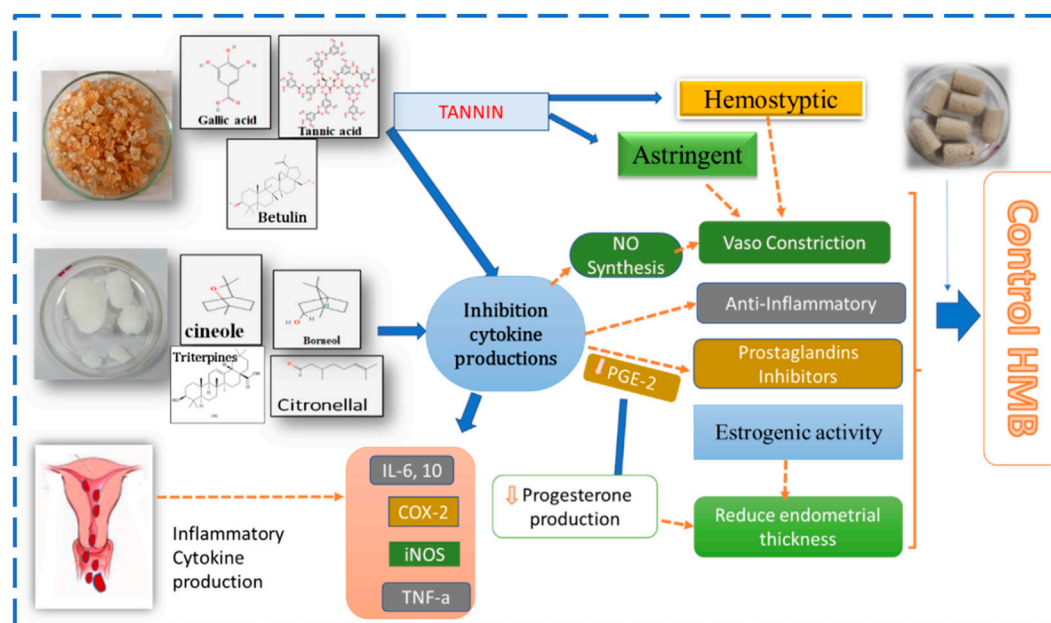


FIGURE 6

Anti-inflammatory mechanism of action of a vaginal suppository of camphor and acacia gum.

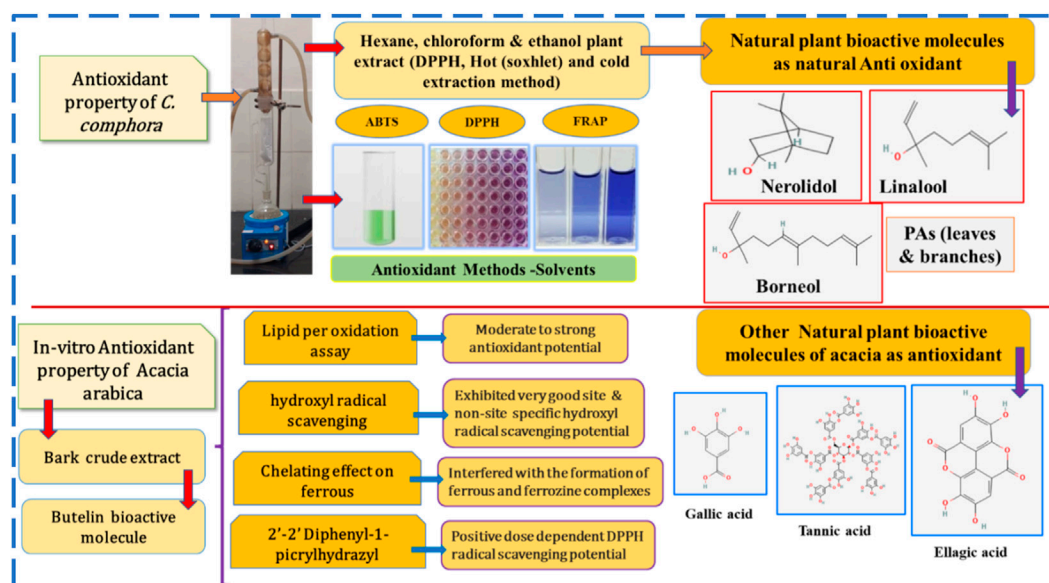


FIGURE 7
Antioxidant activity of camphor and acacia.

ability to locally regulate fibrinolysis is lost, leading to the development of coagulopathy as plasmin generation and subsequent fibrinolysis become systemic. This is the rationale behind the pharmacologic use of tranexamic acid in fibrinolysis disruption (Levy et al., 2018). VEGF-A is dramatically reduced in HMB participants who experience excessive menstrual bleeding (Akhtar et al., 2022). By activating tissue factors, VEGF-A contributes to neovascularization and may induce coagulation pathways. VEGF-A is produced by immune cell types in the endometrium, including macrophages. Therefore, decreased levels could cause extended heavy bleeding patterns and impair endometrial healing in affected women (Berbic et al., 2014). The fibrinolytic system is demonstrated to be over-activated in HMB-affected women during the menstrual stage of their cycle (Maybin and Critchley, 2016). Increased fibrinolysis causes more blood to be lost during endometrial shedding (Maybin and Critchley, 2016). Anti-fibrinolytic drugs reduce subsequent fibrin breakdown by preventing the interaction between plasmin and lysine residues, which slows down the dissolution of clots. Anti-fibrinolytic agents reversibly inhibit lysine binding sites on plasminogen and displace plasminogen from fibrin, and plasmin is prevented from interacting with lysine residues on the fibrin polymer. To alleviate severe menstrual bleeding, anti-fibrinolytic drugs have been suggested (Ac et al., 2018). As per the reports, the anti-fibrinolytic drug tranexamic acid reduces menstrual blood loss by approximately 50% (Maybin and Critchley, 2016). Hemostatic agents can act through platelet aggregation, vasoconstriction, clotting factor activation, or anti-fibrinolytic activity. Bioactive plant metabolites frequently involved in bleeding control are saponins, tannins, glycosides, and other phenolic compounds (Ebrahimi et al., 2020). Plant metabolites and tannins, since antiquity, have been used for their ethnomedicinal properties in traditional medicine. Tannins have been shown in studies to have the potential to

prevent thromboembolic events and fibrinolysis systems. Furthermore, tannins have been shown in studies to have profibrinolytic and Edi antifibrinolytic effects. Tannins can influence platelet and endothelial activity (Marcinićzyk et al., 2022). Acacia gum is rich in tannin, with the bioactive molecules ellagic acid, gallic acid, and tannic acid. According to a study, the polymeric metabolites of *A. arabica* found in the aqueous extracts reduce the PT and aPTT in mice; these plant metabolites exhibit hemostatic effects and hasten blood coagulation properties (Bhatnagar et al., 2013). A study has shown that *A. arabica* gum, along with *Moringa oleifera* pods, showed thrombogenic activity as the weight of the clots was significantly higher than that of tranexamic acid (Bhatnagar et al., 2013). *A. arabica* might probably have thrombotic action and comparatively fewer side effects than hormonal treatment. Therefore, acacia gum and camphor have multidimensional potent prostaglandin inhibitors, antioxidant, immunomodulatory, astringent, styptic, and anti-inflammatory properties (Liu et al., 2020). Hence, the therapeutic effect of the vaginal suppository of acacia gum and camphor on HMB is explained in comparison with tranexamic acid.

4.2 Adverse effects on the SG and TG

Medication safety was assessed by clinical history, physical examinations, measuring vital signs, and monitoring for adverse events. In the SG, three participants complained of a mild burning sensation that persisted for a few seconds to 10 min with no other complaints. In the TG, back pain and headache were complaints by three participants, whereas two participants complained about flatulence. Similarly, adverse effects with tranexamic acid were reported in a previous study (Lukes et al., 2010).

4.3 Strengths of the study

This study holds the distinction of being the first of its kind to validate the efficacy and safety of a vaginal Unani dosage form in HMB. The trial's design was robust, employing a double-blind, randomized, double-dummy clinical approach, demonstrating good compliance with a low attrition rate of only 10%.

4.4 Limitations of the study

A limitation of the study was the omission of the alkaline hematin method, which is considered the standard for calculating menstrual blood loss. However, this method is deemed impractical, time-consuming, and costly. This study focused exclusively on the reproductive age group experiencing heavy menstrual bleeding. Consequently, its applicability cannot be extended to individuals facing peri-menopausal or pubertal heavy menstrual bleeding. Additionally, the majority of participants belonged to the lower-middle-class socioeconomic bracket, limiting the generalization of findings to the upper socioeconomic status. Furthermore, it is important to note that the study's scope does not include populations with specific conditions. These conditions include uterine fibroids exceeding 3 cm and/or numbering more than 3, as well as individuals with polyps, pelvic inflammatory disease, bleeding disorders, severe anemia (Hb < 7 gm%), chronic renal disease, uncontrolled thyroid dysfunction, liver disease, uncontrolled hypertension, and diabetes mellitus. Therefore, in this context, further studies are recommended. Another limitation of the study was the inability to conduct a quantitative analysis of specific bioactive secondary plant metabolites, stability testing of the vaginal suppository, and an assessment of the pharmacokinetics of the drug molecule due to constraints in resources and time. Furthermore, hepatic safety parameters (AST, ALT, and ALP) and renal safety parameters (blood urea and serum creatinine) have to be carried out after intervention to verify the safety of research botanical drugs on hepatic and renal functions.

4.5 Future recommendation

The use of vaginal suppositories may be recommended for women comfortable with complementary and alternative approaches seeking to avoid potential side effects associated with conventional pharmaceuticals. The authors also suggest conducting a quantitative analysis of the specific bioactive secondary metabolites of the plant using diverse mobile phases and evaluating the stability of the finished product. Moreover, assessing the presence of active constituents in the bloodstream could provide insights into comprehensive pharmacokinetic and pharmacodynamic characteristics. To enhance the research drug's efficacy and potency, further Phase-III clinical trials with an extended duration and lengthier follow-up are suggested. Additionally, a comparative analysis between the vaginal suppository and nonsteroidal anti-inflammatory drugs or other conventional treatments would provide valuable insights.

5 Conclusion

We concluded that participants receiving the novel suppository exhibited significant reductions in PBLAC scores and marked improvements in HRQoL SF-36 scores, with a substantial percentage achieving normal menstrual blood loss. Importantly, no adverse events were reported in either group. *A. arabica* gum (*Gond Babul*) and *C. camphora* (*Kafoor*) suppositories emerge as novel and well-supported options for HMB treatment. Furthermore, this study explored the application of AI for the classification of experimental data through machine learning models.

Data availability statement

The raw data supporting the conclusion of this article will be made available by the authors, without undue reservation.

Ethics statement

A scientific review and ethics committee approval with identifier: NIUM/IEC/2019-20/015/ANQ/07 were obtained from the National Institute of Unani Medicine, Bengaluru, and the study was registered at the CTRI (identifier: CTRI/2021/01/030184) before initiating the clinical study. The studies were conducted in accordance with local legislation and institutional requirements. The participants provided their written informed consent to participate in this study. Written informed consent was obtained from the individual(s) for the publication of any potentially identifiable images or data included in this article.

Author contributions

MJAF: data curation, formal analysis, and writing—original draft. AS: data curation, formal analysis, and writing—original draft. MBBH: conceptualization, formal analysis, investigation, project administration, software, and writing—review and editing. SP: conceptualization, formal analysis, investigation, project administration, software, and writing—review and editing. KR: formal analysis, validation, visualization, and writing—original draft. FA: conceptualization, investigation, resources, and writing—original draft. AK: conceptualization, investigation, resources, and writing—original draft. AA: conceptualization, investigation, resources, and writing—original draft. ZA: methodology, validation, visualization, and writing—original draft. ID: methodology, validation, visualization, and writing—original draft. JB: methodology, validation, visualization, and writing—original draft. TS: methodology, validation, visualization, and writing—original draft.

Funding

The authors declare that financial support was received for the research, authorship, and/or publication of this article. This publication work was funded by the Researchers Supporting Project (RSP 2024R339) at King Saud University, Riyadh, Saudi Arabia.

Acknowledgments

The authors would like to thank Prof. Sawan, Singh, Chandel, and Dr. Gul for the help, support, and motivation for the study. We also acknowledge the Ministry of Ayush for providing the facilities for the research work in National Institute of Unani Medicine.

Conflict of interest

The authors declare that the research was conducted in the absence of any commercial or financial relationships that could be construed as a potential conflict of interest.

References

- Abdulhamid, A., Sani, I., Kankiya, I. H., and Fakai, I. M. (2019). Phytochemical screening, analgesic effect and anti-inflammatory activity of crude methanolic stem bark extract of *Acacia nilotica* (linn.). *Asian J. Biol. Sci.* 12, 450–456. doi:10.3923/ajbs.2019.450.456
- Ac, B., Lethaby, A., Farquhar, C., and Hickey, M. (2018). Antifibrinolytics for heavy menstrual bleeding. *Cochrane Database Syst. Rev.* 4, CD000249. doi:10.1002/14651858.CD000249.pub2
- Agneszka, G., and Skrzydlewska, E. (2022). Antioxidative and anti-inflammatory activity of ascorbic acid. *Antioxidants* 11, 1993. doi:10.3390/antiox11101993
- Ahmad, S., Zahiruddin, S., Parveen, B., Basist, P., Parveen, A., Gaurav, , et al. (2021). Indian medicinal plants and formulations and their potential against COVID-19—preclinical and clinical research. *Front. Pharmacol.* 11, 578970. doi:10.3389/fphar.2020.578970
- Akhtar, F., Patel, P. K., Heyat, M. B. B., Yousaf, S., Baig, A. A., Mohona, R. A., et al. (2022). Smartphone addiction among students and its harmful effects on mental health, oxidative stress, and neurodegeneration towards future modulation of anti-addiction therapies: a comprehensive survey based on SLR, research questions, and network visualization. *CNS Neurol. Disord. - Drug Targets* 21. doi:10.2174/1871527321666220614121439
- Ali, A. (2012). *Acacia nilotica*: a plant of multipurpose medicinal uses. *J. Med. Plants Res.* 6, 1492–1496. doi:10.5897/jmpr11.1275
- Ali, N. E., Kaddam, L. A., Alkarib, S. Y., Kaballo, B. G., Khalid, S. A., Higawee, A., et al. (2020). Gum Arabic (*Acacia Senegal*) augmented total antioxidant capacity and reduced C-reactive protein among haemodialysis patients in phase II trial. *Int. J. Nephrol.* 2020, 7214673. doi:10.1155/2020/7214673
- Alli, L. A., Adesokan, A. A., Salawu, O. A., and Akanji, M. A. (2015). Toxicological studies of aqueous extract of *Acacia nilotica* root. *Interdiscip. Toxicol.* 8, 48–54. doi:10.1515/intox-2015-0005
- Al-Jurjani, S. I. (2010). Dhakhira Khwarizm Shāhi (Urdu trans: khan AH). VI. New Delhi: Idarae Kitabus Shifa.
- AlShorman, O., Masadeh, M., Heyat, M. B. B., Akhtar, F., Almahasneh, H., Ashraf, G. M., et al. (2022). Frontal lobe real-time EEG analysis using machine learning techniques for mental stress detection. *J. Integr. Neurosci.* 21, 020. doi:10.31083/jjin2101020
- Am Elnour, A., Es Mirghani, M., Na, K., Alam, Z. M., and H Musa, K. (2018). Study of antioxidant and anti-inflammatory crude methanol extract and fractions of *Acacia seyal* gum. *Am. J. Pharmacol. Pharmacother.* 05. doi:10.21767/2393-8862.100013
- Amos, S., Akah, P. A., Oduke, C. J., Gamaniel, K. S., and Wambede, C. (1999). The pharmacological effects of an aqueous extract from *Acacia nilotica* seeds. *Phytother. Res.* 685, 683–685. doi:10.1002/(sici)1099-1573(199912)13:8<683::aid-pt534>3.0.co;2-x
- Azizkhani, M., Vahid Dastjerdi, M., Tabaraee Arani, M., Pirjani, R., Sepidarkish, M., Ghorat, F., et al. (2018). Traditional dry cupping therapy versus medroxyprogesterone acetate in the treatment of idiopathic menorrhagia: a randomized controlled trial. *Iran. Red. Crescent Med. J.* 20. doi:10.5812/ircmj.60508
- Belal Bin Heyat, M., Akhtar, F., Sultana, A., Tumrani, S., Teelhawod, B. N., Abbasi, R., et al. (2022). Role of oxidative stress and inflammation in insomnia sleep disorder and cardiovascular diseases: herbal antioxidants and anti-inflammatory coupled with insomnia detection using machine learning. *Curr. Pharm. Des.* 28, 3618–3636. doi:10.2174/138161282966622101161636
- Benifa, J. V. B., Chola, C., Muead, A. Y., Hayat, M. A. B., Bin Heyat, M. B., Mehrotra, R., et al. (2023). FMDNet: an efficient system for face mask detection based on lightweight model during COVID-19 pandemic in public areas. *Sensors* 23, 6090. doi:10.3390/s23136090
- Berbic, M., Ng, C. H. M., and Fraser, I. S. (2014). Inflammation and endometrial bleeding. *Climacteric* 17, 47–53. doi:10.3109/13697137.2014.963964
- Bhatnagar, M., Parwani, L., Sharma, V., Ganguli, J., and Bhatnagar, A. (2013). Hemostatic, antibacterial biopolymers from *Acacia arabica* (Lam.) Willd. and *Moringa oleifera* (Lam.) as potential wound dressing materials. *Indian J. Exp. Biol.* 51, 804–810.
- Bin Heyat, M. B., Akhtar, F., Abbas, S. J., Al-Sarem, M., Alqarafi, A., Stalin, A., et al. (2022). Wearable flexible electronics based cardiac electrode for researcher mental stress detection system using machine learning models on single lead electrocardiogram signal. *Biosensors* 12, 427. doi:10.3390/bios12060427
- Chaplin, S. (2018). Assessment and management of heavy menstrual bleeding. *Prescriber* 29, 21–22. doi:10.1002/psb.1687
- Chen, Y., Zhou, Z., and Min, W. (2018). Mitochondria, oxidative stress and innate immunity. *Front. Physiol.* 9, 1487. doi:10.3389/fphys.2018.01487
- Daffalah, A., and al-Mustafa, A. (1996). Investigation of the Anti-inflammatory activity of *Acacia nilotica* and *Hibiscus sabdariffa*. *Am. J. Chin. Med.* 24.
- Ebrahimi, F., Torbati, M., Mahmoudi, J., and Valizadeh, H. (2020). Medicinal plants as potential hemostatic agents. *J. Pharm. Pharm. Sci.* 23, 10–23. doi:10.18433/jpps30446
- Elgailani, I. E. H., and Ishak, C. Y. (2014). Determination of tannins of three common *Acacia* species of Sudan. *Adv. Chem.* 2014, 1–5. doi:10.1155/2014/192708
- Fan, L. Y., Lin, Q., Yang, N. Y., and Chen, L. H. (2020). Analgesic effects of the essential oil from cinnamomum camphora against nitroglycerin-induced migraine in mice. *Indian J. Pharm. Sci.* 82, 166–170. doi:10.36468/pharmaceutical-sciences.634
- Farzana, M., and Sultana, A. (2020). A review of ethnomedicine, phytochemical and pharmacological activities of *Acacia nilotica* (Linn). *J. Pharmacogn. Phytochem.* 12, 84–90.
- Fathima, A., and Sultana, A. (2012). Clinical efficacy of a Unani formulation “Safoof Habis” in menorrhagia: a randomized controlled trial. *Eur. J. Integr. Med.* 4, e315–e322. doi:10.1016/j.eujim.2012.01.007
- Fazmiya, M., Sultana, A., Rahman, K., Heyat, B. B., Akhtar, F., Khan, S., et al. (2022). Current insights on bioactive molecules, antioxidant, anti-inflammatory, and other pharmacological activities of cinnamomum camphora linn. *Oxid. Med. Cell Longev.* 2022, 9354555. doi:10.1155/2022/9354555
- Fu, J., Zeng, C., Zeng, Z., Wang, B., and Gong, D. (2016). Cinnamomum camphora seed kernel oil ameliorates oxidative stress and inflammation in diet-induced obese rats. *J. Food Sci.* 81, H1295–H1300. doi:10.1111/1750-3841.13271
- Garg, N., and Jain, A. (2015). Therapeutic and medicinal uses of katpura- A review. *Int. J. Sci. Res.* 6 (4), 2319–7064.
- Goshtasebi, A., Mazari, Z., Behboudi Gandevani, S., and Naseri, M. (2015). Anti-hemorrhagic activity of *Punica granatum* L. flower (Persian Golnar) against heavy menstrual bleeding of endometrial origin: a double-blind, randomized controlled trial. *Med. J. Islam. Repub. Iran.* 29, 199.
- Gutman, I. (n.d.). In *Methods of enzymatic analysis*. Editor H. U. Bergmeyer. 4th ed (New York: Academic Press).
- Hassanien, M. A. (2019). The protective and antioxidant effects of gum Arabic: a review of recent evidence using the new PubMed system. *Int. J. Community Med. Public Health* 7, 356. doi:10.18203/2394-6040.ijcmph2019592
- Heyat, M. B. B., Lai, D., Khan, F. I., and Zhang, Y. (2019). Sleep bruxism detection using decision tree method by the combination of C4-P4 and C4-A1 channels of scalp EEG. *IEEE Access* 7, 102542–102553. doi:10.1109/ACCESS.2019.2928020

Publisher's note

All claims expressed in this article are solely those of the authors and do not necessarily represent those of their affiliated organizations, or those of the publisher, the editors, and the reviewers. Any product that may be evaluated in this article, or claim that may be made by its manufacturer, is not guaranteed or endorsed by the publisher.

Supplementary material

The Supplementary Material for this article can be found online at: <https://www.frontiersin.org/articles/10.3389/fphar.2024.1331622/full#supplementary-material>

- Higham, J. M., O'Brien Pm, S. R., and Shaw, R. W. (1990). Assessment of menstrual blood loss using a pictorial chart. *Br. J. Obs. Gynaecol.* 97, 734–739. doi:10.1111/j.1471-0528.1990.tb16249.x
- Hussain, T., Murtaza, G., Metwally, E., Kalhor, D. H., Kalhor, M. S., Rahu, B. A., et al. (2021). The role of oxidative stress and antioxidant balance in pregnancy. *Mediat. Inflamm.* 2021, 9962860. doi:10.1155/2021/9962860
- Hussain, T., Tan, B., Yin, Y., Blachier, F., Tossou, M. C. B., and Rahu, N. (2016). Oxidative stress and inflammation: what polyphenols can do for us? *Oxid. Med. Cell. Longev.* 2016, 7432797. doi:10.1155/2016/7432797
- Imdad, S., Firdose, K., and Begum, W. (2017). Effect of Qurse Gulnar in Heavy menstrual bleeding – a randomized single blind standard control study. *IOSR J. Dent. Med. Sci.* 16, 25–31. doi:10.9790/0853-1608122531
- Iqbal, M. S., Abbasi, R., Bin Heyat, M. B., Akhtar, F., Abdelgelil, A. S., Albogami, S., et al. (2022). Recognition of mRNA N4 acetylcytidine (ac4C) by using non-deep vs. Deep learning. *Appl. Sci.* 12, 1344. doi:10.3390/app12031344
- Jahan, D., Begum, W., Roqaiya, M., and Hussaini, Y. K. (2016). Anti-haemorrhagic activity of polyherbal formulation in menorrhagia: a randomized controlled trial. *Altern. Integr. Med.* 5, 3–6. doi:10.4172/2327-5162.1000219
- Johari, H., Abedini, M., and Fallahi, S. (2015). The effect of Camphor (Cinnamomum camphora) on concentration of liver enzymes in female rats. *Int. J. Latest Res. Sci. Technol.* 4, 111–113.
- Kabir al-Din, M. (2007). *Makhzan al-Mufradat*. New Delhi: Idarae Kitabus Shifa.
- Kang, N. J., Han, S. C., Yoon, S. H., Sim, J. Y., Maeng, Y. H., Kang, H. K., et al. (2019). Cinnamomum camphora leaves alleviate allergic skin inflammatory responses *in vitro* and *in vivo*. *Toxicol. Res.* 35, 279–285. doi:10.5487/TR.2019.35.3.279
- Karashima, Y., Damann, N., Prenen, J., Talavera, K., Segal, A., Voets, T., et al. (2007). Bimodal action of menthol on the transient receptor potential channel TRPA1. *J. Neurosci.* 27, 9874–9884. doi:10.1523/JNEUROSCI.2221-07.2007
- Kashefi, F., Khajehei, M., Alavinia, M., Golmakani, E., and Asili, J. (2015). Effect of ginger (Zingiber officinale) on heavy menstrual bleeding: a placebo-controlled, randomized clinical trial. *Phyther. Res.* 29, 114–119. doi:10.1002/ptr.5235
- Kaur, P., Arora, S., and Singh, R. (2022). Isolation, characterization and biological activities of betulin from *Acacia nilotica* bark. *Sci. Rep.* 12, 9370. doi:10.1038/s41598-022-13338-3
- Khan, H., and Muhammad, A. (2018). *Muhit-i-A'zam. Vol II, IV (Urdu trans)*. New Delhi: CCRUM Ministry of Health and Family Welfare, Govt. of India.
- Khan, M. (2006). *Bayaz-e-Khas al Marufilaj-al-Amraaz*. New Delhi: Aijaz publication.
- Lai, D., Zhang, Y., Zhang, X., Su, Y., and Bin Heyat, M. B. (2019). An automated strategy for early risk identification of sudden cardiac death by using machine learning approach on measurable arrhythmic risk markers. *IEEE Access* 7, 94701–94716. doi:10.1109/ACCESS.2019.2925847
- Lee, H. J., Hyun, E. A., Yoon, W. J., Kim, B. H., Rhee, M. H., Kang, H. K., et al. (2006). *In vitro* anti-inflammatory and anti-oxidative effects of Cinnamomum camphora extracts. *J. Ethnopharmacol.* 103, 208–216. doi:10.1016/j.jep.2005.08.009
- Lee, S. H., Kim, D. S., Park, S. H., and Park, H. (2022). Phytochemistry and applications of cinnamomum camphora essential oils. *Molecules* 27, 2695. doi:10.3390/molecules27092695
- Levy, J. H., Koster, A., Quinones, Q. J., Milling, T. J., and Key, N. S. (2018). Antifibrinolytic therapy and perioperative considerations. *Anesthesiology* 128, 657–670. doi:10.1097/ALN.0000000000001997
- Li, Y. R., Fu, C. S., Yang, W. J., Wang, X. L., Feng, D., Wang, X. N., et al. (2018). Investigation of constituents from Cinnamomum camphora (L.) J. Presl and evaluation of their anti-inflammatory properties in lipopolysaccharide-stimulated RAW 264.7 macrophages. *J. Ethnopharmacol.* 221, 37–47. doi:10.1016/j.jep.2018.04.017
- Liu, X., Cruz Rivera, S., Moher, D., Calvert, M. J., Denniston, A. K., Chan, A. W., et al. (2020). Reporting guidelines for clinical trial reports for interventions involving artificial intelligence: the CONSORT-AI extension. *Nat. Med.* 26, 1364–1374. doi:10.1038/s41591-020-1034-x
- Liu, Z., Kong, L., Lu, S., and Zou, Z. (2019). Application of a combined homogenate and ultrasonic cavitation system for the efficient extraction of flavonoids from cinnamomum camphora leaves and evaluation of their antioxidant activity *in vitro*. *J. Anal. Methods Chem.* 2019, 4892635. doi:10.1155/2019/4892635
- Livdand-Forret, A. B., Harvey, P. J., and Larkin-Thier, S. M. (2007). Menorrhagia: a synopsis of management focusing on herbal and nutritional supplements, and chiropractic. *J. Can. Chiropr. Assoc.* 51, 235–246.
- Lukes, A. S., Moore, K. A., Muse, K. N., Gersten, J. K., Hecht, B. R., Edlund, M., et al. (2010). Tranexamic acid treatment for heavy menstrual bleeding: a randomized controlled trial. *Obstet. Gynecol.* 116, 865–875. doi:10.1097/AOG.0b013e3181f20177
- Maerkel, K., Durrer, S., Henseler, M., Schlumpf, M., and Lichtensteiger, W. (2007). Sexually dimorphic gene regulation in brain as a target for endocrine disruptors: developmental exposure of rats to 4-methylbenzylidene camphor. *Toxicol. Appl. Pharmacol.* 218, 152–165. doi:10.1016/j.taap.2006.10.026
- Magnay, J. L., O'Brien, S., Gerlinger, C., and Seitz, C. (2020). Pictorial methods to assess heavy menstrual bleeding in research and clinical practice: a systematic literature review. *BMC Womens. Health* 20, 24–16. doi:10.1186/s12905-020-0887-y
- Majusi, A. (2010). Kamil al-Sana'a al-tibbiyya (Urdu trans: kantoori GH). I. New Delhi: Idarae Kitabus Shifa.
- Marcińczyk, N., Gromotowicz-Popławska, A., Tomczyk, M., and Chabielska, E. (2022). Tannins as hemostasis modulators. *Front. Pharmacol.* 12, 806891. doi:10.3389/fphar.2021.806891
- Massiha, A., and Muradov, P. Z. (2015). Comparison of antifungal activity of extracts of ten plant species and griseofulvin against human pathogenic dermatophytes. *Zahedan J. Res. Med. Sci.* 17. doi:10.17795/zjrms-2096
- Maybin, J. A., and Critchley, H. O. (2016). Medical management of heavy menstrual bleeding. *Women's Heal* 12, 27–34. doi:10.2217/whe.15.100
- M Peake, W. M., and Whiting, M. (2006). Measurement of serum creatinine-current status and future goals. *Clin. Biochem.* 27, 173–184.
- Muhamad, S. H. A., On, S., Sanusi, S. N. A., Hashim, A. A., and Addinna Zai, M. H. (2019). Antioxidant activity of Camphor leaves extract based on variation solvent. *J. Phys. Conf. Ser.* 1349, 012102. doi:10.1088/1742-6596/1349/1/012102
- Mukhtar, F., Mukhtar, H., Syeda, P., and Naaz, A. (2019). *Treatment of menorrhagia with Unani formulation Qurs -e- Habis: a case report*, 19–21. 8.
- Mumford, S. L., Browne, R. W., Schliep, K. C., Schmelzer, J., Plowden, T. C., Michels, K. A., et al. (2016). Serum antioxidants are associated with serum reproductive hormones and ovulation among healthy women. *J. Nutr.* 146, 98–106. doi:10.3945/jn.115.217620
- Nadkarni, K. M. (2004). *Indian plants and drugs: with their medicinal properties and uses*. New Delhi: Srishti Book Distributors.
- Pal, R., Adhikari, D., Heyat, M. B. B., Guragai, B., Lipari, V., Brito Ballester, J., et al. (2022). A novel smart belt for anxiety detection, classification, and reduction using IloMT on students' cardiac signal and MSY. *Bioengineering* 9, 793. doi:10.3390/bioengineering9120793
- Pal, R., Adhikari, D., Heyat, M. B. B., Ullah, I., and You, Z. (2023). Yoga meets intelligent internet of things: recent challenges and future directions. *Bioengineering* 10, 459. doi:10.3390/bioengineering10040459
- Qaraaty, M., Kamali, S. H., Dabaghian, F. H., Zafarghandi, N., Mokaberejad, R., Mobli, M., et al. (2014). Effect of myrtle fruit syrup on abnormal uterine bleeding: a randomized double-blind, placebo-controlled pilot study. *Daru* 22, 45–47. doi:10.1186/2008-2231-22-45
- Qayyum, S., Sultana, A., Bin Heyat, M. B., Rahman, K., Akhtar, F., Haq, A., et al. (2023). Therapeutic efficacy of a formulation prepared with Linum usitatissimum L., plantago ovata forssk., and honey on uncomplicated pelvic inflammatory disease analyzed with machine learning techniques. *Pharmaceutics* 15, 643. doi:10.3390/pharmaceutics15020643
- Saeedi, R., Sultana, A., and Rahman, K. (2020). Medicinal properties of different parts of *Acacia nilotica* linn (Babul), its phytoconstituents and diverse pharmacological activities. *Int. J. Pharm. Pharm. Sci.* 12, 8–14. doi:10.22159/ijpps.2020v12i2.35672
- Safari, V., Kamau, J. K., Nthiga, P. M., Ngugi, M. P., Orinda, G., and Njagi, E. M. (2016). Antipyretic, antiinflammatory and antinociceptive activities of aqueous bark extract of *Acacia nilotica* (L.) delile in albino mice. *J. Pain Manag. Med.* 02. doi:10.35248/2684-1320.16.2.113
- Saleem, S. M., and Jan, S. S. (2021). Modified Kuppusswamy socioeconomic scale updated for the year 2021. *Indian J. Forensic Community Med.* 8, 1–3. doi:10.18231/j.ijfcm.2021.001
- Schumann, G., Canalias, F., Joergensen, P., Kang, D., Lessinger, J., Klauke, , et al. (2010). IFCC reference procedures for measurement of the catalytic concentrations of enzymes: corrigendum, notes and useful advice. International Federation of Clinical Chemistry and Laboratory Medicine (IFCC)–IFCC Scientific Division. *Clin. Chem. Lab. Med.* 48, 615–621. doi:10.1515/CCLM.2010.137
- Sethi, P. (1996). *High performance thin layer chromatography*. 1st ed. New Delhi: CBS Publishers and Distributors.
- Sina, I. (2010). *Al-Qānūn fī'l Tibb*. New Delhi: Idarae Kitabus Shifa.
- Sultana, A., Begum, W., Saeedi, R., Rahman, K., Bin Heyat, M. B., Akhtar, F., et al. (2022a). Experimental and computational approaches for the classification and correlation of temperament (mizaj) and uterine dystemperament (su'-I-mizaj Al-rahim) in abnormal vaginal discharge (sayalan Al-rahim) based on clinical analysis using support vector machine. *Complexity* 2022, 1–16. doi:10.1155/2022/5718501
- Sultana, A., Rahman, K., Bin Heyat, M. B., Sumbul, Akhtar, F., and Muaad, A. Y. (2022b). Role of inflammation, oxidative stress, and mitochondrial changes in premenstrual psychosomatic behavioral symptoms with anti-inflammatory, antioxidant herbs, and nutritional supplements. *Oxid. Med. Cell. Longev.* 2022, 3599246. doi:10.1155/2022/3599246
- Sultana, A., and Rahman, K. U. (2012). Effect of traditional dry cupping therapy on heavy menstrual bleeding in menorrhagia: a preliminary study. *Tang Humanit. Med.* 2, 33.1–33.3. doi:10.5667/tang.2012.0030
- Taghvaei, M., and Jafari, S. M. (2015). Application and stability of natural antioxidants in edible oils in order to substitute synthetic additives. *Int. J. Community Med. Public Heal.* 7, 356. doi:10.1007/s13197-013-1080-1

- Tansaz, M., Memarzadehzavareh, H., Qaraaty, M., Eftekhari, T., Tabarraei, M., and Kamalinejad, M. (2016). Menorrhagia management in Iranian traditional medicine. *J. Evidence-Based Complement. Altern. Med.* 21, 71–76. doi:10.1177/2156587215589522
- Tietz, N., Rinker, A., Shaw, L., Bossert-Reuther, S., Franck, P. F. H., Gella, F. J., et al. (2011). IFCC primary reference procedures for the measurement of catalytic activity concentrations of enzymes at 37 °C. Part 9: reference procedure for the measurement of catalytic concentration of alkaline phosphatase International Federation of Clinical Chemistry and Laboratory Medicine (IFCC) Scientific Division, Committee on Reference Systems of Enzymes (C-RSE) (1). *Clin. Chem. Lab. Med.* 49, 1439–1446. doi:10.1515/CCLM.2011.621
- Trinder, P. (1969). Determination of glucose in blood using glucose oxidase with an alternative oxygen acceptor. *Ann. Clin. Biochem.* 6, 24–27. doi:10.1177/000456326900600108
- Tripathi, P., Ansari, M. A., Gandhi, T. K., Mehrotra, R., Heyat, M. B. B., Akhtar, F., et al. (2022). Ensemble computational intelligent for insomnia sleep stage detection via the sleep ECG signal. *IEEE Access* 10, 108710–108721. doi:10.1109/ACCESS.2022.3212120
- Ullah, H., Bin Heyat, M. B., Akhtar, F., Sumbul, Muaad, A. Y., Islam, M. S., et al. (2022). An end-to-end cardiac arrhythmia recognition method with an effective DenseNet model on imbalanced datasets using ECG signal. *Comput. Intell. Neurosci.* 2022, 9475162. doi:10.1155/2022/9475162
- Wu, M., Ni, L., Lu, H., Xu, H., Zou, S., and Zou, X. (2020). Terpenoids and their biological activities from cinnamomum: a review. *J. Chem.* 2020, 1–14. doi:10.1155/2020/5097542
- Yang, H., Xu, P., Song, W., and Zhai, X. (2021). Anti-tyrosinase and antioxidant activity of proanthocyanidins from *Cinnamomum camphora*. *Int. J. Food Prop.* 24, 1265–1278. doi:10.1080/10942912.2021.1958841
- Yousefi, F., Kashanian, M., Nazem, I., Bioos, S., Sadeghpour, O., Aliasl, J., et al. (2020). Comparison between Golnar product and placebo in heavy menstrual bleeding: a double-blind randomized clinical trial. *Avicenna J. phytomedicine* 10, 523–532. doi:10.22038/ajp.2020.15528
- Zafar, M. M. I., Hassan, F., Naqvi, S. B. S., Muhammad, S., Hasan, F., Jabeen, S., et al. (2012). Evaluation of antibacterial activity of camphor, benzoin, cubebs, fenugreek, apricot and cinnamon leaf against standard cultures and clinical isolates of an array of organisms. *Pak. J. Pharmacol.* 36, 69–75.

Glossary

4-MBC	4-Methyl benzylidene camphor
ABTS assays	2,2'-Azinobis-(3-ethylbenzothiazoline-6-sulfonic acid
aPTT	Activated partial thromboplastin time
COX	Cyclooxygenase
CRP	C-reactive protein
DPPH	2,2-Diphenyl-1-picrylhydrazyl
ER-alpha	Estrogen receptor-alpha
FRAP	Fluorescence recovery after photobleaching
ICAM-1	Intercellular adhesion molecule-1
IGF-I	Insulin-like growth factor-I
IL	Interleukin
iNOS	Inducible nitric oxide synthase
LPS	Lipopolysaccharides
IFN	Gamma interferon
MeOH	Methanol
MMP-9	Matrix metalloproteinase
NF-kB	Nuclear factor kappa-light-chain-enhancer of activated B cells
NO	Nitric oxide
OXPHOS	Oxidative phosphorylation
PGE2	Prostaglandin E2
PGI2	Prostaglandin I2
PPE	Preproenkephalin
PR	Progesterone receptor
PT	Prothrombin time
ROS/RNS	Reactive oxygen species/reactive nitrogen species
TAC	Total antioxidant capacity
TNFα	Tumor necrotizing factor alpha
VEGF-A	Vascular endothelial growth factor-A
CV	Cross validation
AI	Artificial intelligence
KNN	K-nearest neighbor
AB	AdaBoost
NB	Naive Bayes
RF	Random forest
HMB	Heavy menstrual bleeding
SG	Suppository group
TG	Tranexamic group
HRQoL	Health-related quality of life



OPEN ACCESS

EDITED BY

Stalin Antony,
University of Electronic Science and
Technology of China, China

REVIEWED BY

Shihan Wang,
Guang'anmen Hospital, China
Peizheng Yan,
Shandong University of Traditional Chinese
Medicine, China

*CORRESPONDENCE

Xiangdong Zhu,
✉ zhuxiangdong33@163.com
Yonglin Liang,
✉ 875532437@qq.com

[†]These authors have contributed equally to
this work

RECEIVED 13 December 2023

ACCEPTED 26 February 2024

PUBLISHED 04 March 2024

CITATION

Gao Y, Zhang L, Zhang F, Liu R, Liu L, Li X, Zhu X
and Liang Y (2024), Traditional Chinese
medicine and its active substances reduce
vascular injury in diabetes via regulating
autophagic activity.
Front. Pharmacol. 15:1355246.
doi: 10.3389/fphar.2024.1355246

COPYRIGHT

© 2024 Gao, Zhang, Zhang, Liu, Liu, Li, Zhu and
Liang. This is an open-access article distributed
under the terms of the [Creative Commons
Attribution License \(CC BY\)](#). The use,
distribution or reproduction in other forums is
permitted, provided the original author(s) and
the copyright owner(s) are credited and that the
original publication in this journal is cited, in
accordance with accepted academic practice.
No use, distribution or reproduction is
permitted which does not comply with these
terms.

Traditional Chinese medicine and its active substances reduce vascular injury in diabetes via regulating autophagic activity

Yankui Gao^{1†}, Lei Zhang^{1†}, Fei Zhang², Rong Liu³, Lei Liu¹,
Xiaoyan Li¹, Xiangdong Zhu^{4*} and Yonglin Liang^{1*}

¹Department of Basic Medicine, Gansu University of Traditional Chinese Medicine, Lanzhou, China,

²Department of Traditional Chinese Medicine, Fujian University of Traditional Chinese Medicine, Lanzhou, China, ³Department of Traditional Chinese Medicine, Jiangxi University of Traditional Chinese Medicine, Nanchang, China, ⁴Department of Traditional Chinese Medicine, Ningxia Medical University, Yinchuan, China

Due to its high prevalence, poor prognosis, and heavy burden on healthcare costs, diabetic vascular complications have become a significant public health issue. Currently, the molecular and pathophysiological mechanisms underlying diabetes-induced vascular complications remain incompletely understood. Autophagy, a highly conserved process of lysosomal degradation, maintains intracellular homeostasis and energy balance via removing protein aggregates, damaged organelles, and exogenous pathogens. Increasing evidence suggests that dysregulated autophagy may contribute to vascular abnormalities in various types of blood vessels, including both microvessels and large vessels, under diabetic conditions. Traditional Chinese medicine (TCM) possesses the characteristics of “multiple components, multiple targets and multiple pathways,” and its safety has been demonstrated, particularly with minimal toxicity in liver and kidney. Thus, TCM has gained increasing attention from researchers. Moreover, recent studies have indicated that Chinese herbal medicine and its active compounds can improve vascular damage in diabetes by regulating autophagy. Based on this background, this review summarizes the classification, occurrence process, and related molecular mechanisms of autophagy, with a focus on discussing the role of autophagy in diabetic vascular damage and the protective effects of TCM and its active compounds through the regulation of autophagy in diabetes. Moreover, we systematically elucidate the autophagic mechanisms by which TCM formulations, individual herbal extracts, and active compounds regulate diabetic vascular damage, thereby providing new candidate drugs for clinical treatment of vascular complications in diabetes. Therefore, further exploration of TCM and its active compounds with autophagy-regulating effects holds significant research value for achieving targeted therapeutic approaches for diabetic vascular complications.

KEYWORDS

diabetic vascular complications, autophagy, TCM formulations, herbal extracts, active compounds

1 Introduction

Diabetes is a chronic disease characterized by metabolic disorders, primarily involving disturbances in the metabolism of glucose and lipid, and is accompanied by various chronic complications. With the development of global economy and changes in people's lifestyles, the incidence of diabetes has been increasing year by year. According to statistics, type 2 diabetes accounts for the majority of diabetes cases and is often accompanied by one or more chronic complications (Wang P. et al., 2022). Diabetic chronic complications refer to the chronic damage caused by long-term hyperglycemic conditions to tissues and organs in the body, mainly including cardiovascular diseases, diabetic nephropathy, neuropathy, retinopathy, and non-healing wounds. These complications are the main causes of disability and premature death in patients, all of which originate from diabetic vascular complications (Wang C.-Y. et al., 2023). Due to its high prevalence, poor prognosis, and heavy burden on healthcare costs, diabetic vascular complications have become a major public health issue. Currently, the molecular and pathophysiological mechanisms underlying diabetes-induced vascular complications are still not fully elucidated. Although some progress has been made in the clinical treatment of diabetic vascular complications (Chen, 2018), such as controlling blood glucose, lipids, blood pressure, and lifestyle changes, specific therapeutic methods are still lacking.

To date, an increasing number of studies have shown a certain relationship between autophagy and the progression of diabetic vascular complications (Wei et al., 2021). Therefore, in this review, we provide an overview of the latest research progress on autophagy in diabetic vascular complications. Notably, we also introduce various traditional Chinese medicines (TCMs) that improve symptoms and molecular mechanisms of diabetic vascular complications by regulating autophagic flux. Furthermore, TCMs with autophagy-regulating capabilities hold promising prospects as a treatment strategy for diabetic vascular complications.

2 Autophagy

2.1 Classification of autophagy

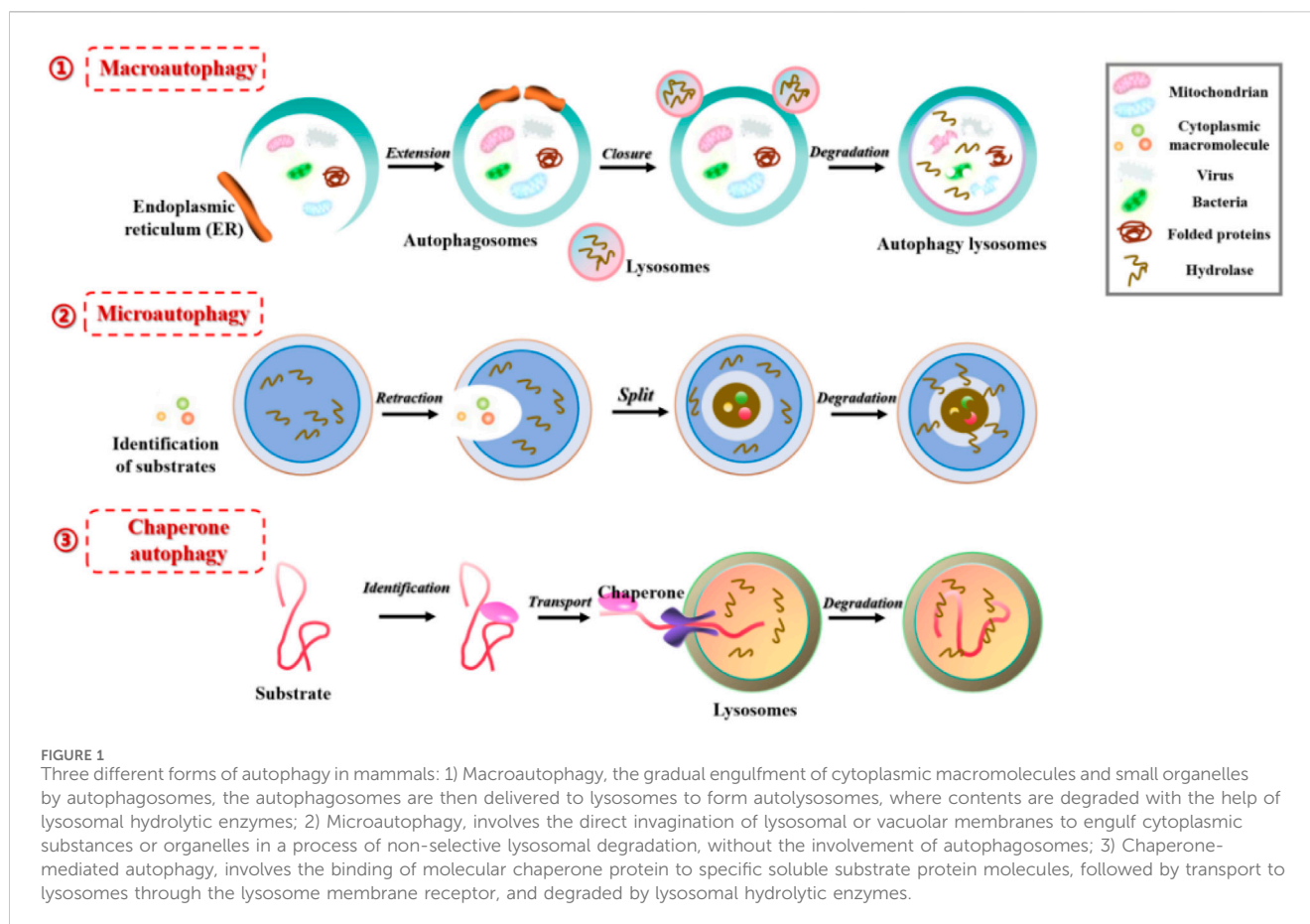
Autophagy is a highly conserved pathway of lysosomal degradation that primarily involves the degradation of autophagosomes recruited to sequester misfolded proteins, damaged organelles, exogenous pathogens, and other substances by lysosomal hydrolytic enzymes. This process facilitates the clearance and recycling (degradation of contents to generate nutrients for cellular growth), thereby ensuring the homeostasis of the intracellular environment. Based on the occurrence process, autophagy can be classified into macroautophagy, microautophagy, and chaperone-mediated autophagy (Figure 1). Macroautophagy refers to the gradual engulfment of cytoplasmic macromolecules and small organelles by autophagosomes, which are double-membraned vesicles that form by extension and closure. The autophagosomes are then delivered to lysosomes to form autolysosomes, where contents are degraded with the help of lysosomal hydrolytic enzymes. Generally, autophagy refers to the macroautophagy.

Microautophagy involves the direct invagination of lysosomal or vacuolar membranes to engulf cytoplasmic substances or organelles in a process of non-selective lysosomal degradation, without the involvement of autophagosomes. Chaperone-mediated autophagy (mainly in mammals) involves the binding of molecular chaperone protein Hsc70 to specific soluble substrate protein molecules with the KFERQ motif, followed by transport to lysosomes through the lysosome membrane receptor LAMP2A, and finally degradation by lysosomal hydrolytic enzymes (Parzych and Klionsky, 2014).

Notably, based on the selectivity of substrate degradation, autophagy can also be divided into selective autophagy and non-selective autophagy (Figure 2). Selective autophagy, as the name suggests, involves the involvement of selective autophagy receptors that directly bind to LC3 (Atg8 in yeast and plant cells), and then deliver specific degradation substrates to autophagosomes for degradation. Currently, types of selective autophagy include mitophagy, endoplasmic reticulum (ER)-phagy, ribophagy, pexophagy, and so on (Li W. et al., 2021; Vargas et al., 2023). Non-selective autophagy mainly refers to the relatively non-selective degradation of substrates. For example, autophagy induced by rapamycin, autophagy induced by nitrogen starvation, autophagy induced by serum starvation, and so on (Seglen et al., 1990).

2.2 The occurrence process of autophagy

The process of autophagy involves a series of consecutive stages, including initiation, nucleation, elongation, fusion, degradation, and recycling. These stages are highly regulated by autophagy-related genes (ATGs) and other auxiliary factors. In the initiation stage of autophagy, organelles such as mitochondria in the cytoplasm are first enclosed by vesicles called "isolation membranes". These isolation membranes mainly originate from the ER and the Golgi apparatus. The vesicles eventually form double-membrane structures called autophagosomes, also known as initial autophagic vacuoles. Autophagosomes fuse with endosomes to form intermediate autophagic vacuoles. Various stimuli, such as oxygen deprivation and nutrient deficiency, induce the formation of autophagosomes, and this step involves two protein complexes: one is the Vps34 complex containing Vps34 (class III PI3K), Beclin1 (Atg6 in yeast), Atg14, and Vps15 (p150). The other is the ULK1 complex containing serine/threonine kinase ULK1 (Atg1 in yeast), which is an important positive regulatory factor in autophagosome formation. Subsequently, the elongation of autophagosomes leads to the formation of unique double-membrane structures called autolysosomes. This step requires the participation of two ubiquitin-like conjugation systems, both of which are catalyzed by Atg7: one system leads to the conjugation of Atg5-Atg12, which forms the Atg5-Atg12-Atg16L complex that can interact with the outer membrane of the extending phagophore. The other system involves the processing of Atg8, a protein encoded by the mammalian homolog of yeast Atg8, which leads to the generation of processed LC3. When autophagy is induced, LC3B is cleaved by the Atg4 protein to generate LC3-I, which is then activated by Atg7 and conjugated to phosphatidylethanolamine (PE) in the membrane to form processed LC3-II. Processed LC3-II is recruited to growing autophagosomes and its integration depends on Atg5-Atg12. Unlike Atg5-Atg12-Atg16L, LC3B-II is present on



both the inner and outer surfaces of autophagosomes. The elongation and closure of autophagosomes both require the involvement of LC3B-II. After the closure of autophagosomes, the Atg16-Atg5-Atg12 complex dissociates from the vesicles, but a fraction of LC3-II remains covalently bound to the membrane. Therefore, LC3-II is commonly used as a marker to monitor the level of autophagy in cells. Once autophagosomes are fully closed to form autolysosomes, their outer membrane fuses with lysosomes to form autolysosomes. The fusion between autophagosomes and lysosomes requires the involvement of lysosomal membrane protein LAMP-1 and small GTPase Rab7. After fusion, the contents of the autophagocytic vesicles (including misfolded proteins, damaged organelles, invasive pathogens, etc.) are degraded by a series of acidic hydrolases in the lysosome. The small molecules produced by degradation, especially amino acids, are transported back to the cytoplasm for protein synthesis and maintain normal cellular biological functions under starvation conditions (Yang and Klionsky, 2009; Glick et al., 2010; Devkota, 2017). After identification, in yeast, the main vacuolar amino acid effluxes during autophagy are Atg22 and other vacuolar permeases (such as Avt3 and Avt4), which help to understand the mechanism of nutrient cycling in the body, and these permeases also represent the final step of degradation and recycling (Abeliovich and Klionsky, 2001; Xu and Du, 2022). During the entire process of autophagy, both the cytoplasm and cell organelles are damaged, the most obvious being mitochondria and the endoplasmic reticulum (Qi and Chen, 2019; Wang S. et al., 2023). Although autophagy does not

directly damage the cell membrane and cell nucleus, there is evidence that after initial fragmentation or digestion, the cell membrane and cell nucleus will eventually become lysosomes to digest and break down themselves, thus achieving a stable internal environment (Saftig and Puertollano, 2021).

2.3 Molecular mechanism of autophagy

Initially, autophagy research was mainly conducted in yeast. In the 1990s, Yoshimori and his team discovered multiple ATGs in the yeast model. They found that almost all yeast ATG homologues were found in higher eukaryotes. In 2003, Klionsky et al. named these genes ATG genes and studied the interactions between the encoded proteins and their autophagic functions. To date, researchers have identified more than 40 genes encoding ATG proteins in yeast, and in mammalian cells, about 20 core ATG genes regulate starvation-induced autophagy. These ATGs are constantly recruited near the vacuoles and assembled into autophagosome precursors. The classification and specific functions of these ATGs can be shown in Table 1. Subsequently, in April 2005, Klionsky edited and published a new journal ("Autophagy"), leading to the increasing number of autophagy-related research papers indexed by PubMed (Ohsumi, 2014). Notably, on 3 October 2016, Japanese scientist Yoshinori Ohsumi was awarded the Nobel Prize in Physiology or Medicine for his "discovery of the mechanism of autophagy", and the autophagy research had since received widespread attention

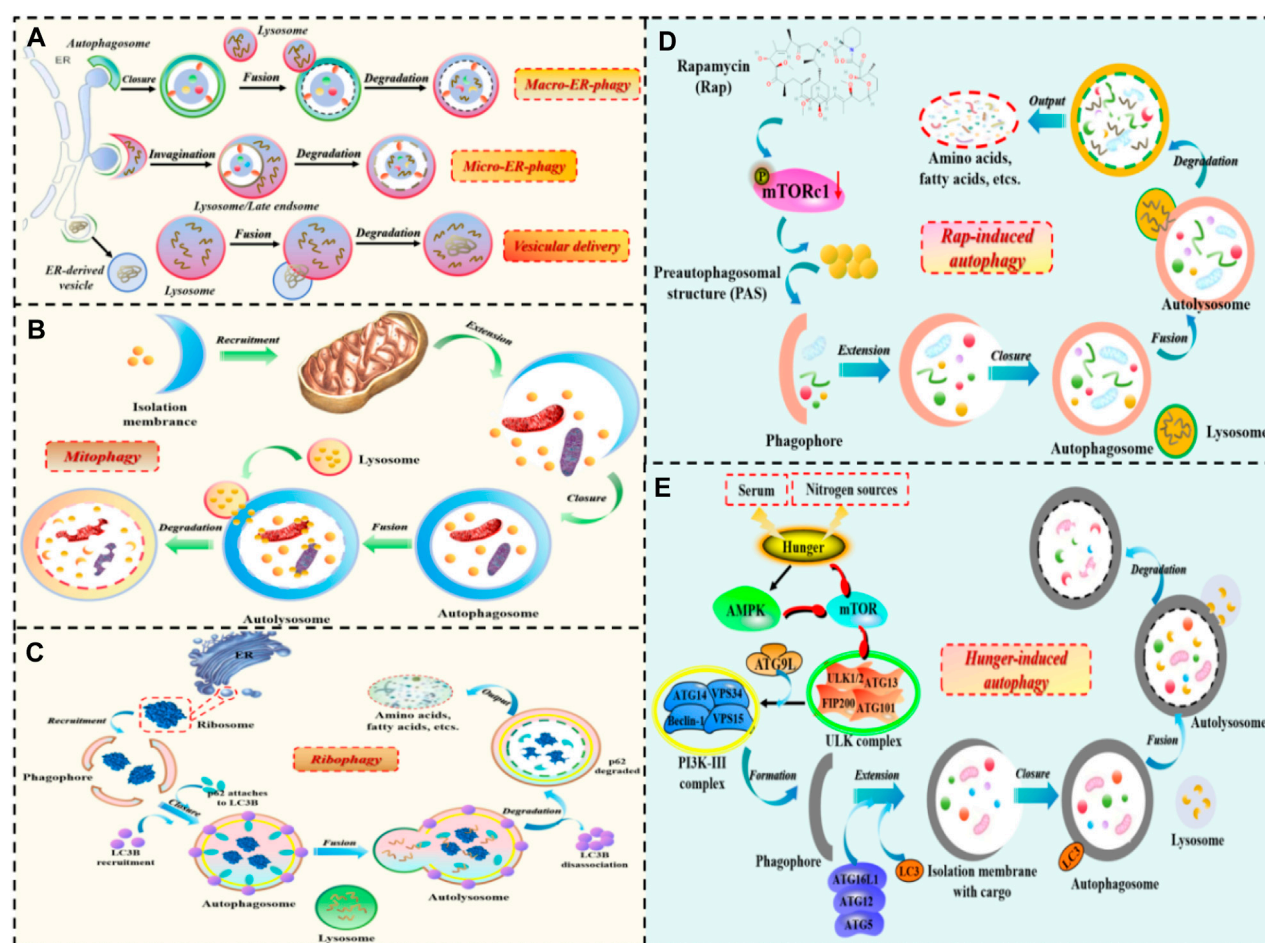


FIGURE 2

The occurrence process of selective autophagy and non-selective autophagy. 1) The process of selective autophagy: (A) ER-phagy; (B) Mitophagy; (C) Ribophagy. 2) The process of non-selective autophagy: (D) Autophagy induced by rapamycin; (E) Autophagy induced by starvation.

from scholars in various fields (Długońska, 2017), with the molecular mechanisms of autophagy gradually being elucidated.

As a common physiological regulatory mechanism in mammalian cells, mTOR and AMPK are the two key molecules regulating autophagy activity in mammals, mainly involving the phosphatidylinositol 3-kinase (PI3K)-AKT-mTOR and AMPK-TSC1/2-mTOR signaling pathways. Additionally, other signaling pathways regulate autophagic activity to a certain extent. For example, 3-methyladenine (3-MA) inhibits autophagy by suppressing the activity of Class III PI3K, Transcription factor EB (TFEB) affects autophagic activity by interfering with the biological processes of lysosomes, Beclin-1 and UVRAG act as positive regulators, anti-apoptotic factor Bcl-2 acts as a negative regulator, and they together form the Class III PI3 complex to regulate autophagy. Death-associated protein kinase (DAPK) and DAPK-related protein kinase (DRP-1) can participate in the induction process of autophagy (Figure 3).

2.3.1 PI3K-AKT-mTOR

There is a close relationship between the PI3K/AKT/mTOR signaling pathway and the cell autophagy response (Xu et al., 2020). Among them, PI3K can phosphorylate intracellular

inositol lipids, regulate intercellular signaling and intracellular vesicle transport. According to their sequence homology and substrate specificity, they can be divided into three categories: Class I PI3K can produce 3-phosphoryl inositol lipids and directly activate signaling pathways. Class II and Class III PI3K regulate intracellular trafficking and autophagy pathway membrane transport, which have indirect effects on cell signaling. Notably, Class I PI3K is a heterodimer of the p110 catalytic subunit and the p85 regulatory subunit, which can be divided into p110α catalytic subunit and p110β catalytic subunit according to the coding gene. The roles of these two subunits in cell autophagy are also different. The p110α catalytic subunit plays an inhibitory role in cell autophagy through the NF-E2 P45-related factor 2-antioxidant response element-dependent pathway and activation of AKT protein. Conversely, the p110β catalytic subunit plays a promoting role in cell autophagy by binding to RAS-related protein 5 and activating forkhead box protein O (FoxO).

AKT is a downstream target of PI3K, which can inhibit the expression of ATG by inhibiting the activity of FoxO transcription factors. ROS level also downregulates the expression of FoxO protein, thereby inhibiting cell autophagy (Cheng, 2019). In

TABLE 1 The classification and function of ATGs.

Mammals	Yeast	Function
ULK1/2	ATG1	It is involved in initiation of autophagy, membrane targeting, membrane curvature sensing, and lipid vesicle tethering
ATG2A/B	ATG2	It is important for ATG9 recruitment to expand autophagosome
ATG3	ATG3	It is involved in LC3 lipidation and maintaining mitochondrial homeostasis
ATG4A-D	ATG4	It is involved in LC3 activation and delipidation
ATG5	ATG5	It is involved in autophagosome formation/elongation and in LC3 activation
Beclin-1	ATG6	It is involved in lipid binding and membrane deformation
ATG7	ATG7	It is involved in LC3 and ATG12 conjugation, and forms a thioester bond with ATG8
MAP1LC3A-C, GABARAPs, GATE-16	ATG8	It is involved in modifier, used as autophagosome marker, recognizes the cargo-specific adaptors
ATG9L1/L2	ATG9	It is involved in phagophore expansion, and interacts with ATG2-WIPI complex
ATG10	ATG10	It is involved in the E2-like enzyme in ATG12 conjugation with ATG5
ATG12	ATG12	It is involved in modifier, forms an E3 complex with ATG5 and ATG16, and interacts with ATG3
ATG13	ATG13	It is involved in initiation of autophagy, targets mTOR signaling pathway, interacts with ATG1, bridges ATG1 and ATG17-ATG31-ATG29, binds to LC3, and interacts with ATG101
ATG14 (Barkor)	ATG14	It is subunit of VPS34-PI3K complex, interacts with Beclin-1 to assemble the autophagic-specific complex, targets membrane and senses membrane curvature, and promotes membrane fusion
ATG16L1/L2	ATG16	It binds to ATG5-ATG12 complex acting as part of the E3 enzyme complex
RB1CC1/FIP200	ATG17	It is involved in initiation of autophagy, interacts with ATG13 and ATG9, forms ternary complex with ATG31 and ATG29; and senses membrane curvature
WIPI1-4	ATG18	It is part of the ATG2-WIPI complex which is important to autophagosome; binds to PI3P; required for the retrograde transport of ATG9; and complexes with ATG2
ATG101	—	Interact with ATG13 and forms the ULK-ATG13-ATG101-FIP200 complex

addition, AKT not only regulates cell autophagy at the transcriptional level, but also participates in the regulation of several autophagy proteins. It is found that AKT had the ability to inhibit cell autophagy independently of mTORC1. Only when a mixture of rapamycin, PI3K and autophagy inhibitors are added with AKT inhibitors can be completely blocked cell autophagy. In the terms of site, AKT phosphorylates ULK1, a protein initiating cell autophagy at S774, which alters its conformation and regulates its intracellular location, resulting in its inactivation (Mohamed et al., 2021). AKT phosphorylates another autophagy protein Beclin-1 at S295, leading to its inactivation, thus inhibiting the formation process of Beclin-1-PI3K complex and blocking cell autophagy. Meanwhile, at the S295 site, using AKT inhibitors and up-regulating PTEN can also prevent Beclin-1 phosphorylation (Wang G. et al., 2021). Thus, AKT can inhibit cell autophagy by phosphorylating ULK1, Beclin-1 and other autophagy proteins to inactivate them.

mTOR can include two types: mTOR Complex 1 (mTORC1) and mTOR Complex 2 (mTORC2), both of which play important roles in cell autophagy (Kim and Guan, 2015). Among them, mTORC1 is mainly involved in the regulation of energy metabolism, cell growth, and the sensing of environmental changes. When the body is in an environment with sufficient

oxygen, energy, and growth factors, the activity of mTORC1 can be activated, resulting in the upregulation of nucleotides, proteins, and fatty acid synthesis, and inhibiting cell autophagy, thereby promoting the accumulation of biomass and cell growth. In contrast, when the body is in an acidic, nutrient-deficient environment, the activity of mTORC1 can be inhibited, thus promoting the initiation of cell autophagy. mTORC2 is activated by growth factors and focuses on regulating the reconstruction of the cytoskeleton and cell survival. As a regulatory protein, both mTORC1 and mTORC2 can participate in the regulation of autophagy, and play essential roles in maintaining the dynamic balance between cell synthesis and degradation processes. Studies have found that mTORC1 mainly inhibits cell autophagy by phosphorylating proteins such as Unc-51-like kinase complex, ATG13, ATG14, protein nuclear receptor binding factor 2, and regulating the activity of transcription factors EB/E3, which are related to the formation and maturation of autophagosomes (Noda, 2017; Rabanal-Ruiz et al., 2017). In contrast, mTORC2 can inhibit cell autophagy by suppressing the protein kinase sgk1 and promoting autophagy by up-regulating the expression of mitochondrial outer membrane voltage-dependent anion channel protein 1 (Ballesteros-Álvarez and Andersen, 2021).

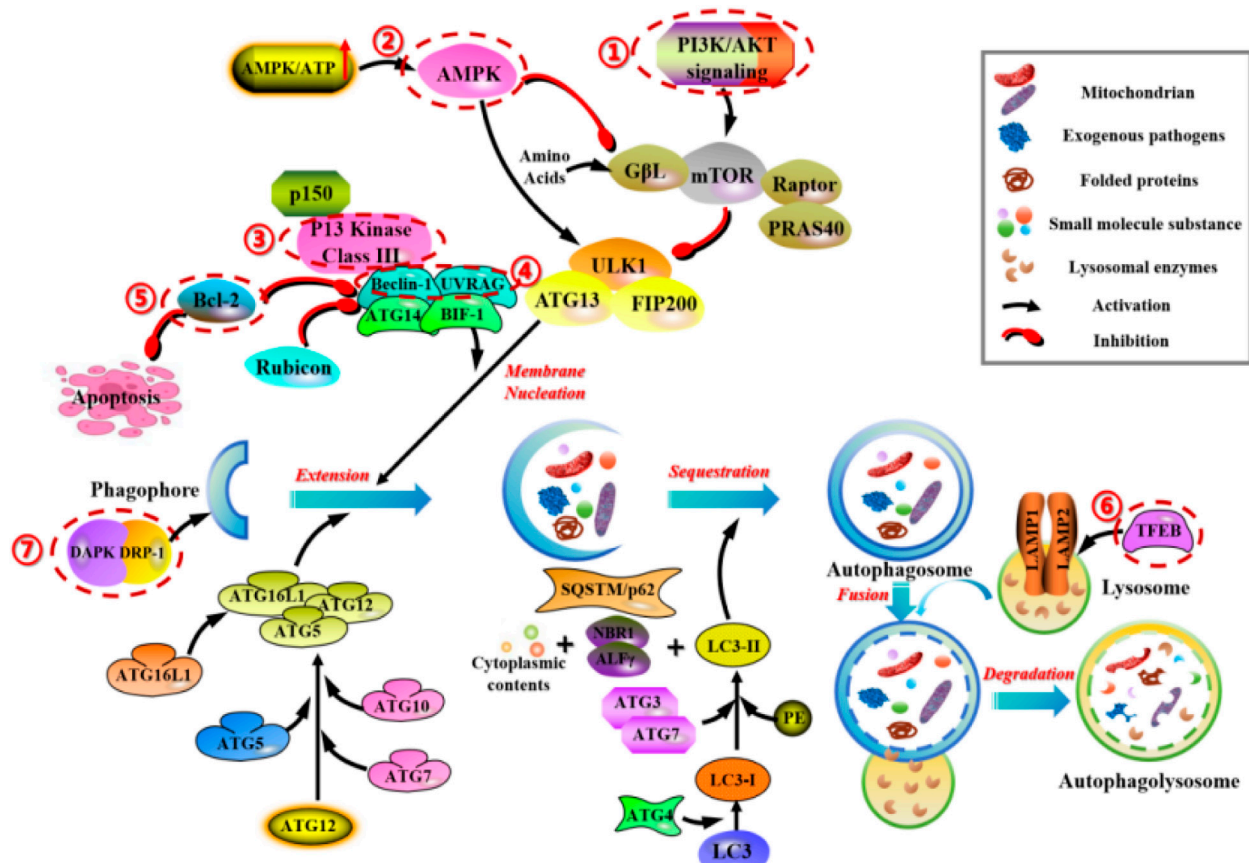


FIGURE 3

Main molecular mechanisms of autophagy in mammals. 1) PI3K/AKT/mTOR regulates the cell-cell signaling and transport of autophagic vesicles. 2) AMPK-TSC1/2-mTOR regulates the energetic stress signaling and transport of autophagic vesicles. 3) 3-methyladenine (3-MA) inhibits autophagy by suppressing the activity of Class III PI3K. 4) Beclin-1 and UVRAG, act as positive regulators, form the Class III PI3 complex to regulate autophagy. 5) Anti-apoptotic factor Bcl-2, acts as a negative regulator, form the Class III PI3 complex to regulate autophagy. 6) TFEB affects autophagic activity by interfering with the biological processes of lysosomes. 7) DAPK and DRP-1 can participate in the induction process of autophagy.

2.3.2 AMPK-TSC1/2-mTOR

mTOR is a major regulatory molecule for cell growth and metabolism, promoting anabolic processes such as ribosome biogenesis and the synthesis of proteins, nucleotides, fatty acids, and lipids, while inhibiting catabolic processes such as autophagy. Dysregulation of mTOR signaling is often associated with numerous human diseases, including diabetes, neurodegenerative diseases, and cancer (Zhu et al., 2019b; Yang et al., 2019; Gremke et al., 2020). mTOR is a serine/threonine kinase belonging to the PI3K-related kinase (PIKK) family and can interact with several proteins to form two distinct complexes, known as mTORC1 and mTORC2. Numerous studies have shown that mTORC1 is a key regulator of autophagy, controlling different steps in the autophagic process (such as nucleation, autophagosome extension, maturation, and termination) (Martens, 2018). Therefore, mTORC1 is a promising target for regulating autophagy. In the activation process of mTORC1, it is often subjected to various stimuli (such as growth factors, nutrients, energy, and stress signals) and activated fundamental signaling pathways (such as PI3K, MAPK, and AMPK). Among them, the AMPK-TSC1/2-mTOR pathway is a classical autophagic pathway. Under conditions of abundant glucose, active mTORC1 inhibits autophagy initiation by

phosphorylating specific sites (Ser 757) of ULK1 and disrupting the interaction between ULK1 and AMPK. In contrast, when glucose is scarce, AMPK is activated, leading to the phosphorylation of mTORC1 by AMPK, subsequent interaction between ULK1 and AMPK, and activation of ULK1 to initiate autophagy (Kim et al., 2011).

2.3.3 Class III PI3K

PI3Ks is a class of kinases that plays a crucial role in cell signaling pathways, specifically catalyzing the phosphorylation of the 3-hydroxyl group of phosphatidylinositol (PtdIns). The catalytic products bind to specific domains on receptor proteins to mediate signal transduction, playing essential roles in processes such as cell growth, division, migration, vesicle trafficking, and autophagy (Farrell et al., 2013). PI3Ks can be divided into three classes (Type I, II, and III) based on their structural characteristics and substrates. Class III PI3K plays a key role in vesicle trafficking and autophagosome formation. Members of Class III PI3K and some of its complexes are highly conserved evolutionarily. In mammals, homologs of PI3KC3, p150, Beclin-1, ATG14L, and UVRAG are Vps34, Vps15, Vps30, Atg14, and Vps38, respectively. Notably, each member of the PI3KC3 complex can

directly or indirectly regulate the activity of Vps34, thereby regulating autophagy. Vps34, as the third class of PI3 kinase in mammals (PIK3C3), phosphorylates phosphatidylinositol (PI) to produce phosphatidylinositol triphosphate (PI3P), which is crucial for the extension of autophagosome membranes and the recruitment of ATG proteins to autophagosomes. Vps34 is activated by binding to Vps15 and further associates with Beclin-1 to form the Vps34-Vps15-Beclin1 complex (Backer, 2008).

2.3.4 TFEB

TFEB is a member of the basic helix-loop-helix leucine zipper transcription factor family MiT/TFE. Members of the MiT/TFE family play crucial roles in many cellular processes, particularly autophagy-lysosome biogenesis, cellular energy homeostasis, and metabolic processes. In vertebrates, the MiT/TFE transcription factor family consists of four evolutionarily conserved members: TFEB, MITF, TFEC, and TFE3. All MiT/TFE proteins, including TFEB, are evolutionarily conserved and can be found in primitive metazoans. TFEB is considered the primary regulator of lysosome biogenesis. TFEB can tightly link autophagy with lysosome biogenesis by regulating the expression of ATGs. Moreover, TFEB can also regulate lysosomal exocytosis. Increasing evidence suggests that dysregulation of TFEB activity leads to impaired autophagy-lysosome function, resulting in numerous human diseases, such as neurodegenerative diseases (including Alzheimer's disease and Parkinson's disease), lysosomal storage disorders, metabolic disorders, cancer and so on (He et al., 2019; Kim et al., 2021; Gu et al., 2022; Tan et al., 2022). Given the crucial role of TFEB in human diseases, regulating TFEB activity may represent a novel therapeutic target for clinical and regenerative applications. Studies have shown that the molecular mechanisms regulating TFEB are closely related to its subcellular localization (cytoplasmic and nuclear shuttling) and signal transduction (Willett et al., 2017). Autophagy is an adaptive response of cells to nutritional stress, and its activation is essential for maintaining homeostasis in the body. Initially, TFEB is mainly localized in the cytoplasm and can be transferred to the nucleus to cope with starvation. Upon re-feeding after hunger, TFEB's re-localization can be restored. Moreover, the upstream molecules of TFEB (such as mTORC1) can also induce its nuclear localization after regulation. It is noteworthy that many stimuli (such as endoplasmic reticulum stress, infection, mitochondrial damage, and inflammation) can also promote TFEB's nuclear localization. The activation and subcellular localization of TFEB are mainly controlled by protein interactions and post-translational modifications. Interestingly, the subcellular localization of TFEB is strictly controlled by phosphorylation. mTOR kinase is a known major kinase that phosphorylates TFEB (at sites S122, S142, and S211) and regulates its intracellular localization. Phosphorylation of TFEB at site S142 is also mediated by ERK2. Recent studies have also found that STUB1 regulates TFEB activity by targeting phosphorylated TFEB (S142 and S211) for ubiquitin-mediated proteasomal degradation (Sha et al., 2017).

2.3.5 Beclin-1 and UVRAG

In yeast, Atg6/Vps30, which is a homolog of the mammalian Beclin-1 protein, is a protein involved in both autophagy and apoptosis pathways in the Vps34 complex. In mammals, Beclin-1

only participates in the autophagy process. In yeast, Atg6/Vps30 does not directly bind to Vps34 but forms a complex with Vps34 through Atg14 or Vps38, respectively participating in autophagy and protein sorting. Human Beclin-1 shares 24.4% homology with yeast Atg6/Vps30 and has been confirmed to play a crucial role only in the autophagy process, without participating in vesicle transport. Researchers have also analyzed the structure of Beclin-1, which contains a BH3 domain, making it a member of the Bcl-2 family and capable of binding to Bcl-2 (Cao and Klionsky, 2007). Furthermore, Beclin-1 contains an ECD domain (a key domain for binding of Beclin-1 to type III PI3K) and a CCD domain. Intermolecular interactions through the CCD domain allow Beclin-1 to form homodimers and heterodimers with UVRAG and Atg14 (Noble et al., 2008). Subsequently, the CCD domain of Beclin-1, a member of the Bcl-2 family, has been analyzed after studying its crystal structure. The results indicate that the surface a-d pairings and charge properties of key residues in the CCD domain directly affect the stability of dimers and the formation of different PI3KC3 complexes (Li et al., 2012). Therefore, Beclin-1 can bind to Bcl-2 and Bcl-XL to regulate apoptosis, as well as form complexes with type III PI3K to play a crucial role in autophagy, serving as an essential protein for communication and coordination between apoptotic and autophagic pathways.

UVRAG was initially discovered in 1990 by Teitz et al. while searching for genes responsible for UV damage resistance and DNA repair in cells, and the cDNA sequence of the protein was only cloned at that time. In 1997, Perelman et al. (1997) localized UVRAG to the 11q13 subregion of human chromosome 11, between D11S916 and D11S906, noting that the region is amplified in various cancers, suggesting a potential relationship between UVRAG and tumorigenesis. The study also analyzed the structure of UVRAG, indicating a CCD domain and a PEST domain, which may contribute to UVRAG's metabolic instability. Ionov et al. (2004) identified two genes, UVRAG and p300, as likely causes of microsatellite instability in colorectal cancer, further confirming the close relationship between UVRAG and various diseases, including tumors. Subsequent research also demonstrated a correlation between UVRAG and microsatellite instability in gastric cancer (Kim et al., 2008). In addition to tumors, UVRAG deficiency can cause situs inversus in the thoracic and abdominal visceral (Iida et al., 2000; Goi et al., 2003). Current molecular biology research suggests that the CCD domain of UVRAG can bind to the CCD domain of Beclin-1 to form heterodimers, thereby stabilizing the Beclin-1-PI3KC3 complex and enhancing PI3KC3 kinase activity. This activation promotes autophagy as a positive regulatory factor. However, UVRAG deficiency may potentially induce cancer by downregulating autophagy (Zhong et al., 2009). Meanwhile, other studies have reported that UVRAG participates in autophagy through vesicle transport. UVRAG can form complexes with C-Vps, which function independently of the UVRAG-VPS34 complex. This complex primarily activates Rab7 GTPase activity, promoting fusion between membranous vesicles, including intracellular vesicle fusion and autophagosome fusion with late endosomes/lysosomes. This process accelerates the degradation of phagocytosed materials, promoting maturation of autophagosomes and the autophagic process (Liang et al., 2008). Therefore, the UVRAG-C-Vps complex can simultaneously promote both vesicle transport and maturation of autophagosomes.

2.3.6 Anti-apoptotic factor Bcl-2

The Bcl-2 protein family can be divided into three subgroups: anti-apoptotic proteins, such as Bcl-2, Bcl-xL and Mcl-1, which contain the common BH1-BH4 structural domain. The pro-apoptotic proteins, such as Bax and Bak, which contain the common BH1-BH3 structural domain. And the pro-apoptotic proteins, such as Bad, Bid, Bim, Noxa, BNIP3 and Puma, which only contain the BH3 structural domain (Kale et al., 2018). Among them, Bcl-2 protein not only participates in cell apoptosis but also participates in cell autophagy and plays a key dual regulatory role in both (Liu et al., 2019b). At present, the classic theory for Bcl-2 regulation of autophagy and apoptosis is through the regulation of Beclin-1 (Xu and Qin, 2019). Beclin-1 is a mammalian autophagy gene homologous to the yeast ATG6/VSP30 autophagy gene and is the earliest discovered key factor in regulating autophagy. It is a BH3-only protein with three important structural domains: BH3, CCD, and ECD. Beclin-1 can bind to multiple proteins through these domains to form complexes that induce the localization of autophagy-related proteins to the autophagosome membrane and regulate the formation and maturation of autophagy. The proteins that make up this complex mainly include VPS34, UVRAG, Ambrl, and Bcl-2. Among them, Bcl-2 contains the same BH3 structural domain as Beclin-1, and Bcl-2 can bind to Beclin-1 through this domain. When Bcl-2 and Beclin-1 form a complex, it can inhibit autophagy. When the classic apoptosis program is activated, activated Caspase-3 cleaves Beclin-1, thereby inhibiting autophagy. However, Lindqvist LM et al. have all found that the anti-apoptotic proteins represented by Bcl-2 do not directly bind to Beclin-1 to directly regulate cell autophagy, but indirectly regulate autophagy by inhibiting Bax/Bak-mediated apoptosis. That is, in the absence of Bax and Bak, Bcl-2 cannot significantly induce cell autophagic death (Lindqvist et al., 2014; Lindqvist and Vaux, 2014).

2.3.7 DAPK and DRP-1

Recent studies had shown that the expression of death-associated protein kinase (DAPK) and DAPK-related protein kinase (DRP-1) could trigger two important non-caspase-dependent cytoplasmic events: 1) membrane vesicle growth (observed in any form of cell death). 2) proliferative autophagy (a typical characteristic of autophagy). And when autophagosomes were found to contain DRP-1, it indicated that this kinase directly participated in the process of autophagy (Inbal et al., 2002).

3 Autophagy in vascular lesions

Clinically, patients with diabetes often exhibit insulin resistance and hyperinsulinemia, which are commonly accompanied by hypertension, dyslipidemia, obesity, and other metabolic syndrome manifestations. Moreover, changes in abnormal vascular endothelial cells, coagulation, and platelet function in diabetes can lead to vascular damage, such as atherosclerosis, thereby causing a series of vascular lesions. Diabetic vascular lesions mainly include microvascular lesions and macrovascular lesions. Among them, microvascular lesions include retinopathy, peripheral neuropathy, and diabetic nephropathy, while macrovascular lesions include coronary heart disease and stroke.

The symptoms produced by diabetic vascular lesions are mainly related to the location and severity of the lesioned vessels. The impact of diabetes on large vessels is mainly manifested as organ ischemia, such as chest stuffiness and chest pain caused by coronary heart disease, hemiplegia and aphasia caused by stroke, and cold feet, numbness, and claudication caused by peripheral arterial disease. When it accumulates to microvessels, it may lead to diabetic nephropathy (proteinuria and increased creatinine level in urine detected by auxiliary examination), retinopathy (blindness), peripheral neuropathy and microvascular disease (decreased sensation in extremity tips, ulcers, and infections). The basic treatment for diabetic vascular complications is to change unhealthy lifestyles while using medications to control blood sugar, hypertension, dyslipidemia, and obesity, which are risk factors for atherosclerosis. Additionally, it involves treating the damage of target organ corresponding to the vascular lesions. However, since diabetes simultaneously damages both large and microvessels throughout the body, the treatment difficulty lies in the fact that most patients have multiple vessels involved in the disease, making it difficult to restore blood supply to the target organs. Therefore, the treatment and prevention of diabetic vascular lesions remain a clinical challenge. Recent studies have increasingly shown that autophagy plays a crucial role in the development of diabetic vascular lesions, mainly involving vascular permeability, angiogenesis, vascular endothelial cell function, and vascular endothelial cell senescence (Salabei and Hill, 2013; Sanhueza-Olivares et al., 2022; Liu et al., 2023). Next, we will further elucidate the relationship between autophagy and these factors, laying the theoretical foundation for the application of autophagy-related preparations in diabetic vascular lesions and broadening the clinical treatment methods for this type of disease.

3.1 The relationship between autophagy and vascular permeability and neovascularization

Diabetic vascular lesions are mainly divided into microvascular lesions and macrovascular lesions. Endothelial cells located in the innermost layer of blood vessels are shaped like spindles or polygons, not only acting as a semi-permeable barrier between blood and vascular smooth muscle, but also serving as effector organs that sense and respond to changes in the external environment. They are important determinants of whole-body and local hemodynamic function and regulation of vascular smooth muscle cell proliferation. Therefore, endothelial cells play a key role in maintaining blood flow, regulating vascular permeability, and controlling the growth and proliferation of vascular smooth muscle cells.

Autophagy is an important metabolic process within cells, playing a crucial role in maintaining cellular homeostasis, clearing damaged proteins and organelles, regulating cell growth and death, and so on. In the terms of vascular permeability and neovascularization, autophagy also plays a certain role. On the one hand, autophagy can regulate vascular permeability. Studies have shown that autophagy plays an important role in regulating the function and stability of endothelial cells. Autophagy can clear harmful substances and damaged proteins in endothelial cells,

and can maintain the stability of intracellular environment, so as to protect the function of endothelial cells. The loss of endothelial cell function will lead to the occurrence and development of atherosclerosis in diabetic patients. However, the mechanism of endothelial cell dysfunction in diabetic patients has not been fully understood. Zhang YK et al.'s research (Zhang et al., 2022) found that liraglutide, a glucagon-like peptide-1 (GLP-1) receptor agonist, acted on the upstream of the PINK1/Parkin pathway, effectively offset high glucose-induced cellular dysfunction by inhibiting the PINK1/Parkin-dependent mitochondrial autophagy. Therefore, it is very necessary to use liraglutide as an adjuvant treatment for type 2 diabetes to reduce the risk of atherosclerosis, and further research is needed to examine the exact molecules, including the SIRT1 upstream of the liraglutide targeted to maintain mitochondrial homeostasis PINK1/parkin pathway. In addition, autophagy can also regulate vascular permeability via adjusting the apoptosis and inflammatory response of endothelial cells. As shown by Zheng YZ et al.'s research (Zheng et al., 2022), melatonin directly reduced the expression of endothelial cell injury markers in HCAECs, thereby alleviating the vascular inflammation induced by *candida albicans* water-soluble components (CAWS) in a Kawasaki disease mouse model. Mechanistically, melatonin promotes autophagy by activating the melatonin/melatonin receptor (MT)/cAMP response element binding protein (CREB) pathway and upregulating AGT3 expression, so as to inhibit cell apoptosis in an autophagy-dependent manner. Moreover, melatonin also reduced the production of pro-inflammatory cytokines in macrophages and indirectly reduced immunopathological damage to HCAECs. This study shows that melatonin protects endothelial cells in Kawasaki disease by inhibiting cell apoptosis in an autophagy-dependent manner and reducing immunopathological damage mediated by macrophages. On the other hand, autophagy also plays a vital role in angiogenesis. Angiogenesis refers to the formation of new blood vessels, which plays a key role in tissue repair and regeneration. Research has found that autophagy can promote the proliferation and migration of vascular endothelial cells, participating in the process of angiogenesis. Autophagy affects the occurrence and development of angiogenesis by regulating vascular endothelial cell growth factors and signaling pathways. 1 α , 25-Dihydroxyvitamin D3 (1,25D) is a hormone form of vitamin D, which has been proven to be beneficial for vascular diseases. As Xiong et al. (2021) found that 1,25D could partially improve the impairment of cell proliferation and migration induced by AGEs in endothelial cells via using CCK8 assay and Trans-well assay. Through tube formation assay, Western blot, and RT-PCR assay, they demonstrated that AGEs impaired angiogenic capacity, which was closely related to the expression changes of angiogenesis-related genes (including VEGFA, VEGFB, VEGFR1, VEGFR2, TGF β 1, MMP2, and MMP9) in endothelial cells. 1,25D could promote the expression of these angiogenic and angiogenic markers. Using DCFH-DA, ELISA, and Western blot assays, they also found that AGEs-induced oxidative stress damaged the angiogenic capacity of endothelial cells, and 1,25D relieved the vascular dysfunction by inhibiting oxidative stress. Notably, excessive autophagy induced by AGEs damaged angiogenesis, which was regulated by 1,25D and AGEs through the PI3K/Akt signaling pathway. This study suggests that AGEs-induced oxidative stress and autophagy can lead to angiogenic disorders, and 1,25D can improve angiogenesis by

inhibiting excessive autophagy and oxidative stress, providing new insights for the treatment of diabetic vascular complications.

All in all, the role of autophagy in vascular permeability and angiogenesis is multifaceted. Autophagy affects the regulation of vascular permeability by regulating the function and stability of vascular endothelial cells. Meanwhile, autophagy also participates in the process of angiogenesis, promoting the formation of new blood vessels. However, further research is needed to reveal the specific mechanisms and regulatory processes.

3.2 The relationship between autophagy and vascular endothelial cell function

Studies had confirmed that long-term hyperglycemic conditions could lead to vascular endothelial dysfunction in the body, and the vascular abnormalities in diabetes patients were closely related to the injury of hyperglycemia-induced vascular endothelial cells (Li F. et al., 2023). In addition, endothelial cell dysfunction could also limit the repair function of endothelial cells and decrease the angiogenic capacity (Eelen et al., 2015; Gimbrone and Garcia-Cardena, 2016), which were considered important pathogenic factors for the development of diabetic cardiovascular diseases.

Autophagy plays an important role in the functional disturbance of endothelial cells. When the function of endothelial cells is disturbed, it may lead to the occurrence and development of vascular diseases. The role of autophagy in the functional disturbance of endothelial cells is mainly reflected in the following aspects: (1) Regulating oxidative stress in endothelial cells: Oxidative stress is one of the important factors leading to functional disturbance of endothelial cells. Autophagy can reduce the degree of oxidative stress in endothelial cells by removing harmful substances and damaged proteins generated by oxidative stress, thereby protecting the cells. As shown in the research by Zhu et al. (2019a), exposure of human umbilical vein endothelial cells (HUVECs) to oxidized low-density lipoprotein (ox-LDL) reduced cell viability, increased the content level of malondialdehyde (MDA), and reduced the content level of superoxide dismutase (SOD) in a concentration-dependent manner. Pre-treatment with salidroside significantly enhanced cell viability and reduced lactate dehydrogenase (LDH) release in HUVECs exposed to ox-LDL. Further research also found that ox-LDL could induce autophagy in HUVECs, and salidroside could further enhance autophagy after pre-treatment. However, salidroside weakened the increase of oxidative stress induced by ox-LDL in HUVECs. Interestingly, ox-LDL reduced the expression levels of SIRT1 and FOXO1 mRNA and protein, and these changes could be reversed by salidroside. This suggests that salidroside has a protective effect on endothelial cells induced by ox-LDL, and the mechanism may be related to increasing SIRT1 and FoxO1 expression to induce autophagy. (2) Maintaining homeostasis of endothelial cells: Autophagy can remove harmful substances and aging proteins in endothelial cells, maintaining stability of the intracellular environment. This helps to protect the function and stability of endothelial cells, reducing the occurrence of functional disturbance. Studies have shown that endothelial cell dysfunction plays a fundamental role in the pathogenesis of atherosclerosis, and autophagy has a protective effect on the occurrence of

atherosclerosis. As Zhang G. et al. (2021) studied the effect of oxLDL/ β 2GPI/anti- β 2GPI complex on autophagy in vascular endothelial cells and explored its potential mechanism. They used HUVECs and mouse brain endothelial cell line (bEnd.3) as the models of vascular endothelial cells. The expression of autophagy protein was detected by Western blot analysis, autophagosome accumulation was observed by TEM, and autophagic flux was detected by RFP-GFP-LC3 adenovirus transfection and chloroquine treatment to inhibit lysosomes, so as to assess the level of autophagy. Western blotting was used to detect the expression of phosphorylated PI3K, phosphorylated AKT, phosphorylated mTOR, and phosphorylated eNOS. 3-Methyladenine (3-MA) and rapamycin were used to assess the role of autophagy in the impairment of endothelial cell function induced by oxLDL/ β 2GPI/anti- β 2GPI complexes. Their results showed that oxLDL/ β 2GPI/anti- β 2GPI complexes inhibited the endothelial autophagy through the PI3K/AKT/mTOR and eNOS signaling pathways and further promoted the endothelial cell dysfunction. The findings of this study provide a new mechanism for vascular endothelial damage in patients with atherosclerosis complicated by antiphospholipid syndrome (APS). (3) Regulating inflammation response in vascular endothelial cells: Inflammation response is one of the common characteristics of vascular endothelial cell dysfunction. Autophagy can inhibit the inflammation response of vascular endothelial cells by regulating inflammation-related signaling pathways, thus reducing the occurrence of functional disorders. Caveolin-1 (Cav-1) expression plays a related role in the formation of atherosclerosis by controlling NO production, vascular inflammation, low-density lipoprotein (LDL) uptake, and extracellular matrix remodeling. As Zhang et al. (2020) studied how Cav-1 expression in aortic endothelium affects autophagy and whether enhanced autophagy is beneficial to the atherosclerosis-protective phenotype observed in Cav-1-deficient mice. Their results showed that Cav-1 deficiency promoted autophagy activation in susceptible areas of aortic endothelium by enhancing autophagic flux. Mechanistically, they found that Cav-1 interacted with the ATG5-ATG12 complex and affected the cellular localization of autophagosome components in lipid rafts, thereby controlling autophagosome formation and autophagic flux. Pharmacological inhibition of autophagy weakened the atherosclerosis protection observed in Cav-1 mice by increasing endothelial inflammation and macrophage recruitment, thus identifying a new molecular mechanism for preventing atherosclerosis progression by Cav-1 deficiency. This study demonstrates that Cav-1 is a relevant regulator of aortic endothelial autophagy and suggests that pharmacological inhibition of Cav-1-activated autophagy may provide a potential therapeutic strategy for cardiovascular diseases including atherosclerosis. (4) Regulating apoptosis and proliferation in vascular endothelial cells: Imbalance in apoptosis and proliferation of vascular endothelial cells is also an important factor in functional disorders. Autophagy can maintain normal growth and death of vascular endothelial cells by regulating cell apoptosis and proliferation-related signaling pathways, thus reducing the occurrence of functional disorders. ANGPTL4 is a member of the angiopoietin-like protein family and participates in the regulation of angiogenesis, lipid metabolism, glucose metabolism, and redox reactions. As Zhan et al. (2022) found

that over-expression of ANGPTL4 in HUVECs enhanced cell proliferation and clonal formation abilities *in vitro*, whereas knockdown of ANGPTL4 had the opposite effect. Moreover, ANGPTL4 expression was upregulated in HUVECs treated with palmitic acid (PA), and over-expression of ANGPTL4 prevented PA-induced endothelial damage. In their exploration of the mechanism, they demonstrated that ANGPTL4 regulated endothelial cell proliferation and apoptosis by modulating autophagy. Additionally, they found that ANGPTL4 levels were downregulated in atherosclerosis mouse serum and were closely related to autophagy-related proteins in atherosclerosis mouse aortic tissue. This study suggests that ANGPTL4 promotes endothelial cell proliferation and inhibits PA-induced endothelial cell damage, thereby preventing the development of atherosclerosis. Furthermore, Fan et al. (2023) evaluated the effects of Homoplagitin (Hom) on vascular endothelial cells by using high-glucose-treated HUVECs and db/db mice. *In vitro*, Hom significantly inhibited cell apoptosis, promoted autophagosome formation and lysosome function, such as lysosome membrane permeability and expression of LAMP1 and cathepsin B. Autophagy inhibitors, such as chloroquine or bafilomycin A1, reversed Hom's anti-apoptotic effects. Moreover, Hom promoted gene expression and nuclear translocation of TFEB. Knockdown of TFEB weakened the up-regulating effects of Hom on lysosome function and autophagy. Hom activated AMPK protein and inhibited the phosphorylation of mTOR, p70S6K, and TFEB proteins. AMPK inhibitors attenuated these effects, and molecular docking suggested a good interaction between Hom and AMPK proteins. Animal studies showed that Hom effectively upregulated the expression of p-AMPK and TFEB proteins, enhanced autophagy, reduced cell apoptosis, and alleviated vascular damage. These findings indicate that Hom can enhance autophagy through the AMPK/mTORC1/TFEB pathway, so as to improve the high glucose-mediated vascular endothelial cell apoptosis.

All in all, autophagy plays a crucial role in vascular endothelial cell dysfunction. Autophagy can protect vascular endothelial cell function and stability by regulating oxidative stress, maintaining cell homeostasis, inhibiting inflammatory responses, and regulating cell apoptosis and proliferation. Therefore, further study of the regulatory mechanisms of autophagy in vascular endothelial cell dysfunction has a great significance, which will help develop new therapeutic strategies to prevent the occurrence of vascular diseases.

3.3 The relationship between autophagy and vascular endothelial senescence

Increasing evidence suggests that persistent hyperglycemia is an important cause of vascular endothelial cell senescence in patients with diabetes (Li et al., 2019; Wang G. et al., 2021; Wan et al., 2022). In the normal physiological conditions, vascular endothelial cells are in a quiescent phase with a low rate of self-renewal. However, exogenous damaging factors (such as high glucose stimulation) can lead cells into the division phase, during which telomeres shorten continuously, resulting in senescence. The main characteristics of senescence include cell enlargement, enhanced SA- β -gal activity, cell cycle arrest, increased expression of

TABLE 2 The active compound counteracts the effects of diabetic vascular damage by modulating autophagic flux.

Herbal extracts	Categories	Autophagy-related targets	In vitro/ In vivo	Model	References
Salvianolic acid B	<i>Salvia miltiorrhiza</i> Bge	Beclin-1, Parkin, Pink1	In vitro and vivo	HG-induced HUVECs and db/db mice	Xiang et al. (2022)
Notoginsenoside R1	<i>Panax notoginseng</i> (Burkill) F. H. Chen ex C. H. Chow	LC3B, P62/SQTM1, Parkin, Pink1	In vitro and vivo	HG-induced rMC-1 and db/db mice	Zhou et al. (2019)
Notoginsenoside Fc	<i>Panax notoginseng</i> (Burkill) F. H. Chen ex C. H. Chow	LC3B, Beclin-1, P62/SQTM1	In vitro and vivo	Sprague-Dawley rat model induced by STZ and RAOECs induced by HG	Liu et al. (2019a)
Glycyrrhizic acid	<i>Glycyrrhiza uralensis</i> Fisch	LC3B, Beclin-1, P62/SQTM1	In vivo	Rat model of type I diabetes	Asseri et al. (2022)
Scutellarin	<i>Scutellaria baicalensis</i> Georgi	LC3B, Beclin-1, P62/SQTM1, ATG5, Parkin, Pink1	In vitro	HG-induced HUVECs	Xi et al. (2021)
Epigallocatechin gallate	<i>Green Tea</i>	LC3B	In vitro	Palmitic acid-induced BAEC	Kim et al. (2013)
Homoplantaginin	<i>Salvia japonica</i> Thunb	LAMP1, Cathepsin B, AMPK, mTOR, TFEB	In vitro and vivo	HG-induced HUVECs and db/db mice	Fan et al. (2023)
Resveratrol	<i>Aloe vera</i> (L.) Burm. f	LC3B, Beclin-1	In vitro	Gly-LDL-induced HUVECs	Sha et al. (2021)
Artesunate	<i>Artemisia caruifolia</i> Buch.-Ham. ex Roxb	LC3B, Beclin-1, P62/SQTM1, AMPK, SIRT1	In vivo	DR rat model induced by STZ	Li et al. (2023b)
Naringin	<i>Citrus reticulata</i> Blanco	mTOR, LC3B, Beclin-1, P62/SQTM1	In vitro	HG/HF-induced HUVECs	Wang et al. (2020a)
Geranylgeranylacetone	<i>Bayberry</i>	mTOR, LC3B	In vivo	Rat retinal I/R model	Zhang et al. (2023a)
Icariin	<i>Epimedium brevicornu</i> Maxim	mTOR, LC3B, P62/SQTM1	In vitro	H ₂ O ₂ -induced BM-EPCs	Tang et al. (2015)
Gypenoside XVII	<i>Gynostemma pentaphyllum</i> (Thunb.) Makino	ATG5, Beclin-1, LC3B, P62/sqtm1	In vivo	db/db mice	Luo et al. (2021)
Lentinan mushroom	<i>Lentinus edodes</i>	Beclin-1	In vitro	HG-induced HUVECs	Yang et al. (2022)

senescence-associated genes and proteins, and increased cell inflammatory secretions. In addition, endothelial cell senescence plays a crucial role in the development of vascular aging and related cardiovascular diseases. Atherosclerotic lesions are often accompanied by endothelial cell senescence. As discovered by Brodsky et al. (2004), vascular endothelial cell senescence was closely related to the severity of vascular lesions in Zucker diabetic rats. Ebselen, as a potent nitrosative stress scavenger, could reduce protein tyrosine nitration modification and delayed vascular endothelial cell senescence, thus alleviating diabetic macrovascular lesions. Moreover, endothelial cell senescence causes decreased vascular elasticity and compliance, serving as one of the major causes of hypertension. Thus, endothelial cell senescence was closely related to diabetic macroangiopathy.

Autophagy plays a vital role in vascular endothelial senescence. Vascular endothelial cells are the inner layer of the vascular wall and play a key role in maintaining vascular function and stability. Following with age, vascular endothelial cells undergo senescence, which may lead to decreased vascular function and the development of related diseases. The role of autophagy in vascular endothelial senescence mainly includes: 1) Clearance of senescent cells and damaged materials: Autophagy can clear senescent vascular endothelial cells, including aged proteins and organelles. This helps to maintain the function and stability of vascular endothelial cells, reducing the negative impact of senescent cells on the surrounding environment. As discovered by Chen et al.

(2014), angiotensin-converting enzyme inhibitors (ACEIs) or angiotensin II type 1 receptor blockers (ARBs) had beneficial effects on high glucose-induced endothelial responses. High glucose activation of the RAS enhanced mitochondrial damage and increased senescence, apoptosis, and autophagic responses in endothelial cells, which were simulated by using angiotensin (Ang) II. However, the negative effects of hyperglycemia were inhibited by ACEI or ARB. Direct mitochondrial damage caused by 3-chlorobenzoyl cyanide (CCCP) resulted in similar adverse effects to high glucose or Ang, and eliminated the protective effects of ACEI or ARB. By impairing autophagy, high glucose-induced senescence and cell apoptosis were accelerated, and the beneficial effects mediated by ACEI or ARB were abolished. In addition, increased FragEL™ DNA fragmentation (TUNEL) positive cells, β-galactosidase activation, and expression of autophagy biomarkers were observed in diabetic patients and rats, which were reduced by ACEI or ARB treatment. These data indicate that autophagy prevents vascular endothelial cell senescence and apoptosis in high glucose-induced endothelial cells through RAS-mitochondrial regulation. 2) Maintenance of vascular endothelial cell function: Autophagy can protect the biological function of vascular endothelial cells by clearing harmful substances and maintaining stability within the cell. Specifically, autophagy can eliminate damaged proteins and organelles in senescent cells, reducing toxic substance accumulation within cells and maintaining normal cell function. Diabetic vascular complications

TABLE 3 A single herb counteracts the effects of diabetic vascular damage by modulating autophagy flux.

Single herbs	Autophagy-related targets	<i>In vitro</i> / <i>In vivo</i>	Model	References
Ginger	Beclin-1, Parkin, Pink1	<i>In vitro</i> , <i>In vivo</i>	HG-induced HUVECs and db/db mice	Li et al. (2021a)
Ginkgo Biloba Leaf Extract	mTOR, P62/SQTM1	<i>In vivo</i>	ApoE ^{−/−} mice model induced by STZ and high-fat diet	Tian et al. (2019)
Large-leaf yellow tea	LC3B, Beclin-1, ATG5, P62/SQTM1	<i>In vivo</i>	Diabetic mice and HG-induced HUVECs	Wang et al. (2022b)
Ginseng-Sanqi-Chuanxiong (GSC) extracts	LC3B, Beclin-1, P62/SQTM1, Parkin, Pink1	<i>In vitro</i>	HG/PA-induced HAEC	Wang et al. (2020b)
Aqueous anise extract	Beclin-1	<i>In vivo</i>	Rat model induced by STZ	Faried and El-Mehi (2020)
Ginseng lotus extract	LC3B, P62	<i>In vivo</i>	Ligate and reperfusion of the left anterior descending artery of rat	Li (2022)

TABLE 4 TCM compounds counteract the effects of diabetic vascular injury by regulating autophagic flux.

Chinese herbal compound preparations	Herbal composition	Autophagy-related targets	<i>In vitro</i> / <i>In vivo</i>	Model	References
Yigan Mingmu decoction	<i>Bupleurum</i> , <i>angelica</i> , <i>white peony</i> , <i>ligusticum wallichii</i> , <i>salvia miltiorrhiza</i> , <i>poria cocos</i> , <i>plantain seed</i> , <i>flos Buddlejae</i> , <i>tribulus terrestris</i> , <i>rhizoma alismatis</i> , <i>motherwort fruit</i> , <i>cassia seed</i>	LC3B	<i>In vivo</i>	SD rat model induced by STZ	Wang (2021)
Danzhi Jiangtang Capsules	<i>Radix pseudostellariae</i> , <i>rehmannia glutinosa</i> , <i>Peony bark</i> , <i>rhizoma alismatis</i> , <i>dodder</i> , <i>leech</i>	Beclin-1, ATG5, LC3B	<i>In vivo</i>	GK lower limb ischemic rats	Ni et al. (2018)
Huoxue Jiedu Jiangtang decoction	<i>Ginseng</i> , <i>ophiopogon japonicus</i> , <i>schisandra chinensis</i> , <i>cornus officinalis</i> , <i>birthplace</i> , <i>rhizoma dioscoreae</i> , <i>rheum officinale</i> , <i>turtle shell</i> , <i>peach kernel</i> , <i>peony bark</i> , <i>coptis chinensis</i>	LC3B, Beclin-1	<i>In vivo</i>	Rat model induced by STZ and high-fat diet	Fu et al. (2023)
Mingmu Xiaomeng tablets	<i>Pearl powder</i> , <i>grape</i> , <i>zinc acid</i>	LC3B, P62/SQTM1	<i>In vivo</i>	Rat model induced by STZ	Fang (2020)
Huangqi Gegen Decoction Combined with Gualou Decoction	<i>Astragalus membranaceus</i> , <i>pueraria lobata</i> , <i>fructus trichosanthis</i> , <i>myrrh</i> , <i>licorice</i>	Beclin-1	<i>In vivo</i>	SD rat model induced by STZ and high-fat diet	Bi, (2023)
Buyang Huanwu Decoction	<i>Astragalus membranaceus</i> , <i>angelica sinensis tail</i> , <i>red peony</i> , <i>earthworm</i> , <i>ligusticum wallichii</i> , <i>peach kernel</i> , <i>safflower</i>	LC3B, Beclin-1	<i>In vitro</i>	HG-induced HRCECs	Shi et al. (2022)

are usually defined by vascular endothelial lesions. However, whether endothelial cells can switch from a quiescent state to a highly active state under high glucose stimulation, hindering vascular stability, and whether this process is related to diabetic vascular complications remain unclear. Survivin had been identified as an anti-apoptotic protein in tumors or epithelial cells, promoting proliferation or inhibiting cell apoptosis. Therefore, Xu et al. (2018) investigated the effects of high glucose on endothelial cell function and the potential involvement of survivin. They found that high glucose did not cause endothelial damage, but significantly promoted vascular endothelial cell proliferation and angiogenic capacity, indicating endothelial cell dysfunction characterized by a bias towards high activity. Simultaneously, upregulation of survivin was detected along with increased key components of the autophagic pathway, including LC3, Beclin-1, and p62. YM155 was a specific survivin inhibitor that could eliminate high glucose-induced endothelial hyperactivation. The application of

autophagy inhibitor (3 MA) and agonist (rapamycin) supported the idea that survivin could act as a downstream effect or autophagy. These data suggest that the survivin/autophagy axis is a potential therapeutic target for diabetic vascular complications. 3) Regulating inflammatory response of vascular endothelial cells: Aging vascular endothelial cells often produce more inflammatory factors, leading to increased inflammation. Autophagy can inhibit the inflammatory response of vascular endothelial cells and reduce the occurrence of vascular endothelial senescence by regulating inflammation-related signaling pathways. Studies have shown that neutrophil migration from the circulation to infected or injured sites is a crucial immune response, which requires the disruption of endothelial cells on the inner side of blood vessels. Unregulated neutrophil transendothelial migration is pathogenic, but its physiological termination molecular basis is still unknown. As Reglero-Real et al. (2021) demonstrated that venular endothelial cells in inflamed tissues could exhibit strong autophagic responses, which are time-consistent with the peak of

neutrophil transport and strictly localized to endothelial cell contacts. Meanwhile, in a mouse inflammation model, genetic ablation of autophagy in endothelial cells led to excessive neutrophil TEM and uncontrolled leukocyte migration, while pharmacological induction of autophagy inhibited neutrophil infiltration into tissues. Mechanistically, autophagy regulated the remodeling of endothelial cell junctions and the expression of key endothelial cell adhesion molecules, thus promoting intracellular transport and degradation. This study suggests that autophagy is an important regulator of leukocyte transport mechanisms in endothelial cells aimed at terminating physiological inflammation. Diabetic retinopathy (DR) is a chronic, progressive, and potentially harmful retinal disease associated with persistent hyperglycemia. Yu et al. (2023) established a DR model using high glucose-treated human retinal microvascular endothelial cells (HRMECs) and stachydrine (STA, a water-soluble alkaloid extracted from *Leonurus heterophyllus*) treatment in rats. They used corresponding kits to determine levels of ROS and inflammatory factors (including TNF- α , IL-1 β , and IL-6), CCK-8 and EDU staining assays to analyze cellular growth, and immunofluorescence and Western blot techniques to detect the expression levels of LC3B-II, p62, p-AMPK α , AMPK α , and SIRT1 proteins. The results showed that STA decreased ROS and inflammatory factor levels in HRMECs treated with high glucose. Furthermore, after STA treatment, the protein levels of Beclin-1, LC3B-II, p-AMPK α , and SIRT1 increased in HRMECs treated with high glucose and STA-treated rat retinal tissues, while the level of p62 protein decreased. This study indicates that STA can effectively alleviate inflammation and promote DR progression via activating the AMPK/SIRT1 signaling pathway *in vitro* and *in vivo*.

All in all, autophagy plays an important role in endothelial aging within blood vessels. Autophagy can maintain the function and stability of endothelial cells by clearing aged cells and damaged substances, as well as regulating inflammatory responses, thereby maintaining the health state of endothelial cells. Therefore, further research on the regulatory mechanism of autophagy in endothelial cell aging may help develop new therapeutic strategies to delay vessel aging and related diseases.

4 Active compounds from Chinese herbs relieve diabetic vasculopathy by regulating autophagy

In recent years, more and more scholars have pointed out that Chinese herbs have a feature of “multi-component, multi-target, multi-pathway”, which not only conforms to the holistic thinking in traditional Chinese medicine but also fits the complex and changeable process of diabetes and its complications. In addition, according to the research of modern pharmacology, Chinese herbs and their active compounds not only have broad biological activities (such as antioxidant, anti-inflammatory, and anti-tumor) (Wang et al., 2013; Luo et al., 2019; Zhang Q. et al., 2021), but these substances have also been proven to be relatively safe, especially with less toxicity to liver and kidney (Yang et al., 2018; Liu et al., 2020; Zulkifli et al., 2023). Therefore, Chinese herbs (including single-flavor drugs and compound formulations) and their active substances are increasingly considered alternative sources for regulating patients with diabetes and its complications (Table 2–4).

4.1 Compound Chinese herbal formulas alleviate diabetic vasculopathy by regulating autophagy

Yigan Mingmu decoction has the functions of soothing the liver and improving eyesight, as well as promoting blood circulation and diuresis. It is a Chinese herbal compound formulation that can improve retinal lesions in diabetic patients. Some researchers have confirmed through *in vivo* and *in vitro* experiments that Yigan Mingmu decoction can reduce the relative expression of TXNIP on Müller cells in the retina, keeping its autophagic level in balance, so as to damage mitochondria produced by oxidative stress can be eliminated through complete autophagy pathways, thus avoiding the release of inflammatory factors and reducing apoptosis and necrosis of cells, thereby exerting protective effects on the retina (Wang S. et al., 2021).

Danzhi Jiangtang Capsules is a Chinese herbal compound formula that has been used at Anhui Provincial Hospital of TCM for decades. In previous studies, it was found that Danzhi Jiangtang Capsules could alleviate calcification of diabetic rat lower limb endothelial cells, and the mechanism was to downregulate the expression of β -catenin in the nucleus, reduce the synthesis of β -catenin protein, thereby inhibiting the transcription of downstream cell phenotype genes, so as to achieve the purpose of preventing endothelial cell vascular calcification (Ni et al., 2023). In addition, Danzhi Jiangtang Capsules could activate the VEGF/Akt/eNOS and Ang/Tie2 signaling pathways that are suppressed in diabetic vascular lesions, thereby promoting the dissociation of the basement membrane of blood vessels, preparing for the initiation of angiogenesis, and ultimately promoting the regeneration of lower limb blood vessels (Li, 2017; Ni et al., 2020). Notably, a recent study found that Danzhi Jiangtang Capsules could promote angiogenesis and treat diabetic lower extremity vascular lesions by inhibiting the expression level of genes related to the mTOR pathway, inducing the formation of autophagosomes, and activating autophagy. Meanwhile, based on the network pharmacology and the molecular docking technology, it was found that Danzhi Jiangtang Capsules had multiple components, multiple targets, and multiple pathways for treating diabetic complications. Among them, 12 key components (including quercetin, luteolin, kaempferol, crocetin, paeoniflorin, ursolic acid, isorhamnetin, β -sitosterol, jingniping glycoside, gardnerin A, alexin, and hyperin) and 17 core targets (including AKT1, TNF, IL6, IL1B, VEGFA, TP53, CASP3, JUN, EGFR, STAT3, FN1, PPARG, MYC, MMP9, PTGS2, CXCL8, and CCL2) were enriched. Its mechanism of action might be related to inhibiting inflammation, reducing oxidative stress, regulating cell apoptosis, adjusting immune response, and autophagy regulation (Ni et al., 2018).

Interestingly, TCM formula not only has a certain effect on microcirculation vessels, but also has protective effects on large blood vessels, which are gradually being studied by scholars. Huoxue Jiedu Jiangtang decoction is a traditional Chinese herbal formula that can improve the large blood vessel lesions of diabetic patients. Previous studies had shown that Huoxue Jiedu Jiangtang decoction could reduce the inflammation response in diabetic rats, reduce

aortic cell apoptosis, inhibit the coupling of endoplasmic reticulum stress and inflammation response, so as to improve the arterial damage caused by diabetes (Fu et al., 2019; Cao et al., 2020). Notably, recent research had shown that Huoxue Jiedu Jiangtang decoction could affect the development of diabetic atherosclerosis through the autophagy pathway. As Fu et al. (2023) used streptozotocin (STZ) abdominal injection and high-fat feeding to establish a diabetic model and used aortic balloon injury to establish an atherosclerosis model. Meanwhile, blood was taken to detect glycated hemoglobin and serum triglyceride (TG), low-density lipoprotein cholesterol (LDL-C) levels, H&E staining was used to observe the pathological morphology of the aorta, and transmission electron microscopy (TEM) was used to observe autophagy phenomena and ultrastructures in aortic cells. RT-PCR was used to detect the expression levels of IRE-1, TRAF2, and GRP78 mRNA in aortic tissue, and Western blot was used to detect the expression of Beclin1 and LC3II proteins in aortic tissue. This study showed that Huoxue Jiedu Jiangtang decoction could protect the aorta by inhibiting ER stress caused by diabetic metabolic disorders, regulating endoplasmic reticulum homeostasis, and inhibiting excessive autophagy of aortic endothelial cells.

4.2 Single-flavor drug alleviates diabetic vasculopathy by regulating autophagy

Ginger, as a common and widely used spice, is rich in various chemical components, including phenolic compounds, terpenes, polysaccharides, lipids, organic acids, and fibrils (Zhou et al., 2021). Recent studies had found that ginger could have a certain effect on the vascular system. On the one hand, using cell cultures or animal models had shown that the active ingredients in ginger could alleviate oxidative stress and inflammation, increase NO synthesis, inhibit the proliferation of vascular smooth muscle cells, promote cholesterol excretion by macrophages, inhibit angiogenesis, block voltage-dependent Ca^{2+} channels, and induce autophagy (Li C. et al., 2021). On the other hand, in some clinical trials, ginger had been shown to have beneficial effects on blood lipids, inflammatory cytokines, blood pressure, and platelet aggregation (Daniels et al., 2022). These studies pointed to the potential benefits of ginger and its components in the treatment of vascular-related diseases (including hypertension, coronary artery disease, diabetes and so on).

In addition, studies had shown that ginkgo biloba extract could restore autophagic flux through the mTOR signaling pathway to inhibit ER stress, thus reducing atherosclerosis in diabetic ApoE^{-/-} mice induced by STZ (Tian et al., 2019).

High glucose-induced vascular endothelial cell injury plays an important role in the development of diabetic vascular complications. Studies had shown that yellow tea had a protective effect on vascular endothelial cells. As Wang et al. (2022) studied the effect of n-butanol fraction of Huoshan large-left yellow tea extract (HLYTE) on high glucose-induced vascular endothelial cell injury by using HUVECs and diabetic mice as research subjects. In this study, they found that the extract of HLYTE could upregulate autophagy through the AMPK/mTOR pathway and inhibit oxidative stress response, thereby protecting vascular endothelial cells from high glucose-induced injury.

4.3 Active compounds alleviate diabetic vasculopathy by regulating autophagy

There is growing evidence that active compounds abundant in TCM can alleviate diabetic vascular injury through autophagy pathway. Salvianolic acid B is a non-protein amino acid in *Salvia miltiorrhiza* Bge. With a wide range of biological activities. Recent studies had found that Salvianolic acid B could alleviate diabetic endothelial and mitochondrial dysfunction by down-regulating endothelial cell apoptosis and mitochondrial autophagy (including Beclin-1, Parkin, Pink1 targets), thereby improving diabetic-induced vascular complications (Xiang et al., 2022).

Notoginsenoside R1 is a novel saponin extracted from *Panax notoginseng* (Burkill) F. H. Chen ex C. H. Chow with pharmacological properties, including treating diabetic encephalopathy, improving microcirculation disorders, and so on. As Zhou et al. (2019) found that the retinal vascular degeneration, retinal thickness reduction, and retinal function impairment in db/db mice were significantly alleviated after 12 weeks of oral administration of notoginsenoside R1 (30 mg/kg). Meanwhile, pre-treatment with notoginsenoside R1 significantly inhibited apoptosis of retinal Müller cells (rMC-1) in high glucose-induced rats and db/db mice, and suppressed oxidative stress and inflammation by inhibiting VEGF expression and increasing PEDF expression. Moreover, pre-treatment with notoginsenoside R1 upregulated the levels of PINK3 and Parkin in high glucose-induced rMC-1 cells and db/db mouse retinal cells, increased the LC3-II/LC3-I ratio, downregulated the levels of p62/SQSTM1, and enhanced the co-localization of GFP-LC1 puncta and MitoTracker in rMC-3 cells. In summary, this study demonstrated that notoginsenoside R1 could improve diabetic retinopathy by activating mitochondrial autophagy through PINK1-dependent mechanism. Notoginsenoside Fc is another novel saponin isolated from the leaves of *Panax notoginseng* (Burkill) F. H. Chen ex C. H. Chow. Numerous pharmacological activities of notoginsenoside Fc, such as anti-oxidant, anti-inflammatory, and anti-tumor effects, have been confirmed by many scholars as folk medicine or dietary supplement (Huang and Tian, 2016; Gong and Zhuang, 2022; Niu et al., 2023). In the terms of blood vessels, notoginsenoside Fc not only effectively counteracts the aggregation of platelet, but also shows potential benefits for re-endothelialization (Liu et al., 2018; Zhang X.-F. et al., 2023). Notably, interventional therapies, such as percutaneous transluminal angioplasty and endovascular stent implantation, have been widely used for treating diabetic peripheral vascular complications. However, re-endothelialization is an essential process after vascular injury during interventional therapy, and hyperglycemia in diabetes plays a crucial role in disrupting endothelial layer integrity, leading to delayed re-endothelialization and excessive intimal proliferation. Interestingly, as Liu et al. (2019a) found that notoginsenoside Fc could accelerate re-endothelialization after vascular injury in diabetic rats by promoting endothelial cell autophagy (including LC3B, Beclin-1, P62/SQSTM1 targets), indicating that notoginsenoside Fc might have therapeutic benefits for early endothelial damage and restenosis after intervention for diabetes-related vascular diseases.

Glycyrrhizic acid is the main active component of TCM *Glycyrrhiza uralensis* Fisch. Previous studies had shown that

glycyrrhizic acid had a wide range of pharmacological effects, such as anti-oxidation, anti-inflammation, anti-viral, anti-cancer, and so on (Wang and Du, 2016; Sun et al., 2019; Asseri et al., 2022; Zhang Y. et al., 2023). In addition, many pieces of evidence had confirmed that glycyrrhizic acid could have certain improvement effects on diabetes and its related complications. It was reported that diabetes complications could further affect many organs and systems, including oral tissues and salivary glands. Among them, salivary glands played a vital role in maintaining oral homeostasis, and the parotid gland, submandibular gland, and sublingual gland were the main salivary glands responsible for synthesizing saliva. During the development of diabetes, the salivary glands could be negatively affected, leading to reduce saliva secretion, periodontal tissue damage, and reduce salivary function, oral mucosal lesions. Notably, recent studies had shown that glycyrrhizic acid might improve diabetes-induced sublingual gland damage by regulating oxidative stress, autophagy (including LC3B, Beclin-1, P62/SQTM1 targets), and angiogenesis, so as to restore the homeostasis of oral environment (Asseri et al., 2022).

Scutellarin is one of the main active components of TCM *Scutellaria baicalensis* Georgi. It has been reported that scutellarin has been used to treat cardiovascular diseases and vascular dysfunction caused by diabetes (Sun et al., 2017; Su et al., 2022; Huang et al., 2023). In addition, scutellarin also has a protective effect on vascular endothelial cells, preventing hyperglycemia. As Xi et al. (2021) exposed HUVECs to a high-sugar environment to induce *in vitro* vascular endothelial cell damage, and evaluated cell viability by using the MTT assay, Hoechst33342 staining, and flow cytometry to measure the degree of cell apoptosis, using immunofluorescence staining, TEM, and Western blot to determine the changes in mitochondrial autophagic flux, their findings revealed that scutellarin could protect vascular endothelial cells from high-sugar-induced damage by up-regulating mitochondrial autophagy through the PINK1/Parkin signaling pathway, and also provided a theoretical basis and experimental support for scutellarin as a candidate drug for diabetes-induced vascular dysfunction.

5 Conclusions and future directions

With the development of modern society, the number of patients with diabetic complications and vascular lesions is increasing. Due to the extremely complex etiology of diabetic vascular lesions, single-treatment methods based on autophagy are often ineffective, while TCM has unique advantages in the treatment of diabetic vascular lesions. There are two main reasons for this phenomenon: on the one hand, since the mechanism of autophagy can involve multiple signaling pathways, it is often difficult for drugs with a single target to consider multiple pathways. Moreover, Chinese herbal medicine can not only play a role through multiple targets, but also consider multiple targets of autophagy in diabetic vascular lesions. On the other hand, Chinese herbal medicine and its active ingredients have been proven to be safe, especially the toxic damage to the liver and kidneys is relatively small. For example, Yigan Mingmu decoction, Danzhi Jiangtang capsules, and Huoxue Jiedu Jiangtang decoction have been used in China for thousands of years. Notably, in view of

the TCM preparation in the complex components, cumbersome process and other objective problems, in recent years, many scholars have attempted to separate active ingredients from clinically effective Chinese herbal compound preparations through chemical methods, and apply these active ingredients to cell or animal experiments to elucidate the mechanism of action of Chinese herbal preparations.

At present, there are many shortcomings in the research on autophagy regulation in diabetic vascular lesions in Chinese herbal medicine. The research on autophagy regulation mechanism of diabetic vascular lesions in Chinese herbal medicine is still in the stage of observational research, lacking in-depth exploration of mechanism. This is partly due to the use of natural products in Chinese herbal medicine, which are characterized by confusion. Therefore, more standardization and larger-scale clinical studies are needed to promote the more widespread acceptance of Chinese herbal medicine treatment for patients with diabetic vascular lesions.

Author contributions

YG: Data curation, Formal Analysis, Writing—original draft. LZ: Data curation, Formal Analysis, Writing—original draft. FZ: Data curation, Investigation, Methodology, Writing—review and editing. RL: Investigation, Methodology, Writing—review and editing. LL: Investigation, Methodology, Writing—review and editing. XL: Investigation, Methodology, Software, Writing—review and editing. XZ: Conceptualization, Writing—review and editing. YL: Conceptualization, Funding acquisition, Writing—review and editing.

Funding

The author(s) declare that financial support was received for the research, authorship, and/or publication of this article. This present study was supported by the National Natural Science Foundation of China, Grant/Award Number: 82360914, and the Gansu Provincial Department of Education Project, Grant/Award Number: 2021CYZC-03.

Conflict of interest

The authors declare that the research was conducted in the absence of any commercial or financial relationships that could be construed as a potential conflict of interest.

Publisher's note

All claims expressed in this article are solely those of the authors and do not necessarily represent those of their affiliated organizations, or those of the publisher, the editors and the reviewers. Any product that may be evaluated in this article, or claim that may be made by its manufacturer, is not guaranteed or endorsed by the publisher.

References

- Abeliovich, H., and Klionsky, D. J. (2001). Autophagy in yeast: mechanistic insights and physiological function. *Microbiol. Mol. Biol. Rev.* 65, 463–479. doi:10.1128/MMBR.65.3.463-479.2001
- Asseri, S. M., Elsherbiny, N. M., El-Sherbiny, M., Sherif, I. O., Alsamman, A. M., Maysarah, N. M., et al. (2022). Glycyrrhizic acid ameliorates submandibular gland oxidative stress, autophagy and vascular dysfunction in rat model of type 1 diabetes. *Sci. Rep.* 12, 725. doi:10.1038/s41598-021-04594-w
- Backer, J. M. (2008). The regulation and function of Class III PI3Ks: novel roles for Vps34. *Biochem. J.* 410, 1–17. doi:10.1042/BJ20071427
- Ballesteros-Álvarez, J., and Andersen, J. K. (2021). mTORC2: the other mTOR in autophagy regulation. *Aging Cell* 20, e13431. doi:10.1111/accel.13431
- Bi, D.-Y. (2023). Study on the mechanism of action of Astragalus Gegen decoction and Gualuo decoction based on SIRT1 signal on diabetic atherosclerotic rats. *Liaoning Univ. Trad. Chin. Med.* 5, 1–70. doi:10.27213/d.cnki.glnzc.2023.000626
- Brodsky, S. V., Gealekman, O., Chen, J., Zhang, F., Togashi, N., Crabtree, M., et al. (2004). Prevention and reversal of premature endothelial cell senescence and vasculopathy in obesity-induced diabetes by ebsele. *Circ. Res.* 94, 377–384. doi:10.1161/01.RES.0000111802.09964.EF
- Cao, G.-Y., Liu, T.-Z., Wang, W.-Z., Wang, L., Liu, Y.-J., and Li, N. (2020). Effect of Huoxue detoxification and hypoglycemic formula on the balance of pro-inflammatory/Anti-inflammatory factors in patients with acute coronary syndrome of diabetes mellitus and non-revascularization. *Mod. J. Integr. Trad. Chin. West Med.* 29, 1430–1433. doi:10.3969/j.issn.1008-8849.2020.13.015
- Cao, Y., and Klionsky, D. J. (2007). Physiological functions of Atg6/Beclin 1: a unique autophagy-related protein. *Cell Res.* 17, 839–849. doi:10.1038/cr.2007.78
- Chen, F., Chen, B., Xiao, F.-Q., Wu, Y.-T., Wang, R.-H., Sun, Z.-W., et al. (2014). Autophagy protects against senescence and apoptosis via the RAS-mitochondria in high-glucose-induced endothelial cells. *Cell Physiol. Biochem.* 33, 1058–1074. doi:10.1159/000358676
- Chen, J.-J. (2018). Research progress in clinical drug therapy in patients with diabetic vascular disease. *Card. Dis. Elect. J. Integra Trad. Chin. West Med.* 6, 22. doi:10.16282/j.cnki.cn11-9336/r.2018.06.013
- Cheng, Z. (2019). The FoxO-autophagy Axis in health and disease. *Trends Endocrinol. Metab.* 30, 658–671. doi:10.1016/j.tem.2019.07.009
- Daniels, C. C., Isaacs, Z., Finelli, R., and Leisegang, K. (2022). The efficacy of Zingiber officinale on dyslipidaemia, blood pressure, and inflammation as cardiovascular risk factors: a systematic review. *Clin. Nutr. ESPEN* 51, 72–82. doi:10.1016/j.clnesp.2022.08.031
- Devkota, S. (2017). The autophagy process. *Oncotarget* 8, 18623. doi:10.18632/oncotarget.15951
- Đluhońska, H. (2017). Autophagy as a universal intracellular process. A comment on the 2016 Nobel prize in Physiology or medicine. *Ann. Parasitol.* 63, 153–157. doi:10.17420/ap6303.100
- Eelen, G., de Zeeuw, P., Simons, M., and Carmeliet, P. (2015). Endothelial cell metabolism in normal and diseased vasculature. *Circ. Res.* 116, 1231–1244. doi:10.1161/CIRCRESAHA.116.302855
- Fan, L., Zhang, X., Huang, Y., Zhang, B., Li, W., Shi, Q., et al. (2023). Homoplantagin attenuates high glucose-induced vascular endothelial cell apoptosis through promoting autophagy via the AMPK/TFEB pathway. *Phytother. Res.* 37, 3025–3041. doi:10.1002/ptr.7797
- Fang, Y.-W. (2020). The mechanism of autophagy on diabetic retinopathy is regulated through the PI3K/Akt/mTOR pathway. *Guangzhou Univ. Chin. Med.* 2, 1–85. doi:10.27044/d.cnki.ggzuz.2020.000841
- Farié, M. A., and El-Mehi, A. E. S. (2020). Aqueous anise extract alleviated the pancreatic changes in streptozotocin-induced diabetic rat model via modulation of hyperglycaemia, oxidative stress, apoptosis and autophagy: a biochemical, histological and immunohistochemical study. *Folia Morphol. Warsz.* 79, 489–502. doi:10.5603/FM.a2019.0117
- Farrell, F. O., Rusten, T. E., and Stenmark, H. (2013). Phosphoinositide 3-kinases as accelerators and brakes of autophagy. *FEBS J.* 280, 6322–6337. doi:10.1111/febs.12486
- Fu, X.-Z., Huang, W.-H., Wang, N.-L., Li, X.-C., Qiu, H.-X., Cao, Q.-X., et al. (2019). Experimental study on the effect of blood detoxification and hypoglycemic formula on atherosclerotic endoplasmic reticulum stress in diabetic rats. *Chin. J. Integra Med. Cardio-Cereb Dis.* 17, 3702–3707.
- Fu, X.-Z., Jiang, X.-F., Chen, J.-J., and Shen, Y.-Y. (2023). The effect of blood activation, detoxification and hypoglycemic formula on diabetic atherosclerosis was discussed based on the theory of autophagy. *Mod. J. Interga Trad. Chin. West Med.* 32, 1899–1905.
- Gimbrone, M. A., and Garcia-Cardena, G. (2016). Endothelial cell dysfunction and the pathobiology of atherosclerosis. *Circ. Res.* 118, 620–636. doi:10.1161/CIRCRESAHA.115.306301
- Glick, D., Barth, S., and Macleod, K. F. (2010). Autophagy: cellular and molecular mechanisms. *J. Pathol.* 221, 3–12. doi:10.1002/path.2697
- Goi, T., Kawasaki, M., Yamazaki, T., Koneri, K., Katayama, K., Hirose, K., et al. (2003). Ascending colon cancer with hepatic metastasis and cholecystolithiasis in a patient with situs inversus totalis without any expression of UVRAG mRNA: report of a case. *Surg. Today* 33, 702–706. doi:10.1007/s00595-002-2567-y
- Gong, W.-L., and Zhuang, H.-T. (2022). Research progress on anti-tumor effect of panax notoginseng saponins. *J. Pharm. Res.* 41, 183–186. doi:10.13506/j.cnki.jpr.2022.03.011
- Gremke, N., Polo, P., Dort, A., Schneikert, J., Elmshäuser, S., Brehm, C., et al. (2020). mTOR-mediated cancer drug resistance suppresses autophagy and generates a druggable metabolic vulnerability. *Nat. Commun.* 11, 4684. doi:10.1038/s41467-020-18504-7
- Gu, Z., Cao, H., Zuo, C., Huang, Y., Miao, J., Song, Y., et al. (2022). TFEB in Alzheimer's disease: from molecular mechanisms to therapeutic implications. *Neurobiol. Dis.* 173, 105855. doi:10.1016/j.nbd.2022.105855
- He, R., Wang, M., Zhao, C., Shen, M., Yu, Y., He, L., et al. (2019). TFEB-driven autophagy potentiates TGF- β induced migration in pancreatic cancer cells. *J. Exp. Clin. Cancer Res.* 38, 340. doi:10.1186/s13046-019-1343-4
- Huang, B., Han, R., Tan, H., Zhu, W., Li, Y., Jiang, F., et al. (2023). Scutellarin ameliorates diabetic nephropathy via TGF- β 1 signaling pathway. *Biol. Pharm. Bull.* b23-00390. doi:10.1248/bpb.b23-00390
- Huang, J.-L., and Tian, D.-X. (2016). Research progress on anti-inflammatory immunopharmacology of notoginseng saponins. *Chin. J. Trad. Chin. Med. Pharm.* 31, 4657–4660.
- Iida, A., Emi, M., Matsuoka, R., Hiratsuka, E., Okui, K., Ohashi, H., et al. (2000). Identification of a gene disrupted by inv(11)(q13.5;q25) in a patient with left-right axis malformation. *Hum. Genet.* 106, 277–287. doi:10.1007/s004390051038
- Inbal, B., Bialik, S., Sabanay, I., Shani, G., and Kimchi, A. (2002). DAP kinase and DRP-1 mediate membrane blebbing and the formation of autophagic vesicles during programmed cell death. *J. Cell Biol.* 157, 455–468. doi:10.1083/jcb.200109094
- Ionov, Y., Nowak, N., Perucho, M., Markowitz, S., and Cowell, J. K. (2004). Manipulation of nonsense mediated decay identifies gene mutations in colon cancer Cells with microsatellite instability. *Oncogene* 23, 639–645. doi:10.1038/sj.onc.1207178
- Kale, J., Osterlund, E. J., and Andrews, D. W. (2018). BCL-2 family proteins: changing partners in the dance towards death. *Cell Death Differ.* 25, 65–80. doi:10.1038/cdd.2017.186
- Kim, H.-S., Montana, V., Jang, H.-J., Pargura, V., and Kim, J. (2013). Epigallocatechin gallate (EGCG) stimulates autophagy in vascular endothelial cells: a potential role for reducing lipid accumulation. *J. Biol. Chem.* 288, 22693–22705. doi:10.1074/jbc.M113.477505
- Kim, J., Kim, S. H., Kang, H., Lee, S., Park, S.-Y., Cho, Y., et al. (2021). TFEB-GDF15 axis protects against obesity and insulin resistance as a lysosomal stress response. *Nat. Metab.* 3, 410–427. doi:10.1038/s42255-021-00368-w
- Kim, J., Kundu, M., Viollet, B., and Guan, K.-L. (2011). AMPK and mTOR regulate autophagy through direct phosphorylation of Ulk1. *Nat. Cell Biol.* 13, 132–141. doi:10.1038/ncb2152
- Kim, M. S., Jeong, E. G., Ahn, C. H., Kim, S. S., Lee, S. H., and Yoo, N. J. (2008). Frameshift mutation of UVRAG, an autophagy-related gene, in gastric carcinomas with microsatellite instability. *Hum. Pathol.* 39, 1059–1063. doi:10.1016/j.humpath.2007.11.013
- Kim, Y. C., and Guan, K.-L. (2015). mTOR: a pharmacologic target for autophagy regulation. *J. Clin. Invest.* 125, 25–32. doi:10.1172/JCI73939
- Li, C., Li, J., Jiang, F., Tzvetkov, N. T., Horbanczuk, J. O., Li, Y., et al. (2021a). Vasculoprotective effects of ginger (Zingiber officinale Roscoe) and underlying molecular mechanisms. *Food Funct.* 12, 1897–1913. doi:10.1039/d0fo02210a
- Li, F., Yuan, L., Shao, N., Yang, X., Yang, S., He, L., et al. (2023a). Changes and significance of vascular endothelial injury markers in patients with diabetes mellitus and pulmonary thromboembolism. *BMC Pulm. Med.* 23, 183. doi:10.1186/s12890-023-02486-5
- Li, J.-J. (2022). Based on mitochondrial function, the effect and mechanism of ginseng lotus extract in protecting microvessels and preventing non-reflow were studied. *Chin. Acad. Chin. Med. Sci.* 2022, 58. doi:10.27658/d.cnki.gzzzy.2022.000058
- Li, J.-L. (2017). Study on the clinical intervention of lower limb vascular lesions in early diabetes mellitus and the effect of Dan Leech hypoglycemic capsule on the expression of Ang1, Ang2 and Tie2 proteins in rats. *Anhui Univ. Trad. Chin. Med.* 3, 1–74.
- Li, L., Chen, J., Zhou, Y., Zhang, J., and Chen, L. (2023b). Artesunate alleviates diabetic retinopathy by activating autophagy via the regulation of AMPK/SIRT1 pathway. *Arch. Physiol. Biochem.* 129, 943–950. doi:10.1080/13813455.2021.1887266
- Li, S., Zhan, J.-K., Wang, Y.-J., Lin, X., Zhong, J.-Y., Wang, Y., et al. (2019). Exosomes from hyperglycemia-stimulated vascular endothelial cells contain versican that regulate calcification/senescence in vascular smooth muscle cells. *Cell Biosci.* 9, 1. doi:10.1186/s13578-018-0263-x
- Li, W., He, P., Huang, Y., Li, Y.-F., Lu, J., Li, M., et al. (2021b). Selective autophagy of intracellular organelles: recent research advances. *Theranostics* 11, 222–256. doi:10.7150/thno.49860

- Li, X., He, L., Che, K. H., Funderburk, S. F., Pan, L., Pan, N., et al. (2012). Imperfect interface of Beclin1 coiled-coil domain regulates homodimer and heterodimer formation with Atg14L and UVRAG. *Nat. Commun.* 3, 662. doi:10.1038/ncomms1648
- Liang, C., Lee, J., Inn, K., Gack, M. U., Li, Q., Roberts, E. A., et al. (2008). Beclin1-binding UVRAG targets the class C Vps complex to coordinate autophagosomal maturation and endocytic trafficking. *Nat. Cell Biol.* 10, 776–787. doi:10.1038/ncb1740
- Lindqvist, L. M., Heinlein, M., Huang, D. C. S., and Vaux, D. L. (2014). Prosurvival Bcl-2 family members affect autophagy only indirectly, by inhibiting Bax and Bak. *Proc. Natl. Acad. Sci. U. S. A.* 111, 8512–8517. doi:10.1073/pnas.1406425111
- Lindqvist, L. M., and Vaux, D. L. (2014). BCL2 and related prosurvival proteins require BAK1 and BAX to affect autophagy. *Autophagy* 10, 1474–1475. doi:10.4161/auto.29639
- Liu, H., Wang, X., Gao, H., Yang, C., and Xie, C. (2023). Physiological and pathological characteristics of vascular endothelial injury in diabetes and the regulatory mechanism of autophagy. *Front. Endocrinol. (Lausanne)* 14, 1191426. doi:10.3389/fendo.2023.1191426
- Liu, J., Jiang, C., Ma, X., Feng, L., and Wang, J. (2019a). Notoginsenoside Fc accelerates reendothelialization following vascular injury in diabetic rats by promoting endothelial cell autophagy. *J. Diabetes Res.* 2019, 9696521. doi:10.1155/2019/9696521
- Liu, J., Liu, W., and Yang, H. (2019b). Balancing apoptosis and autophagy for Parkinson's disease therapy: targeting BCL-2. *ACS Chem. Neurosci.* 10, 792–802. doi:10.1021/acscchemneuro.8b00356
- Liu, J.-J., Ma, X., Feng, L.-S., and Wang, J.-B. (2018). Protective effect of notoginsenoside Fc on vascular endothelial cell against injury induced by high glucose. *J. Med. Res.* 47, 112–115+120. doi:10.11969/j.issn.1673-548X.2018.08.026
- Liu, R., Li, X., Huang, N., Fan, M., and Sun, R. (2020). Toxicity of traditional Chinese medicine herbal and mineral products. *Adv. Pharmacol.* 87, 301–346. doi:10.1016/bbs.apha.2019.08.001
- Luo, H., Vong, C. T., Chen, H., Gao, Y., Lyu, P., Qiu, L., et al. (2019). Naturally occurring anti-cancer compounds: shining from Chinese herbal medicine. *Chin. Med.* 14, 48. doi:10.1186/s13020-019-0270-9
- Luo, Y., Dong, X., Lu, S., Gao, Y., Sun, G., and Sun, X. (2021). Gypenoside XVII alleviates early diabetic retinopathy by regulating Müller cell apoptosis and autophagy in db/db mice. *Eur. J. Pharmacol.* 895, 173893. doi:10.1016/j.ejphar.2021.173893
- Martens, S. (2018). A division of labor in mTORC1 signaling and autophagy. *Sci. Signal* 11, eaav3530. doi:10.1126/scisignal.aav3530
- Mohamed, D. Z., El-Sisi, A. E.-D., Sokar, S. S., Shebl, A. M., and Abu-Risha, S. E.-S. (2021). Targeting autophagy to modulate hepatic ischemia/reperfusion injury: a comparative study between octreotide and melatonin as autophagy modulators through AMPK/PI3K/AKT/mTOR/ULK1 and Keap1/Nrf2 signaling pathways in rats. *Eur. J. Pharmacol.* 897, 173920. doi:10.1016/j.ejphar.2021.173920
- Ni, Y.-Q., Fang, C.-H., Li, J.-Y., Shi, H., Yu, D.-D., Liu, G.-J., et al. (2023). Effect of Danzhi Jiangtang Capsule on regulating β -catenin protein on high phosphorus-induced calcification of vascular endothelial cell in lower limb in diabetic mice. *J. Tianjin Univ. Trad. Chin. Med.* 42, 81–86. doi:10.11656/j.issn.1673-9043.2023.01.16
- Ni, Y.-Q., Fang, C.-H., and Shi, H. (2020). Effect and mechanism of Danzhi Jiangtang Capsule on diabetic angiogenesis through regulating VEGF signaling pathway. *J. Beijing Univ. Trad. Chin. Med.* 43, 141–147. doi:10.3969/j.issn.1006-2157.2020.02.008
- Ni, Y.-Q., Zhao, J.-D., Liu, J., Guo, C.-L., and Fang, C.-H. (2018). The role and mechanism of mTOR-autophagy-mediated antihyperglycemic capsule in regulating angiogenesis of femoral artery endothelial cells in rats with diabetic vascular injury. *Chin. Assoc. Chin. Med.* 5, 218–219.
- Niu, S.-R., Wang, F.-Z., Cui, W.-Y., Me, Y., Kong, Z.-Q., Fan, B., et al. (2023). Research progress on the extraction, separation and purification of active ingredients of Panax notoginseng and its antioxidant activity. *J. Food Saf. Qual.* 14, 163–171. doi:10.19812/j.cnki.jfsq11-5956/ts.2023.19.017
- Noble, C. G., Dong, J.-M., Manser, E., and Song, H. (2008). Bcl-xL and UVRAG cause a monomer-dimer switch in Beclin1. *J. Biol. Chem.* 283, 26274–26282. doi:10.1074/jbc.M804723200
- Noda, T. (2017). Regulation of autophagy through TORC1 and mTORC1. *Biomolecules* 7, 52. doi:10.3390/biom7030052
- Ohsumi, Y. (2014). Historical landmarks of autophagy research. *Cell Res.* 24, 9–23. doi:10.1038/cr.2013.169
- Parzych, K. R., and Klionsky, D. J. (2014). An overview of autophagy: morphology, mechanism, and regulation. *Antioxid. Redox Signal* 20, 460–473. doi:10.1089/ars.2013.5371
- Perelman, B., Dafni, N., Naiman, T., Eli, D., Yaakov, M., Feng, T. L., et al. (1997). Molecular cloning of a novel human gene encoding a 63-kDa protein and its sublocalization within the 11q13 locus. *Genomics* 41, 397–405. doi:10.1006/geno.1997.4623
- Qi, Z., and Chen, L. (2019). Endoplasmic reticulum stress and autophagy. *Adv. Exp. Med. Biol.* 1206, 167–177. doi:10.1007/978-981-15-0602-4_8
- Rabanal-Ruiz, Y., Otten, E. G., and Korolchuk, V. I. (2017). mTORC1 as the main gateway to autophagy. *Essays Biochem.* 61, 565–584. doi:10.1042/EBC20170027
- Reglero-Real, N., Pérez-Gutiérrez, L., Yoshimura, A., Rolas, L., Garrido-Mesa, J., Barkaway, A., et al. (2021). Autophagy modulates endothelial junctions to restrain neutrophil diapedesis during inflammation. *Immunity* 54, 1989–2004.e9. doi:10.1016/j.immuni.2021.07.012
- Saftig, P., and Puertollano, R. (2021). How lysosomes sense, integrate, and cope with stress. *Trends Biochem. Sci.* 46, 97–112. doi:10.1016/j.tibs.2020.09.004
- Salabei, J. K., and Hill, B. G. (2013). Implications of autophagy for vascular smooth muscle cell function and plasticity. *Free Radic. Biol. Med.* 65, 693–703. doi:10.1016/j.freeradbiomed.2013.08.003
- Sanhueza-Olivares, F., Troncoso, M. F., Pino-de la Fuente, F., Martínez-Bilbao, J., Riquelme, J. A., Norambuena-Soto, I., et al. (2022). A potential role of autophagy-mediated vascular senescence in the pathophysiology of HFpEF. *Front. Endocrinol. (Lausanne)* 13, 1057349. doi:10.3389/fendo.2022.1057349
- Seglen, P. O., Gordon, P. B., and Holen, I. (1990). Non-selective autophagy. *Semin. Cell Biol.* 1, 441–448.
- Sha, W., Liu, M., Sun, D., Qiu, J., Xu, B., Chen, L., et al. (2021). Resveratrol improves Gly-LDL-induced vascular endothelial cell apoptosis, inflammatory factor secretion and oxidative stress by regulating miR-142-3p and regulating SPRED2-mediated autophagy. *Aging (Albany NY)* 13, 6878–6889. doi:10.18632/aging.202546
- Sha, Y., Rao, L., Settembre, C., Ballabio, A., and Eissa, N. T. (2017). STUB1 regulates TFEB-induced autophagy-lysosome pathway. *EMBO J.* 36, 2544–2552. doi:10.15252/emboj.201796699
- Shi, Y., Chen, Z.-Y., Chen, K.-M., Hu, Y.-H., Hu, J., and Chen, S. (2022). Effect of Buyang Huanwu decoction on miR-21-mediated autophagy of human retinal microvascular endothelial cells in a high-glucose environment. *Recent Adv. Ophthalmol.* 42, 858–862. doi:10.13389/j.cnki.rao.2022.0177
- Su, Y., Fan, X., Li, S., Li, Z., Tian, M., and Li, S. (2022). Scutellarin improves type 2 diabetic cardiomyopathy by regulating cardiomyocyte autophagy and apoptosis. *Dis. Markers* 2022, 3058354. doi:10.1155/2022/3058354
- Sun, X.-P., Wan, L.-L., Yang, Q.-J., Huo, Y., Han, Y.-L., and Guo, C. (2017). Scutellarin protects against doxorubicin-induced acute cardiotoxicity and regulates its accumulation in the heart. *Arch. Pharm. Res.* 40, 875–883. doi:10.1007/s12272-017-0907-0
- Sun, Z.-G., Zhao, T.-T., Lu, N., Yang, Y.-A., and Zhu, H.-L. (2019). Research progress of glycyrrhizic acid on antiviral activity. *Mini Rev. Med. Chem.* 19, 826–832. doi:10.2174/1389557519666190119111125
- Tan, A., Prasad, R., Lee, C., and Jho, E.-H. (2022). Past, present, and future perspectives of transcription factor EB (TFEB): mechanisms of regulation and association with disease. *Cell Death Differ.* 29, 1433–1449. doi:10.1038/s41418-022-01028-6
- Tang, Y., Jacobi, A., Vater, C., Zou, L., Zou, X., and Stiehler, M. (2015). Icaritin promotes angiogenic differentiation and prevents oxidative stress-induced autophagy in endothelial progenitor cells. *Stem Cells* 33, 1863–1877. doi:10.1002/stem.2005
- Tian, J., Popal, M. S., Liu, Y., Gao, R., Lyu, S., Chen, K., et al. (2019). Ginkgo biloba leaf extract attenuates atherosclerosis in streptozotocin-induced diabetic ApoE^{-/-} mice by inhibiting endoplasmic reticulum stress via restoration of autophagy through the mTOR signaling pathway. *Oxid. Med. Cell Longev.* 2019, 8134678. doi:10.1155/2019/8134678
- Vargas, J. N. S., Hamasaki, M., Kawabata, T., Youle, R. J., and Yoshimori, T. (2023). The mechanisms and roles of selective autophagy in mammals. *Nat. Rev. Mol. Cell Biol.* 24, 167–185. doi:10.1038/s41580-022-00542-2
- Wan, Y., Liu, Z., Wu, A., Khan, A. H., Zhu, Y., Ding, S., et al. (2022). Hyperglycemia promotes endothelial cell senescence through AQR/PLAU signaling Axis. *Int. J. Mol. Sci.* 23, 2879. doi:10.3390/ijms23052879
- Wang, C.-Y., An, X.-L., Lv, C.-J., Yuan, M., and Liu, J.-F. (2023a). Risk factors for macrovascular disease in patients with type 2 diabetes mellitus. *Chin. J. Integra Med. Cardio-Cereb Dis.* 21, 3607–3609.
- Wang, G., Han, B., Zhang, R., Liu, Q., Wang, X., Huang, X., et al. (2021a). C1q/TNF-Related protein 9 attenuates atherosclerosis by inhibiting hyperglycemia-induced endothelial cell senescence through the ampka/KLF4 signaling pathway. *Front. Pharmacol.* 12, 758792. doi:10.3389/fphar.2021.758792
- Wang, K., Peng, S., Xiong, S., Niu, A., Xia, M., Xiong, X., et al. (2020a). Naringin inhibits autophagy mediated by PI3K-Akt-mTOR pathway to ameliorate endothelial cell dysfunction induced by high glucose/high fat stress. *Eur. J. Pharmacol.* 874, 173003. doi:10.1016/j.ejphar.2020.173003
- Wang, P., Huang, Y., Ren, J., Rong, Y., Fan, L., Zhang, P., et al. (2022a). Large-leaf yellow tea attenuates high glucose-induced vascular endothelial cell injury by up-regulating autophagy and down-regulating oxidative stress. *Food Funct.* 13, 1890–1905. doi:10.1039/d1fo03405g
- Wang, Q., Kuang, H., Su, Y., Sun, Y., Feng, J., Guo, R., et al. (2013). Naturally derived anti-inflammatory compounds from Chinese medicinal plants. *J. Ethnopharmacol.* 146, 9–39. doi:10.1016/j.jep.2012.12.013
- Wang, S., Long, H., Hou, L., Feng, B., Ma, Z., Wu, Y., et al. (2023b). The mitophagy pathway and its implications in human diseases. *Signal Transduct. Target Ther.* 8, 304. doi:10.1038/s41392-023-01503-7

- Wang, S., Wuniquiemu, T., Tang, W., Teng, F., Bian, Q., Yi, L., et al. (2021b). Luteolin inhibits autophagy in allergic asthma by activating PI3K/Akt/mTOR signaling and inhibiting Beclin-1-PI3KC3 complex. *Int. Immunopharmacol.* 94, 107460. doi:10.1016/j.intimp.2021.107460
- Wang, X. (2021). Mechanism of intervention of Yigan Mingmu decoction on autophagy of Müller cells in a model of diabetic retinopathy edema in SD rats. *Hunan Univ. Trad. Chin. Med.* 3, 1–77. doi:10.27138/d.cnki.ghuzc.2021.000464
- Wang, X., Zhang, J.-Q., Xiu, C.-K., Yang, J., Fang, J.-Y., and Lei, Y. (2020b). Ginseng-sangqi-chuanxiong (GSC) extracts ameliorate diabetes-induced endothelial cell senescence through regulating mitophagy via the AMPK pathway. *Oxid. Med. Cell Longev.* 2020, 7151946. doi:10.1155/2020/7151946
- Wang, Y.-M., and Du, G.-Q. (2016). Glycyrrhizic acid prevents enteritis through reduction of NF- κ B p65 and p38MAPK expression in rat. *Mol. Med. Rep.* 13, 3639–3646. doi:10.3892/mmr.2016.4981
- Wang, Y.-Q., Zhang, C.-H., and Huang, S.-F. (2022b). Analysis of the occurrence of complications of type 2 diabetes mellitus in the elderly and its influencing factors. *Beijing Med. J.* 44, 269–272. doi:10.15932/j.0253-9713.2022.03.018
- Wei, H.-J., Zhang, C., Yang, S.-H., Zheng, Y., Shen, J.-L., Liu, Y., et al. (2021). Autophagy is involved in the research progress of diabetic vasculopathy. *Chin. J. Compar Med.* 31, 132–140.
- Willett, R., Martina, J. A., Zewe, J. P., Wills, R., Hammond, G. R. V., and Puertollano, R. (2017). TFEB regulates lysosomal positioning by modulating TMEM55B expression and JIP4 recruitment to lysosomes. *Nat. Commun.* 8, 1580. doi:10.1038/s41467-017-01871-z
- Xi, J., Rong, Y., Zhao, Z., Huang, Y., Wang, P., Luan, H., et al. (2021). Scutellarin ameliorates high glucose-induced vascular endothelial cells injury by activating PINK1/Parkin-mediated mitophagy. *J. Ethnopharmacol.* 271, 113855. doi:10.1016/j.jep.2021.113855
- Xiang, J., Zhang, C., Di, T., Chen, L., Zhao, W., Wei, L., et al. (2022). Salvianolic acid B alleviates diabetic endothelial and mitochondrial dysfunction by down-regulating apoptosis and mitophagy of endothelial cells. *Bioengineered* 13, 3486–3502. doi:10.1080/21655979.2022.2026552
- Xiong, Y., Zhou, F., Liu, Y., Yi, Z., Wang, X., Wu, Y., et al. (2021). 1 α ,25-Dihydroxyvitamin D3 promotes angiogenesis by alleviating AGEs-induced autophagy. *Arch. Biochem. Biophys.* 712, 109041. doi:10.1016/j.abb.2021.109041
- Xu, D.-D., and Du, L.-L. (2022). Fission yeast autophagy machinery. *Cells* 11, 1086. doi:10.3390/cells11071086
- Xu, H.-D., and Qin, Z.-H. (2019). Beclin 1, bcl-2 and autophagy. *Adv. Exp. Med. Biol.* 1206, 109–126. doi:10.1007/978-981-15-0602-4_5
- Xu, Y.-X., Huang, C., Liu, M., Chen, N., Chen, W., Yang, C., et al. (2018). Survivin regulated by autophagy mediates hyperglycemia-induced vascular endothelial cell dysfunction. *Exp. Cell Res.* 364, 152–159. doi:10.1016/j.yexcr.2018.01.037
- Xu, Z., Han, X., Ou, D., Liu, T., Li, Z., Jiang, G., et al. (2020). Targeting PI3K/AKT/mTOR-mediated autophagy for tumor therapy. *Appl. Microbiol. Biotechnol.* 104, 575–587. doi:10.1007/s00253-019-10257-8
- Yang, B., Xie, Y., Guo, M., Rosner, M. H., Yang, H., and Ronco, C. (2018). Nephrotoxicity and Chinese herbal medicine. *Clin. J. Am. Soc. Nephrol.* 13, 1605–1611. doi:10.2215/CJN.11571017
- Yang, F., Qin, Y., Wang, Y., Meng, S., Xian, H., Che, H., et al. (2019). Metformin inhibits the NLRP3 inflammasome via AMPK/mTOR-dependent effects in diabetic cardiomyopathy. *Int. J. Biol. Sci.* 15, 1010–1019. doi:10.7150/ijbs.29680
- Yang, Q.-W., Ni, H.-Y., Wu, L., and Mei, H.-L. (2022). The protective effect of lentinan regulating autophagy on HUVEC injury induced by high glucose and its mechanism. *Chin. Pharm. Bull.* 38, 1182–1189. doi:10.12360/CPB202106014
- Yang, Z., and Klionsky, D. J. (2009). An overview of the molecular mechanism of autophagy. *Curr. Top. Microbiol. Immunol.* 335, 1–32. doi:10.1007/978-3-642-00302-8_1
- Yu, J., Ke, L., Zhou, J., Ding, C., Yang, H., Yan, D., et al. (2023). Stachydrine relieved the inflammation and promoted the autophagy in diabetes retinopathy through activating the AMPK/SIRT1 signaling pathway. *Diabetes Metab. Syndr. Obes.* 16, 2593–2604. doi:10.2147/DMSO.S420253
- Zhan, W., Tian, W., Zhang, W., Tian, H., and Sun, T. (2022). ANGPTL4 attenuates palmitic acid-induced endothelial cell injury by increasing autophagy. *Cell Signal* 98, 110410. doi:10.1016/j.cellsig.2022.110410
- Zhang, G., He, C., Wu, Q., Xu, G., Kuang, M., Wang, T., et al. (2021a). Impaired autophagy induced by oxLDL/ β 2GPI/anti- β 2GPI complex through PI3K/AKT/mTOR and eNOS signaling pathways contributes to endothelial cell dysfunction. *Oxid. Med. Cell Longev.* 2021, 6662225. doi:10.1155/2021/6662225
- Zhang, L., Xue, K., Fan, P., Chen, C., Hu, J., Huang, J., et al. (2023a). Geranylgeranylacetone-induced heat shock protein70 expression reduces retinal ischemia-reperfusion injury through PI3K/AKT/mTOR signaling. *Exp. Eye Res.* 229, 109416. doi:10.1016/j.exer.2023.109416
- Zhang, Q., Liu, J., Duan, H., Li, R., Peng, W., and Wu, C. (2021b). Activation of Nrf2/HO-1 signaling: an important molecular mechanism of herbal medicine in the treatment of atherosclerosis via the protection of vascular endothelial cells from oxidative stress. *J. Adv. Res.* 34, 43–63. doi:10.1016/j.jare.2021.06.023
- Zhang, X., Ramirez, C. M., Aryal, B., Madrigal-Matute, J., Liu, X., Diaz, A., et al. (2020). Cav-1 (Caveolin-1) deficiency increases autophagy in the endothelium and attenuates vascular inflammation and atherosclerosis. *Arterioscler. Thromb. Vasc. Biol.* 40, 1510–1522. doi:10.1161/ATVBAHA.120.314291
- Zhang, X.-F., Li, T., and Fan, H.-Y. (2023b). Research progress on the pharmacological effects of notoginseng saponins on the cardiovascular system. *J. Jilin Med. Coll.* 44, 149–152. doi:10.13845/j.cnki.issn1673-2995.2023.02.028
- Zhang, Y., Sheng, Z., Xiao, J., Li, Y., Huang, J., Jia, J., et al. (2023c). Advances in the roles of glycyrrhizic acid in cancer therapy. *Front. Pharmacol.* 14, 1265172. doi:10.3389/fphar.2023.1265172
- Zhang, Y., Wang, S., Chen, X., Wang, Z., Wang, X., Zhou, Q., et al. (2022). Liraglutide prevents high glucose induced HUVECs dysfunction via inhibition of PINK1/Parkin-dependent mitophagy. *Mol. Cell Endocrinol.* 545, 111560. doi:10.1016/j.mce.2022.111560
- Zheng, Y., Huang, S., Zhang, J., Hou, J., Wu, F., Wang, W., et al. (2022). Melatonin alleviates vascular endothelial cell damage by regulating an autophagy-apoptosis axis in Kawasaki disease. *Cell Prolif.* 55, e13251. doi:10.1111/cpr.13251
- Zhong, Y., Wang, Q. J., Li, X., Yan, Y., Backer, J. M., Chait, B. T., et al. (2009). Distinct regulation of autophagic activity by Atg14L and Rubicon associated with Beclin 1-phosphatidylinositol-3-kinase complex. *Nat. Cell Biol.* 11, 468–476. doi:10.1038/ncb1854
- Zhou, P., Xie, W., Meng, X., Zhai, Y., Dong, X., Zhang, X., et al. (2019). Notoginsenoside R1 ameliorates diabetic retinopathy through PINK1-dependent activation of mitophagy. *Cells* 8, 213. doi:10.3390/cells8030213
- Zhou, P.-F., Li, W.-Z., and Wen, X.-Y. (2021). Research progress on chemical composition and pharmacological activity of ginger. *J. Trad. Chin. Veterinary Med.* 40, 93–96. doi:10.13823/j.cnki.jtcvm.2021.01.023
- Zhu, Z., Li, J., and Zhang, X. (2019a). Salidroside protects against ox-LDL-induced endothelial injury by enhancing autophagy mediated by SIRT1-FoxO1 pathway. *BMC Complement. Altern. Med.* 19, 111. doi:10.1186/s12906-019-2526-4
- Zhu, Z., Yang, C., Iyaswamy, A., Krishnamoorthi, S., Sreenivasmurthy, S. G., Liu, J., et al. (2019b). Balancing mTOR signaling and autophagy in the treatment of Parkinson's disease. *Int. J. Mol. Sci.* 20, 728. doi:10.3390/ijms20030728
- Zulkifli, M. H., Abdullah, Z. L., Mohamed Yusof, N. I. S., and Mohd Fauzi, F. (2023). *In silico* toxicity studies of traditional Chinese herbal medicine: a mini review. *Curr. Opin. Struct. Biol.* 80, 102588. doi:10.1016/j.sbi.2023.102588



OPEN ACCESS

EDITED BY

Abd El-Latif Hesham,
Beni-Suef University, Egypt

REVIEWED BY

Yasufumi Katanasaka,
University of Shizuoka, Japan
Ravi Sonkar,
Boston University, United States

*CORRESPONDENCE

Eko Fuji Ariyanto,
✉ fuji@unpad.ac.id

RECEIVED 06 January 2024

ACCEPTED 22 March 2024

PUBLISHED 05 April 2024

CITATION

Ariyanto EF (2024), The efficacy of botanical drugs in orchestrating epigenetic modifications for ameliorating metabolic disorders.
Front. Pharmacol. 15:1366551.
doi: 10.3389/fphar.2024.1366551

COPYRIGHT

© 2024 Ariyanto. This is an open-access article distributed under the terms of the [Creative Commons Attribution License \(CC BY\)](#). The use, distribution or reproduction in other forums is permitted, provided the original author(s) and the copyright owner(s) are credited and that the original publication in this journal is cited, in accordance with accepted academic practice. No use, distribution or reproduction is permitted which does not comply with these terms.

The efficacy of botanical drugs in orchestrating epigenetic modifications for ameliorating metabolic disorders

Eko Fuji Ariyanto*

Department of Biomedical Sciences, Faculty of Medicine, Universitas Padjadjaran, Bandung, Indonesia

KEYWORDS

botanical drugs, epigenetics, DNA methylation, histone modifications, non-coding RNA, metabolic disorder

Introduction

Metabolic diseases remain the most worrying global health problem as their prevalence is increasing globally every year (Choi et al., 2008). Moreover, most metabolic diseases and their complications including coronary artery disease, diabetes mellitus, hypertension, and obesity are chronic and associated with a very high financial burden. Consequently, various efforts have been made to develop safe drugs with mild side effects for long-term consumption.

Epigenetics are changes in gene expression without changes in DNA sequences and plays a role in cellular processes in various diseases (Ling and Ronn, 2019; Guo et al., 2021). Epigenetic changes can be caused by at least three mechanisms including DNA methylation, post-translational histone modifications, and regulation of gene expression by non-coding RNA (ncRNA) which can be microRNA (miRNA), long non-coding RNA (lncRNA), etc (Xiao et al., 2019). Increased DNA methylation at gene promoters causes decreased gene expression, increased ncRNA activity reduces gene expression through degradation of messenger RNA (mRNA), while the effect of histone modifications on gene expression is more variable depending on the type and location of substrate attachment to the histone tail (Xiao et al., 2019). Epigenetics plays an important role in the development of many metabolic diseases (Tikoo et al., 2008; Stančáková and Laakso, 2016; Ling and Ronn, 2019; Rizzacasa et al., 2019; Samblas et al., 2019; Wu et al., 2023) and since they are reversible, restoring epigenetic status to normal provides opportunities for developing pharmacotherapies for metabolic diseases (Hamm and Costa, 2015).

Currently, botanical drug is an interesting topic of discussion for the treatment of metabolic diseases because of its low toxicity and promising therapeutic effects (Ariyanto et al., 2023a; Ariyanto et al., 2023b; Wu et al., 2023). Botanical drugs are composed of many compounds, some of which provide therapeutic effects (Ariyanto et al., 2023a; Ariyanto et al., 2023b; Wu et al., 2023) and are usually consumed in the form of decoction, pills, powder, etc. extracted from the leaves, fruit, roots, or stems of plants (Wu et al., 2023).

Several studies have determined the effect of botanical drugs on metabolic diseases but its effectiveness in modifying the epigenetic status of molecular pathways involved in the pathogenesis and pathophysiology of metabolic diseases has not yet been revealed. This article aims to comprehensively analyze the efficacy of botanical drugs in treating metabolic diseases through epigenetic changes to provide insight into research and development strategies for botanical drugs as a pharmacotherapy for metabolic diseases.

Previous studies have shown that botanical drugs can produce epigenetic changes through several mechanisms including modulating DNA methylation, posttranslational

histone modifications, as well as ncRNA-mediated gene regulation by modulating the expression or activity of DNA methyltransferase (DNMT) and histone deacetylase (HDAC) (Wu et al., 2023). DNMT catalyzes DNA methylation while HDAC catalyzes the release of acetyl groups from histones to inhibit gene expression (Verdin et al., 2003; Mirza et al., 2013).

Botanical drugs that modulate DNA methylation

Several studies have reported the effect of botanical drugs in changing DNA methylation levels to improve metabolic disease conditions. Zhou showed that geniposide present in *Hedyotis diffusa*, *Radix scrophulariae*, *Eucommia ulmoides*, and *Paederia scandens* has antiatherosclerotic effects through regulating DNA methylation (Zhou, 2019). Ma et al showed that resveratrol has important benefits in preventing cardiovascular disease because it can inhibit homocysteine-induced PTEN hypermethylation to inhibit smooth muscle cell proliferation, one of the stages of atherogenesis (Ma et al., 2018). Another study indicated the role of curcumin in increasing the methylation of the RNA18S5 gene through activation of DNMT2 which produces atheroprotective effects (Lewinska et al., 2015). An *in vivo* study reported the role of naoluoxintong (NLXT) in a rat model of ischemic stroke with middle cerebral artery occlusion (MCAO) (Hong et al., 2021). NLXT regulated *NogoA*, *NgR1*, *NgR2*, *RhoA*, and *Rock2* gene expression through downregulation of DNA methylation (Hong et al., 2021).

Botanical drugs that modulate posttranslational histone modifications

Resveratrol, a metabolite contained in melinjo seeds, improved outcomes in type 2 diabetes mellitus patients through epigenetic modification (Bo et al., 2018). Administering 40 mg and 500 mg for 6 months to type 2 diabetes mellitus patients increased Sirtuin-1 (Sirt1) expression which was associated with a decrease in H3K56 acetylation and body fat (Bo et al., 2018). Naringenin and hesperetin, Quzhou Fructus aurantia-derived metabolites, inhibited AMPK-mediated p300 induction to decrease histone acetylation, thereby decreasing *Txnip* expression in pancreatic β cells in diabetic mice and the INS-1 pancreatic β cell line (Wang et al., 2021).

Several *in vivo* studies reported the potential of esculetin, a derivative of coumarin, in improving diabetes mellitus and its complications through epigenetic modification (Kadakol et al., 2015; Kadakol et al., 2017). Esculetin administered at doses of 50 and 100 mg/kg/day for 2 weeks reduced dimethylation at lysine 4 of histone 3 (H3K4me2) and H3K36me2, as well as acetylation at lysine 27 of histone 3 (H3K27ac) in the hearts of type 2 diabetes mice (Kadakol et al., 2015). The administration of 50 mg/kg/day esculetin for 6 weeks also improved cardiomyopathy caused by type 2 diabetes mellitus by reducing levels of H3K9ac, H2AK119ub, and H2BK120ub (Kadakol et al., 2017). Therefore, esculetin has the potential to be developed for the treatment of diabetes mellitus and its complications through epigenetic modifications, especially in histones.

In vivo studies in mouse models and *in vitro* studies reported that icariin pretreatment (4 μ M) prevented ischemia/reperfusion (I/R)-induced injury by increasing the activity of sirtuin-1, a histone deacetylase, which then reduced FOXO1 (Wu et al., 2018). This mechanism improved the quality of heart contractions, limited the size of cardiac infarction, and leakage of creatine kinase-MB from damaged myocardium, as well as reduced oxidative stress in heart cell mitochondria (Wu et al., 2018). Moreover, administration of sirtuin-1 inhibitors and *Sirt1* siRNA reduced the visible cardioprotective effects (Wu et al., 2018).

Suxiao Jiuxin pill (SJP) is a botanical drug that contains tetramethylpyrazine and borneol and has often been used as a therapy for coronary artery disease in China (Ruan et al., 2018). In the context of cell-cell communication in the heart, exosomes play a pivotal role in cardiac mesenchymal stem cell and cardiomyocyte communication, some of which can occur through the modulation of epigenetic changes (Ruan et al., 2018). Ruan et al showed that SJP treatment can cause changes in C-MSC-derived exosomes to increase H3K27me3 and decrease *Utx* expression, as well as increase *Pcna* expression, a marker of cardiomyocyte proliferation in HL-1 cells, a mouse cardiomyocyte line (Ruan et al., 2018).

Anacardic acid was reported to have an inhibitory effect on histone acetylation in a cardiac hypertrophy mice model. Administration of 3.75 mg/kg anacardic acid improved cardiac hypertrophy through modulating histone acetylation (Li et al., 2019) by inhibiting the expression of p300 and p300/CBP-associated factor (PCAF), thereby reducing H3K9ac levels and normalizing the transcriptional activity of Mef2 (Li et al., 2019). Anacardic acid also inhibits the activity of histone acetylases in mouse cardiac hypertrophy, causing changes in the expression of several important genes in the heart and reducing cardiac hypertrophy (Peng et al., 2017).

In vitro studies reported the effectiveness of kaempferol and piperine in inhibiting adipocyte differentiation and increasing lipolytic gene expression, respectively, through epigenetic modification (Park et al., 2019; Park et al., 2022). Administration of 100 μ M kaempferol inhibited the expression of several *Pparg* target adipogenic genes including *Adipoq*, *Fabp4*, and *Lpl* by reducing H3K27me3 deposition in the gene promoter region during 3T3-L1 adipocyte differentiation (Park et al., 2022). Administration of 50 μ M piperine for 8 days to the 3T3-L1 cell line decreased H3K27me3 enrichment in *Pparg*, decreased H3K9ac, and increased *Ezh2*, increasing the expression of *Ezh2*-associated lipolytic genes (Park et al., 2019).

Qian Yang Yu Yin (QYYY) granules improve renal injury conditions through epigenetic regulation in HEK293T cells whose proliferation was induced by Ang II as a renal damage model (Zhang et al., 2020). QYYY inhibits the proliferation of HEK293T cells, acetyl-cortactin, and DNA methylation, as well as increasing *Sirt1* and H3K4me3 (Zhang et al., 2020).

Botanical drugs that modulate ncRNA

Several *in vivo* studies demonstrated the role of botanical drugs in improving the pathological conditions of metabolic

diseases through miRNA regulation. Supplementation with plant-derived polyphenols reduces weight gain, liver steatosis, insulin resistance, and histopathological damage in diet-induced fatty liver disease in hyperlipidemic mice through regulation of the miRNA paralogs miR-103/107 and miR-122 which then modulated glucose and lipid metabolism (Joven et al., 2012). Supplementation with 0.05% lycopene for 8 weeks inhibited liver steatosis in high-fat-fed mice through miRNA-21 induction, which then caused *Fabp7* degradation and decreased fatty acid-binding protein 7 (FABP7) expression (Ahn et al., 2012). Another *in vivo* study unraveled that the administration of 40 mg/kg Xuesaitong increased myocardial blood vessel formation in a myocardial infarction mouse model through inhibiting miR-3158-3p targeting *Nur77* (Liao et al., 2023).

Yang et al. showed the effect of administering 25 μ mol/L dihydromyricetin in increasing endothelial nitric oxide (NO) synthesis and inhibiting atherosclerosis through inhibiting miR-21 in the apolipoprotein E-deficient mice model (Yang et al., 2020). Inhibition of miR-21 further increased the expression of the gene encoding dimethylarginine dimethylaminohydrolase-1, which in turn decreased asymmetric dimethylarginine and increased endothelial NO synthase to increase NO production (Yang et al., 2020). *In vivo* research on a rat myocardial infarction model showed that Wenxin granules improved myocardial infarction by regulating miR-1 and protein kinase C (PKC)-mediated signal transduction which protected gap junctions and increased the ventricular fibrillation threshold (Wu et al., 2017).

A study using human coronary artery endothelial cell-derived exosomes found that chrysin treatment reduced endothelial cell-derived miR-92a-containing exosomes which then caused an increase in *Klf2* expression for an atheroprotective effect (Lin et al., 2021). Yunpi Heluo decoction improved insulin resistance in Zucker diabetic fatty rats by reducing miR-29a-3p expression causing increased *Irs1* expression, a target of miR-29a-3p (Mao et al., 2019), thereby increasing the protein expression of IRS1, protein kinase B, and pyruvate dehydrogenase lipoamide kinase isozyme 1 (PDK1) (Mao et al., 2019). Another study found that quercetin, perillyl alcohol, and berberine improved pathological conditions in pulmonary arterial hypertension by regulating miR-204 and miR-27a, as well as factors that play a role in inflammation, fibrosis, and apoptosis (Rajabi et al., 2021). Moreover, Cao et al. suggested the role of *Astragalus polysaccharide* in accelerating the differentiation of C3H10T 1/2 cells into brown adipocytes through the regulation of miR-1258-5p and *Cux1* (Cao et al., 2021).

Discussion

The burgeoning field of botanical drugs has garnered significant attention in recent years due to its perceived potential and effectiveness in the treatment of metabolic diseases. Several investigations and empirical data discussed earlier provide detailed insights into the potential and effectiveness of botanical

drugs in managing metabolic diseases. Several studies have indicated that even at low doses, botanical drugs can yield significant effects, suggesting considerable efficacy.

Despite the promising outcomes observed in the previous studies, the precise molecular mechanisms underlying the therapeutic effects of botanical drugs remain incompletely understood. A key area of inquiry pertains to the epigenetic alterations and gene regulation induced by secondary metabolites. Delving deeper into these mechanisms necessitates elucidating, for instance, the specific binding proteins or transcription factors involved in mediating posttranslational histone modifications, modulating gene expression, and, subsequently, producing biological effects. This intricate interplay between secondary metabolites and molecular pathways warrants further exploration through more advanced molecular and biochemical analyses.

Moreover, alongside unraveling the molecular intricacies, it is crucial to conduct rigorous investigations into the safety profile of botanical drugs. While botanical drugs offer potential therapeutic benefits, ensuring their safety is paramount. Comprehensive toxicity studies and pharmacological evaluations are essential to ascertain any potential adverse effects associated with prolonged usage or interactions with other medications and compounds. Such thorough assessments are fundamental for mitigating risks and promoting the responsible use of botanical drugs in clinical settings.

Furthermore, the exploration of potential side effects and drug interactions extends beyond individual metabolites to encompass their synergistic effects and interactions with conventional pharmaceuticals. Understanding how botanical drugs interact with other molecules, including prescription drugs, is essential for preventing adverse reactions and optimizing therapeutic outcomes. Integrating pharmacokinetic and pharmacodynamic studies can provide valuable insights into the bioavailability, metabolism, and potential drug interactions of herbal formulations.

While empirical evidence highlights the therapeutic potential of botanical drugs in managing metabolic diseases, further research is imperative to elucidate the underlying molecular mechanisms and ensure their safety and efficacy. By leveraging advanced scientific methodologies and conducting comprehensive evaluations, we can unlock the optimal therapeutic potential of botanical drugs while safeguarding patient health and wellbeing.

Conclusion

Botanical drugs in relatively small doses produce beneficial effects in various pathological conditions involved in metabolic diseases by changing the level of DNA methylation or post-translational histone modifications, or modulating ncRNAs. However, further studies elaborating more specific molecular mechanisms, safety, adverse effects and potential interactions with other molecules are required to accelerate the development of novel drugs.

Author contributions

EA: Conceptualization, Funding acquisition, Investigation, Resources, Validation, Writing–original draft, Writing–review and editing.

Funding

The author(s) declare financial support was received for the research, authorship, and/or publication of this article. This study was funded by Universitas Padjadjaran grant for EA.

Acknowledgments

I would like to thank Universitas Padjadjaran for supporting this study.

References

- Ahn, J., Lee, H., Jung, C. H., and Ha, T. (2012). Lycopene inhibits hepatic steatosis via microRNA-21-induced downregulation of fatty acid-binding protein 7 in mice fed a high-fat diet. *Mol. Nutr. Food Res.* 56 (11), 1665–1674. doi:10.1002/mnfr.201200182
- Ariyanto, E. F., Danil, A. S., Rohmawaty, E., Sujatmiko, B., and Berbudi, A. (2023a). Effect of resveratrol in melinjo seed (gnetum gnemon L.) extract on type 2 diabetes mellitus patients and its possible mechanism: a review. *Curr. Diabetes Rev.* 19 (2), e280222201512. doi:10.2174/1573399818666220228160908
- Ariyanto, E. F., Wirajati, F., Rahman, P. H., Berbudi, A., and Rohmawaty, E. (2023b). Mechanism of action of Indonesian medicinal plants in inhibiting 3T3-L1 adipocyte differentiation: a review. *J. Appl. Pharm. Sci.* 13 (05), 050–057. doi:10.7324/JAPS.2023.6711
- Bo, S., Togliatto, G., Gambino, R., Ponzio, V., Lombardo, G., Rosato, R., et al. (2018). Impact of sirtuin-1 expression on H3K56 acetylation and oxidative stress: a double-blind randomized controlled trial with resveratrol supplementation. *Acta Diabetol.* 55 (4), 331–340. doi:10.1007/s00592-017-1097-4
- Cao, Y., Deng, B., Zhang, S., Gao, H., Song, P., Zhang, J., et al. (2021). Astragalus polysaccharide regulates brown adipogenic differentiation through miR-1258-5p-modulated cut-like homeobox 1 expression. *Acta Biochim. Biophys. Sin. (Shanghai)* 53 (12), 1713–1722. doi:10.1093/abbs/gmab151
- Choi, B. C., McQueen, D. V., Puska, P., Douglas, K. A., Ackland, M., Campostrini, S., et al. (2008). Enhancing global capacity in the surveillance, prevention, and control of chronic diseases: seven themes to consider and build upon. *J. Epidemiol. Commun. Health* 62, 391–397. doi:10.1136/jech.2007.060368
- Guo, W., Ma, H., Wang, C. Z., Wan, J. Y., Yao, H., and Yuan, C. S. (2021). Epigenetic studies of Chinese herbal medicine: pleiotropic role of DNA methylation. *Front. Pharmacol.* 12, 790321. doi:10.3389/fphar.2021.790321
- Hamm, C. A., and Costa, F. F. (2015). Epigenomes as therapeutic targets. *Pharmacol. Ther.* 151, 72–86. doi:10.1016/j.pharmthera.2015.03.003
- Hong, L., Chen, W., He, L., Tan, H., Peng, D., Zhao, G., et al. (2021). Effect of Naoluxintong on the NogoA/RhoA/ROCK pathway by down-regulating DNA methylation in MCAO rats. *J. Ethnopharmacol.* 281, 114559. doi:10.1016/j.jep.2021.114559
- Joven, J., Espinel, E., Rull, A., Aragonès, G., Rodríguez-Gallego, E., Camps, J., et al. (2012). Plant-derived polyphenols regulate expression of miRNA paralogs miR-103/107 and miR-122 and prevent diet-induced fatty liver disease in hyperlipidemic mice. *Biochim. Biophys. Acta* 1820 (7), 894–899. doi:10.1016/j.bbagen.2012.03.020
- Kadakol, A., Malek, V., Goru, S. K., Pandey, A., and Gaikwad, A. B. (2015). Esculetin reverses histone H2A/H2B ubiquitination, H3 dimethylation, acetylation and phosphorylation in preventing type 2 diabetic cardiomyopathy. *J. Funct. Foods* 17, 127–136. doi:10.1016/j.jff.2015.05.017
- Kadakol, A., Malek, V., Goru, S. K., Pandey, A., and Gaikwad, A. B. (2017). Telmisartan and esculetin combination ameliorates type 2 diabetic cardiomyopathy by reversal of H3, H2A, and H2B histone modifications. *Indian J. Pharmacol.* 49, 348–356. doi:10.4103/ijp.IJP_710_16
- Lewinska, A., Wnuk, M., Grabowska, W., Zabek, T., Semik, E., Sikora, E., et al. (2015). Curcumin induces oxidation-dependent cell cycle arrest mediated by SIRT7 inhibition of rDNA transcription in human aortic smooth muscle cells. *Toxicol. Lett.* 233 (3), 227–238. doi:10.1016/j.toxlet.2015.01.019
- Li, S., Peng, B., Luo, X., Sun, H., and Peng, C. (2019). Anacardic acid attenuates pressure-overload cardiac hypertrophy through inhibiting histone acetylases. *J. Cell Mol. Med.* 23 (4), 2744–2752. doi:10.1111/jcmm.14181
- Liao, J., Shao, M., Wang, Y., Yang, P., Fu, D., Liu, M., et al. (2023). Xuesaitong promotes myocardial angiogenesis in myocardial infarction mice by inhibiting MiR-3158-3p targeting Nur77. *Aging (Albany NY)* 15 (10), 4084–4095. doi:10.18632/aging.204671
- Lin, C. M., Wang, B. W., Pan, C. M., Fang, W. J., Chua, S. K., Cheng, W. P., et al. (2021). Chrysin boosts KLF2 expression through suppression of endothelial cell-derived exosomal microRNA-92a in the model of atheroprotection. *Eur. J. Nutr.* 60 (8), 4345–4355. doi:10.1007/s00394-021-02593-1
- Ling, C., and Ronn, T. (2019). Epigenetics in human obesity and type 2 diabetes. *Cell Metab.* 29, 1028–1044. doi:10.1016/j.cmet.2019.03.009
- Ma, S. C., Zhang, H. P., Jiao, Y., Wang, Y. H., Zhang, H., Yang, X. L., et al. (2018). Homocysteine-induced proliferation of vascular smooth muscle cells occurs via PTEN hypermethylation and is mitigated by resveratrol. *Mol. Med. Rep.* 17 (4), 5312–5319. doi:10.3892/mmr.2018.8471
- Mao, Z. J., Weng, S. Y., Lin, M., and Chai, K. F. (2019). Yunpi Heluo decoction attenuates insulin resistance by regulating liver miR-29a-3p in Zucker diabetic fatty rats. *J. Ethnopharmacol.* 243, 111966. doi:10.1016/j.jep.2019.111966
- Mirza, S., Sharma, G., Parshad, R., Gupta, S. D., Pandya, P., and Ralhan, R. (2013). Expression of DNA methyltransferases in breast cancer patients and to analyze the effect of natural compounds on DNA methyltransferases and associated proteins. *J. Breast Cancer* 16, 23–31. doi:10.4048/jbc.2013.16.1.23
- Park, U., Hwang, J., Youn, H., Kim, E., and Um, S. (2019). Piperine inhibits adipocyte differentiation via dynamic regulation of histone modifications. *Phytother. Res.* 33, 2429–2439. doi:10.1002/ptr.6434
- Park, U. H., Hwang, J. T., Youn, H., Kim, E. J., and Um, S. J. (2022). Kaempferol antagonizes adipogenesis by repressing histone H3K4 methylation at PPARγ target genes. *Biochem. Biophys. Res. Commun.* 617, 48–54. doi:10.1016/j.bbrc.2022.05.098
- Peng, C., Luo, X., Li, S., and Sun, H. (2017). Phenylephrine-induced cardiac hypertrophy is attenuated by a histone acetylase inhibitor anacardic acid in mice. *Mol. Biosyst.* 13 (4), 714–724. doi:10.1039/c6mb00692b
- Rajabi, S., Najafipour, H., Jafarnejad-Farsangi, S., Joukar, S., Beik, A., Askaripour, M., et al. (2021). Quercetin, perillyl alcohol, and berberine ameliorate right ventricular disorders in experimental pulmonary arterial hypertension: effects on miR-204, miR-27a, fibrotic, apoptotic, and inflammatory factors. *J. Cardiovasc Pharmacol.* 77 (6), 777–786. doi:10.1097/FJC.0000000000001015
- Rizzacasa, B., Amati, F., Romeo, F., Novelli, G., and Mehta, J. L. (2019). Epigenetic modification in coronary atherosclerosis: JACC review topic of the week. *J. Am. Coll. Cardiol.* 74 (10), 1352–1365. doi:10.1016/j.jacc.2019.07.043
- Ruan, X. F., Li, Y. J., Ju, C. W., Shen, Y., Lei, W., Chen, C., et al. (2018). Exosomes from Suxiao Juxin pill-treated cardiac mesenchymal stem cells decrease H3K27 demethylase UTX expression in mouse cardiomyocytes *in vitro*. *Acta Pharmacol. Sin.* 39 (4), 579–586. doi:10.1038/aps.2018.18
- Samblas, M., Milagro, F. I., and Martínez, A. (2019). DNA methylation markers in obesity, metabolic syndrome, and weight loss. *Epigenetics* 14 (5), 421–444. doi:10.1080/15592294.2019.1595297
- Stančáková, A., and Laakso, M. (2016). Genetics of type 2 diabetes. *Endocr. Dev.* 31, 203–220. doi:10.1159/000439418
- Tikoo, K., Meena, R. L., Kabra, D. G., and Gaikwad, A. B. (2008). Change in post-translational modifications of histone H3, heat-shock protein-27 and MAP kinase

Conflict of interest

The author declares that the research was conducted in the absence of any commercial or financial relationships that could be construed as a potential conflict of interest.

Publisher's note

All claims expressed in this article are solely those of the authors and do not necessarily represent those of their affiliated organizations, or those of the publisher, the editors and the reviewers. Any product that may be evaluated in this article, or claim that may be made by its manufacturer, is not guaranteed or endorsed by the publisher.

- p38 expression by curcumin in streptozotocin-induced type I diabetic nephropathy. *Br. J. Pharmacol.* 153, 1225–1231. doi:10.1038/sj.bjp.0707666
- Verdin, E., Dequiedt, F., and Kasler, H. G. (2003). Class II histone deacetylases: versatile regulators. *Trends Genet.* 19, 286–293. doi:10.1016/S0168-9525(03)00073-8
- Wang, S. W., Sheng, H., Bai, Y. F., Weng, Y. Y., Fan, X. Y., Zheng, F., et al. (2021). Inhibition of histone acetyltransferase by naringenin and hesperetin suppresses Txnip expression and protects pancreatic β cells in diabetic mice. *Phytomedicine* 88, 153454. doi:10.1016/j.phymed.2020.153454
- Wu, A., Zhao, M., Lou, L., Zhai, J., Zhang, D., Zhu, H., et al. (2017). Effect of Wenxin granules on gap junction and MiR-1 in rats with myocardial infarction. *Biomed. Res. Int.* 2017, 3495021. doi:10.1155/2017/3495021
- Wu, B., Feng, J. Y., Yu, L. M., Wang, Y. C., Chen, Y. Q., Wei, Y., et al. (2018). Icaritin protects cardiomyocytes against ischaemia/reperfusion injury by attenuating sirtuin 1-dependent mitochondrial oxidative damage. *Br. J. Pharmacol.* 175 (21), 4137–4153. doi:10.1111/bph.14457
- Wu, Y. Y., Xu, Y. M., and Lau, A. T. Y. (2023). Epigenetic effects of herbal medicine. *Clin. Epigenetics* 15 (1), 85. doi:10.1186/s13148-023-01481-1
- Xiao, Y., Su, M., Ou, W., Wang, H., Tian, B., Ma, J., et al. (2019). Involvement of noncoding RNAs in epigenetic modifications of esophageal cancer. *Biomed. Pharmacother.* 117, 109192. doi:10.1016/j.biopha.2019.109192
- Yang, D., Yang, Z., Chen, L., Kuang, D., Zou, Y., Li, J., et al. (2020). Dihydromyricetin increases endothelial nitric oxide production and inhibits atherosclerosis through microRNA-21 in apolipoprotein E-deficient mice. *J. Cell Mol. Med.* 24 (10), 5911–5925. doi:10.1111/jcmm.15278
- Zhang, S. F., Mao, X. J., Jiang, W. M., and Fang, Z. Y. (2020). Qian Yang Yu Yin Granule protects against hypertension-induced renal injury by epigenetic mechanism linked to Nicotinamide N-Methyltransferase (NNMT) expression. *J. Ethnopharmacol.* 255, 112738. doi:10.1016/j.jep.2020.112738
- Zhou, Q. B. (2019). Double effect of geniposide on gene methylation of foam cells derived from RAW264.7 induced by ox-LDL. *Chin. J. Integr. Traditional West. Medicine* 39 (7), 853–858.



OPEN ACCESS

EDITED BY

Stalin Antony,
University of Electronic Science and
Technology of China, China

REVIEWED BY

Bin-Nan Wu,
Kaohsiung Medical University, Taiwan
Amro M. Soliman,
University of Alberta, Canada

*CORRESPONDENCE

Youquan Gu,
✉ guyq940@163.com

RECEIVED 22 January 2024

ACCEPTED 25 March 2024

PUBLISHED 08 April 2024

CITATION

Zhang G, Wang Q, Jiang B, Yao L, Wu W,
Zhang X, Wan D and Gu Y (2024), Progress of
medicinal plants and their active metabolites in
ischemia-reperfusion injury of stroke: a novel
therapeutic strategy based on regulation of
crosstalk between mitophagy and ferroptosis.
Front. Pharmacol. 15:1374445.
doi: 10.3389/fphar.2024.1374445

COPYRIGHT

© 2024 Zhang, Wang, Jiang, Yao, Wu, Zhang,
Wan and Gu. This is an open-access article
distributed under the terms of the [Creative
Commons Attribution License \(CC BY\)](#). The use,
distribution or reproduction in other forums is
permitted, provided the original author(s) and
the copyright owner(s) are credited and that the
original publication in this journal is cited, in
accordance with accepted academic practice.
No use, distribution or reproduction is
permitted which does not comply with these
terms.

Progress of medicinal plants and their active metabolites in ischemia-reperfusion injury of stroke: a novel therapeutic strategy based on regulation of crosstalk between mitophagy and ferroptosis

Guozhen Zhang^{1,2}, Qiang Wang³, Bing Jiang⁴, Lihe Yao³,
Wenjuan Wu³, Xiaoyan Zhang², Dongjun Wan² and
Youquan Gu^{1,3*}

¹College of the First Clinical Medicine, Lanzhou University, Lanzhou, Gansu, China, ²Department of Neurology, People's Liberation Army Joint Logistics Support Force 940th Hospital, Lanzhou, Gansu, China, ³Department of Neurology, First Hospital of Lanzhou University, Lanzhou, Gansu, China, ⁴Department of Integrated Chinese and Western Medicine, Gansu University of Traditional Chinese Medicine, Lanzhou, Gansu, China

The death of cells can occur through various pathways, including apoptosis, necroptosis, mitophagy, pyroptosis, endoplasmic reticulum stress, oxidative stress, ferroptosis, cuproptosis, and disulfide-driven necrosis. Increasing evidence suggests that mitophagy and ferroptosis play crucial regulatory roles in the development of stroke. In recent years, the incidence of stroke has been gradually increasing, posing a significant threat to human health. Hemorrhagic stroke accounts for only 15% of all strokes, while ischemic stroke is the predominant type, representing 85% of all stroke cases. Ischemic stroke refers to a clinical syndrome characterized by local ischemic-hypoxic necrosis of brain tissue due to various cerebrovascular disorders, leading to rapid onset of corresponding neurological deficits. Currently, specific therapeutic approaches targeting the pathophysiological mechanisms of ischemic brain tissue injury mainly include intravenous thrombolysis and endovascular intervention. Despite some clinical efficacy, these approaches inevitably lead to ischemia-reperfusion injury. Therefore, exploration of treatment options for ischemic stroke remains a challenging task. In light of this background, advancements in targeted therapy for cerebrovascular diseases through mitophagy and ferroptosis offer a new direction for the treatment of such diseases. In this review, we summarize the progress of mitophagy and ferroptosis in regulating ischemia-reperfusion injury in stroke and emphasize their potential molecular mechanisms in the pathogenesis. Importantly, we systematically elucidate the

role of medicinal plants and their active metabolites in targeting mitophagy and ferroptosis in ischemia-reperfusion injury in stroke, providing new insights and perspectives for the clinical development of therapeutic drugs for these diseases.

KEYWORDS

mitophagy, ferroptosis, ischemia-reperfusion injury in stroke, medicinal plants, active metabolites

1 Introduction

As a common and severe neurological systemic disease, stroke can be categorized into ischemic stroke and hemorrhagic stroke. Globally, the incidence of both types of stroke is increasing annually, leading to a significant rise in mortality and disability, especially in low- and middle-income countries. Hemorrhagic stroke accounts for only 15% of all strokes, while ischemic stroke is the predominant type, representing 85% of all strokes (Feske, 2021; Montañó et al., 2021). Ischemic stroke refers to a clinical syndrome characterized by local ischemic and hypoxic necrosis of brain tissue due to various cerebrovascular lesions, leading to rapid onset of corresponding neurological deficits. Currently, specific therapeutic approaches for the pathophysiological mechanisms of ischemic brain tissue injury mainly include intravenous thrombolysis and endovascular intervention therapy (Rabinstein, 2020). Although these methods have shown some clinical efficacy, they inevitably lead to ischemia-reperfusion injury. Therefore, it is an urgent global need to explore the comprehensive pathogenic mechanisms and effective diagnostic and therapeutic methods for ischemic stroke. Increasing evidence suggests that ischemia-reperfusion injury is an important link in the pathogenesis of ischemic stroke, and in this process, the regulation of cellular physiological processes such as mitophagy and ferroptosis becomes particularly crucial (Liu et al., 2013; Zhang et al., 2022a; She et al., 2023). Ischemia-reperfusion injury in cerebral stroke results from cellular damage due to insufficient cerebral blood flow, exacerbated by oxidative stress and inflammatory reactions during reperfusion. Mitophagy and ferroptosis, as important intracellular regulatory mechanisms, have received increasing attention from scholars in recent years. Activation of mitophagy during the process of ischemic stroke reperfusion injury helps clear dysfunctional mitochondria, alleviate oxidative stress, and exert a protective effect. Studies have shown that by regulating the signaling pathways related to mitophagy, it is possible to alleviate neuronal cell damage caused by ischemic stroke reperfusion and thus slow down the progression of stroke (Zhou et al., 2015; Hwang et al., 2023). Additionally, ferroptosis, as a novel form of cell death caused by the accumulation of intracellular iron ions, is closely related to the release and accumulation of local iron ions in ischemic stroke reperfusion injury. Inhibiting ferroptosis can alleviate cell membrane damage and neuroinflammatory reactions, offering new insights into the treatment strategies for stroke (Liu et al., 2023c; 2023b).

Cell death serves as a vital component of the entire cell life cycle and is essential for individual growth, development, and survival. Cell death occurs regularly in normal tissues and is necessary to maintain metabolic balance. Previous studies have shown that cell death pathways can be largely classified into two classic forms: apoptosis and necrosis (Kopeina and Zhivotovsky, 2022). Apoptosis

is a highly regulated form of programmed cell death that can occur during multicellular organism development, throughout the life cycle, and in response to cellular stress. Apoptosis is primarily mediated by the “protease-rich” Caspase family. In addition, other proteins (including pro-apoptotic and anti-apoptotic proteins) also play essential roles (Fleisher, 1997). Dysregulation of cell apoptosis has been observed in various disease states (including autoimmune diseases, neurodegenerative diseases, and cancer) (Giovannetti et al., 2008; Wong, 2011; Erekat, 2022). Necrosis is a type of non-programmed cell death that mainly occurs in acute injury, infection, and when apoptosis is inhibited, characterized by cell swelling and dissolution. Pathologically, necrotic cells can release cell contents into the surrounding environment and recruit phagocytes to clear dead cells through triggering inflammation. However, uncontrolled necrosis can also cause severe tissue damage, such as gangrene (Festjens et al., 2006). In recent years, with the continuous development of molecular biology techniques, numerous novel forms of cell death have emerged, such as mitophagy (Lu et al., 2023a), ferroptosis (Dixon and Pratt, 2023), cuproptosis (Kahlson and Dixon, 2022), disulfide-driven necrosis (Liu et al., 2023d), and so on.

The concept of mitophagy was proposed by Lemasters in 2005. Under stressors such as reactive oxygen species (ROS) exposure, mitochondrial DNA mutations accumulate, leading to decreased mitochondrial membrane potential and depolarization damage. This ultimately results in cell death. In this severe survival situation, mitochondria have to “kill” to maintain mitochondrial and cellular homeostasis and prevent damaged mitochondria from causing further harm to the cell. To do so, cells selectively encapsulate and degrade damaged or dysfunctional mitochondria within the cell. Mitophagy can be divided into four key steps: (1) Depolarization of damaged mitochondria, resulting in loss of membrane potential. (2) Mitochondria are encapsulated by autophagosomes to form mitophagosomes. (3) Mitophagosomes fuse with lysosomes. (4) The contents of mitochondria are degraded by lysosomal enzymes, and acidic hydrolases from lysosomes or vacuoles flow into the autophagosomes to degrade damaged mitochondria. Increasing research suggests that selective clearance of dysfunctional mitochondria through mitophagy plays a crucial role in maintaining mitochondrial quantity, quality homeostasis, and cell survival (Lu et al., 2023b).

The concept of ferroptosis was first proposed by Dixon et al. in 2012, mainly used to describe the cell death mechanism induced by Earstin, characterized by the inhibition of intracellular cysteine transport, leading to glutathione consumption and inactivation of glutathione peroxidase 4 (GPX4) (Tang et al., 2021). Unlike apoptosis, autophagy, and necrosis, ferroptosis is a form of programmed cell death regulated by iron ions, characterized by increased intracellular iron ions, accumulation of lipid peroxides

and related metabolic products, and peroxidation of polyunsaturated fatty acids in the plasma membrane. Morphologically, ferroptosis involves significant shrinkage of mitochondria, increased density of double-layer membrane structure, and loose or disappeared cristae formation. Biochemically, GPX4 activity decreases, excessive glutathione consumption, lipids in the cell are oxidized by divalent iron ions in a manner similar to the Fenton reaction, resulting in the production of large amounts of ROS. Genetically, ferroptosis is associated with abnormal expression of multiple genes, particularly those related to iron regulation, including RPL8, IREB2, ATP5G3, CS, TTC35, ACSF2, and so on (Hadian and Stockwell, 2020). It is noteworthy that with the continuous development of molecular biology techniques, regulation of this type of cell death has been extensively studied. In numerous cell experiments, ferroptosis inducers have been confirmed to mainly belong to the RAS selective killing factor family, represented by Earstin and RSL3. Inhibitors have been developed relatively more extensively, including classic ferrostatin-1, iron chelator deferoxamine, antioxidant Trolox, mitogen extracellular signal-regulated kinase (ERK) inhibitor U0126, and so on (Zeng et al., 2023). Thus, these ferroptosis-related regulators are expected to become a new direction for disease prevention and treatment.

In fact, there is a close relationship between mitophagy and ferroptosis, as they both participate in the regulation of cell function and intracellular homeostasis. On one hand, excessive free iron can lead to mitochondrial dysfunction, thereby triggering mitophagy. The goal of mitophagy is to package damaged mitochondria into autophagosomes and degrade them through lysosomes, thus preventing harmful substances from leaking out of the cell. This process can regulate intracellular iron ion levels to some extent, thereby influencing the occurrence and progression of ferroptosis (Lin et al., 2023). On the other hand, ferroptosis may also have a certain impact on mitophagy. Some studies have shown that during the process of ferroptosis, oxidative stress levels in the cell increase, which may affect mitochondrial stability and initiate mitophagy (Li et al., 2023a). Furthermore, some molecular signaling pathways related to iron metabolism may participate in the regulation of mitophagy (Bi et al., 2024). Overall, the relationship between ferroptosis and mitophagy involves complex signaling pathways and molecular mechanisms. Current research is continuously deepening, and understanding these interactions may help reveal the molecular mechanisms of cell death and cell self-regulation, which may have important implications for the treatment of related diseases. Increasing evidence suggests that mitophagy and ferroptosis play essential roles in the occurrence and development of ischemia-reperfusion injury in stroke (Li et al., 2021b; Shen et al., 2021).

In summary, mitophagy and ferroptosis play important roles in the pathophysiological processes of stroke, providing new avenues for the treatment of stroke and its complications. Therefore, this article systematically reviews the mechanisms of mitophagy and ferroptosis. Furthermore, we have studied their roles in ischemic stroke reperfusion injury. Importantly, this article also systematically elucidates the roles of medicinal plants and their active metabolites in targeting mitophagy and ferroptosis in ischemic stroke reperfusion injury, providing new directions and

insights for the clinical development of therapeutic drugs for such diseases.

2 The pathogenesis of mitophagy and ferroptosis

2.1 The pathogenesis of mitophagy

Mitochondria are dynamic organelles with diverse functions, playing crucial roles in cellular metabolism and survival, including involvement in necrotic cell death and programmed apoptosis. Mitophagy is a cellular protective mechanism that removes excess or dysfunctional mitochondria, maintaining a fine-tuned balance of mitochondria to ensure intracellular homeostasis. There is increasing evidence that mitophagy, as an acute tissue stress response, plays a crucial role in maintaining the health of the mitochondrial network. Due to the critical importance of timely removal of abnormal mitochondria for cell survival, cells have evolved multiple pathways for mitophagy to ensure its timely activation in various environments. A better understanding of the mechanisms of mitophagy in various diseases is crucial for the treatment and design of therapeutic targets for diseases. Here, we summarize the molecular mechanisms mediated by mitophagy, thereby maintaining the dynamic balance of mitochondria at the systemic and organ levels, laying a theoretical foundation for the development of precision medical new treatment strategies based on the research progress of mitophagy signal transduction (Figure 1).

2.1.1 PINK1/Parkin signaling pathway

PINK1 is a protein kinase located in the inner mitochondrial membrane (IMM) that promotes Parkin phosphorylation and facilitates its transfer to mitochondria. When mitochondrial damage occurs and leads to depolarization, PINK1 accumulates significantly, phosphorylating Mfn2 to enhance its binding ability with Parkin, upregulating its autophosphorylation level, or phosphorylating and ubiquitinating Parkin. This promotes Parkin's transfer from the cytoplasm to mitochondria. Under this condition, Parkin can form a substrate polyubiquitin chain through the E3 ligase complex by interacting with the activated Ub and voltage-dependent anion channel 1 (VDAC1). Subsequently, Parkin can be recognized and bound by the ubiquitin-binding protein p62/SQSTM1 and microtubule-associated protein 1 light chain 3 (LC3), aggregating ubiquitinated proteins in new autophagosomes and fusing with lysosomes to form autophagic lysosomes. These lysosomes degrade and clear damaged mitochondria through acidic hydrolases within the body. As Wang HY et al. (Wang et al., 2019) found, electroacupuncture therapy can improve nitro/oxidative stress-induced mitochondrial dysfunction and reduce the accumulation of damaged mitochondria by promoting mitophagy through the Pink1/Parkin-mediated pathway, thereby protecting cells from neuronal damage in brain ischemia-reperfusion. It is noteworthy that the non-dependent mitophagy pathway on Parkin is still under investigation. For example, Szarhel R et al. (Szargel et al., 2016) demonstrated that PINK1 can accumulate in the outer mitochondrial membrane (OMM) and recruit SIAH-1 through the mediation of Synphilin-1, leading to

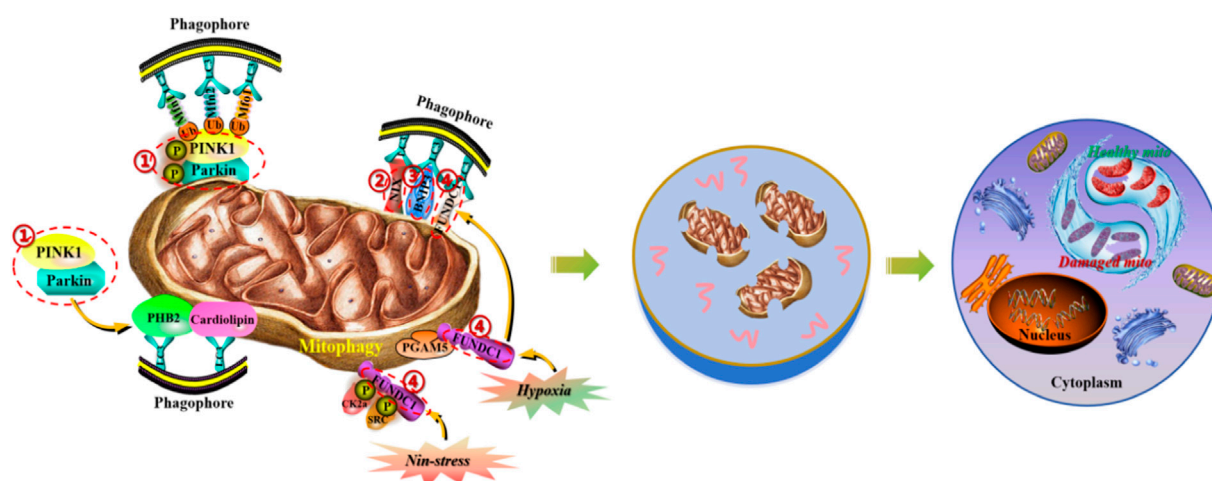


FIGURE 1

Molecular mechanisms of mitophagy in the maintenance of mitochondrial homeostasis. (1) PINK1/Parkin signaling pathway induces mitochondrial autophagy by regulating the activity of p62/SQSTM1 and LC3 proteins. (2) NIX protein, located on the outer membrane of mitochondria, induces mitochondrial autophagy by directly binding to LC3. (3) BNIP3 protein, as the HIF- α target gene, can synergistically induce mitochondrial autophagy with NIX protein. (4) FUNDC1 protein, located on the outer membrane of mitochondria, induces mitochondrial autophagy by dephosphorylation and binding to LC3.

ubiquitination of damaged mitochondria and accelerating the autophagic process.

2.1.2 NIX protein

NIX is a protein mainly located in the OMM and belongs to the anti-apoptotic B-cell lymphoma-2 homology domain 3. It can directly bind to LC3 to induce mitophagy. Research has shown that NIX is crucial for mitochondrial clearance during erythrocyte maturation, as mitochondrial depolarization, massive generation of ROS, and hypoxia can induce NIX expression, thereby activating the mitophagic pathway (Wu et al., 2021b; Li et al., 2021c).

2.1.3 BNIP3 protein

BNIP3 is a target gene of hypoxia-inducible factor 1 α (HIF-1 α). When ischemic stroke occurs, hypoxic conditions activate HIF-1 α , leading to upregulated expression of NIX and BNIP3 in cells, and thus activating the mitophagic pathway. As Fu ZJ et al. (Fu et al., 2020) found, knocking out HIF-1 α in renal tubules can significantly inhibit ischemia-reperfusion-induced mitophagy, exacerbating renal tubular apoptosis and injury. In contrast, adenoviral-mediated overexpression of BNIP3 significantly reverses the reduction of mitophagy and prevents renal injury enhancement in mice with ischemia-reperfusion injury, indicating a protective role of HIF-1 α -BNIP3-mediated mitophagy in renal tubular cells by inhibiting acute kidney injury cell apoptosis and ROS production. Other studies have reported that NIX/BNIP3 is involved in ischemia-reperfusion-induced mitophagy, but excessive upregulation of BNIP3 can lead to cell death, and NIX may only participate in the regulation of the basic level of mitophagy under physiological conditions (Zhang and Ney, 2009).

2.1.4 FUNDC1 protein

FUNDC1 is a trimeric transmembrane protein located in the outer mitochondrial membrane. It exists stably in the outer

membrane under normal conditions and does not mediate mitophagy. When mitochondrial damage or dysfunction occurs, the expression levels of FUNDC1 and LC3 increase, and FUNDC1 can induce mitophagy by dephosphorylation. As Zhou H et al. (Zhou et al., 2018) discovered, inhibiting mitophagy through the mTORC1-ULK1-FUNDC1 pathway can protect against myocardial ischemia-reperfusion injury, suggesting the potential existence of a similar mechanism in brain ischemia-reperfusion injury.

2.2 The pathogenesis of ferroptosis

Since the description of ferroptosis as an iron-dependent non-apoptotic cell death form in 2012, there has been increasing interest in the process and function of ferroptosis. Ferroptosis can occur through two major pathways: exogenous or transporter-dependent pathways and endogenous or enzyme-regulated pathways. Ferroptosis is caused by an imbalance in the production of oxidants and antioxidants, driven by the abnormal expression and activity of various redox enzymes involved in the generation or detoxification of free radicals and lipid oxidation products. Therefore, ferroptosis is precisely regulated at multiple levels, including the epigenetic, transcriptional, post-transcriptional, and post-translational layers. In this review, we summarize the current knowledge of the comprehensive molecular mechanisms of ferroptosis and describe how dysregulated ferroptosis can participate in the development of diseases (Figure 2).

2.2.1 GPX4 protein

GPX4, also known as phospholipid hydrogen peroxide glutathione peroxidase (PHGPx), is the fourth member of the selenium-containing GPX family. The GPX4 protein has a molecular weight of approximately 19 kDa and is composed of

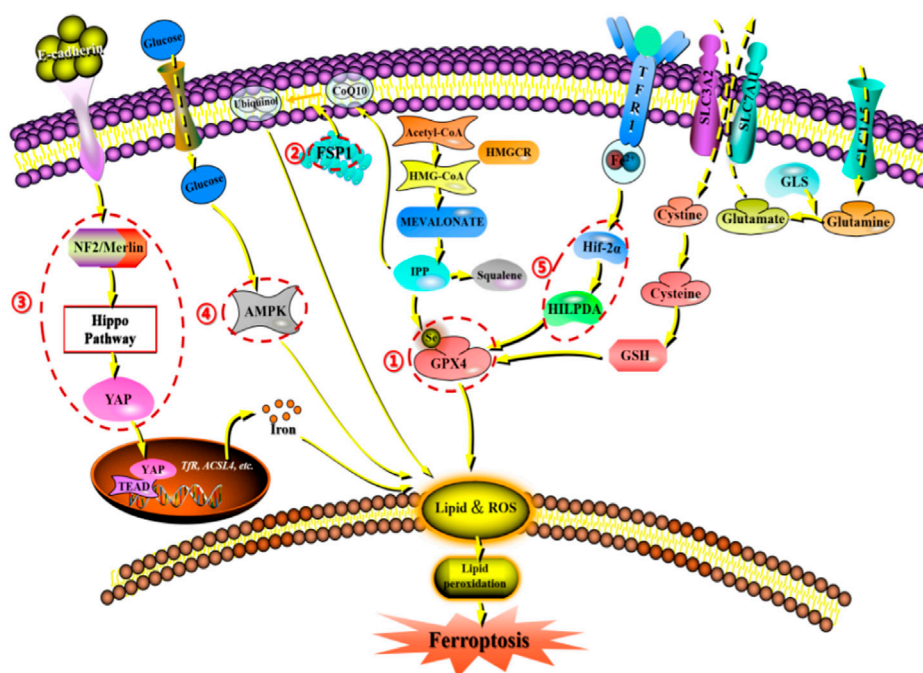


FIGURE 2

Network crosstalk of molecular mechanisms during ferroptosis development. (1) GPX protein regulates ferroptosis by clearing lipid peroxide products on the membrane. (2) FSPA gene regulates ferroptosis by acting on reducing and oxidizing substrates. (3) E-cadherin/NF2/Hippo/YAP signaling pathway regulates ferroptosis by mediating the activity of ferroptosis regulatory factors. (4) AMPK signaling pathway regulates ferroptosis by initiating an energy stress protective program. (5) HIF-2 α /The HILPDA signaling pathway regulates ferroptosis by affecting phospholipid peroxidation.

about 170 amino acids. Several GPX family members, including GPX1-GPX8, have been found in mammals. However, only GPX4 exhibits the ability to clear membrane lipid peroxy radicals, which is closely related to its unique amino acid sequence and spatial structure. Studies have shown that increasing the intracellular selenium content can synergistically activate transcription factors TFAP2c and Sp1 to promote GPX4 expression in neurons. Persistent oxidative stress can cause GSH depletion, which leads to the impairment of the GSH-dependent reduction of the selenocysteine active site in GPX4 and the formation of dehydroalanine and irreversible inactivation of GPX4 through the β -cleavage process. In addition, selenamide formed between selenite and nearby amino acids can protect the enzyme from irreversible inactivation. Multiple ferroptosis inducers ultimately lead to GPX4 depletion through covalent modification of the selenocysteine active site, interference with methionine metabolism, and iron-dependent oxidative stress mechanisms (Liu et al., 2023e). Notably, according to a 2014 targeted metabolomics study, overexpression or knockdown of GPX4 can regulate the lethality of 12 ferroptosis inducers to cells (Yang et al., 2014). Thus, GPX4 has been confirmed as a key regulatory factor for ferroptosis. Mechanistically, GPX4 utilizes its catalytic activity to weaken the toxicity of lipid peroxides and maintain the stability of the lipid bilayer. RSL3, as an inhibitor of GPX4, can covalently bind to GPX4 and inactivate it, leading to the accumulation of intracellular peroxides and ultimately triggering ferroptosis (Li et al., 2021a). Furthermore, as a cofactor for GPX4 to convert peroxides to alcohols, the lack of glutathione can cause cysteine

deficiency, which will directly inactivate GPX4 and trigger ferroptosis (Ursini and Maiorino, 2020).

2.2.2 FSP1 gene

FSP1 is a target gene of transcription factors NRF2, CRBP, and PPAR α . Interestingly, it has been reported that in T-lymphoblastoid lymphoma cells, long non-coding RNA MEG3 (maternally expressed gene 3) upregulates FSP1 expression, while miR-214 downregulates FSP1 expression, and both types of RNA are also involved in tumor development (Brewer, 2023). Increasing evidence indicates that FSP1 expression levels are positively correlated with ferroptosis resistance in hundreds of tumor cell lines and mainly manifest in FSP1-mediated ferroptosis resistance in lung cancer cell culture and mouse xenograft tumors (Hendricks et al., 2023). Therefore, FSP1 expression is crucial for predicting the efficacy of ferroptosis-inducing drugs in cancer, and FSP1 inhibitors have been identified as a potential strategy to overcome ferroptosis resistance in many cancers. In addition to transcriptional regulation, little is known about how the redox enzyme activity of FSP1 is regulated and how its subcellular localization controls its function in different physiological and pathological processes. However, FSP1 can act on both reducing and oxidizing substrates (such as NADH, NADPH, CoQ10, and α -tocopherol), indicating that its regulatory process is complex (Lv et al., 2023).

2.2.3 E-cadherin/NF2/Hippo/YAP signaling pathway

The role of the E-cadherin-NF2-Hippo-YAP pathway in regulating ferroptosis is of great significance. The regulation of

ferroptosis by cell density in epithelial cells is mediated by E-cadherin-mediated intercellular contact. This intercellular interaction can activate the intracellular Hippo signaling pathway through the tumor suppressor protein NF2 (also known as Merlin), thereby inhibiting the nuclear translocation and transcription activity of tumor protein YAP. As YAP targets multiple ferroptosis regulatory factors, including ACSL4 and transferrin receptor TfR1, the occurrence of ferroptosis ultimately depends on the activity of the Hippo pathway. Inhibition of the Hippo pathway and activation of YAP can accelerate the process of ferroptosis (Wu et al., 2019a; Wang et al., 2022).

2.2.4 AMPK signaling pathway

Energy and metabolic stress cause energy loss, leading to the loss of control of the systemic cascades required to maintain homeostasis, such as energy-dependent transmembrane ion concentration imbalance, ultimately resulting in cell death. In addition, metabolic stress induced by glucose starvation promotes ROS accumulation in cells, indicating that glucose starvation may promote ferroptosis. Interestingly, glucose starvation inhibits cell ferroptosis, a protective effect that often depends on the activity of the energy-sensing kinase AMPK. Therefore, when glucose is deficient, the AMPK pathway can be activated, initiating an energy stress protection program to counteract ferroptosis. This process involves the impairment of PUFA biosynthesis, which is essential for lipid peroxide-induced ferroptosis. Studies have shown that the activation of the energy stress protection program can protect the kidney from ischemia-reperfusion injury. This AMPK-dependent protective mechanism may be the first line of defense against organ damage caused by energy exhaustion, which often accompanies organ injury (Lee et al., 2020).

2.2.5 HIF-2 α /HILPDA signaling pathway

It is well-known that ferroptosis is caused by phospholipid peroxidation. The question then arises as to whether the process of ferroptosis is dependent on oxygen concentration. Early experiments showed that Erastin-induced ferroptosis was not affected in a 1% oxygen environment, indicating that hypoxia does not inhibit ferroptosis. However, recent studies have shown that hypoxia can actually increase the sensitivity of cells to ferroptosis, such as in clear cell carcinoma cells that are highly sensitive to GPX4 inhibitor-induced ferroptosis. This sensitivity is mediated by the HIF-2 α subtype through the induction of hypoxia-inducible lipid droplet-associated proteins (HILPDA) and PUFA lipid remodeling (Gao et al., 2023). Therefore, it is speculated that the HIF-2 α /HILPDA signaling pathway-driven sensitivity to ferroptosis in cells may represent a novel method for eliminating newly formed hypoxic tumors.

3 The role of mitophagy and ferroptosis in ischemic reperfusion injury of stroke

3.1 The role of mitophagy in ischemic-reperfusion injury of stroke

The brain is the most metabolically active organ in the body, with the brain's oxygen consumption accounting for 20%–30% of

the body's total oxygen consumption and a 24-h glucose consumption of approximately 108 g. The brain's energy mainly comes from aerobic metabolism of glucose, with almost no energy reserves. Therefore, the brain tissue is highly sensitive to ischemia and hypoxic damage. Studies have shown that the lack of ATP generation caused by ischemia and hypoxia is the main cause of cell and brain tissue death after ischemic stroke (Schädlich et al., 2023). Given the high energy demand of the brain, it is particularly important for mitochondria to produce a large amount of ATP through the respiratory chain and oxidative phosphorylation to ensure mitochondrial morphology and function, and to provide stable and continuous energy supply. Ischemic stroke is a complex series of pathological processes. When ischemic stroke occurs, mitochondria in the ischemic and hypoxic environment have insufficient ATP generation, continuous opening of ion channels causes Ca²⁺ influx, lipase and protease are activated, the mitochondrial respiratory chain is dysfunctional, and a large amount of reactive oxygen species are produced, leading to mitochondrial structural changes and functional impairment (Sims and Muyderman, 2010).

Mitochondria are key organelles that maintain cellular metabolism, regulating the number, morphology, quality, and distribution of mitochondria within cells through activities such as division, fusion, and autophagy. When cerebral ischemia occurs, mitochondrial division and fusion transiently maintain structural integrity and normal function. During ischemic stroke, mitochondria promote the separation of damaged mitochondria through division to maintain mitochondrial health. Studies have shown that significant mitochondrial division can be observed following ischemic stroke and during the ischemia-reperfusion injury period. When ischemic stroke occurs, mitochondrial dysfunction triggers abnormal mitochondrial division and fusion, affecting mitochondrial dynamics and leading to cell death. Optic atrophy 1 (OPA1), as a mitochondrial inner membrane protein, primarily mediates IMM fusion, and research has shown that maintaining the stability of transmembrane long form L-OPA1 located on the inner membrane of mitochondria, so as to reduce neuronal apoptosis and protect ischemic brain tissue. By observing the effect of L-OPA1 on rats with middle cerebral artery occlusion (MCAO) model, it was found that L-OPA1 over-expression could restore mitochondrial morphology and ultrastructure, improve mitochondrial dysfunction, and protect neurons. It is generally believed that mitochondrial fusion can repair mildly damaged mitochondria and promote mitochondrial fusion by up-regulating OPA1 expression levels, thereby providing neuroprotection after ischemia-reperfusion injury. Drp1 is located on the surface of OMM and plays a crucial role in ischemic stroke, and downregulation of Drp1 can inhibit mitochondrial fission and reduce brain injury. As Zhang YH et al. (Zhang et al., 2018) observed the effects of crocin on the mitochondrial dynamics of hypoxia-reoxygenation injured human neuroblastoma cells (SH-SY5Y), it was found that crocin can inhibit Drp1 expression and upregulate OPA1 expression, thereby protecting neurons and cells by suppressing mitochondrial division and fusion abnormalities. Other studies have shown that ginkgolide K has a significant inhibitory effect on Drp1, and in the MCAO model, ginkgolide K can alleviate neuronal damage by preventing GSK3 β and Drp1 translocation to mitochondria (Zhou et al., 2017).

Additionally, Grohm *et al.* (Grohm *et al.*, 2010) found that mitochondrial fusion could repair mild damage and decrease the infarct size, indicating that mitochondrial dynamics played an important role in the ischemic stroke. Inhibiting mitochondrial division or promoting fusion may offer new therapeutic targets for treating such diseases. It is noteworthy that following ischemic stroke, the accumulation of ROS within cells can cause mitochondrial depolarization, thereby initiating autophagy. Increasing research suggests that mitochondrial autophagy is closely associated with ischemic stroke, cardiovascular disease, and neurodegenerative disorders (Shao *et al.*, 2020; Ajoalabady *et al.*, 2022; Li *et al.*, 2023b). Some studies related to stroke suggest that mitochondrial autophagy appears to be a cell survival mechanism because its ability to engulf and clear damaged mitochondria facilitates the maintenance of organelle integrity and cellular energy supply, reduces cellular and neuronal death, and thus serves as a neuroprotective agent to ameliorate clinical symptoms after stroke. Research has confirmed that in stroke models, BNIP3 and NIX interact, and downregulating BNIP3 leads to weakened mitochondrial autophagy, while NIX activation shows similar changes. As Yuan Y *et al.* (Yuan *et al.*, 2017) discovered, in ischemia-reperfusion models, knocking out NIX decreased mitochondrial autophagy, exacerbated brain damage, indicating that NIX had neuroprotective effects and suggesting that mitochondrial autophagy mediated by BNIP3/NIX might be a potential therapeutic target for ischemic stroke. However, mitochondrial autophagy is not always protective, excessive mitochondrial autophagy can lead to cell death. For example, Zhang YF and others (Zhang *et al.*, 2020) found that peroxynitrite (ONOO) mediated Drp1 recruitment to damaged mitochondria, causing excessive mitochondrial autophagy and exacerbating cerebral ischemia-reperfusion injury, indicating that ONOO-mediated mitochondrial autophagy activation might be a key therapeutic target for improving ischemic stroke prognosis. Thus, mitochondrial autophagy is a double-edged sword. On one hand, it can maintain cellular homeostasis by clearing damaged mitochondria. On the other hand, excessive autophagy can lead to excessive mitochondrial degradation.

In conclusion, the interplay between mitochondrial dynamics and mitochondrial autophagy plays a crucial role in the ischemic stroke. Mitochondria not only produce ATP, but also serve as an important source of ROS, which is a determining factor in the degree of ischemia-reperfusion injury. Although ischemic stroke leads to mitochondrial dysfunction and destructive effects, when reperfusion occurs, the rapid restoration of oxygen levels causes excessive activation of the mitochondrial electron transport chain, leading to increased levels of ROS and exacerbating cerebral ischemic damage. Therefore, prolonging the reperfusion window and providing neuroprotection are crucial for disease treatment. Furthermore, mitochondrial autophagy serves as an early defensive mechanism in ischemia-reperfusion injury, clearing damaged mitochondria and reducing the stimulation and damage to normal mitochondria. However, when autophagy is excessive or blocked, it may exacerbate the damage. Therefore, reasonably regulating the mitochondrial autophagy flux during different stages of ischemic stroke is essential for disease treatment and prognosis.

3.2 The role of ferroptosis in ischemia-reperfusion injury of stroke

During ischemic brain tissue, increased ROS, weakened antioxidant defense, excessive free radical production, inactivation of antioxidant enzymes, and consumption of antioxidants lead to various harmful events, including lipid and protein peroxidation, DNA damage, and cell death. Multiple studies have shown that ferroptosis plays a regulatory role in ischemic brain damage (mainly in neurons) and mediates the occurrence and development of rat ischemic brain injury, with inhibition of ferroptosis reducing rat ischemic brain damage. As Tuo QZ *et al.* (Tuo *et al.*, 2017) discovered, increased iron load after cerebral ischemia exacerbates cell death in brain tissue, and administration of ferroptosis inhibitors such as Ferrostatin-1 (Fer-1) and Liproxstatin-1 (Lip-1) protected mice from ischemia-reperfusion injury caused by middle cerebral artery occlusion, confirming that ferroptosis can lead to neuron death after ischemic brain injury. Interestingly, further findings suggested that tau gene knockout mice were protected from ferroptosis after ischemia-reperfusion injury, suggesting that tau-iron interaction may be one of the mechanisms underlying ferroptosis. In a rat middle cerebral artery occlusion model, increased iron concentration in the damaged brain region may be caused by vascular leakage nearby, leading to the influx of transferrin, which increases the saturation of plasma transferrin and exhibits neuroprotective effects. Lan B *et al.* (Lan *et al.*, 2020) found that the expression of divalent metal ion transporter 1 (DMT1) was upregulated in the rat middle cerebral artery occlusion model, and DMT1 inhibition suppressed ferroptosis and alleviated cerebral ischemic damage. During the ischemic period, the expression of brain transferrin receptor 1 (TFR1) increased, and extracts from the traditional Chinese medicine Naotai formula can reduce TFR1 expression to inhibit ferroptosis and improve brain damage. GPX4 and GSH are endogenous ferroptosis inhibitors that are closely related to cerebral ischemia. In ischemic rats, low GPX4 levels lead to ferroptosis, while increased GPX4 levels can improve cerebral damage. Phellandrene is a drug used to treat cerebral ischemia, and it can inhibit ferroptosis by enhancing GPX4 expression and reducing hippocampal neuron damage in the process of cerebral ischemia-reperfusion injury. Lipoxygenases (LOXs) are key enzymes that oxidize polyunsaturated fatty acids (PUFAs) to cause lipid peroxidation and ferroptosis. They are highly expressed after cerebral ischemia and can be inhibited to alleviate damage. There are several subtypes of LOXs, including 12/15-LOX. In the middle cerebral artery occlusion model, 12/15-LOX expression increased, and inhibition of 12/15-LOX can reduce neuron death, thus improving neuron recovery.

In summary, cerebral ischemia can induce ferroptosis, which in turn exacerbates cerebral ischemic damage. Inhibition of ferroptosis can alleviate this ischemic damage. However, the regulatory mechanisms involving brain ferroptosis remain unclear, including the upstream regulatory mechanisms of iron overload, GPX4, and 12/15-LOX. It is still uncertain whether ferroptosis directly causes cell death or indirectly causes it through other mechanisms, which requires further exploration by scholars.

3.3 The role of crosstalk between mitophagy and ferroptosis in ischemia-reperfusion injury of stroke

Reperfusion injury after cerebral ischemia is a complex pathological process caused by the restoration of blood supply following ischemia, involving various mechanisms such as oxidative stress, inflammatory responses, cellular apoptosis, and so on. Recently, it has been found that mitophagy and ferroptosis are also two closely related modes of cell death associated with cerebral ischemia-reperfusion injury. Currently, research on the crosstalk mechanisms between them is gradually unfolding. However, this research field is relatively new, with continuous new discoveries being made.

Mitophagy is a specific autophagic process that primarily functions to maintain mitochondrial quality and cellular homeostasis by eliminating damaged mitochondria. On the other hand, ferroptosis is a non-apoptotic form of cell death that depends on iron, characterized by the accumulation of lipid peroxides and inactivation of antioxidant repair systems. Some studies have suggested that in a model of ischemia-reperfusion injury in stroke, the activity of mitophagy may be regulated and interact with the iron metabolism and ferroptosis signaling pathways. As Lin QS *et al.* (Lin *et al.*, 2023) found that mitophagy could regulate iron ion levels through the ROS/HO-1/GPX4 axis, thereby alleviating cisplatin-induced ferroptosis in renal tubular epithelial cells. Another study indicated that the activity of mitophagy may be inhibited during the progression of ischemia-reperfusion injury in stroke, leading to excessive accumulation of iron ions in cells and subsequently inducing ferroptosis (Tian *et al.*, 2023). On the other hand, the dysregulation of iron metabolism and the occurrence of ferroptosis also control the autophagic flux of mitochondria in the ischemia-reperfusion injury model of stroke. According to research, mitophagy may lead to an increase in free iron content within neurons by degrading ferritin, thereby promoting iron-dependent neuronal death (Ajoolabady *et al.*, 2021; Bi *et al.*, 2021). The main mechanism appears to involve the inhibition of JNK protein phosphorylation by FUNDC1 protein (Wu *et al.*, 2019b), which is believed to suppress the transcription of Nuclear receptor coactivator-4 (NCOA4) (Guo *et al.*, 2021a), leading to increased degradation of cytoplasmic ferritin and release of free Fe²⁺, thereby inducing iron-dependent cell death (Peng *et al.*, 2016). In summary, there is an active crosstalk between mitophagy and ferroptosis in ischemia-reperfusion injury in stroke, mainly manifested in three aspects: (1) Damaged mitochondria may release a large amount of iron ions into the cytoplasm, triggering iron-dependent lipid peroxidation and promoting ferroptosis. (2) Levels of ROS are significantly increased in ischemia-reperfusion injury in stroke. ROS can not only directly damage mitochondria, leading to mitophagy, but also promote lipid peroxidation reactions and enhance ferroptosis. Therefore, ROS may be an important bridge linking mitophagy and ferroptosis. (3) Mitophagy and ferroptosis may mutually regulate each other through sharing certain signaling pathways. For example, nuclear factor E2-related factor 2 (Nrf2) is not only a key regulator of the antioxidant stress response, but also a modulator of iron metabolism. Its activation can simultaneously affect mitophagy and ferroptosis. Further research can focus on the role and mechanism of Nrf2 in regulating these two modes of cell death.

In conclusion, there is a complex crosstalk regulation mechanism between mitophagy and ferroptosis in cerebral ischemia-reperfusion injury, and the modulation of mitophagic activity may affect iron metabolism and the occurrence of ferroptosis, while abnormal levels of iron ions also affect the activity of mitophagy. Therefore, further research will help to reveal this crosstalk of regulatory mechanism, providing new targets and strategies for the treatment of ischemia-reperfusion injury in stroke.

4 Medicinal plants and their active metabolites alleviate cerebral ischemia-reperfusion injury by targeting mitophagy and ferroptosis

In recent years, an increasing number of researchers have pointed out that medicinal plants have the characteristics of “multi-component, multi-target, and multi-pathway,” which is precisely in line with the complexity and variability of the evolution process of cerebral stroke and its complications. Moreover, according to modern pharmacological research, medicinal plants and their active metabolites not only have extensive biological activities (such as antioxidant, anti-inflammatory, and anti-tumor), but they have also been proven to be relatively safe, especially compared to western drugs in terms of liver and kidney toxicity damage. Therefore, the research and development of medicinal plants (including single-medicinal plant and traditional Chinese herbal compound preparations) and their active metabolites are very promising (Tables 1–6), which greatly brings hope for patients with cerebral stroke and its complications.

4.1 Traditional Chinese herbal compound preparations alleviate cerebral ischemia-reperfusion injury by regulating mitophagy

Taohong Siwu decoction (THSWD) has the efficacy of promoting blood circulation and removing blood stasis and is a commonly used traditional Chinese medicine compound formulation for treating ischemic stroke. It is composed of *Paeonia lactiflora* Pall., *Conioselinum anthriscoides* (H.Boissieu) Pimenov and Kljuykov, *Rehmannia glutinosa* (Gaertn.). The ratio of DC., *Prunus persica* (L.) Batsch, *Angelica sinensis* (Oliv.) Diels, and *Carthamus creticus* L. is 3:2:4:3:3:2. Notably, Shi Y *et al.* (Shi *et al.*, 2023) studied the protective effects and mechanisms of THSWD on PC12 cells injured by oxygen-glucose deprivation/reperfusion (OGD/R) *in vitro*. They used the PC12 cell OGD/R model to simulate *in vitro* neuron ischemia-reperfusion injury, and evaluated the severity of PC8 cell damage by CCK-8, flow cytometry, and lactate dehydrogenase (LDH) assays. They also observed the ultrastructure of mitochondria and ferroptosis by transmission electron microscopy, and assessed mitochondrial function using ATP and mitochondrial membrane potential (MMP) detection kits. Additionally, they detected cell autophagy and NLRP3 inflammasome-related proteins by western blot and immunofluorescence staining. The results showed that THSWD

TABLE 1 Traditional Chinese herbal compound preparations alleviate the degree of cerebral ischemia-reperfusion injury by regulating mitophagic flux.

Chinese herbal compound preparations	Medicinal plants	Autophagy-related targets	In vitro/ In vivo	Model	References
Taohong Siwu decoction	<i>Bupleurum chinense</i> DC., <i>Angelica sinensis</i> (Oliv.) Diels	LC3B	In vivo	MCAO/ R-induced SD rat model	Shi et al. (2023)
	<i>Paeonia lactiflora</i> Pall., <i>Conioselinum anthriscoides</i> “Chuanxiong”, <i>Salvia miltiorrhiza</i> Bunge				
	<i>Smilax glabra</i> Roxb., <i>Plantago asiatica</i> L., <i>Buddleja officinalis</i> Maxim.				
	<i>Tribulus terrestris</i> L., <i>Alisma plantago-aquatica</i> L., <i>Leonurus japonicus</i> Houtt.,				
	<i>Senna tora</i> (L.) Roxb				
Xiao-Xu-Ming decoction	<i>Ephedra sinica</i> Stapf	LC3, Beclin1, Lamp1, SQSTM1/p62	In vivo	MCAO/ R-induced SD rat model	Lan et al. (2018)
	<i>Stephania tetrandra</i> S.Moore, <i>Panax ginseng</i> C.A.Mey				
	<i>Scutellaria baicalensis</i> Georgi				
	<i>Neolitsea cassia</i> (L.) Kosterm				
	<i>Glycyrrhiza glabra</i> L.				
	<i>Paeonia lactiflora</i> Pall., <i>Conioselinum anthriscoides</i> “Chuanxiong”				
	<i>Juglans regia</i> L.				
	<i>Aconitum carmichaelii</i> Debeaux, <i>Saposhnikovia divaricata</i> (Turcz.) Schischk., <i>Zingiber officinale</i> Roscoe				
Longhu Xingnao granules	<i>Pheretima</i> , <i>Ambrum</i> , <i>Astragalus membranaceus</i> (Fisch.) Bunge, <i>Angelica sinensis</i> (Oliv.) Diels, <i>Conioselinum anthriscoides</i> “Chuanxiong”, <i>Juglans regia</i> L., <i>Paeonia lactiflora</i> Pall., <i>Gastrodia elata</i> Blume, <i>Typha domingensis</i> Pers., <i>Rheum officinale</i> Baill., <i>Panax bipinnatifidus</i> Seem., <i>Ziziphus jujuba</i> Mill	LC3B, Beclin-1, BNIP-3	In vivo	MCAO/ R-induced SD rat model	Zhang et al. (2022b)
Huoxue Rongluo decoction	<i>Spatholobus suberectus</i> Dunn	LC3B, Pink1, Parkin, SQSTM1/p62, TOMM20	In vitro	OGD/R-induced PC12 cell model	Yan et al. (2023)
	<i>Pourthiaea villosa</i> (Thunb.) Decne., <i>Rehmannia glutinosa</i> (Gaertn.) DC., <i>Curcuma aeruginosa</i> Roxb., <i>Polygonatum cyrtoneura</i> Hua				
	<i>Boswellia sacra</i> Flück., <i>Commiphora myrrha</i> (T.Nees) Engl., <i>Conioselinum anthriscoides</i> “Chuanxiong”				
Huazhuo Jiedu Huoxue Tongluo decoction	<i>Coptis chinensis</i> Franch.	Pink1, Parkin	In vivo	MCAO/ R-induced SD rat model	Sun et al. (2023)
	<i>Smilax glabra</i> Roxb., <i>Alisma plantago-aquatica</i> L.,				
	<i>Salvia miltiorrhiza</i> Bunge, <i>Paeonia lactiflora</i> Pall., <i>Angelica sinensis</i> (Oliv.) Diels, <i>Dianthus chinensis</i> L., <i>Curcuma aromatica</i> Salisb., <i>Conioselinum anthriscoides</i> “Chuanxiong”, <i>Pheretima</i> , <i>Glycyrrhiza glabra</i> L				
Qizhi granules	<i>Astragalus membranaceus</i> (Fisch.) Bunge, <i>Reynoutria multiflora</i> (Thunb.) Moldenke, <i>Whitmania pigra</i> Whitman, <i>Juglans regia</i> L., <i>Curcuma phaeocaulis</i> Valetton, <i>Sparganium stoloniferum</i> , Buch. -Ham., <i>Senna tora</i> (L.) Roxb.,	LC3B, SQSTM1/p62	In vivo	MCAO/ R-induced SD rat model	Duan et al. (2023)
	<i>Crataegus pinnatifida</i> Bunge, <i>Trionyx sinensis</i> Wiegmann				

TABLE 2 Traditional Chinese herbal compound preparations alleviate the degree of cerebral ischemia-reperfusion injury by regulating ferroptosis levels.

Chinese herbal compound preparations	Medicinal plants	Ferroptosis-related targets	In vitro/ In vivo	Model	References
Xingnaojing injection	<i>Moschus</i> , <i>Curcuma aromatica</i> Salisb., <i>Gardenia jasminoides</i> J. Ellis, <i>Dryobalanops aromatica</i> C.F.Gaertn	GPX4, FPN, TFR, DMT1	In vitro, in vivo	Hypoxia SH-SY5Y cell model, MCAO/R-induced SD rat model	Liu et al. (2023a)
Naotai formula	<i>Pheretima</i> , <i>Astragalus membranaceus</i> (Fisch.) Bunge, <i>Ligusticum sinense</i> Oliv., <i>Bombyx mori</i> Linnaeus	BMP6, SMADs, FPN, SLC40A1, GSH, GPX4	In vitro	OGD/R-induced BV2 cell model	Liao et al. (2023)
Compound tongluo decoction	<i>Pleuropterus multiflorus</i> (Thunb.) Nakai, <i>Polygonatum cyrtonema</i> Hua, <i>Ecklonia kurome</i> , <i>Bombyx mori</i> Linnaeus, <i>Euonymus alatus</i> (Thunb.) Sieb, <i>Gastrodia elata</i> Blume, <i>Whitmania pigra</i> Whitman	SHH, Gli1, GPX4, ACSL4, ALOX5	In vitro, in vivo	OGD/R-induced hippocampal neurons cell model, MACO/R-induced rat model	Hui et al. (2022)
Wenyang Fuyuan decoction	White appendage, <i>Astragalus membranaceus</i> (Fisch.) Bunge, <i>Codonopsis pilosula</i> (Franch.) Nannf., <i>Dianthus chinensis</i> L., <i>Epimedium brevicornu</i> Maxim., <i>Panax notoginseng</i> (Burkill) F. H. Chen ex C. H. Chow, <i>Zingiber o-jicinale</i> Rosc., <i>Glycyrrhiza glabra</i> L	TFR1, GSH, IRP1, FPN	In vivo	MCAO/R-induced SD rat model	Li et al. (2023)
Buyang Huanwu decoction	<i>Astragalus membranaceus</i> (Fisch.) Bunge, <i>Angelica sinensis</i> (Oliv.) Diels, <i>Paeonia lactiflora</i> Pall., <i>Pheretima</i> , <i>Conioselinum anthriscoides</i> "Chuanxiong," <i>Juglans regia</i> L., <i>Carthamus tinctorius</i> L	TfR1, DMT1, FPN1, GPX4	In vitro, in vivo	OGD/R-induced HT22 cell model, MCAO/R-induced SD rat model	Cai (2023)

TABLE 3 A single medicinal plant alleviates the degree of cerebral ischemia-reperfusion injury by modulating mitophagic flux.

Single medicinal plants	Autophagy-related targets	In vitro/In vivo	Model	References
Dengzhan Xixin injection	LC3B, SQSTM1/p62, TOM20, Pink1, Parkin	In vivo	MCAO/R-induced SD rat model	Yang et al. (2022)
Saffron extract	LC3B, AMPK, mTOR	In vitro	OGD/R induced HT22 cell model	Huang et al. (2019)
Ginkgo biloba extract	Beclin1, LC3B, SQSTM1/p62	In vivo	MCAO/R-induced SD rat model	Zang et al. (2023)

TABLE 4 A single medicinal plant alleviates the degree of cerebral ischemia-reperfusion injury by modulating ferroptosis levels.

Single medicinal plants	Autophagy-related targets	In vitro/In vivo	Model	References
<i>Paeoniae Radix Rubra</i>	GPX4, FTH1	In vitro, in vivo	HT22 cell line following oxidative stress model, MCAO injury SD rat model	Zhao et al. (2023a)
Neutral polysaccharide from <i>Gastrodia elata</i>	GPX4	In vitro, in vivo	OGD/R induced HT22 cell model IS mouse model	Zhang et al. (2023)
Roots of <i>Astragalus</i>	Fn, FHC, FLC, Tf, TfR, DMT1, LTCC, TRPC6, FPN1, SLC3A2, GPX4	In vivo	MCAO/R-induced SD rat model	Chen et al. (2022)

treatment improved the survival rate of OGD/R-damaged PC12 cells, reduced cell damage and apoptosis. Moreover, the expression of ATP, MMP, and autophagy markers (LC3-II/LC3-I, Beclin1, Atg5) and mitochondrial autophagy markers (Parkin and PINK-1) was significantly increased, while the levels of ROS, NLRP3 inflammasome, and pro-inflammatory cytokines were significantly decreased. These beneficial effects of THSWD on mitochondrial autophagy and NLRP3 inflammasome were reversed by mitochondrial division inhibitory factor 1 (Mdivi-1). The study indicates that THSWD can protect PC3 cells from OGD/

R damage by enhancing mitochondrial autophagy and inhibiting the activation of NLRP12 inflammasome, which provides a certain theoretical basis for the application of THSWD in ischemic stroke and reperfusion injury.

Xiao-Xu-Ming decoction (XXMD), with the efficacy of warming the Yang, promoting blood circulation, and removing blood stasis, has been widely used in the treatment of ischemic stroke, and its clinical effect is significant. It is composed of herbs such as ephedra, aristolochia, panax ginseng, scutellaria baicalensis, cinnamon, licorice, peony, ligusticum chuanxiong, apricot kernel, aconitum,

TABLE 5 The active metabolite alleviates the degree of cerebral ischemia-reperfusion injury by modulating mitophagic flux.

Metabolites	Medicinal plants	Autophagy-related targets	In vitro/ In vivo	Model	References
Ligustilide	<i>Conioselinum anthriscoides</i> “Chuanxiong” and <i>Angelica sinensis</i> (Oliv.) Diels	Parkin, Pink1	In vitro, in vivo	OGD/R-induced hippocampal neurons cell model, MCAO/R-induced SD rat model	Mao et al. (2022)
Artemisinin	<i>Artemisia Annua</i> L	PHB2, Tomm20, SQSTM1/p62, LC3B	In vitro	OGD/R-induced SH-SY5Y cell model	Jiang et al. (2022)
Jionoside A1	<i>Rehmannia glutinosa</i> (Gaertn.) DC.	LC3B, SQSTM1/p62, Nix, Parkin, FUNCD1	In vitro, in vivo	OGD/R-induced cell model, tMCAO/R-induced SD rat model	Yu et al. (2023)
Ginsenoside compound K	<i>Panax ginseng</i> C.A.Mey	LC3B, Tomm20	In vitro, in vivo	OGD/R-induced PC12 cell model, MCAO/R-induced SD rat model	Huang et al. (2023)
Panax notoginseng saponins	<i>Panax Notoginseng</i> (Burk.) F. H. Chen Ex C. Chow	Parkin, Pink1	In vivo	MCAO/R-induced SD rat model	Xiao et al. (2022)
Curcumin	<i>Curcuma longa</i> L.	LC3B	In vitro, in vivo	OGD/R-induced neurons cell model, MCAO/R-induced SD rat model	Wang and Xu (2020)
Naringin	<i>Citrus reticulata</i> Blanco	LC3B, Parkin	In vitro, in vivo	OGD/R-induced SH-SY5Y cell model, MCAO/R-induced SD rat model	Feng et al. (2018)
Garciesculenxanthone B	<i>Garcinia hanburyi</i> Hook.f.	Parkin, Pink1, LC3B,SQSTM1/p62, Tomm20, Timm23, MFN1	In vitro, in vivo	OGD/R-induced HeLa and SH-SY5Y cell model, MCAO/R-induced mice model	Wu et al. (2021a)
Salidroside	<i>Rhodiola rosea</i> L	Parkin, Pink1, LC3B, p62, Tomm20	In vitro, in vivo	OGD/R-induced neuronal cell model, MCAO/R-induced C57BL/6 mice model	Gu et al. (2020)
Esculetin	<i>Aesculus chinensis</i> Bunge	Bnip3, Beclin1, Pink1, Parkin, LC3B	In vivo	tMCAO/R-induced mice model	Xu et al. (2019)
Baicalin	<i>Scutellaria baicalensis</i> Georgi	Drp1, AMPK, SQSTM1/p62	In vitro, in vivo	OGD/R-induced PC12 cell model, MCAO/R-induced SD rat model	Li et al. (2017)
Resveratrol	<i>Polygoni Cuspidati Rhizoma Et Radix</i>	LC3B, Timm23, Tomm20, Pink1, Parkin	In vitro	OGD/R-induced primary cortical neurons cell model	Ye et al. (2021)
Oridonin	<i>Isodon rubescens</i> (Hemsl.) H.Hara	RIPK3, AMPK, Pink1, Parkin, LC3B, SQSTM1/p62	In vivo	tMCAO/R-induced mice model	Li et al. (2023c)
Rehmapicroside	<i>Rehmannia glutinosa</i> (Gaertn.) DC.	Parkin, Pink1, SQSTM1/p62, LC3B	In vitro, in vivo	OGD/R-induced PC12 cell model, MCAO/R-induced SD rat model	Zhang et al. (2020)

radix saposhnikoviae, and ginger. Previous studies have shown that XXMD can protect neurons, blood vessels, and mitochondria from cerebral ischemia-reperfusion-induced damage (Zhu et al., 2010; Lan et al., 2013, 2014). However, it remains unclear whether XXMD can regulate mitochondrial autophagy after cerebral ischemia-reperfusion. Therefore, Lan R et al. (Lan et al., 2018) investigated the effects of XXMD on mitochondrial autophagy and mitochondrial function after cerebral ischemia-reperfusion. They used triphenyltetrazolium chloride (TTC) staining to measure the infarct area, hematoxylin and eosin (HE) staining and Nissl staining to assess cerebral ischemic damage, and transmission electron microscopy to observe the ultrastructural characteristics of mitochondria and mitochondrial autophagy in ischemic cerebral cortex. Subsequently, they also detected mitochondrial autophagy by immunofluorescence labeled with LC3B and VDAC1, observed the formation of autophagosomes labeled with LC3B and Lamp1, and analyzed the expression levels of LC3B, Beclin1, and Lamp1 proteins by western blot. The results showed that the neurological score worsened and cell ischemic damage was severe in MCAO rats.

However, these phenomena were significantly reversed by XXMD. In addition, XXMD significantly downregulated mitochondrial autophagy and reduced the expression levels of LC3B, Beclin1, and Lamp1 proteins induced by cerebral ischemia-reperfusion. This study suggests that XXMD exerts neuroprotective effects by down-regulating the expression levels of LC3B, Beclin1, and Lamp1 proteins, thereby reducing mitochondrial activation and improving mitochondrial function in cerebral ischemia-reperfusion injury.

4.2 Traditional Chinese herbal compound preparations alleviate cerebral ischemia-reperfusion injury by regulating ferroptosis

Xingnaojing injection (XNJ) is made of natural musk, gold, gardenia, borneol and other herbs through scientific methods, which has the effect of clearing heat, cooling blood, and promoting blood circulation. XNJ is a neuroprotective traditional Chinese medicine

TABLE 6 The active metabolite alleviates the degree of cerebral ischemia-reperfusion injury by modulating ferroptosis levels.

Metabolites	Medicinal plants	Ferroptosis-related targets	In vitro/In vivo	Model	References
β -Caryophyllene	<i>Dianthus chinensis</i> L.	ACSL4, COX2, GPX4	In vitro, in vivo	OGD/R-induced primary astrocytes model, MCAO/R-induced SD rat model	Hu et al. (2022)
Carthamin yellow	<i>Carthamus tinctorius</i> L.	ACSL4, FTH1, GPX4, TFR1	In vivo	MCAO/R-induced SD rat model	Guo et al. (2021b)
Baicalein	<i>Scutellaria baicalensis</i> Georgi	GPX4, ACSL4, ACSL3	In vitro, in vivo	OGD/R-induced HT22 cell model, tMCAO/R-induced mice model	Li et al. (2022a)
Rehmannioside A	<i>Rehmannia glutinosa</i> (Gaertn.) DC.	SLC7A11, GPX4	In vitro, in vivo	H2O2-induced SH-SY5Y cell model, MCAO/R-induced SD rat model	Fu et al. (2022)
Dihydromyricetin	<i>Nekemias megalophylla</i> (Diels and Gilg) J.Wen and Z.L.Nie	GPX4, ACSL4, PEBP1	In vitro, in vivo	OGD/R-induced HT22 cell model, MCAO/R-induced SD rat model	Xie et al. (2022)
Astragaloside IV	<i>Hedysarum Multijugum</i> Maxim	GPX4, GSH	In vitro, in vivo	OGD/R-induced SH-SY5Y cell model, MCAO/R-induced SD rat model	Wang et al. (2023a)
Kaempferol	<i>Kaempferiae Rhizoma</i>	SLC7A11, GPX4	In vitro	OGD/R-induced neuronal injury	Yuan et al. (2021)
Procyanidins	<i>Vitis vinifera</i> L.	GPX4, SLC7A11	In vivo	MCAO/R-induced mice model	Chen et al. (2023)
Galangin	<i>Alpiniae Officinarum Rhizome</i>	SLC7A11, GPX4	In vivo	Using bilateral common carotid artery ligation in gerbils	Guan et al. (2021)
Vitexin	<i>Vitidis Negundo Folium</i>	Tfr1, SLC7A11, GPX4	In vitro, in vivo	OGD/R-induced neuron cell model, MCAO/R-induced SD rat model	Guo and Shi (2023)
Oxysophoridine	<i>Sophora flavescens</i> Aiton	ACSL4, TFR1, FTH1, GPX4	In vitro, in vivo	OGD/R-induced HT22 cell model, MCAO/R-induced SD rat model	Zhao et al. (2023b)
Ginkgolide B	<i>Ginkgo biloba</i> L.	ACSL4, GPX4, FTH1, NCOA4	In vitro, in vivo	OGD/R-induced PC12 cell model, tMCAO/R-induced SD rat model	Yang et al. (2024)
Resveratrol	<i>Oroxylum indicum</i> (L.) Kurz	SLC7A11, TFR1, GPX4, ACSL4, PTGS2	In vivo	MCAO/R-induced SD rat model	Li et al. (2022b)
Berberine	<i>Coptis chinensis</i> Franch	GPX1	In vivo	MCAO/R-induced mice model	Wang et al. (2023b)
Soybean isoflavones	<i>Glycine max</i> (L.) Merr	GPX4	In vivo	MCAO/R-induced SD rat model	Li et al. (2023d)

Abbreviations: MCAO/R, middle cerebral artery occlusion/reperfusion; SD, sprague dawley; OGD/R, oxygen-glucose deprivation/reoxygenation; tMCAO/R, transient middle cerebral artery occlusion/reperfusion.

injection, which has been widely used in the treatment of stroke. Liu HQ *et al.* (Liu et al., 2023a) explored the potential mechanism of XNJ in ferroptosis-mediated cerebral ischemia using proteomics and *in vitro* and *in vivo* experiments. They found that XNJ treatment reduced the infarct volume and brain tissue damage in MCAO rats. Nissl staining also showed that compared with MCAO rats, the brain tissue Nissl bodies in XNJ-treated rats were clear, increased by 3.54 times, indicating that XNJ improved the cerebral damage and neurological deficit in MCAO rats. Proteomics identified 101 differentially expressed proteins (DEPs) shared by both conditions. Interestingly, these DEPs were closely related to ferroptosis according to bioinformatics analysis. Further studies showed that after XNJ treatment, the expressions of GPX4, ferroportin (FPN), and heme oxygenase-1 (HO-1) were upregulated, while the expressions of cyclooxygenase-2 (COX-2), transfer receptors (TFR), and divalent metal transporter-1 (DMT1) were downregulated, which relieved MCAO-induced cerebral ischemia. In addition, *in vitro* experiments showed that XNJ increased the survival rate of hypoxic injured SH-SY5Y cells. XNJ increased the level of GPX4 after cell hypoxia, inhibited the protein expression of COX-2 and TFR. Additionally, XNJ of different

concentrations (0.25%, 0.5%, 1%) decreased the ROS content in hypoxic cells, indicating that XNJ can inhibit hypoxia-induced cell damage by regulating the expression of ferroptosis-related proteins and reducing ROS production. This study suggests that XNJ can promote the recovery of neurological function in MCAO rats and hypoxic SH-SY5Y cells by regulating ferroptosis.

Naotai formula (NTF) is a novel traditional Chinese medicine therapy for ischemic stroke, showing beneficial effects in inhibiting inflammation and lipid peroxidation synthesis. Liao J *et al.* (Liao et al., 2023) established an OGD/R model using BV2 microglial cells and detected the effects of NTF on inflammation and ferroptosis in OGD/R-damaged BV2 microglial cells using immunofluorescence, fluorescence probe method, DCFH-DA flow cytometry, enzyme-linked immunosorbent assay (ELISA), and western blot technology. The results showed that microglial M1 polarization promotes the secretion of pro-inflammatory cytokines and exacerbates ferroptosis and brain damage after OGD/R surgery. However, the BMP6 inhibitor LND-193189 reversed these effects. Similarly, NTF promotes the shift of microglia from M1 to M2. In addition, NTF effectively inhibits the expression of ferromodulin, BMP6 and SMADs, and promotes the expression levels of

ferroportin (FPN, SLC40A1) and GPX4. This study indicates that microglial M1/M2 polarization plays a crucial role in inflammation and ferroptosis during OGD/R. The BMP6/SMADs signaling pathway is a potential therapeutic target for microglial transformation-induced inflammation and ferroptosis. Notably, NTF can alleviate inflammation and ferroptosis in BV2 microglial cells by regulating the BMP6/SMADs signaling pathway in OGD/R-induced damage.

Compound tongluo decoction (CTLD) is a traditional Chinese medicine formula with various pharmacological activities, including improving cerebral ischemia symptoms. To further explore the potential mechanism of CTLD in relieving cerebral ischemia, Hui Z *et al.* (Hui *et al.*, 2022) established MCAO rat models and OGD/R cell models for research. The expression of endoplasmic reticulum (ER) stress, ferroptosis, Sonic Hedgehog (SHH) pathway-related proteins, and angiogenesis-related proteins were analyzed by Western blot. The expression of CD31 was detected by immunofluorescence to study angiogenesis. Furthermore, immunohistochemistry was used to detect the expression of GRP78 and XBP-1 in brain tissue. Prussian blue staining was applied to detect iron deposition in brain tissue. ELISA kits were used to measure ROS, malondialdehyde (MDA), and superoxide dismutase (SOD) levels. Angiogenesis was analyzed by tube formation assays. The results showed that CTLD and 4-phenylbutyric acid (4-PBA, a ER stress inhibitor) can alleviate cerebral ischemia symptoms. At the molecular level, CTLD and 4-PBA rescued ER stress and ferroptosis but promoted the SHH signaling pathway in cerebral infarction rats. Interestingly, cerebral infarction showed high levels of angiogenesis, and CTLD exacerbated angiogenesis but 4-PBA inhibited it. In addition, CTLD inhibited ER stress and ferroptosis but promoted angiogenesis in OGD/R-induced PC12 cells, which was partially reversed by the SHH signaling antagonist SANT-1. Overall, this study revealed that CTLD may alleviate cerebral ischemia symptoms by activating the SHH pathway in cerebral infarction rats, inhibiting ER stress-induced ferroptosis, and promoting angiogenesis.

4.3 Single-medicinal plant alleviate cerebral ischemia-reperfusion injury by regulating mitochondrial autophagy

Dengzhan Xixin injection (DX) is an herbal extract derived from the medicinal plant *Brachypodium distachyon*, which has been widely used in the clinical treatment of sequelae of cerebral ischemia. Lv Y *et al.* (Lv *et al.*, 2022) detected the main components of DX by high-performance liquid chromatography (HPLC) and established an SD rat brain ischemia-reperfusion injury model using MCAO. They found that DX mainly contains baicalein, 3,4-O-dicaffeoylquinic acid, 3,5-O-dicaffeoylquinic acid, 4,5-O-dicaffeoylquinic acid, caffeic acid, and 5-O-caffeoylquinic acid. Compared with the model group, DX significantly alleviated neurological deficits, reduced rCBF deficiency, and cerebral infarction symptoms. Furthermore, the pathological changes and neuron loss in the rat MCAO model were significantly improved after DX administration. Simultaneously, DX decreased the increased levels of ROS and MDA while increasing the level of SOD. Notably, DX treatment led to the collapse of ATP and the

MMP system, as well as a decrease in the relative copy number of mitochondrial DNA (mtDNA). Increasing the number of autophagosomes helped maintain the ultrastructure of mitochondria. The representative components of DX had potential binding sites for mitochondrial autophagy/apoptosis-related proteins. DX increased the protein expression of LC3B, PINK1, and Parkin while reducing the levels of p62 and TOM20. In addition, DX limited the TUNEL-positive cell rate, decreased the expression of Bax, Cyto-c, and cleaved Caspase-3, and increased the level of Bcl-2. This study confirmed that the protection of DX against cerebral ischemia is attributed to up-regulating mitochondrial autophagy and inhibiting mitochondria-mediated cell apoptosis, thus effectively improving rat cerebral ischemia-reperfusion injury.

4.4 Single-medicinal plant alleviate cerebral ischemia-reperfusion injury by regulating ferroptosis

Paeonia lactiflora, a natural medicinal plant, has been widely used in clinical practice in China to promote blood circulation and eliminate blood stasis. However, its effects on cerebral ischemia are rarely reported. To evaluate the potential therapeutic effects of *P. lactiflora* extracts on cerebral ischemia and explore its potential mechanisms, Zhao FY *et al.* (Zhao *et al.*, 2023a) conducted a study to preliminarily screen the active ingredients and provide an experimental basis for the potential application of *P. lactiflora* as a novel therapeutic drug. They found that *P. lactiflora* extracts can reduce the infarct volume and improve the neurological deficit in rats, as well as upregulate the expression of GPX4, FTH1, Beclin1, LC3 II, and p-Akt in the hippocampus. Meanwhile, *in vitro* studies showed that *P. lactiflora* extracts could alleviate H₂O₂-induced HT22 cell damage by regulating cell factors, such as MDA, GSH, and ROS, accompanied by increased protein expression of GPX4 and Beclin1. Notably, the PI3K/Akt signaling pathway can be inhibited by the PI3K inhibitor LY294002. Further studies confirmed that the effective components of *P. lactiflora* extracts in regulating ferroptosis and autophagy are mainly defined as albiflorin, paeoniflorin, benzoylpaeoniflorin, oleanolic acid, and hesperetin. These data suggest that *P. lactiflora* extracts exert neuroprotective effects by inhibiting ferroptosis and activating autophagy through the PI3K/Akt signaling pathway. This study not only lays a theoretical foundation for the potential application of *P. lactiflora* extracts as a novel therapeutic drug but also provides insights into the PI3K/Akt-related ferroptosis and autophagy as therapeutic targets for cerebral ischemia.

The crosstalk between ferroptosis and neuroinflammation plays a significant role in the pathogenesis of cerebral ischemia-reperfusion injury. Studies have shown that neutral polysaccharides (NPGE) from medicinal plant *Gastrodia elata* have significant effects on oxidative stress and inflammation (Zhu *et al.*, 2019). To investigate the potential impact of NPGE on neuropathology in ischemic brain reperfusion injury, Zhang YG *et al.* (Zhang *et al.*, 2023) conducted a series of experiments by using a mouse model of ischemic stroke and HT22 cells induced by OGD/R. They found that NPGE treatment could reduce neurologic impairment, reduce infarct volume, alleviate brain edema, and promote the survival of OGD/R-induced HT22 cells in ischemic

stroke mice. At the molecular level, NPGE treatment relieved neuron iron death by upregulating GPX4 levels, reducing ROS and MDA, reducing excessive accumulation of Fe^{2+} , improving glutathione levels, and SOD activity. In addition, NPGE treatment inhibited neuroinflammation by downregulating the levels of IL-1 β , IL-6, TNF- α , NLRP3, and HMGB1. Simultaneously, NPGE treatment alleviated Erastin-induced HT22 cell iron death and inflammation. Furthermore, NPGE upregulated the expression of NRF2 and HO-1, promoting NRF2 translocation to the cell nucleus. Lastly, they also used the NRF2 inhibitor brusatol to verify that the NRF2/HO-1 signaling pathway mediated NPGE's anti-iron cell proliferation and anti-inflammatory properties. In summary, their research results demonstrated the protective effects of NPGE and emphasized its therapeutic potential as a component of a drug for treating ischemic brain reperfusion injury.

The dried root of the medicinal plant *Astragalus membranaceus* is commonly used as a traditional Chinese medicine and has been widely used in clinical practice for the treatment of stroke, cerebral ischemia, qi deficiency, and hypertension (Fu et al., 2014; Chen et al., 2020; Zhang et al., 2021). The Bu Yang Huan Wu Tang, which has been used in traditional Chinese medicine to treat stroke for more than 200 years, has a significant effect on cerebral ischemia, with *A. membranaceus* as the main ingredient. Therefore, Chen J et al. (Chen et al., 2022) studied the regulation of *A. membranaceus* on transmembrane iron transport proteins and iron-related factors in rat cerebral ischemia reperfusion injury. They established a rat cerebral ischemia reperfusion injury model by using MCAO to block the blood supply of the bilateral cerebral middle cerebral artery in two male SD rats. Subsequently, they explored the regulation of *A. membranaceus* on iron transmembrane transport under conditions of cerebral ischemia reperfusion injury. Next, they used TTC staining to measure the infarct area, H&E staining to observe the histological structure of the brain tissue, and Nissl staining to assess neuronal damage. Then, they observed iron transport proteins, including ferritin (Fn), ferritin heavy chain (FHC), ferritin light chain (FLC), transferrin (Tf), transferrin receptors (TfR), DMT1, L-type calcium channels (LTCC), transient receptor potential canonical 6 (TRPC6), and FPN1, by immunohistochemistry and western blotting. Western blotting was used to detect the expression of membrane sodium-dependent cystine/glutamate reverse transport protein system Xc (System Xc) light chain subunit (XCT) and heavy chain subunit (SLC3A2), GPX4, nuclear factor erythroid 2-related factor (NFE2L2), HO-1, and iron-responsive element-binding protein 2 (IREB2) in rat brain tissue. The results showed that *A. membranaceus* reduced the infarct area and neuronal damage in the rat model after surgery. Similarly, *A. membranaceus* treatment could regulate the expression of iron transport proteins. Therefore, *A. membranaceus* was able to reduce the expression of Fn, FHC, FLC, Tf, TfR, DMT1, and TRPC6 in rats after cerebral ischemia reperfusion injury, and increase the expression of FPN1 through a Tf/TfR-independent pathway. This study suggests that *A. membranaceus* stimulation inhibits the iron death process by regulating key iron death factors, such as XCT, SLC3A2, GPX4, NFE2L2, HO-1, and IREB2. In summary, the root of *A. membranaceus* regulates transmembrane iron transport and iron death, thereby improving cerebral ischemia-reperfusion injury.

4.5 Metabolites alleviate cerebral stroke ischemia-reperfusion injury by regulating mitochondrial autophagy

Increasing evidence indicates that abundant metabolites in medicinal plants can mitigate cerebral stroke ischemia-reperfusion injury through regulating mitochondrial autophagy (Pineda-Ramírez et al., 2020; Ahsan et al., 2021). Ligustalactylone (LIG) is a natural compound extracted from *Chinese angelica* and *ligusticum*, which exhibits neuroprotective activity after cerebral ischemia-reperfusion injury. As reported by Mao ZG et al. (Mao et al., 2022), using MCAO/R as an animal model and OGD/R as an *in vitro* model, they investigated the neuroprotective effects of LIG on MCAO/R rats by performing neurobehavioral scoring, TTC staining, and HE staining. They reflected mitochondrial function by measuring the levels of ROS, MMP, and Na-K-ATPase activity and observed mitochondrial autophagy under transmission electron microscopy and fluorescence microscopy. Western blot analysis was used to examine the protein expression changes in mitochondrial autophagy mediated by PINK1/Parkin. Subsequently, cell transfection was employed to explore the specific mechanism of LIG neuroprotection and mitochondrial autophagy. The results showed that LIG enhanced mitochondrial function *in vivo* and *in vitro* by promoting mitochondrial autophagy, thereby alleviating cerebral ischemia-reperfusion injury. However, PINK1 deficiency and midivi-1 (a mitochondrial division inhibitor) further exacerbated ischemia-induced brain damage, mitochondrial dysfunction, and neuron injury, thereby eliminating the enhanced mitochondrial autophagy under cerebral ischemia-reperfusion injury. This study indicates that LIG can improve neuron damage in ischemic stroke by promoting mitochondrial autophagy through PINK1/Parkin, and targeting PINK1/Parkin-mediated mitochondrial autophagy and LIG therapy may be a promising therapeutic strategy for ischemic stroke.

Studies have shown that oxidative stress plays a crucial role in cerebral ischemia-reperfusion injury. Artemisinin (ART) is a natural metabolite extracted from medicinal plant *Artemisia annua*. Recent research indicates that ART not only has a potent antimalarial effect (Chaturvedi et al., 2010), but also exhibits antioxidant stress activity (Ahmed-Laloui et al., 2022). As reported by Jiang MH et al. (Jiang et al., 2022), they constructed an *in vitro* model of cerebral ischemia-reperfusion injury by using OGD/R. Subsequently, they assessed cell damage by using CCK-8 and LDH release, and evaluated the oxidative stress-induced damage and ART's protective effects by using measurements of ROS, MDA, SOD, GSH, and MMP. The results showed that OGD/R treatment exacerbated oxidative stress damage, while ART reversed the effects of OGD/R, suggesting that autophagy might be closely related to oxidative stress. To confirm whether the antioxidant stress effects of ART were related to PHB2-mediated autophagy, they measured the protein expression of PHB2, TOMM20, p62, and the conversion of LC3I to LC3II. They found that the protein expression of PHB2, TOMM20, p62, and the LC3II/LC3I ratio was significantly correlated with OGD/R treatment. After OGD/R treatment, the colocalization of PHB2 and LC3, TOMM20 and LC3 decreased, and ART reversed these changes. Silencing PHB2 reduced the protective effects of ART on OGD/R-induced oxidative stress damage, as well as the protein expression

of PHB2, TOMM20, and LC3II/LC3I and the colocalization of PHB2 and LC3B, TOMM20 and LC3B. Subsequently, they found that ART increased the conversion of LC3I to LC3II after chloroquine-induced inhibition of the lysosomal pathway, silenced PHB2, thereby inhibiting the conversion of LC3I to LC3II and impairing mitochondrial autophagy. This study demonstrates that ART alleviates OGD/R-induced oxidative stress damage through PHB2-mediated mitochondrial autophagy in human neuroblastoma SH-SY5Y cell line, providing new insights for the treatment of oxidative damage induced by cerebral ischemia-reperfusion in clinical practice.

Jionoside A1, a substance found in the traditional Chinese herb *Radix Rehmanniae Praeparata*, may possess neuroprotective properties. As reported by Yu XY *et al.* (Yu *et al.*, 2023), they constructed *in vitro* and *in vivo* models by using OGD/R and temporary middle cerebral artery occlusion (tMCAO), respectively, and intervened with Jionoside A1 treatment and small interfering RNA (siRNA) to reduce Nix expression. The results showed that Jionoside A1 could alleviate stroke ischemia-reperfusion injury by promoting Nix-mediated mitochondrial autophagy. This study provides new experimental information for the research on ischemic stroke ischemia-reperfusion injury and lays a certain theoretical basis for its application.

Ginsenoside compound K (GCK) is a major active metabolite in *ginseng* and has shown good safety and bioavailability in clinical trials, possessing neuroprotective effects on cerebral ischemic stroke (Oh and Kim, 2016). However, its potential role in preventing cerebral stroke ischemia-reperfusion injury remains unclear. Huang QX *et al.* (Huang *et al.*, 2023) confirmed through *in vitro* and *in vivo* models that GCK pretreatment could alleviate Drp1 mitochondrial translocation, mitochondrial autophagy, mitochondrial apoptosis, and neuronal bioenergetic imbalance, thus inhibiting stroke ischemia-reperfusion injury. Furthermore, GCK treatment could decrease the binding affinity of Mfn1 and Mfn2, inhibit Mfn1/Mfn2-mediated ubiquitination and degradation, and increase the protein level of Mfn2 in cerebral ischemia-reperfusion injury. In summary, these data indicate that GCK may be a promising therapeutic agent that can antagonize stroke ischemia-reperfusion injury through Mfn1/Mfn2-mediated mitochondrial dynamics and bioenergetics.

4.6 Metabolites alleviate cerebral stroke ischemia-reperfusion injury by regulating ferroptosis

Ischemic stroke is a complex brain disease regulated by multiple cell death processes, including apoptosis, autophagy, and ferroptosis. β -Caryophyllene (BCP) is a natural bicyclic sesquiterpene rich in *essential oils* and has been shown to have potential pharmacological benefits in various diseases, including ischemic stroke (Fidyt *et al.*, 2016; Yang *et al.*, 2017; Scandiffio *et al.*, 2020). As reported by Hu QW *et al.* (Hu *et al.*, 2022), ferroptosis was involved in the process of ischemia-reperfusion-induced neural damage, indicating that this novel cell death might provide new therapeutic options for the clinical treatment of ischemic stroke. *In vivo* studies have demonstrated that BCP improves neurological scoring, infarct volume, and pathological characteristics after

MCAO/R surgery. Furthermore, BCP significantly enhanced NRF2 nuclear translocation, activated the NRF2/HO-1 pathway, and prevented ferroptosis. Interestingly, similar results were obtained *in vitro*, where BCP reduced ROS generation and iron accumulation induced by OGD/R. Notably, the NRF2 inhibitor ML385 reversed the neuroprotective effects of BCP. These data indicate that ferroptosis plays a crucial role in cerebral ischemia-reperfusion injury, and this is the first time that a significant neuroprotective effect of BCP in reducing ischemic stroke damage has been discovered, which is closely related to the regulation of ferroptosis, possibly involving the activation of the NRF2/HO-1 axis.

Carthamin yellow (CY) is a flavonoid metabolite extracted from *safflower*, which has been shown to alleviate myocardial ischemia and reperfusion injury. However, it remains unclear whether CY can improve ischemic stroke. Guo HH *et al.* (Guo *et al.*, 2021b) investigated the preventive effect of CY on experimental ischemic stroke using MCAO model rats. They found that after 2a0weeks of CY treatment, the neurological deficit score, brain water content, and infarct area were reduced, and MAP-2 immunoreactivity in the cerebral cortex was increased. Furthermore, CY treatment resulted in the inactivation of the cortical NF- κ B/NLR family pyrin domain containing three inflammatory signaling pathways, as well as decreased serum levels of TNF- α , IL-1 β , and IL-6. Additional studies revealed that CY treatment inhibited the accumulation of Fe²⁺ and reactive oxygen species, as well as reversed the expression levels of acyl-CoA synthetase long chain family member 4, transferrin receptor 1, glutathione peroxidase 4, and ferritin heavy chain 1 protein in the brain. CY treatment also reversed the levels of glutathione, superoxide dismutase, and malondialdehyde in the serum. In conclusion, this study demonstrates that CY can protect rats from ischemic stroke damage, which may be achieved through alleviating inflammation and ferroptosis.

Baicalein, a major bioactive metabolite isolated from the root bark of the medicinal plants *Scutellaria baicalensis*, has been investigated for its potential role in ischemic stroke. Li M *et al.* (Li *et al.*, 2022a) studied the potential effects of baicalein on cerebral ischemia-reperfusion injury using HT22 cells induced by OGD/R, tMCAO mice, and RSL3-simulated HT22 cells. They found that baicalein increased the viability of OGD/R-treated HT22 cells in the tMCAO model mice and significantly improved cerebral ischemia-reperfusion injury. Additionally, baicalein decreased the levels of iron, lipid peroxidation, and morphological features of ferroptosis in the brain tissue of tMCAO model mice, indicating that baicalein can alleviate cerebral ischemia-reperfusion injury *in vitro* and *in vivo* by inhibiting ferroptosis. Further studies confirmed the inhibitory activity of baicalein on ferroptosis in RSL3-stimulated HT22 cells. The results of western blotting showed that baicalein inhibited ferroptosis by regulating the expression levels of GPX4, ACSL4, and ACSL3 in OGD/R-treated cells, tMCAO mice, and RSL3-stimulated HT22 cells. These data suggest that baicalein can reverse cerebral ischemia-reperfusion injury by resisting ferroptosis, possibly through the regulation of the GPX4/ACSL4/ACSL3 axis, which reflects the potential of baicalein as a therapeutic agent for cerebral ischemia-reperfusion injury.

Reypolysaccharide A is derived from medicinal plant *Radix Rehmanniae Praeparata*, which is widely used as an important

component of a variety of medicinal plants in China, and is mainly used for the treatment of cerebral arteriosclerosis, stroke and senile dementia (Zhang et al., 2008). Recent studies have shown that Reypolysaccharide A can improve memory and neuronal damage. As Fu C et al. (Fu et al., 2022) first revealed the DEP in patients with ischemic stroke by using the RayBio protein array. They then established a cognitive impairment model in rats using a 14-day MCAO treatment and intraperitoneal injection of 80 mg/kg Reypolysaccharide A, as well as exposing SH-SY5Y cells to H₂O₂ for 24 h and treating them with 80 μ M Reypolysaccharide A for 24 h. Subsequently, they assessed the neuroprotective effects of Reypolysaccharide A by detecting the infarct volume *in vivo* (TTC staining), the neurological deficit (Garcia score) and learning memory (morris water maze test), and cell viability *in vitro* (CCK-8 and LDH). Meanwhile, the biochemical methods were used to detect the activities of SOD, MDA and myeloperoxidase (MPO) in rats, as well as the levels of GSH, oxidized glutathione (GSSG) and nicotinamide adenine dinucleotide phosphate (NADPH) in cell. And the DCFH-DA was used to measure the level of ROS. Finally, the expression levels of MPO, PI3K, p-PI3K, Akt, p-Akt, HO-1, Nrf 2, SLC7A11, and GPX 4 proteins in the rat cerebral cortex were detected by the western blotting technology. The results of the *in vivo* study showed that compared with the model group, the cognitive impairment and neurological deficits in the Reypolysaccharide A treatment group were significantly improved, and the cerebral infarction of MCAO rats was reduced. In addition, the results of the *in vivo* study showed a significant increase in cell viability and a decrease in toxicity induced by the H₂O₂ + Reypolysaccharide A group. Further studies showed that the expressions of p-PI3K, p-Akt, Nrf2, HO-1 and SLC7A11 proteins in the Reypolysaccharide A-treated group were significantly higher than those in the model group. These data suggest that Reypolysaccharide A has neuroprotective effects and improves cognitive impairment after cerebral ischemia by inhibiting ferroptosis and activating the PI3K/AKT/Nrf2 and SLC7A11/GPX4 signaling pathways, and these findings also provide valuable insights into the pathogenesis and therapeutic targets of ischemic stroke.

5 Conclusion and future directions

Mitochondrial autophagy and ferroptosis are newly discovered types of programmed cell death associated with the development of cerebral ischemia-reperfusion injury. Pharmacological activators of mitochondrial autophagy and pharmacological inhibitors of ferroptosis can alleviate early brain damage caused by ischemia-reperfusion. However, when the disease progresses to the middle and late stages, it inevitably increases the load on the organs and triggers excessive and persistent mitochondrial autophagy and ferroptosis in the body, resulting in the production of ROS and inflammation, further causing cortical cell death, exacerbating the destruction of the blood-brain barrier, and promoting the entry of more bacteria or viruses into the brain, ultimately exacerbating the malignant cycle of the disease. Therefore, specifically inhibiting the processes of mitochondrial autophagy and ferroptosis may improve middle and later stage cerebral ischemia-reperfusion injury. It is thus

particularly important to regulate the processes of mitochondrial autophagy and ferroptosis reasonably based on the disease development stage. Although many advances have been made in understanding the mechanisms and roles of mitochondrial autophagy and ferroptosis in brain diseases, further clinical application of targeted therapy for these processes is still in the early stages. Their specific roles remain to be investigated in the context of brain diseases, including many that were not covered in this review (such as cerebral arteriosclerosis, epilepsy, Alzheimer's disease and so on). Therefore, we believe that more research, including cell experiments, animal experiments, and clinical studies, is needed to understand the roles of different cell death processes in brain diseases more thoroughly, thus providing new clinical treatment methods for brain diseases. Interestingly, many brain diseases are associated with one or more cell death processes, including other patterns not mentioned in this review, such as necroptosis, endoplasmic reticulum stress, oxidative stress, pyroptosis, cupric death, and disulfide death. Therefore, further research is needed to determine the specific cell death mechanisms involved in brain diseases, thus developing treatment approaches relevant to the disease context. Future studies should focus on the interplay between cell death processes in brain diseases.

Given the complex etiology of cerebral ischemia-reperfusion injury, single-targeted therapy based on mitochondrial autophagy or ferroptosis is often unsatisfactory. However, medicinal plants have unique advantages in treating cerebral ischemia-reperfusion injury. This can be attributed to two main aspects: Firstly, the mechanisms of mitochondrial autophagy and ferroptosis involve multiple signaling pathways (including PINK1/Parkin, AMPK, E-cadherin/NF2/Hippo/YAP, HIF-2 α /HILPDA, and so on), and it is sometimes difficult for a single-targeted drug to address all pathways. Fortunately, increasing evidence shows that many medicinal plants and their active metabolites can not only act through multiple targets but also consider multiple targets (such as NIX, BNIP3, FUNDC1, GPX4, FSP1, and so on) in cerebral ischemia-reperfusion injury, such as mitochondrial autophagy and ferroptosis. Secondly, medicinal plants and their active metabolites have been proven to be safe, especially with fewer toxic effects on liver and kidney damage compared to western medications. For instance, traditional Chinese herbal compound preparations such as Taohong Siwu decoction, Xiao-Xu-Ming decoction, and compound tongluo decoction have been used for thousands of years in China, and their clinical efficacy is relatively optimistic. It is worth noting that in recent years, many researchers have attempted to isolate active ingredients from clinically effective herbal formulas by chemical methods and apply them to cell or animal experiments to elucidate their molecular mechanisms. To date, research on the regulation of mitochondrial autophagy and ferroptosis in herbal plants related to cerebral ischemia-reperfusion injury still has many limitations, and the study of mitochondrial autophagy and ferroptosis regulation in cerebral ischemia-reperfusion injury is still in the observational research stage, lacking deeper exploration of mechanisms. Therefore, more standardized and larger-scale clinical studies are needed to promote the wider acceptance of medicinal plant therapy in patients with cerebral ischemia-reperfusion injury and hope that these medicinal plants and their active metabolites can withstand experimental scrutiny

and bring benefits to patients with cerebral ischemia-reperfusion injury as soon as possible.

Author contributions

GZ: Formal Analysis, Writing—original draft. QW: Data curation, Investigation, Writing—review and editing. BJ: Data curation, Investigation, Writing—review and editing. LY: Formal Analysis, Methodology, Writing—review and editing. WW: Formal Analysis, Methodology, Writing—review and editing. XZ: Visualization, Writing—review and editing. DW: Visualization, Writing—review and editing. YG: Conceptualization, Funding acquisition, Writing—review and editing.

Funding

The author(s) declare that financial support was received for the research, authorship, and/or publication of this article. This work

was supported by The Fund of The First Hospital of Lanzhou University (No. ldyyn2020-108); Natural Science Foundation of Gansu Province (No. 20JR10RA671).

Conflict of interest

The authors declare that the research was conducted in the absence of any commercial or financial relationships that could be construed as a potential conflict of interest.

Publisher's note

All claims expressed in this article are solely those of the authors and do not necessarily represent those of their affiliated organizations, or those of the publisher, the editors and the reviewers. Any product that may be evaluated in this article, or claim that may be made by its manufacturer, is not guaranteed or endorsed by the publisher.

References

- Ahmed-Laloui, H., Zaak, H., Rahmani, A., Kashi, I., Chemat, S., Miara, M. D., et al. (2022). Assessment of artemisinin and antioxidant activities of three wild *Artemisia* species of Algeria. *Nat. Prod. Res.* 36, 6344–6352. doi:10.1080/14786419.2022.2025803
- Ahsan, A., Liu, M., Zheng, Y., Yan, W., Pan, L., Li, Y., et al. (2021). Natural compounds modulate the autophagy with potential implication of stroke. *Acta Pharm. Sin. B* 11, 1708–1720. doi:10.1016/j.apsb.2020.10.018
- Ajoolabady, A., Chiong, M., Lavandero, S., Klionsky, D. J., and Ren, J. (2022). Mitophagy in cardiovascular diseases: molecular mechanisms, pathogenesis, and treatment. *Trends Mol. Med.* 28, 836–849. doi:10.1016/j.molmed.2022.06.007
- Ajoolabady, A., Hamid, A., Libby, P., Tuomilehto, J., Gregory, Y. H. L., Penninger, J. M., et al. (2021). Ferritinophagy and ferroptosis in the management of metabolic diseases. *Trends Endocrinol. Metab.* 32, 444–462. doi:10.1016/j.tem.2021.04.010
- Bi, Y., Ajoolabady, A., Demillard, L., Yu, W., Hilaire, M. L., Zhang, Y. M., et al. (2021). Dysregulation of iron metabolism in cardiovascular diseases: from iron deficiency to iron overload. *Biochem. Pharmacol.* 190, 114661. doi:10.1016/j.bcp.2021.114661
- Bi, Y., Liu, S., Qin, X., Abudureyimu, M., Wang, L., Zou, R., et al. (2024). FUNDC1 interacts with GPX4 to govern hepatic ferroptosis and fibrotic injury through a mitophagy-dependent manner. *J. Adv. Res.* 55, 45–60. doi:10.1016/j.jare.2023.02.012
- Brewer, G. (2023). FSP1 in cancer: not just a phase. *Nat. Rev. Cancer* 23, 578. doi:10.1038/s41568-023-00607-0
- Cai, G.-Y. (2023). Study on the mechanism of Buyang Huanwu decoction in resisting cerebral ischemia-reperfusion injury through ferroptosis. *Chengde Med. Coll.* 285, 1–93. doi:10.27691/d.cnki.gcdyx.2023.000113
- Chaturvedi, D., Goswami, A., Saikia, P. P., Barua, N. C., and Rao, P. G. (2010). Artemisinin and its derivatives: a novel class of anti-malarial and anti-cancer agents. *Chem. Soc. Rev.* 39, 435–454. doi:10.1039/b816679j
- Chen, J., Ma, D., Bao, J., Zhang, Y., and Deng, G. (2022). Roots of *Astragalus propinquus* schischkin regulate transmembrane iron transport and ferroptosis to improve cerebral ischemia-reperfusion injury. *Evid. Based Complement. Altern. Med.* 2022, 7410865. doi:10.1155/2022/7410865
- Chen, L., Huang, J., Yao, Z.-M., Sun, X.-R., Tong, X.-H., Hu, M., et al. (2023). Procyanidins alleviated cerebral ischemia/reperfusion injury by inhibiting ferroptosis via the Nrf2/HO-1 signaling pathway. *Molecules* 28, 3582. doi:10.3390/molecules28083582
- Chen, Z., Liu, L., Gao, C., Chen, W., Vong, C. T., Yao, P., et al. (2020). Astragali Radix (Huangqi): a promising edible immunomodulatory herbal medicine. *J. Ethnopharmacol.* 258, 112895. doi:10.1016/j.jep.2020.112895
- Dixon, S. J., and Pratt, D. A. (2023). Ferroptosis: a flexible constellation of related biochemical mechanisms. *Mol. Cell* 83, 1030–1042. doi:10.1016/j.molcel.2023.03.005
- Duan, F.-F., Lu, X.-J., Ju, L.-L., Zhuang, X.-T., Sun, X.-W., Liu, T.-Y., et al. (2023). Effect of qizhi capsule on the expression levels of autophagy-related factors of LC3 and p62 in CIRI rats. *Lishizhen Med. Mat. Med. Res.* 34, 13–16. doi:10.3969/j.issn.1008-0805.2023.01.04
- Erekat, N. S. (2022). Apoptosis and its therapeutic implications in neurodegenerative diseases. *Clin. Anat.* 35, 65–78. doi:10.1002/ca.23792
- Feng, J., Chen, X., Lu, S., Li, W., Yang, D., Su, W., et al. (2018). Naringin attenuates cerebral ischemia-reperfusion injury through inhibiting peroxynitrite-mediated mitophagy activation. *Mol. Neurobiol.* 55, 9029–9042. doi:10.1007/s12035-018-1027-7
- Feske, S. K. (2021). Ischemic stroke. *Am. J. Med.* 134, 1457–1464. doi:10.1016/j.amjmed.2021.07.027
- Festjens, N., Vanden Berghe, T., and Vandenabeele, P. (2006). Necrosis, a well-orchestrated form of cell demise: signalling cascades, important mediators and concomitant immune response. *Biochim. Biophys. Acta* 1757, 1371–1387. doi:10.1016/j.bbabi.2006.06.014
- Fidy, K., Fiedorowicz, A., Strzdała, L., and Szumny, A. (2016). β -caryophyllene and β -caryophyllene oxide-natural compounds of anticancer and analgesic properties. *Cancer Med.* 5, 3007–3017. doi:10.1002/cam4.816
- Fleisher, T. A. (1997). Apoptosis. *Ann. Allergy Asthma Immunol.* 78, 245–249. doi:10.1016/S1081-1206(10)63176-6
- Fu, C., Wu, Y., Liu, S., Luo, C., Lu, Y., Liu, M., et al. (2022). Rehmannioside A improves cognitive impairment and alleviates ferroptosis via activating PI3K/AKT/Nrf2 and SLC7A11/GPX4 signaling pathway after ischemia. *J. Ethnopharmacol.* 289, 115021. doi:10.1016/j.jep.2022.115021
- Fu, J., Wang, Z., Huang, L., Zheng, S., Wang, D., Chen, S., et al. (2014). Review of the botanical characteristics, phytochemistry, and pharmacology of *Astragalus membranaceus* (Huangqi). *Phytother. Res.* 28, 1275–1283. doi:10.1002/ptr.5188
- Fu, Z.-J., Wang, Z.-Y., Xu, L., Chen, X.-H., Li, X.-X., Liao, W.-T., et al. (2020). HIF-1 α -BNIP3-mediated mitophagy in tubular cells protects against renal ischemia/reperfusion injury. *Redox Biol.* 36, 101671. doi:10.1016/j.redox.2020.101671
- Gao, X., Hu, W., Qian, D., Bai, X., He, H., Li, L., et al. (2023). The mechanisms of ferroptosis under hypoxia. *Cell Mol. Neurobiol.* 43, 3329–3341. doi:10.1007/s10571-023-01388-8
- Giovannetti, A., Pierdominici, M., Di Iorio, A., Cianci, R., Murdaca, G., Puppo, F., et al. (2008). Apoptosis in the homeostasis of the immune system and in human immune mediated diseases. *Curr. Pharm. Des.* 14, 253–268. doi:10.2174/138161208783413310
- Grohm, J., Plesnila, N., and Culmsee, C. (2010). Bid mediates fission, membrane permeabilization and peri-nuclear accumulation of mitochondria as a prerequisite for oxidative neuronal cell death. *Brain Behav. Immun.* 24, 831–838. doi:10.1016/j.bbi.2009.11.015
- Gu, C.-J., Li, L.-W., Huang, Y.-F., Qian, D.-F., Liu, W., Zhang, C.-L., et al. (2020). Salidroside ameliorates mitochondria-dependent neuronal apoptosis after spinal cord ischemia-reperfusion injury partially through inhibiting oxidative stress and promoting mitophagy. *Oxid. Med. Cell Longev.* 23, 3549704. doi:10.1155/2020/3549704
- Guan, X., Li, Z., Zhu, S., Cheng, M., Ju, Y., Ren, L., et al. (2021). Galangin attenuated cerebral ischemia-reperfusion injury by inhibition of ferroptosis through activating the SLC7A11/GPX4 axis in gerbils. *Life Sci.* 264, 118660. doi:10.1016/j.lfs.2020.118660

- Guo, H., Zhu, L., Tang, P., Chen, D., Li, Y., Li, J., et al. (2021a). Carthamin yellow improves cerebral ischemia-reperfusion injury by attenuating inflammation and ferroptosis in rats. *Int. J. Mol. Med.* 47, 52. doi:10.3892/ijmm.2021.4885
- Guo, L., and Shi, L. (2023). Viteixin improves cerebral ischemia-reperfusion injury by attenuating oxidative injury and ferroptosis via Keap1/Nrf2/HO-1 signaling. *Neurochem. Res.* 48, 980–995. doi:10.1007/s11064-022-03829-0
- Guo, W., Zhao, Y. H., Li, H. X., and Lei, L. (2021b). NCOA4-mediated ferritinophagy promoted inflammatory responses in periodontitis. *J. Periodontol. Res.* 56, 523–534. doi:10.1111/jre.12852
- Hadian, K., and Stockwell, B. R. (2020). SnapShot: ferroptosis. *Cell* 181, 1188–1188.e1. doi:10.1016/j.cell.2020.04.039
- Hendricks, J. M., Doubravsky, C. E., Wehri, E., Li, Z., Roberts, M. A., Deol, K. K., et al. (2023). Identification of structurally diverse FSP1 inhibitors that sensitize cancer cells to ferroptosis. *Cell Chem. Biol.* 30, 1090–1103.e7. doi:10.1016/j.chembiol.2023.04.007
- Hu, Q., Zuo, T., Deng, L., Chen, S., Yu, W., Liu, S., et al. (2022). β -Caryophyllene suppresses ferroptosis induced by cerebral ischemia reperfusion via activation of the NRF2/HO-1 signaling pathway in MCAO/R rats. *Phytomedicine* 102, 154112. doi:10.1016/j.phymed.2022.154112
- Huang, Q., Li, J., Chen, J., Zhang, Z., Xu, P., Qi, H., et al. (2023). Ginsenoside compound K protects against cerebral ischemia/reperfusion injury via Muf1/Mfn2-mediated mitochondrial dynamics and bioenergy. *J. Ginseng Res.* 47, 408–419. doi:10.1016/j.jgr.2022.10.004
- Huang, Z., Xu, J., Huang, X., Sun, G., Jiang, R., Wu, H., et al. (2019). Crocin induces anti-ischemia in middle cerebral artery occlusion rats and inhibits autophagy by regulating the mammalian target of rapamycin. *Eur. J. Pharmacol.* 857, 172424. doi:10.1016/j.ejphar.2019.172424
- Hui, Z., Wang, S., Li, J., Wang, J., and Zhang, Z. (2022). Compound Tongluo Decoction inhibits endoplasmic reticulum stress-induced ferroptosis and promoted angiogenesis by activating the Sonic Hedgehog pathway in cerebral infarction. *J. Ethnopharmacol.* 283, 114634. doi:10.1016/j.jep.2021.114634
- Hwang, I., Kim, B.-S., Lee, H. Y., Cho, S.-W., Lee, S. E., and Ahn, J.-Y. (2023). PA2G4/EBP1 ubiquitination by PRKN/PARKIN promotes mitophagy protecting neuron death in cerebral ischemia. *Autophagy* 20, 365–379. doi:10.1080/15548627.2023.2259215
- Jiang, M., Lai, X., Zhang, Y., Shen, M., Ma, H., Liu, A., et al. (2022). Artemisinin alleviates cerebral ischemia/reperfusion-induced oxidative damage via regulating PHB2-mediated autophagy in the human neuroblastoma SH-SY5Y cell line. *Oxid. Med. Cell Longev.* 2022, 6568748. doi:10.1155/2022/6568748
- Kahlon, M. A., and Dixon, S. J. (2022). Copper-induced cell death. *Science* 375, 1231–1232. doi:10.1126/science.abo3959
- Kopeina, G. S., and Zhivotovsky, B. (2022). Programmed cell death: past, present and future. *Biochem. Biophys. Res. Commun.* 633, 55–58. doi:10.1016/j.bbrc.2022.09.022
- Lan, B., Ge, J.-W., Cheng, S.-W., Zheng, X.-L., Liao, J., He, C., et al. (2020). Extract of Naotaiyang, a compound Chinese herbal medicine, protects neuron ferroptosis induced by acute cerebral ischemia in rats. *J. Integr. Med.* 18, 344–350. doi:10.1016/j.joim.2020.01.008
- Lan, R., Xiang, J., Wang, G.-H., Li, W.-W., Zhang, W., Xu, L.-L., et al. (2013). Xiao-Xu-Ming decoction protects against blood-brain barrier disruption and neurological injury induced by cerebral ischemia and reperfusion in rats. *Evid. Based Complement. Altern. Med.* 2013, 629782. doi:10.1155/2013/629782
- Lan, R., Zhang, Y., Wu, T., Ma, Y.-Z., Wang, B.-Q., Zheng, H.-Z., et al. (2018). Xiao-Xu-Ming decoction reduced mitophagy activation and improved mitochondrial function in cerebral ischemia and reperfusion injury. *Behav. Neurol.* 2018, 4147502. doi:10.1155/2018/4147502
- Lan, R., Zhang, Y., Xiang, J., Zhang, W., Wang, G.-H., Li, W.-W., et al. (2014). Xiao-Xu-Ming decoction preserves mitochondrial integrity and reduces apoptosis after focal cerebral ischemia and reperfusion via the mitochondrial p53 pathway. *J. Ethnopharmacol.* 151, 307–316. doi:10.1016/j.jep.2013.10.042
- Lee, H., Zandkarimi, F., Zhang, Y., Meena, J. K., Kim, J., Zhuang, L., et al. (2020). Energy-stress-mediated AMPK activation inhibits ferroptosis. *Nat. Cell Biol.* 22, 225–234. doi:10.1038/s41556-020-0461-8
- Li, J., Jia, Y.-C., Ding, Y.-X., Bai, J., Cao, F., and Li, F. (2023a). The crosstalk between ferroptosis and mitochondrial dynamic regulatory networks. *Int. J. Biol. Sci.* 19, 2756–2771. doi:10.7150/ijbs.83348
- Li, J., Yang, D., Li, Z., Zhao, M., Wang, D., Sun, Z., et al. (2023b). PINK1/Parkin-mediated mitophagy in neurodegenerative diseases. *Ageing Res. Rev.* 84, 101817. doi:10.1016/j.arr.2022.101817
- Li, L., Song, J.-J., Zhang, M.-X., Zhang, H.-W., Zhu, H.-Y., Guo, W., et al. (2023c). Oridonin ameliorates caspase-9-mediated brain neuronal apoptosis in mouse with ischemic stroke by inhibiting RIPK3-mediated mitophagy. *Acta Pharmacol. Sin.* 44, 726–740. doi:10.1038/s41401-022-00995-3
- Li, L.-Q., Zhang, D., Yuan, L., Xiang, J.-J., Chen, W., and Hu, Y.-Q. (2023). Ischemia reperfusion injury Wenyang Fuyuan formula ischemic stroke Mitochondrial iron death Neurological deficit scores miR-137 mimic. *Shanxi Trad. Chin. Med.* 44, 1354–1359. doi:10.3969/j.issn.1000-7369.2023.10.005
- Li, M., Meng, Z., Yu, S., Li, J., Wang, Y., Yang, W., et al. (2022a). Baicalein ameliorates cerebral ischemia-reperfusion injury by inhibiting ferroptosis via regulating GPX4/ACSL4/ACSL3 axis. *Chem. Biol. Interact.* 366, 110137. doi:10.1016/j.cbi.2022.110137
- Li, S., He, Y., Chen, K., Sun, J., Zhang, L., He, Y., et al. (2021a). RSL3 drives ferroptosis through NF- κ B pathway activation and GPX4 depletion in glioblastoma. *Oxid. Med. Cell Longev.* 2021, 2915019. doi:10.1155/2021/2915019
- Li, S., Li, L., Min, S., Liu, S., Qin, Z., Xiong, Z., et al. (2023d). Soybean isoflavones alleviate cerebral ischemia/reperfusion injury in rats by inhibiting ferroptosis and inflammatory cascade reaction. *Nan Fang. Yi Ke Da Xue Xue Bao* 43, 323–330. doi:10.12122/j.issn.1673-4254.2023.02.23
- Li, S., Sun, X., Xu, L., Sun, R., Ma, Z., Deng, X., et al. (2017). Baicalin attenuates *in vivo* and *in vitro* hyperglycemia-exacerbated ischemia/reperfusion injury by regulating mitochondrial function in a manner dependent on AMPK. *Eur. J. Pharmacol.* 815, 118–126. doi:10.1016/j.ejphar.2017.07.041
- Li, T., Tan, Y., Ouyang, S., He, J., and Liu, L. (2022b). Resveratrol protects against myocardial ischemia-reperfusion injury via attenuating ferroptosis. *Gene* 808, 145968. doi:10.1016/j.gene.2021.145968
- Li, X., Ma, N., Xu, J., Zhang, Y., Yang, P., Su, X., et al. (2021b). Targeting ferroptosis: pathological mechanism and treatment of ischemia-reperfusion injury. *Oxid. Med. Cell Longev.* 2021, 1587922. doi:10.1155/2021/1587922
- Li, Y., Zheng, W., Lu, Y., Zheng, Y., Pan, L., Wu, X., et al. (2021c). BNIP3L/NIX-mediated mitophagy: molecular mechanisms and implications for human disease. *Cell Death Dis.* 13, 14. doi:10.1038/s41419-021-04469-y
- Liao, J., Wei, M., Wang, J., Zeng, J., Liu, D., Du, Q., et al. (2023). Naotaiyang formula attenuates OGD/R-induced inflammation and ferroptosis by regulating microglial M1/M2 polarization through BMP6/SMADs signaling pathway. *Biomed. Pharmacother.* 167, 115465. doi:10.1016/j.biopha.2023.115465
- Lin, Q., Li, S., Jin, H., Cai, H., Zhu, X., Yang, Y., et al. (2023). Mitophagy alleviates cisplatin-induced renal tubular epithelial cell ferroptosis through ROS/HO-1/GPX4 axis. *Int. J. Biol. Sci.* 19, 1192–1210. doi:10.7150/ijbs.80775
- Liu, H., An, N., Wang, L., Li, Y., Song, K., Sun, Y., et al. (2023a). Protective effect of Xingnaojing injection on ferroptosis after cerebral ischemia injury in MCAO rats and SH-SY5Y cells. *J. Ethnopharmacol.* 301, 115836. doi:10.1016/j.jep.2022.115836
- Liu, H., Zhang, T.-A., Zhang, W.-Y., Huang, S.-R., Hu, Y., and Sun, J. (2023b). Rhein attenuates cerebral ischemia-reperfusion injury via inhibition of ferroptosis through NRF2/SLC7A11/GPX4 pathway. *Exp. Neurol.* 369, 114541. doi:10.1016/j.expneurol.2023.114541
- Liu, H., Zhao, Z., Yan, M., Zhang, Q., Jiang, T., and Xue, J. (2023c). Calycosin decreases cerebral ischemia/reperfusion injury by suppressing ACSL4-dependent ferroptosis. *Arch. Biochem. Biophys.* 734, 109488. doi:10.1016/j.abb.2022.109488
- Liu, K., Sun, Y., Gu, Z., Shi, N., Zhang, T., and Sun, X. (2013). Mitophagy in ischaemia/reperfusion induced cerebral injury. *Neurochem. Res.* 38, 1295–1300. doi:10.1007/s11064-013-1033-0
- Liu, X., Zhuang, L., and Gan, B. (2023d). Disulfidptosis: disulfide stress-induced cell death. *Trends Cell Biol.* S0962-8924 (23), 00141–1. doi:10.1016/j.tcb.2023.07.009
- Liu, Y., Wan, Y., Jiang, Y., Zhang, L., and Cheng, W. (2023e). GPX4: the hub of lipid oxidation, ferroptosis, disease and treatment. *Biochim. Biophys. Acta Rev. Cancer* 1878, 188890. doi:10.1016/j.bbcan.2023.188890
- Lu, Y., Li, Z., Zhang, S., Zhang, T., Liu, Y., and Zhang, L. (2023a). Cellular mitophagy: mechanism, roles in diseases and small molecule pharmacological regulation. *Theranostics* 13, 736–766. doi:10.7150/thno.79876
- Lu, Y., Li, Z., Zhang, S., Zhang, T., Liu, Y., and Zhang, L. (2023b). Cellular mitophagy: mechanism, roles in diseases and small molecule pharmacological regulation. *Theranostics* 13, 736–766. doi:10.7150/thno.79876
- Ly, Y., Liang, C.-H., Sun, Q.-C., Zhu, J., Xu, H.-Y., Li, X.-Q., et al. (2023). Structural insights into FSP1 catalysis and ferroptosis inhibition. *Nat. Commun.* 14, 5933. doi:10.1038/s41467-023-41626-7
- Mao, Z., Tian, L., Liu, J., Wu, Q., Wang, N., Wang, G., et al. (2022). Ligustilide ameliorates hippocampal neuronal injury after cerebral ischemia reperfusion through activating PINK1/Parkin-dependent mitophagy. *Phytomedicine* 101, 154111. doi:10.1016/j.phymed.2022.154111
- Montaña, A., Hanley, D. F., and Hemphill, J. C. (2021). Hemorrhagic stroke. *Handb. Clin. Neurol.* 176, 229–248. doi:10.1016/B978-0-444-64034-5.00019-5
- Oh, J., and Kim, J.-S. (2016). Compound K derived from ginseng: neuroprotection and cognitive improvement. *Food Funct.* 7, 4506–4515. doi:10.1039/c6fo01077f
- Peng, H., Fu, S. Z., Wang, S. Y., Xu, H. X., Dhanasekaran, M., Chen, H. G., et al. (2016). Ablation of FUNDC1-dependent mitophagy renders myocardium resistant to paraquat-induced ferroptosis and contractile dysfunction. *Biochim. Biophys. Acta Mol. Basis Dis.* 1868, 166448. doi:10.1016/j.bbdis.2022.166448
- Pineda-Ramírez, N., Alquisiras-Burgos, I., Ortiz-Plata, A., Ruiz-Tachiúin, M.-E., Espinoza-Rojas, M., and Aguilera, P. (2020). Resveratrol activates neuronal autophagy through AMPK in the ischemic brain. *Mol. Neurobiol.* 57, 1055–1069. doi:10.1007/s12035-019-01803-6
- Rabinstein, A. A. (2020). Update on treatment of acute ischemic stroke. *Contin. (Minneapolis)* 26, 268–286. doi:10.1212/CON.0000000000000840

- Scandiffio, R., Geddo, F., Cottone, E., Querio, G., Antoniotti, S., Gallo, M. P., et al. (2020). Protective effects of (E)- β -Caryophyllene (BCP) in chronic inflammation. *Nutrients* 12, 3273. doi:10.3390/nu12113273
- Schädlich, I. S., Winzer, R., Stabernack, J., Tolosa, E., Magnus, T., and Rissiek, B. (2023). The role of the ATP-adenosine axis in ischemic stroke. *Semin. Immunopathol.* 45, 347–365. doi:10.1007/s00281-023-00987-3
- Shao, Z., Dou, S., Zhu, J., Wang, H., Xu, D., Wang, C., et al. (2020). The role of mitophagy in ischemic stroke. *Front. Neurol.* 11, 608610. doi:10.3389/fneur.2020.608610
- She, R., Liu, D., Liao, J., Wang, G., Ge, J., and Mei, Z. (2023). Mitochondrial dysfunctions induce PANoptosis and ferroptosis in cerebral ischemia/reperfusion injury: from pathology to therapeutic potential. *Front. Cell Neurosci.* 17, 1191629. doi:10.3389/fncel.2023.1191629
- Shen, L., Gan, Q., Yang, Y., Reis, C., Zhang, Z., Xu, S., et al. (2021). Mitophagy in cerebral ischemia and ischemia/reperfusion injury. *Front. Aging Neurosci.* 13, 687246. doi:10.3389/fnagi.2021.687246
- Shi, Y., Liu, Q., Chen, W., Wang, R., Wang, L., Liu, Z.-Q., et al. (2023). Protection of Taohong Siwu Decoction on PC12 cells injured by oxygen glucose deprivation/reperfusion via mitophagy-NLRP3 inflammasome pathway *in vitro*. *J. Ethnopharmacol.* 301, 115784. doi:10.1016/j.jep.2022.115784
- Sims, N. R., and Muyderman, H. (2010). Mitochondria, oxidative metabolism and cell death in stroke. *Biochim. Biophys. Acta* 1802, 80–91. doi:10.1016/j.bbdis.2009.09.003
- Sun, K., Huo, R.-Q., Han, Y.-F., Li, F.-Z., and Tian, J.-B. (2023). Effects of Huazhuo Jiedu Huoxue Tongluo Formula on mitochondrial autophagy related protein PINK1 and Parkin in rats with cerebral ischemia-reperfusion injury. *Chin. J. Trad. Chin. Med. Pharm.* 38, 1014–1019.
- Szargel, R., Shani, V., Abd Elghani, F., Mekies, L. N., Liani, E., Rott, R., et al. (2016). The PINK1, synphilin-1 and SHAH-1 complex constitutes a novel mitophagy pathway. *Hum. Mol. Genet.* 25, 3476–3490. doi:10.1093/hmg/ddw189
- Tang, D., Chen, X., Kang, R., and Kroemer, G. (2021). Ferroptosis: molecular mechanisms and health implications. *Cell Res.* 31, 107–125. doi:10.1038/s41422-020-00441-1
- Tian, H.-Y., Huang, B.-Y., Nie, H.-F., Chen, X.-Y., Zhou, Y., Yang, T., et al. (2023). The interplay between mitochondrial dysfunction and ferroptosis during ischemia-associated central nervous system diseases. *Brain Sci.* 13, 1367. doi:10.3390/brainsci13101367
- Tuo, Q.-Z., Lei, P., Jackman, K. A., Li, X.-L., Xiong, H., Li, X.-L., et al. (2017). Tau-mediated iron export prevents ferroptotic damage after ischemic stroke. *Mol. Psychiatry* 22, 1520–1530. doi:10.1038/mp.2017.171
- Ursini, F., and Maiorino, M. (2020). Lipid peroxidation and ferroptosis: the role of GSH and GPX4. *Free Radic. Biol. Med.* 152, 175–185. doi:10.1016/j.freeradbiomed.2020.02.027
- Wang, F., Liu, Y., Ni, F., Jin, J., Wu, Y., Huang, Y., et al. (2022). BNC1 deficiency-triggered ferroptosis through the NF2-YAP pathway induces primary ovarian insufficiency. *Nat. Commun.* 13, 5871. doi:10.1038/s41467-022-33323-8
- Wang, H.-Y., Chen, S.-H., Zhang, Y.-M., Xu, H., and Sun, H. (2019). Electroacupuncture ameliorates neuronal injury by Pink1/Parkin-mediated mitophagy clearance in cerebral ischemia-reperfusion. *Nitric Oxide* 91, 23–34. doi:10.1016/j.niox.2019.07.004
- Wang, L., Liu, C., Wang, L., and Tang, B. (2023a). Astragaloside IV mitigates cerebral ischaemia-reperfusion injury via inhibition of P62/Keap1/Nrf2 pathway-mediated ferroptosis. *Eur. J. Pharmacol.* 944, 175516. doi:10.1016/j.ejphar.2023.175516
- Wang, W., and Xu, J. (2020). Curcumin attenuates cerebral ischemia-reperfusion injury through regulating mitophagy and preserving mitochondrial function. *Curr. Neurovasc. Res.* 17, 113–122. doi:10.2174/1567202617666200225122620
- Wang, X., Zhang, J., Wang, S., Song, Z., Sun, H., Wu, F., et al. (2023b). Berberine modulates gut microbiota to attenuate cerebral ferroptosis induced by ischemia-reperfusion in mice. *Eur. J. Pharmacol.* 953, 175782. doi:10.1016/j.ejphar.2023.175782
- Wong, R. S. Y. (2011). Apoptosis in cancer: from pathogenesis to treatment. *J. Exp. Clin. Cancer Res.* 30, 87. doi:10.1186/1756-9966-30-87
- Wu, H., Wang, Y., Li, W. H., Chen, H., Du, L., Liu, D., et al. (2019a). Deficiency of mitophagy receptor FUNDC1 impairs mitochondrial quality and aggravates dietary-induced obesity and metabolic syndrome. *Autophagy* 15, 1882–1898. doi:10.1080/15548627.2019.1596482
- Wu, J., Minikes, A. M., Gao, M., Bian, H., Li, Y., Stockwell, B. R., et al. (2019b). Intercellular interaction dictates cancer cell ferroptosis via NF2-YAP signalling. *Nature* 572, 402–406. doi:10.1038/s41586-019-1426-6
- Wu, M., Lu, G., Lao, Y.-Z., Zhang, H., Zheng, D., Zheng, Z.-Q., et al. (2021a). Garciculenxanthone B induces PINK1-Parkin-mediated mitophagy and prevents ischemia-reperfusion brain injury in mice. *Acta Pharmacol. Sin.* 42, 199–208. doi:10.1038/s41401-020-0480-9
- Wu, X., Zheng, Y., Liu, M., Li, Y., Ma, S., Tang, W., et al. (2021b). BNIP3L/NIX degradation leads to mitophagy deficiency in ischemic brains. *Autophagy* 17, 1934–1946. doi:10.1080/15548627.2020.1802089
- Xiao, Q., Kang, Z., Liu, C., and Tang, B. (2022). Panax notoginseng saponins attenuate cerebral ischemia-reperfusion injury via mitophagy-induced inhibition of NLRP3 inflammasome in rats. *Front. Biosci. Landmark Ed.* 27, 300. doi:10.31083/j.fbl2711300
- Xie, J., Zhang, T., Li, P., Wang, D., Liu, T., and Xu, S. (2022). Dihydromyricetin attenuates cerebral ischemia reperfusion injury by inhibiting SPHK1/mTOR signaling and targeting ferroptosis. *Drug Des. Devel. Ther.* 16, 3071–3085. doi:10.2147/DDDT.S378786
- Xu, B., Zhu, L., Chu, J., Ma, Z., Fu, Q., Wei, W., et al. (2019). Esculetin improves cognitive impairments induced by transient cerebral ischaemia and reperfusion in mice via regulation of mitochondrial fragmentation and mitophagy. *Behav. Brain Res.* 372, 112007. doi:10.1016/j.bbr.2019.112007
- Yan, S.-Y., Yang, R.-Y., Chen, Y., Liu, L.-J., Gao, X.-F., and Zhou, D.-S. (2023). Study on the effects and mechanism of drug-containing serum huoxue rongluo decoction in mitochondrial autophagy in oxygen-glucose deprivation/reoxygenation-damaged PC12 cells. *Chin. J. Inf. Trad. Chin. Med.* 30, 101–107. doi:10.19879/j.cnki.1005-5304.202207029
- Yang, L., Tao, Y., Luo, L., Zhang, Y., Wang, X., and Meng, X. (2022). Dengzhan Xixin injection derived from a traditional Chinese herb *Erigeron breviscapus* ameliorates cerebral ischemia/reperfusion injury in rats via modulation of mitophagy and mitochondrial apoptosis. *J. Ethnopharmacol.* 288, 114988. doi:10.1016/j.jep.2022.114988
- Yang, M., Lv, Y., Tian, X., Lou, J., An, R., Zhang, Q., et al. (2017). Neuroprotective effect of β -caryophyllene on cerebral ischemia-reperfusion injury via regulation of necroptotic neuronal death and inflammation: *in vivo* and *in vitro*. *Front. Neurosci.* 11, 583. doi:10.3389/fnins.2017.00583
- Yang, W. S., SriRamaratnam, R., Welsch, M. E., Shimada, K., Skouta, R., Viswanathan, V. S., et al. (2014). Regulation of ferroptotic cancer cell death by GPX4. *Cell* 156, 317–331. doi:10.1016/j.cell.2013.12.010
- Yang, Y., Wu, Q., Shan, X., Zhou, H., Wang, J., Hu, Y., et al. (2024). Ginkgolide B attenuates cerebral ischemia-reperfusion injury via inhibition of ferroptosis through disrupting NCOA4-FTH1 interaction. *J. Ethnopharmacol.* 318, 116982. doi:10.1016/j.jep.2023.116982
- Ye, M., Wu, H., and Li, S.-G. (2021). Resveratrol alleviates oxygen/glucose deprivation/reoxygenation-induced neuronal damage through induction of mitophagy. *Mol. Med. Rep.* 23, 73. doi:10.3892/mmr.2020.11711
- Yu, X., Liu, X., Mi, X., Luo, X., Lian, Z., Tang, J., et al. (2023). Jionoside A1 alleviates ischemic stroke ischemia/reperfusion injury by promoting Nix-mediated mitophagy. *Cell Mol. Biol. (Noisy-le-grand)* 69, 237–245. doi:10.14715/cmb/2023.69.8.37
- Yuan, Y., Zhai, Y.-Y., Chen, J.-J., Xu, X.-F., and Wang, H.-M. (2021). Kaempferol ameliorates oxygen-glucose deprivation/reoxygenation-induced neuronal ferroptosis by activating nrf2/slc7a11/GPX4 Axis. *Biomolecules* 11, 923. doi:10.3390/biom11070923
- Yuan, Y., Zheng, Y., Zhang, X., Chen, Y., Wu, X., Wu, J., et al. (2017). BNIP3L/NIX-mediated mitophagy protects against ischemic brain injury independent of PARK2. *Autophagy* 13, 1754–1766. doi:10.1080/15548627.2017.1357792
- Zang, R., Ling, F., Wu, Z., Sun, J., Yang, L., Lv, Z., et al. (2023). Ginkgo biloba extract (EGB-761) confers neuroprotection against ischemic stroke by augmenting autophagic/lysosomal signaling pathway. *J. Neuroimmunol.* 382, 578101. doi:10.1016/j.jneuroim.2023.578101
- Zeng, F., Nijati, S., Tang, L., Ye, J., Zhou, Z., and Chen, X. (2023). Ferroptosis detection: from approaches to applications. *Angew. Chem. Int. Ed. Engl.* 62, e202300379. doi:10.1002/anie.202300379
- Zhang, C.-H., Yang, X., Wei, J.-R., Chen, N.-M.-H., Xu, J.-P., Bi, Y.-Q., et al. (2021). Ethnopharmacology, phytochemistry, pharmacology, toxicology and clinical applications of radix astragali. *Chin. J. Integr. Med.* 27, 229–240. doi:10.1007/s11655-019-3032-8
- Zhang, J., and Ney, P. A. (2009). Role of BNIP3 and NIX in cell death, autophagy, and mitophagy. *Cell Death Differ.* 16, 939–946. doi:10.1038/cdd.2009.16
- Zhang, Q., Jia, M., Wang, Y., Wang, Q., and Wu, J. (2022a). Cell death mechanisms in cerebral ischemia-reperfusion injury. *Neurochem. Res.* 47, 3525–3542. doi:10.1007/s11064-022-03697-8
- Zhang, R.-X., Li, M.-X., and Jia, Z.-P. (2008). *Rehmannia glutinosa*: review of botany, chemistry and pharmacology. *J. Ethnopharmacol.* 117, 199–214. doi:10.1016/j.jep.2008.02.018
- Zhang, Y., He, Y., Wu, M., Chen, H., Zhang, L., Yang, D., et al. (2020). Rehmapicroside ameliorates cerebral ischemia-reperfusion injury via attenuating peroxynitrite-mediated mitophagy activation. *Free Radic. Biol. Med.* 160, 526–539. doi:10.1016/j.freeradbiomed.2020.06.034
- Zhang, Y., Ye, P., Zhu, H., Gu, L., Li, Y., Feng, S., et al. (2023). Neutral polysaccharide from *Gastrodia elata* alleviates cerebral ischemia-reperfusion injury by inhibiting ferroptosis-mediated neuroinflammation via the NRF2/HO-1 signaling pathway. *CNS Neurosci. Ther.* 30, e14456. doi:10.1111/cns.14456
- Zhang, Y.-H., Yao, M.-J., Cong, W.-H., and Liu, J.-X. (2018). Effect of extraction of saffron crocus on mitochondrial dynamics in ischemia/reperfusion rats. *Chin. Pharm. Bull.* 34, 770–775. doi:10.3969/j.issn.1001-1978.2018.06.008

- Zhang, Z.-W., Liao, L.-Y., Yang, H., Zeng, J.-S., Hu, J., Gao, Y., et al. (2022b). Protective effect of longhu xingnao granule mediated mitochondrial autophagy on brain neurons in rats with cerebral ischemia-reperfusion injury. *Guid. J. Trad. Chin. Med. Pharm.* 28, 23–29. doi:10.13862/j.cn43-1446/r.2022.11.005
- Zhao, F., Peng, C., Li, H., Chen, H., Yang, Y., Ai, Q., et al. (2023a). Paeoniae Radix Rubra extract attenuates cerebral ischemia injury by inhibiting ferroptosis and activating autophagy through the PI3K/Akt signalling pathway. *J. Ethnopharmacol.* 315, 116567. doi:10.1016/j.jep.2023.116567
- Zhao, J., Ma, M., Li, L., and Fang, G. (2023b). Oxysophoridine protects against cerebral ischemia/reperfusion injury via inhibition of TLR4/p38MAPK-mediated ferroptosis. *Mol. Med. Rep.* 27, 44. doi:10.3892/mmr.2023.12931
- Zhou, H., Wang, J., Zhu, P., Zhu, H., Toan, S., Hu, S., et al. (2018). NR4A1 aggravates the cardiac microvascular ischemia reperfusion injury through suppressing FUNDC1-mediated mitophagy and promoting Mff-required mitochondrial fission by CK2 α . *Basic Res. Cardiol.* 113, 23. doi:10.1007/s00395-018-0682-1
- Zhou, M., Xia, Z.-Y., Lei, S.-Q., Leng, Y., and Xue, R. (2015). Role of mitophagy regulated by Parkin/DJ-1 in remote ischemic postconditioning-induced mitigation of focal cerebral ischemia-reperfusion. *Eur. Rev. Med. Pharmacol. Sci.* 19, 4866–4871.
- Zhou, X., Wang, H.-Y., Wu, B., Cheng, C.-Y., Xiao, W., Wang, Z.-Z., et al. (2017). Ginkgolide K attenuates neuronal injury after ischemic stroke by inhibiting mitochondrial fission and GSK-3 β -dependent increases in mitochondrial membrane permeability. *Oncotarget* 8, 44682–44693. doi:10.18632/oncotarget.17967
- Zhu, H., Liu, C., Hou, J., Long, H., Wang, B., Guo, D., et al. (2019). Gastrodia elata blume polysaccharides: a review of their acquisition, analysis, modification, and pharmacological activities. *Molecules* 24, 2436. doi:10.3390/molecules24132436
- Zhu, X.-H., Li, S.-J., Hu, H.-H., Sun, L.-R., Das, M., and Gao, T.-M. (2010). Neuroprotective effects of xiao-xu-ming decoction against ischemic neuronal injury *in vivo* and *in vitro*. *J. Ethnopharmacol.* 127, 38–46. doi:10.1016/j.jep.2009.09.054



OPEN ACCESS

EDITED BY

Stalin Antony,
University of Electronic Science and
Technology of China, China

REVIEWED BY

Yang Xie,
Brigham and Women's Hospital and Harvard
Medical School, United States
Xianju Huang,
South-Central Minzu University, China

*CORRESPONDENCE

Gang Fan,
✉ fangang1111@163.com
Ugen Tenzin,
✉ 1043091135@qq.com
Tsedien Nhamdriel,
✉ 536913114@qq.com

[†]These authors have contributed equally to
this work

RECEIVED 08 February 2024

ACCEPTED 22 April 2024

PUBLISHED 21 May 2024

CITATION

Tao Y, Peng F, Wang L, Sun J, Ding Y, Xiong S,
Tenzin U, MiMa, Nhamdriel T and Fan G (2024),
Ji-Ni-De-Xie ameliorates type 2 diabetes
mellitus by modulating the bile acids
metabolism and FXR/FGF15 signaling pathway.
Front. Pharmacol. 15:1383896.
doi: 10.3389/fphar.2024.1383896

COPYRIGHT

© 2024 Tao, Peng, Wang, Sun, Ding, Xiong,
Tenzin, MiMa, Nhamdriel and Fan. This is an
open-access article distributed under the terms
of the [Creative Commons Attribution License](https://creativecommons.org/licenses/by/4.0/)
(CC BY). The use, distribution or reproduction in
other forums is permitted, provided the original
author(s) and the copyright owner(s) are
credited and that the original publication in this
journal is cited, in accordance with accepted
academic practice. No use, distribution or
reproduction is permitted which does not
comply with these terms.

Ji-Ni-De-Xie ameliorates type 2 diabetes mellitus by modulating the bile acids metabolism and FXR/FGF15 signaling pathway

Yiwen Tao^{1†}, Fang Peng^{1†}, Lijie Wang¹, Jiayi Sun², Yin Ding¹,
Shuangfeng Xiong¹, Ugen Tenzin^{3*}, MiMa⁴, Tsedien Nhamdriel^{4*}
and Gang Fan^{1,5*}

¹State Key Laboratory of Southwestern Chinese Medicine Resources, School of Ethnic Medicine and School of Pharmacy, Chengdu University of Traditional Chinese Medicine, Chengdu, China, ²Innovative Institute of Chinese Medicine and Pharmacy, Chengdu University of Traditional Chinese Medicine, Chengdu, China, ³Dege County Tibetan Hospital (Institute of Tibetan Medicine), Dege, China, ⁴Department of Tibetan Medicine, University of Tibetan Medicine, Lhasa, China, ⁵Meishan Hospital of Chengdu University of Traditional Chinese Medicine, Meishan, China

Introduction: Ji-Ni-De-Xie (JNDX) is a traditional herbal preparation in China. It is widely used to treat type 2 diabetes mellitus (T2DM) in traditional Tibetan medicine system. However, its antidiabetic mechanisms have not been elucidated. The aim of this study is to elucidate the underlying mechanism of JNDX on bile acids (BAs) metabolism and FXR/FGF15 signaling pathway in T2DM rats.

Methods: High-performance liquid chromatography-triple quadrupole mass spectrometry (HPLC-QQQ-MS) and UPLC-Q-Exactive Orbitrap MS technology were used to identify the constituents in JNDX. High-fat diet (HFD) combined with streptozotocin (45 mg·kg⁻¹) (STZ) was used to establish a T2DM rat model, and the levels of fasting blood-glucose (FBG), glycosylated serum protein (GSP), homeostasis model assessment of insulin resistance (HOMA-IR), LPS, TNF- α , IL-1 β , IL-6, TG, TC, LDL-C, HDL-C, and insulin sensitivity index (ISI) were measured to evaluate the anti-diabetic activity of JNDX. In addition, metagenomic analysis was performed to detect changes in gut microbiota. The metabolic profile of BAs was analyzed by HPLC-QQQ-MS. Moreover, the protein and mRNA expressions of FXR and FGF15 in the colon and the protein expressions of FGF15 and CYP7A1 in the liver of T2DM rats were measured by western blot and RT-qPCR.

Results: A total of 12 constituents were identified by HPLC-QQQ-MS in JNDX. Furthermore, 45 chemical components in serum were identified from JNDX via UPLC-Q-Exactive Orbitrap MS technology, including 22 prototype components and 23 metabolites. Using a T2DM rat model, we found that JNDX (0.083, 0.165 and 0.33 g/kg) reduced the levels of FBG, GSP, HOMA-IR, LPS, TNF- α , IL-1 β , IL-6, TG, TC, and LDL-C, and increased ISI and HDL-C levels in T2DM rats. Metagenomic results demonstrated that JNDX treatment effectively improved gut microbiota dysbiosis, including altering some bacteria (e.g., *Streptococcus* and *Bacteroides*) associated with BAs metabolism. Additionally, JNDX improved BAs disorder in T2DM rats, especially significantly increasing cholic acid (CA) levels and decreasing ursodeoxycholic acid (UDCA) levels. Moreover, the protein

and mRNA expressions of FXR and FGF15 of T2DM rats were significantly increased, while the expression of CYP7A1 protein in the liver was markedly inhibited by JNDX.

Discussion: JNDX can effectively improve insulin resistance, hyperglycemia, hyperlipidemia, and inflammation in T2DM rats. The mechanism is related to its regulation of BAs metabolism and activation of FXR/FGF15 signaling pathway.

KEYWORDS

Tibetan medicine, Ji-Ni-De-Xie, bile acid metabolism, FXR/FGF15 signaling, type 2 diabetes mellitus,



GRAPHICAL ABSTRACT

1 Introduction

Diabetes mellitus is a chronic metabolic disease characterized by hyperglycemia primarily caused by deficiency of insulin secretion and utilization (Wu et al., 2022). Currently, diabetes mellitus has a high incidence and serious complications, which seriously affects the quality of life of patients. Type 2 diabetes mellitus (T2DM) accounts for 90% of diabetes cases. The major characteristics of T2DM are insulin resistance and hyperglycaemia (Wu et al., 2023). Currently, a rapidly growing of T2DM has become a health problem affecting nearly half a billion people worldwide (Magliano et al., 2021; Zhang et al., 2023). Therefore, it is necessary to develop effective drugs for the prevention and treatment of T2DM.

Bile acids (BAs) have a strong correlation with diabetes. The composition and level changes of BAs could be observed in patients with insulin resistance or T2DM (Du et al., 2022). Additionally, some studies have found that gastrointestinal homeostasis is jointly regulated by BAs and gut microbes, and the imbalance of this interaction may lead to the development of T2DM and other pathologies (Guo et al., 2022). As intestinal signaling molecules, BAs promote fibroblast growth factor-15 (FGF15, murine homologous gene of human FGF19), a gastrointestinal hormone, transmitting signals by activating the farnesoid X receptor (FXR),

and play a vital role in glycolipid metabolism and energy metabolism (Meiring et al., 2022; Tawulie et al., 2023). Furthermore, cholesterol 7 α hydroxylase (CYP7A1), as a rate-limiting enzyme in the classical BAs synthesis pathway, determines the rate of BAs synthesis and converts cholesterol to 7 α -hydroxycholesterol (Chiang, 2013). Simultaneously, CYP7A1 activation is negatively regulated by FXR receptors. When FXR is activated in the liver or intestines, the expression of FGF15 increases, which in turn inhibits the expression of CYP7A1, thereby reducing the synthesis of BAs (Yan et al., 2022). Currently, synthetic FXR agonists such as obeticholic acid have been shown to be effective against insulin resistance and have been applied in clinical as a potential therapy for T2DM (Kuipers et al., 2014). Besides, FXR antagonists such as NDB and HS218 could effectively reduce blood glucose in obese mice and suppress the expression of gluconeogenic gene in db/db mice (Zhao et al., 2021). These researches suggest that FXR and BAs metabolism occupy a significant role in glycolipid metabolism.

Tibetan medicine is the most complete medical system in the ethnic minority medical system in China, with a history of more than 3,800 years. The unique medical theory and abundant medicinal plant resources on the Qinghai-Tibet Plateau provide favorable conditions for the treatment of diseases with Tibetan medicine (Zhao et al., 2021). In recent years, the study of

TABLE 1 Medicinal information of Ji-Ni-De-Xie (JNDX).

Chinese name	Tibetan name (transliteration)	Latin name	Family name	Parts used
Xiao Bo Pi	མཁའ་བོ་པི། (Jie Xing)	<i>Berberis kansuensis</i> C.K.Schneid.	Berberidaceae	Stem bark
Jiang Huang	ཡུང་བ། (Yong Wa)	<i>Curcuma longa</i> L.	Zingiberaceae	Rhizome
Yu Gan Zi	ཡུ་གན་ཟི། (Ju Ru La)	<i>Phyllanthus emblica</i> L.	Euphorbiaceae	Fruit
Ji Li	ཇི་ལི། (Sai Ma)	<i>Tribulus terrestris</i> L.	Zygophyllaceae	Fruit
Hong Hua	ཁོང་ཁུ་མ། (Ku Kong)	<i>Carthamus tinctorius</i> L.	Compositae	Flower
He Zi	ཁེ་ཟི། (A Ru La)	<i>Terminalia chebula</i> Retz.	Combretaceae	Fruit
Duo Hua Huang Qi	སྡེ་ལྷ་མོ་རྩ། (Sa Sai)	<i>Astragalus floridus</i> Bunge	Leguminosae	Herb
Ya Zui Hua	ཡ་ཟུའ་མ། (Ba Xia Ga)	<i>Adhatoda vasica</i> Nees	Acanthaceae	Branch and leaf

Note: The family name and Latin name from “The Plant List” Webservers (<http://www.theplantlist.org>).

Tibetan medicine in treating diabetes has been paid more and more attention. Some Tibetan herbs and preparations have been shown to be effective in treating T2DM and its complications, such as Tibetan medicine Lvluo, *Berberis kansuensis* Schneid, and Shibawei Hezi Liniao pills (Liu, 2018; Xu et al., 2021; Zheng et al., 2021). Ji-Ni-De-Xie (JNDX) is a hospital preparation prepared by the Tibetan Medicine Hospital in Dege County, Sichuan Province, China. It is comprised of *B. kansuensis* C.K.Schneid., *Curcuma longa* L., *Phyllanthus emblica* L., *Tribulus terrestris* L., *Carthamus tinctorius* L., *Terminalia chebula* Retz., *Astragalus floridus* Bunge, and *Adhatoda vasica* Nees (Table 1). It has been clinically employed in treating diabetes for over a decade, boasting a robust clinical foundation that ensures its safety and efficacy (Li et al., 2015; Luo et al., 2022a). Although the efficacy of JNDX in the treatment of T2DM is definite, its specific anti-diabetic mechanism remains unclear. Hence, to better understand the therapeutic effects and potential mechanisms of JNDX on T2DM, we established a T2DM rat model induced by a high-fat diet (HFD) combined with streptozotocin (STZ). In addition, targeted metabolomics based on high-performance liquid chromatography-triple quadrupole mass spectrometry (HPLC-QQQ-MS), metagenomics, real-time quantitative polymerase chain reaction (RT-qPCR), and Western blotting were combined to explore the potential mechanisms of JNDX in improving T2DM from the perspective of regulating BAs metabolism. The results of this study will provide important reference for the clinical application and drug development of JNDX.

2 Materials and methods

2.1 Materials

Ji-Ni-De-Xie was obtained from Dege County Tibetan Hospital (Institute of Tibetan Medicine) (Sichuan, China). Metformin hydrochloride tablets were purchased from Sino American Shanghai Shiguibao Pharmaceutical Co., Ltd (Shanghai, China) (Lot number: ABS9845); STZ (Lot number: WXBD7077V) was purchased from Sigma-Aldrich Co., St (Louis, United States). The enzyme-linked immunosorbent assay (ELISA) kits of insulin (Ins) (No. MM-0587R1), glycosylated serum protein (GSP) (No. MM-0735R1), tumor necrosis factor- α (TNF- α) (No. MM-0180R1),

lipopolysaccharide (LPS) (No. MM-0647R1), glucagon-like peptide 1 (GLP-1) (No. MM-0033R2), and FGF15 (No. MM-0938R1) were obtained from Jiangsu Meimian Industrial Co., Ltd (Jiangsu, China). The ELISA kits of interleukin-6 (IL-6) (No. EK306/3-96) and IL-1 β (No. EK301B/3-96) were provided by MULTISCIENCES (LIANKE) Biotech, Co., Ltd (Zhejiang, China). Triglyceride (TG) (No. C061-a), total cholesterol (TC) (No. C063-a), low-density lipoprotein cholesterol (LDL-C, No. C070-a), and high-density lipoprotein cholesterol (HDL-C) (No. C069-a) were purchased from Changchun Huili Biotech CO., LTD. Primary antibodies FXR/NR1H4 Rabbit mAb (1:1500, A24015, ABclonal Technology, China), Rabbit anti-CYP7A1 (1:1000, bs-21430R, Bioss, China), and anti-FGF15 (1:1000, sc-398338, Santa Cruz Biotechnology Inc., United States). Secondary antibodies goat anti-rabbit (1:10000, bs-0295G-HRP, Bioss, China) and HRP goat anti-mouse IgG (H + L) (1:10000, AS003, ABclonal Technology, China). β -actin (1:1000, GB15003, Servicebio, China).

2.2 Preparation and composition analysis of JNDX

JNDX was ground and sifted through No. 3 sieve, and then accurately weighed 0.1 g into 100 mL conical bottle. 50 mL 50% methanol was added into bottle, and then ultrasound was performed for 30min. After cooling, make up the weight with 50% methanol, and filter the supernatant with 0.22 μ m microporous filter membrane.

The chemical constituents of JNDX were analyzed by HPLC-QQQ-MS (Agilent 1260, Agilent Technologies Inc., United States). The analysis was performed using a WondaSil C₁₈-WR chromatographic column (4.6 \times 250 mm, 5 μ m). Then, the mobile phase was water containing 0.1% formic acid A)–methanol B). The column temperature was 25°C and the sample volume was 5.0 μ L. The gradient program’s specific condition was set as follows: 0–1 min, 10%–45% B; 1–3 min, 45%–70% B; 3–4 min, 70%–70% B; 4–5 min, 70%–75% B; 5–7 min, 75%–75% B; 7–10 min, 75%–95% B; 10–20 min, 95% B. The mass spectrum conditions were as follows: electrospray ion source (ESI), high purity nitrogen (dry gas) as a collision gas, with a flow rate of 11 L·min^{–1}; capillary voltage was set at 4000 V (+) and 2500 V (–); temperature was maintained at 300°C with a pressure of 15 psi. Simultaneous determination of positive and negative ions was conducted in multiple reaction monitoring (MRM) mode.

TABLE 2 Experimental dosages of rats *in vivo*.

Group	Volume of administration (mL/kg)	Dosage (g/kg/d)	concentration (g/mL)	Equivalent to multiple of clinical dosage
Normal	10.000	-	-	-
Model		-	-	-
Metformin		0.250	0.025	10.000
JNDX-H		0.330	0.330	10.000
JNDX-M		0.165	0.165	5.000
JNDX-L		0.083	0.083	2.500

2.3 Animals and treatment

Male Sprague-Dawley rats (weight 160–180 g, SPF level) and HFD were purchased from Chengdu Dashuo Experimental Animal Co., Ltd. [Laboratory animal license number SCXK (Sichuan) 2020-030, Sichuan, China] and then adaptively housed in 25°C ± 2°C and relative humidity 50%–60% for 1 week. The rats were held in the Experimental Animal Center of Chengdu University of Traditional Chinese Medicine, and the water and diet were unrestricted supplied. The experimental unit license number is SYXK (Sichuan) 2020-124. Chengdu University of Traditional Chinese Medicine's Animal Ethics Committee consented its approval to this research (the ethical approval number: 2018–15). The study was conducted in compliance with the guidelines set out by the National Health Institutes of China.

According to JNDX instruction, the adult clinical oral administration dose of JNDX is 1 to 2 pills/day (mass is 1.1537 g/pill). Thus, the maximum dose for adults is 0.0330 g/kg/d (assuming a body weight of 70 kg), and the high dose for rats in the present study is 0.330 g/kg/d, the medium dose is 0.165 g/kg/d, and the low dose is 0.083 g/kg/d (Chen, 2006). The specific groups and dosages are shown in Table 2. The JNDX powder was sieved through the 4th screen, and 0.05% sodium carboxymethyl cellulose (CMC-Na) solvent was used to dissolve the powder and metformin (positive control group) respectively.

2.4 Analysis of the chemical composition in rat serum after JNDX intervention by UPLC-Q-Exactive Orbitrap MS

After grinding, 50 g of JNDX was weighed and mixed with 10 times the volume of 50% ethanol. It was then heated and reflux-extracted twice for 2 h each time. The filtrate was mixed and concentrated under reduced pressure, resulting in a JNDX extract with a concentration of 0.625 g·mL⁻¹. Sprague-Dawley rats were randomly divided into normal group and JNDX group. The JNDX group received an oral gavage of 12.5 g·kg⁻¹ of JNDX extract, while the normal group received an equivalent volume of distilled water for three consecutive days. Oral gavage was administered twice daily, with the rats fasting but not restricted from water intake for 12 h before the final administration. Blood samples (0.5 mL) were collected from the orbital vein at 0.25 h, 0.5 h, 1 h, 1.5 h, 2 h, 3 h,

5 h, and 8 h after the final gavage, centrifuged at 3500 rpm for 10 min, and the serum was collected and stored at –80°C. For the JNDX group, 1 mL of serum was collected and mixed with 3 mL of acetonitrile to precipitate proteins. After centrifuging at 11000 rpm for 10 min, the supernatant was dried with nitrogen gas at 37°C. The residue was reconstituted with 200 µL of methanol, centrifuged at 11000 rpm for 10 min, and the supernatant was filtered through a 0.22 µm microporous membrane. Finally, we analyzed the filtrate using ultra high performance liquid chromatography with four stage rod/electrostatic field orbital trap high resolution mass spectrometry (UPLC-Q-Exactive Orbitrap MS) (Thermo-Fisher, United States).

The mass spectrometry conditions were as follows: using HESI ion source, positive ion detection mode with a spray voltage of +3500 V; negative ion detection mode with a spray voltage of –3000 V; sheath gas flow rate of 35.0 Arb, auxiliary gas flow rate of 10.0 Arb, and capillary temperature of 320°C. Full MS/dd-MS² scan mode was employed with a Full MS resolution of 70,000 and dd-MS² resolution of 17,500. The scan range was from m/z 100 to 1500.

High-performance liquid chromatography analysis was performed using a ZORBAX SB-C₁₈ chromatographic column (150 mm × 2.1 mm, 1.8 µm). Then, the mobile phase was methanol A)–water containing 0.1% formic acid B). The column temperature was 30°C and the sample volume was 5.0 µL. The gradient program's specific condition was set as follows: 0–20 min, 5%–20% A; 20–30 min, 50%–80% A; 30–35 min, 80%–95% A; 35–45 min, 95% A; 45–50 min, 95%–5% A (Luo et al., 2022a).

2.5 Induction of T2DM rats

Sprague-Dawley male rats were randomly divided into 2 groups, 8 were normal group, and the rest were model screening group for T2DM rats. The rats in the model group were fed with HFD for 4 weeks and then fasted for 12 h. On the following day, 1% STZ buffer solution (45 mg·kg⁻¹) was prepared for intraperitoneal injection in the model screening group. Besides, the rats in the normal group were injected with an equivalent amount of 0.1 mol·L⁻¹ citric acid-sodium citrate buffer solution (pH = 4.1). After STZ injection, the rats had free access to food and water, and fasting blood-glucose (FBG) was measured after fasting for 12 h at 72 h, 2 weeks, and 4 weeks, respectively. The FBG of each rat was measured three times by blood glucose meter (Anwen + code, Sinocare Inc.). The rats with three FBG indices greater than or

TABLE 3 Real-time quantitative polymerase chain reaction primer sequences used in this study.

Gene	Forward primers (5'–3')	Reverse primers (5'–3')
FXR	CATCATGGCTTCGGTTCAG	TCCCCACCTTCCTTCCATC
FGF15	AAGTGGAGTGGGCGTATTGT	AGTGGACCTTCATCCGACAC
GAPDH	AAGTTCAACGGCACAGTCAA	TCTCGTCTCTGGAAGATGG

equal to 11.0 mmol·L⁻¹ and the index of FBG steadily were considered as T2DM model rats.

A total of 40 model rats were selected and randomly divided into 5 groups: model group (model), metformin group (metformin), JNDX high-dose group (JNDX-H), JNDX medium-dose group (JNDX-M), and JNDX low-dose group (JNDX-L), with 8 rats in each group. All model rats were raised together with 8 rats in the normal group (normal). During the experiment, the normal group was fed with ordinary diet, and the model group and the JNDX group were fed with HFD.

2.6 Biochemical indicators assay

After the successful modeling of STZ in Sprague-Dawley rats, the rats were given continuous administration of JNDX for 40 days. Subsequently, the rats were fasted for 12 h and then FBG was measured by glucose meter. Blood samples were collected from abdominal aorta, and then the whole blood was left for 2 h, and centrifuged at 3500 rpm at 4°C for 15 min to obtain the serum. The serum was stored at – 80°C for detection. The contents of TG, TC, LDL-C, and HDL-C were measured by an automatic biochemical analyzer (BK-200, Shandong Biobase Scientific Instrument Co., LTD.). The ELISA kits were performed to detect the levels of GSP and Ins and then calculated the value of ho-meostasis model assessment of insulin resistance (HOMA-IR) and insulin sensitivity index (ISI). All experimental procedures were followed strictly with manufacturer's instructions. HOMA-IR and ISI were calculated according to the following formulas:

$$\text{ISI} = \text{Ln} [1 / (\text{FBG} (\text{mmol}/\text{mL}) \times \text{Ins} (\mu\text{U}/\text{mL}))]$$

$$\text{HOMA} - \text{IR} = \text{FBG} (\text{mmol}/\text{L}) \times \text{Ins} (\mu\text{U}/\text{mL}) / 22.5$$

(Xu et al., 2021).

2.7 Gut microbiota analysis

Fecal sample DNA of rats was extracted from Magnetic Soil and Stool DNA Kit (TIANGEN BIOTECH Co., LTD., Beijing, China) and metagenomic sequencing was performed. The DNA samples were fragmented into 350 bp fragments using ultrasonication for Illumina sequencing and subsequent PCR amplification. Following clustering, the library preparations were sequenced using the NovaSeq 6000 sequencing platform with PE150 read length.

The relative abundance information of gut microbiota was imported into R software (Version 4.2.2) for statistical analysis. The R package phyloseq was used to calculate α -diversity. α -diversity was studied to explore the complexity of species diversity using Shannon index (Lkhagva et al., 2021). Principal coordinates analysis (PCoA) based on Bray Curtis distance was conducted to explore the characteristics of gut microbiota. Anosim analysis was used to compare the similarities and differences in the composition of gut microbiota between the model and JNDX groups. Functional predictions of gut microbiota were performed using Kyoto Encyclopedia of Genes and Genomes (KEGG) and DIAMOND software (Kanehisa, et al., 2006; 2014; Buchfink, et al., 2015) based on metagenomic sequencing data. The Linear Discriminant Analysis Effect Size (LEfSe) software was employed to calculate the differences in functional pathways among groups at the family, genus, and species levels (LDA score >4.0, $p < 0.05$) (Segata, et al., 2011).

2.8 Effect of JNDX on BAs in T2DM rats based on HPLC-QQQ-MS analysis

The cryopreserved serum samples were thawed at room temperature and swirled evenly. Then, 100 μL serum sample was precisely measured and 10 μL internal standard (1.00 $\mu\text{g}\cdot\text{mL}^{-1}$) (Cholic acid-d₄, Lot number: ISO-13098, Nanjing Beiyu Biotechnology Co., LTD.) and 200 μL chromatograph-grade acetonitrile were added. The mixture swirled at room temperature for 2 min, stood for 10 min, and centrifuged at 11 000 rpm at 4°C for 10 min. The supernatant was processed through 0.22 μm microporous filter membrane. The serum samples of rats in each group were analyzed by a triple quadrupole mass spectrometer (Agilent G6420A, Agilent Technologies Inc., United States). The analysis method was established on the basis of our previous research work (Yi, 2022).

2.9 Enzyme-linked immunosorbent assay

The levels of LPS, IL-6, IL-1 β , TNF- α , GLP-1, and FGF15 were estimated using ELISA kits. The experiment process was carried out in strict accordance with the manufacturer's instructions.

2.10 RNA isolation and real-time quantitative polymerase chain reaction analysis

100 mg of the tissue was taken and fully grinded in 1 mL of pre-cooled lysis buffer. Total RNA was extracted from tissue using Trizol (Lot number: 9109, TAKARA). The concentration of total RNA was measured by ultramicro quantitative nucleic acid protein detector (EVA 3100, Monad Biotechnology Co. LTD., Jiangsu, China). Subsequently, 1 μg RNA template was prepared for reverse transcription using a M-MLV Reverse Transcriptase kit (M170A, Promega Biotech Co., Ltd., Beijing, China) and iScript™ cDNA Synthesis Kit (1708890, Bio-Rad Laboratories, Inc., United States) was used to synthesize cDNA. Finally, RT-qPCR was performed via fluorescent quantitative PCR instrument (CFX Connect, Bio-Rad Laboratories, Inc., United States). The total reaction system of fluorescence quantitative detection was 10 μL . In

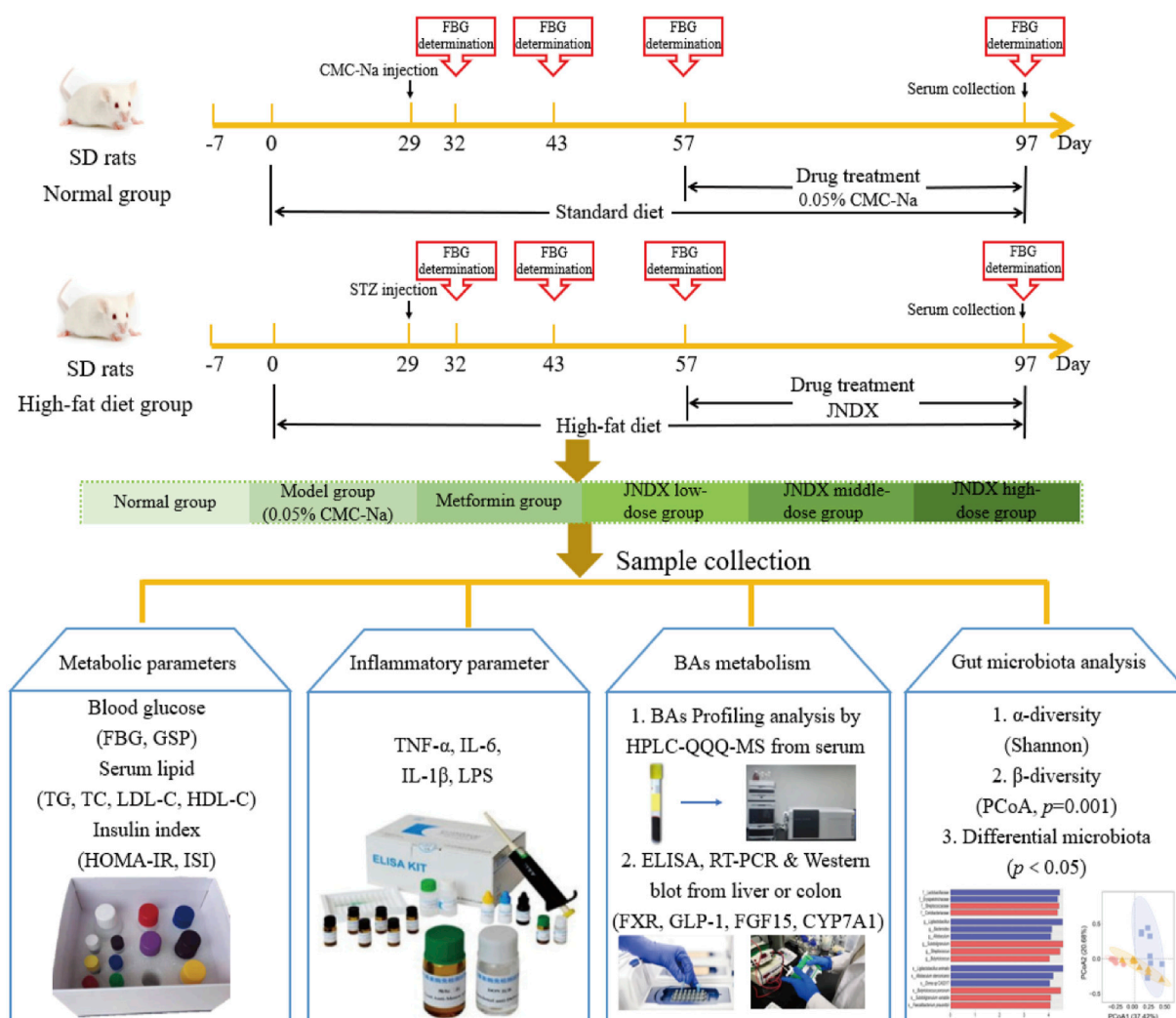


FIGURE 1
The specific experimental procedure in this study.

addition, the amplification steps were as following: 95°C, 5 min for initial denaturation step, and 95°C, 10 s to 60°C, 30 s for 40 cycles of denaturation, and anneal at 65°C–95°C, 0.5°C/5 s. The primer sequences in this study were presented in Table 3. The 96-well plate was put into the fluorescence quantitative PCR instrument, and the detection was set on the Bio-Rad CFX Manager. The expression multiple was calculated using the $\Delta\Delta CT$ method, and the differences in the samples of relative mRNA expression were normalization by reference genes (GAPDH): $\Delta CT = CT_{\text{target gene}} - CT_{\text{reference gene}}$, $\Delta\Delta CT = \Delta CT_{\text{treatment sample}} - \Delta CT_{\text{control sample}}$, the analyzed formula = $2^{-\Delta\Delta CT}$ (Su et al., 2023).

2.11 Western blot analysis

Animal tissues were homogenized and lysed using freezing grinder (JXFSTPRP-CL, Shanghai Jingxin Industrial Development Co., Ltd., Shanghai, China) and RIPA lysis buffer (AR0102S, BOSTER, China). Then, the samples were centrifuged at 10,000 g

for 10 min at 4°C. The supernatant of each sample was obtained and the protein concentration of the sample was measured with BCA kit (AR0146, BOSTER, China). Whereafter, the SDS-PAGE sample loading buffer (AR1112-10, BOSTER, China) was added in total protein and denatured at 100°C for 10 min to obtain WB samples. 10% PAGE high resolution color gel was prepared to separate proteins of different molecular weight, and the isolated proteins were transferred to polyvinylidene difluoride (PVDF) membranes, which were then blocked with 5% BSA at room temperature for 90 min. The membranes were placed in incubator box containing primary antibody at 4°C overnight: FXR (1:1500), CYP7A1 (1:1000), and FGF15 (1:1000). On the second day, after the recovery of the primary antibody, membranes were washed three times with TBST. Next, membranes covered with the second antibody (1:10000) and incubated for 90 min at room temperature. After incubation, the membranes were washed three times and exposed to ultra-sensitive ECL chemiluminescent substrate kit (BL520A, Biosharp, China). Finally, visualizer (ChampChemi 610 Plus, Beijing Sage Creation, China) was employed to visualize the protein bands and ImageJ

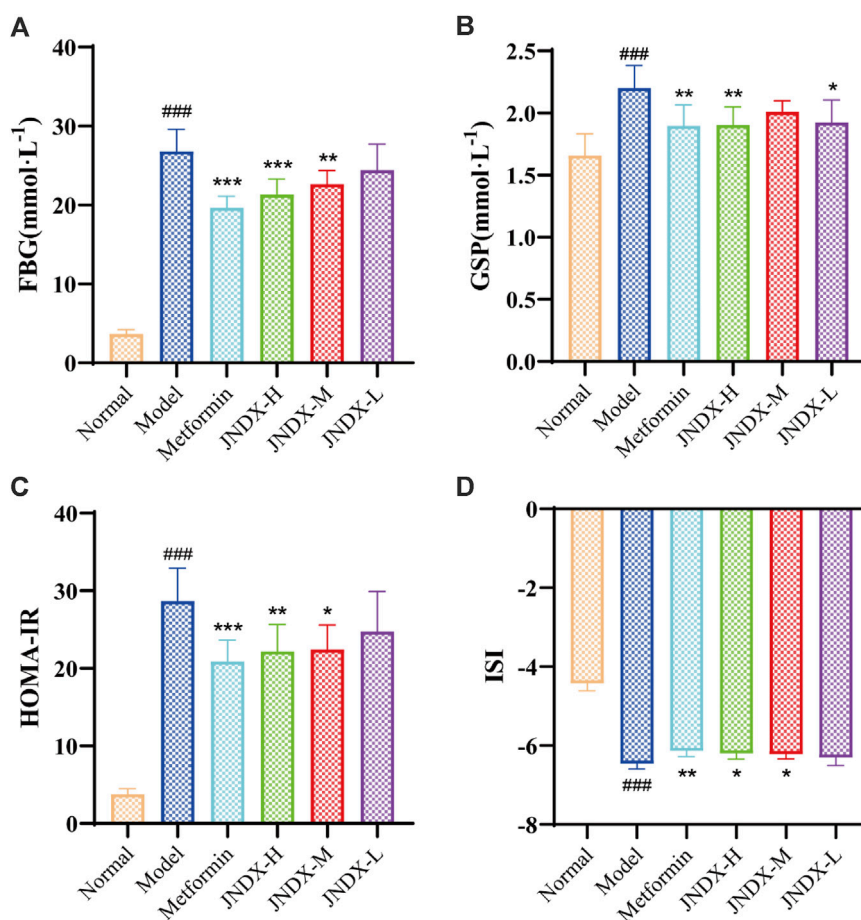


FIGURE 2
Effects of JNDX on FBG (A), GSP (B), HOMA-IR (C), and ISI (D). All data were represented as mean \pm SD. # $p < 0.05$, ## $p < 0.01$, ### $p < 0.001$ vs the Normal group, * $p < 0.05$, ** $p < 0.01$, *** $p < 0.001$ vs the Model group.

software (version 1.37V, NIH, United States) was performed to quantify the relative gray value of bands.

2.12 Statistical analyses

The data were presented as means \pm standard deviation (SD). GraphPad Prism 8 (San Diego, CA, United States) was performed for the statistical analysis. One-way analysis of variance (ANOVA) was conducted to determine the p -value, with statistical significance established at a p -value < 0.05 .

3 Results

3.1 HPLC-QQQ-MS analysis of chemical constituents in JNDX

The chemical constituents of JNDX were analyzed by HPLC-QQQ-MS technique. A total of 12 constituents (magnoflorine, berberine, curcumin, jateorrhizine, demethoxycurcumin, gallic acid, chebulagic acid, ferulic acid 4-O- β -D-glucopyranoside, hydroxysafflor

yellow A, rutin, ferulic acid, and ellagic acid) were identified in JNDX by comparing their retention time and mass spectrum information with standard compounds. In addition, the contents of the 12 constituents in JNDX were calculated according to their calibration curves established by the corresponding standard compounds. The results showed that gallic acid had the highest content (18.11 mg·g⁻¹), followed by chebulagic acid (4.98 mg·g⁻¹), magnoflorine (3.27 mg·g⁻¹), ellagic acid (3.17 mg·g⁻¹), ferulic acid 4-O- β -D-glucopyranoside (3.07 mg·g⁻¹), and ferulic acid (1.83 mg·g⁻¹). The content determination results, mass spectrometry information and chromatogram of JNDX are shown in [Supplementary Table S1](#), [S2](#) and [Supplementary Figure S1](#).

3.2 UPLC-Q-Exactive Orbitrap MS analysis of chemical compounds in rat serum after JNDX intervention

A total of 45 chemical compounds in rat serum after JNDX intervention were identified using UPLC-Q-Exactive Orbitrap MS technology, including 22 prototype components and 23 metabolites. The detailed chemical compounds in rat serum and the diagram of

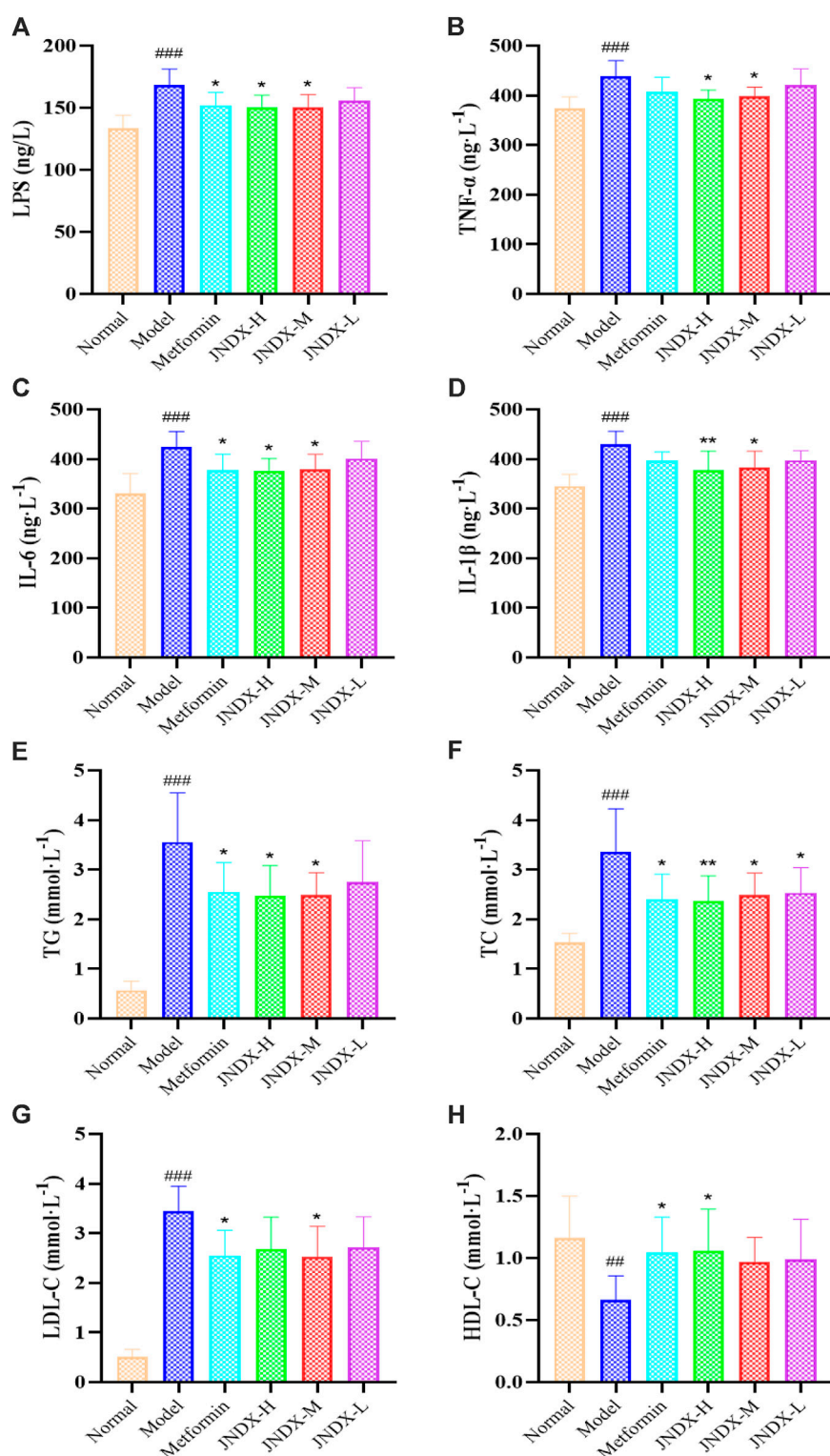


FIGURE 3
Effects of JNDX on LPS (A), pro-inflammatory cytokines TNF-α (B), IL-6 (C), and IL-1β (D), and lipid indices TG (E), TC (F), LDL-C (G), and HDL-C (H). All data were represented as mean ± SD. * $p < 0.05$, ** $p < 0.01$, *** $p < 0.001$ vs the Normal group, * $p < 0.05$, ** $p < 0.01$, *** $p < 0.001$ vs the Model group.

positive and negative ion flow are shown in [Supplementary Figure S2](#) and [Supplementary Table S3](#). These components included berberine, magnoflorine, ferulic acid, ellagic acid, jateorrhizine,

demethoxycurcumin, and curcumin. They mainly originated from the combination of *B. kansuensis* C.K.Schneid., *C. longa* L., *P. emblica* L., and *T. chebula* Retz., suggesting that these four herbs

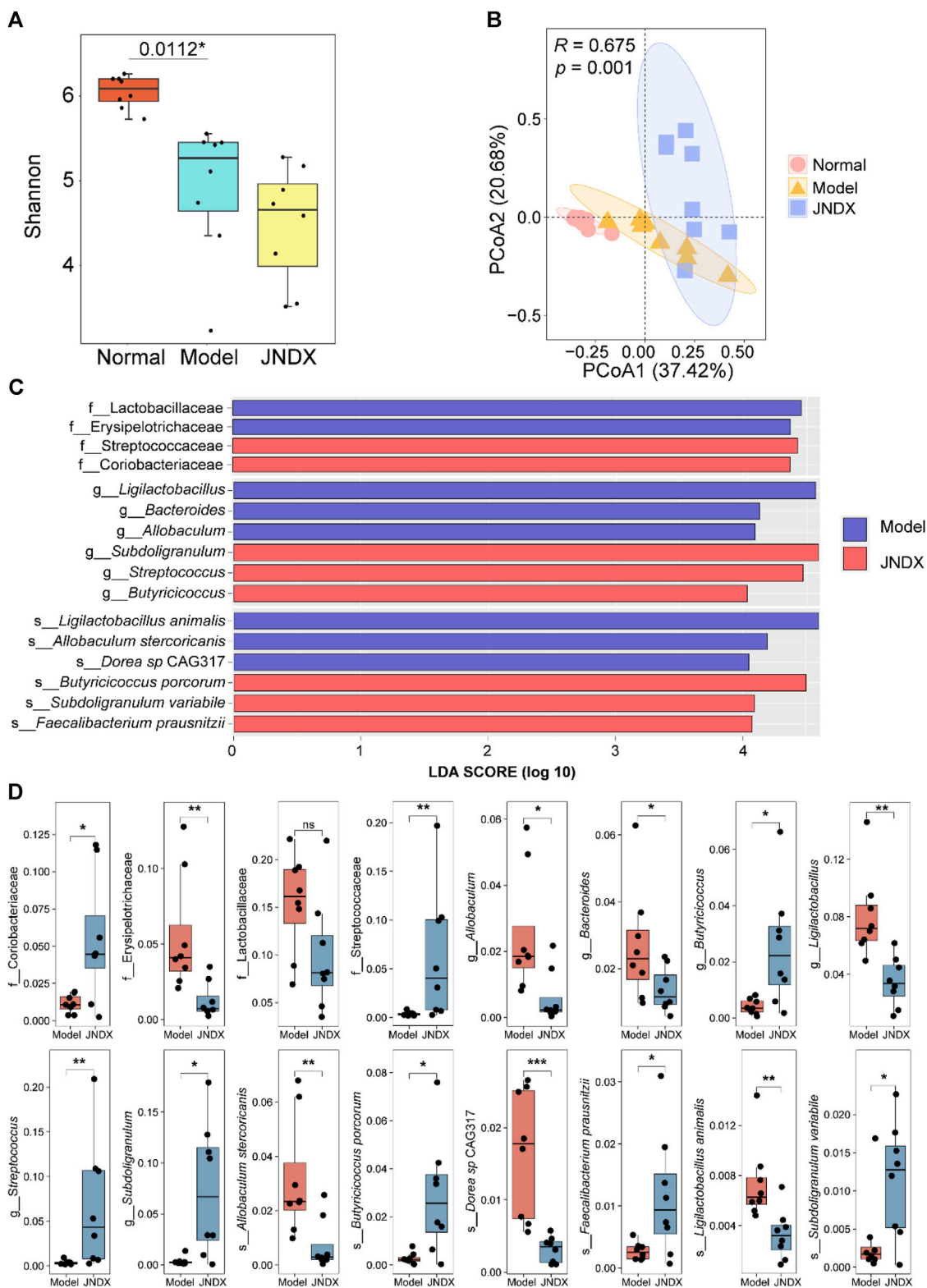


FIGURE 4
Effects of JNDX on gut microbiota. **(A)** Differences in gut bacterial diversity among the 3 groups of rats based on Shannon index. **(B)** Principal coordinates analysis (PCoA) analysis based on Bray Curtis distance was performed to explore the gut microbiota characteristics between the 3 groups. $R > 0$ indicates that the between-group differences were greater than the within-group differences. Reliability of statistical analyses was expressed as p -value. **(C)** LEfSe analysis showed significant enrichment of gut microbiota in the model and JNDX groups at the family, genus, and species levels. Taxa with LDA scores >4 are shown. **(D)** Kruskal Wallis variance analysis showed the differential expression of gut microbiota between the model group and the JNDX group.

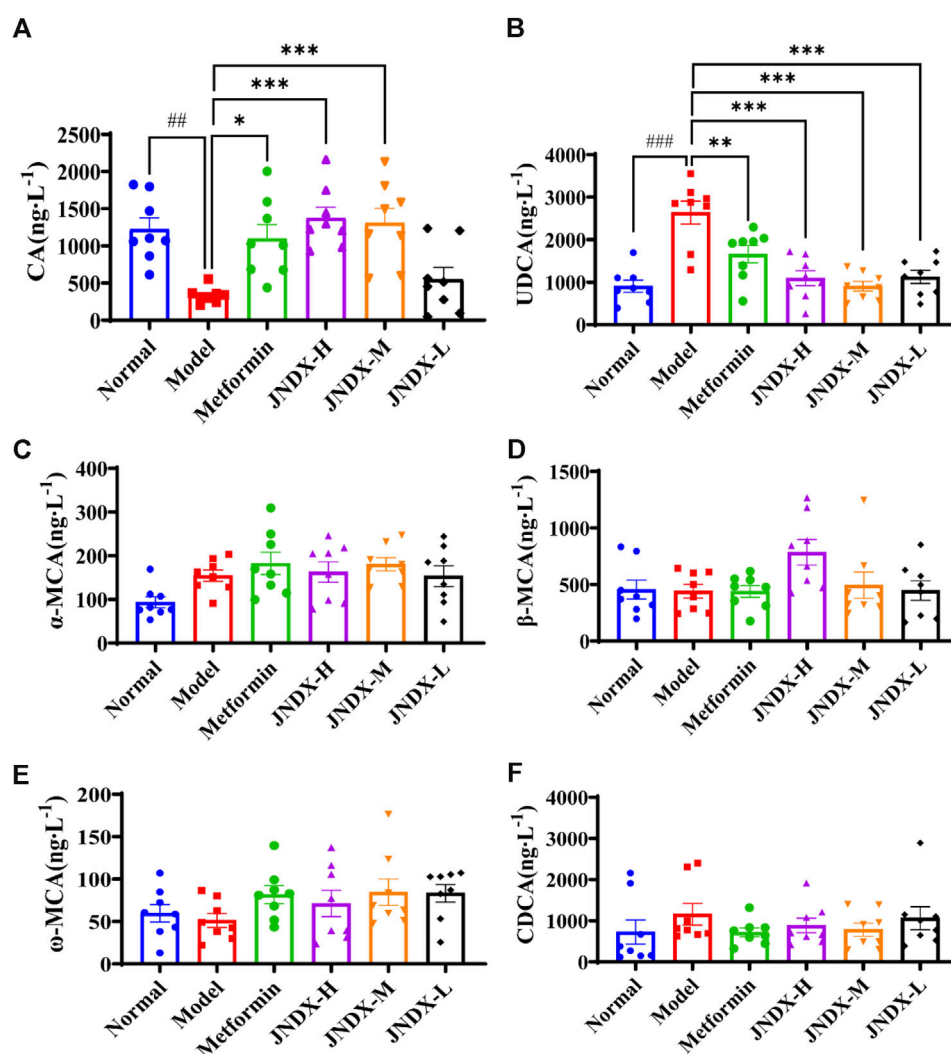


FIGURE 5
(Continued).

contributed significantly to the treatment of T2DM with JNDX. In conclusion, the results indicate that berberine, magnoflorine, ferulic acid, ellagic acid, jateorrhizine, demethoxycurcumin, and curcumin may be the effective components of JNDX treating T2DM.

3.3 JNDX reduced blood glucose, ameliorate insulin resistance, and insulin sensitivity in T2DM rats

After the successful modeling of T2DM rats, the typical diabetes symptoms of eating more, drinking more water, excreting more, while the weight loss were obvious. Figure 1 depicts the specific experimental procedure. The effect of JNDX on T2DM rats was evaluated by measuring relevant blood glucose and insulin-related indices. Figure 2A shows that FBG is significantly higher in model group than in normal group ($p < 0.001$). After 40 days of administration, both the high dose and medium dose groups of JNDX could significantly reduce FBG ($p < 0.01$), while the effect of

FBG reduction was not significantly different in the low dose group. These results indicate that JNDX could significantly reduce FBG in T2DM rats. In addition, GSP was similar to glycosylated hemoglobin and reflected the average blood glucose concentration over the past 1–3 weeks. The results indicate that the GSP level of the T2DM rats in the model group is significantly higher than that in the normal group ($p < 0.001$). After 40 days of administration, GSP content was obviously decreased at JNDX-H and JNDX-L group compared with model group ($p < 0.05$) (Figure 2B).

Ins value of rats in each group were measured by kit. HOMA-IR and ISI were calculated according to FBG and ins of rats after the last administration. Results are shown in Figures 2C, D. Compared with the normal group, the HOMA-IR of the model group was markedly increased ($p < 0.001$), and the ISI was significantly decreased ($p < 0.001$). Compared with the model group, HOMA-IR was obviously decreased ($p < 0.05$), while the ISI was increased observably ($p < 0.05$) in JNDX-H and JNDX-M groups. The results suggest that JNDX can improve insulin resistance and insulin sensitivity in T2DM rats.

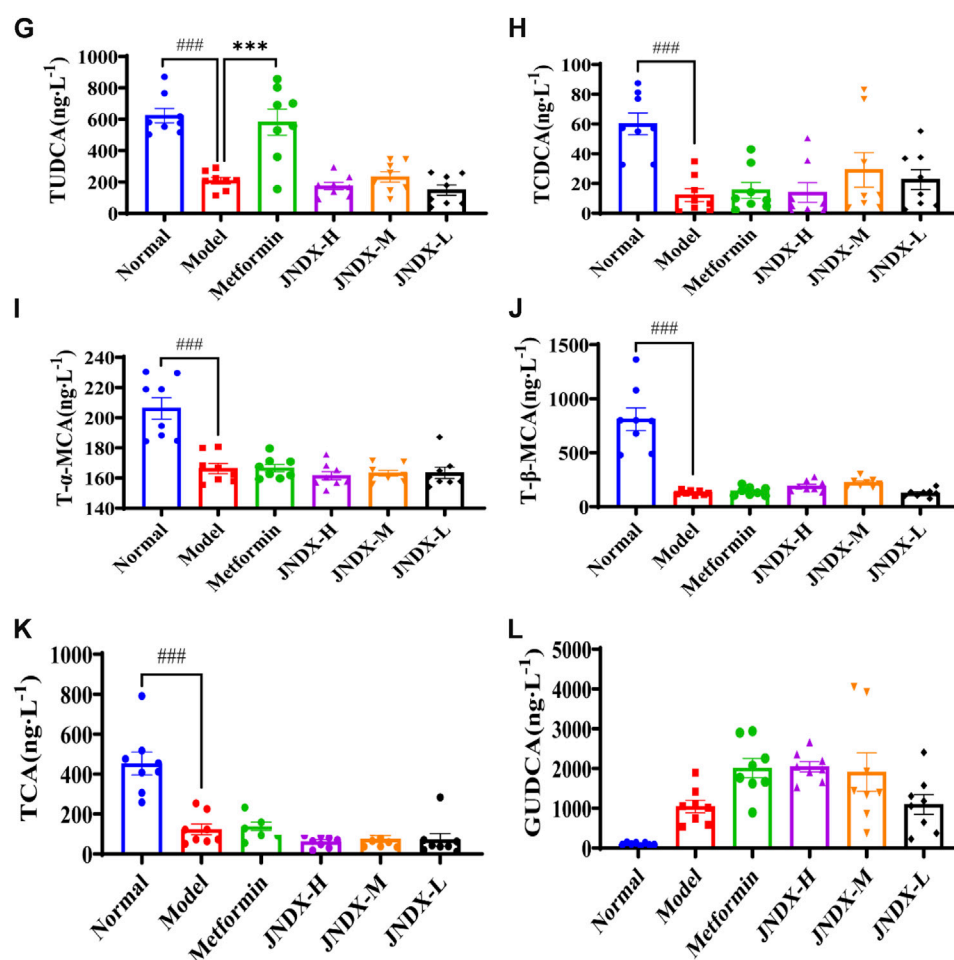


FIGURE 5
(Continued).

3.4 Effects of JNDX on LPS and inflammatory cytokines in T2DM rats

To further investigate the effect of JNDX on inflammation in T2DM rats. We found that the serum levels of LPS, IL-1 β , TNF- α , and IL-6 were significantly increased in model group (Figures 3A–D). Both high- and medium-dose JNDX markedly decreased the level of LPS, IL-1 β , TNF- α , and IL-6 ($p < 0.05$), whereas the low-dose JNDX decrease mildly in these indexes. These results demonstrate that JNDX can improve inflammation in T2DM rats.

3.5 Effects of JNDX on blood lipids (TG, TC, LDL-C and HDL-C) in T2DM rats

Through the detection of blood lipid indexes of rats in each group, we found that TG, TC, and LDL-C of T2DM rats in model group were upregulated compared with normal rats ($p < 0.001$). Nevertheless, after JNDX intervention, these indicator levels were reversed (Figures 3E–G). Besides, the expression of HDL-C was

lower in the model group than in the normal group, and JNDX-H could noticeably increase the level of HDL-C ($p < 0.05$) (Figure 3H). These results suggest that JNDX can ameliorate the blood lipid in T2DM rats.

3.6 Effects of JNDX on gut microbiota in T2DM rats

Metagenomic analysis of fecal samples was performed to assess the effect of JNDX on gut microbiota in T2DM rats. The Shannon index was significantly different between the normal and model groups ($p = 0.0112$). There was no significant difference between the model and the JNDX group (Figure 4A). The results showed that JNDX had little effect on the α diversity of gut microbiota. However, PCoA analysis showed a clear separation among the three groups, suggesting that JNDX significantly affected the composition of the gut microbiota (PCoA1, 37.42%, PCoA2, 20.68%, $p = 0.001$) (Figure 4B). The relative abundance of gut microbiota in normal, model, and JNDX groups at the family, genus, and species levels are presented in Supplementary Figure S3

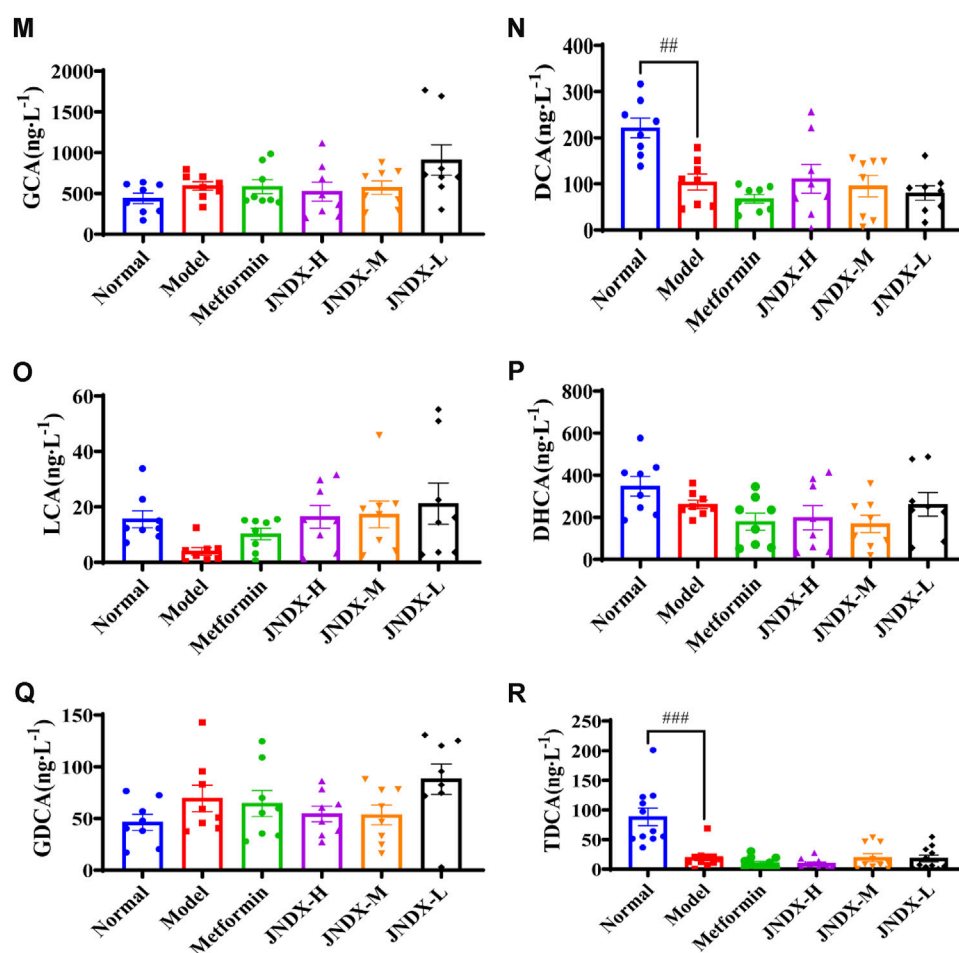


FIGURE 5
(Continued). Effects of JNDX on serum BAs in T2DM rats. Comparison of differences in 18 serum BAs among different groups of rats (A) CA, (B) UDCA, (C) α -MCA, (D) β -MCA, (E) ω -MCA, (F) CDCA, (G) TUDCA, (H) TCDCA, (I) T- α -MCA, (J) T- β -MCA, (K) TCA, (L) GUDCA, (M) GCA, (N) DCA, (O) LCA, (P) DHCA, (Q) GDCA, (R) TDCA, all data were represented as mean \pm SD. * p < 0.05, ** p < 0.01, *** p < 0.001 vs the normal group, # p < 0.05, ## p < 0.01, ### p < 0.001 vs the model group.

and [Supplementary Table S4](#). [Figures 4C, D](#) show significant enrichment of gut microbiota in model and JNDX rats at the family, genus, and species levels based on LEfSe analysis. The results suggest that JNDX can improve the gut microbiota disorder in T2DM rats by increasing the relative abundance of some bacteria (*Coriobacteriaceae*, *Streptococcaceae*, *Butyricoccus*, *Streptococcus*, *Subdoligranulum*, *Butyricoccus porcorum*, *Faecalibacterium prausnitzii*, and *Subdoligranulum variabile*) and decreasing the relative abundance of some bacteria (*Erysipelotrichaceae*, *Lactobacillaceae*, *Allobaculum*, *Bacteroides*, *Ligilactobacillus*, *Allobaculum stercoricanis*, *Dorea* sp CAG317, and *Ligilactobacillus animalis*). Among them, *Butyricoccus*, *B. porcorum*, and *F. prausnitzii* have been proven to be beneficial bacteria, promoting improvement in T2DM ([Heinken et al., 2014](#); [Xu et al., 2015](#)). Additionally, *Allobaculum* and *Bacteroides* have been demonstrated to be harmful bacteria, detrimental to the treatment of T2DM ([Wang et al., 2020](#); [Chen et al., 2023](#)). Notably, some bacteria such as *Streptococcus* and *Bacteroides* are closely associated with BAs metabolism, indicating that JNDX may further influence BAs profile in T2DM rats.

3.7 Effects of JNDX on bile acids metabolism in T2DM rats

HPLC-QQQ-MS analyzed 18 BAs, including cholic acid (CA), dihydrocaffeic acid (DHCA), glycocholic acid (GCA), and glycooursodeoxycholic acid (GUDCA), etc. in the serum of rats. The data of each group were analyzed by GraphPad Prism software, and the results are shown in [Figure 5](#). The total BAs, total primary BAs, and total secondary BAs are illustrated in [Supplementary Figure S4](#). Compared to the normal group, the contents of 6 primary BAs [CA, taurooursodeoxycholic acid (TUDCA), taurochenodeoxycholic acid (TCDCA), tauro- α -muricholic acid (T- α -MCA), tauro- β -muricholic acid (T- β -MCA), and taurocholic acid (TCA)] in the model group were significantly decreased (p < 0.05), and the secondary BAs such as deoxycholic acid (DCA) and taurodeoxycholic acid (TDCA) were also markedly reduced (p < 0.001) compared to the normal group. Besides, the primary BAs ursodeoxycholic acid (UDCA) was significantly increased (p < 0.001) and CA was remarkable decreased (p < 0.01) in

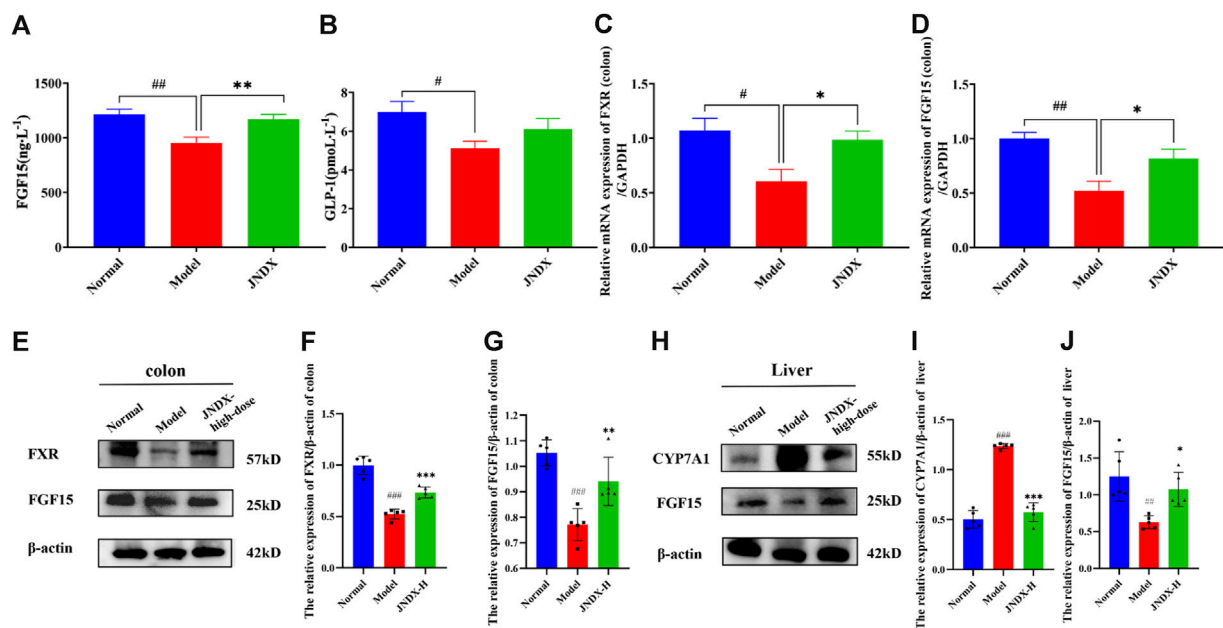


FIGURE 6 Effects of JNDX on serum FGF15 (A) and GLP-1 (B) in T2DM rats. T2DM rats were treated with JNDX to observe its impacts on the relative mRNA expression of FXR (C) and FGF15 (D), as well as FXR and FGF15 protein levels in the colon (E–G), and CYP7A1 and FGF15 protein levels in the liver (H–J). All data were represented as mean ± SD. * $p < 0.05$, ** $p < 0.01$, *** $p < 0.001$ vs the Normal group, * $p < 0.05$, ** $p < 0.01$, *** $p < 0.001$ vs the Model group.

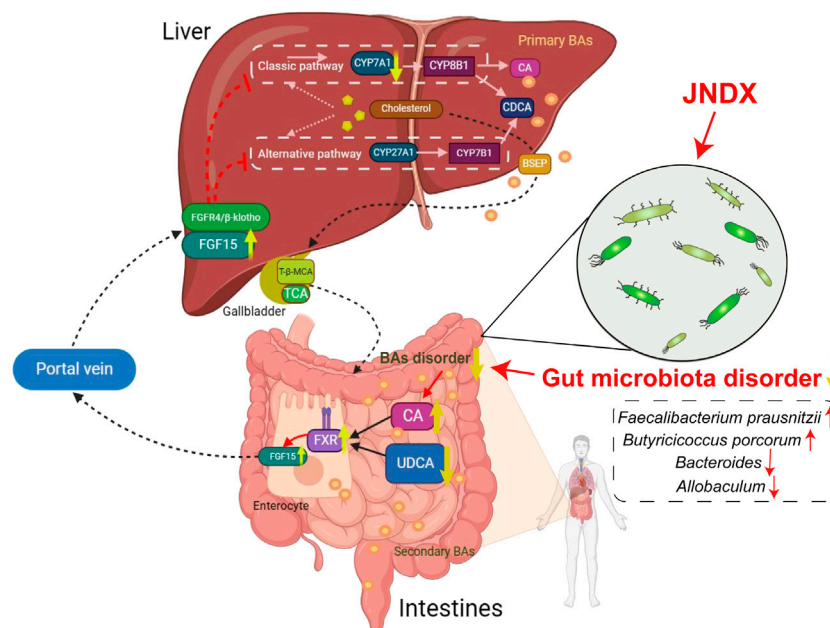


FIGURE 7 An overview diagram of the impact of JNDX on gut-liver axis and FXR/FGF15 signaling. 1) In the intestine: JNDX improves gut microbiota and bile acids metabolism (e.g., CA and UDCA) disorders, and then activates FXR, thereby promoting the production of FGF15. 2) In hepatocytes: FGF15 binds to the liver FGFR4/β-klotho receptor via the portal vein, inhibiting the generation of CYP7A1, thereby reducing BAs synthesis in the liver. CYP7A1 serves as the rate-limiting enzyme for BAs synthesis in classical way; CYP27A1 is the vital enzyme for alternative synthesis of CDCA; Primary BAs are mainly transported by BSEP to the gallbladder for storage.

comparison to those in the normal group. Nevertheless, compared with the model group, UDCA level was significantly decreased ($p < 0.001$) and CA level was

significantly increased ($p < 0.001$) observably in JNDX group. The results indicate that JNDX can affect BAs metabolism.

3.8 Effects of JNDX on the FXR-FGF15 signaling pathway in T2DM model rats

3.8.1 Effect of JNDX on serum FGF15 and GLP-1 in T2DM rats

The results showed that FGF15 and GLP-1 in model group were declined significantly ($p < 0.05$) compared with normal group. Besides, compared with model group, FGF15 was distinctly risen after 40 days of administration of JNDX ($p < 0.01$) (Figure 6A). Although there was no markedly difference in serum GLP-1 among all groups, it had some improvement effect as well (Figure 6B). The results reflect that JNDX can increase the expression of FGF15 in T2DM rats.

3.8.2 Effect of JNDX on FXR and FGF15 mRNA expression in the intestine of T2DM rats

The expression of related mRNA (FXR, FGF15) in the FXR/FGF15 pathway was detected by RT-qPCR. we found that the mRNA levels of FXR and FGF15 in the colon of the model group were significantly reduced ($p < 0.05$) compared with the normal group. After 40 days of JNDX intervention, the levels of FXR and FGF15 were upregulated ($p < 0.05$) (Figures 6C, D). The results show that JNDX can increase the relative mRNA expression of FXR and FGF15 in intestinal with T2DM rats.

3.8.3 Effect of JNDX on FXR/FGF15 pathway related protein expression in intestine and liver of T2DM rats

FXR was a key receptor for BAs. It was highly expressed in the liver and intestines. Notably, activating intestinal FXR, which was once speculated to be a helpful therapy, treats metabolic diseases. In our study, we detected FXR and FGF15 proteins in rat's colon and CYP7A1 and FGF15 proteins in rat's liver in the FXR/FGF15 pathway. The results showed that in the model group, the levels of FXR and FGF15 in T2DM rat were remarkable reduction, whereas the expression of CYP7A1 was observably increased compared with the normal group ($p < 0.001$). After intervening of high dose JNDX, the levels of FXR and FGF15 were increased ($p < 0.01$) (Figures 6E–G, J) and CYP7A1 was downregulated in comparison to those in the model group ($p < 0.001$) (Figures 6H, I). These results reveal that JNDX ameliorates the symptoms of T2DM rats via regulating the FXR/FGF15 signal pathway.

4 Discussion

In the present study, we successfully established a T2DM rat model by combining HFD and STZ (45 mg/kg), and the results showed that the T2DM model group had obvious characteristics of higher blood lipids and blood glucose compared to normal group. In addition, the elevated levels of FBG, GSP, HOMA-IR, ISI, TG, TC, LDL-C, LPS, TNF- α , IL-1 β , and IL-6 indicated increased insulin resistance, decreased insulin sensitivity, and increased inflammation in T2DM rats. Furthermore, the BAs profile and gut microbiota of T2DM rats were significantly disturbed. We subsequently found a decrease in the protein and mRNA expressions of FXR (colon) and FGF15 (colon, liver), while the protein level of CYP7A1 (liver) increased in T2DM rats. Interestingly, these indicators were reversed after taking JNDX.

T2DM is a chronic condition that affects the way your body processes blood glucose. Insulin is a hormone produced by the pancreas that helps glucose from food enter the body's cells to be used for energy. When people have T2DM, their bodies either resist the effects of insulin or do not produce enough insulin to maintain normal glucose levels. As a result, glucose accumulates in the bloodstream instead of being used for energy, leading to high blood sugar levels (Al-kuraishy et al., 2023). The general treatment for T2DM may include oral medications, insulin therapy, and lifestyle modifications. Metformin, tolbutamide and GLP-1 agonists (e.g., exenatide and repaglinide) are employed in reducing the hyperglycemia at present (Uppal et al., 2018). Nevertheless, these drugs will produce some adverse reactions, such as vomiting, headache, and diarrhea (Doyle and Egan, 2007). Traditional herbal medicine has been used to treat diabetes for many years, and the advantage of it lies in its comprehensive use of various ingredients and effects of herbs, focusing on the overall balance and individual treatment. Importantly, traditional herbs are highly regarded for their low side effects and good efficacy, making them a preferred choice for treating diabetes compared to other anti-diabetic drugs (Li et al., 2021). Hence, it is meaningful to study the anti-diabetic effect and mechanism of traditional Tibetan medicine.

In recent years, research on Tibetan medicine for the treatment of diabetes has gradually received attention. Diabetes is a modern medical term, which in Tibetan medical theory, can be classified as a “Jing Ni Sa Ku” (གཞི་ནི་ས་ཀུ་ཤིང་རྩ་ལྷན་པོ་ནད་པོ་) disease. The diagnosis of T2DM in the “Four Medical Classics” divides diabetes into three major types and a total of 20 subtypes based on the color, odor, and nature of urine (four types of Long རྩ་ལྷན་པོ་, six types of Chiba རྩ་ལྷན་པོ་, and ten types of Peigen པེ་གེན་པོ་) (Zhong, 2014). Currently, some Tibetan medicinal materials and compound preparations have been studied and used for the prevention and treatment of T2DM and its complications, such as JNDX. As a hospital preparation, the clinical function of JNDX has been shown to be effective. Moreover, in our previous research, we investigated the chemical composition and quality criteria of JNDX, and predicted its therapeutic target for T2DM through network pharmacology (Peng et al., 2022; Luo et al., 2022a; Li et al., 2015). However, the possible mechanisms of JNDX treating T2DM have not yet been explored. Hence, we established a T2DM rat model to investigate the underlying mechanisms of JNDX *in vivo*.

The commonly used method for modeling T2DM in male rats involves inducing insulin resistance through a HFD and subsequently impairing pancreatic β -cell function by injecting a small dose of STZ (Skovso, 2014). This model has been noted for its effective and economic advantages (Ghasemi et al., 2014). In this study, the T2DM rats consistently showed FBG levels exceeding 11.0 mmol/L, along with typical diabetic symptoms such as polyphagia, polydipsia, and polyuria throughout the modeling period. Furthermore, many clinical studies have observed elevated levels of inflammatory mediators in the blood circulation of T2DM patients (Huang et al., 2022). Therefore, T2DM is closely associated with hyperglycemia, hyperlipidemia, and inflammation. We detected the levels of FBG, GSP, HOMA-IR, ISI, TG, TC, LDL-C, HDL-C, LPS, TNF- α , IL-1 β , and IL-6 to evaluate the anti-diabetic effect of JNDX. Among them, the increasing of LPS could bind with leukocytes in the bloodstream, thereby inducing the expression of pro-inflammatory cytokines TNF- α , IL-1 β , and IL-6 and resulting in inflammatory response (Guan et al., 2023). Furthermore, impaired pancreatic function in diabetic patients often leads to abnormal lipid

metabolism, so evaluating lipid parameters (TG, TC, LDL-C, and HDL-C) in T2DM patients has clinical value (Bai et al., 2021). Studies have indicated that the levels of TG, TC, and LDL-C in diabetic patients are higher than those in non-diabetic individuals, while the level of HDL-C is lower (Zhou et al., 2023). Therefore, reducing blood glucose, blood lipid levels, and inflammation is a beneficial approach to improving T2DM.

In the present study, gut microbiota dysbiosis is significantly improved in T2DM rats after 40 days of JNDX administration, including increased relative abundance of *Butyricoccus* and *F. prausnitzii*, and decreased relative abundance of *Allobaculum* and *Bacteroides*. Among them, *F. prausnitzii* is a well-known bacterium that produces butyrate, and the production of butyrate contributes to maintaining gut health (Heinken et al., 2014). Besides, a study has found the similar results that some traditional Chinese herbal formulas rich in *F. prausnitzii* have the potential to alleviate T2DM (Xu et al., 2015). Moreover, *Butyricoccus* is also a bacterium that produces butyrate, which has a positive effect on improving T2DM. Furthermore, in the regulation of the gut microbiota, an increase in certain harmful bacteria could aggravate gut microbiota dysbiosis. *Bacteroides* enterotype is an independent risk factor for T2DM, which attributes to elevated LPS levels leading to diminished insulin sensitivity (Wang et al., 2020). *Allobaculum* has been shown to produce trimethylamine oxide, which can not only promote fat production by inhibiting the BA-mediated hepatic FXR signaling, but also induce insulin resistance, thus impacting blood glucose homeostasis and the occurrence and development of T2DM (Chen et al., 2023). Furthermore, *Streptococcus thermophilus* MN-ZLW-002 regulates gut microbiota by adjusting the composition of BAs and reduces the levels of high lipid and glucose. (Luo et al., 2022b).

BAs have been proven to be closely associated with T2DM. Our study demonstrates that JNDX can improve BAs disorder in T2DM rats. In addition, BAs can ameliorate the T2DM symptoms by relieving inflammatory response, promoting insulin secretion, relieving endoplasmic reticulum stress, and inhibiting insulin resistance (Staley et al., 2017; Maghsoodi et al., 2019). BAs are classified into primary and secondary BAs based on their origins. CA and chenodeoxycholic acid (CDCA), the primary BAs, are general synthesized in the human liver. It is noteworthy that bile salt hydrolase (BSH) enzymatically converts primary conjugated BAs into unconjugated BAs. Subsequently, through epimerization, UDCA is generated, followed by the formation of secondary BAs through hydroxylation catalyzed by 7 α -hydroxylase. Secondary BAs such as DCA and lithocholic acid (LCA) are produced in the human body. Nevertheless, in rodents, secondary BAs can be generated including DCA and LCA (Xiang et al., 2021). Primary and secondary BAs together constitute the bile acid spectrum (Prawitt et al., 2011; Zhao et al., 2020). Many clinical and animal experiments have found changes in the BAs spectrum of T2DM patients and animals. The investigation demonstrates that the T2DM group showed significant changes in the content of primary BAs (e.g., CA, UDCA, and T- α -MCA) and secondary BAs (e.g., DCA, TUDCA, and TDCA), compared to the normal group (Meier, 2012; Fang et al., 2015; Wahlström et al., 2016). Additionally, CA and CDCA increase the expression of FXR receptors in liver tissue, promoting the secretion of GLP-1, which beneficially impacts glucose metabolism. By contrast, studies have noted that increased levels of most conjugated BAs (GCA, GCDCA, TCA, and

TCDCa) are associated with an increased risk of T2DM (Lu et al., 2021). Some studies have indicated that CA is an agonist of FXR, while UDCA acts as an antagonist of FXR (Du et al., 2022; Li et al., 2024). Accordingly, our research findings suggest that the elevation of CA and reduction of UDCA levels in circulating serum activate FXR expression, thereby modulating the FXR/FGF15 pathway, affecting BAs synthesis, and improving T2DM.

Modern research has indicated that BAs regulate and activate multiple host metabolic pathways through FXR. The metabolic pathways regulated by FXR mainly include glucose, sterol metabolism, and lipid, and are believed to have the potential to improve conditions such as obesity, liver damage, and chronic inflammatory diseases (Xiang et al., 2021). Several studies have indicated that FXR activation contributes to the improvement of T2DM, and the “BAs – intestinal FXR/FGF15” signaling pathway is an important mechanism through which FXR exerts its effects. An intestinal-restricted FXR agonist (fexaramine) has been found to promote browning of mouse adipose tissue, reducing obesity, inflammation, and insulin resistance (Shapiro et al., 2018). Activation of intestinal FXR can induce the release of FGF15, which reaches liver cells via the portal vein. Then, FGF15 is bound with the liver FGF4/ β Klotho receptor, inhibiting the expression of CYP7A1, thereby suppressing the synthesis of BAs in the liver (Liu et al., 2023). The specific mechanism of anti-diabetes is shown in Figure 7. Other studies have found that FGF15/19 released from the small intestine inhibits hepatic gluconeogenesis by suppressing the CREB-PGC-1 α pathway (Potthoff et al., 2011). Furthermore, research has suggested that sleeve gastrectomy (SG) serves as a preferred surgical approach by surgeons for treating diabetes mellitus, typically ameliorating hepatic glucose metabolism and improving T2DM via the intestinal-liver crosstalk mediated by FGF15. Following SG, there is an elevation in BAs, which can activate the FXR/FGF15 pathway and then specifically stimulate hepatic FGF4 and its corresponding signaling pathways, promoting hepatic glycogen synthesis, and inhibiting gluconeogenesis (Wei et al., 2023).

This study indicates that JNDX noticeably improves the dysbiosis of gut microbiota and affects BAs (CA and UDCA) metabolism in T2DM rats, both of which have been shown in modern research to activate the “BAs–FXR/FGF15” pathway, thereby improving T2DM. A study has also indicated that increased expression of FXR and FGF15 in the intestine, along with decreased expression of CYP7A1 in the liver, contributed to treating T2DM in rats (Tawulie et al., 2023), which was consistent with the findings of this research. In conclusion, this study reasonably confirms that JNDX treatment for T2DM can exert its effects by regulating the BAs metabolism and FXR/FGF15 signaling.

5 Conclusion

Our study firstly explored the potential mechanisms of JNDX in improving T2DM *in vivo*. The results showed that JNDX could effectively improve insulin resistance, hyperglycemia, hyperlipidemia, and inflammation in T2DM rats. Additionally, the protein and mRNA levels of FXR and FGF15 increased after JNDX treatment, while the expression of CYP7A1 decreased. These results suggest that the mechanism by which JNDX ameliorates T2DM may be related to

its improvement of BAs metabolic disorders and activation of FXR/FGF15 pathway. Our findings contribute to a better understanding of the therapeutic effect of JNDX on T2DM and provide a scientific basis for its clinical application and drug development.

Data availability statement

The data presented in the study are deposited in the NCBI repository (<https://www.ncbi.nlm.nih.gov/>), accession number PRJNA1110576.

Ethics statement

The animal study was approved by Chengdu University of Traditional Chinese Medicine's Animal Ethics Committee. The study was conducted in accordance with the local legislation and institutional requirements.

Author contributions

YT: Writing—original draft, Writing—review and editing, Investigation, Visualization. FP: Investigation, Writing—review and editing, Conceptualization, Methodology, Validation. LW: Writing—original draft, Visualization. JS: Resources, Writing—review and editing. YD: Writing—review and editing, Visualization. SX: Writing—review and editing, Data curation. UT: Conceptualization, Project administration, Writing—review and editing. M: Supervision, Writing—review and editing. TN: Funding acquisition, Supervision, Writing—review and editing. GF: Conceptualization, Funding acquisition, Project administration, Supervision, Writing—original draft, Writing—review and editing.

References

- Al-kuraishy, H. M., Al-Gareeb, A. I., Saad, H. M., and Batiha, G. E.-S. (2023). The potential effect of metformin on fibroblast growth factor 21 in type 2 diabetes mellitus (T2DM). *Inflammopharmacology* 31, 1751–1760. doi:10.1007/s10787-023-01255-4
- Bai, Y., Wang, S., and Li, G. (2021). To explore the level of serum lipid test in diabetic obese patients and its clinical application value. *Health Everyone* 20, 86–87.
- Buchfink, B., Xie, C., and Huson, D. H. (2015). Fast and sensitive protein alignment using DIAMOND. *Nat. Methods* 12, 59–60. doi:10.1038/nmeth.3176
- Chen, Q. (2006) *Research methods in pharmacology of Chinese materia medica*. Beijing: People's Medical Publishing House.
- Chen, X. L., Cai, K., Zhang, W., Su, S. L., Zhao, L. H., Qiu, L. P., et al. (2023). Bear bile powder ameliorates type 2 diabetes via modulation of metabolic profiles, gut microbiota, and metabolites. *Front. Pharmacol.* 13, 1090955. doi:10.3389/fphar.2022.1090955
- Chiang, J. Y. L. (2013). "Bile acid metabolism and signaling." in *Comprehensive physiology*. Editor R. Terjung (Hoboken, New Jersey, United States: Wiley), 1191–1212. doi:10.1002/cphy.c120023
- Doyle, M. E., and Egan, J. M. (2007). Mechanisms of action of glucagon-like peptide 1 in the pancreas. *Pharmacol. Ther.* 113, 546–593. doi:10.1016/j.pharmthera.2006.11.007
- Du, L., Li, Q., Yi, H., Kuang, T., Tang, Y., and Fan, G. (2022). Gut microbiota-derived metabolites as key actors in type 2 diabetes mellitus. *Biomed. Pharmacother.* 149, 112839. doi:10.1016/j.biopha.2022.112839
- Fang, S., Suh, J. M., Reilly, S. M., Yu, E., Osborn, O., Lackey, D., et al. (2015). Intestinal FXR agonism promotes adipose tissue browning and reduces obesity and insulin resistance. *Nat. Med.* 21, 159–165. doi:10.1038/nm.3760
- Ghasemi, A., Khalifi, S., and Jedi, S. (2014). Streptozotocin-nicotinamide-induced rat model of type 2 diabetes (review). *Acta Physiol. hung.* 101, 408–420. doi:10.1556/APHysiol.101.2014.4.2
- Guan, Q., Jiang, X., and Li, X. (2023). Effect of potentilla anserina polysaccharide on inflammatory response and apoptosis of cardiomyocytes induced by LPS by regulating expression of miR-421. *Chin. J. Immunol.* 39, 81–85. doi:10.3969/j.issn.1000-484X.2023.01.015
- Guo, X., Okpara, E. S., Hu, W., Yan, C., Wang, Y., Liang, Q., et al. (2022). Interactive relationships between intestinal flora and bile acids. *Int. J. Mol. Sci.* 23, 8343. doi:10.3390/ijms23158343
- Heinken, A., Khan, M. T., Paglia, G., Rodionov, D. A., Harmsen, H. J., and Thiele, I. (2014). Functional metabolic map of *Faecalibacterium prausnitzii*, a beneficial human gut microbe. *J. Bacteriol.* 196, 3289–3302. doi:10.1128/JB.01780-14
- Huang, H., Zhu, L., and Hu, H. (2022). Effect of sitagliptin on blood glucose level, islet function and inflammatory response in patients with T2DM. *Smart Healthc.* 8, 87–89. doi:10.19335/j.cnki.2096-1219.2022.14.030
- Kanehisa, M., Goto, S., Hattori, M., Aoki-Kinoshita, K. F., Itoh, M., Kawashima, S., et al. (2006). From genomics to chemical genomics: new developments in KEGG. *Nucleic Acids Res.* 34, D354–D357. doi:10.1093/nar/gkj102
- Kanehisa, M., Goto, S., Sato, Y., Kawashima, M., Furumichi, M., and Tanabe, M. (2014). Data, information, knowledge and principle: back to metabolism in KEGG. *Nucleic Acids Res.* 42, D199–D205. doi:10.1093/nar/gkt1076
- Kuipers, F., Bloks, V. W., and Groen, A. K. (2014). Beyond intestinal soap—bile acids in metabolic control. *Nat. Rev. Endocrinol.* 10, 488–498. doi:10.1038/nrendo.2014.60

Funding

The author(s) declare that financial support was received for the research, authorship, and/or publication of this article. The work was supported by the financial support from the Key Research and Development Program of Sichuan Province (No. 2022YFS0434), the Research Funding Project for Constructing and Training Doctoral Program of Traditional Chinese Medicine (Tibetan Medicine) in 2023 (Nos BSDJS-23-11 and BSDJS-23-01), and the National Key Research and Development Program of China (Nos 2023YFC3504400 and 2023YFC3504403).

Conflict of interest

The authors declare that the research was conducted in the absence of any commercial or financial relationships that could be construed as a potential conflict of interest.

Publisher's note

All claims expressed in this article are solely those of the authors and do not necessarily represent those of their affiliated organizations, or those of the publisher, the editors and the reviewers. Any product that may be evaluated in this article, or claim that may be made by its manufacturer, is not guaranteed or endorsed by the publisher.

Supplementary material

The Supplementary Material for this article can be found online at: <https://www.frontiersin.org/articles/10.3389/fphar.2024.1383896/full#supplementary-material>

- Li, M., Ding, L., Hu, Y.-L., Qin, L.-L., Wu, Y., Liu, W., et al. (2021). Herbal formula LLKL ameliorates hyperglycaemia, modulates the gut microbiota and regulates the gut-liver axis in Zucker diabetic fatty rats. *J. Cell. Mol. Med.* 25, 367–382. doi:10.1111/jcmm.16084
- Li, T., Ding, N., Guo, H., Hua, R., Lin, Z., Tian, H., et al. (2024). A gut microbiota-bile acid axis promotes intestinal homeostasis upon aspirin-mediated damage. *Cell Host Microbe* 32, 191–208.e9. doi:10.1016/j.chom.2023.12.015
- Li, Y., Xiong, G., Lv, X., Wu, J., Duan, L., Fan, G., et al. (2015). Study on quality standard of Tibetan medicine *Ji-Ni De-Xie*. *World Sci. Technology/Modernization Traditional Chin. Med. Materia Medica* 17, 1551–1555. doi:10.11842/wst.2015.07.036
- Liu, F., Yao, Y., Wang, Q., Zhang, F., Wang, M., Zhu, C., et al. (2023). Nigakionone alleviates DSS-induced experimental colitis via regulating bile acid profile and FXR/NLRP3 signaling pathways. *Phytother. Res. PTR* 37, 15–34. doi:10.1002/ptr.7588
- Liu, Y. (2018). Research progress on treatment of diabetes with Tibetan medicine Lvluo-hua. *Plateau Sci. Res.* 2 (03), 69–75. doi:10.16249/j.cnki.2096-4617.2018.03.011
- Lkhagva, E., Chung, H. J., Ahn, J. S., and Hong, S. T. (2021). Host factors affect the gut microbiome more significantly than diet shift. *Microorganisms* 9, 2520. doi:10.3390/microorganisms9122520
- Lu, J., Wang, S., Li, M., Gao, Z., Xu, Y., Zhao, X., et al. (2021). Association of serum bile acids profile and pathway dysregulation with the risk of developing diabetes among normoglycemic Chinese adults: findings from the 4C study. *Diabetes Care* 44, 499–510. doi:10.2337/dc20-0884
- Luo, Y., Cheng, R., Liang, H., Miao, Z., Wang, J., Zhou, Q., et al. (2022b). Influence of high-fat diet on host animal health via bile acid metabolism and benefits of oral-fed *Streptococcus thermophilus* MN-ZLW-002. *Exp. Anim.* 71, 468–480. doi:10.1538/expanim.21-0182
- Luo, Y., Zeng, Y., Peng, J., Xu, X., Zhang, K., Yu, J., et al. (2022a). Chemical composition analysis of Tibetan medicine *Ji-ni-de-xie* based on UPLC-Q-Executive Orbitrap MS technology. *Chin. J. New Drugs* 31, 1727–1735.
- Maghsoodi, N., Shaw, N., Cross, G. F., Alaghband-Zadeh, J., Wierzbicki, A. S., Pinkney, J., et al. (2019). Bile acid metabolism is altered in those with insulin resistance after gestational diabetes mellitus. *Clin. Biochem.* 64, 12–17. doi:10.1016/j.clinbiochem.2018.11.016
- Magliano, D. J., Boyko, E. J., and Committee, I. D. A. (2021). IDF DIABETES ATLAS. Available at: <https://www.ncbi.nlm.nih.gov/books/NBK581934/> (Accessed January 7, 2024).
- Meier, J. J. (2012). GLP-1 receptor agonists for individualized treatment of type 2 diabetes mellitus. *Nat. Rev. Endocrinol.* 8, 728–742. doi:10.1038/nrendo.2012.140
- Meiring, S., Meessen, E. C. E., van Baar, A. C. G., Holleman, F., Nieuwdorp, M., Olde Damink, S. W., et al. (2022). Duodenal mucosal resurfacing with a GLP-1 receptor agonist increases postprandial unconjugated bile acids in patients with insulin-dependent type 2 diabetes. *Am. J. Physiol. Endocrinol. Metab.* 322, E132–E140. doi:10.1152/ajpendo.00337.2021
- Peng, F., Peng, J., Zhang, K., Luo, Y., Zhao, Z., and Fan, G. (2022). Study on the mechanism of Tibetan medicine *Ji Ni De Xie* in the treatment of type II diabetes mellitus based on network pharmacology and molecular docking. *Pharm. Clin. Chin. Materia Medica* 13, 51–56.
- Potthoff, M. J., Boney-Montoya, J., Choi, M., He, T., Sunny, N. E., Satapati, S., et al. (2011). FGF15/19 regulates hepatic glucose metabolism by inhibiting the CREB-PGC-1 α pathway. *Cell Metab.* 13, 729–738. doi:10.1016/j.cmet.2011.03.019
- Prawitt, J., Caron, S., and Staels, B. (2011). Bile acid metabolism and the pathogenesis of type 2 diabetes. *Curr. Diab. Rep.* 11, 160–166. doi:10.1007/s11892-011-0187-x
- Segata, N., Izard, J., Waldron, L., Gevers, D., Miropolsky, L., Garrett, W. S., et al. (2011). Metagenomic biomarker discovery and explanation. *Genome Biol.* 12, R60. doi:10.1186/gb-2011-12-6-r60
- Shapiro, H., Kolodziejczyk, A. A., Halstuch, D., and Elinav, E. (2018). Bile acids in glucose metabolism in health and disease. *J. Exp. Med.* 215, 383–396. doi:10.1084/jem.20171965
- Skovso, S. (2014). Modeling type 2 diabetes in rats using high fat diet and streptozotocin. *J. Diabetes Investig.* 5, 349–358. doi:10.1111/jdi.12235
- Staley, C., Weingarden, A. R., Khoruts, A., and Sadowsky, M. J. (2017). Interaction of gut microbiota with bile acid metabolism and its influence on disease states. *Appl. Microbiol. Biotechnol.* 101, 47–64. doi:10.1007/s00253-016-8006-6
- Su, J., Tao, Y., Liu, J., Sun, J., Zeng, Y., Meng, X., et al. (2023). Tibetan medicine *Qi-Sai-Er-Sang-Dang-Song* Decoction inhibits TNF- α -induced rheumatoid arthritis in human fibroblast-like synoviocytes via regulating NOTCH1/NF- κ B/NLRP3 pathway. *J. Ethnopharmacol.* 310, 116402. doi:10.1016/j.jep.2023.116402
- Tawulie, D., Jin, L., Shang, X., Li, Y., Sun, L., Xie, H., et al. (2023). Jiang-Tang-San-Huang pill alleviates type 2 diabetes mellitus through modulating the gut microbiota and bile acids metabolism. *Phytomedicine* 113, 154733. doi:10.1016/j.phymed.2023.154733
- Uppal, S., Italiya, K. S., Chitkara, D., and Mittal, A. (2018). Nanoparticle-based drug delivery systems for small molecule anti-diabetic drugs: an emerging paradigm for effective therapy. *Acta Biomater.* 81, 20–42. doi:10.1016/j.actbio.2018.09.049
- Wahlström, A., Sayin, S. I., Marschall, H.-U., and Bäckhed, F. (2016). Intestinal crosstalk between bile acids and microbiota and its impact on host metabolism. *Cell Metab.* 24, 41–50. doi:10.1016/j.cmet.2016.05.005
- Wang, J., Li, W., Wang, C., Wang, L., He, T., Hu, H., et al. (2020). Enterotype Bacteroides is associated with a high risk in patients with diabetes: a pilot study. *J. Diabetes Res.* 2020, 6047145. doi:10.1155/2020/6047145
- Wei, M., Cao, W.-B., Zhao, R.-D., Sun, D.-P., Liang, Y.-Z., Huang, Y.-D., et al. (2023). Fibroblast growth factor 15, induced by elevated bile acids, mediates the improvement of hepatic glucose metabolism after sleeve gastrectomy. *World J. Gastroenterol.* 29, 3280–3291. doi:10.3748/wjg.v29.i21.3280
- Wu, J., Yang, K., Fan, H., Wei, M., and Xiong, Q. (2023). Targeting the gut microbiota and its metabolites for type 2 diabetes mellitus. *Front. Endocrinol.* 14, 1114424. doi:10.3389/fendo.2023.1114424
- Wu, L., Gao, Y., Su, Y., Li, J., Ren, W. C., Wang, Q. H., et al. (2022). Probiotics with anti-type 2 diabetes mellitus properties: targets of polysaccharides from traditional Chinese medicine. *Chin. J. Nat. Med.* 20, 641–655. doi:10.1016/S1875-5364(22)60210-3
- Xiang, J., Zhang, Z., Xie, H., Zhang, C., Bai, Y., Cao, H., et al. (2021). Effect of different bile acids on the intestine through enterohepatic circulation based on FXR. *Gut Microbes* 13, 1949095. doi:10.1080/19490976.2021.1949095
- Xu, J., Lian, F., Zhao, L., Zhao, Y., Chen, X., Zhang, X., et al. (2015). Structural modulation of gut microbiota during alleviation of type 2 diabetes with a Chinese herbal formula. *ISME J.* 9, 552–562. doi:10.1038/ismej.2014.177
- Xu, T., Ge, Y., Du, H., Li, Q., Xu, X., Yi, H., et al. (2021). Berberis kansuensis extract alleviates type 2 diabetes in rats by regulating gut microbiota composition. *J. Ethnopharmacol.* 273, 113995. doi:10.1016/j.jep.2021.113995
- Yan, X., Zhang, Y., Peng, Y., and Li, X. (2022). The water extract of *Radix scutellariae*, its total flavonoids and baicalin inhibited CYP7A1 expression, improved bile acid, and glycolipid metabolism in T2DM mice. *J. Ethnopharmacol.* 293, 115238. doi:10.1016/j.jep.2022.115238
- Yi, H. (2022) *Pharmacodynamics of Tibetan medicine eight flavors of berberis jamesiana forest capsule in the treatment of type 2 diabetes*. dissertation/master's thesis. Chengdu, Sichuan: Chengdu University of Traditional Chinese Medicine.
- Zhang, Y., Han, S., Liu, C., Zheng, Y., Li, H., Gao, F., et al. (2023). THADA inhibition in mice protects against type 2 diabetes mellitus by improving pancreatic β -cell function and preserving β -cell mass. *Nat. Commun.* 14, 1020. doi:10.1038/s41467-023-36680-0
- Zhao, L., Lou, H., Peng, Y., Chen, S., Fan, L., and Li, X. (2020). Elevated levels of circulating short-chain fatty acids and bile acids in type 2 diabetes are linked to gut barrier disruption and disordered gut microbiota. *Diabetes Res. Clin. Pract.* 169, 108418. doi:10.1016/j.diabres.2020.108418
- Zhao, T., Wang, J., He, A., Wang, S., Chen, Y., Lu, J., et al. (2021). Mebhydrolin ameliorates glucose homeostasis in type 2 diabetic mice by functioning as a selective FXR antagonist. *Metabolism* 119, 154771. doi:10.1016/j.metabol.2021.154771
- Zheng, L., Wang, G., and Wu, Q. (2021). Effect of Eighteen Flavor Myrobalan Diuretic pills on the signaling pathway RAGE-NF- κ B in renal tissues of male rats with diabetic nephropathy. *Chin. high Alt. Med. Biol.* 42, 120–125. doi:10.13452/j.cnki.jqmc.2021.02.008
- Zhong, G. (2014). Analysis of Tibetan Medicine's understanding and treatment of type 2 diabetes. *China Tibetol.* 2, 152–155.
- Zhou, S., Xu, H., Zhu, J., Fan, X., and Zhang, J. (2023). Clinical efficacy and metabolomics study of Wendan Decoction in the treatment of phlegm-dampness obstructive sleep apnea-hypopnea syndrome with type 2 diabetes mellitus. *J. Ethnopharmacol.* 317, 116775. doi:10.1016/j.jep.2023.116775

Glossary

BAs	bile acids	TNF-α	tumor necrosis factor-α
BSA	bovine serum albumin	TUDCA	tauroursodeoxycholic acid
BSH	bile salt hydrolase	T-α-MCA	tauro-α-muricholic acid
CA	cholic acid	T-β-MCA	tauro-β-muricholic acid
CYP7A1	Cholesterol 7α hydroxylase	UDCA	ursodeoxycholic acid
DCA	deoxycholic acid	UPLC-Q-Exactive Orbitrap MS	ultra high performance liquid chromatography with four stage rod/electrostatic field orbital trap high resolution mass spectrometry
DHCA	dihydrocaffeic acid		
ELISA	enzyme-linked immunosorbent assay		
FBG	fasting blood-glucose		
FGF15	fibroblast growth factor 15		
FXR	farnesol X receptor		
GCA	glycocholic acid		
GLP-1	glucagon-like peptide 1		
GSP	glycosylated serum protein		
GUDCA	glycoursodeoxycholic acid		
HDL-C	high-density lipoprotein cholesterol		
HFD	high-fat diet		
HOMA-IR	ho-meostasis model assessment of insulin resistance		
HPLC-QQ-MS	high-performance liquid chromatography-triple quadrupole mass spectrometry		
IL-1β	interleukin-1β		
IL-6	interleukin-6		
Ins	insulin		
ISI	insulin sensitivity index		
JNDX	Ji-Ni-De-Xie		
LCA	lithocholic acid		
LDL-C	low-density lipoprotein cholesterol		
LPS	lipopolysaccharide		
mRNA	messenger RNA		
PVDF	polyvinylidene difluoride		
RT-qPCR	real-time quantitative polymerase chain reaction		
SD	Sprague-Dawley		
SG	sleeve gastrectomy		
STZ	streptozotocin		
T2DM	type 2 diabetes mellitu		
TBST	Tris Buffered Saline with Tween 20		
TC	total cholesterol		
TCA	taurocholic acid		
TCDCa	taurochenodeoxycholic acid		
TDCA	taurodeoxycholic acid		
TG	triglyceride		



OPEN ACCESS

EDITED BY

Stalin Antony,
University of Electronic Science and
Technology of China, China

REVIEWED BY

Wang Lingchong,
Nanjing University of Chinese Medicine, China
Wonhyo Seo,
Ewha Womans University, Republic of Korea
Young-Sun Lee,
Korea University, Republic of Korea

*CORRESPONDENCE

Tom Ryu,
✉ tomryu1@schmc.ac.kr
Beom Sun Chung,
✉ bschung@yonsei.ac.kr

RECEIVED 30 January 2024

ACCEPTED 11 June 2024

PUBLISHED 28 June 2024

CITATION

Yang K, Ryu T and Chung BS (2024), Psyllium
fiber improves hangovers and inflammatory
liver injury by inhibiting intestinal drinking.
Front. Pharmacol. 15:1378653.
doi: 10.3389/fphar.2024.1378653

COPYRIGHT

© 2024 Yang, Ryu and Chung. This is an open-
access article distributed under the terms of the
[Creative Commons Attribution License \(CC BY\)](https://creativecommons.org/licenses/by/4.0/).
The use, distribution or reproduction in other
forums is permitted, provided the original
author(s) and the copyright owner(s) are
credited and that the original publication in this
journal is cited, in accordance with accepted
academic practice. No use, distribution or
reproduction is permitted which does not
comply with these terms.

Psyllium fiber improves hangovers and inflammatory liver injury by inhibiting intestinal drinking

Keungmo Yang¹, Tom Ryu^{2*} and Beom Sun Chung^{3*}

¹Division of Gastroenterology and Hepatology, Department of Internal Medicine, College of Medicine, The Catholic University of Korea, Seoul, Republic of Korea, ²Department of Internal Medicine, Institute for Digestive Research, Digestive Disease Center, Soonchunhyang University College of Medicine, Seoul, Republic of Korea, ³Department of Anatomy, Yonsei University Wonju College of Medicine, Wonju, Republic of Korea

Introduction: Excessive alcohol intake often results in hangovers and inflammatory liver damage, posing a significant health concern. Current treatment options for hangovers are still insufficient, highlighting the urgent need for new therapeutic approaches. Psyllium fiber (PF) is well-known for its gastrointestinal benefits, but its effect on hangovers is less explored.

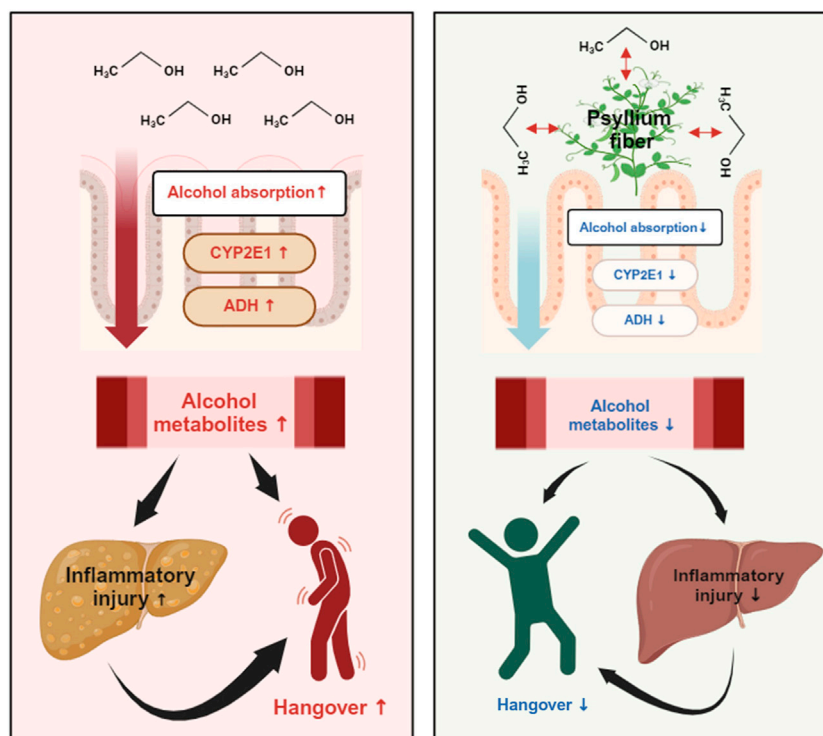
Methods: We utilized a mouse model with a single binge drinking (4 g/kg) to induce hangover and inflammatory liver injury. Intestine and liver injury were serologically and histologically estimated. Hangover symptoms were assessed using cylinder and footprint tests to objectively quantify hangover symptoms in mice.

Results: Binge drinking significantly activated alcohol-metabolizing enzymes in the small intestine and liver, leading to inflammatory damage. Concurrently, there was a rise in alcohol metabolites such as acetaldehyde and acetone, which exhibited a positive correlation with hangover symptoms in mice. Interestingly, the oral administration of PF (100 mg/kg) alongside alcohol consumption significantly reduced the activity of these enzymes and lowered the levels of alcohol metabolites. Mice treated with PF exhibited a considerable improvement in hangover symptoms and a reduction in hepatic inflammation, compared to control groups. Furthermore, *in vitro* experiments using HepG2 cell lines and semipermeable membranes demonstrated that PF effectively inhibits alcohol absorption into the body.

Discussion: In conclusion, PF demonstrates a potential protective effect against alcohol-induced hangover and liver injury by inhibiting the absorption of alcohol and lowering hangover-related alcohol metabolites. This study suggests that PF could serve as an effective therapeutic option for mitigating the adverse effects of excessive alcohol consumption.

KEYWORDS

psyllium fiber, hangover, alcohol-induced liver injury, inflammation, alcohol absorption



GRAPHICAL ABSTRACT

Graphical summary of the study.

1 Introduction

In recent years, the significant rise in chronic alcohol consumption has emerged as a major global health concern, contributing to a spectrum of alcohol-associated liver diseases including steatosis, steatohepatitis, cirrhosis, and hepatocellular carcinoma (Kim et al., 2020). Meanwhile, in the regard of acute alcohol consumption, people suffer from acute intoxication called hangover, which is characterized by an unpleasant feeling and symptoms, and it is first described by the British writer William Hickey in 1,768 as an aftermath of heavy alcohol drinking (Swift and Davidson, 1998). Although the symptoms of hangover include distress, fatigue, thirst, palpitation, tremor, sickness, diarrhea, and headache, they have interindividual variability and affect functional and psychiatric problems (Prat et al., 2009). Amount of alcohol costs is \$7.5 billion per year, and the diminished occupational productivity caused by hangover-like symptoms lost \$1.4 billion each year in Canada (Single et al., 1998). More than 1 million workdays are deleted per year due to the symptoms of hangover in Finland (Järvillehto et al., 1975). Moreover, the majority of alcohol-related workplace issues are attributed to light to moderate drinkers, with hangover being the primary morbidity rather than long-term consequences of chronic alcohol consumption, such as alcohol-associated liver diseases (Stockwell, 1998).

Physiologic mechanisms of alcohol hangover include direct effects of alcohol, and alcohol metabolism such as acetaldehyde toxicity (Swift and Davidson, 1998). Alcohol-induced diuresis by inhibiting antidiuretic hormone or vasopressin, and that leads the

body to electrolyte imbalance and dehydration (Eisenhofer et al., 1985). Additionally, alcohol itself can irritate the gastrointestinal wall and disrupt the normal gut barrier, resulting in upper abdominal pain, nausea, and vomiting (Lieber, 1995). Furthermore, vasodilation related headache could be occurred with alcohol intoxication and alteration of secretion of several neurotransmitters with alcoholic effect would be implicated in the pathogenesis of headache (Parantainen, 1983).

Alcohol is metabolized by two-step process. The first enzyme that is called alcohol dehydrogenase (ADH) changes alcohol to an acetaldehyde, then second enzyme called aldehyde dehydrogenase (ALDH) metabolizes acetaldehyde to acetic acid. The speed of conversions is controlled by the concentration of nicotinamide adenine dinucleotide. Furthermore, excessive alcohol breakdown requires cytochrome P 450 2E1 (CYP2E1) and co-factor nicotinamide adenine dinucleotide phosphate (Mackus et al., 2020). Among them, acetaldehyde, an intermediate product of alcohol metabolism, is known to causes toxic effects, including tachycardia, skin flushing, nausea and headache. Interestingly, in some people genetic variants with the ALDH enzyme release become ill after consuming small amounts of alcohol (Swift and Davidson, 1998; Brooks and Zakhari, 2014). Furthermore, alcohol withdrawal, the presence of congeners, concurrent use of other drugs, and individual differences may exacerbate hangover symptoms.

Although interventions for hangover symptoms are searched with several results in the internet, including aspirin, bananas, exercise, hair of the dog, ibuprofen, shower, and sleep, effective way to relieve hangover was not studied scientifically so far.

Recently, several interesting phytomedicinal interventions were introduced for decrease hangover feeling, and that included *Borago officinalis*, *Cynara scolymus*, *Opuntia ficus-indica* (Pittler et al., 2003; Wiese et al., 2004; Pittler et al., 2005). Nevertheless, all the compounds had insignificant efficacy for hangover relief or was not designed as a strictly controlled study (Pittler et al., 2005). Psyllium fiber consists of gel-forming arabinoxylan, a polymer rich arabinose, which is rarely digested in human gastrointestinal tract (Jalanka et al., 2019). Psyllium fiber is well-known laxatives that have capacity for effective water holding and prevent from dehydration of bowel (McRorie Jr and McKeown, 2017). This gel-forming fiber is also studied as an intervention for obesity and diabetes (Gibb et al., 2015; Gibb et al., 2023).

The study proposes that psyllium fiber, known for its hydrophilic properties and gel-forming ability, could be an effective remedy for hangovers. This hypothesis is based on the idea that psyllium fiber can influence alcohol absorption in the intestines through osmosis. Given these properties, we aim to investigate whether psyllium fiber can alleviate hangover symptoms and alcohol-induced liver injury by modulating alcohol absorption in the gut.

2 Methods

2.1 Psyllium fiber

In this experiment, a widely recognized commercial product (Whole Psyllium Husks, NOW Foods, Inc., Bloomington, IL) within its expiration date was utilized. This product contains psyllium fiber sourced from the seeds of *Plantago ovata* Forssk [Plantaginaceae]. The selection of this product was based on its extensive use and established reliability, ensuring the consistency and reproducibility of the experimental results.

2.2 Animal experiment

The Institute Animal Care and Use Committee (IACUC) in Yonsei University Wonju College of Medicine approved all animal experiments (IACUC number: YWC-230614-2). The mice were managed on the regular light-dark cycle (12 h each) in a specific pathogen-free (SPF) facility. The SPF facility's temperature and humidity were consistently maintained at around $22^{\circ}\text{C} \pm 2^{\circ}\text{C}$ and 40%–60%, respectively. Wild-type (WT) mice with C57BL/6J background were purchased from Orient Bio Inc. (Seongnam, Republic of Korea). Single binge drinking of ethanol (4 g/kg body weight) was performed to induce hangovers and inflammatory liver injury in the 8-week-old male mice. To assess the effects on hangovers, the mice were either given a vehicle or psyllium fiber (100 mg/kg) by oral gavage together with the binge drinking. The study grouped 24 mice into four different categories, with each group consisting of 6 mice per cage.

2.3 Cell culture

Human hepatocellular carcinoma cells (HepG2) were purchased from the ATCC (Manassas, VA). The standard

medium used was Dulbecco's Modified Eagle Medium (DMEM), supplemented with 10% fetal bovine serum (FBS) and antibiotics (penicillin 10,000 units/mL, streptomycin 10,000 $\mu\text{g/mL}$). The cells were cultured in 6-well plates at a density of approximately 200,000 cells per well in 2 mL of standard medium for *in vitro* experiments. This particular seeding density was chosen to ensure adequate cell-to-cell contact and optimal cell growth, while avoiding over-confluence that could lead to cellular stress and altered cellular responses. HepG2 cells were incubated at 37°C in a humidified atmosphere of 5% CO_2 to ensure optimal growth conditions.

2.4 Biochemical measurement

The mice were sacrificed after 12 h of the binge drinking, and their venous blood samples were collected in vacuum tubes containing ethylenediaminetetraacetic acid anticoagulant (V-tube, AB Medical, Republic of Korea) and centrifuged at 14,000 rpm for 5 min. The supernatant was analyzed using gas chromatography on an Agilent 7890 B Gas Chromatograph (Agilent Technologies, Santa Clara, CA, United States). The levels of alanine aminotransferase (ALT), aspartate aminotransferase (AST), triglycerides (TG), and total cholesterol (TC) were analyzed using Fuji Dry-Chem 3,500 (Fuji Film, Tokyo, Japan).

2.5 Quantitative PCR

Total RNA was isolated from either liver tissues or cells using either the RNeasy Mini Kit (Qiagen) or the TRIzol reagent (Thermo Fisher Scientific), following the manufacturer's instructions. This RNA was then uniformly reverse-transcribed into cDNA using the ReverTra Ace[®] qPCR RT Master Mix with gDNA Remover (Toyobo). For the quantitative real-time PCR (qRT-PCR), the SYBR Green Real-time PCR Master Mix (Toyobo), was employed in with Quantstudio 3 (PCR Instrument system; Thermo Fisher Scientific). To standardize the relative expression levels of each interested genes, the expression level of 18S rRNA was utilized as a reference. The detailed information of the forward and reverse primer pairs used are presented in [Supplementary Table S1](#).

2.6 Histological analyses

For uniformity in histological analysis across all samples, the same areas of the medial and left liver lobes as well as the jejunum area of the intestine were consistently collected from each mouse. The tissue samples were then fixed in 10% neutral buffered formalin (Sigma-Aldrich) for an overnight period. Following a thorough deparaffinization and rehydration process, the tissues were sectioned into 4 μm slices and subsequently stained using hematoxylin (Sigma-Aldrich) and eosin (Biognost) solutions. Imaging of the stained tissues was performed using an Olympus BX51 light microscope, and the DP2-BSW software was employed for the analysis of the captured images.

2.7 Immunostaining

Paraffin-embedded liver tissue sections from mice were used for immunostaining analysis. The process began with deparaffinization and rehydration of the samples, followed by their immersion in a 10 mM citrate buffer (pH 6.0). For antigen retrieval, the samples underwent microwave exposure for 5 min. To prevent non-specific binding, the tissues were treated with 10% donkey serum for an hour. Overnight incubation at 4°C was then carried out with primary antibodies diluted between 1:50 to 1:200 in PBS containing 0.1% Tween-20. For immunohistochemistry staining, the samples were incubated with either anti-Rabbit IgG (Vector Laboratories) or anti-Mouse IgG (Vector Laboratories) for an hour at room temperature. The DAB substrate kit (Vector Laboratories) was used to develop the further reactions, and the slides were sealed with Balsam (Sigma-Aldrich). In the case of immunofluorescent staining, the samples were treated with Alexa Fluor® 488 or Alexa Fluor® 594 conjugated secondary antibodies (Abcam) for an hour at room temperature and then covered with DAPI mounting solution (Abcam). The imaging of these samples was carried out using an Olympus BX51 microscope (Olympus, Tokyo, Japan). For image analysis, DP2-BSW software was utilized.

2.8 Western blot analyses

Proteins were extracted from tissues using RIPA lysis buffer, which includes 10% glycerol, 10% SDS, 1 mM Na₃VO₄, 1 mM PMSF, 150 mM NaCl, and 30 mM Tris (pH 7.5), along with phosphatase inhibitor and protease cocktail (Thermo Fisher Scientific). These proteins were then separated using 10% SDS-polyacrylamide gel electrophoresis. For transferring the proteins from the gel, a nitrocellulose membrane (Thermo Fisher Scientific) was utilized. After the transfer, this nitrocellulose membrane was subjected to blocking with a 5% skim milk solution for an hour at room temperature. Following this, the membranes were treated overnight at 4°C with primary antibodies diluted in PBS (1:500 to 1:2,000). On the next day, the membranes were incubated with secondary antibodies for 1 h at room temperature. The SuperSignal™ West Pico PLUS Chemiluminescent substrate (Thermo Fisher Scientific) was applied to visualize the immunoreactive bands.

2.9 Isolation of liver mononuclear cells

The liver tissues of the mice were homogenized using a 70 µm mesh filter cell strainer. This is followed by centrifugation at 40 g for 5 min to remove hepatocytes. The supernatant obtained is then washed and resuspended in 40% Percoll (GE Healthcare). This cell lysate was subsequently centrifuged at 1,400 g and 4°C for 30 min to further purify the sample. Red blood cells were lysed using an RBC lysis buffer (BioLegend). The isolated liver mononuclear cells (MNCs) were then washed in sterile PBS and their numbers were quantified.

2.10 Flow cytometry analyses

The liver mononuclear cells (MNCs) isolated from mice were initially stained with CD16/CD32 (mouse Fc blocker) (BD

Bioscience) and then with the LIVE/DEAD™ fixable aqua dead cell stain kit for 405 nm excitation (Thermo Fisher Scientific) to differentiate between living and dead cells. Subsequently, these cells were labeled with various fluorescence-tagged antibodies: eFluor 450-conjugated CD45 (Thermo Fisher Scientific), APC-Cy7-conjugated CD11b (BD Biosciences), FITC-conjugated F4/80 (eBioscience), PE-Cy7-conjugated Ly-6G (BD Biosciences), and PE-conjugated Siglec-F (BD Biosciences). The fluorescence-labeled cells were then analyzed using a FACS Aria III flow cytometer (BD Bioscience). Data regarding the proportions of neutrophils (CD11b⁺Ly6G⁺), eosinophils (CD11b⁺SiglecF⁺), and macrophages (F4/80⁺CD11b⁺) were examined using FlowJo software (FlowJo LLC) through a pseudo-color analysis plot.

2.11 Semipermeable membrane experiment

To simulate alcohol diffusion through the cell membrane, a semipermeable membrane experiment was designed. The semipermeable membrane (Innovating Science) was composed of regenerated cellulose derived from cotton linters, which are among the purest naturally occurring sources of cellulose. This membrane permits the passage of particles up to 14,000 Da. Ethanol, with a molecular weight of approximately 46 Da, was able to diffuse through the semipermeable membrane, and its concentration was measured over time. The semipermeable pocket contained 50 mL of normal saline with 5 g of psyllium fiber.

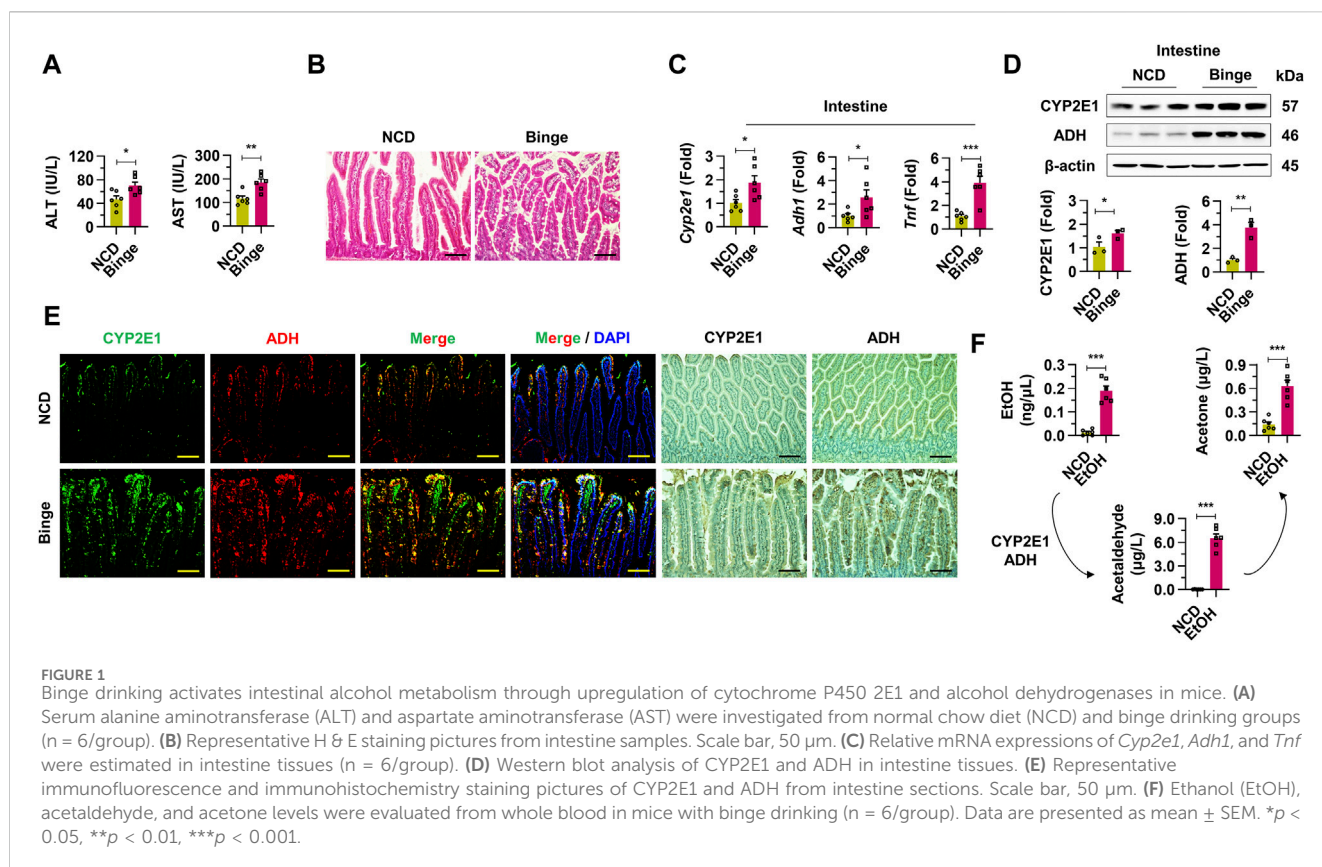
2.12 Statistical analysis

All collected data were analyzed using Prism software, version 8.0 (GraphPad Software), and are represented as mean ± SEM. In the *in vivo* experiments, any mice that experienced severe problems, such as mortality post-binge drinking, were excluded in further analysis. Statistical differences between two groups were determined using the unpaired Student's *t*-test. For comparisons involving multiple groups, One-way Analysis of Variance (ANOVA) was employed, along with *post hoc* tests like Tukey's and Dunnett's. A *p*-value of less than 0.05 was considered statistically significant.

3 Results

3.1 Binge drinking activates alcohol metabolism in intestines

In this research, we employed a binge drinking (4 g/kg body weight) model to induce hangover symptoms and alcohol-induced liver damage in mice. Compared to the normal chow diet (NCD) group, the binge drinking mice exhibited significantly elevated serum ALT and AST levels, suggesting liver damage (Figure 1A). H&E staining demonstrated epithelial cell damage and steatosis in the intestinal tissues of the binge group relative to the NCD group (Figure 1B). The mRNA expressions of Cyp2e1, Adh1, and Tnf were markedly upregulated in the intestines of the binge group (Figure 1C). Protein levels of CYP2E1 and ADH showed a substantial increase in the intestines of the binge-exposed mice,



as confirmed by Western blot analysis (Figure 1D). Similarly, enhanced expression of CYP2E1 and ADH in the intestines of the binge drinking mice was evident through immunofluorescence and immunohistochemistry staining (Figure 1E). Furthermore, elevated levels of ethanol, acetaldehyde, and acetone in the blood provided further evidence of activated alcohol metabolism following binge drinking (Figure 1F). These findings collectively indicate that binge drinking significantly induces damage to intestinal cells and activates alcohol metabolism in the intestines.

3.2 Inflammatory liver injury was induced by binge drinking

There were no significant changes in total body weight and liver to body weight ratio observed between two groups (Supplementary Figure S1A). Elevated serum triglyceride (TG) levels were observed in the binge drinking mice, while total cholesterol (TC) levels showed no significant difference when compared to the NCD group (Figure 2A; Supplementary Figure S1B). mRNA expressions of *Cyp2e1*, *Adh1*, *Tnf*, and *Il1b* were significantly upregulated in the whole liver tissues of the binge group, indicating enhanced metabolic activity (Figure 2B). Interestingly, the number of liver mononuclear cells (MNCs) significantly increased after alcohol consumption (Supplementary Figure S1C). Consistently, with alcohol administration, there was evidence of hepatocyte damage and mild steatosis around the central veins (CV) of the liver, along with activation of enzymes associated with alcohol

metabolism (Figure 2C; Supplementary Figure S1D). An increased frequency of neutrophils from hepatic MNCs in the binge group indicated an inflammatory response, while the frequency of macrophages and eosinophils showed no significant change (Figure 2D; Supplementary Figure S1E). qRT-PCR analysis further confirmed the inflammatory state with elevated expression levels of *Tnf*, *Cxcl1*, and *Il1b* in liver MNCs (Figure 2E). Taken together, these results underline the specific pathological and inflammatory effects of binge alcohol consumption on liver tissue.

3.3 Alcohol metabolites are associated with hangover symptoms in mice

In the assessment of the impact of binge drinking on behavior and metabolism, we utilized various tests. The cylinder test depicted in Figure 3A involves two positions: static and forelimb touch. Binge drinking led to a decrease in the number of touches in the cylinder test over various time points, suggesting impaired motor function (Figure 3B). Correlative analysis showed a significant negative correlation between increased alcohol metabolites and decreased motor activity in the cylinder test results (Figure 3C). The footprint test serves as another quantitative approach for objectively measuring hangover symptoms by analyzing gait changes, captured through the tracking of movements in the forelimb and hindlimb (Figure 3D). Six hours after binge drinking, the footprint test revealed specific alterations in the gait of mice, such as a reduced stride length and an increased stride width, mimicking the staggered

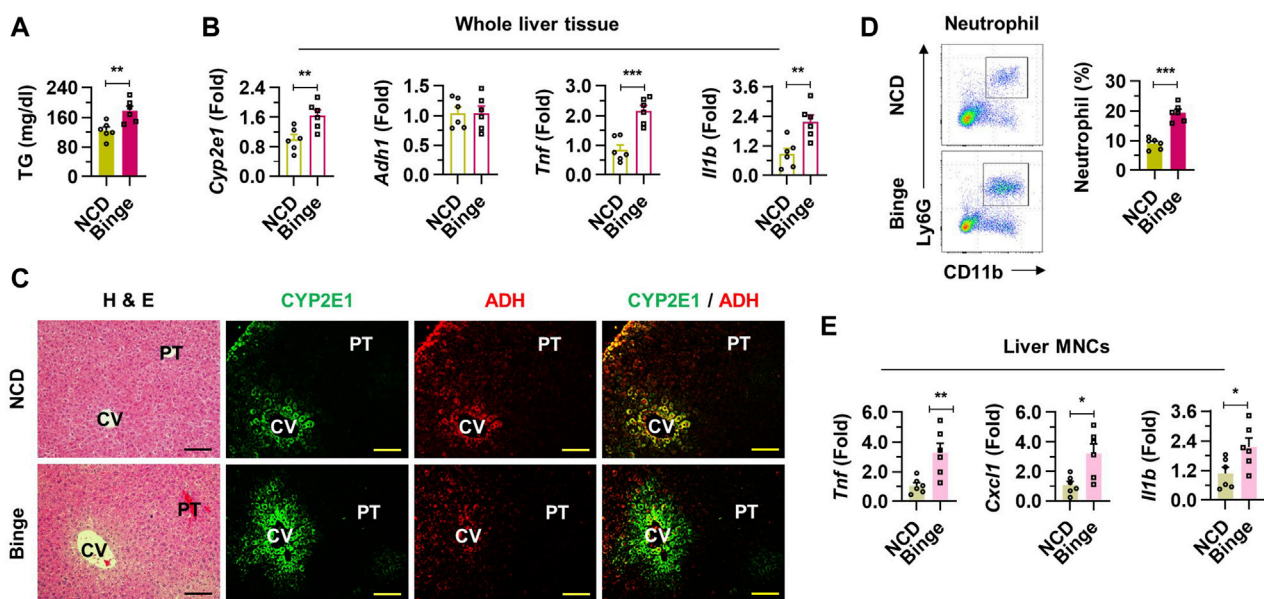


FIGURE 2

Inflammatory liver injury was induced by binge drinking in mice. **(A)** Serum triglyceride (TG) levels were measured after binge drinking ($n = 6/\text{group}$). **(B)** Relative mRNA expressions of *Cyp2e1*, *Adh1*, *Tnf*, and *Il1b* were analyzed in whole liver tissues ($n = 6/\text{group}$). **(C)** Representative H & E and immunofluorescence (CYP2E1 and ADH) staining pictures in liver sections. Central vein (CV) and portal triad (PT). Scale bar, 50 μ m. **(D)** Frequencies of neutrophils from isolated liver mononuclear cells (MNCs) were estimated by fluorescence activated cell sorting. **(E)** qRT-PCR of *Tnf*, *Cxcl1*, and *Il1b* in liver MNCs ($n = 6/\text{group}$). Data are presented as mean \pm SEM. * $p < 0.05$, ** $p < 0.01$, *** $p < 0.001$.

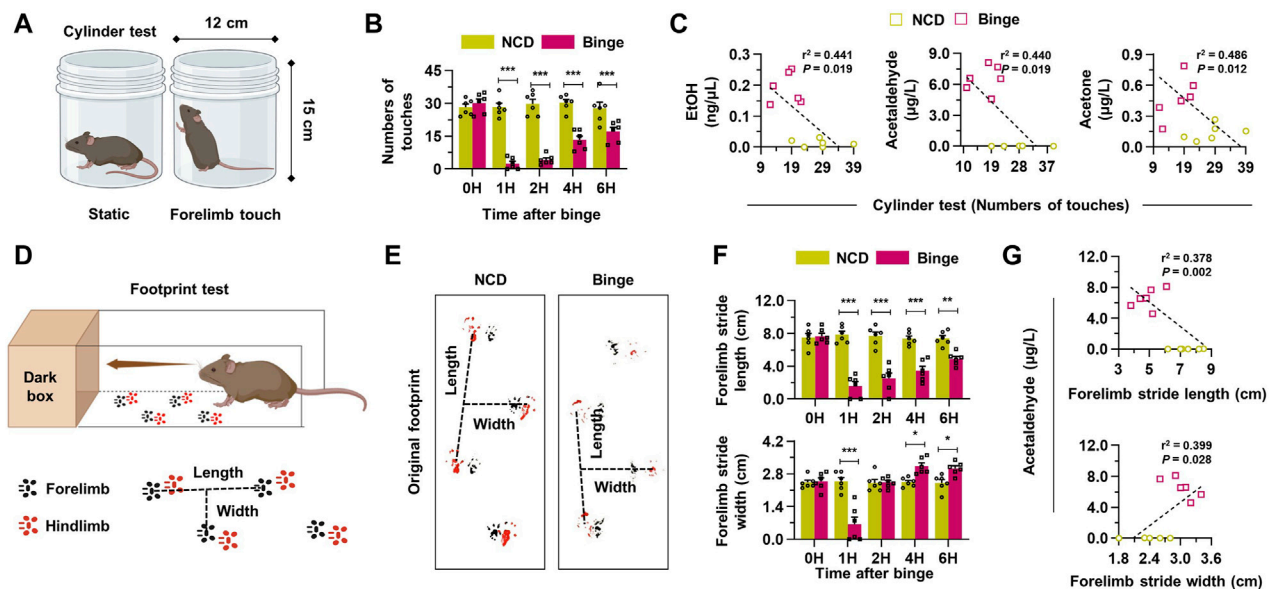
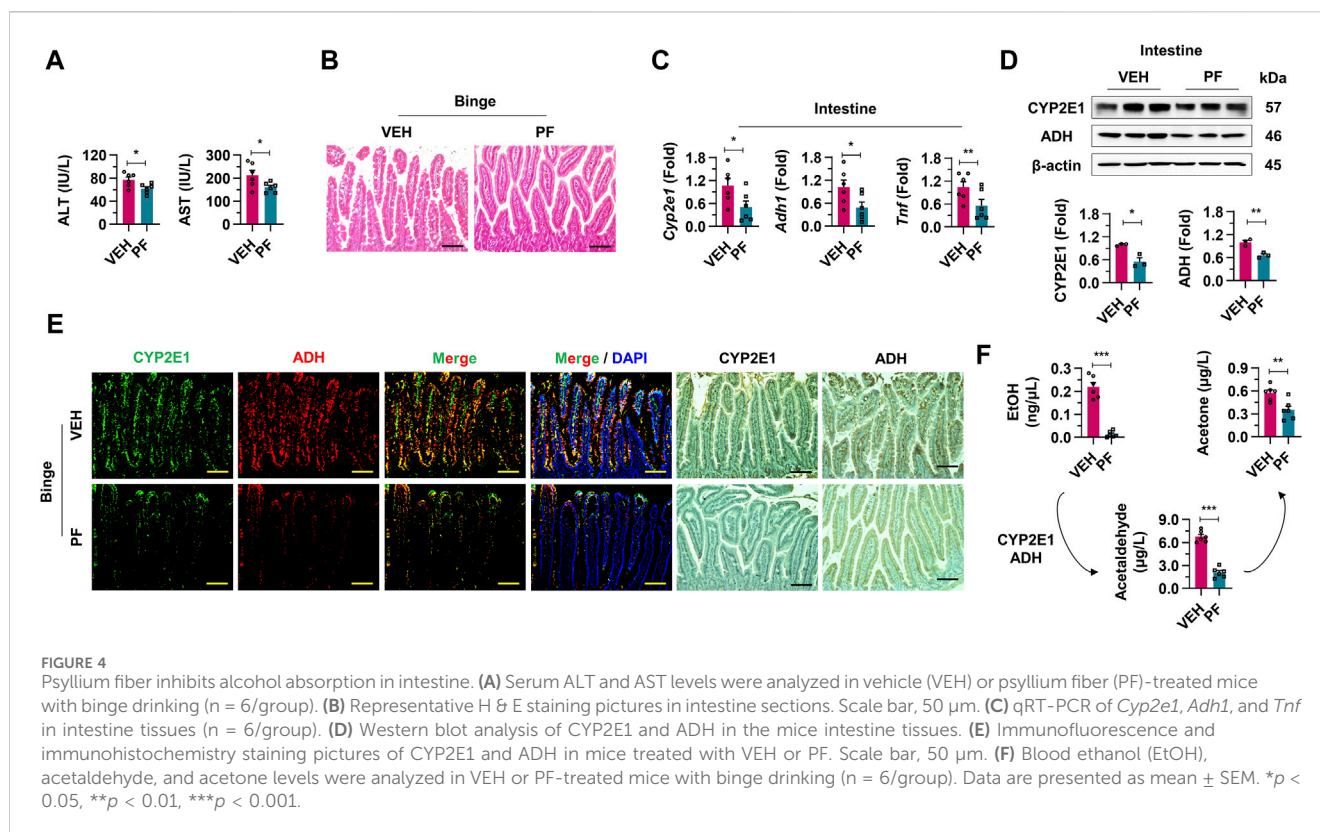


FIGURE 3

Binge drinking elevates the production of alcohol metabolites, leading to hangover behaviors. **(A)** A schematic figure of cylinder test (static position or forelimb touch) in mice. **(B)** Binge drinking leads to a decrease in the number of touches in the cylinder test at various time points ($n = 6/\text{group}$). **(C)** Correlative analysis was conducted to assess the relationship between alcohol metabolites and the results of the cylinder tests in both the NCD and binge-drinking groups ($n = 6/\text{group}$). **(D)** A diagram illustrating the footprint test in mice (black: forelimb, red: hindlimb). **(E)** Representative pictures of the footprint test taken 6 h after binge drinking. **(F)** Forelimb stride length and width according to the different time points after binge drinking ($n = 6/\text{group}$). **(G)** Correlative analysis between footprint tests and blood acetaldehyde levels ($n = 6/\text{group}$). Data are presented as mean \pm SEM. * $p < 0.05$, ** $p < 0.01$, *** $p < 0.001$.



gait commonly observed in individuals under the influence of alcohol (Figure 3E). A significant correlation was noted between forelimb stride lengths and blood alcohol metabolite levels, showing a negative relationship, while stride width displayed a positive correlation with metabolite levels, indicating significant changes in gait patterns linked to increased alcohol metabolites (Figure 3F; Supplementary Figure S2A). Similarly, the analysis of hindlimb strides also indicated results consistent with those of the forelimb, further demonstrating the motor impairments induced by binge drinking (Supplementary Figure S2C). Thus, binge drinking in mice effectively resulted in impaired motor function and altered gait patterns, mimicking hangover symptoms, which were associated with increased alcohol metabolites.

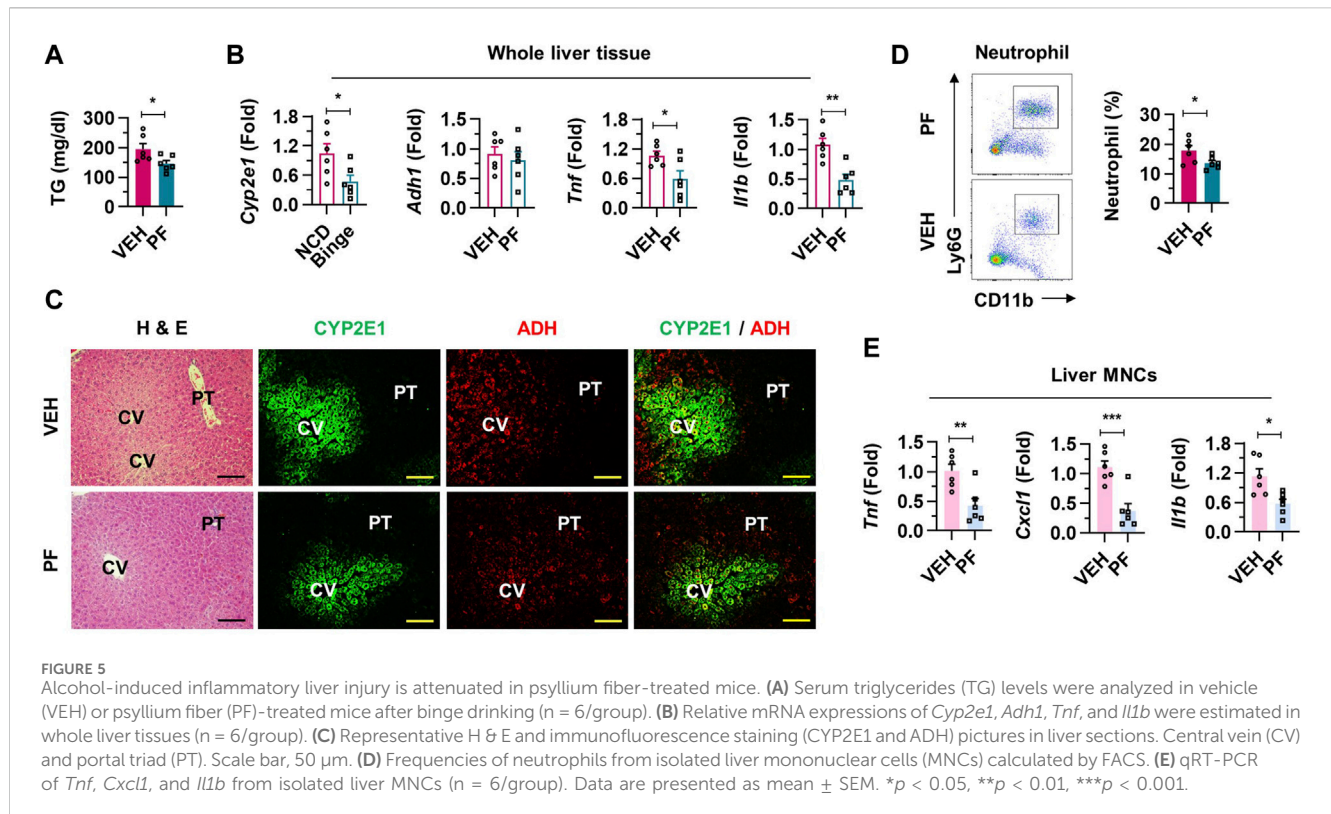
3.4 Psyllium fiber inhibits alcohol absorption in intestine

To evaluate the efficacy of psyllium fiber in modulating the effects of alcohol absorption, mice subjected to binge drinking were administered with vehicle or psyllium fiber (Figure 4). First, a significant reduction in both AST and ALT levels was observed in the group treated with psyllium fiber compared to the vehicle group (Figure 4A). After evaluating serological inflammatory markers, psyllium fiber was found to reduce alcohol-induced damage to intestinal epithelial cells and steatosis. These findings underscore the histopathological benefits of psyllium fiber in preserving the integrity of the intestinal mucosa upon alcohol exposure (Figure 4B). In qRT-PCR and Western blot analyses, mice treated with psyllium fiber displayed a notable decrease in

mRNA and protein expression levels of CYP2E1 and ADH compared to the vehicle-treated group. This reduction indicates that PF may exert a regulatory effect on the metabolic pathways engaged in alcohol processing in the intestine (Figures 4C, D). Immunostaining analysis also showed diminished localization and expression of CYP2E1 and ADH enzymes in the intestinal tissues of psyllium fiber-treated mice, aligning with the qRT-PCR and Western blot data (Figure 4E). Lastly, psyllium fiber treatment remarkably decreased the blood levels of ethanol, acetaldehyde, and acetate, indicating that psyllium fiber effectively reduced alcohol absorption in the intestine (Figure 4F).

3.5 Alcohol-induced hepatic inflammation is attenuated after psyllium fiber treatment

Next, we investigated the impact of psyllium fiber on hepatic inflammation induced by binge drinking. Psyllium fiber treatment did not significantly affect total body weight or the liver to body weight ratio (Supplementary Figure S3A). There was a notable reduction of serum TG levels without the alteration of TC levels (Figure 5A; Supplementary Figure S3B). Psyllium fiber treatment resulted in the downregulation of pro-inflammatory genes such as *Cyp2e1*, *Adh1*, *Tnf*, and *Il1b*, indicating inhibited alcohol-metabolizing activity and inflammatory signaling in the liver tissues (Figure 5B). This decrease in the number of hepatic MNCs is consistent with the anti-inflammatory effects observed at the molecular level (Supplementary Figure S3C). Histological analysis revealed reduced damage in hepatocytes and decreased steatosis around the CVs in the psyllium fiber-treated mice.



Furthermore, a decline in the expression of alcohol-metabolizing enzymes CYP2E1 and ADH was observed (Figure 5C; Supplementary Figure S3D). Flow cytometry analysis of isolated liver MNCs from the psyllium fiber-treated group showed a significant reduction in neutrophil frequency, without notable changes in the counts of macrophages and eosinophils, further supporting the anti-inflammatory properties of psyllium fiber in alcohol-induced liver injury (Figure 5D; Supplementary Figure S3E). As expected, RT-PCR showed that psyllium fiber treatment significantly reduced the expression of pro-inflammatory cytokines in liver MNCs (Figure 5E). Therefore, our findings demonstrate that psyllium fiber treatment effectively attenuates alcohol-induced hepatic inflammation.

3.6 Psyllium fiber improves hangover symptoms with reduced alcohol metabolites

The behavioral effects of psyllium fiber on improving hangover symptoms following binge drinking were analyzed through a series of motor function tests. Supplementary videos show representative cylinder test performances of the normal mice, the binge group treated with vehicle, and the binge group treated with psyllium fiber, respectively (Supplementary Videos S1–S3). Psyllium fiber treatment significantly increased the number of touches in the cylinder test following alcohol consumption, suggesting an improvement in motor coordination and balance in treated mice (Figure 6A). Correlation analyses demonstrated a remarkable relationship in the psyllium fiber group, where an increase in the number of touches in the cylinder test was associated with a decrease

in alcohol metabolites, suggesting that the psyllium fiber may enhance recovery from motor impairment following binge drinking (Figure 6B). The footprint test conducted 6 h after alcohol consumption indicated that psyllium fiber-treated mice exhibited improved motor function, characterized by an increase in stride length and a decrease in stride width, reflecting enhanced gait stability (Figure 6C). In the comparison of forelimb and hindlimb strides, the psyllium fiber group displayed an increase in stride length and a decrease in stride width (Figure 6D; Supplementary Figure S4A). In the psyllium fiber group, correlation analysis of forelimb and hindlimb footprint tests showed that as alcohol metabolites decreased, stride length increased and stride width decreased, suggesting an improvement in gait stability and a reduction in staggered walking commonly associated with hangover symptoms (Figure 6E; Supplementary Figures S4B, C). In summary, psyllium fiber alleviates hangover symptoms induced by binge drinking, as evidenced by improved motor functions and reduced alcohol metabolites.

3.7 Psyllium fiber suppresses the alcohol absorption into the cells

To further demonstrate the hypothesis that psyllium fiber holds alcohol and thereby inhibits its absorption into cells, additional *in vitro* experiments were conducted. When HepG2 cells were treated with ethanol, there was a marked increase in the mRNA levels of CYP2E1 and ADH1, which are essential enzymes in alcohol metabolism. In contrast, due to the inhibitory effect of psyllium fiber on ethanol absorption across the intestinal wall, a noticeable

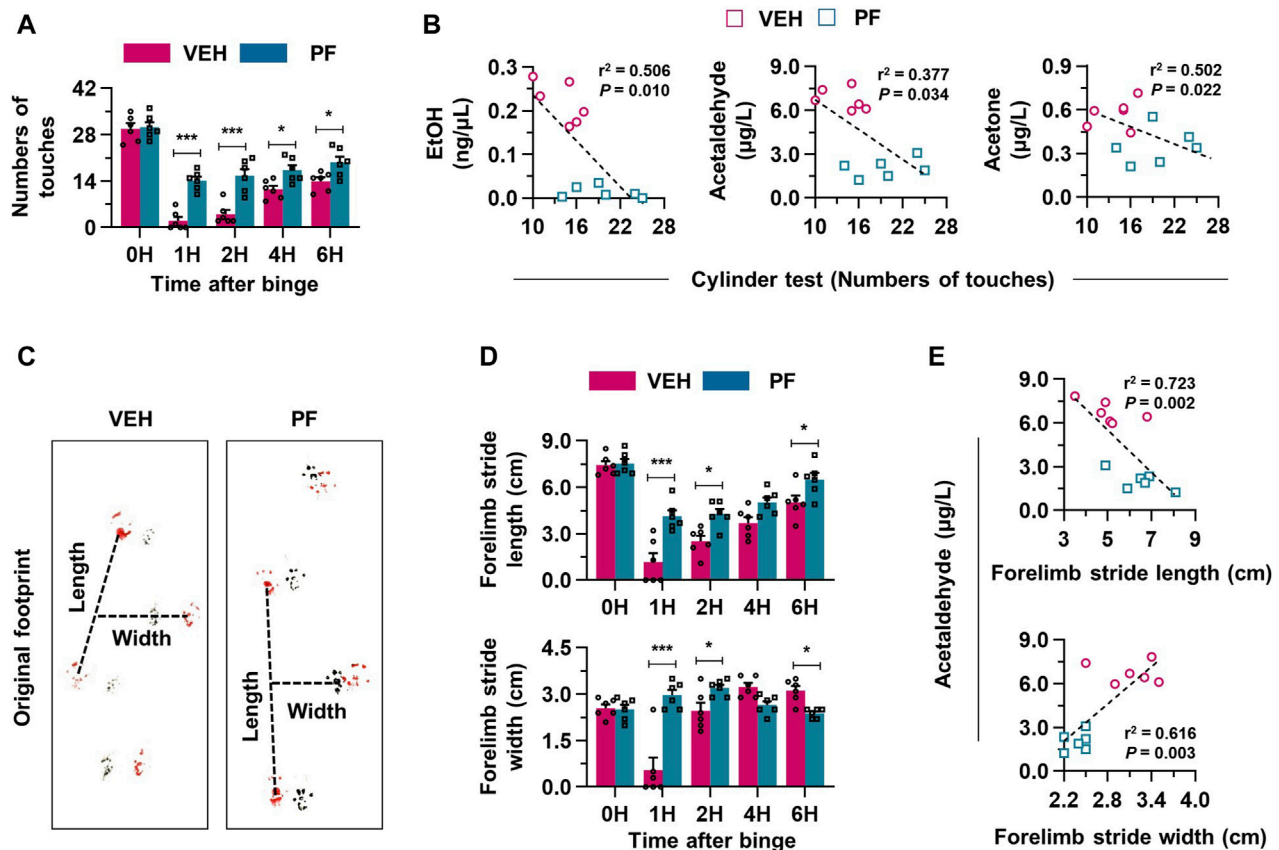


FIGURE 6

Psyllium fiber effectively improves hangover symptoms with decreased alcohol metabolites. (A) Psyllium fiber (PF) increased the number of touches in the cylinder test at different time points ($n = 6/\text{group}$). (B) Correlation analysis was performed among alcohol metabolites and cylinder tests in vehicle (VEH) or PF-treated groups ($n = 6/\text{group}$). (C) Representative pictures of the footprint test taken 6 h after binge drinking. (D) Forelimb stride length and width were compared at the different time points after binge drinking ($n = 6/\text{group}$). (E) Correlative analysis between forelimb stride tests and acetaldehyde levels ($n = 6/\text{group}$). Data are presented as mean \pm SEM. * $p < 0.05$, ** $p < 0.01$, *** $p < 0.001$.

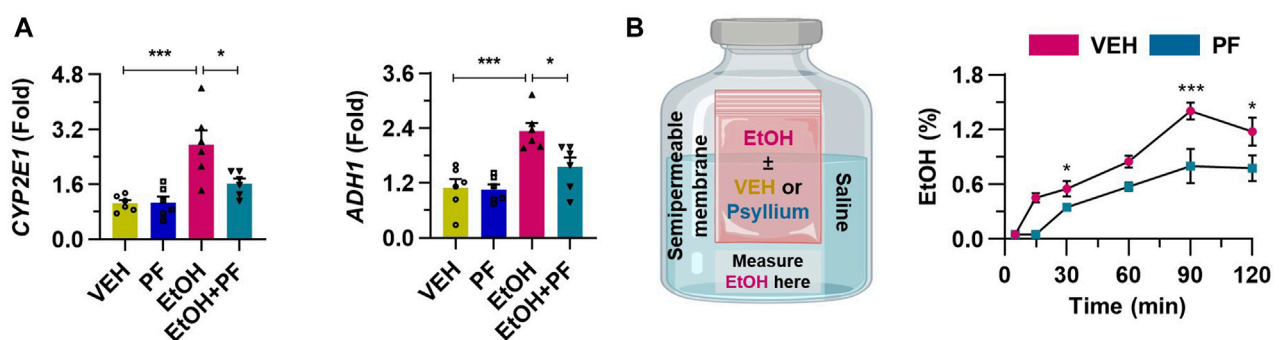


FIGURE 7

Psyllium fiber inhibits the alcohol absorption into the cells. (A) qRT-PCR of *CYP2E1* and *ADH1* in cultured HepG2 cells treated with 100 mM ethanol (EtOH) or 1 mM psyllium fiber (PF) for 6 h ($n = 6/\text{group}$). (B) Ethanol concentration was consecutively measured using a semipermeable membrane in samples treated with vehicle (VEH) or 10 mM psyllium fiber (PF) ($n = 4/\text{group}$). Data are presented as mean \pm SEM. * $p < 0.05$, ** $p < 0.01$, *** $p < 0.001$.

decrease in the expression of these metabolic enzymes was observed (Figure 7A). In the semipermeable membrane, experiment, the treatment with psyllium fiber significantly suppressed the movement of alcohol through the membrane (Figure 7B). This

indicates that psyllium fiber may hold onto alcohol, preventing its passage through the membrane, which could imply the ability of psyllium fiber to inhibit the absorption of alcohol in the gastrointestinal tract.

4 Discussion

In our study, we provide several lines of evidences that psyllium fiber decreases intestinal metabolism of alcohol after acute drink of alcohol and relieves hangover symptoms (Graphical Abstract). The experimental data using mice suggested that binge drinking upregulates expressions of enzymes including CYP2E1 and ADH within the wall of jejunum and administration of psyllium fiber reduces the expressions. Moreover, impaired motor function of mice with binge drinking dramatically recovered with additional consumption of psyllium fiber with alcohol regarding to the data in this study including the gait dynamic of mice (Kale et al., 2004; Hansen and Pulst, 2013). We also revealed the hepatoprotective effect of psyllium fiber against acute inflammation induced by alcohol drinking using qRT-PCR, flow cytometry, and immunofluorescence staining. In the *in vitro* experiment, we examined the protective mechanisms of psyllium husk fiber on the gut and liver when exposed to alcohol-induced damage. This investigation involved treating HepG2 cell lines and employing semipermeable osmosis membranes to elucidate the details of the process.

A recent interesting study introduced the concept of “intestinal drinking” and it refers to the continue absorption of alcohol in the gut barrier until the defecation, the final release of the fecal materials. The study found that acetaldehyde levels in the blood peaked after binge drinking, and consecutive defecation significantly downregulated the concentration. Furthermore, the study revealed that neutrophil count in the blood and hangover related symptoms such as nausea, headache, and fatigue gradually decreased with the defecation in the next morning of binge drinking. The study emphasized that termination of alcohol absorption within the gastrointestinal wall would relieve hangover related factors (Ryu et al., 2023).

Ethanol is metabolized not only in the liver, but also in the gastrointestinal wall and the fact suggest the gut barrier as the first gatekeeper of alcohol consumption in human body. Ethanol could be metabolized with mucosal cell by ADH and microsomal ethanol oxidizing system (Seitz et al., 1994). A study concluded that ADH and ALDH isozymes are differentially expressed in the jejunum and the result suggest that the small bowel could be the first pass metabolism of alcohol and cytotoxic acetaldehyde would play a pivotal role in gastrointestinal tract (Chiang et al., 2009). Furthermore, gut-liver crosstalk caused by increased gut permeability in alcohol associated liver disease, and inflammatory response induced by upregulated expression of TNF- α , IL-1 β and IL-6 in distal ileum with chronic exposure to alcohol support the importance of alcohol metabolism of the intestinal wall (Shim and Jeong, 2020). Collectively, this study aims to highlight the potential efficacy of medical interventions targeting the gastrointestinal wall in alleviating hangover symptoms following binge drinking. We propose the concept of faster alcohol deprivation in the gut with psyllium fiber as a promising approach to mitigate hangover severity.

Psyllium fiber is one of the fiber laxatives that work by increasing the weight and hydrophilic characteristics of stool, thereby softening the consistency of the stool. It is a soluble fiber that blends with water and forms a gelatin-like substance in gastrointestinal tract. Soluble fibers including psyllium fiber is one of the safe and well-tolerated laxatives of which adverse events are rarely occurred with mild abdominal distension (Jensen et al., 2013; Singh et al., 2021). A

review article addressed that psyllium as level II evidence and grade B recommendation as a laxatives (Rao and Brenner, 2021). This bulking agent that is a non-absorbable in gastrointestinal tract, absorbs water and enhances intestinal peristalsis deemed safe even during pregnancy (Clementi and Weber-Schöndorfer, 2015).

Previous studies examining hangover improvement have highlighted the increased activities of alcohol-metabolizing enzymes with various medical interventions. A recent study addressed the plant-base extract mixture (*M. crystallinum*, *P. lobata* flower, and *A. indica*) could decrease blood acetaldehyde level and hangover symptoms such as thirst and tiredness, and mechanistic study revealed that blood ADH and ALDH level significantly increased right after the alcohol consumption with the treatment (Jung et al., 2023). Several studies suggest that herbal medicines including *Camellia sinensis*, *Houttuynia cordata*, *Nelumbo nucifera* G., and *Opuntia ficus indica* suggest that activation of ADH and ALDH could be the key mechanism of the hangover relief (Moslemi et al., 2023). Furthermore, fermented smilax china root extract, and fermented persimmon juice also emphasized the importance of increased expression of alcohol metabolizing enzymes with medical intervention after acute alcohol consumption (Zhou et al., 2019; Boby et al., 2021). Nevertheless, our study aims the downregulation of the ethanol metabolizing enzymes, interrupting the absorption of alcohol through the gastrointestinal wall and we analyzed the consequences of the psyllium fiber administration, a bulk forming laxatives.

Recent studies highlight the significance of the gut-liver axis in alcohol-associated liver disease, underscoring the potential of psyllium fiber intervention to not only alleviate hangover symptoms but also mitigate the inflammatory insults to the liver induced by excessive alcohol metabolism. Binge drinking not only leads to risky behavioral habits, impaired cardiovascular system, and gut inflammation, but also induces increased intestinal permeability, upregulated serum nitric oxide, excess of lipid peroxidation products, and sinusoidal endothelia cell dysfunction, thereby results in worsened liver injury and increased portal pressure (Mathurin and Deltenre, 2009). In this research, we investigated the protective effect of psyllium fiber against absorption of alcohol from the gastrointestinal tract, which might reduce the ethanol exposure to the liver via portal vein or systemic circulation. By downregulating “intestinal drinking,” psyllium fiber may not only alleviate hangover symptoms but also exert a hepatoprotective effect against acute liver inflammation. This was evidenced by histologic findings and flow cytometry analysis, which demonstrated a reduction in neutrophil infiltration with the medical intervention. Also, we conducted *in vitro* experiment that could explain the liver protection of psyllium fiber using HepG2 cell line and expression of alcohol metabolizing enzymes such as CYP2E1 and ADH.

Our findings also emphasized the osmotic effect of psyllium fiber, that result in retention of water in the gastrointestinal tract, and it could also hold alcohol that has hydrophilic characteristics. We specified this mechanism utilizing semipermeable membrane experiment. Ethanol plus vehicle or ethanol plus psyllium fiber were inserted in the semipermeable pocket, and the pocket was soaked in the saline bottle. Psyllium fiber effectively held water and additional ethanol, thereby inhibiting the leakage of ethanol from inside of pocket to the saline bottle (Figure 7B). The experimental data suggest that

administered psyllium fiber could hold water and hydrophilic ethanol by composing gelled structure throughout the gastrointestinal tract. This experimental mechanism is consistent with the mode of action as a laxatives of psyllium, which is explained by water retaining in the small intestine, and increasing water flow into the distal ileum and ascending colon, resulting increase in the fluidity of the colonic materials (Jalanka et al., 2019).

There may be concerns that alleviating hangover symptoms could potentially exacerbate alcoholism by encouraging further alcohol consumption. However, existing literature suggests that hangover, often accompanied by depressed mood, is a part of the vicious cycle of alcoholism (Wiese et al., 2000; Penning et al., 2010). Thus, relieving hangover symptoms could potentially disrupt this cycle. Moreover, research indicates that the elimination of alcohol and acetaldehyde through defecation may offer a solution not only for alleviating hangover symptoms but also for addressing alcohol abuse (Ryu et al., 2023).

The present study has several limitations that warrant acknowledgment. First, we could not conduct obtain human blood samples after binge drinking. For the further investigation, human cohort study with or without psyllium fiber after alcohol consumption would be required. Next, the effect of psyllium fiber was limited to the gut protection and hepatoprotective effect after binge drinking. In future experiments, it would be beneficial to explore the potential hangover protection mechanisms involving other organs, such as the brain or bone marrow, which are known to interact with the liver during acute alcohol-induced damage.

Based on the extensive experimental data gathered in this study, we propose that the administration of psyllium husk could serve as an effective treatment option for alleviating hangover symptoms and providing additional protection to the gastrointestinal tract and liver against acute alcohol-induced damage. Further supplementary experiments are warranted to explore the potential application of psyllium fiber as a safe and effective medical intervention for hangovers in real-world scenarios.

Data availability statement

The original contributions presented in the study are included in the article/**Supplementary Material**, further inquiries can be directed to the corresponding authors.

Ethics statement

The animal study was approved by the Institute Animal Care and Use Committee (IACUC) in Yonsei University Wonju College

of Medicine (IACUC number: YWC-230614-2). The study was conducted in accordance with the local legislation and institutional requirements.

Author contributions

KY: Conceptualization, Investigation, Methodology, Writing–original draft. TR: Conceptualization, Funding acquisition, Methodology, Supervision, Writing–review and editing. BSC: Conceptualization, Funding acquisition, Methodology, Supervision, Writing–review and editing.

Funding

The author(s) declare that financial support was received for the research, authorship, and/or publication of this article. This work was supported by the National Research Foundation of Korea (NRF) grant funded by the Korea government (MSIT) (No. 2021R1G1A1092673). And it was also supported by Basic Science Research Program through the National Research Foundation of Korea (NRF) funded by the Ministry of Education (No. RS-2023-00238039).

Conflict of interest

The authors declare that the research was conducted in the absence of any commercial or financial relationships that could be construed as a potential conflict of interest.

Publisher's note

All claims expressed in this article are solely those of the authors and do not necessarily represent those of their affiliated organizations, or those of the publisher, the editors and the reviewers. Any product that may be evaluated in this article, or claim that may be made by its manufacturer, is not guaranteed or endorsed by the publisher.

Supplementary material

The Supplementary Material for this article can be found online at: <https://www.frontiersin.org/articles/10.3389/fphar.2024.1378653/full#supplementary-material>

References

- Boby, N., Lee, E.-B., Abbas, M. A., Park, N. H., Lee, S. P., Ali, M. S., et al. (2021). Ethanol-induced hepatotoxicity and alcohol metabolism regulation by GABA-enriched fermented smilax China root extract in rats. *Foods* 10, 2381. doi:10.3390/foods10102381
- Brooks, P. J., and Zakhari, S. (2014). Acetaldehyde and the genome: beyond nuclear DNA adducts and carcinogenesis. *Environ. Mol. Mutagen.* 55, 77–91. doi:10.1002/em.21824
- Chiang, C. P., Wu, C. W., Lee, S. P., Chung, C. C., Wang, C. W., Lee, S. L., et al. (2009). Expression pattern, ethanol-metabolizing activities, and cellular localization of alcohol and aldehyde dehydrogenases in human pancreas: implications for pathogenesis of alcohol-induced pancreatic injury. *Alcohol. Clin. Exp. Res.* 33, 1059–1068. doi:10.1111/j.1530-0277.2009.00927.x
- Clementi, M., and Weber-Schöndorfer, C. (2015). "Gastro-intestinal medications, hypolipidemic agents and spasmolytics," in *Drugs during pregnancy and lactation* (Elsevier), 93–113.
- Eisenhofer, G., Lambie, D. G., Whiteside, E. A., and Johnson, R. H. (1985). Vasopressin concentrations during alcohol withdrawal. *Br. J. Addict.* 80, 195–199. doi:10.1111/j.1360-0443.1985.tb03271.x

- Gibb, R. D., McRorie, Jr J. W., Russell, D. A., Hasselblad, V., and D'Alessio, D. A. (2015). Psyllium fiber improves glycemic control proportional to loss of glycemic control: a meta-analysis of data in euglycemic subjects, patients at risk of type 2 diabetes mellitus, and patients being treated for type 2 diabetes mellitus. *Am. J. Clin. Nutr.* 102, 1604–1614. doi:10.3945/ajcn.115.106989
- Gibb, R. D., Sloan, K. J., and McRorie, Jr J. W. (2023). Psyllium is a natural nonfermented gel-forming fiber that is effective for weight loss: a comprehensive review and meta-analysis. *J. Am. Assoc. Nurse Pract.* 35, 468–476. doi:10.1097/JXX.0000000000000882
- Hansen, S. T., and Pulst, S. M. (2013). Response to ethanol induced ataxia between C57BL/6J and 129X1/SvJ mouse strains using a treadmill based assay. *Pharmacol. Biochem. Behav.* 103, 582–588. doi:10.1016/j.pbb.2012.10.010
- Jalanka, J., Major, G., Murray, K., Singh, G., Nowak, A., Kurtz, C., et al. (2019). The effect of psyllium husk on intestinal microbiota in constipated patients and healthy controls. *Int. J. Mol. Sci.* 20, 433. doi:10.3390/ijms20020433
- Järvillehto, T., Laakso, M.-L., and Virsu, V. (1975). Human auditory evoked responses during hangover. *Psychopharmacologia* 42, 173–177. doi:10.1007/BF00429549
- Jensen, J. K., Johnson, N., and Wilkerson, C. G. (2013). Discovery of diversity in xylan biosynthetic genes by transcriptional profiling of a heteroxylan containing mucilaginous tissue. *Front. Plant Sci.* 4, 183. doi:10.3389/fpls.2013.00183
- Jung, S. H., Lee, Y. H., Lee, E. K., Park, S. D., Shim, J. J., Lee, J. L., et al. (2023). Effects of plant-based extract mixture on alcohol metabolism and hangover improvement in humans: a randomized, double-blind, paralleled, placebo-controlled clinical trial. *J. Clin. Med.* 12, 5244. doi:10.3390/jcm12165244
- Kale, A., Amende, I., Meyer, G. P., Crabbe, J. C., and Hampton, T. G. (2004). Ethanol's effects on gait dynamics in mice investigated by ventral plane videography. *Alcohol. Clin. Exp. Res.* 28, 1839–1848. doi:10.1097/01.alc.0000148103.09378.81
- Kim, H.-H., Choi, S. E., and Jeong, W.-I. (2020). Oxidative stress and glutamate excretion in alcoholic steatosis: metabolic synapse between hepatocyte and stellate cell. *Clin. Mol. Hepatology* 26, 697–704. doi:10.3350/cmh.2020.0152
- Lieber, C. S. (1995). Medical disorders of alcoholism. *N. Engl. J. Med.* 333, 1058–1065. doi:10.1056/NEJM199510193331607
- Mackus, M., Loo, A. J., Garssen, J., Kraneveld, A. D., Scholey, A., and Verster, J. C. (2020). The role of alcohol metabolism in the pathology of alcohol hangover. *J. Clin. Med.* 9, 3421. doi:10.3390/jcm9113421
- Mathurin, P., and Deltenre, P. (2009). Effect of binge drinking on the liver: an alarming public health issue? *Gut* 58, 613–617. doi:10.1136/gut.2007.145573
- McRorie, Jr J. W., and McKeown, N. M. (2017). Understanding the physics of functional fibers in the gastrointestinal tract: an evidence-based approach to resolving enduring misconceptions about insoluble and soluble fiber. *J. Acad. Nutr. Dietetics* 117, 251–264. doi:10.1016/j.jand.2016.09.021
- Moslemi, M., Jannat, B., Mahmoudzadeh, M., Ghasemlou, M., and Abedi, A. S. (2023). Detoxification activity of bioactive food compounds against ethanol-induced injuries and hangover symptoms: a review. *Food Sci. Nutr.* 11, 5028–5040. doi:10.1002/fsn3.3520
- Parantainen, J. (1983). Prostaglandins in alcohol intolerance and hangover. *Drug alcohol dependence* 11, 239–248. doi:10.1016/0376-8716(83)90016-9
- Penning, R., van Nuland, M., Fliervoet, L., Olivier, B., and Verster, J. (2010). The pathology of alcohol hangover. *Curr. Drug Abuse Rev.* 3, 68–75. doi:10.2174/1874473711003020068
- Pittler, M. H., Verster, J. C., and Ernst, E. (2005). Interventions for preventing or treating alcohol hangover: systematic review of randomised controlled trials. *Bmj* 331, 1515–1518. doi:10.1136/bmj.331.7531.1515
- Pittler, M. H., White, A. R., Stevinson, C., and Ernst, E. (2003). Effectiveness of artichoke extract in preventing alcohol-induced hangovers: a randomized controlled trial. *CMAJ* 169, 1269–1273.
- Prat, G., Adan, A., and Sánchez-Turet, M. (2009). Alcohol hangover: a critical review of explanatory factors. *Hum. Psychopharmacol. Clin. Exp.* 24, 259–267. doi:10.1002/hup.1023
- Rao, S. S., and Brenner, D. M. (2021). Efficacy and safety of over-the-counter therapies for chronic constipation: an updated systematic review. *Am. J. gastroenterology* 116, 1156–1181. doi:10.14309/ajg.0000000000001222
- Ryu, T., Yang, K., and Chung, B. S. (2023). Defecation alleviates hangover by terminating intestinal drinking. *Archives Med. Sci. AMS* 19, 1909–1912. doi:10.5114/aoms/174445
- Seitz, H., Gärtner, U., Egerer, G., and Simanowski, U. (1994). Ethanol metabolism in the gastrointestinal tract and its possible consequences. *Alcohol Alcohol. Oxf. Oxf. Suppl.* 2, 157–162.
- Shim, Y.-R., and Jeong, W.-I. (2020). Recent advances of sterile inflammation and inter-organ cross-talk in alcoholic liver disease. *Exp. Mol. Med.* 52, 772–780. doi:10.1038/s12276-020-0438-5
- Singh, A., Benjakul, S., Prodpran, T., and Nuthong, P. (2021). Effect of psyllium (*Plantago ovata* Forsk) husk on characteristics, rheological and textural properties of threadfin bream surimi gel. *Foods* 10, 1181. doi:10.3390/foods10061181
- Single, E., Robson, L., Xie, X., and Rehm, J. (1998). The economic costs of alcohol, tobacco and illicit drugs in Canada, 1992. *Addiction* 93, 991–1006. doi:10.1046/j.1360-0443.1998.9379914.x
- Stockwell, T. (1998). Towards guidelines for low-risk drinking: quantifying the short- and long-term costs of hazardous alcohol consumption. *Alcohol. Clin. Exp. Res.* 22, 63S–69S. doi:10.1111/j.1530-0277.1998.tb04375.x
- Swift, R., and Davidson, D. (1998). Alcohol hangover: mechanisms and mediators. *Alcohol health Res. world* 22, 54–60.
- Wiese, J., McPherson, S., Odden, M. C., and Shlipak, M. G. (2004). Effect of *Opuntia ficus indica* on symptoms of the alcohol hangover. *Archives Intern. Med.* 164, 1334–1340. doi:10.1001/archinte.164.12.1334
- Wiese, J., Shlipak, M. G., and Browner, W. S. (2000). The alcohol hangover. *Ann. Intern. Med.* 132, 897–902. doi:10.7326/0003-4819-132-11-200006060-00008
- Zhou, C., Li, J., Mao, K., Gao, J., Li, X., Zhi, T., et al. (2019). Anti-hangover and anti-hypertensive effects *in vitro* of fermented persimmon juice. *CyTA-Journal Food* 17, 960–966. doi:10.1080/19476337.2019.1680578

Frontiers in Pharmacology

Explores the interactions between chemicals and living beings

The most cited journal in its field, which advances access to pharmacological discoveries to prevent and treat human disease.

Discover the latest Research Topics

[See more →](#)

Frontiers

Avenue du Tribunal-Fédéral 34
1005 Lausanne, Switzerland
frontiersin.org

Contact us

+41 (0)21 510 17 00
frontiersin.org/about/contact



Frontiers in Pharmacology

